DEPOSITIONAL PROCESSES

IN SALDANHA BAY AND LANGEBAAN LAGOON

B.W. FLEMMING

Thesis submitted in fulfilment of the requirements for the degree of Doctor of Philosophy in the Faculty of Science at the University of Cape Town.

AUGUST, 1977

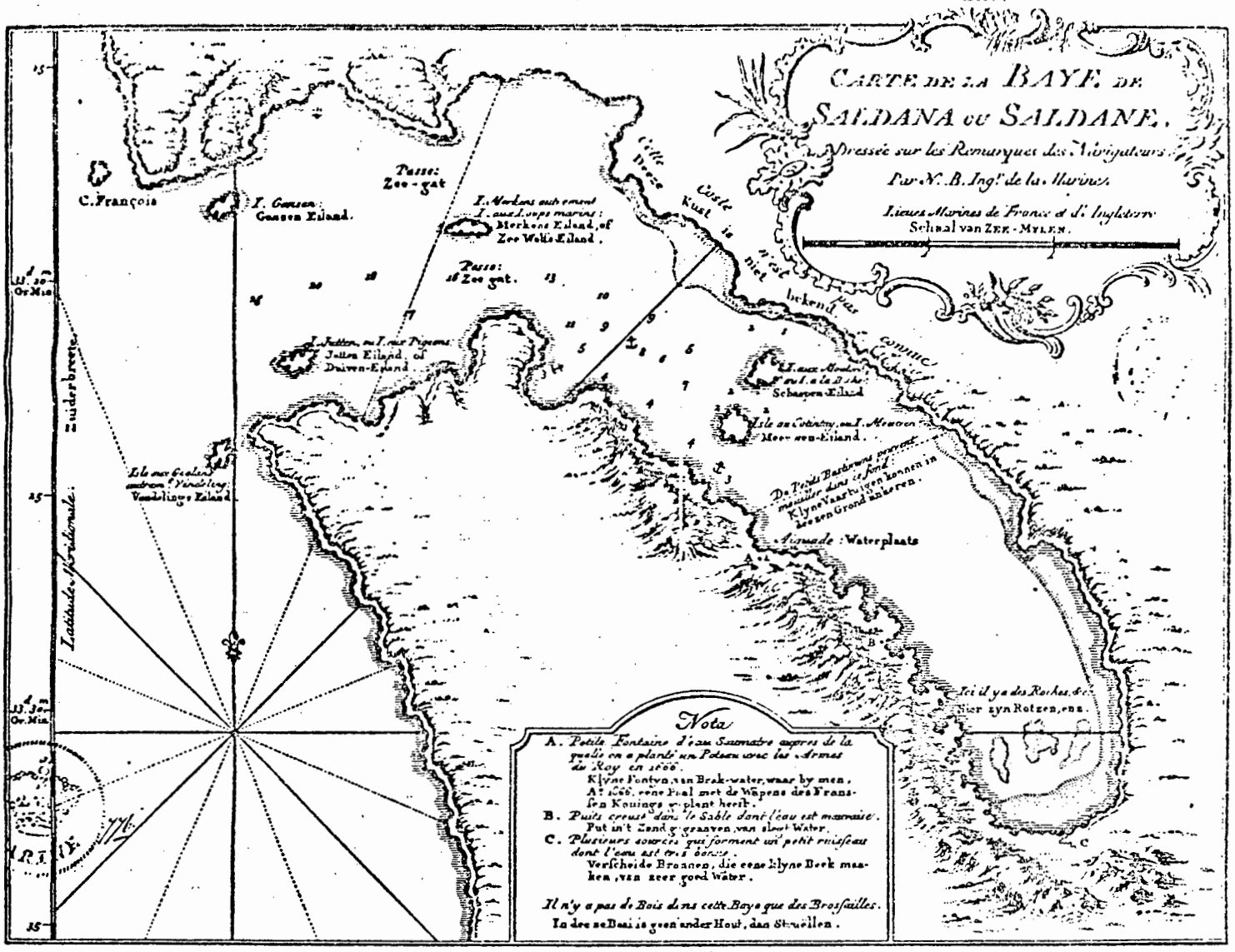

FRONTISPIECE :

An early map of Saldanha Bay and Langebaan Lagoon drawn by N. Bellini at about 1755 (Cape Archives).

ABSTRACT

This study deals with the physical aspects of sedimentation in Saldanha Bay and Langebaan Lagoon. On the basis of detailed textural investigations the depositional history of the study area has been established. The sediments in the bay and in the lagoon consist of a fine terrigenous quartz population and a coarser skeletal carbonate population, which have been mixed in various proportions. In order to gain size parameters that are more closely related to the hydraulic nature of depositional processes observed in the marine environment, grain size analyses were performed with an automatically recording settling tube system. The instrument was developed in the course of this study. Construction costs were kept extremely low without, however, impairing the scientific requirements of the instrument.

Over 500 sediment samples were recovered on a closely- spaced grid; in each case, a size analysis was performed on the total sample and on the insoluble, terrigenous fraction. By subtracting the terrigenous size distribution from that of the total sediment, the relevant size parameters of the bioclastic component were calculated. In this manner 1500 individual size distributions were avaible for interpretation.

In Saldanha Bay, a number of distinct energy zones can be distinguished which are clearly related to the wave-refraction pattern. A centrally-exposed zone is lined on both sides by semi-exposed zones, which in turn are followed by a sheltered zone in the northen bay and a lagoon/bay transitional zone in the south. The transitional zone is characterized by the interaction of ocean-waves and tidal ebb-currents leaving the lagoonal system via the outflow channels that are situated in the southern, wave-sheltered part of Saldanha Bay.

Physiographically the bay consists of a narrow, inshore sand prism that merges with thicker sand bodies that have accumulated in the northen, sheltered parts of the bay and in the bay/lagoon transitional zone, where a tidal delta is well defined. Both semi-exposed zones are covered by a thin veneer of sediment, usually under 0,5m thick. In the centrally-exposed parts of the bay an extensive abrasion platform is observed. It stretches between the inshore sand prism, which terminates approximately along the 11m depth contour, and the onset of the South Channel sand sheet at about -15m.

This physiographically-defined energy gradient is also reflected in the sediment distribution patterns. The coarsest sediments are found on the abrasion platform and along the exposed shorelines of the outer bay, especially in the vicinity of the North Channel. With the exception of the tidal delta in the south which consists of fine-grained sands, the remainder of the bay is charactized by very fine sands which appear to mantle the entire depositional system.

The individual spreading patterns of the terrigenous and the bioclastic components indicate that most of the bioclastic sediments are supplied from local sources, focusing around the abrasion platform and the North Channel. These are predominantly medium to coarse-grained. The terrigenous component, on the other hand, is clearly associated with the tidal delta at the mouth of Langebaan Lagoon. It is fine to very fine-grained and has been carried into the bay from the lagoon by the tidal ebb-current.

The depositional processes in Saldanha Bay are therefore characterized by two progressively mixing, hydraulic populations. A coarser, predominantly bioclastic population, supplied from sources within the bay, is mixed with a finer, predominantly terrigenous population that was supplied from Langebaan Lagoon. The degree of mixing is to a large extent controlled by the hydraulic response of each sedimentary component to the transport mechanism. Besides being coarser, the irregularly-shaped bioclastic particles experience a higher drag and are thus preferentially transported in bedload, whereas the finer-grained and better-rounded, terrigenous quartz particules are transported in bottom suspension. As a result, the carbonate content of the sediments decreases markedly towards the more sheltered parts of the bay.

In contrast, Langebaan Lagoon is a current-dominated environment. Current velocities reach 130 cm/sec at the mouth of the lagoon, and are ebb dominated. Four physiographic units are distinguished: 1) tidal channels, 2) subtidal flats and channel bars, 3) intertidal flats, 4) salt marshes. The energy gradient in the lagoon is reflected by the areal distribution of these units. In the northen parts of the lagoon, i.e. in proximity of the outflow channels, tidal channels and subtidal bars predominate. There are no intertidal flats or salt marshes. The central section is dominated by intertidal flats and tidal channels, whereas the southern section consists mainly of salt marshes. In most channels of the central and northen lagoon, flow velocities are high enough to generate underwater dunes which reach up to 2m in height and 40m in wavelength.

The distribution patterns of modern sediments in Langebaan Lagoon only partially reflect the north/south gradient indicated by the physiographic subdivisions. Instead the sediments are east/west aligned, dividing the lagoon longitudinally into two provinces, seperated by the central channel. The eastern half is predominantly fine-grained whereas the western half comprises medium-grained sediments. The relationship between individual size parameters reflects the process of progressive mixing between the two hydraulic populations in the south and centre. In the north this trend appears to be reversed, whereby the finer population is progressively eliminated as current velocities increase. In the eastern outflow channel a new hydraulic population has evolved which is distinctly different from either parent population.

Carbonate contents of lagoonal sediments are distinctly lower than those of the bay. However, there is a strong gradient in concentration from north to south. In the north the bioclastic component contributes up to 50% to the total sediment whereas in the very south it rarely reaches the 5% level. This selective concentration can be related to progressive shape-sorting in the process of hydraulic transport. This study indicates that the individual groups retain their size-distribution characteristics independently of each other, irrespective of the size-sorting mechanism to which they are exposed. This feature is not reflected by the size-distribution characteristics of the total sediment.

There is strong evidence in Langebaan Lagoon for a former high stand of the Holocene sea-level. The modern sediment distribution appears to reflect the inherited relict pattern, indicating that the modern system has remained essentially stable for some time. On the basis of radiocarbon dates, as well as stratigraphic and physiographic evidence, the Holocene evolution of the lagoon was reconstructed. It would appear that the post-glacial sea-level crossed its present level some 6500 years B.P., reaching a maximum of about +3m between 5000 and 6000 years ago. In this phase the late-Pleistocene dune landscape was drowned and selectively scoured, thereby producing the modern lagoon. The subsequent regression lasted until about 2000 years B.P.. Since that time there appears to have been little change in the entire system.

ACKNOWLEDGEMENTS

The project was initially sponsored by the Deutscher Akademischer Austauschdienst in conjunction with the National Department of Education, who kindly granted a postgraduate scholarship enabling me to further my studies in South Africa. The University of Cape Town in general, and the Department of Geology in particular deserve acknowledgement for providing work space and laboratory facilities. In July 1974 the project received a financial boost by the Department of Planning and the Environment in support of the aquisition of base-line data in the area before large-scale development affected the natural situation. In August 1974, encouraged by Prof. E.S.W. Simpson, I joined the staff of the newly founded National Research Institute of Oceanology (NRIO), under whose auspices the project continued until its completion.

Special thanks are due to the National Iron and Steel Corporation (ISCOR), who made their survey vessels freely available for diving operations in Saldanha Bay. I am greatly indebted to Mr. Jan van T'Hoff of Lievense Construction Co. for his kind hospitality and effort in organizing the ship time. I wish to thank the Sea Fisheries Branch, Department of Industries, for allowing the use of their laboratory in Saldanha and the South African Navy for providing space at their Langebaan base "SAS Flamingo". The Geological Survey, Department of Mines, provided the side-scan sonar instrument, used for sea bed surveys in the bay and the lagoon, and the National Phosphate Development Corporation (PHOSCOR) carried aut the P_2O_5 and the K_2O determinations. Both institutions are thanked for their help.

I am particularly grateful to Chief Petty Officer Reginald Willan and his wife Tiny for their generous hospitality at their Langebaan home and to my brother, Mr. Herbert Flemming, who sacrificed many weeks of his spare time to assit me in the field and the laboratory. I am greatly indebted to Dr. Alan Thum of the Zoology Department, University of Cape Town, for encouraging and financing the construction of the settling tube system for grain size analysis, to Dr. George Branch for his advice in matters concerning marine biology, and to Mr. John Allen, who assisted me as coxswain and buddy diver on several occasions.

Thanks are due to Mrs. Judy Woodford, Mr. Mathew Smith, and Mr. Jacobus Williams, who assisted me with draughting work, laboratory work, and photo-

graphic work respectively. Ms Shirley Wheeler and Mrs. Sylvia Strachan helped with last-minute draughting work, for which I am very grateful. Dr. Gordon Moir and Mr. Dave Reid are thanked for their considerable help with modifications to the computer program used for psi-transformation of settling tube data. The radiocarbon dates were carried out by Dr. J.C. Vogel of the CSIR in Pretoria. I wish to thank Mrs. G. Krummeck for her invisible helping hand throughout the years of this study. Special acknowledgement is due to Mrs. Hanni van den Heever who kindly typed the long manuscript.

Last but not least I wish to thank my supervisor, Dr. W.G. Siesser, for his critical assessment and useful comments to the manuscript, and to all my friends and colleagues at the Geology Department, University of Cape Town, who have contributed to the work through fruitful discussions and advice.

Finally I wish to recall the moral and material support of my parents, who saw me through the long years at university and my admirable teachers, Prof. Dr. E. Seibold, Prof. Dr. G. Einsele, and Prof. Dr. E. Walger, whose combined effort in conveying basic sedimentological thinking to me did not, after all, seem in vain.

CONTENTS

LIST OF TABLES

LIST OF FIGURES

LIST OF PLATES

CHAPTER 1. INTRODUCTION

Research in the marine sciences has for a long time been a remotely controlled exercise, and the lack of direct contact with the object under scrutiny has always been regarded as an unfortunate but inevitable shortcoming. With the advent of SCUBA it became possible for the scientist to observe, experiment and record "in situ".

Although the average scuba-equipment sets a practical depth limit of about 50 m it has opened up a significant and highly interesting section of the aquatic environment. Many geological and biological phenomena, for example, are directly or indirectly related to physical and chemical processes active within this part of the marine environment.

The new technique achieved particular popularity among marine biologists and is today regarded as an indispensable tool for the marine ecologist (Riedl, 1968). In marine geology, on the other hand, diving has remained a sporadic and individualistic undertaking in spite of some highly successful studies (e.g. Menard et al., 1954; Vause, 1959; Imbrie and Buchanan, 1965; Clifton et al., 1971; Boothroyd and Hubbard, 1974). Only in a few institutions has research diving in recent years become a routine procedure for investigations in shallow-water sedimentology. The present study was carried out with the specific aim of integrating diving into the systematic investigation of physical sedimentary processes in a shallow-marine environment. Many of the conclusions reached in the course of this study are the result of "in situ" observations.

The study area is ideally suited for the purpose of underwater investigations. Saldanha Bay and Langebaan Lagoon, situated about 100 km north of Cape Town (Fig. 1), are readily accessible from land or sea. The lagoon and large parts of the bay are protected from heavy surf action by rocky headlands and strong wave refraction.

The climatic setting of the study area is of considerable interest. Tidal sedimentation in warm and hot climates have received relatively little attention (Allen, 1970). Furthermore, the sediments of the area comprise a mixture of terrigenous quartz and skeletal carbonates.

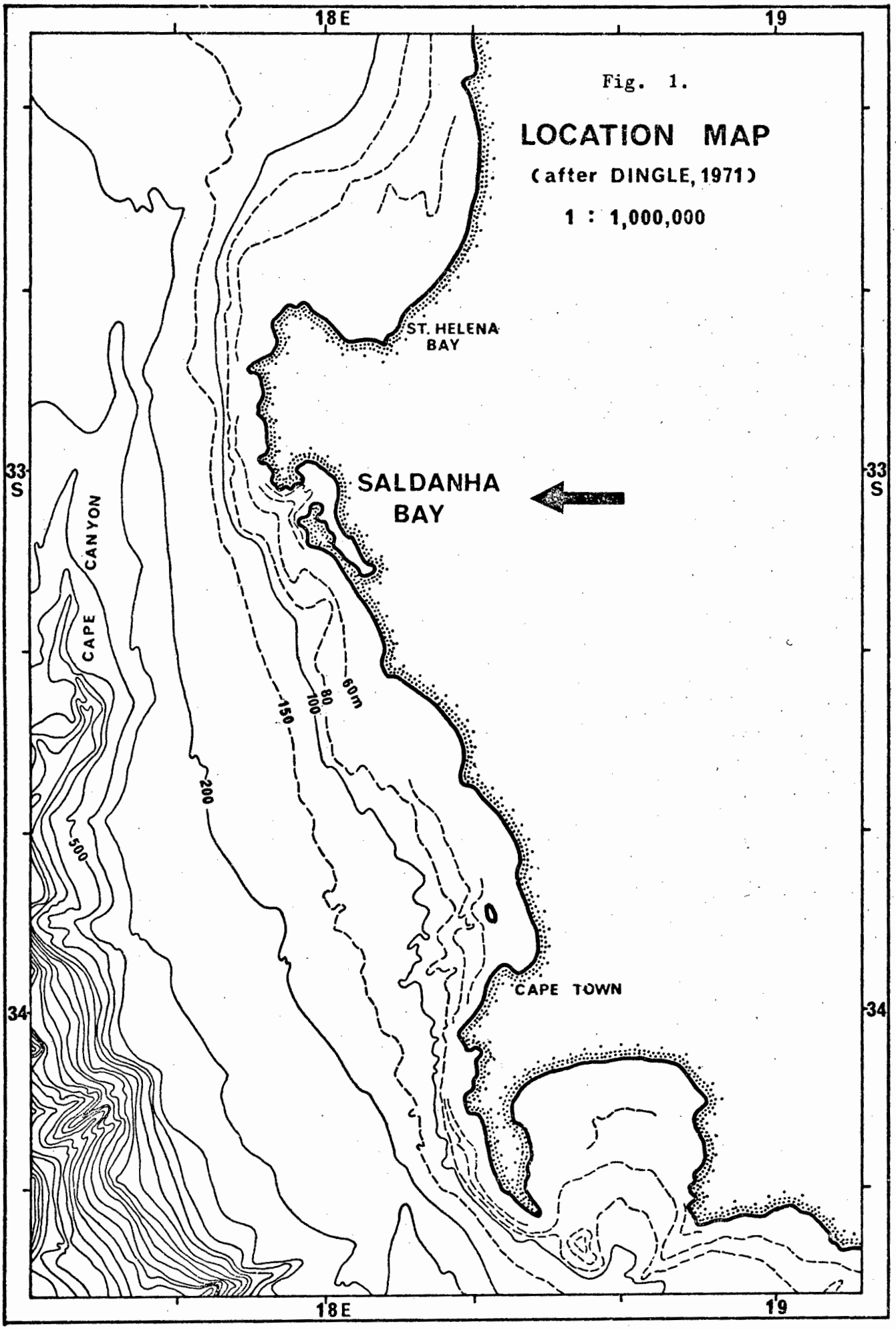

Fig. 1.

LOCATION MAP

(after DINGLE, 1971)

1 : 1,000,000

Klein (1975) has noted that up to date there exists only a single study dealing with mixed carbonate-siliciclastic tidal sediments (Larsonneur, 1975). In addition, Saldanha Bay and Langebaan Lagoon are exposed to distinctly different energy regimes; the former is wave dominated while the latter is controlled by tidal currents. A comparative study of depositional processes characterizing each area would be of interest because it could provide some relevant information on the variability of closely related depositional environments and their recognition in the fossil record.

A marginal aspect that has triggered acute public interest in the area in recent years is the large-scale development of Saldanha Bay into an iron-ore export terminal. Environmentalists and ecologists have expressed concern, especially about the future of Langebaan Lagoon in the wake of human interference and industrial pollution. The present study can therefore be viewed as providing sedimentological base-line data for future assessments of the environmental impact resulting from progressive urban and industrial development in an hitherto unspoiled natural environment.

This study will commence with a brief introduction into the regional setting of the area and continue with a detailed account of the investigational procedures adopted in the field and in the laboratory. Particular emphasis is given to the construction and calibration of an automatically recording settling tube system for the hydraulic grain size analysis of sands. A basic aim in the development of this instrument was the combination of two major demands - low cost and sufficient accuracy. It will be demonstrated that both requirements are fully met, thus providing a reliable and highly accurate instrument that can be routinely used in laboratories operating on low research budgets.

The study will proceed with the presentation and discussion of detailed sedimentological data from Saldanha Bay and Langebaan Lagoon. Both chapters contain further information on environmental aspects specifically relevant to the interpretation of the sedimentological data. After a presentation of the spatial distribution patterns of various grain-size parameters, their genetic relationships are investigated in terms of depositional processes that might adequately explain the observed patterns. Close attention will be given in each case to specific hydraulic

relationships between the two sedimentary components. Depositional environments, subenvironments, facies, and subfacies recognized on this basis are classified and described in terms of environmental characteristics and the lithology of the sediments. A final chapter summarizes the main findings and conclusions in a discussion of the Late Quarternary history of the system with special reference to the Holocene evolution of Langebaan Lagoon.

Until recently the marine geology of the area has received little attention and relevant literature is cited at appropriate places of the text. The writer has presented some of his data at two separate conferences - the Symposium on Research in the Natural Sciences at Saldanha, held at Saldanha in February 1976, and the International Tidalite Conference, held in Johannesburg in July 1976. Both contributions have in the meantime been published as parts of the respective conference proceedings (Flemming, 1977a and 1977b).

CHAPTER 2. REGIONAL SETTING OF THE STUDY AREA

2.1. CLIMATE

The study area lies in the northward extension of the mediterranean climatic belt touching the coastal areas of the southwestern Cape Province (Schulze, 1965). Rainfall is restricted to the winter months and summers are hot and dry. Precipitation is usually concentrated over short periods (Fig. 2B), and reaches peak values of 50 mm/month during May, June, and July and lowest values of 10 mm/month during November, December, January, February and March (Fig. 2A). The long-term yearly average amounts to about 300 mm and, as a result, the climate is semi-arid. Drainage in the immediate vicinity of the study area is very restricted and there is no significant freshwater inflow that would result from surface runoff. The effective catchment area is considerably smaller than the potential catchment area defined by the watershed (Fig. 3). This feature becomes particularly important when considering the sediment budget of the region. Substantial supply of modern terrigenous material is practically absent and the sediments are therefore predominantly of coastal-marine origin.

Wind patterns are summarized in Fig. 4. By far the most important component is formed by the southwesterly winds that form a local derivative of the Southeast Trade Winds which blow persistently during the summer months (Sept. - April) and intermittently during the winter months. Although these winds are frequently strong, reaching 25 km/h for over 90 days/year, they rarely reach gale force over the study area. In the winter months wind patterns are more variable, and rainfall is controlled by cyclonic northwesterly winds frequently reaching severe gale forces for short periods of time. Seasonal temperature fluctuations are low compared to those at higher latitudes. Minimum temperatures are usually well above freezing point whereas maximum temperatures can reach above 30°C.

2.2. HYDROLOGY

The study area faces the southeastern Atlantic Ocean which is controlled by the Benguela Current (Clowes, 1950; Bang, 1974). Large

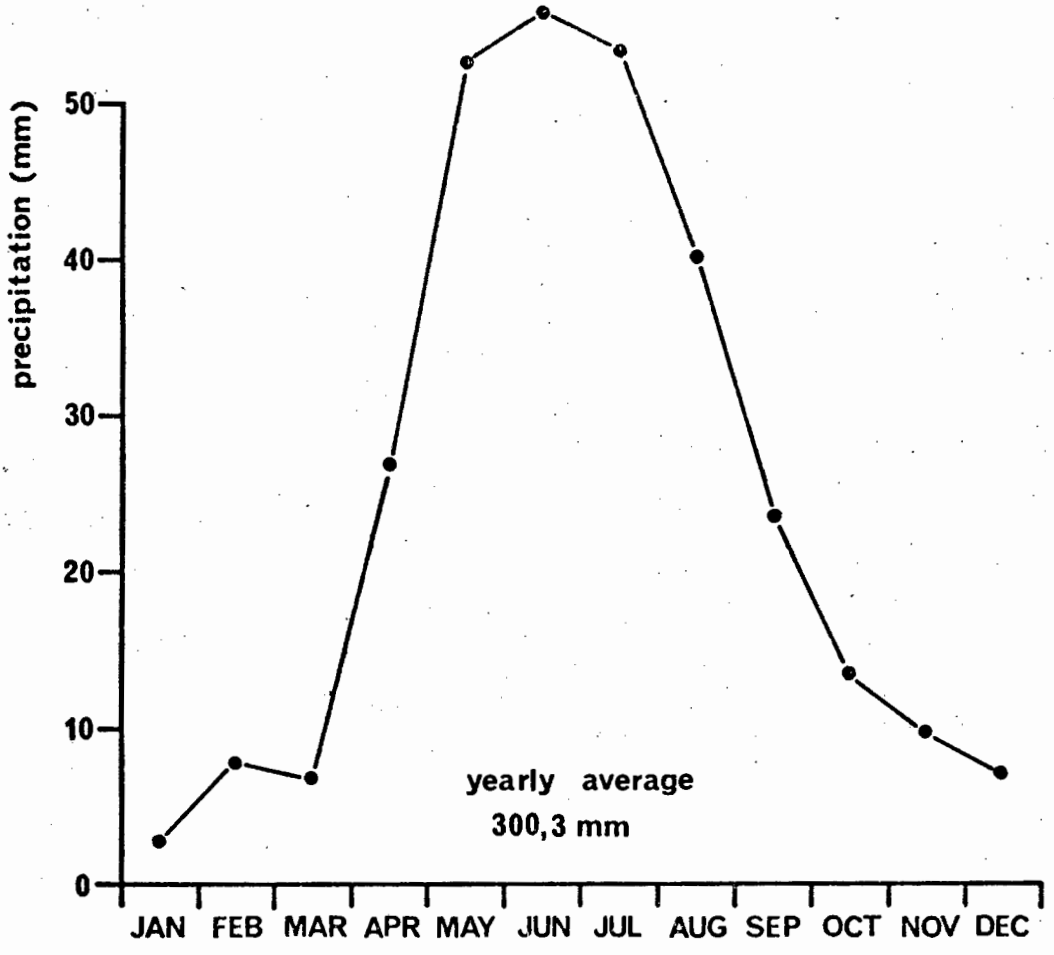

A : Monthly averages of precipitation over a period of 21 years; 1940 – 1961.

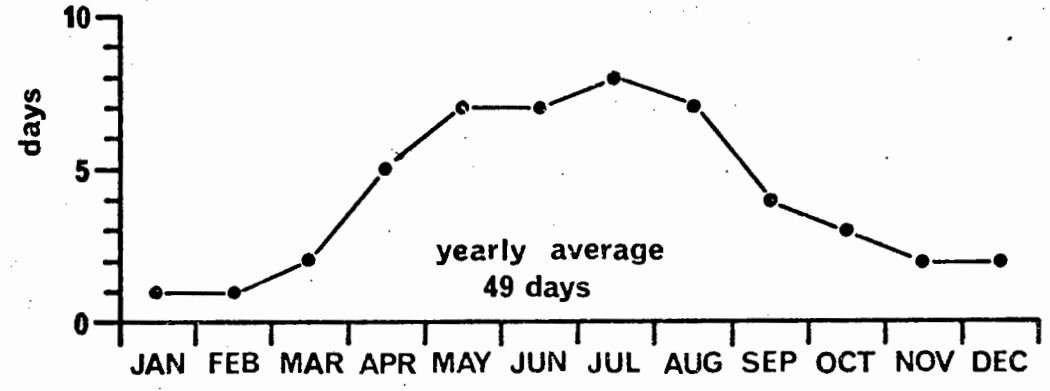

B : Nr. of days with rain; monthly averages over a period of 21 years; 1940 – 1961

Fig. 2.. Precipitation in the study area.

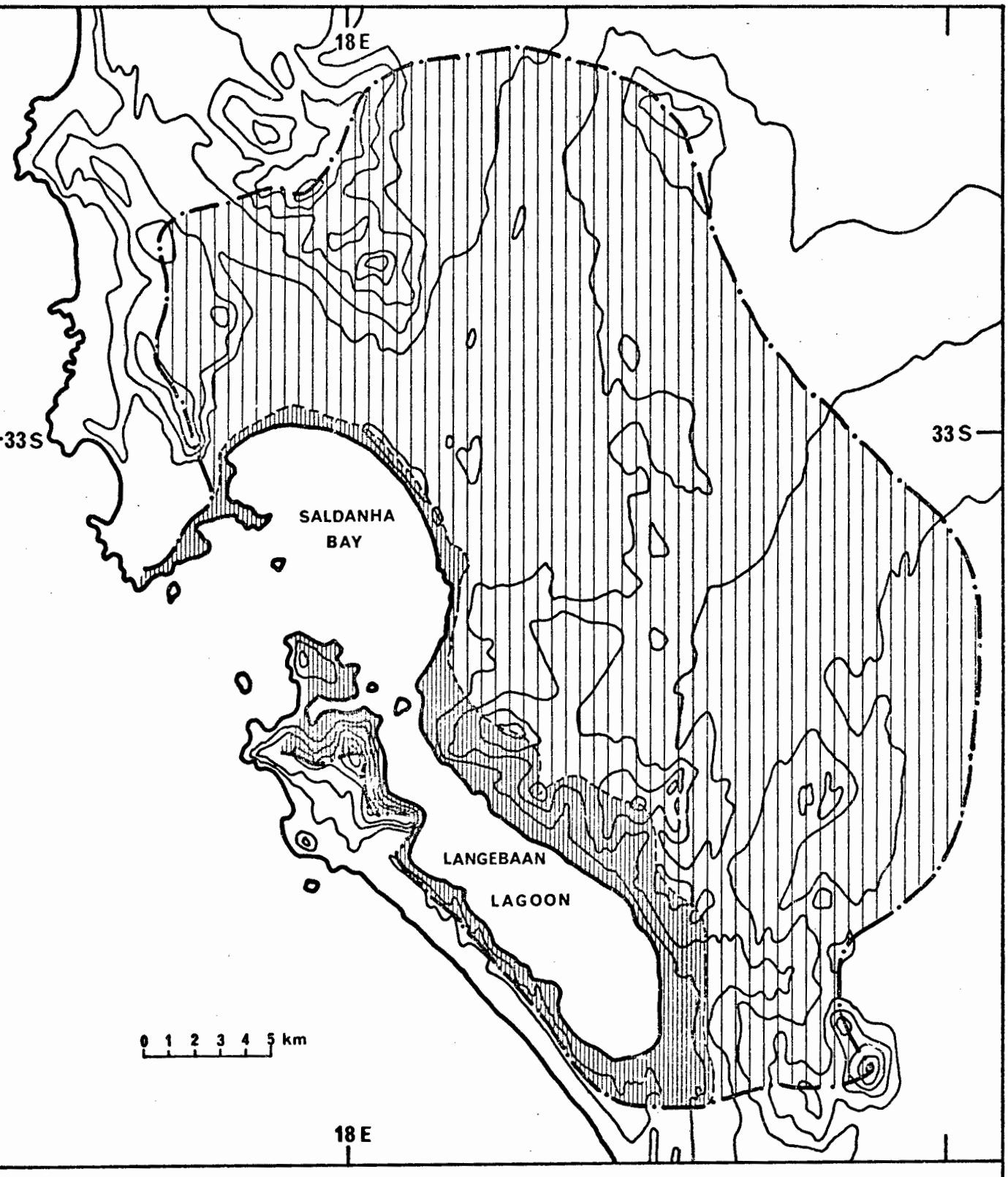

Fig. 3. Drainage in the vicinity of Saldanha Bay and Langebaan Lagoon.

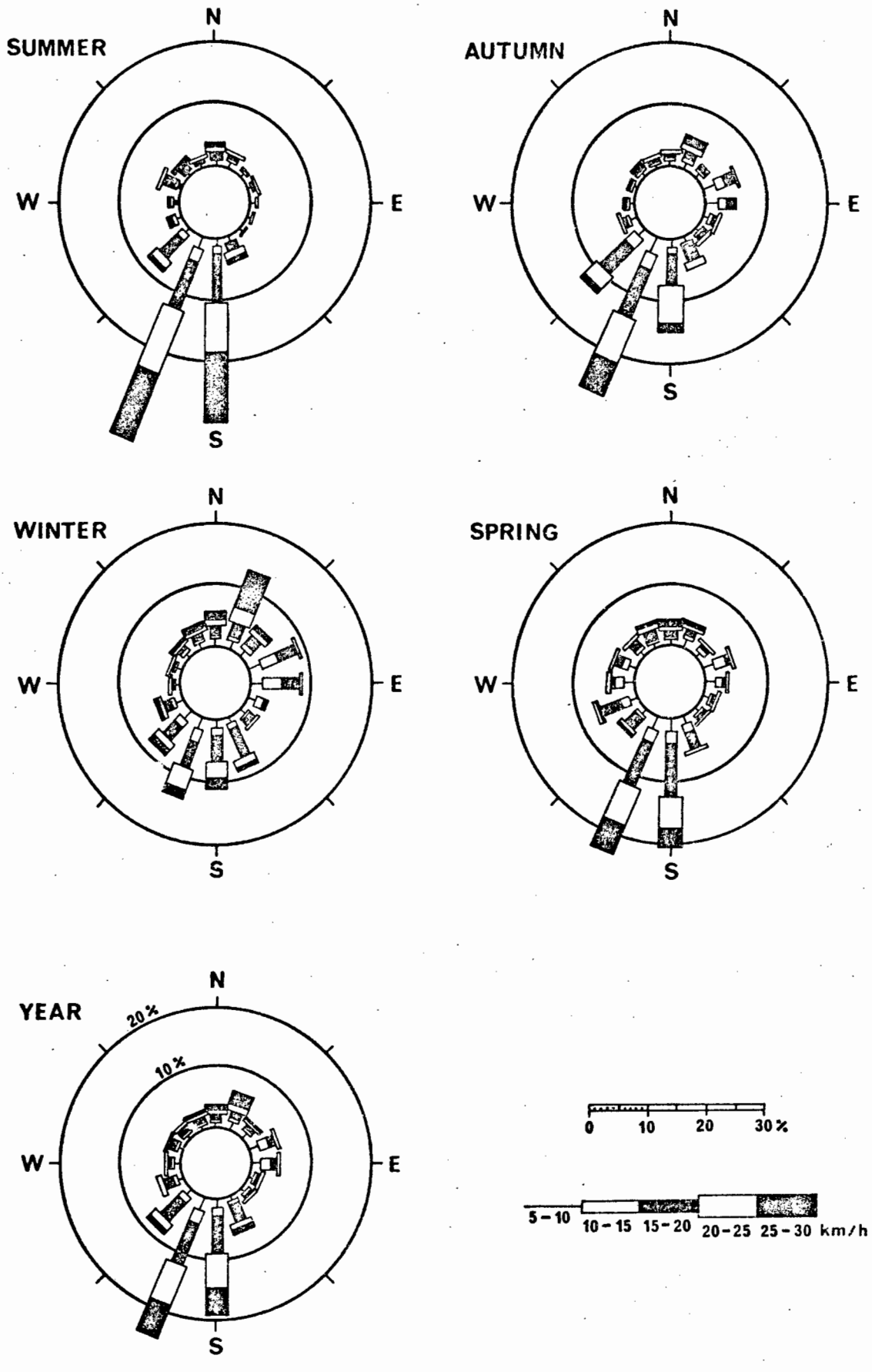

Fig. 4. Average wind conditions at Elandspunt.

cells of cold, upwelling waters develop regularly along the west coast during summer, responding to the strong southeasterly winds that are directed offshore. Although Saldanha Bay and Langebaan Lagoon are normally exposed to a southwesterly component of this wind, upwelling has also been observed just outside the embayment (Pearce and Smith, 1974).

A clear relationship between wind and current patterns has so far not been established but it would appear that, over longer periods, the inshore waters respond to the prevailing winds which, when strong enough, will affect the whole water column to a depth of at least 50 m. In summer, when weather conditions remain stable over long time periods, mass movement will occur predominantly in a northerly direction, although Duncan and Nell (1969) have observed inshore counter currents at the surface. In winter, on the other hand, the general direction of water movement seems to change direction more frequently, depending on the local weather cycle controlled by the rate at which cyclonic lowèpressure cells pass through the area.

Shannon and Stander (1977) have observed that there appears to be little direct interchange between the open sea and the bay, at least as far as their thermohaline characteristics are concerned. Solar radiation has a marked influence on the waters of Saldanha Bay and Langebaan Lagoon, and interaction with the open sea seems to occur only along the boundary of the latter water body and the tide controlled, forward and backward slopping water mass of the bay. The bay can be distinguished from the lagoon thermally, although lagoonal waters penetrate some distance into the southern bay during each ebb cycle. It will be seen later that this feature is also reflected in the distribution pattern of the mud fraction in the modern sediments. Whereas surface water temperatures outside Saldanha Bay rarely exceed 15°C in winter (Clowes, 1950), the respective values for the inner bay are 18°C and 16°C. In Langebaan Lagoon winter temperatures are generally stable around 17°C, whereas summer temperatures range from 17°C at the mouth to over 25°C in the south.

Salinity levels in the bay are very similar to those in the open sea both in summer and in winter, averaging around 34.9 parts/thousand. In summer a plume of slightly more saline water (> 35 parts/thousand) is frequently observed in the southeastern bay, reflecting the influx of lagoonal waters during the ebb tide cycle. In Langebaan Lagoon salinities

increase progressively with distance from the mouth, reaching at least 37 parts/thousand on the open flats of the southern lagoon. Summer and winter salinities for selected stations in Langebaan Lagoon are listed in Table 1.

Tidal currents follow a semi-diurnal cycle and the region falls into the globally defined microtidal range (Davies, 1972). Currents are strong in Langebaan Lagoon, reaching 1.3 m/sec at the mouth, but rarely exceed 15 cm/sec in Saldanha Bay itself. Here wave action appears to be the major energy source. The wave pattern is strongly dominated by swells from the SW and SSW (Fig. 5). The most frequent wave heights are between 2.5 and 3.5 m (Fig. 5A) and wave periods are dominated by 13 - 15 sec waves (Fig. 5B). Excessively high waves are rare and waves with a height of 5 m or more occur for a cumulative total of only 6 days/year (Kluger, 1972). As a result the wave climate is extremely constant, and this feature provides an excellent basis for an assessment of the relevant energy levels controlling sediment dispersal in Saldanha Bay.

Theoretical wave-refraction patterns, calculated for the open sea and the outer bay, are presented by Kluger (1972). The theoretical refraction patterns for swells from the SW and SSW are illustrated in Fig. 6A and 6B respectively. The predictions for the inner bay match very well with the pattern reconstructed by the writer from aerial photographs. A close relationship was observed between sediment distribution and relative energy levels outlined by the wave refraction pattern.

TABLE 1

Salinity ranges in various parts Langebaan Lagoon
(in parts per thousand)

STATION	WINTER	SUMMER
Inlet	33	34
Kraalbaai	32	34
Bottelary (open flats)	30	34.5
Bottelary (tidal pool)	21	57.5
Churchhaven	32	35
Geelbek	33	36.5
Salt Marsh (extreme south)	22	48

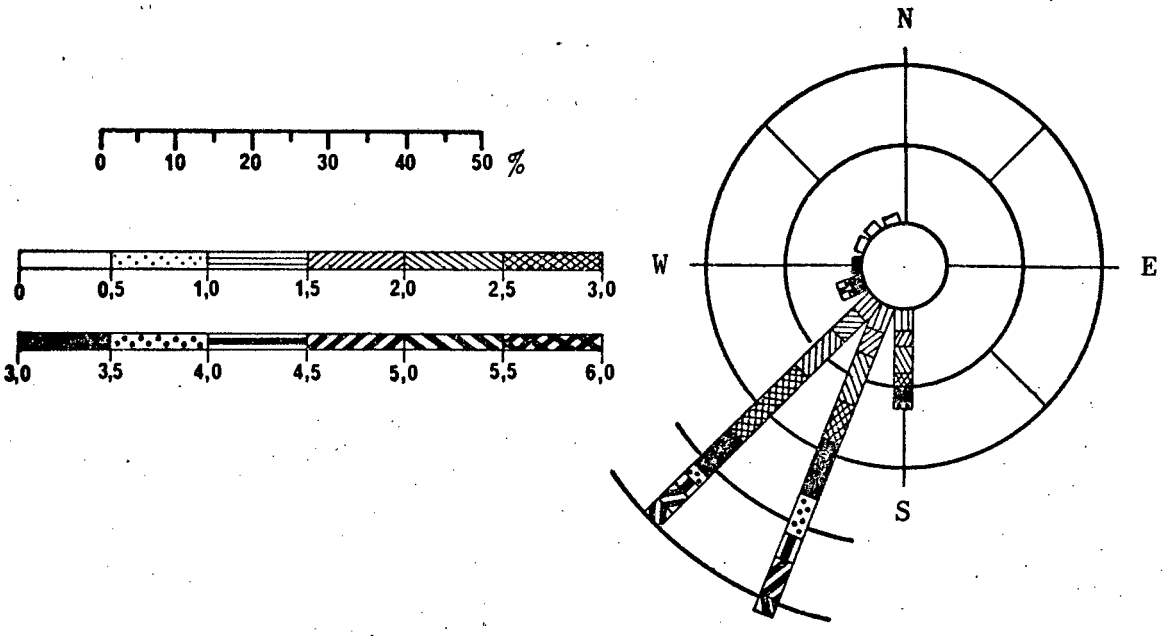

Fig. 5-A. Average wave heights near Saldanha Bay.

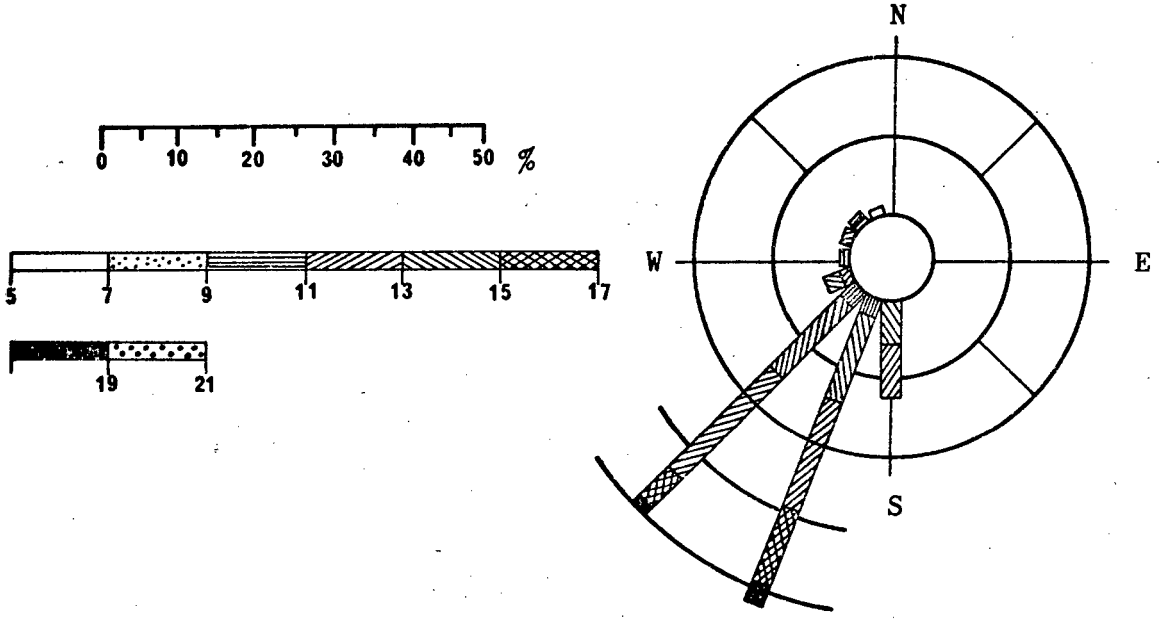

Fig. 5-B. Average wave periods near Saldanha Bay.

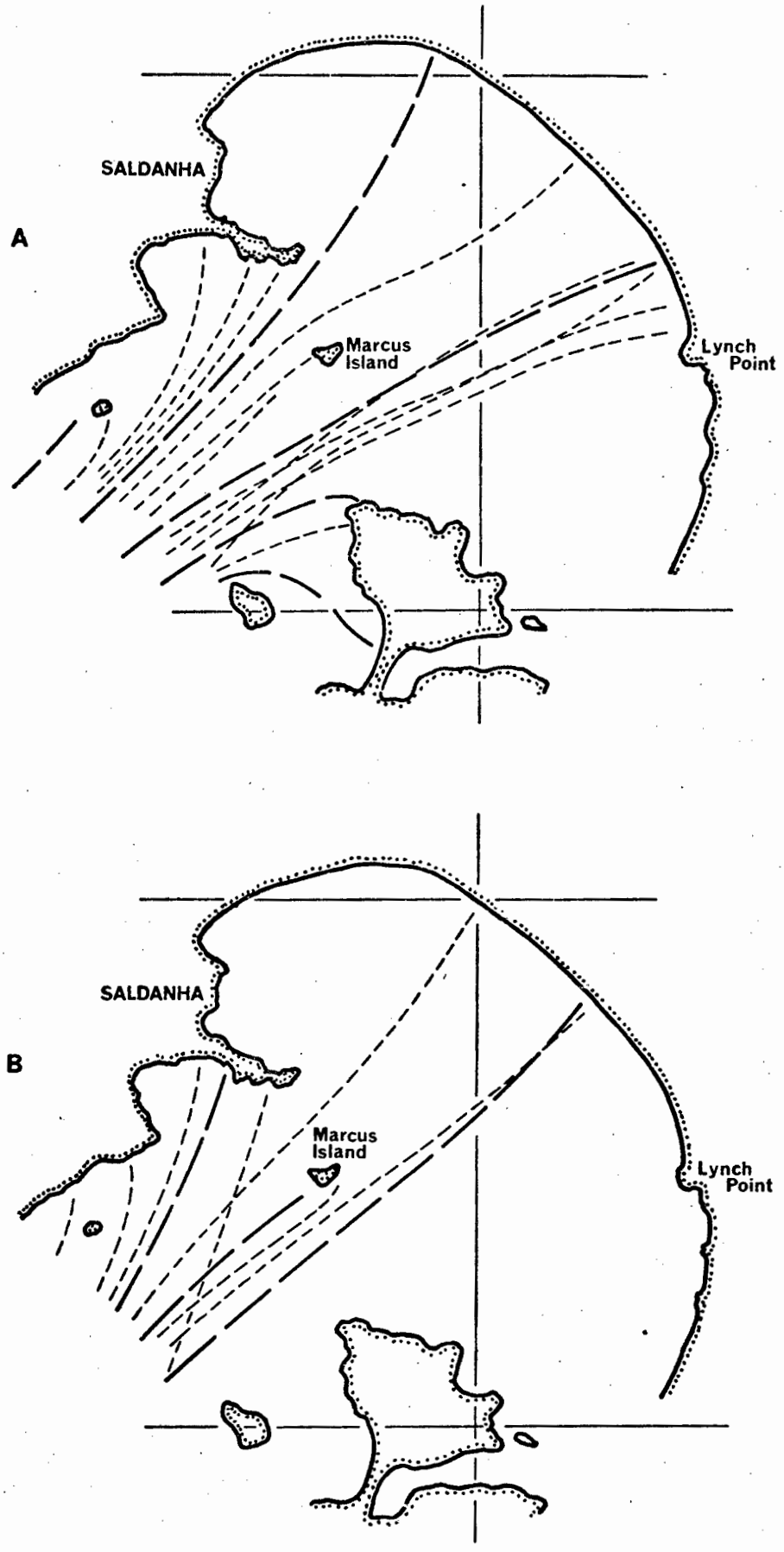

Fig. 6. Theoretical wave-refraction patterns in Saldanha Bay.

A. Waves approaching from SW.
B. Waves approaching from SSW.

(after Kluger, 1972)

2.3 GEOLOGY AND GEOMORPHOLOGY

The regional setting is illustrated in a generalized map of the onshore and offshore geology for the area, between the Cape Peninsula in the south, and Elandsbaai in the north (Fig. 7). The map is based on data compiled by Dingle (1971). The local geological framework is relatively simple. Relief is controlled by dome-like outcrops of the granite basement (Fig. 8). These granites form the southern and northern headlands which define and control the deep-water entrance to Saldanha Bay. The northern section of Langebaan Lagoon is also lined by high granite hills. These socalled Darling granites formed 500-550 million years ago (Visser and Schoch, 1973) as intrusive bodies penetrating into Malmesbury shales which, after a prolonged period of planation, were covered by Table Mountain Sandstones. None of these older sediments are preserved in the study area, with the exception of some small remains of Malmesbury rocks at the mouth of Rietbaai and on Skaapeilands near Langebaan. Millions of years of uninterrupted erosion have resulted in total denudation down to the granite basement along this coastal section.

The immediate hinterland forms an elevated, relict wave-cut platform cut into Malmesbury shales sometime during the Upper Cretaceous or early Tertiary, in the wake of the break-up of western Gondwanaland. During the Tertiary and the Quarternary the low-lying areas were infilled with sediments indicating coastal-marine conditions. These deposits show evidence of numerous marine transgressions and regressions since the late Tertiary. As a result, most of the coastal sediments will have been recycled several times. In many depressions the modern landsurface exposes extensive calcrete sheets which must have formed during low stands of the sea. They have recently been traced seawards by geophysical methods (Du Plessis and De la Cruz, 1977) and the writer has encountered calcrete outcrops on numerous occasions while diving in the central part of Saldanha Bay.

Various aspects of the onshore geology are discussed by Du Toit (1917), Krige (1927), Haughton (1932), Talbot (1947), Mabutt (1956), Haughton (1969), Hendy (1970, Kensley (1972), Siesser (1972), Davies (1973), Visser and Schoch (1973) and Tankard (1974).

The geomorphology of the subaerial and submarine terrain appears to be a direct expression of the geological response to marine and subaerial

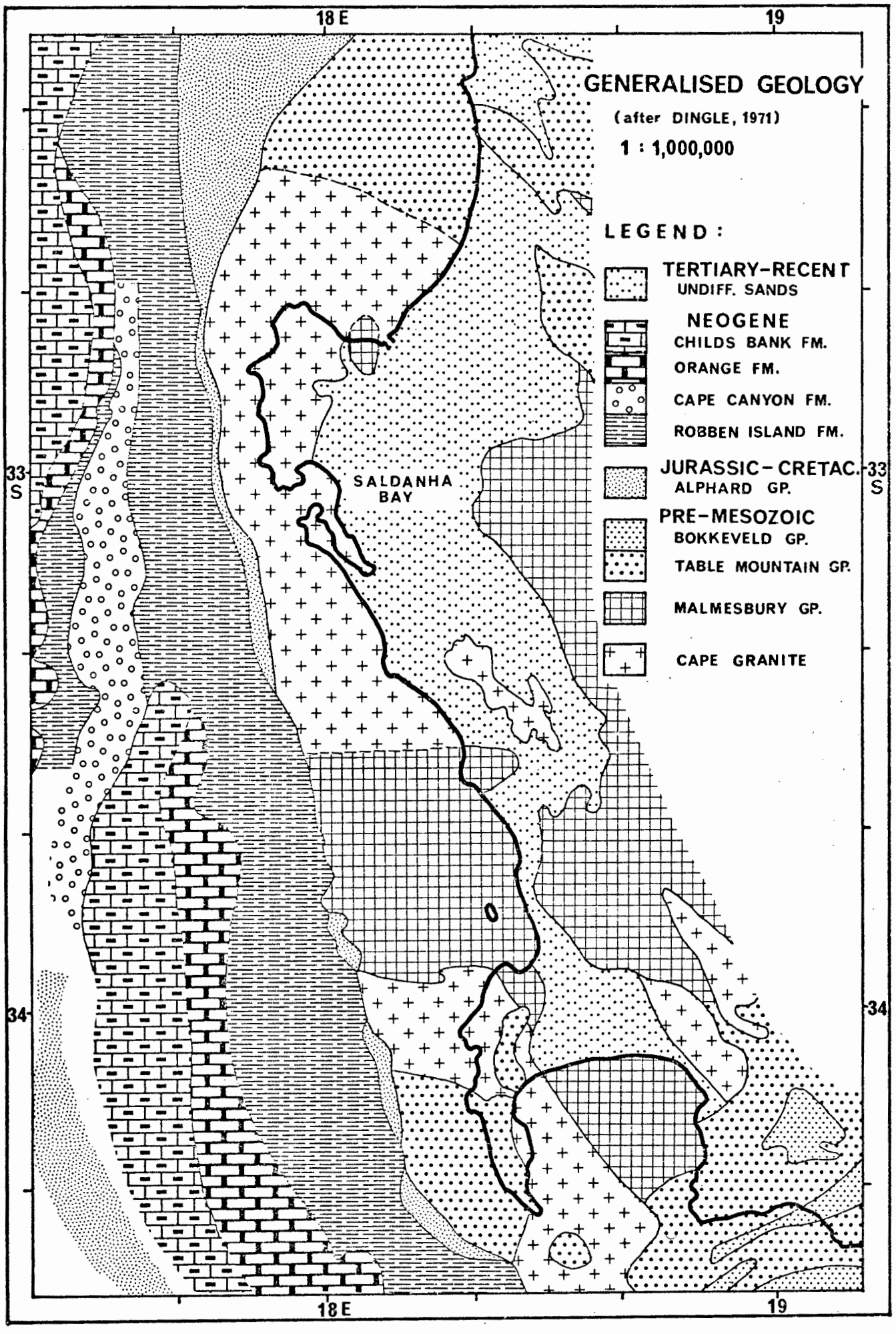
18 E
19
GENERALISED GEOLOGY
(after DINGLE, 1971)
1 : 1,000,000
LEGEND :
TERTIARY-RECENT
UNDIFF. SANDS
NEOGENE
CHILDS BANK FM.
ORANGE FM.
CAPE CANYON FM.
ROBBEN ISLAND FM.
JURASSIC - CRETAC.
ALPHARD GP.
PRE-MESOZOIC
BOKKEVELD GP.
TABLE MOUNTAIN GP.
MALMESBURY GP.
CAPE GRANITE
SALDANHA BAY
33 S
34
18 E
19

Fig. 7.

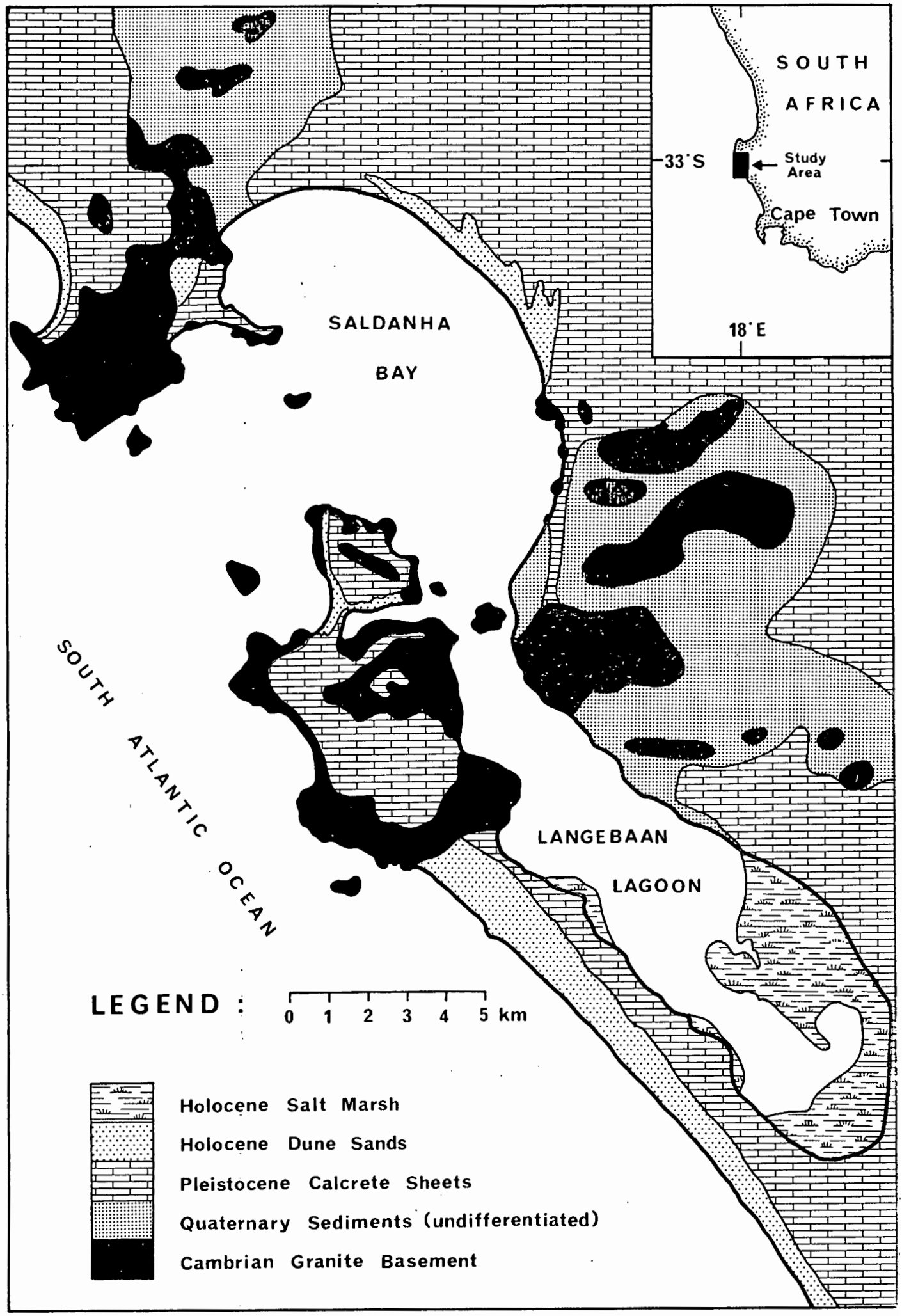

Fig. 8. Local geology.

erosion processes. Thus, in the course of the Flandrian transgression, much of the seaward-extending calcrete and fossil dune material was truncated, reworked and removed by wave abrasion and tidal current scouring (Du Plessis and De la Cruz, 1977). The regional late Pleistocene history and coastal morphology are discussed by Tankard (1976). Tankard discusses a number of interesting features relevant to the late Quaternary evolution of Saldanha Bay and Langebaan Lagoon. Palaeo-environmental aspects of the Saldanha Bay area are also discussed by Siesser (1976) and Birch (1977b). In the present study the writer is able to provide further evidence towards a better understanding of the late Pleistocene history of the area in general, and of the Holocene evolution of Langebaan Lagoon in particular.

CHAPTER 3. METHODS

3.1. FIELD WORK

In Saldanha Bay sample positions were selected in a stratified random manner from a local Decca High-Fix navigational grid. All sample stations were chosen at intersections of the hyperbolic net in order to simplify navigation. By this procedure, 190 stations were chosen such that the overall sample density in the inner bay amounted to about one sample per 500 m square (Fig. 9).

The navigation system has an accuracy of better than 10 m and the true sample positions should therefore in all cases lie within the black dot marked on Fig. 9. To demonstrate this accuracy the writer at one time returned to a previous sample position and was able to relocate the exact sample point on the sea-bed. An additional 20 samples were recovered in the outer bay using a modified Van Veen grab. The positions of these samples were determined by conventional Decca.

In Langebaan Lagoon 220 sample positions were selected along 27 transects spaced about 500 m apart such that all the physiographic units distinguished on aerial photographs were adequately covered (Fig. 10). Sample positions were determined by two-angle measurements using a sextant. The accuracy of the instrument is demonstrated by the consistent alignment of fix-points along the predetermined transects. The exact sample positions with their code numbers, geographic coordinates, and water depths for both Saldanha Bay and Langebaan Lagoon are listed in Appendix 1.1. and Appendix 1.2. respectively.

In the inner bay and in Langebaan Lagoon all samples were recovered "in situ" using SCUBA. At each site four randomly placed cores were taken penetrating 6.5 cm into the sediment. Each core provides on average about 90 g of sediment. The sample depth is less than the expected minimum disturbance by wave action, current activity and bioturbation. This procedure ensured that only modern surface sediments were sampled, thereby avoiding potential contamination by underlying relict sediments. The four individual samples were later mixed into one bulk sample with a total mass of 350 - 400 g of sediment. In this way the probable sample error was

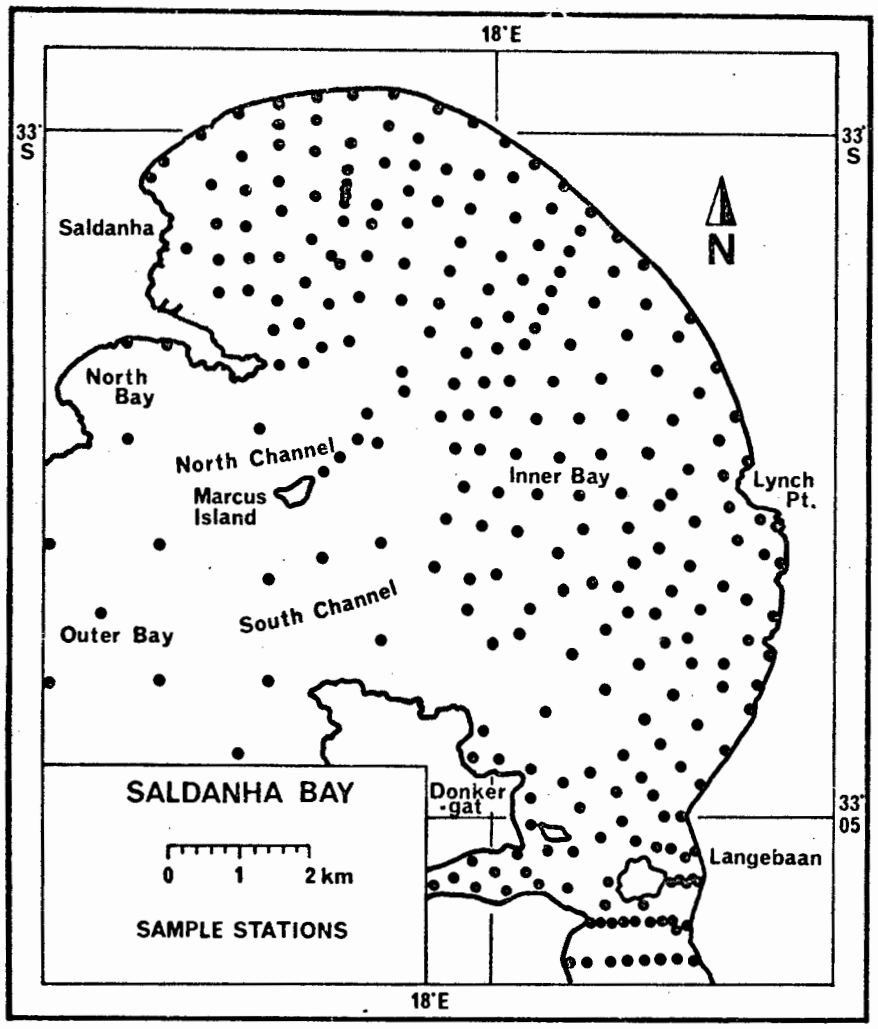
18°E
33° S
33° S
Saldanha
N
North Bay
North Channel
Marcus Island
Inner Bay
Lynch Pt.
Outer Bay
South Channel
SALDANHA BAY
0 1 2 km
SAMPLE STATIONS
Donker-gat
33° 05
Langebaan
18°E

Fig. 9.

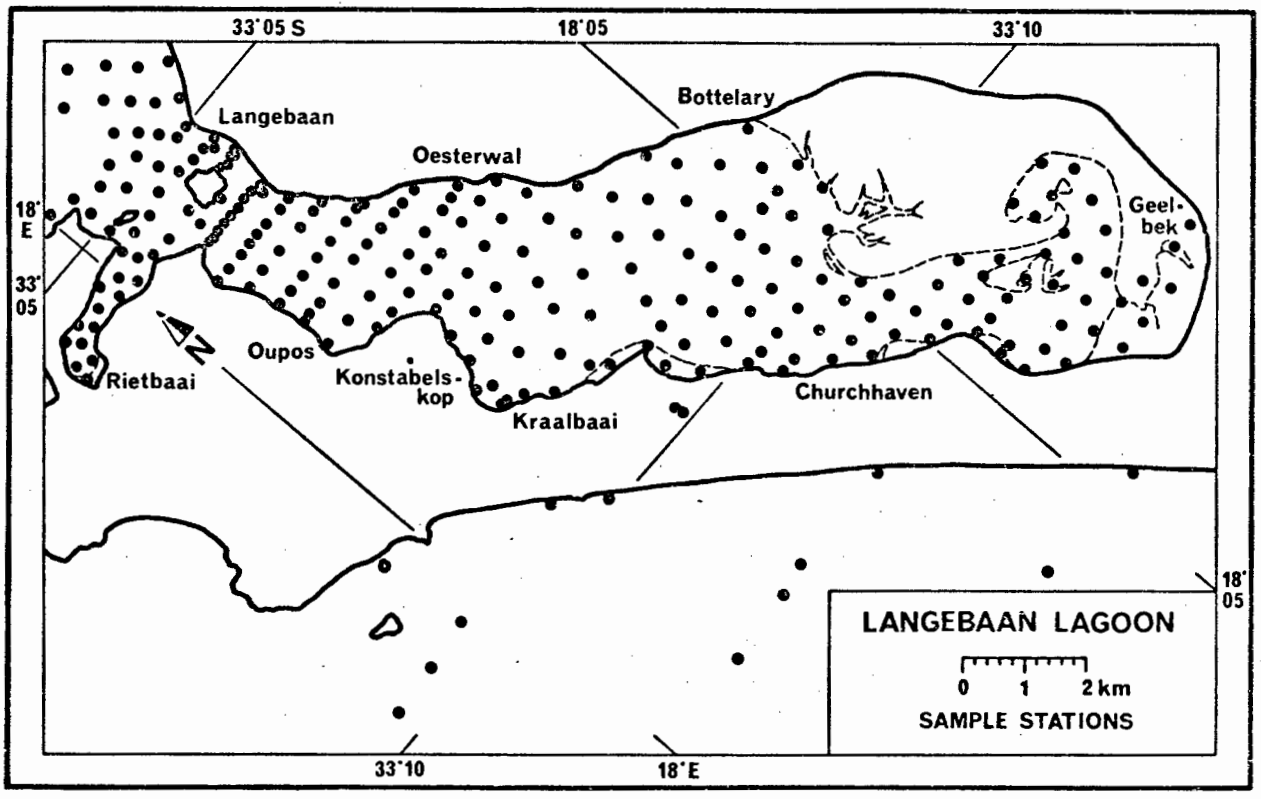
33°05 S
18°05
33°10
Bottelary
Langebaan
Oesterwal
18° E
33° 05
Geel-bek
Oupos
Rietbaai
Konstabels-kop
Kraalbaai
Churchhaven
18° 05
LANGEBAAN LAGOON
0 1 2 km
SAMPLE STATIONS
33°10
18°E

Fig. 10.

reduced by 50% (Krumbein and Pettijohn, 1938; see also Fig. 11).

A major advantage of "in situ" sampling is the exact replication of the sampling procedure at each point. In this manner the sample material reaches the highest possible degree of comparability. In addition the operator can relate his sample position to the general sea-bed conditions in the immediate vicinity. Abnormalities and other specific environmental conditions can be taken into consideration when evaluating the data. The corers are sealed on site, thus preventing any loss of material in the transfer process.

Specific observations, e.g. the occurrence and size of bedforms, rock outcroppings, sediment thicknesses, and biological activity were recorded on plastic sheets attached to a plastic board. Other instruments comprise a compass for orientation and measurement of strike directions and a spirit-level clinometer for the determination of dip angles. Sediment samples for size analysis were supplemented by a selected number of square-box cores (Reineck, 1962; Bouma, 1968; Reineck and Rosenboom, 1969). Relief casts prepared from epoxy-impregnated square-box cores facilitate the study of internal sedimentary structures and their relationship to the environment of deposition. In Langebaan Lagoon they form a strong element in the characterization of specific sedimentary facies.

Current measurements were taken at three stations in Langebaan Lagoon (Fig. 10). Each station was occupied throughout a tidal cycle, and measurements were made at 20 min intervals near the surface and about 1 m above the channel bed. Salinities (Table 1) were determined at various points in Langebaan Lagoon, near the end of a summer season and soon after heavy rainfalls during a winter season.

Side-scan sonar surveys were carried out in the central section of Saldanha Bay in order to establish the exact extent of the abrasion platform observed while diving and in the channel system of Langebaan Lagoon, where major bedforms were expected to develop in response to the high flow velocities. Principles of operation and interpretation of sonographs are discussed in detail by Flemming (1976a). In this study the interpretation of side-scan sonar records was greatly facilitated and complemented by the diving. Some features, especially a number of large bedforms, were investigated further on the basis of the side-scan information. The track

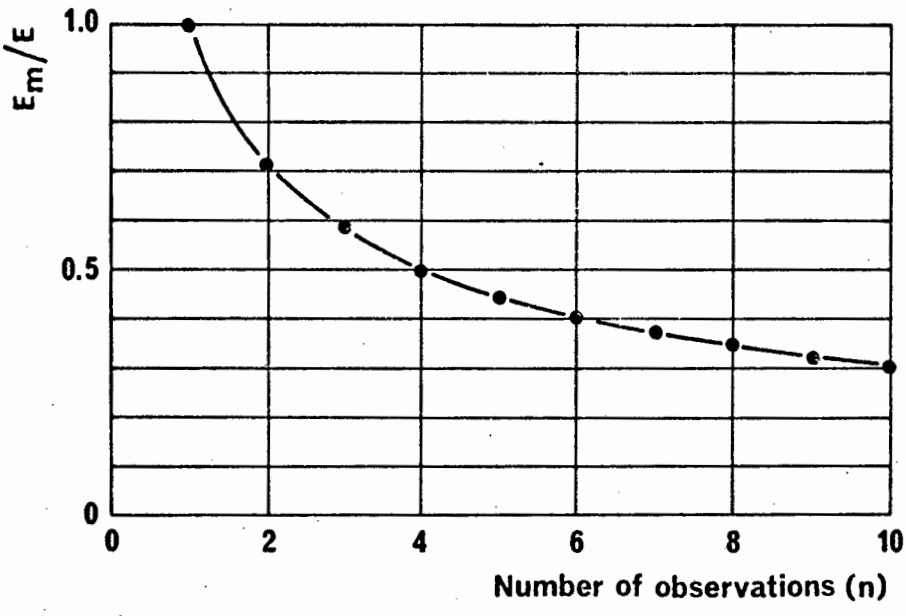

Fig. 11. The error of the mean of a set of observations (n) varies inversely as the square root of the number of observations ($1/\sqrt{n} = Em/E$).

chart with the positions of event marks are presented in Appendix 1.3.

3.2. LABORATORY WORK

The bulk sediment samples were dialized, dried and split into six sub-samples to be used in the various analytical subroutines. The mud content was not removed prior to drying and splitting, because of its overall low content (Folk, 1968). This ensured that each subroutine utilized a subsample of the total sediment, thus maintaining the maximum degree of camparability of the individual results. The preparation of the sample material strictly followed the routine procedures discussed by Müller (1967), Folk (1968) and Carver (1971).

With the exception of carbonate contents of the sediment, geochemical analyses form a subordinate parameter group in this study, which concentrates predominantly on the physical processes of sediment transport and deposition. Organic Carbon was determined from wet oxidation by hot chromic acid and subsequent titration of excess acid against ferrous sulphate. The method is discussed in detail by Morgans (1956) and Olausson (1975). In a recent study Gaudette et al. (1974) have shown that the titration method correlated well with results obtained by the LECO combustion method used in many laboratories. Phosphate (P_2O_5) and Potash (K_2O) determinations were carried out by the Phosphate Development Corporation (PHOSCOR), Phalaborwa. The former was determined spectrophotometrically with an ammonium-vanadate-molybdate method, and the latter by x-ray fluorescence spectrometry.

The content of acid-solubles in the sediment, which are here equated with the $CaCO_3$-content, was established by measuring the weight loss after acid leaching. Although this method is the least accurate way of determining the carbonate content (Siesser and Rogers, 1970) it is considered sufficiently accurate for the purpose of this study. Carbonate contents were not required for geochemical purposes, but simply as an indicator for the proportional contribution of the bioclastic sedementary component to the sediments of the study area. The simplicity and rapidity of the weight-loss method allowed the determination of carbonate contents for all 500 sediment samples.

The mud content of the sediments was determined by fluidizing the mud fraction with H_2O_2 and subsequently separating the coarse and fine

fractions by wet sieving through a 63-micron sieve. Since the overall mud content was very low in the majority of cases, the mud fraction was not further analyzed. A general impression of clay-silt ratios for a number of selected samples can be obtained from Birch (1972).

The coarse fraction (> 63 microns) was split down to the quantity required for a settling tube analysis, usually 2-2.5 g for medium and fine sands and 3-4 g for coarser sediments. The exact procedures of settling tube analyses are discussed in the following section. Hydraulic size analyses were performed on all 500 samples. Each sample was processed in duplicate; one analysis was performed on the total sediment and another on the carbonate-free component (i.e. the terrigenous component). By subtracting the size distribution of the terrigenous particle group from that of the total sediment the complete size distribution of the bioclastic component was calculated. The calculation process is extremely time-consuming and in order to obtain information on all 500 samples, the procedure was simplified by categorizing relative proportions at a limited number of intervals. This has introduced a slight inaccuracy into the statistical parameters like mean diameter, sorting and skewness. Percentage calculations, e.g., the proportions of individual size fractions, are not affected by this procedure and therefore reflect true values.

Paradoxically, the error introduced into the statistical parameters does not impair the interpretations and conclusions reached on the basis of these values. In cases where the bioclastic component exceeds 50% of the total the calculated values will be slightly higher (i.e. the true values will be smaller) and, where it contributes less than 50%, the calculated values will be slightly smaller (i.e. the true values will be higher). Between 40% and 60% the error is small. At concentration levels over 60% the effects, in terms of the interpretation, are overestimated. However, only 10% of all samples fall into this category. At concentration levels below 40%, on the other hand, the effects are underestimated and thus, in over 80% of all cases, the true effects would further emphasize the conclusions reached.

In this manner, a total of 1500 size distributions and their statistical parameters were available for a comparative study of the relationships between the two main sediment components and their combined effect on the total sediment. A comparison between sieving and settling

Fig. 12. Flow chart of analytical laboratory procedures

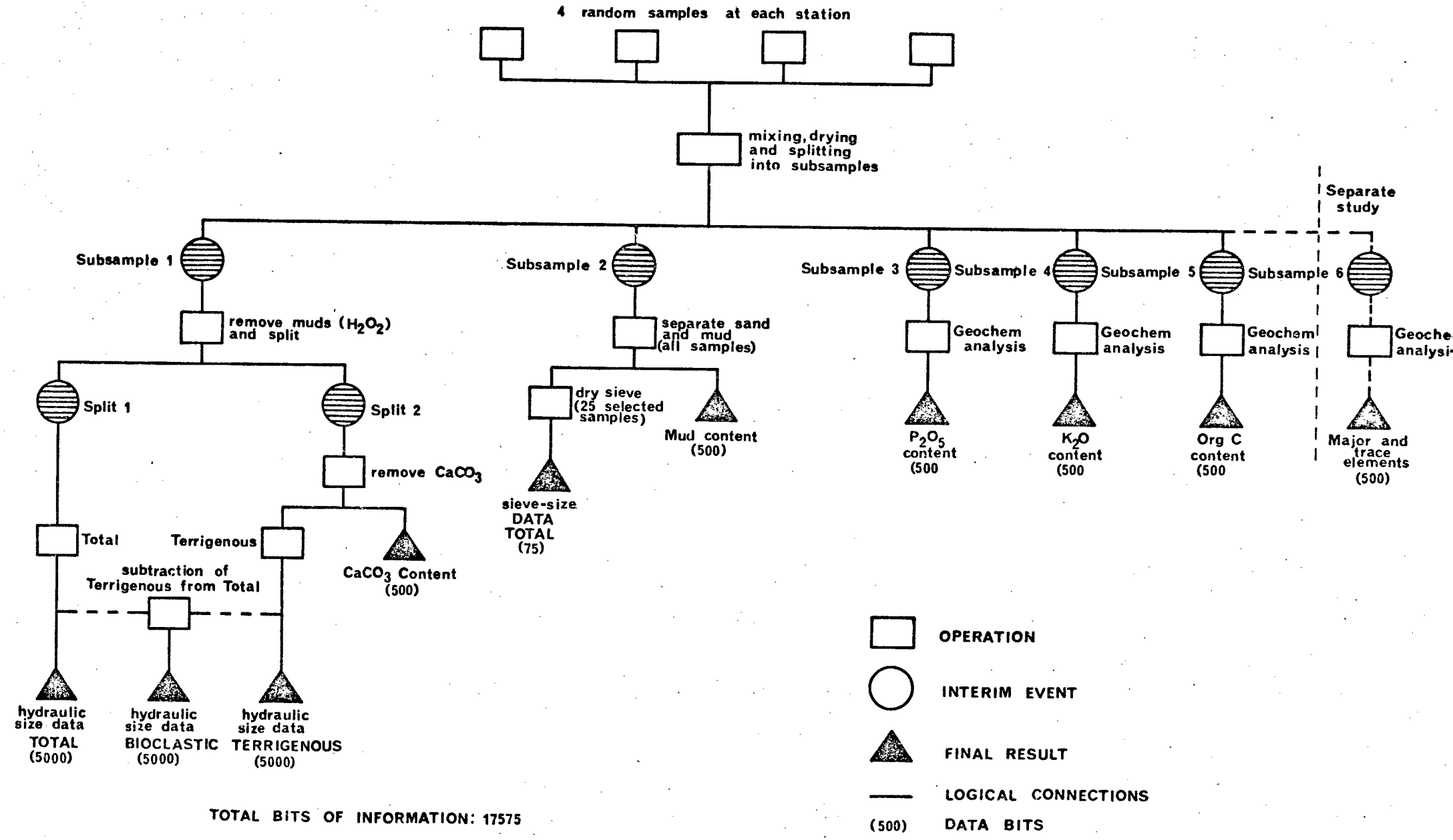

TOTAL BITS OF INFORMATION: 17575

results on the basis of 25 selected samples is presented in the following section.

The general analytical procedure is illustrated in the flow chart of Fig. 12. It should be noted that the distribution patterns of the individual sedimentary parameters were in each case contoured from identical sample densities, i.e. on the basis of all sample stations indicated on Fig. 9 and Fig. 10. All the pertinent grain-size parameters are listed in Appendix 3. Geochemical data are listed in Appendix 4.

3.3. CONSTRUCTION AND CALIBRATION OF AN AUTOMATICALLY RECORDING SETTLING-TUBE FOR THE HYDRAULIC GRAIN-SIZE ANALYSIS OF SANDS

3.3.1. Introduction

The sheer effort and time involved in routine grain size analyses utilizing the conventional sieve method has always been a major limiting factor in detailed sedimentological investigations. As a result, many studies are based on insufficient sample densities and, in addition, statistical parameters are usually calculated from cumulative curves extra-polated from 0.5-phi sieve intervals. Although the latter is not too serious (e.g. Seward-Thompson and Hails, 1973), sample density is certainly a critical factor when investigating depositional sedimentary environments.

It is the aim of this section to discuss the development and systematic application of an alternative method of grain size analysis, that not only eliminates both limitations, but in addition, provides better results for the study of depositional processes. In recent years an increasing number of sedimentologists have resorted to settling techniques for grain-size analysis. Various types of constructions have been described in the literature (e.g. Inman, 1955; Rabatin et al., 1956; Poole, 1957; Bachmann, 1959; Plankeel, 1962; Scott et al., 1963; Buckley, 1964; Janke, 1965; Bieneck et al., 1965; Schlee, 1966; Walger, 1966; Sengupta and Veenstra, 1968; Bascomb, 1968; Cook, 1969; Felix, 1969; Brezina, 1969; Channon, 1971; Sanford and Swift, 1971; Gibbs, 1974; Reed et al., 1975). In most cases the instruments measure the settling velocities of the sedimentary particles in some way or other, but not all the instruments can satisfy the strict scientific requirements discussed by Gibbs (1972).

The settling-tube system developed by the writer for this study has been designed to keep the construction costs at a minimum, while at the same time meeting the scientific requirements as stated by Gibbs (1972). These are discussed in Section 3.3.3. The instrument measures the settling velocities of individual particles in water; the results are then transformed into a grain size equivalent utilizing a computer. The resulting grain size parameter is known as the "sedimentation diameter" or "settling diameter" of a sediment particle. The hydraulic nature of this diameter is normally unrelated to its sieve counterpart; it should therefore not be regarded as a simple replacement of the latter, but rather as a new approach to the grain size problem (Kennedy and Koh, 1961).

The instrument described here is easy to construct and simple to operate. It gives a superior resolution to the sieve method and is considerably less time-consuming. Material costs of the system discussed here, excluding the pen recorder, did not exceed R300.00 at the time of construction in 1974. This is far less than a complete set of experimental sieves. The instrument should be one of the most inexpensive of its kind.

3.3.2. A Critique of Methods

A brief critique of the sieve and settling methods should make it clear that the concept of grain-size is problematical. There is no unique approach that would justify the preference of any particular method. The wide use of sieve analyses is simply a matter of convention, justifiable by the simple fact that it was the only practical method available. Several attempts have been made to express a theory of sieving (Krumbein and Pettijohn, 1938; Mitzutani, 1963; Sahu, 1965; Griffiths, 1967; Ludwick and Henderson, 1968). In principle the sieve diameter is defined as the least cross-sectional diameter of a particle. In theory, all the particles of a sediment should collect on the next smaller sieve as defined by this diameter. Strictly this definition can hold for spherical particles only; however, in nature this is the exception rather than the rule, and sieve diameters are therefore controlled by a combination of shape and the intermediate diameter of particle.

Sieve results are known for their excellent statistical reproducibility. However, Sengupta and Veenstra (1968) have conducted an instructive experiment in which the grains of individual size fractions were stained with different colours and then remixed and resieved. Only 88% of the coloured grains

reappeared in the size fractions to which they originally belonged. Furthermore, Ludwick and Henderson (1968) extensively studied the effects of particle shape on the outcome of sieve results and their findings are most disturbing. It would appear that the common presentation of sieve frequency data in histogram form does not in fact reflect the true size distribution of the sediment. In reality the individual fractions form overlapping, bell-shaped distributions, the cumulative effects of which are completely disregarded. As a result sieve size distributions can, in extreme cases, be underestimated by up to one whole phi-interval.

In addition to this serious, system-inherent shortcoming of the sieve method, it is clear that the vague geometric definition of the sieve diameter can result in purely coincidental accumulations of oddly shaped particles of various densities in the same size fractions and this, besides being unrelated to any natural process of sedimentation, does in most cases not even meet the requirements of its own theory. This becomes particularly relevant when dealing with irregularly shaped particles such as skeletal carbonates or heavy-mineral concentrates (Fontein, 1960; Nelson, 1977).

Grain-size analysis utilizing settling techniques is guided by the realization that most sediments are deposited in the process of hydraulic transport (Bagnold, 1968). This had already been recognized by Odén (1915), Rubey (1933) and Rouse (1936). However, technical problems prevented the construction of sufficiently accurate instrumentation and only after 1940 did this approach receive new attention (Doeglas, 1946). Although Emery (1938) devised a method of grain-size classification using the settling procedure, it is interesting to note that his intention was not to define a "sedimentation diameter" but rather to find a more rapid method that would give results comparable to sieving. To achieve this, various shape factors were introduced and the "Emery Tube" was calibrated accordingly. Even in more recent times some approaches follow this example (Poole, 1957; Nelsen, 1974). Although the reasoning behind the original approach was acceptable, it is no longer justifiable when considering the scientific shortcomings of sieve results as outlined above.

In practice, a sediment sample is introduced into a vertical water column and the settling times of the particles are measured as they accumulate on a pan suspended from a transducer that will measure, in some manner, the cumulative effect of the settling particles. The accumulating weight is

automatically recorded against time through an amplification device that feeds a pen recorder. In this manner a continuous cumulative curve is recorded which requires further refinement because of its time distortion. The settling velocities are then converted into grain sizes relative to a chosen standard, usually quartz or glass spheres (Zeigler and Gill, 1959; Gibbs et al., 1971). The "size" of each grain at any particular point on the curve is thereby expressed in terms of the diameter of a sphere that has the same settling velocity (Fig. 13). All particles that have identical settling velocities are regarded as being hydraulically equivalent as far as settling in still water is concerned.

Statistically the settling results are treated as an ideal sediment. In computing the size distribution of a sediment sample, it is essential to record the water temperature because density and viscosity of the fluid will affect the settling velocity of a particle (Wadell, 1934 and 1936). The size distribution thus obtained reflects the hydraulic sorting process of particles settling through still water, irrespective of particle shape and density. To what extent this idealized process can reproduce the natural mechanism of size-sorting remains to be investigated (Sanford and Swift, 1971). In the meantime, settling procedures for size analysis are the only means of obtaining hydraulically related size data.

It will be noted that both methods of grain size analysis are based "per definitionem" on the nominal diameters of spheres whereby density is taken into account only in the settling procedure, not in sieving. In theory, therefore, both methods should produce identical size distributions for a sample of quartz or glass spheres. This was confirmed experimentally by using glass spheres which were first sieved at 0.25 phi-intervals and then processed in the settling tube. Both curves are very similar (Fig. 14B). The effects of shape and density are illustrated in Fig. 14-A and 14-C.

From the experimental results it can be concluded that grain size distributions obtained by these two methods will diverge progressively with increasing divergence of shape from a spherical diameter, as well as increasing divergence of density from a monomineralic quartz assemblage. Since most natural sediments are composed of polymineralic as well as multi-shaped particles, it can be concluded that the "settling diameter" is indeed a more meaningful grain size parameter when studying depositional

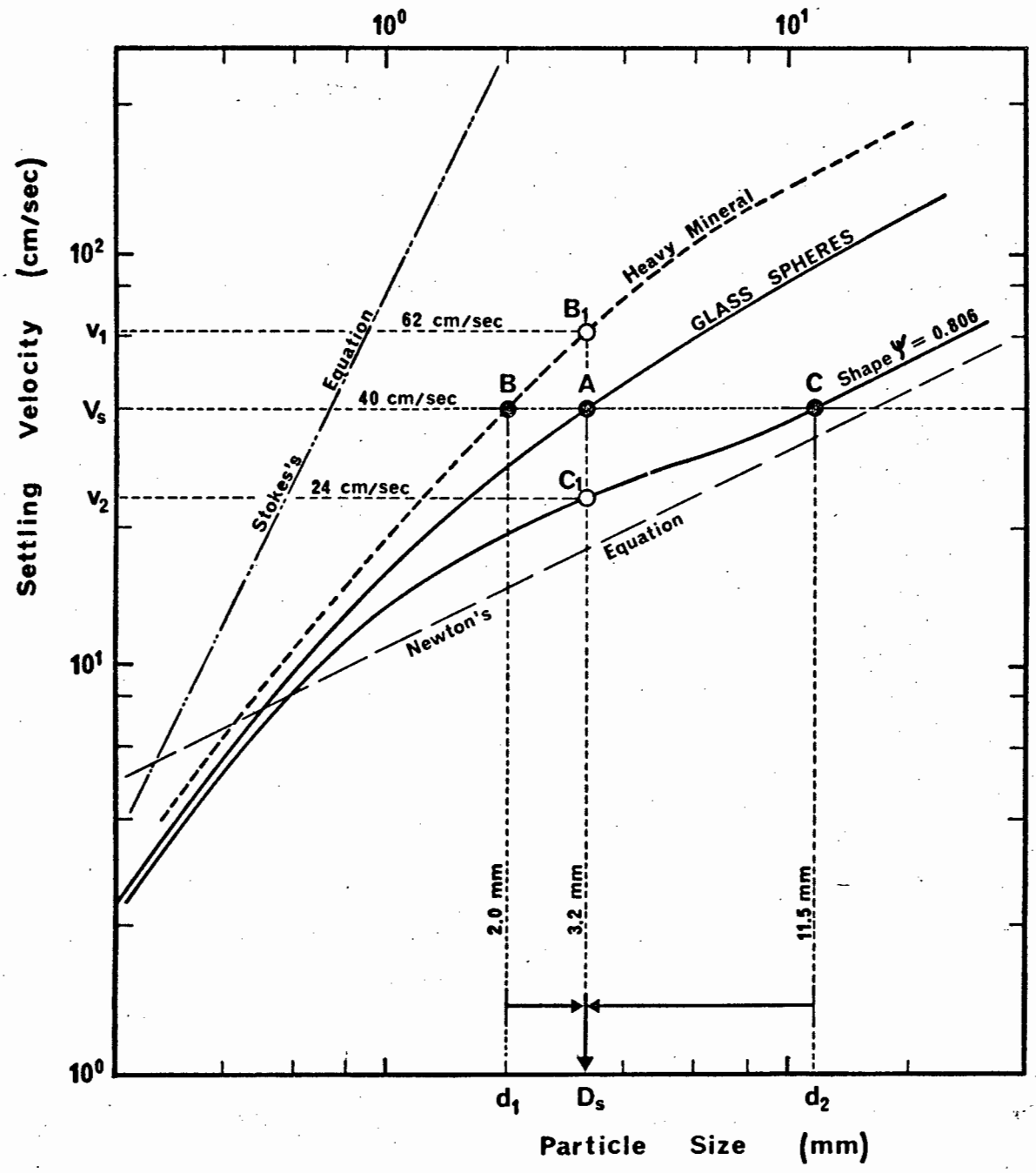

Fig. 13. The principle of hydraulic equivalence : Definition Sketch. Particles A_1, B_1, and C_1 have the same intermediate diameter but different settling velocities (V_s=40 cm/sec; V_1=62 cm/sec; V_2=24 cm/sec). Particles A, B, and C are hydraulically equivalent, i.e. they have the same settling velocity (V_s=40 cm/sec) although their intermediate diameters differ (D_s=3.2 mm: d_1=2 mm; d_2=11.5 mm).

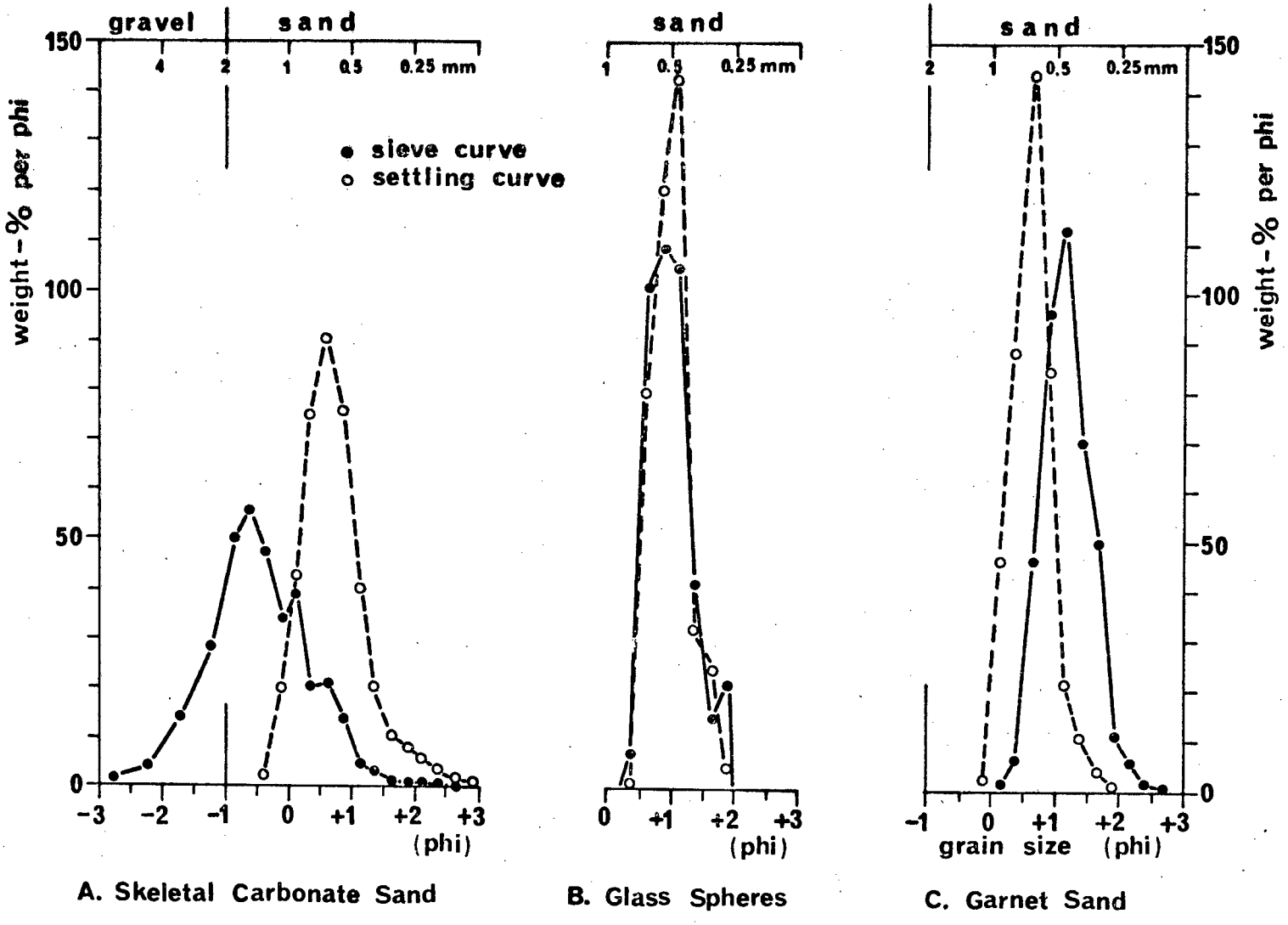

Fig. 14. A comparison of sieve and settling results for three different sediment types

sedimentary environments. It should, therefore, be given preference to the sieve diameter.

In a recent study Reed et al.(1975) have rightly called for caution in the interpretation of hydrodynamic conditions from curve shapes obtained from sieve results (Fisher, 1965; 1969), because the hydraulic incompatibility of sieve data could lead to purely artificial trends in the cumulative curves. Nevertheless, a number of studies, notably that of Folk and Ward (1957), have been extremely successful in the interpretation of depositional processes based on the results of sieving. Possibly, differences in shape and density were negligible in these cases.

Sections 3.3.3. - 3.3.8. deal with the mechanical design, the electronic design, operational procedures, calibration, error assessments, and resolution limits of the settling tube system. They are contained in Appendix 2.

3.4. COMPARISON OF SIEVE AND SETTLING RESULTS

In order to demonstrate the systematic difference between sieving and settling, 25 selected sediment samples were first sieved at 0.5 phi-intervals and then processed in the settling tube. The size frequency data of both was then compared in a number of scatter plots (Fig. 29). In Fig. 29-A mean sieve diameters are plotted against mean settling diameters. With the exception of two samples which scatter more widely, the general trend would suggest that in the study area the deviation between the two methods increases with increasing grain size. In terms of hydraulic equivalence sieve results increasingly overestimate the average grain size of sediments towards the coarser size classes.

In Fig. 29-B the respective sorting values are compared. Again a definite trend is observed. Whereas very well sorted sediments tend to produce similar results it would seem that, on average, sieve results progressively underestimate sorting values towards the poorer sorting categories. Skewness values, on the other hand, do not seem to vary systematically (Fig. 29-C). All the individual size parameters of the sieve and settling results are listed in Appendix 2.3.

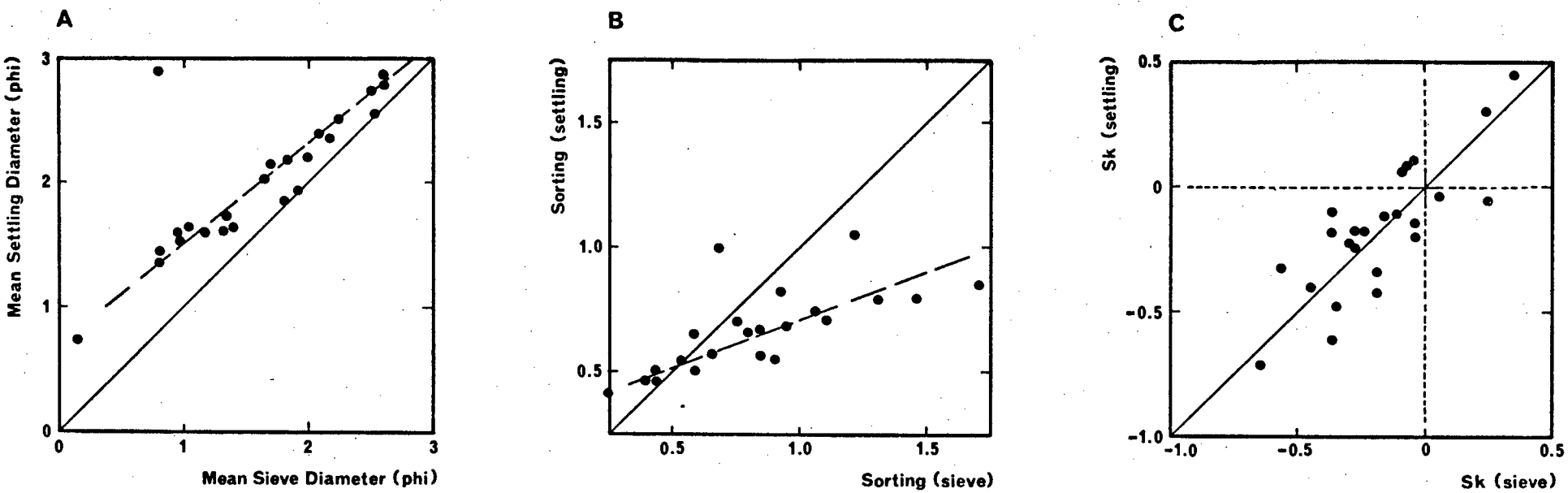

Fig. 29. A comparison between sieve and settling tube results

The observed deviations between the two methods are generally assumed to be caused by differences in shape and densities of the particles. The sediments of the study area are composed of a mixture of quartz and skeletal carbonates which both have similar densities, and it is therefore concluded that the observed difference is predominantly a shape effect. Experimental studies on the effects of particle shape on settling velocities have thus far been restricted to individual grains (e.g. Maiklem, 1968; Braithwaite, 1973) and there exists a serious lack of information on bulk shape effects on the size distributions of sediments consisting of a multitude of differently shaped particles. Extreme shape effects can be expected especially in skeletal sands, in which fragmentation is to a large extent controlled by the mineralogical structure or micro-architecture of the shell material (Folk and Robles, 1964; Force, 1969). In order to determine the hydraulic response of such sediments, their bulk settling behaviour becomes particularly important (e.g. Maiklem, 1968), as it is practically impossible to determine the effect of each individual particle.

To demonstrate the bulk shape effects on particle size distributions, a number of experiments were performed in which the bulk settling behaviour of individual sedimentary components were compared to the results of sieving. Fig. 30-A and 30-B show the respective frequency polygons of sieve and settling data of a mixed carbonate-quartz sediment from a high energy beach. In both cases the two components have very similar size distributions although the settling results are considerably finer than the sieve results. The size shift amounts to 0.48 phi-intervals in the case of the quartz and 0.59 phi-intervals in the case of the carbonates.

Even more dramatic are the results of a study in which a pure skeletal sand was sieved at 0.25 phi-intervals and subsequently processed in the settling tube (Fig. 31). The sieve results characterize the sediment as poorly sorted with a mean diameter of about 1.8 mm ($\overline{X}$ = -0.85 phi) whereas the settling results qualify the same sediment as being well sorted with a mean diameter of only 0.6 mm ($\overline{X}$ = +0.73 phi), i.e. the hydraulic equivalence of the sedimentary particles in this sediment record a mean diameter that is 66% finer than their geometrically defined mean size.

In extension of the above experiments, the writer separated genetically related sedimentary components from various 0.5 phi sieve fractions, then

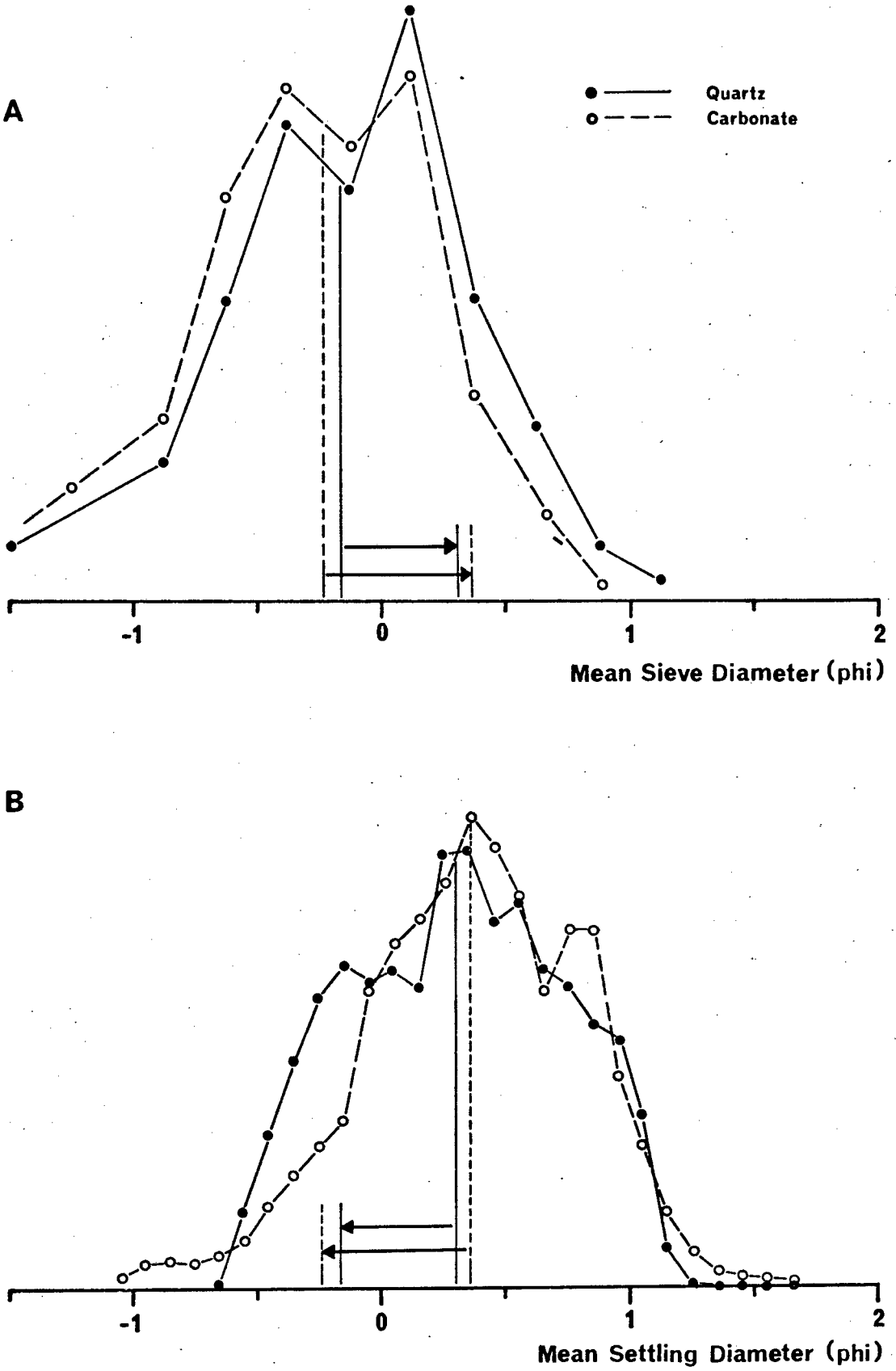

Fig. 30. Size-frequency distributions of sediment from a high-energy beach environment

A. Sieve diameters
B. Settling diameters

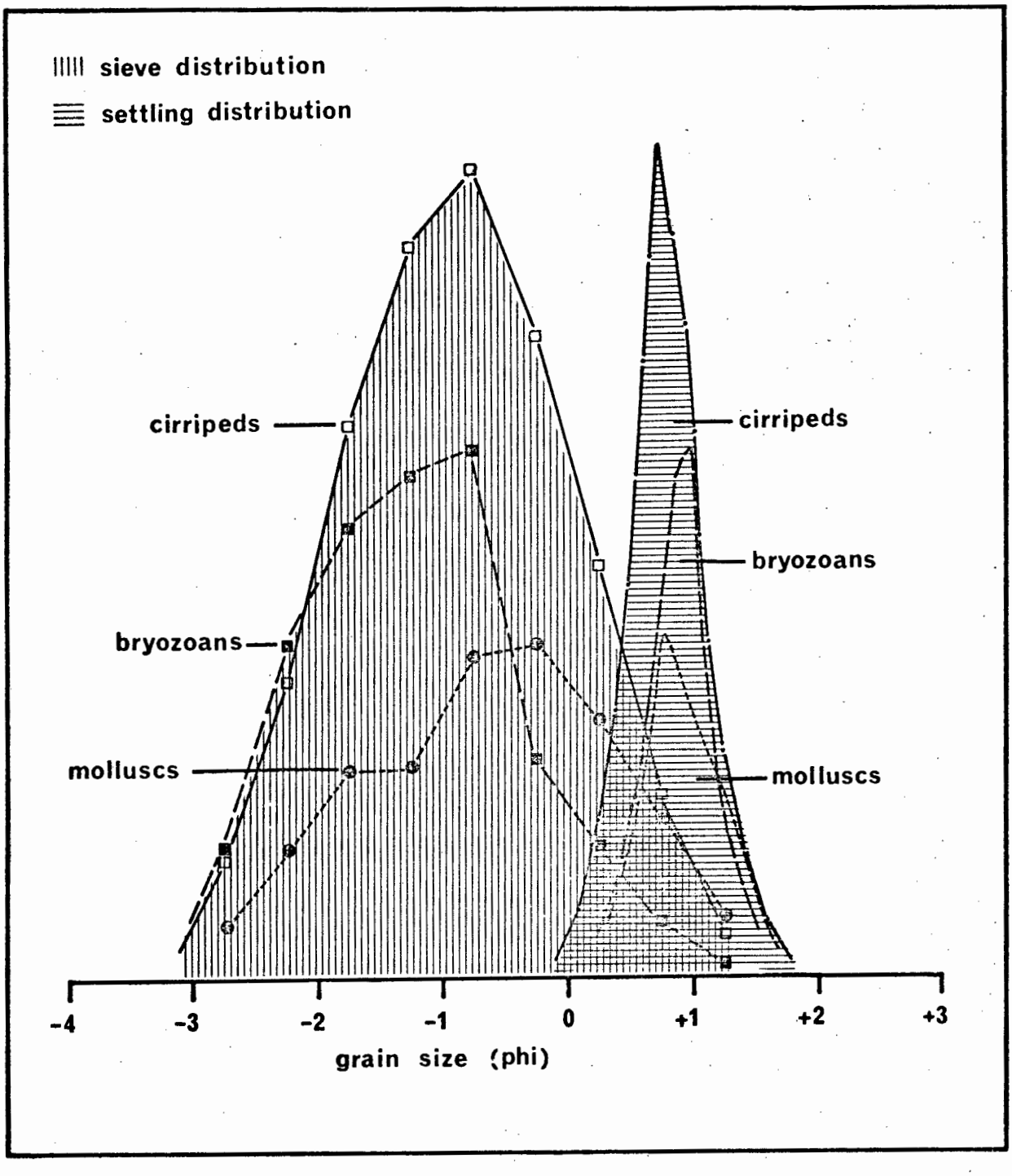

Fig. 31. Diagram illustrating the difference between sieve and settling results. Note the striking difference in mean diameters and sorting characteristics.

settled each half-phi component group through the tube. Studies of this nature may provide hydraulic data suitable for the conversion of coarse fraction component data based on sieve fractions as performed by many authors (e.g. Shepard and Moore, 1954 and 1955; Shepard, 1956; Purdy, 1963; Boillot, 1964; Van Andel, 1967; Sarnthein, 1971; Einsele and Werner, 1972).

In this particular investigation cirriped fragments, bryozoans, and molluscs were separated. Together they often contribute over 90% to the bioclastic fraction in local sediments (Siesser, 1972; Flemming, 1976b). The combined sieve and settling results are presented in Fig. 32. Included are also data points for the previously discussed high energy beach sediments (i.e. smooth cirriped fragments and rough quartz). The diagram also demonstrates the general effect of density in form of a single data point obtained from size analysis of a garnet sand. The increasing effect of bulk particle shape with increasing particle size is particularly well illustrated. Each shape group follows a fairly well defined trend, bryozoans showing the strongest deviation. Similar trends were observed when converting settling data presented by Folk and Robles (1964) in their study of Isla Perez sediments (Fig. 33).

These results leave no alternative but the conclusion that sieve data obtained from irregularly shaped particles should be treated with great caution. It seems doubtful that they contain any significant information about the hydrodynamic processes involved in their deposition. Although this fact was already noted by Folk and Robles (1964), size description of bioclastic sediments based on sieve results continue to be widely applied. Very few authors (e.g. Nelson, 1977) have attempted to eliminate at least extreme shape effects by removing the bioclastic component by acid-leaching prior to sieving. It should be noted, however, that the remaining insoluble fraction can still be composed of irregularly shaped particles which, when sieved, will not produce hydraulically equivalent data. Considering the present instrumental capabilities, it would seem that settling procedures are the only practical and reliable means by which hydraulically related size parameters can be obtained.

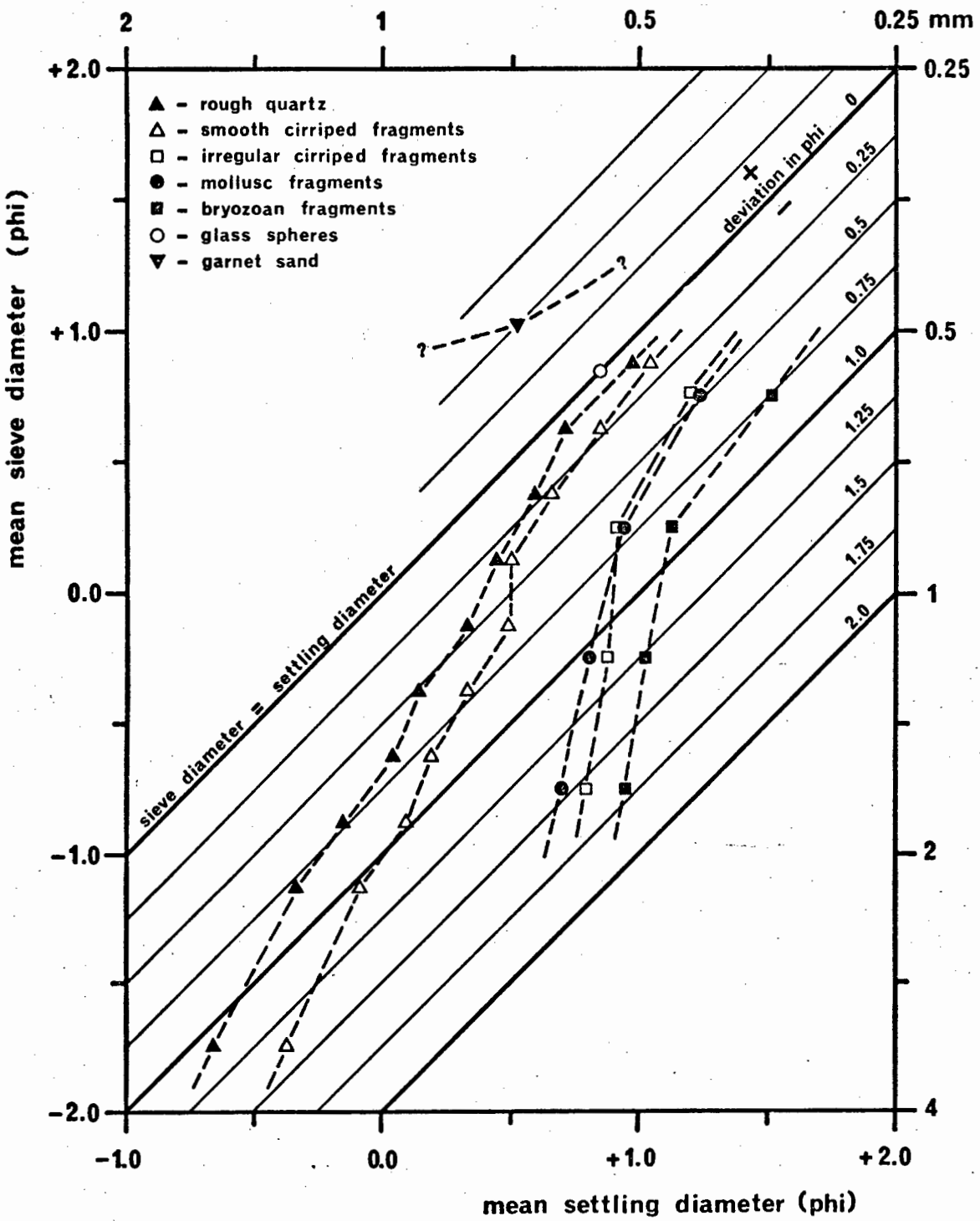

Fig. 32. The effect of particle shape on sieve and settling results for individual sedimentary components. Note the diverging trend with increasing grain size.

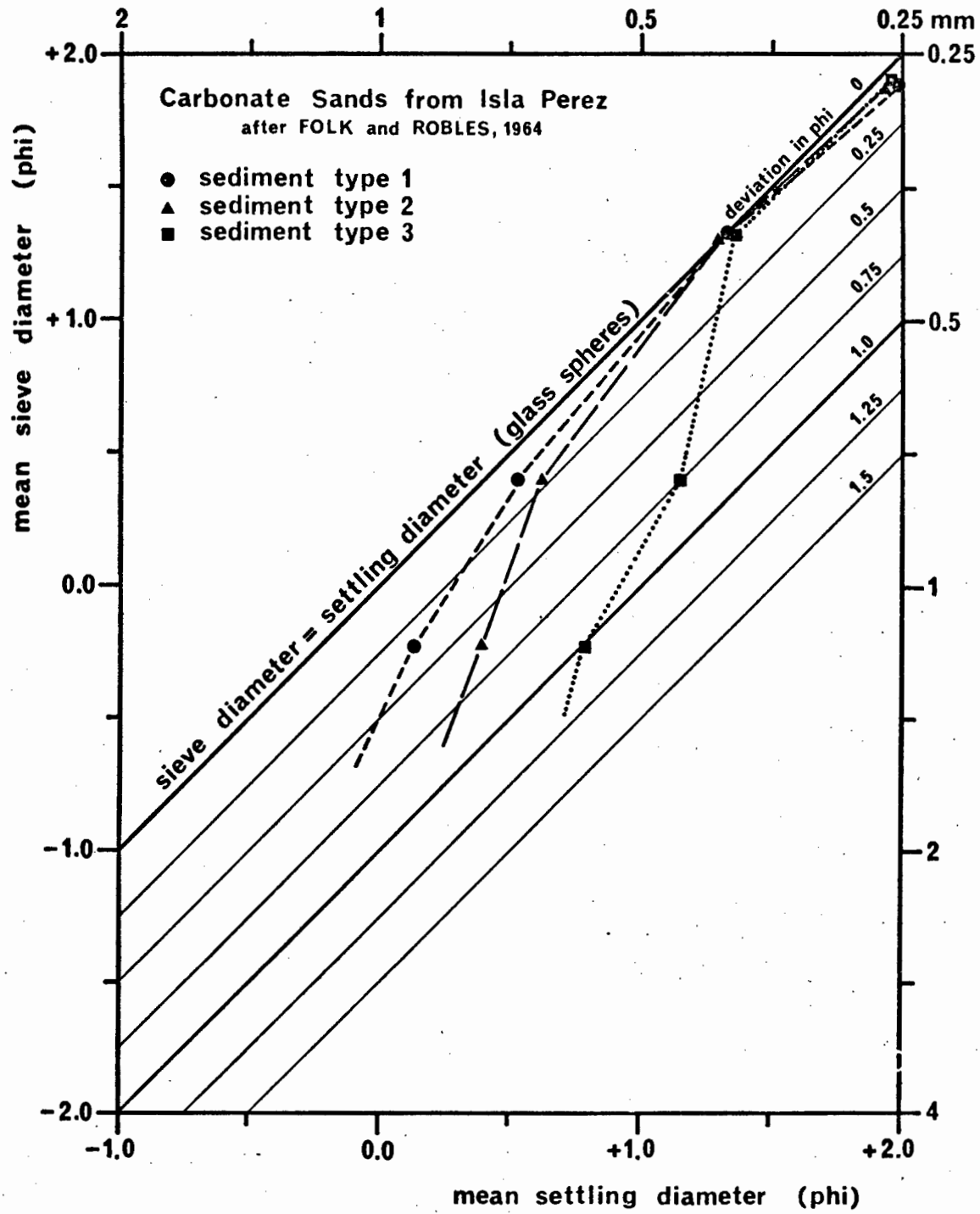

Fig. 33. The effect of Particle shape on sieve and settling results calculated from data compiled by Folk and Robles (1964)

3.5. REMARKS ON THE USE OF RELATIVE SORTING

3.5.1 Introduction

The standard deviation of a grain size distribution, more frequently referred to as the sorting of a sediment, is one of the more commonly used grain size parameters in sedimentological research. Some authors regard it as an indicator of the maturity of a sediment, usually in association with progressive size-sorting as a function of distance from source (e.g. Krumbein, 1937; Reiche, 1950; Folk, 1951; Kennedy, 1951). More recently, however, Folk (1968) and Pettijohn et al. (1972) have expressed reservations about the uncritical use of this concept, pointing out that sorting, in some cases, simply reflects an inhereted property of the sediment.

Nonetheless, sorting is widely recognized as providing useful information about sedimentary environments and the processes controlling their formation. For example, it forms an important parameter in the facies model approach to modern depositional environments (e.g. Reineck and Singh, 1973). Flume studies concerning the generation and control of bedform structures have revealed that certain sorting characteristics could be related to the settling velocities of sedimentary particles involved in their formation (Brush, 1965; Jopling, 1965; Simons et al., 1965). However, some features of standard sorting trends, especially their relationship to mean grain size, are incompatible with their conventional interpretations, thus calling for some caution in their unconditional application.

It is the purpose of this section to discuss the main limitations of standard sorting in its commonly used form, and to propose its replacement by a genetically related parameter known as "relative sorting" (Walger, 1962). Relative sorting is independent of size and is easily calculated from an empirical equation. Moreover, a new classification of sorting categories is proposed. It is systematically developed from the relative sorting scale and is closely related to the standard sorting classification used for terrigenous sediments (Folk and Ward, 1957; Folk, 1966). It is also applicable to bioclastic sediments (Friedman, 1962), especially if based on hydraulic size data.

Relative sorting coefficients can be calculated from Table 3 (Appendix 8) in combination with an equation to be discussed below. By

TABLE 3

Elementary sorting (QD_e) values at 0.1 phi size intervals between 0.063 mm and 2.0 mm

SIZE CLASS	MEAN DIAMETER		QD_e
	microns	phi	
VERY COARSE SAND	2000	-1.0	1.20
	1866	-0.9	1.15
	1741	-0.8	1.10
	1625	-0.7	1.05
	1516	-0.6	1.00
	1414	-0.5	0.95
	1320	-0.4	0.91
	2131	-0.3	0.86
	1149	-0.2	0.82
	1072	-0.1	0.78
	1000	0.0	0.74
COARSE SAND	933	0.1	0.69
	871	0.2	0.65
	812	0.3	0.62
	758	0.4	0.58
	707	0.5	0.55
	660	0.6	0.51
	616	0.7	0.48
	574	0.8	0.45
	536	0.9	0.43
	500	1.0	0.40
MED. SAND	467	1.1	0.37
	435	1.2	0.35
	406	1.3	0.33
	379	1.4	0.31
	354	1.5	0.28
MED. SAND	330	1.6	0.27
	308	1.7	0.25
	287	1.8	0.24
	268	1.9	0.23
	250	2.0	0.21
FINE SAND	233	2.1	0.20
	218	2.2	0.19
	203	2.3	0.19
	190	2.4	0.18
	177	2.5	0.18
	165	2.6	0.18
	154	2.7	0.19
	144	2.8	0.19
	134	2.9	0.20
	125	3.0	0.21
VERY FINE SAND	117	3.1	0.23
	109	3.2	0.24
	102	3.3	0.26
	95	3.4	0.28
	88	3.5	0.30
	83	3.6	0.33
	77	3.7	0.37
	72	3.8	0.40
	67	3.9	0.44
	63	4.0	0.47

plotting mean size against standard sorting and against relative sorting, the point clusters of the total sample, the terrigenous component, and the bioclastic component were compared. The abbreviations chosen to distinguish the various sorting notations have no genetic meaning here but simply follow examples already used in the literature (e.g. Walger, 1963; Seibold, 1963). Instead of plotting the median diameter as average size parameter, the writer prefers the use of the mean size which appears to be hydraulically more significant (Bagnold, 1968).

3.5.2. Previous Work

As a statistical function the standard deviation or sorting (QD) of a sediment, whether derived by graphical means (e.g. Trask, 1932; Krumbein and Pettijohn, 1938; Folk and Ward, 1957; Friedman, 1962) or by the method of moments (e.g. Krumbein and Pettijohn, 1938; Griffiths, 1961; Pettijohn et al., 1972; Blatt et al., 1973), does not distinguish individual size intervals to which it is applied, but treats all size classes equivalently.

However, it was already observed by Krumbein and Pettijohn (1937), Inman (1949), Emery and Stevenson (1950), Griffiths (1951) and Vause (1959) that sediments from equivalent environments showed apparently different degrees of sorting as a function of grain size. This peculiar feature was not further investigated until Walger (1962) demonstrated, by plotting numerous examples from various parts of the world, that there was indeed a systematic dependence of the degree of sorting on average size. Fine sand appears to achieve the best sorting values whereas coarser and finer sediments become progressively less well sorted (Fig. 34). It thus appears that sediments exposed to optimal environmental conditions will approach a size-dependent optimum beyond which their standard deviation will not improve any further.

Walger (1962), in an attempt to fit a visual curve to the optimum sorting trend, studied the size distributions of individual sand lamina of beach sediments following the assumption that those, if any, should be optimally sorted. The results confirmed this deduction and a curve, that fitted the data very well, was defined by an empirical equation in which the ratio between standard sorting and the assumed optimum sorting is equal to unity. Walger (1962) related this curve to the elementary sorting (QD_e) of a sediment of given size. It defines a dimensionless, relative degree

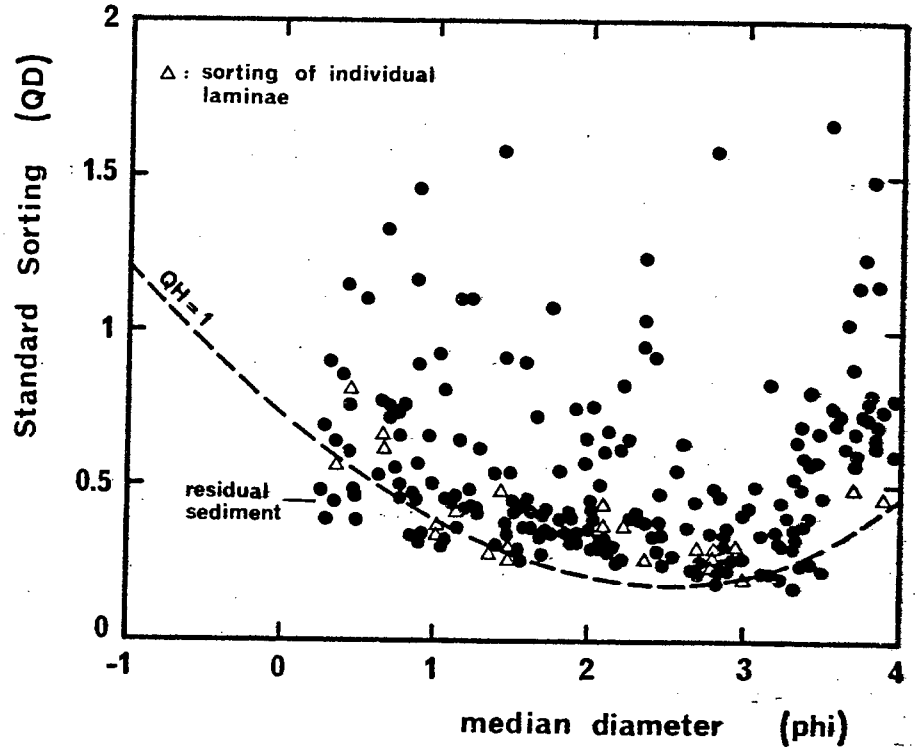

Fig. 34. Standard sorting (QD) as a function of the median diameter. Samples originate from various localities. QH=1 was defined as the elementary sorting coefficient (after Walger, 1962).

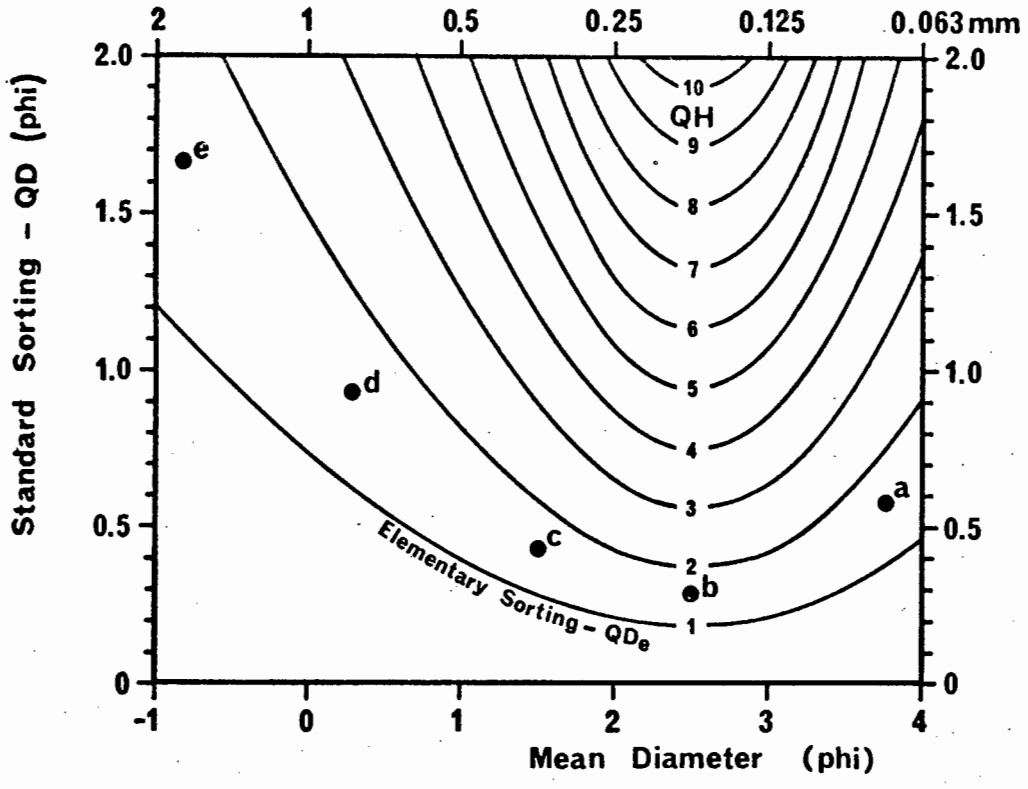

Fig. 35-A. The relationship between mean size, standard sorting (QD), and relative sorting (QH).

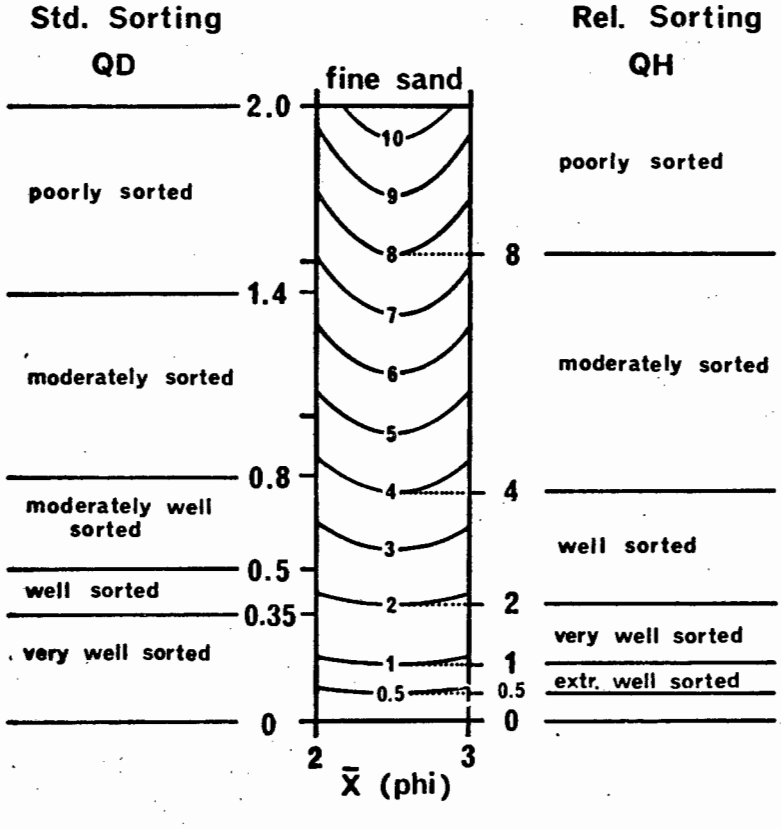

Fig. 35-B. The newly proposed scale of relative sorting in comparison to the conventional standard sorting scale.

of sorting (QH) which is independent of the average size of the sediment. Thus, the optimum sorting that a sediment of given size can achieve is expressed by the equation

$$QD / QD_e = 1 \qquad (1)$$

Any deviations from the elementary sorting will be expressed as multiples of one. The writer has constructed a diagram illustrating the relationship between mean size, standard sorting, and relative sorting (Fig. 35-A). Table 3 (Appendix 8) allows the quick conversion of standard sorting coefficients into elementary sorting, and by substitution in the equation

$$QH = QD / QD_e \qquad (2)$$

the relative sorting coefficient is calculated.

The above discussion indicates that size-sorting appears to be controlled by transport mechanisms, and that identical relative sorting coefficients for different grain sizes should, as a result, be treated equivalently. Thus, the points a, b, c, d and e in Fig. 35-A have all reached the same level of relative sorting (QH = 1.5), yet standard sorting classifies each point as belonging to a different sorting category. Point a would be moderately well sorted, point b very well sorted, point c well sorted, point d moderately sorted, and point e would be poorly sorted. Clearly, the interpretation of sorting trends would differ vastly in both cases.

3.5.3. QD vs. QH in Natural Sediments

In order to support the case for relative sorting, 220 samples from Langebaan Lagoon were evaluated by plotting standard sorting as well as relative sorting coefficients against mean size (Fig. 36-A and 36-B). The majority of samples are well to moderately well sorted and although Fig. 36-A does indicate the existence of a definite trend within the finer size classes, its continuation and overall relationship to the whole point cluster remains obscure. Fig. 36-B, on the other hand, presents a greatly enhanced picture. The point cluster is now clearly arranged in an inverted V-shaped formation with two upward converging arms, suggesting the existence of at least two distinctly different hydraulic populations.

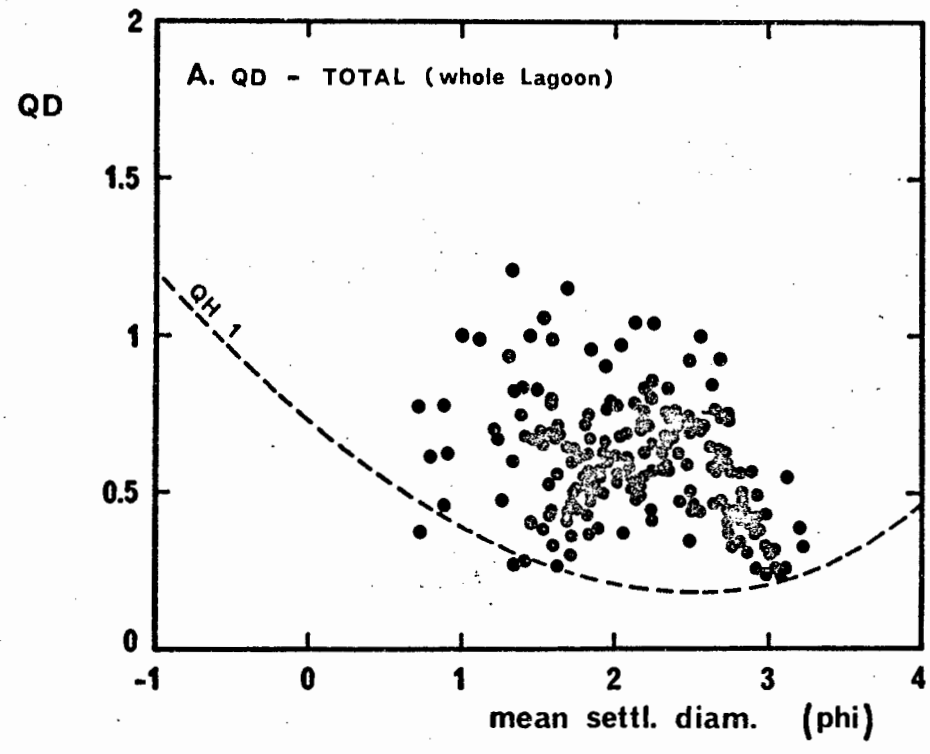

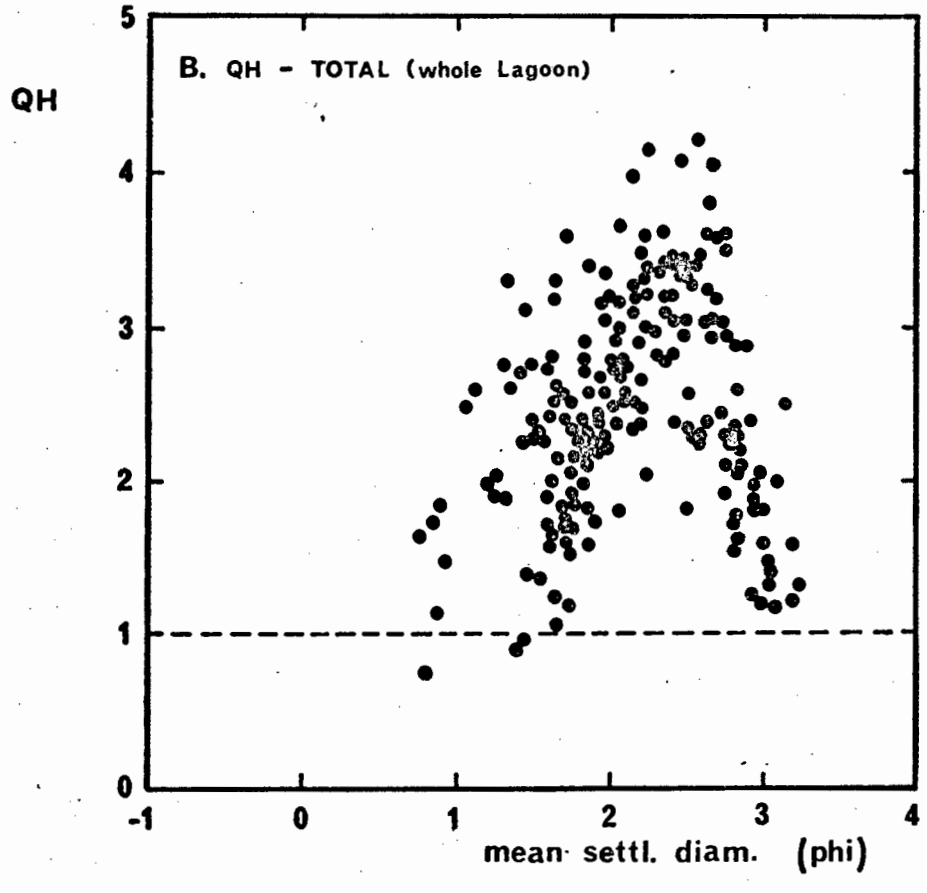

Fig. 36. The relationship between the mean settling diameter and sorting in Langebaan Lagoon.

A. QD vs. Mean settling diameter.
B. QH vs. Mean settling diameter.

This aspect was further investigated by plotting separately all samples belonging to different depositional environments in the lagoon. Fig. 37-A and 37-B represent the QD and QH-plots respectively of intertidal sediments in which each physiographic unit is characterized by a different symbol. The existence of at least two hydraulic populations is confirmed. The trend of eastern tidal flat samples (black circles) is now clearly defined in the QD-plot; but western tidal flat sediments (black squares) and southern tidal flats (open triangles) appear as group clusters. Not so in the QH-plot (Fig. 37-B); here all groups define clear trends.

The next step of the investigation was to determine the extent to which mean diameter and sorting of the total sediment were controlled by each of the sedimentary components and how this was reflected in QD and QH-plots respectively. Fig. 38-A and 38-B represent the QD and QH-patterns of the terrigenous component whereas Fig. 39-A and 39-B represent the respective bioclastic sorting trends. A striking difference exists between the two components. Both the QD and the QH-plots of the terrigenous group show well-defined trends with the QH-pattern displaying a better enhancement. The bioclastic counterparts are in comparison poorly defined. The bioclastic QH-pattern, however, allows a better recognition of general trends (Fig. 39-B). In addition, there are certain differences in the orientation of some details between the terrigenous and the bioclastic components.

Since shape is the only significant difference between the two component groups, the writer concludes that shape factors appear to control the hydraulic response of sedimentary particles in a somewhat different manner than the settling velocities alone would suggest.

The above examples suggest that relative sorting is indeed a more useful parameter when investigating the sorting characteristics of sediments in relation to depositional processes. It should be noted that significant enhancement is observed in the relative sorting patterns in spite of the fact that the samples under consideration are localized near the fine sand fraction. In this region the realignment of data points due to the linear transformation of QH-coefficients will show the least difference to QD-patterns. The further away the mean diameters are located from the fine sand interval, the stronger will the realignment effect be.

Although Walger (1962) concluded that QH = 1 was the optimum degree

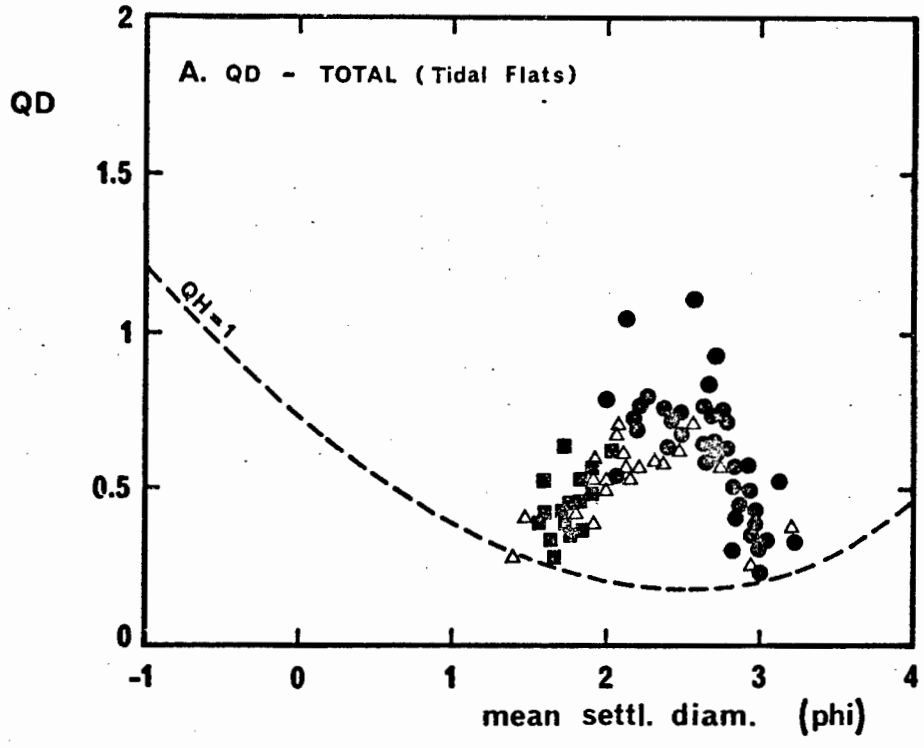

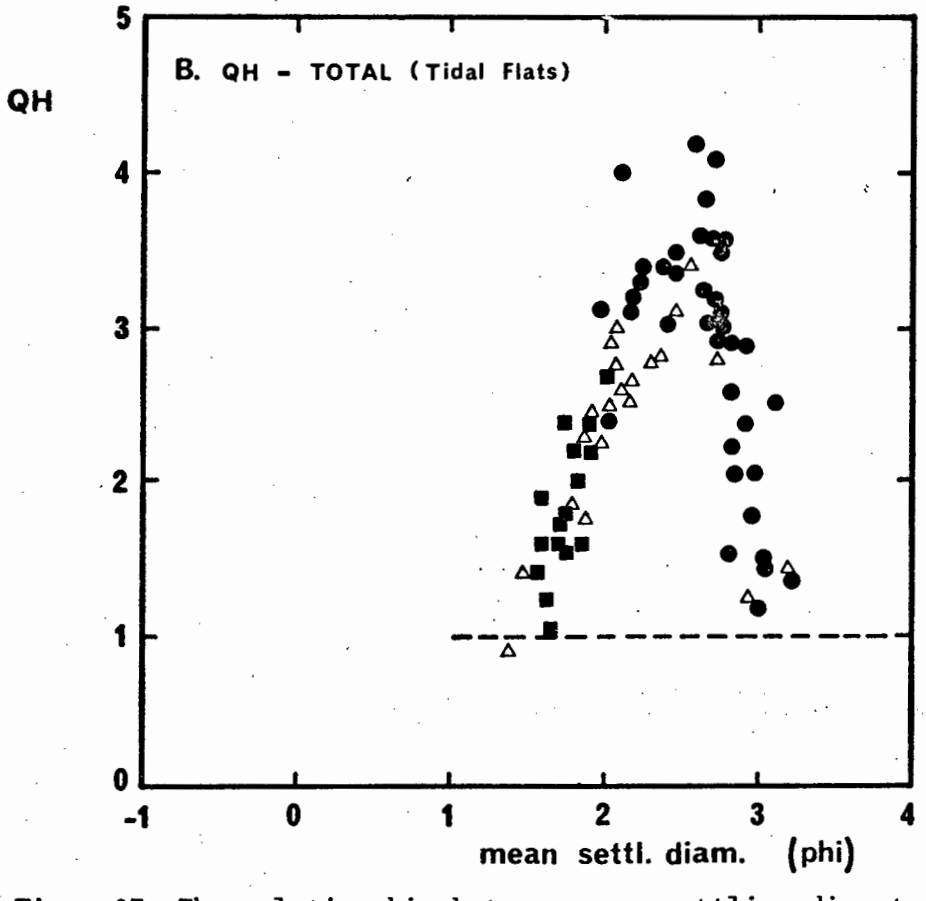

Fig. 37. The relationship between mean settling diameter and sorting in tidal-flat sediments of Langebaan Lagoon.

A. QD vs. Mean settling diameter.
B. QH vs. Mean settling diameter.

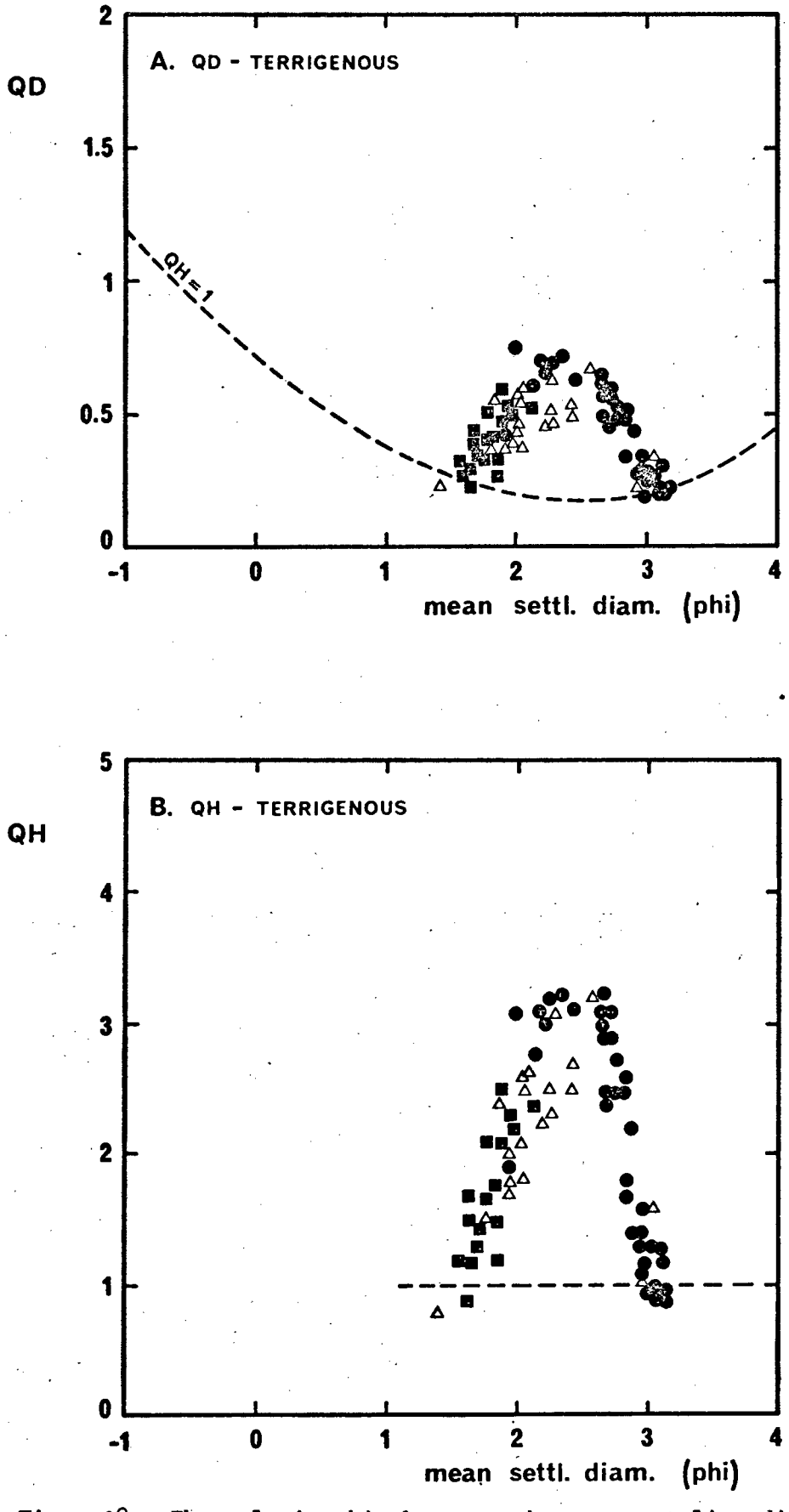

Fig. 38. The relationship between the mean settling diameter and sorting of the terrigenous component in tidal-flat sediments of Langebaan Lagoon.

A. QD vs. Mean settling diameter.
B. QH vs. Mean settling diameter.

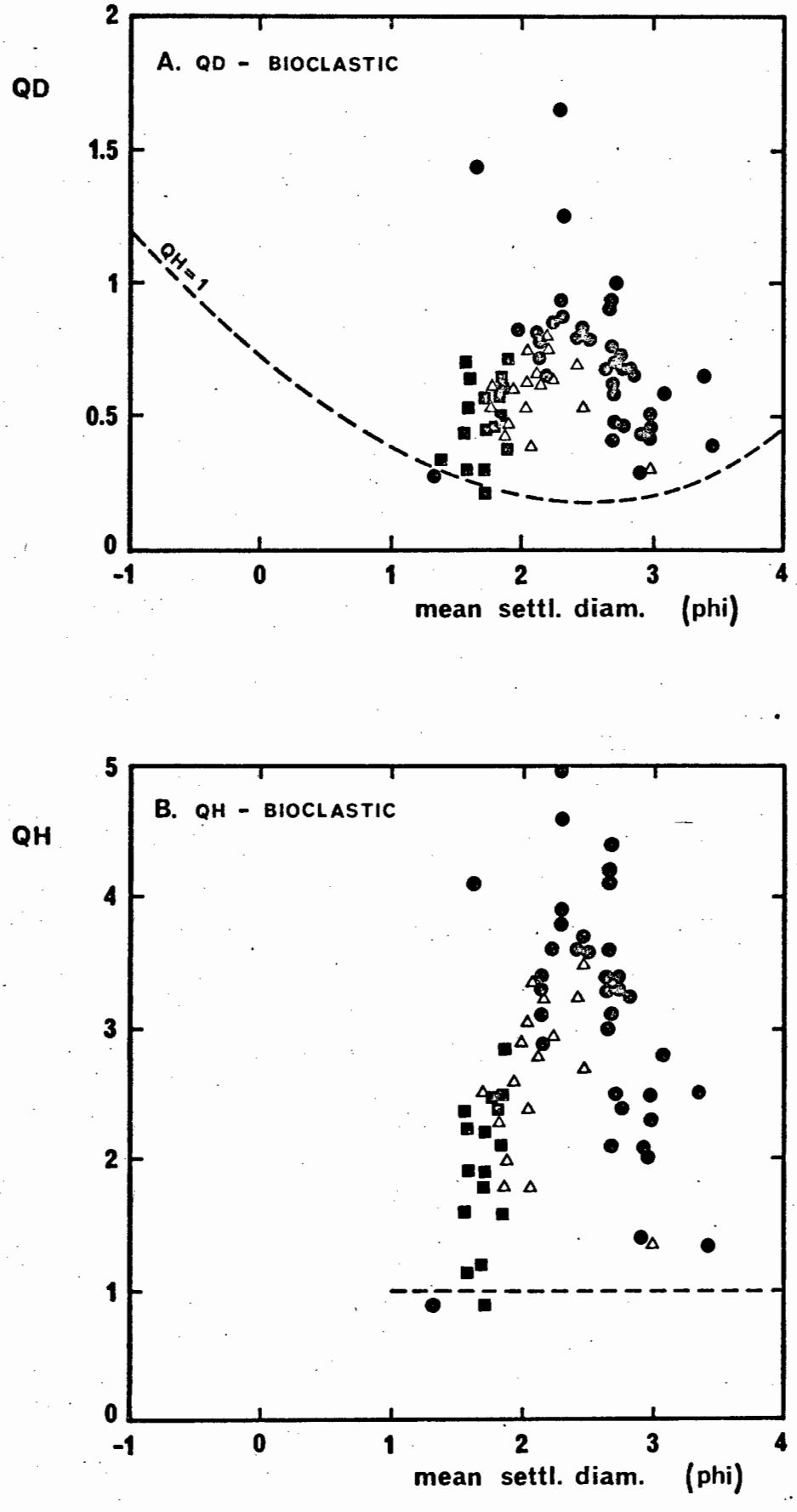

Fig. 39. The relationship between the mean settling diameter and sorting of the bioclastic component in tidal-flat sediments of Langebaan Lagoon.

A. QD vs. Mean settling diameter.
B. QH vs. Mean settling diameter.

of sorting for sediments of any mean size there is evidence that QH = 0.5 might be a better approximation of elementary sorting. The writer found that by plotting QH-values of the terrigenous quartz component of very find sands from a wave-dominated regime (Saldanha Bay), these consistently fell between 0.5 and 1.0 (Fig. 40-A). The bioclastic pattern (Fig. 40-B), on the other hand, seems to be completely independent of the terrigenous component in its sorting characteristics. The size distributions, although skewed, are not truncated, thereby eliminating the possibility of their representing residual sediments which were shown to be better sorted (Walger, 1962).

These results would strongly suggest that the individual shape groups of mixed sediments, of the type investigated in this study, respond as independent hydraulic subpopulations. This tentative rule is reminiscent of the "rule of independent supply" of individual sedimentary components concluded from coarse fraction studies by Van Andel and Veevers (1967) and Sarnthein (1971). It may well explain the mechanism controlling this phenomenon. Better rounded and more spherical components will thus achieve a better elementary sorting than the more irregularly shaped ones. In combination they produce the optimum sorting of QH approaching 1.0 as observed by Walger (1962). Size-sorting, it seems, is not independent of particle shape. This conclusion is strongly supported by observations of shape effects on sedimentary size parameters and depositional processes in Langebaan Lagoon to be discussed in a later chapter.

3.5.4. Classification of QH-Categories

The systematic application of relative sorting coefficients has created the problem of defining meaningful QH-intervals in terms of a relative sorting scale. A new classification is suggested which relates sorting intervals of both QD and QH in the fine sand column (Fig. 35-B). The new proposal is on one hand very similar to the traditional QD-classification, but at the same time, follows a consistent pattern within the QH-scale. Each interval, starting with the elementary sorting coefficient of 0.5, is double the preceeding interval as indicated in Table 4. It thus follows a $\log_2$-relationship similar to that of the phi-scale.

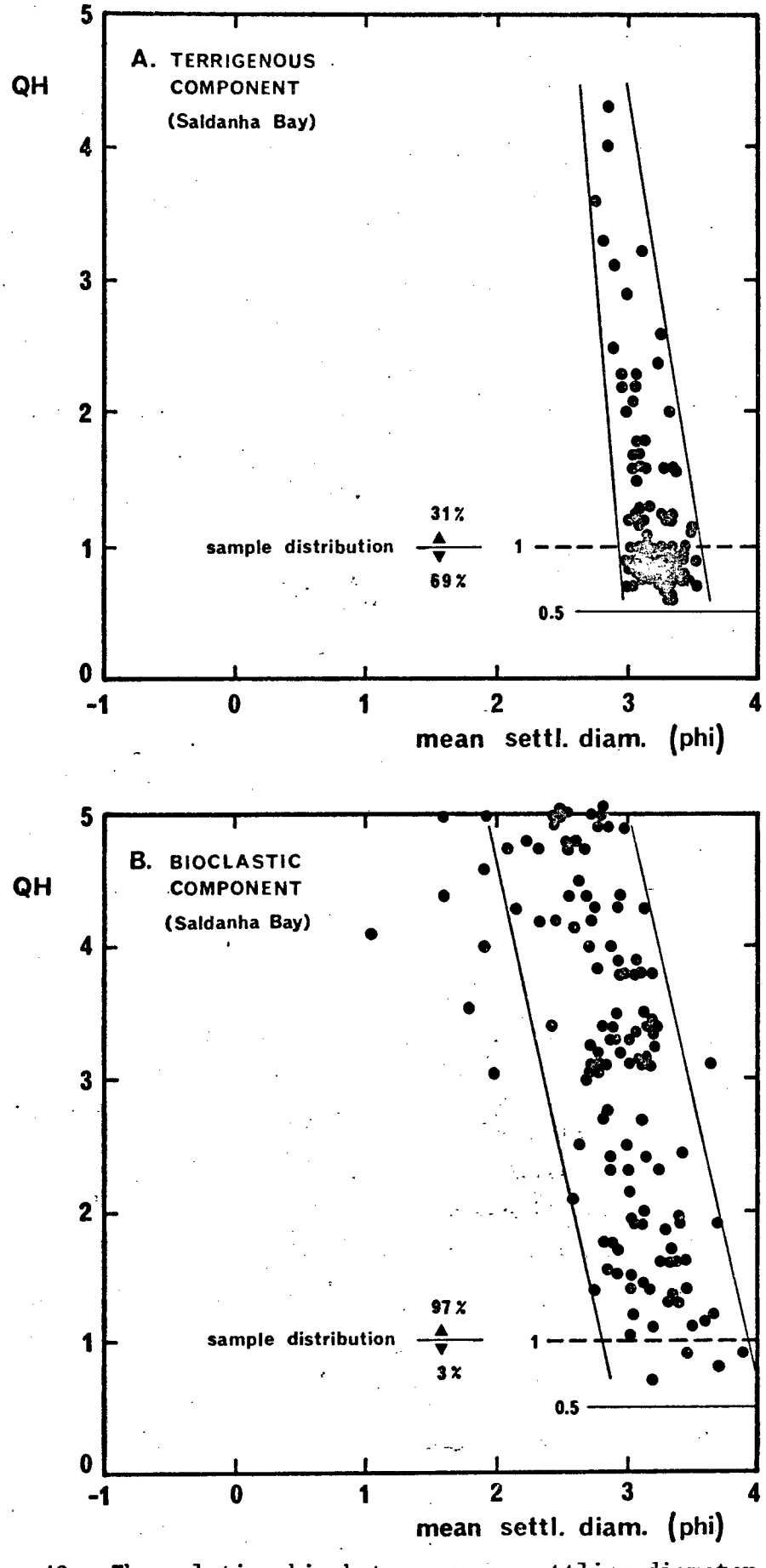

Fig. 40. The relationship between mean settling diameter and sorting in Saldanha Bay.

A. QH vs. mean settling diameter of the terrigenous component.
B. QH vs. mean settling diameter of the bioclastic component.

TABLE 4

Relative Sorting Categories

0.5 - 1.0	extremely well sorted
1.0 - 2.0	very well sorted
2.0 - 4.0	well sorted
4.0 - 8.0	moderately sorted
8.0 - 16.0	poorly sorted
16.0 - 32.0	very poorly sorted

3.5.5. A Hydraulic Model for Sorting

No serious attempt has been made thus far to provide a satisfactory explanation for the size-dependent sorting pattern when applying the standard QD-scale. The writer feels that a model relating sorting to the modes of transport and deposition, i.e. to the mechanism controlling size-sorting, could provide an adequate answer to the problem.

The dynamic relationship between current velocity and grain size can be summarized in a modified Hjulström Diagram (Hjulström, 1935; Sundborg, 1956; Allen, 1965). The diagram (Fig. 41) is an approximation for the size-velocity relationship at 1 m above the bottom and is based on field observations. It does not claim accurately to predict threshold conditions for incipient motion as this would require current measurements in the immediate vicinity of the sediment grains (e.g. Shields, 1935; Menard, 1950; Vanoni, 1964; Bagnold, 1968; Gust and Walger, 1975). However, it does serve to illustrate the situation at fully developed boundary conditions, i.e. when the mechanism of size-sorting should have its maximum effect.

The fine sand fraction, which under optimal conditions appears to be best sorted, lies exactly at that point in the size-velocity diagram at which the critical sedimentation velocity curves meet (i.e. at a size of about 150 microns and a velocity of about 24 cm/sec). This curve demarcates deposition from bedload and deposition from suspension. Thus, fine sand will deposit over a very small velocity gradient with only a brief phase of bedload transport in its coarser portion whereas its finer portion deposits directly from suspension. Because of this fact, fine sand can,

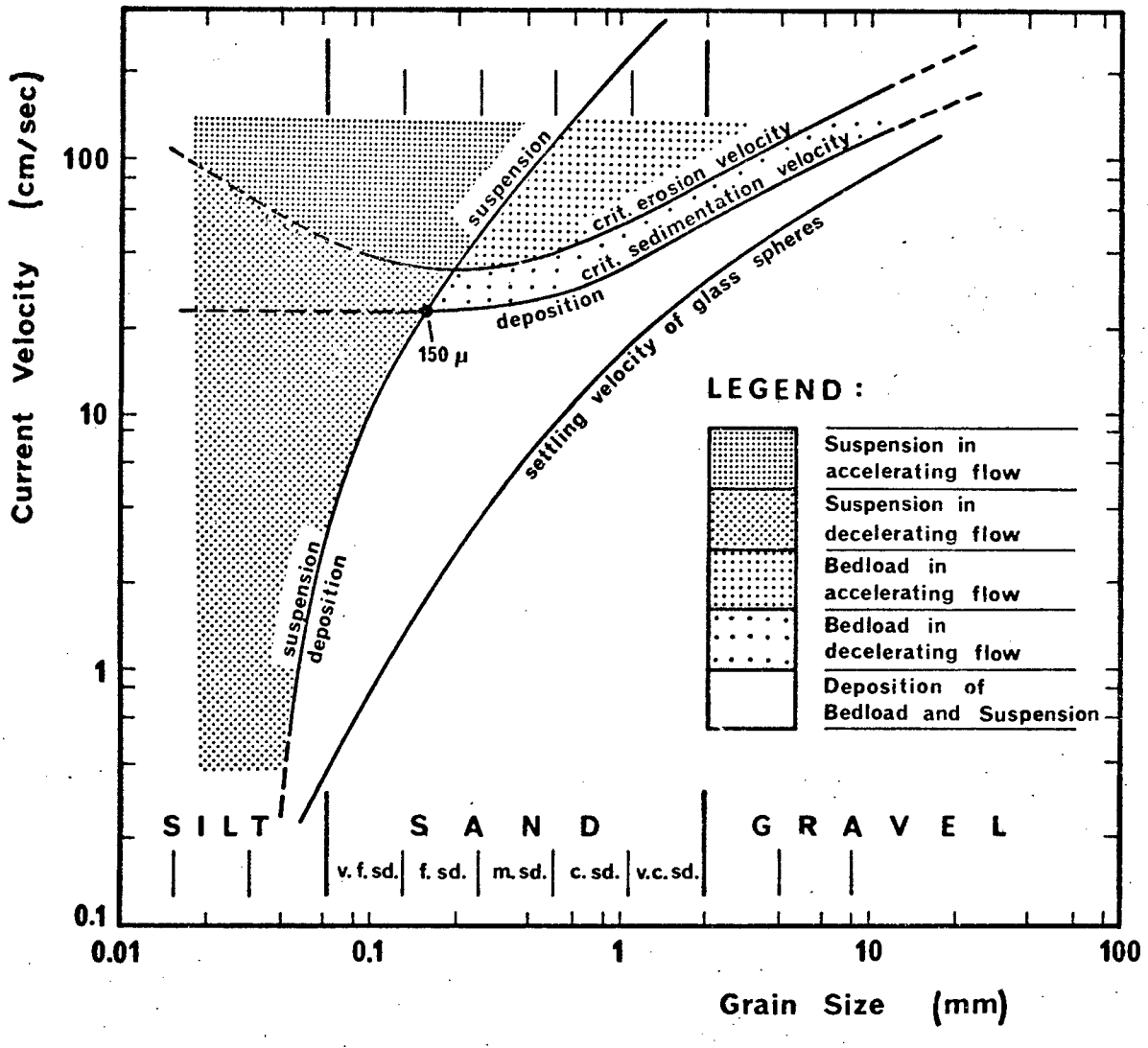

Fig. 41. Size-velocity diagram illustrating the modes of transport and deposition (modified after Allen, 1965).
N.B. The diagram reflects the conditions at a fully developed boundary layer with current velocities measured at 1 m above the bed.

under optimal conditions, achieve the best separation from all other size classes, thereby explaining its excellent sorting characteristics. Coarser sediments require increasingly larger velocity gradients and have, in addition, prolonged bedload phases in which separation of individual size classes is greatly obstructed. Finer sediments, especially from medium silts downward, will deposit almost simultaneously at very low velocities because of the almost vertical velocity gradient. Both finer and coarser sediments are, therefore, increasingly prevented from achieving a similar degree of size-sorting as the fine sand fraction, even under optimal conditions. The mode of transport thus acts as an important control mechanism of size-sorting. It will be shown later that particle shape is another significant parameter in this process.

A different factor which could act as an additional control mechanism is provided by the critical erosion velocity. Fine sand is normally the first sediment for which the critical shear velocity is reached. As a result, the frequency of movement of fine sand, and therefore its size-sorting potential, lies far above that of any other size class.

3.6. APPLICATION OF SOME SEDIMENTATION MODELS

In order to interpret the observed depositional patterns and to gain a better understanding of the dynamic processes leading to them, the writer has used a number of sedimentation models, all of which have been previously applied with varying degrees of success in the literature. The very term "model" implies that it represents a greater or lesser simplification of a real situation and, in most cases, the complexity of natural processes have prevented satisfactory "model solutions".

Most sedimentation models are empirical in nature and whereas some are physically and mathematically well founded, others have remained qualitative or semi-quantitative at best. Applying model solutions must, therefore, be viewed in the context of these limitations; the degree of success will depend entirely on the consistency with which the data can be expressed in terms of available concepts. The writer is fully aware of this problem and realizes that new or modified models could result in different explanations than those presented in this study.

3.6.1. Sediment-Wave Interaction

Saldanha Bay is a wave-controlled regime and sedimentary processes are thus expected to reflect the depositional response to wave-induced currents. Tidal currents and wind currents are superimposed on the wave pattern, but their velocities do not seem to exceed 15 cm/sec at the sea-bed (Shannon and Stander, 1977). Although their overall influence is not considered to be important, they might become significant on a local scale where residual water movements might be increased to a level at which sediment movement is possible.

There is excellent wave data available for the study area (Kluger, 1971); the most frequent wave heights and wave periods lie around 3 m and 14 sec respectively. According to Komar (1976), the resulting relationship between water depth, wave height, and wave length would allow the application of the "Airy Wave Theory" (small amplitude wave theory) to the deep water, intermediate water, and shallow water conditions in Saldanha Bay. This relationship is expressed in Fig. 42.

Under average wave conditions the transition from intermediate to shallow water in Saldanha Bay would occur at approximately 15 m of water depth, i.e. where $h/L < 0.05$, h being the water depth and L being the deep water wave length. The whole study area therefore lies within, or very close to, shallow water wave conditions, as defined by wave theory. The dissipation of orbital velocities in this situation differs fundamentally from that in deeper water. In this situation, velocities do not decrease exponentially as predicted in the model of Rankine (Kondrat'ev, 1953; Zenkovich, 1967), which is frequently used under different environmental conditions (Reineck and Singh, 1973). In shallow water the orbital diameter does not decrease with increasing water depth and, as a result, orbital motion is considerably greater to that in deeper water at any given depth for the same wave conditions.

In many studies of this kind (e.g. Zenkovich, 1967; Reineck and Singh, 1973), it was assumed that near-bottom current velocity was reflected by the mean orbital velocity for that water depth. This value was then reduced by 25 - 30% in order to compensate for orbital deformation. However, near-bottom currents do not describe an orbit but an oscillatory movement parallel to the sea-bed, in which the velocity profile develops from zero motion through a

velocity peak and back to zero motion in the direction of wave propagation, and then repeats a similar motion in the opposite direction. This model is illustrated in Fig. 43-A. It is immediately clear that the mean velocity used in the Rankine-Model does not adequately reflect the pattern of near-bottom flow. Sediment of a given size will begin to move once its critical shear velocity is reached in the accelerating phase and will continue moving until its critical sedimentation velocity is reached in the decelerating phase of each oscillatory component. The Rankine-Model will, therefore, underestimate the peak velocity value by up to 50%. The error will increase with increasing asymmetry of the two components (Fig. 43-B). This situation is frequently observed close inshore and is characterized by net onshore movement of water (Komar, 1976). Since the onshore component can mobilize larger sediment particles than the offshore component, there will be a net transport of coarse material into shallow water, while finer sediments tend to move offshore. Field observations in Saldanha Bay support the latter concept.

Near-bottom oscillatory currents based on this approach were calculated for different wave parameters in Saldanha Bay, in order to assess which wave parameters were in control of the depositional processes observed in the area. Although the general picture obtained in this manner is in good agreement with depositional patterns, the model does not accommodate boundary layer phenomena. As a result, the relationship between near-bottom flow, generated by different wave regimes, and the observed sediment distribution patterns, is correct only in a relative sense. In this context, the peak velocity components presented in a later section (Section 4.2.) are probably a good reflection of the flow conditions just above the boundary layer. The true shear velocity, on the other hand, is that velocity component that acts directly on the sedimentary particle. As it forms part of the boundary layer it will be considerably lower than the near-bottom velocities calculated from various wave parameters.

Unfortunately, it is not possible at this stage to accurately predict boundary layer flow conditions from wave parameters. Teleki (1972) concludes that the boundary layer phenomena in oscillatory currents are poorly understood, and Komar and Miller (1973) indicate that laminar boundary layers may, in fact, play a more important role in oscillatory flows than in steady flows.

Considering this fundamental shortcoming, the writer considers attempts to calculate equilibrium grain sizes for given wave parameters as premature.

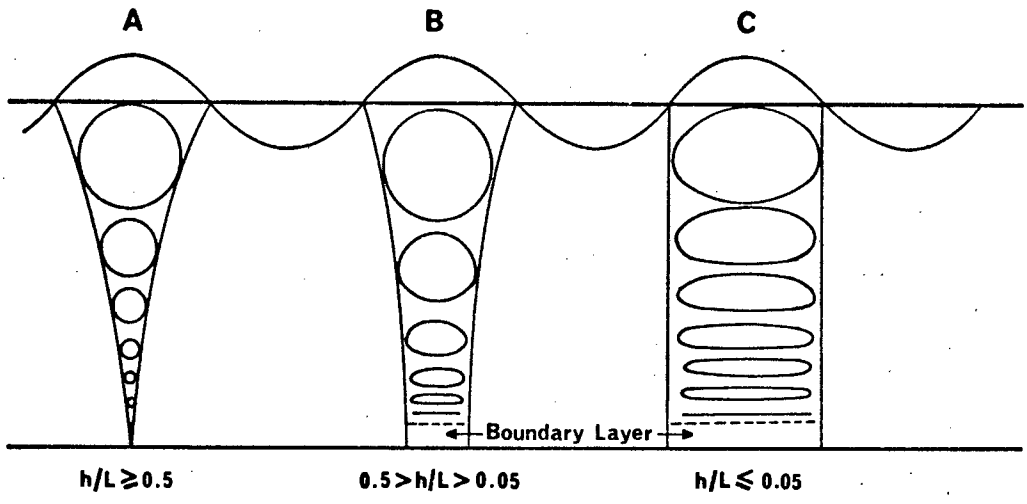

Fig. 42. The dissipation of wave energy with water depth.

A. Deep-water situation
B. Intermediate-water conditions
C. Shallow-water conditions

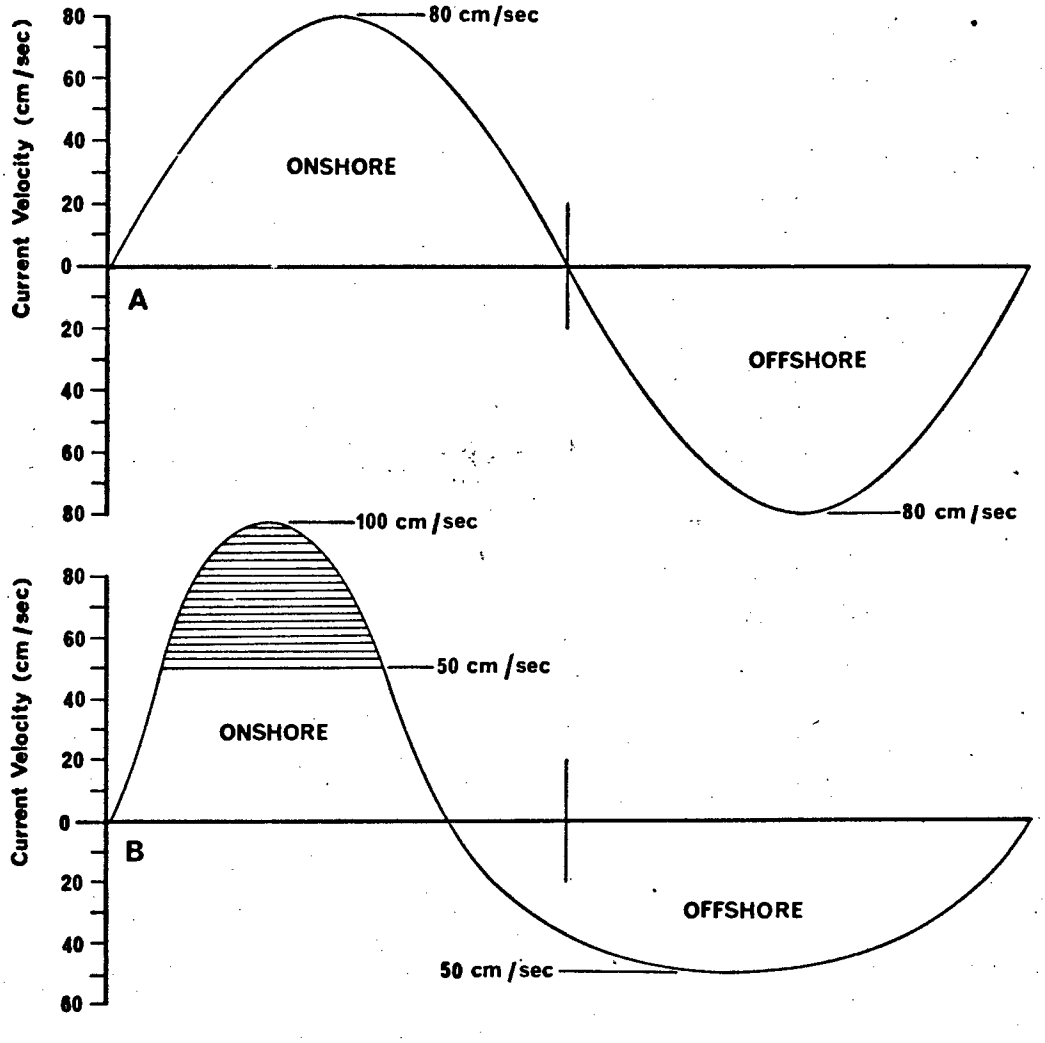

Fig. 43. Time-velocity curves of near-bottom oscillatory currents.

A. Idealized symmetrical case.
B. Strong time-velocity asymmetry.

(after Komar, 1976)

This conclusion is supported by a recent study in which Graf (1976) has compared measured and predicted grain size patterns in the nearshore region of Lake Michigan, making use of the "null-point model" of Munch-Peterson (1950), Johnson and Eagleson (1966) and Swift (1970). The "null-point" is defined as that situation at which all the forces acting on a sedimentary particle cancel out. It was shown that the theoretical formula, developed for equilibrium size prediction under constant wave conditions, consistently overestimated grain sizes, especially as sizes increased. It would appear that even this highly complex formula fails to account for boundary layer phenomena.

There are a number of independent criteria that suggest that sedimentary processes in Saldanha Bay are close to equilibrium and, in order to assess the relationship between the calculated near-bottom velocities and the observed grain sizes, the writer has used 10 cm/sec as a minimum threshold value for fine sediments on an even bed. This value is taken from a size-velocity graph for wave-induced bedforms presented by Allen (1970). It will be shown in Section 4.2. how this value and the calculated near-bottom velocities relate to the equilibrium concept.

3.5.2. Sediment-Current Interaction

In contrast to Saldanha Bay where sedimentation is dominated by waves, sedimentary processes in Langebaan Lagoon are controlled by tidal currents. Two models are frequently used to illustrate the interaction between sediments and one-directional flows. One concept has already been discussed to some extent in Section 3.5.5. (Fig. 41). It represents a modified size-velocity model based on the original work of Hjulström (1935). It defines the approximate velocity situations for erosion and sedimentation of various grain sizes at fully developed boundary conditions. It is easier to apply than the model developed by Bagnold (1966), in which stream power is related to grain size. Stream power is defined as a function of current velocity and bed shear-stress; however, since shear-stress measurements are rarely available from natural environments, the model has little value for comparative purposes in this case.

Although the modified Hjulström diagram probably overestimates threshold velocities to some extent, it serves well to illustrate the response of lagoonal sediments to the tidal flow.

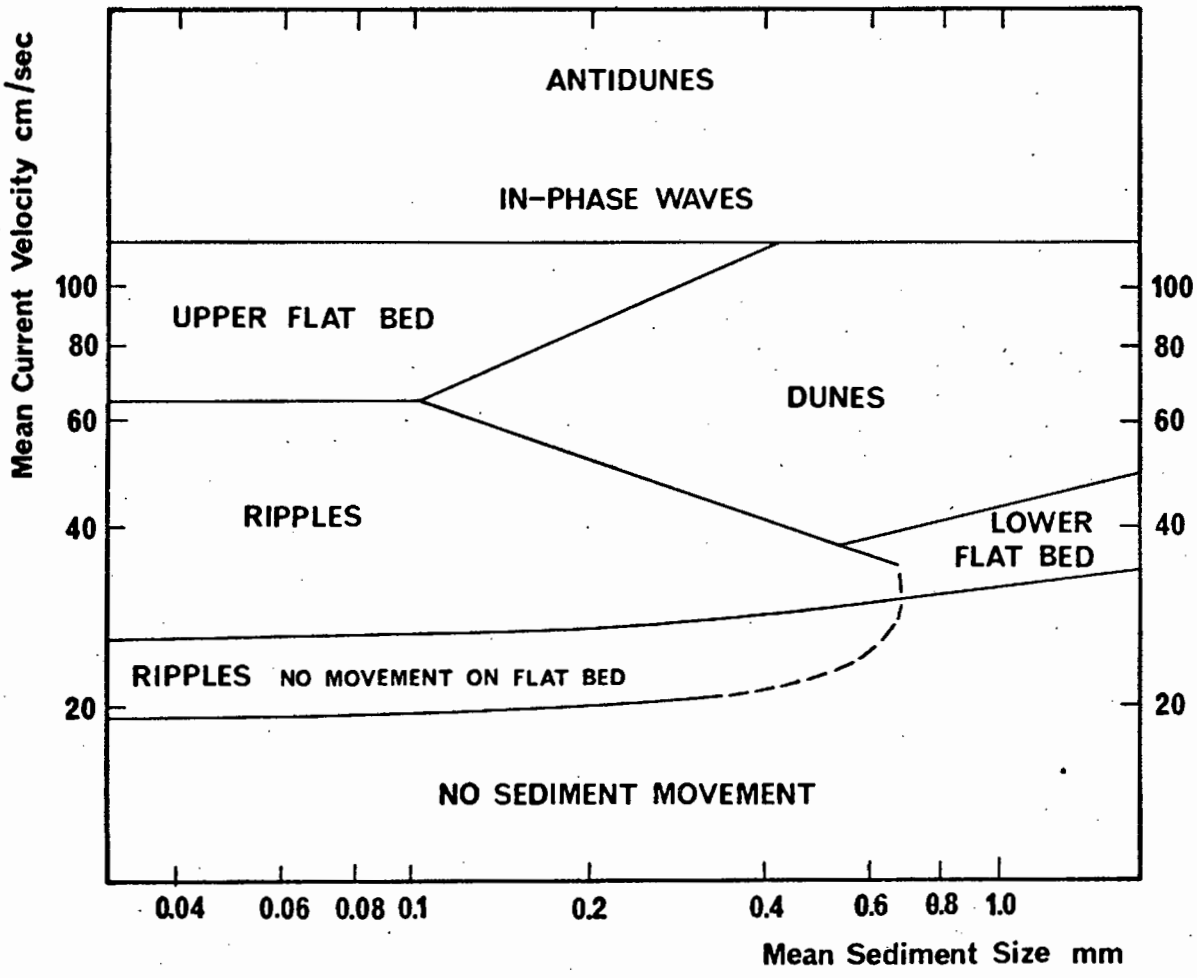

Fig. 44. Schematic size-velocity diagram with related bedforms. (after Southard, 1975)

In the above approach, the main objective was to define the size-velocity relationship at the threshold of sediment movement. Another approach relates sedimentary bedforms to current velocities (e.g. Allen, 1967; Southard, 1975). Although threshold conditions are also observed, the main attention is given to bedform development (Fig. 44). The model is particularly useful as it allows a comparison of observed bedforms with the predicted pattern, thereby defining upper and lower limits of flow conditions in various parts of the lagoonal channels. Fig. 44 can be visualized as an expanded view of the central section of Fig. 41, although the lower boundaries do not coincide exactly. It is interesting to observe the close agreement between the two diagrams and perhaps Fig. 44 gives a better definition of the threshold conditions. On the other hand, the threshold in Fig. 44 was defined on the basis of flume experiments; flow development in flumes and wide, open channels may not necessarily coincide.

Sediment-current interaction, however, is not only reflected by size-velocity relationships but also by size distribution characteristics of sediments. As was pointed out earlier, the mechanism of sediment transport was shown to be directly involved in size-sorting. Folk and Ward (1957) have demonstrated that there is a strict control of size distribution parameters in the course of sediment mixing. Fig. 45-A illustrates the relationship between mean diameter, sorting, skewness and kurtosis in the mixing process of two lognormal populations of different mean sizes. Thus, sorting progressively decreases as the degree of mixing increases, reaching its poorest level where the two populations are equally mixed. At the same time, the finer population initially becomes negatively skewed while the coarser population becomes positively skewed. At the point of equal mixing the distribution is again symmetrical. Kurtosis develops in each case from a mesokurtic curve shape to a leptokurtic one and then back to a mesokurtic one, from where it becomes progressively more platykurtic towards the point of equal mixing.

Fig. 45-B illustrates the same relationship in three-dimensional form, whereby the regression curve through the point cluster describes a helical structure with its central axis running parallel to the mean diameter co-ordinate (X-axis) above the zero-skewness level. Also shown are the projected images of the helix when viewed perpendicular to the individual planes defined by the axes of the mean diameter with that of sorting (XY-plane), the mean diameter with that of skewness (XZ-plane), and that

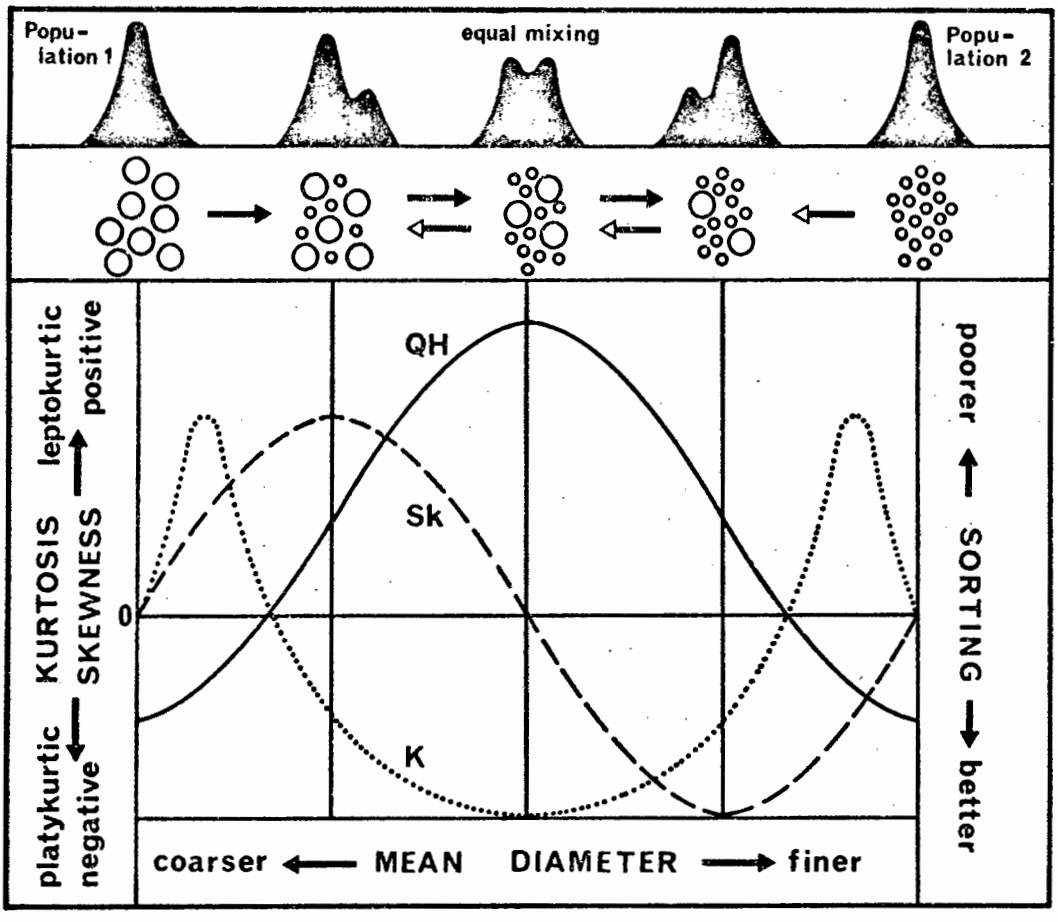

A

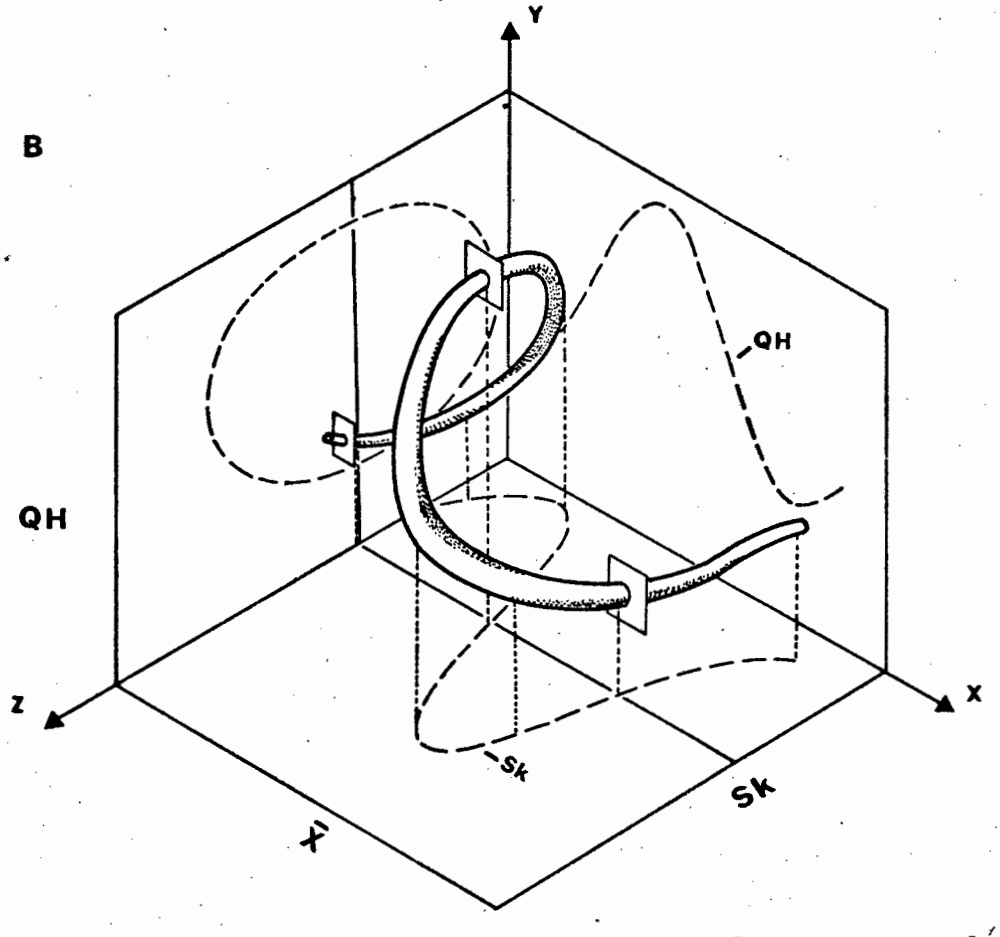

Fig. 45-A. The relationship between the textural parameters of sediments consisting of two progressively mixing hydraulic populations.

45-B. The same relationship in three-dimensional form. Note the helical trend of the data points (after Folk and Ward, 1957).

of sorting with the axis of skewness (YZ-plane). Each plane represents a two-dimensional projection of three-dimensionally arranged data points. All scatter plots involving the various size parameters must be understood in this manner if they are to be correctly interpreted.

It will be shown later in this study that the sediments of Saldanha Bay, and especially those of Langebaan Lagoon, present images that can be interpreted in terms of the above model.

3.6.3. Modes of Sediment Transport

Modes of sediment transport have received considerable attention by hydraulic engineers, and it is well documented that sediments are transported either as bedload or as suspended load (Sundborg, 1956; Raudkivi, 1967; Graf, 1971; Shen, 1971). Various methods have been devised to estimate the competence of modern streams with respect to their transport capacity. However, sedimentologists are often faced with the problem of having to establish retrospectively the hydraulic regime that was in control of a particular depositional feature.

Passega (1957) has presented a model which appears to provide just that information. Supporting his approach with numerous well documented examples, Passega demonstrates that the major transport modes from which sediments were deposited can be reconstructed by plotting the coarsest one percent of the size distribution against the median diameter (CM-Diagram). Depending on the position of the points in this diagram, he distinguishes transport modes such as rolling, rolling and suspension, suspension and rolling, graded suspension and uniform suspension (Fig. 46).

A number of studies have achieved good results in the interpretation of depositional processes in the fluvial and marine environment utilizing this model (Passega, 1964; Passega et al., 1967; Passega, 1969; Sigl, 1973). In the present study, the model has been successfully applied in the interpretation of depositional processes and has provided strong evidence for the differential response of individual sedimentary shape components in Saldanha Bay and Langebaan Lagoon. Although the model still lacks a sound physical explanation, it appears to reliably reflect the conditions of transport just before the sediment is deposited.

A similar approach, utilizing straight line segments of cumulative grain size curves, was suggested by Visher (1965; 1969). Visher distinguishes a traction population, one or two saltation populations and a suspension population. Although a number of studies have subsequently recognized straight line segments, the writer was not able to distinguish these with sufficient confidence to justify their systematic use. Furthermore, the model has recently been criticised on methodological grounds (Reed et al., 1975). Visher has based all his interpretations on sieve data and although this might not be too serious in some cases, e.g. fluvial sediments, it must certainly fail in a marine environment where irregularly shaped particles form part of the sediment. In this case sieve results are incompatible with the hydraulic nature of the sediments (see also Section 3.3.2).

For the purpose of this study the terminology of Passega (1964) has been slightly modified in order to make its application more practical. In the course of sediment transport, two hydraulically distinct modes are observed - material in bedload and material in suspension (Shen, 1971). The bedload can be further subdivided into a bottom layer in which particles predominantly roll or slide. This lowest portion of the bedload, also known as surface creep, or the traction carpet, is obviously identical with Passega's rolling category. It will henceforth be referred to as the traction carpet. Its lower limit has been arbitrarily defined at a coarsest percentile of 0-phi.

The suspension + rolling category appears to be identical with the region of bottom suspension in which particles from the bed continuously leap into the flow. This process is also known as saltation. Often there are two saltation populations present, one that makes lower and shorter jumps and another that makes higher and longer jumps. In order to link up with Passega's terminology, this part of the bedload has been termed bottom suspension whereby it was convenient to distinguish a lower bottom suspension (saltation population 1) and an upper bottom suspension (saltation population 2).

The division line between the two has been drawn at +0.65 phi. Thus, the lower bottom suspension ranges from a coarsest percentile level of 0-phi to +0.65-phi, the upper bottom suspension from +0.65-phi to +1.3-phi. At finer grain-size levels there is true suspension which Passega (1957) has

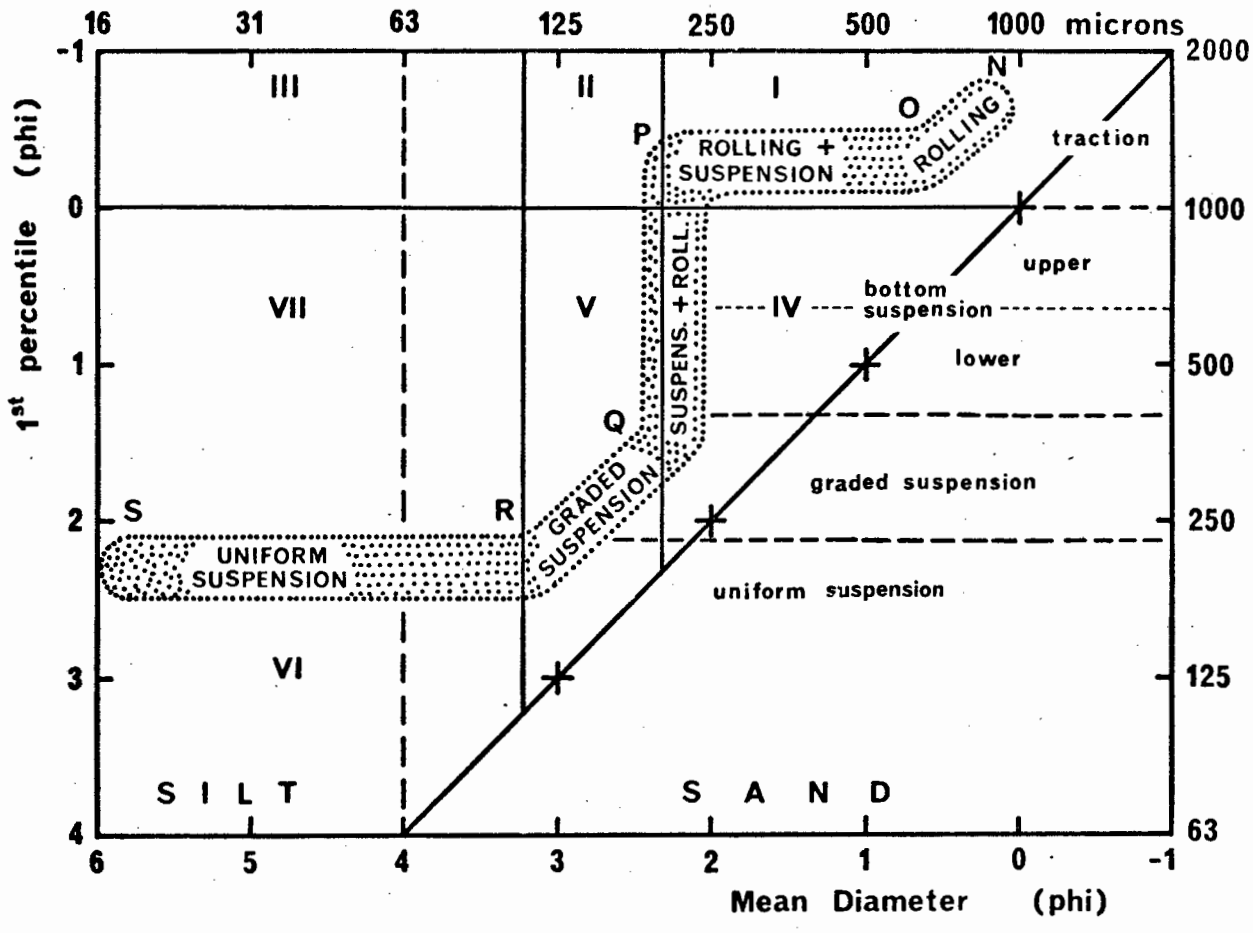

Fig. 46. Modes of sediment transport inferred from the relationship between the 1st-percentile and the mean diameter of the sediment (modified after Passega, 1957).

divided into a graded suspension between +1.3-phi and +2.3-phi, and a uniform suspension at levels finer than +2.3-phi.

The writer wishes to emphasize that the size limitations of the individual transport modes is quite arbitrary, since there will normally be a complete gradation between individual levels. An important aspect, however, is that the classification is sequential and, as such, it should be a sensitive indicator of changing transport patterns. It will be demonstrated in the course of this study that the individual modes, as defined above, actually present well defined, sequential patterns in Saldanha Bay and Langebaan Lagoon.

3.6.4. Grain-Size Images

The previous sections were predominantly concerned with physical process-response models such as threshold of motion, size-velocity relationships, and modes of transport. The following sections will deal more with empirical relationships between individual sedimentary parameters and their environment of deposition. By nature, these are descriptive and serve the purpose of distinction between the sedimentary characteristics of different depositional environments.

An early approach to this effect was presented by Friedman (1961) who was able to distinguish dune and beach sediments simply by plotting mean diameters against skewness. Shepard and Young (1961), on the other hand, found that this was reliable only in regions with predominantly onshore winds. The area investigated in the present study is exposed to onshore winds and thus the model was tested for its predictive potential. The outcome was highly significant in that the predictive value of the model for the unconditional recognition of the two environments was conclusively refuted.

Fig. 47 demonstrates that the model neatly separates two different environments; however, the environments do not represent dunes and beaches as the model requires, but western and eastern tidal flat sediments respectively. A point of interest is the fact that the western tidal flats are composed of reworked dune material. The model does, therefore, seem to reliably predict the source to which a sediment is related and, in this restricted sense, it may serve a useful purpose.

It would appear that Friedman (1961) was able to distinguish between the two environments only because he knew where the sediment originated from. Under these circumstances, however, it becomes quite irrelevant to demonstrate this by any other means. The model does, therefore, not predict environments but only the source to which a sediment may be related.

Another study with similar implications was recently presented by Jones and Cameron (1976). In this case, graphic sediment statistics of samples recovered from conceptually pre-defined environments were investigated by discriminant function analysis. The experiment was initially performed on sieve data and subsequently repeated on settling data. The method correctly grouped 96% of the sieve data into their pre-defined subenvironments, whereas the settling results were correctly grouped in only 72% of all cases. The authors concluded that the conventional sieve method appeared to provide better results for the classification of subenvironments.

This conclusion is significant for two reasons. Firstly, as in the case of the Friedman Model, the grouping results were meaningful only because the sample origin was known beforehand. The approach must necessarily fail on similar grounds as the previous one. For similar reasons, the method can never achieve predictive value. Secondly, by ignoring the fact that settling results are hydraulically more meaningful, the far more important conclusion, namely that the conceptually defined subenvironments were physically not as different as the sieve data might imply, eluded them altogether.

A different approach was adopted by Doeglas (1968). By plotting various textural parameters against the median diameter (e.g. Q_1 and Q_3 against Md), a clear and seemingly significant grain size image emerged. Q_1 and Q_3 represents the median diameter. The former two parameters are related to the sorting of a sediment, whereas the latter reflects the average size of the frequency distribution. Doeglas then proceeds to plot median against median - an exercise that lacks any logic.

In an attempt to find a clear and meaningful presentation of the grain size images of different sedimentary environments, the writer has modified the approach of Doeglas (1968) and has combined it with the approach

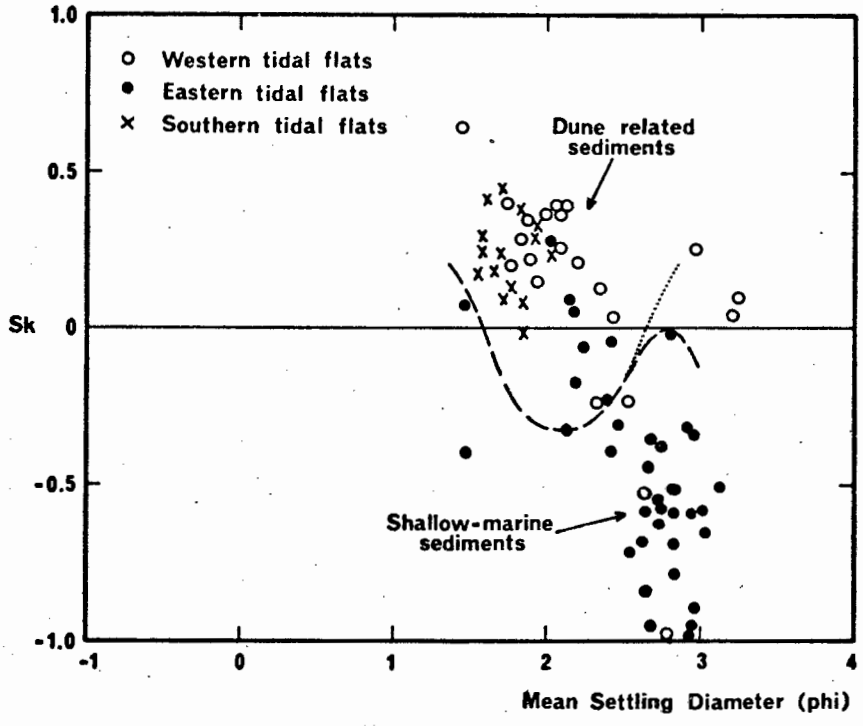

Fig. 47. The apparant distinction between beach and dune sediments (after Friedman, 1961). The model separates eastern and western tidal-flat sediments instead.

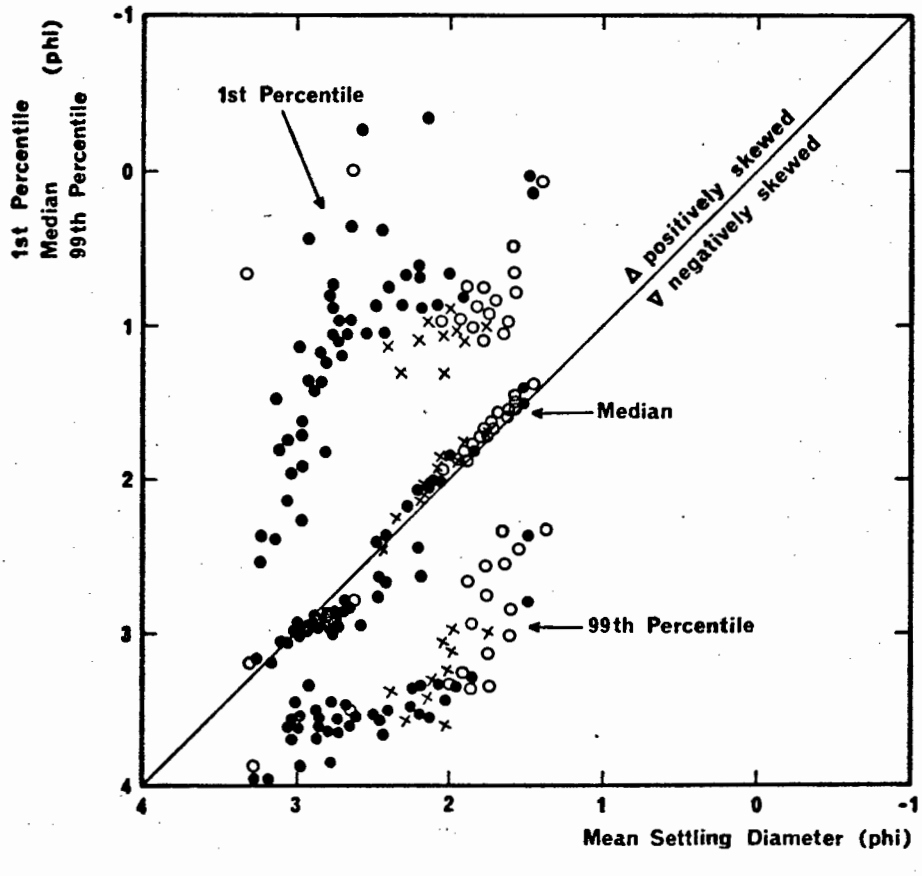

Fig. 48. Grain-size image of intertidal flat sediments in Langebaan Lagoon.

of Passega (1969) in an expanded CM-Diagram. The new diagram provides considerably more information than either approach individually. Fig. 48 can serve as an example. Three parameters, the first percentile, the median diameter and the ninetyninth percentile are plotted against the mean diameter of the sediment.

As outlined earlier, the 1st percentile and the mean will indicate the predominant mode of transport. The 99th percentile represents the finest material deposited and, since the two tails together approximate the overall spread of a size distribution, the 1st and the 99th percentiles should illustrate the sorting of the sediment. The closer the two values lie together the better the sorting should be and the further they lie apart the poorer the sorting should become. This inferred relationship was tested by plotting the difference between the two values against the sorting of the sediment (Fig. 49). The relationship is excellently recorded and it is concluded that the combination of the 1st and the 99th percentiles serve the same purpose as the 25th and 75th percentiles used by Doeglas (1968). Thus, by plotting both the 1st and the 99th percentile against the mean diameter, a grain size image is achieved that, not only expresses a similar relationship as that intended by Doeglas, but, in addition, provides fundamental genetic information about the depositional processes in the course of which the sediment was deposited.

This initial diagram was then further expanded by adding the mediam diameter to the diagram. Statistically the relationship between the mean and the median will indicate in which direction a size distribution is skewed (viz. Pettijohn et al., 1972). The resulting plot now presents a grain size image which conveys almost all the important aspects of individual size distributions like mean, median, sorting and skewness. In addition, it relates individual samples to each other in a scatter plot that reflects the depositional processes controlling the environment. In this form the grain size images of individual depositional units can be compared in a meaningful manner.

3.6.5. Depositional Environments and Facies Models

The term "environment" is generally used in a physiographical sense (Blatt et al., 1973). It denotes the totality of physical and chemical conditions by which one physiographically defined region can be distinguished from another. Unfortunately, there is no generally accepted terminology

(Hedgepeth, 1957) and the term "environment" is often used in a rather loose form. Thus, the world oceans are normally referred to as the "marine environment", yet any physiographically defined portion of the marine environment is usually also referred to as an "environment". In order to avoid confusion, the term "environment" will be henceforth used in the latter sense. In this context Saldanha Bay forms a coastal-bay environment and Langebaan Lagoon forms a coastal-lagoon environment.

In sedimentological terms each environment is characterized by at least one major process-response mechanism, although in most cases there will be a number of such mechanisms acting either independently in different parts of the system, or sequentially within the same area. In this context sedimentary environments reflect the dynamic conditions controlling local depositional processes (Reineck and Singh, 1973).

In Saldanha Bay and Langebaan Lagoon several units can be distinguished which appear to be characterized by specific depositional processes. Each unit is described as a "subenvironment" of the whole system, while individual sedimentary features within a subenvironment have been described as "sedimentary facies".

The concept of sedimentary facies was originally developed by Walther (1894). In principle this concept was described by Moore (1949) as an "areally restricted part of a designated stratigraphic unit which exhibits characters significantly different from those of other parts of the unit". Although this is not the only sense in which the term "facies" has been used (viz. Moore, 1957; Dunbar and Rogers, 1957; Teichert, 1958; Weller, 1960; Krumbein and Sloss, 1963; Selley, 1970), it is particularly well suited for a detailed description of the depositional characteristics in the study area, especially in Saldanha Bay.

Some environments and subenvironments are characterized by such a typical sequence of depositional features that they have taken on a model character. Each association of specific features has been expressed in terms of a so-called "facies model". Facies models, developed mainly on the basis of modern examples, have been particularly successful in the recognition of ancient sedimentary environments. Some excellent summaries of various aspects of this approach have been published, e.g. Richter (1936), Seilacher (1953, 1954, 1964), Schäfer (1956, 1962), Pettijohn (1957),

Potter (1959), Reineck (1963), Pettijohn and Potter (1964), Conybeare and Crook (1968), Allen (1970), Selley (1970), Rigby and Hamblin (1972), Reineck and Singh (1973), Blatt et al, (1973), Ginsburg (1975). The depositional features observed in Langebaan Lagoon appear to be particularly well suited for a facies model approach.

The fundamental framework of the facies model approach is based on primary sedimentary structures. These are formed by physical, chemical and biological processes, either independently or in combination, whereby the former two are usually classified as inorganic sedimentary structures, while the latter are summarized under organic sedimentary structures (Pettijohn, 1957; Conybeare and Crook, 1968), bioturbation structures (Richter, 1936), or biogenic sedimentary structures (Seilacher, 1962). Both groups leave their marks on the surface as well as within the sediment. In principle the primary structures observed in the study area can be viewed as the outcome of interacting physical and biological processes. These are, in each case, a reliable indicator of the specific energy levels controlling the depositional processes in the environment.

Bioturbation, i.e. the disturbance of the sediment by the burrowing activity of organisms, can be viewed as a process in which physically produced structures are progressively destroyed by biological activity. Since both processes are co-active, the classification of internal sedimentary structures is based on the degree of bioturbation as a descriptive standard (Reineck, 1963; Reineck and Singh, 1973). Hence biological and physical internal structures are discussed together.

Biological structures have received close attention because of their ecological implications. Significant contributions in this field, especially in the distinction of surface structures and internal structures, were made by Seilacher (1953 and 1962) and Schäfer (1956). The terminology used in this study has to a large extent been adapted from these authors. The degree of bioturbation, in combination with textural features, was used to characterize the various depositional units. In accordance, the stratonomic approach of Seilacher (1953), occasionally supported by ecological considerations, was adopted. Only the major organisms involved in bioturbation are discussed, whereby taxonomic references are based on the work of Day (1958 and 1969).

3.6.6. Lithology

A lithological classification of the sediments in Saldanha Bay and Langebaan Lagoon faces the problem of inadequate terminology. The sediments of the study area consist of a mixture of skeletal carbonates and terrigenous quartz. Petrological classifications, however, are designed, either for carbonate rocks (e.g. Dunham, 1962; Folk, 1965), or quartz-sandstones (e.g. Pettijohn et al., 1972).

With few exceptions, the sample material of the study area consists of sand-sized particles, and petrographically the sediment would, therefore, pass as an "arenitic rock" or simply as an "arenite". Mud is present in many samples, although mostly in quantities under 1%. Using the three component groups as respective endmembers, a triangular diagram was constructed (Fig. 50). Whereas the mud remains a marginal component in practically all samples, skeletal carbonates and terrigenous quartz are mixed in all grades between 5% and 95%.

The triangular diagram was subdivided following the textural example of Shepard (1954), and the terminology was taken from Krumbein and Sloss (1963). On the basis of this classification, the sediments of the whole study area qualify, either as slightly calcareous quartzarenites, calcareous quartzarenites, quartzose calcarenites, or slightly quartzose calcarenites. Füchtbauer (1959) has presented a more detailed subdivision than the one quoted above, but it was found to be less practical for the purpose of areal classification.

Petrographically some calcarenites would qualify, in terms of the classification of Dunham (1962), as "lime grainstones" or as "lime packstones". However, in order to avoid unnecessary confusion, the writer has decided to use a single, genetically consistent terminology. Calcarenites, as described in this study, can therefore be regarded synonomous with "sand-sized skeletal lime grainstones" in cases of very low mud content, or as "sand-sized skeletal lime packstones" in cases where the mud content is higher.

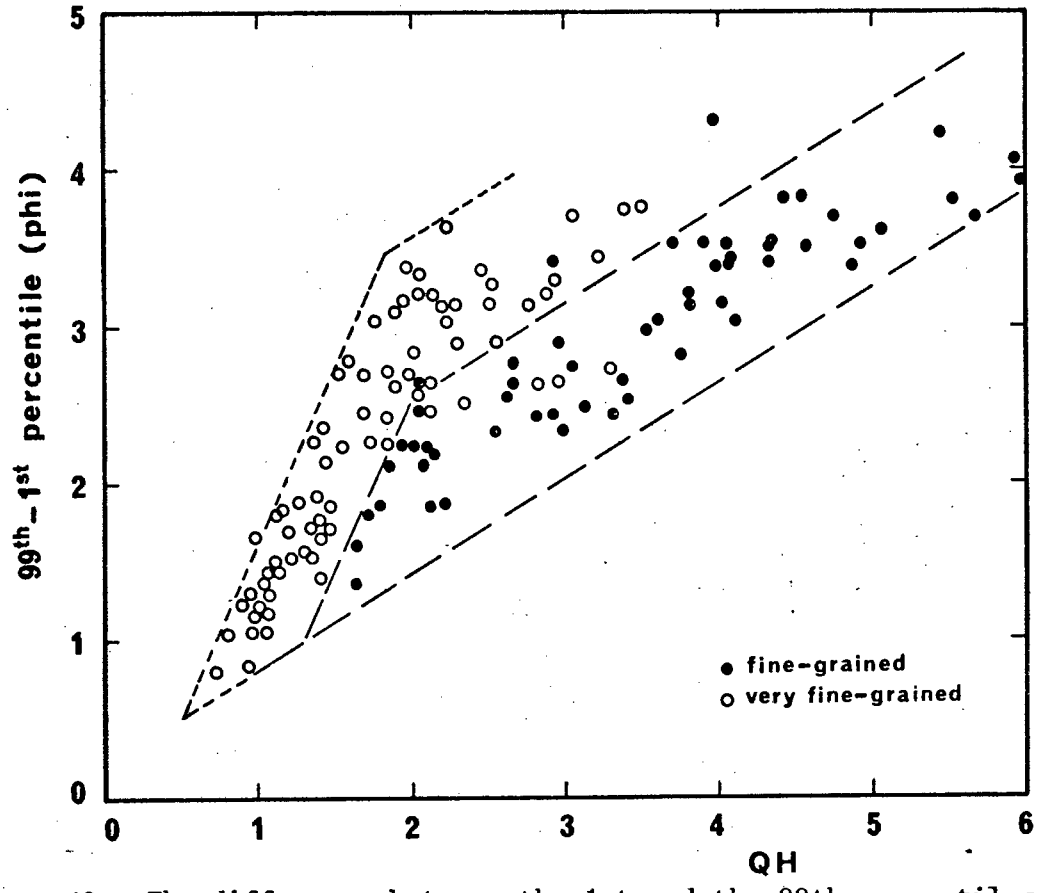

Fig. 49. The difference between the 1st and the 99th percentiles clearly reflects the sorting characteristics of the sediment.

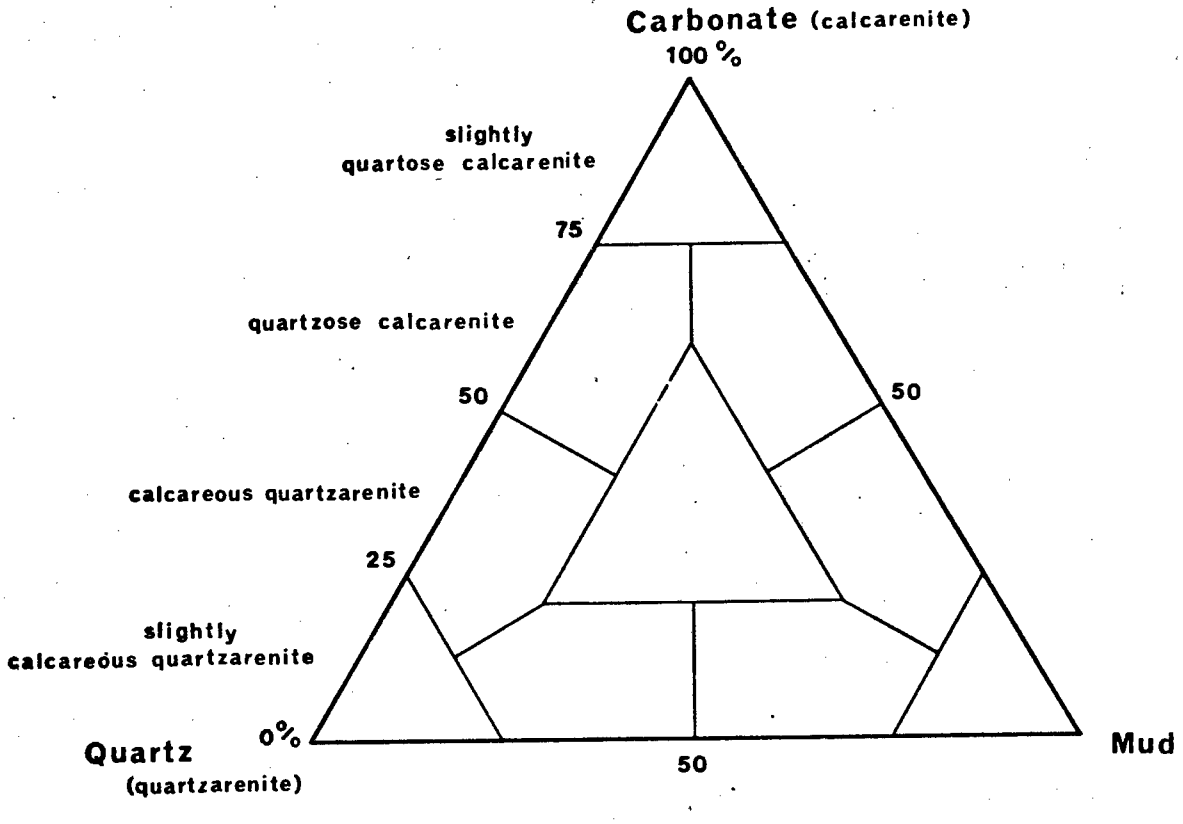

Fig. 50. Lithological classification.

CHAPTER 4. SALDANHA BAY

4.1. PHYSIOGRAPHIC FEATURES

A striking feature of Saldanha Bay is the apparent symmetry of its planimetric shape as defined by the shoreline. The elliptical character of this shape can, in fact, be expressed in terms of two converging logarithmic spiral curves around the spiral centres X and Y (Fig. 51-A). Each spiral forms a mirror image of the other along the plane $Z - Z_1$. The closeness of fit between the shoreline and the two log.spirals is demonstrated in Fig. 51-B.

Significantly, the overall shape has been extremely well maintained, in spite of some interference with the wave refraction pattern in the shadow of Marcus Island. In response, there is a slight bulge in the shoreline at the point where the two wave orthogonals A_1 and A_2 meet the beach (Fig. 52-A). Slight deviations are also caused by a number of rocky promonteries along the southeastern shoreline of Saldanha Bay, e.g. Lynch Point.

Another important feature can be observed in the southern bay at the point where the eastern embankment of the lagoonal outflow-channel meets the shoreline of the bay. This point, which obviously defines an equilibrium situation between the forces of the tidal ebb current and the refracted ocean waves, is situated on the log.spiral curve. It would thus appear that the geometry of the shoreline in coastal embayments, such as Saldanha Bay, is a strict function of the energy dissipation controlled by the wave refraction pattern.

The curvi-linear expression of coastlines controlled by waves refracting around headlands was first described by Jennings (1955). Davies (1958) and Silvester (1960) were the next authors to draw attention to this peculiar phenomenon. Yasso (1962 and 1965) then demonstrated that this relationship could, in fact, be expressed by a logarithmic spiral curve, and Silvester (1970) proved the consistency of this feature by systematically fitting logarithmic spiral curves to numerous experimentally produced shorelines. Other authors who have successfully fitted log.spiral curves to natural shorelines are LeBlond (1972) and

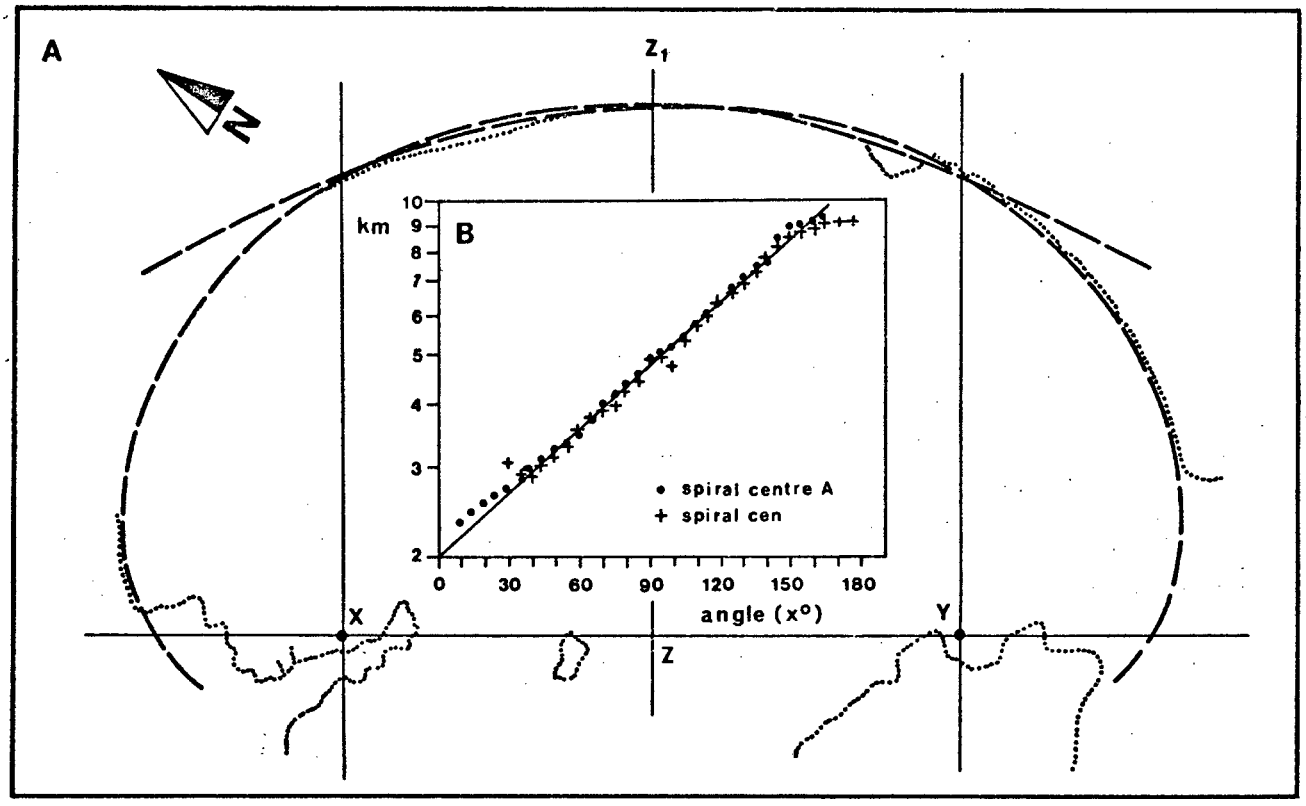

Fig. 51. Coastline geometry.

A. Planimetric shape of Saldanha Bay.
B. Coastline fit with a logarithmic spiral curve.

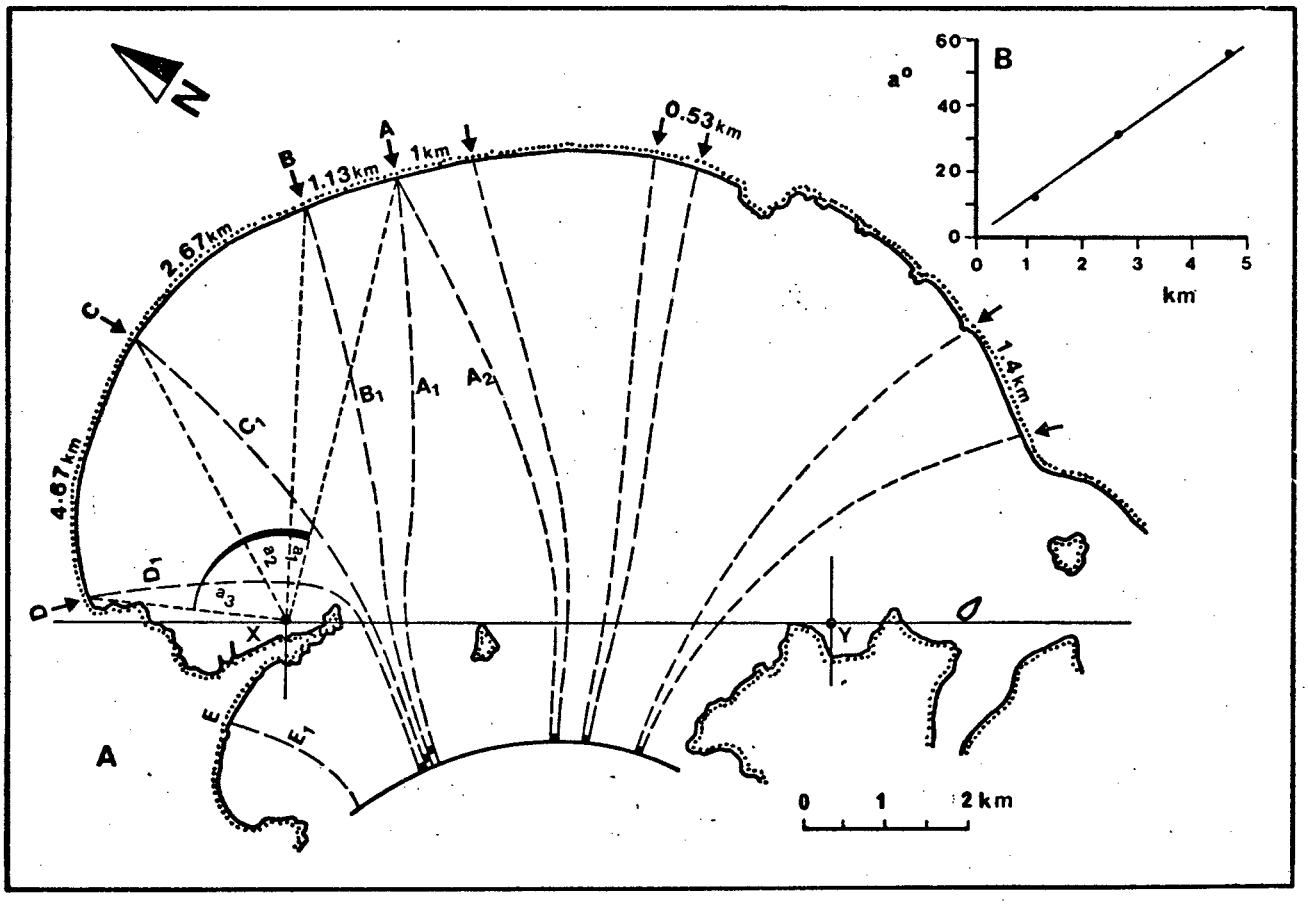

Fig. 52-A. The relationship between wave refraction and energy dispersion.

52-B. The relationship between radial angles and distances along the shoreline between equal energy increments.

Bremner and LeBlond (1974). In spite of the powerful evidence supporting the spiral concept (viz.) Silvester, 1974), the curve-fitting approach is rejected by Tanner (1976) on the grounds that it lacks any basis in theory, calling it an accident of geometry.

In this study the writer has found evidence which, if substantiated by further investigations, could provide a sound theoretical basis to the log.spiralphenomenon. In Fig. 52-A a number of wave paths were selected such that they were equally spaced at the entrance to the bay (d = 0.1 km). With the aid of aerial photographs, their respective refraction paths were traced to the points along the shoreline where each orthogonal meets the beach (points A, B, C, D). The wave energy originally contained in each 0.1 km increment at the mouth of the bay, is progressively spread between each set of orthogonals as the wave is refracted. Since wave refraction increases towards the sheltered parts of the bay, the originally equal energy increments are spread over increasingly larger distances. This is well illustrated by the increasing distance between each set of orthogonals from point A to point D (d_1 = 1.13 km, d_2 = 2.67 km, d_3 = 4.67 km). Each point was then linked with a radial vector extended from the spiral centre X, and the angles between each set of radial vectors was determined ($a_1 = 12°$, $a_2 = 31°$, $a_3 = 55°$). It was found that each radial angle is directly proportional to the distance along the shoreline between each respective set of orthogonals, whereby 1 km distance is equivalent to a radial angle of about 12° (Fig. 52-B).

This intricate relationship between wave refraction and logarithmic spiral geometry can hardly be accidental. It would appear that the progressive dissipation of energy by waves refracting around headlands proceeds exponentially, whereby the equilibrium shoreline follows a logarithmic spiral law.

The lateral dissipation of wave energy is also reflected by the progressively decreasing depth to which the shoreface is controlled by wave action. In Saldanha Bay the onset of the inshore sand prism lies at -7 m along orthogonal A, at -5 m along orthogonal B, at -3 m along orthogonal C and at -1 m along orthogonal D. In the most exposed part of the inner bay the inshore sand prism extends to -11 m, while in North Bay it can be traced to about -16 m. It would thus appear that at least the

inshore section of Saldanha Bay is in equilibrium with the energy spectrum of ocean waves entering the system.

The bathymetry of Saldanha Bay indicates that, not only the inshore section of the bay is equilibrated, but probably most of the remaining bay as well (Fig. 53). In the most exposed parts of the bay the depth profile (Fig. 54, Profile 5) begins with a relatively steep shoreface having a slope gradient of 1:62. Between -11 m and -15 m the gradient decreases sharply to only 1:530, indicating the presence of a terrace. It will be shown later that this terrace actually represents a well developed wave-cut platform.

Between -16 m and -20 m the average gradient of 1:366 is again slightly steeper. It is interrupted between -20 m and -22 m where a sudden step is observed. This feature is not obvious everywhere at the surface, but Du Plessis and De la Cruz (1977) have traced the same phenomenon on shallow seismic profiles. These authors have related this feature to a relict coastal cliff cut by a -20 m to -23 m Würm II Interstadial sea level. A similar cliff at about the same depth was reported by Murray et al. (1970) from the Southwest African coastline, and Flemming (1976b) related the planation of Rocky Bank to a sea level standing -20 m to -25 m below the present.

Away from the exposed part of the bay, isobaths shift progressively further offshore in response to the decreasing energy. This is illustrated in Fig. 54 (Inset), in which selected depth profiles have been drawn along their corresponding wave orthogonals. Along Profile 5, which runs through the exposed zone, the -10 m isobath is situated at a distance of 0.9 km from the shore. To the north and south of Profile 5, this distance increases to 1.270 km along Profile 4 and 1.200 km along an offset of Profile 6, 1.930 km along Profile 3 and 1.730 km along Profile 7, while along Profile 2 a distance of 2.270 km is recorded. Profile 1 in North Bay can serve as an example for a high energy coast where the distance to the -10 m isobath is reduced to only 0.330 km. On the whole, this picture suggests equilibrium conditions.

The occurrence and distribution of specific sea-bed features, such as rock outcrops and major sediment types, were investigated by side-scan sonar. The results are presented in Fig. 55, together with isopachs of

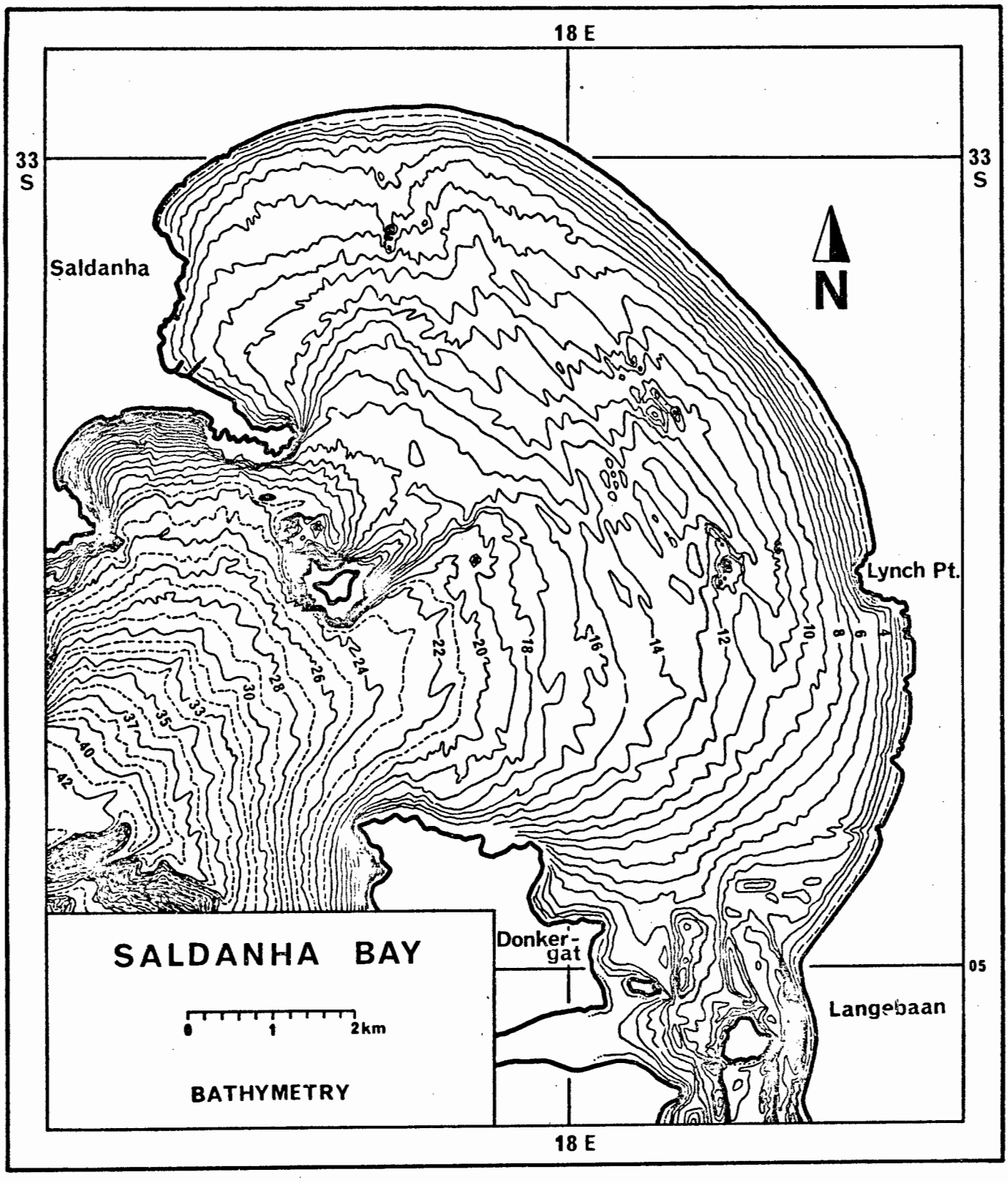

Fig. 53. Bathymetry of Saldanha Bay at 1 m depth intervals. Chart datum approximates the mean low-tide level.

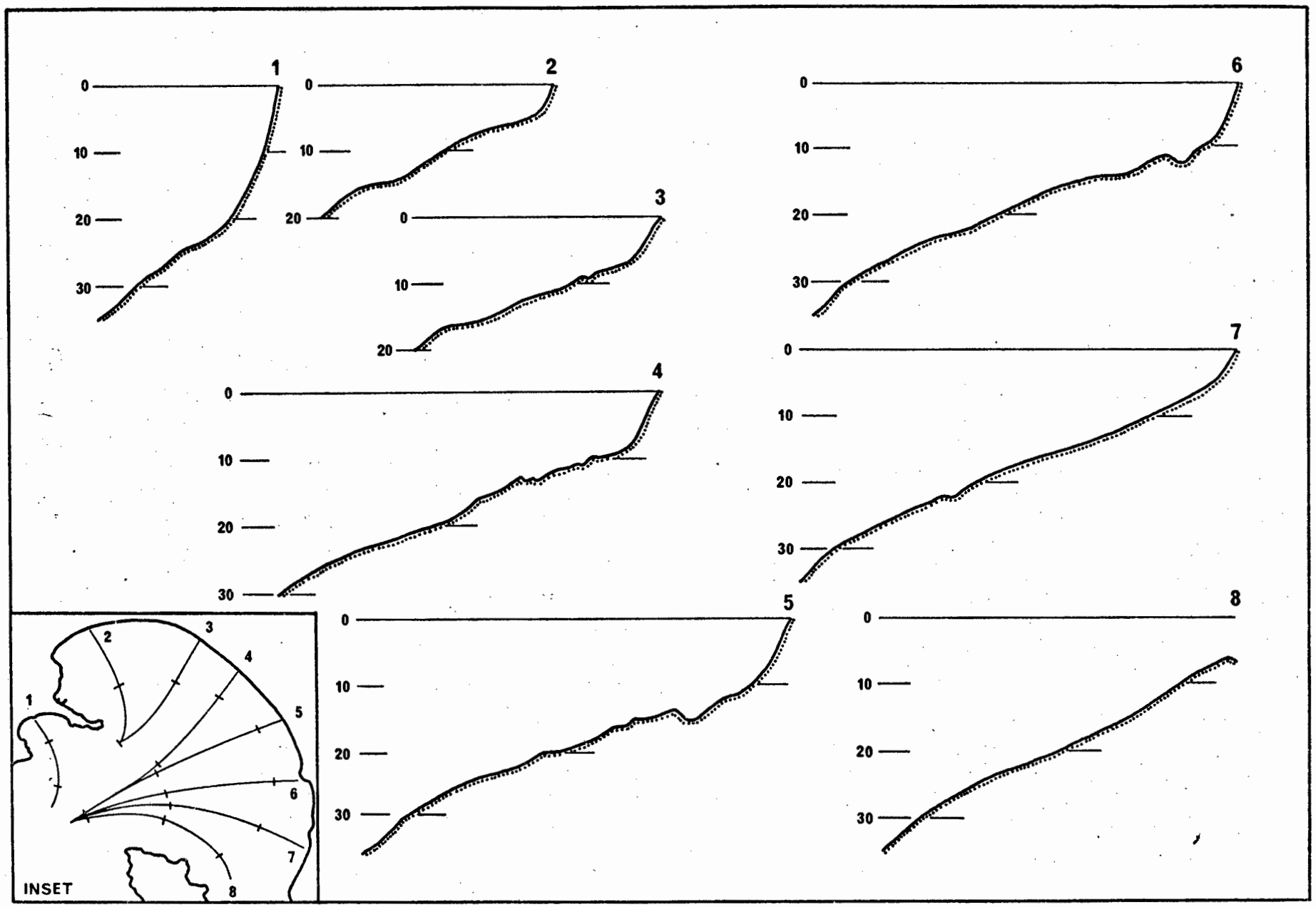

Fig. 54. Selected bathymetric profiles through Saldanha Bay. Profile positions are indicated in the Inset Map.

unconsolidated surface sediments based on shallow seismic data presented by Du Plessis and De la Curz (1977). Their results were slightly modified in order to accommodate additional information obtained by the writer when performing his underwater investigations. A detailed discussion of the operation and interpretation of side-scan sonar records, including data from Saldanha Bay, is presented by Flemming (1976a). In this particular study, the interpretation of sonographs benefited considerably from the knowledge gained by "in situ" observations. A track chart illustrating the limits of the survey is added in Appendix 1.3.

The most striking feature of the underwater terrain is the exact definition of the abrasion platform in the centrally exposed section of Saldanha Bay. Although the approximate limits of the abrasion platform had also been established by diving, the side-scan data have provided important additional information. With the exception of a few known granite outcrops, e.g. Lynch Blinder, Inner Lynch, Seven Blinders, the whole platform consists of exposed calcrete. Plate 1 illustrates the micro-topography produced by abrasion processes of calcrete. It is not as smooth as in some softer rocks, e.g. glacial marls (Flemming and Wefer, 1973), nor does it show the typical parallel pattern produced by bedded rock, outcropping at oblique angles (Belderson et al., 1972; Flemming, 1976a).

In some places, there appear to be low ridges striking in a SE - NW direction, although the feature is not consistent. Similar trends can be inferred from the bathymetric map (Fig. 53). Underwater observations along the northern inshore margin of the abrasion platform have indicated that at least some of these ridges can be associated with collapsed, undercut cliffs related to a former sea level stand at about -12 m.

Fringing the inshore boundary of the abrasion platform are extensive gravel patches which are recorded as even dark areas with sharp boundaries (Plate 1-). Diving has shown these to consist almost entirely of fragmented shell material. They occur in elongated patches and strips oriented subparallel to the direction of the swell and the whole surface is usually ripple marked. Crest to crest spacings of up to 1.5 m were recorded, which is a typical gravel wavelength. Since material of this size is mobile "en masse" only under considerable energy conditions, the deposits can be related to storm-surge activity with a strong onshore directed velocity-asymmetry of the near-bottom oscillatory currents. Under these conditions,

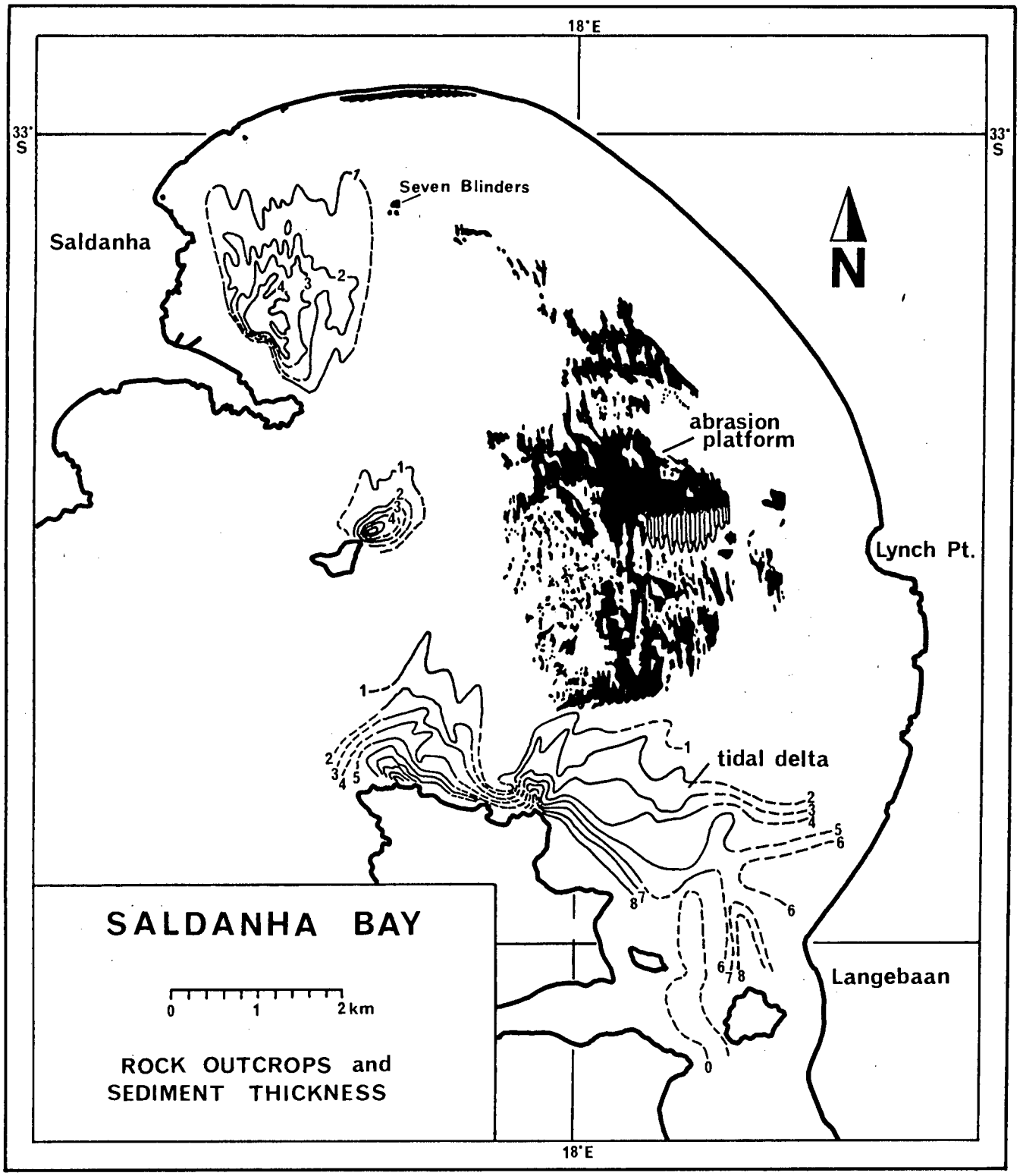

Fig. 55. Physiographic subdivisions of Saldanha Bay.

PLATE 1

A. Sonograph of the abrasion platform.
Note alternating calcrete bands (dark) and sand strips (light).

B. Sonograph of the transition from the abrasion platform to the inshore sand prism.
Note dredger traces on left.

C. Sonograph of the transition from the abrasion platform to the inshore sand prism.
Note the gravel ribbons at centre-left.

D. Sonograph of shell gravels at the inshore margin of the abrasion platform.

Plate 1

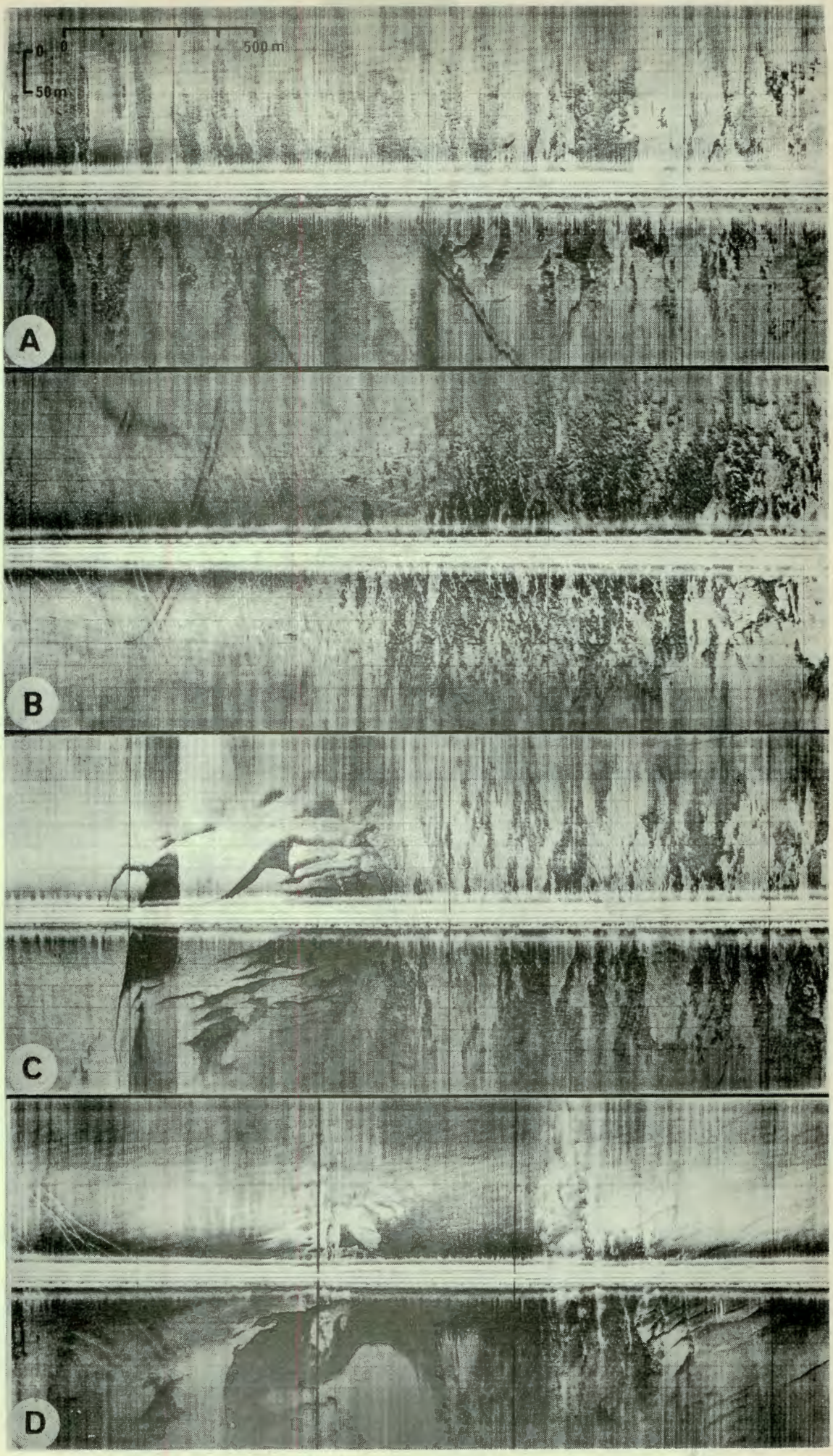

coarser material is mobilized by the onshore current component, whereas the offshore component often fails to reach the critical threshold velocity. In this manner, the coarser material is gradually transported inshore up to a point where the sea-bed slope becomes too steep and the energy needed to overcome the gradient is insufficient. In the exposed parts of Saldanha Bay this situation is reached between -10 m and -12 m.

The abrasion platform and associated gravel patches occur only in the central section of Saldanha Bay facing the wide South Channel. The area facing the North Channel on the other hand is almost completely blanketed with a veneer of finer sediments. The only exceptions are a narrow belt of calcrete along the 10 m isobath and coarse sediments in the entrance to the North Channel. Energy distribution in the bay is such that an abrasion platform is maintained only in the most exposed parts of the bay. The seaward extension of the abrasion platform is terminated approximately along the 15 m isobath by an onlapping sand sheet. The continuation of the abrasion platform remains transparent up to about -18 m, as revealed by numerous isolated calcrete outcrops penetrating the sand cover. This feature indicates that the sand sheet forms part of a transgressive sequence commencing with a thin, basal conglomerate formed by the residual sediments on the abrasion platform. This is followed by the sand sheet described above. In deeper water, increasingly more muddy sediments form the end member of the cycle. The shoreward extension of the sand sheet is terminated along the 15 m isobath where wave energy is sufficient to prevent substantial sedimentation. This depth limit at the same time defines the maximum depth to which the abrasion platform can develop under optimal conditions.

Seven Blinders, a granite outcrop in the northern part of Saldanha Bay (Fig. 56), was investigated in more detail by an underwater survey. Besides recovering rock and sediments samples, 50 measurements were made of the strike directions of the joints in the granite. The joint pattern is illustrated on Fig. 56. The sediment in the immediate vicinity of Seven Blinders is coarse, although further afield very fine sand predominates. This feature is ascribed to the winnowing action of frictional turbulence generated in the vicinity of the rock outcrops. Coarse shell fragments occur in the sediment amongst the rocks and in the shoreward shadow of the whole outcrop. Seaward of Seven Blinders shelly material is conspicuously absent.

Sediment thickness in Saldanha Bay varies considerably but larger

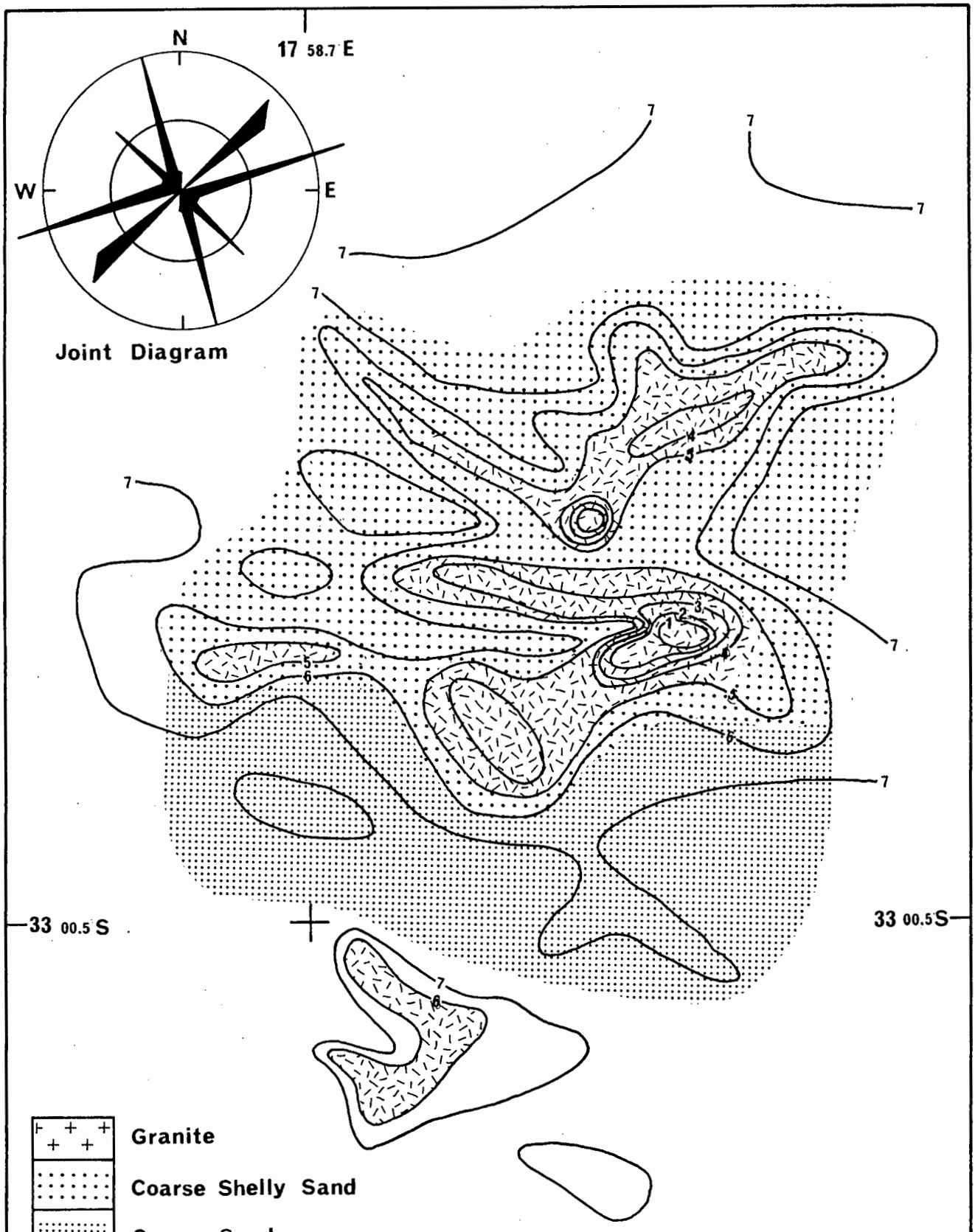

Fig. 56.

SEVEN BLINDERS

SALDANHA BAY

0 10 20 m

accumulations occur in well defined areas. There is a thick (>4 m) sediment deposit of unconsolidated sediments in the sheltered part of the northern bay. There is an analogous deposit in the south, although sedimentation in this area is expected to be strongly influenced by the tidal ebb current from Langebaan Lagoon. Its proximity to the outflow channels, and its distinct textural characteristics, suggest a tidal delta origin for this deposit.

Between the abrasion platform and the shore there is a sediment wedge, usually over 1 m thick, which extends north and south parallel to the shore until it merges with the sheltered sandbodies in the north and the south of Saldanha Bay. The extensive, but thin sandveneer (<0.5 m) covering the northern, less exposed part of the bay has already been pointed out. It is situated between the abrasion platform of the centrally exposed part of the bay and the sheltered northern sections, in which thicker sediment has accumulated. Shorewards this area is bounded by the inshore sand prism, while its seaward boundary is formed by the North Channel. A similar zone is not recognized in the south. Here the inshore sand prism appears to merge directly with the tidal delta.

Two smaller but nevertheless important sedimentary bodies are situated at the entrance to the inner bay. One lies in the shadow of Marcus Island where sediments up to 6 m thick have accumulated. Most of this sediment consists of fragmented shell material, which was evidently produced along the exposed parts of the island and subsequently transported into the leeward shoals by wave action. Wave orthogonals converge behind the island, thereby creating an energy low in which coarse material is deposited. The other deposit is situated along the southern margin of the South Channel towards the north of Elandspunt. Here a large fan reaches into the channel (Fig. 57). The deposit is obviously linked to the dune belt stretching across the peninsula from the beach of Juttenbaai to the South Channel. The whole phenomenon forms an extraordinary example of modern sediment recycling. Sand is blown off the beach in Juttenbaai and is carried across the peninsula, only to be returned to the sea in the South Channel. An overall height of 60 m is overcome, whereby the coarsest material drops out at the foot of the steep ascent. The mean diameter then remains constant until it enters the water, from where it progressively decreases towards the centre of the channel. An important feature of the fan is its deflection towards the west, reflecting ebb-current control along the southern margin of the

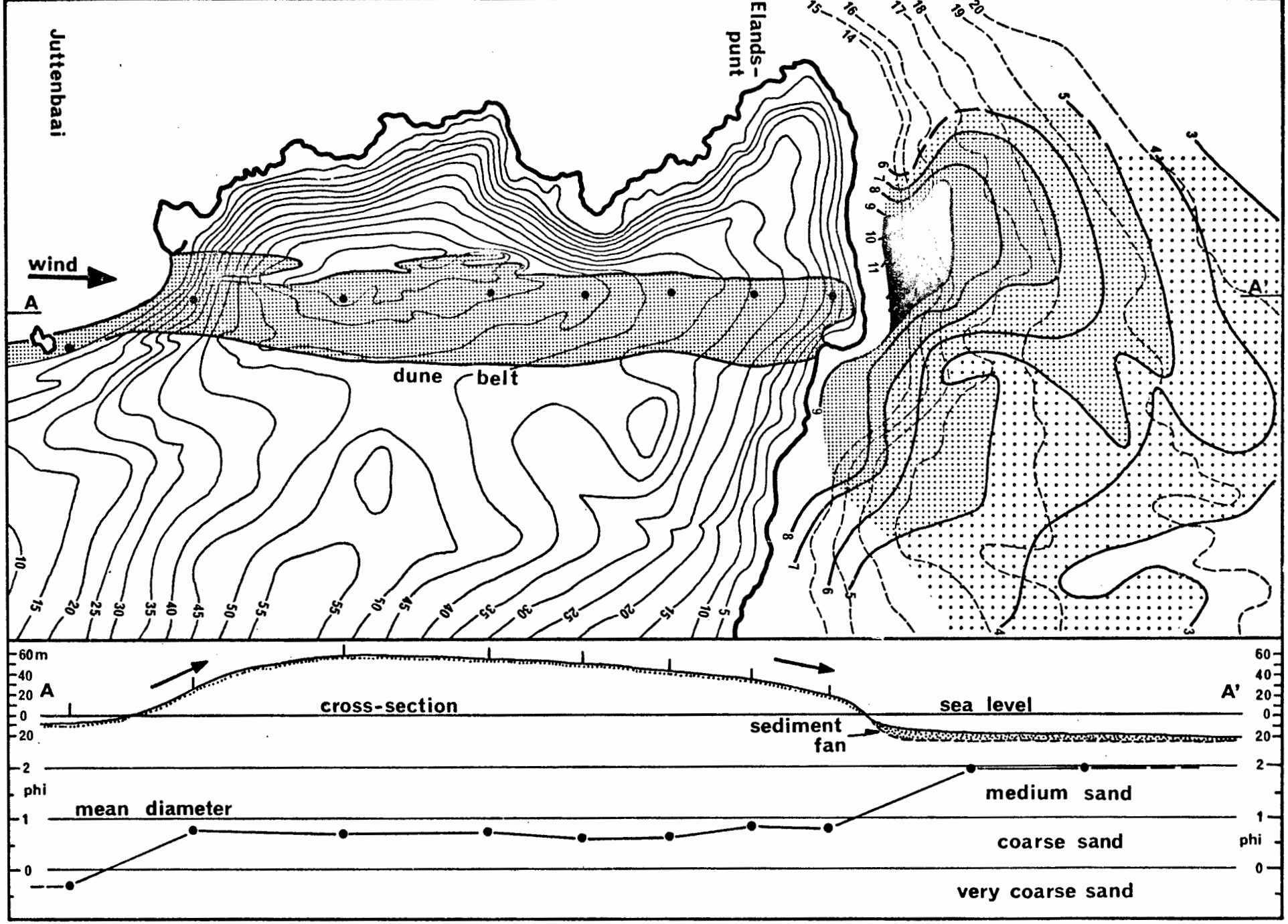

Fig. 57. Sediment transport across Donkergat peninsula.

South Channel.

A final point to be discussed in this section deals with an assessment of abrasion rates in the submerged calcrete sequence. There is sedimentary evidence to be discussed in a later section of this study, indicating that the abrasion platform has reached its base level at -15 m. An interesting observation in this connection is the existence of numerous scour hollows, especially on the inshore part of the abrasion platform. Du Plessis and De la Cruz (1977) report thatthe calcrete layer (Q_2), which follows immediately below the modern unconsolidated sediments (Q_1), is missing shorewards of the -11 m isobath. Since the Q_2-layer dips seawards, it would appear that on the abrasion platform the calcrete has been progressively eroded until it was partially reworked and ultimately truncated at its inshore extension. Locally, where abrasion has penetrated to the softer Q_3-layer, removal of sediment has produced the "geological windows" today recognized as scour hollows (Fig. 58-A). The Q_3-layer is rich in shell material, and it is suggested that the inshore shell gravels discussed earlier were eroded from this local source.

Considering the time span of the Flandrian transgression, it would be of considerable interest to establish the time required for the construction of a mature abrasion platform. In Table 5 directly measured abrasion rates in cm/year are plotted for two different types of rocks. The first column, based on data discussed by Horikawa and Sunamura (1970), lists abrasion rates in mudstones and tuffaceous sandstones along the Japanese coast at various water depths. Column two provides similar data from glacial marls and boulder clays measured in the western Baltic by Wefer and Flemming (1976). In both cases the wave regime is very similar, with wave heights between 0.5 - 1.5 m and wave periods under 8 sec. These values are presented in graph form in Fig. 58-B. According to the observations, boulder clays abrade at twice the rate of mudstones under similar wave regimes. While the former would require only 2000 years to be reduced to an equilibrated abrasion platform, the latter would need 4000 years.

If calcrete were considered to have a similar resistance to abrasion as the mudstones, then, under similar wave conditions, it would take 4000 years to produce an equilibrated abrasion platform. Since average wave parameters in the study area are considerably larger than those on which the calculation is based, the rate of abrasion in the calcrete could

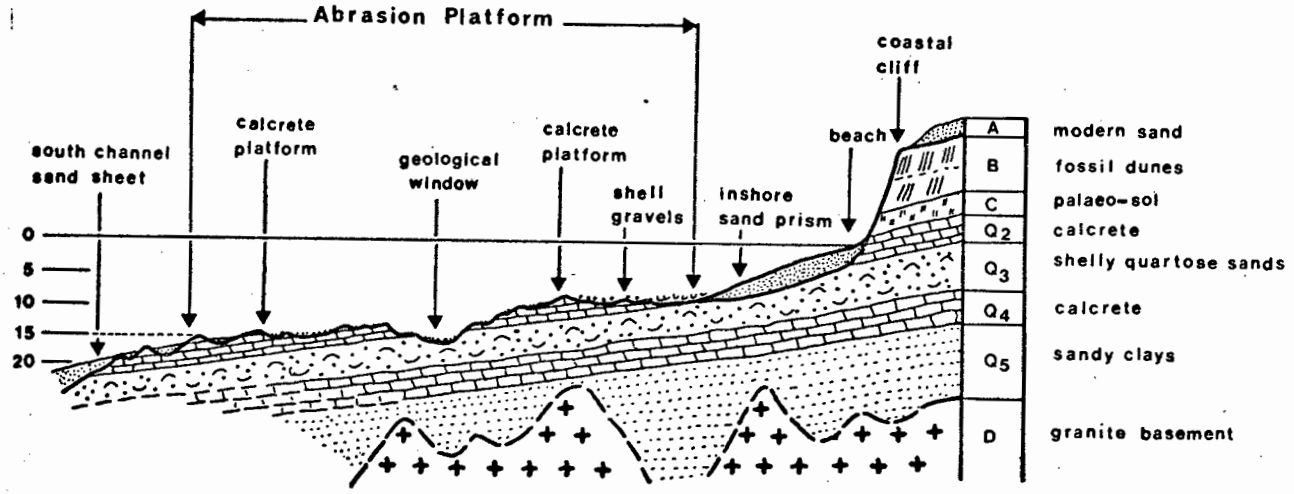

Fig. 58-A. Schematic cross-section through the abrasion platform of Saldanha Bay. The stratigraphic subdivision is partly based on Du Plessis and De la Cruz (1977).

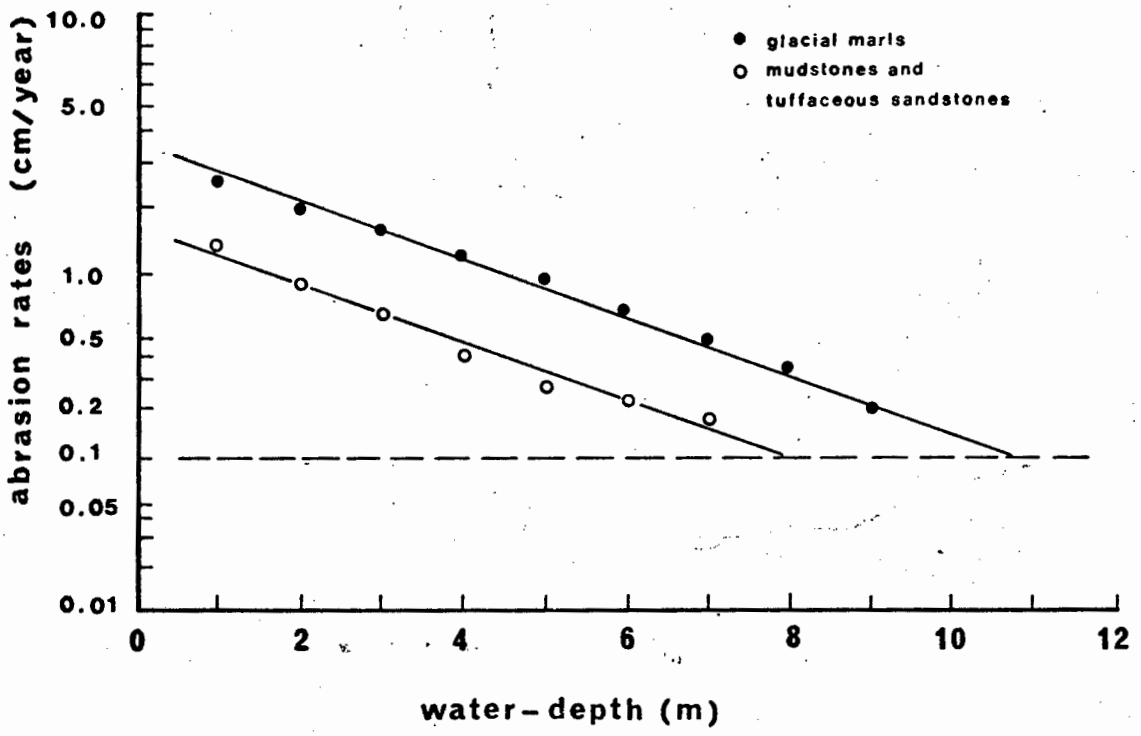

Fig. 58-B. Abrasion rates measured in different rock types.

achieve values as high as those observed in the glacial marls. Thus, a time span of 2000 - 4000 years would be sufficient to account for the abrasion platform observed in Saldanha Bay. Evidence to be discussed in a later section suggests that the Holocene sea level had recovered to its present position some 6400 years B.P. On the basis of these considerations, it is concluded that the abrasion platform is entirely a Holocene feature.

TABLE 5

Erosion rates in submarine bedrock

	MUDSTONE AND TUFFACEOUS SANDSTONE (after Horikawa and Sunamura, 1970)	GLACIAL MARL AND BOULDER CLAY (after Wefer and Flemming, 1976
WATER DEPTH (m)	ABRASION RATES (cm/year)	ABRASION RATES (cm/year)
0	1.65	3.40
1	1.40	2.50
2	0.90	2.00
3	0.65	1.60
4	0.40	1.25
5	0.27	0.95
6	0.23	0.70
7	0.18	0.50
8	-	0.35
9	-	0.20
10	-	0.10

4.2. WAVE REFRACTION AND RELATIVE ENERGY LEVELS

The depositional processes in Saldanha Bay are predominantly controlled by wave action. In order to gain a better understanding of the wave regime, a model approach has been adopted in which the distribution of energy in relationship to wave refraction was investigated. Relative energy levels

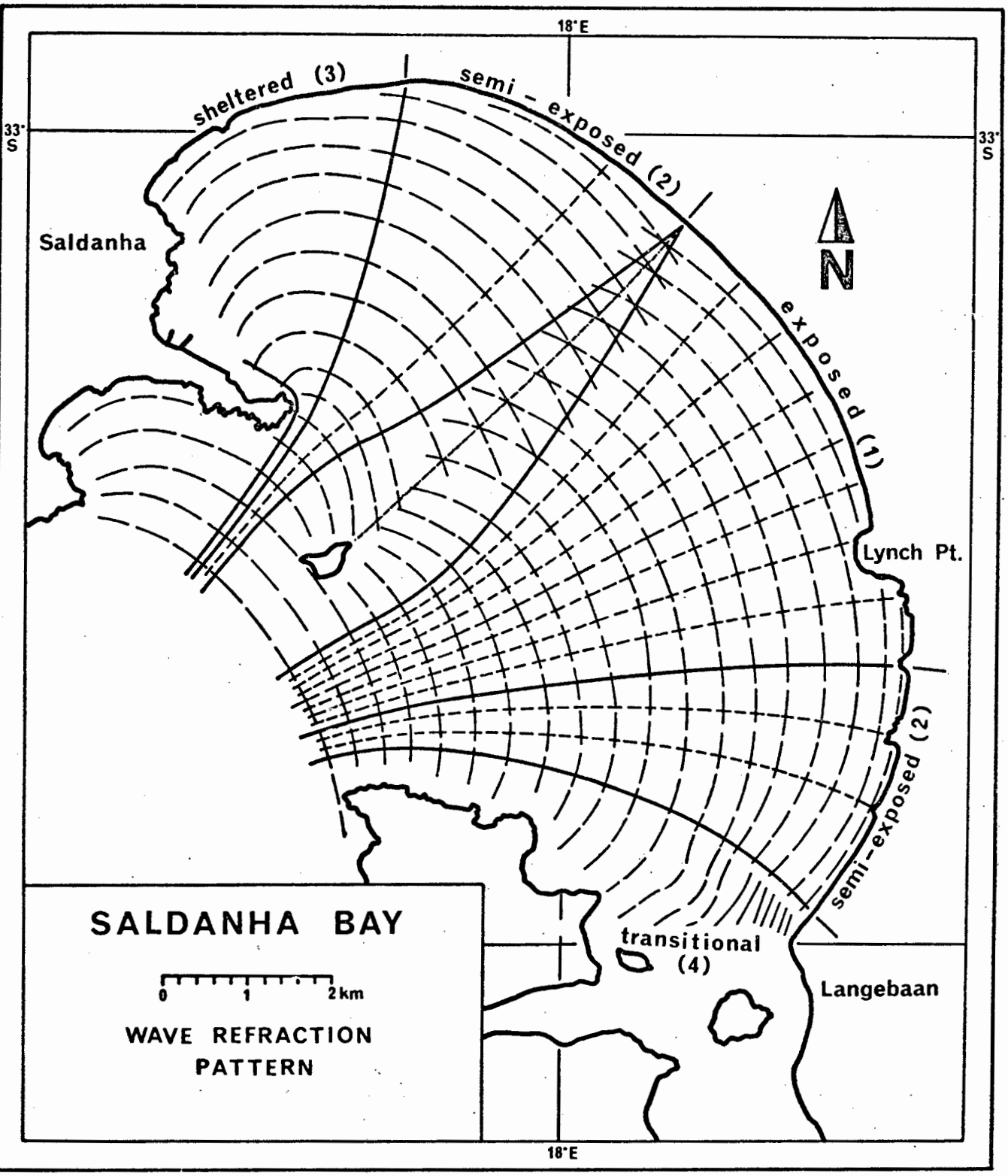

Fig. 59. Wave refraction in Saldanha Bay

were then utilized to calculate the oscillatory currents near the sea-bed.

A wave refraction diagram for the inner part of Saldanha Bay is presented in Fig. 59. The reconstruction is based on aerial photographs and compares well with the theoretical pattern introduced in Section 2.2. (Fig. 6-A). It is somewhat simplified, in that it does not include crossing orthogonals and other distortions caused by refraction processes in the outer bay. It should be noted that the refraction pattern was developed from orthogonals that were spaced at equal intervals along a wave-front in the outer bay. Each orthogonal then follows its independent path, depending on the effect of refraction from point to point in the direction of wave propogation. The wider the spacing becomes, the lower will be the remaining energy within an increment of constant dimensions.

The strongest refraction is observed in the northern entrance where the waves pass through the North Channel. The highest residual energy observed per unit space along the shoreline occurs just north of Lynch Point. It is interesting to observe that this section of the shoreline is the only place in Saldanha Bay where beach cusps were observed. A first visual estimation of expected energy gradients shows good agreement with the physiographic differentiation observed on the sea-bed (Fig. 55). On the basis of this differentiation, four major regions can be distinguished: 1) a centrally exposed zone, 2) two semi-exposed zones, 3) a sheltered zone in the north, and 4) a lagoon-bay transitional zone in the south.

The above wave refraction model only accounts for wave energy and does not include tidal currents, wind stress currents, or edge wave effects such as standing waves oscillating at different periods. Fig. 60-A gives an example of a modal oscillation pattern that might be expected in Saldanha Bay (after Wilson, 1976). The phenomenon is based on the geometrical analogy of a semi-circular basin with a paraboloidal bed configuration. It will be noted that the nodal centre, node 1, and anti-node 4 lie on the same axis chosen for the log-spiral approach to the shoreline configuration, and that the nodal centre coincides with the point through which the mirron plane $Z - Z_1$ in Fig. 51 passes.

Tidal current movements were studied with the aid of drogues (Shannon and Stander, 1977), and Fig. 60-B gives an indication of current velocities

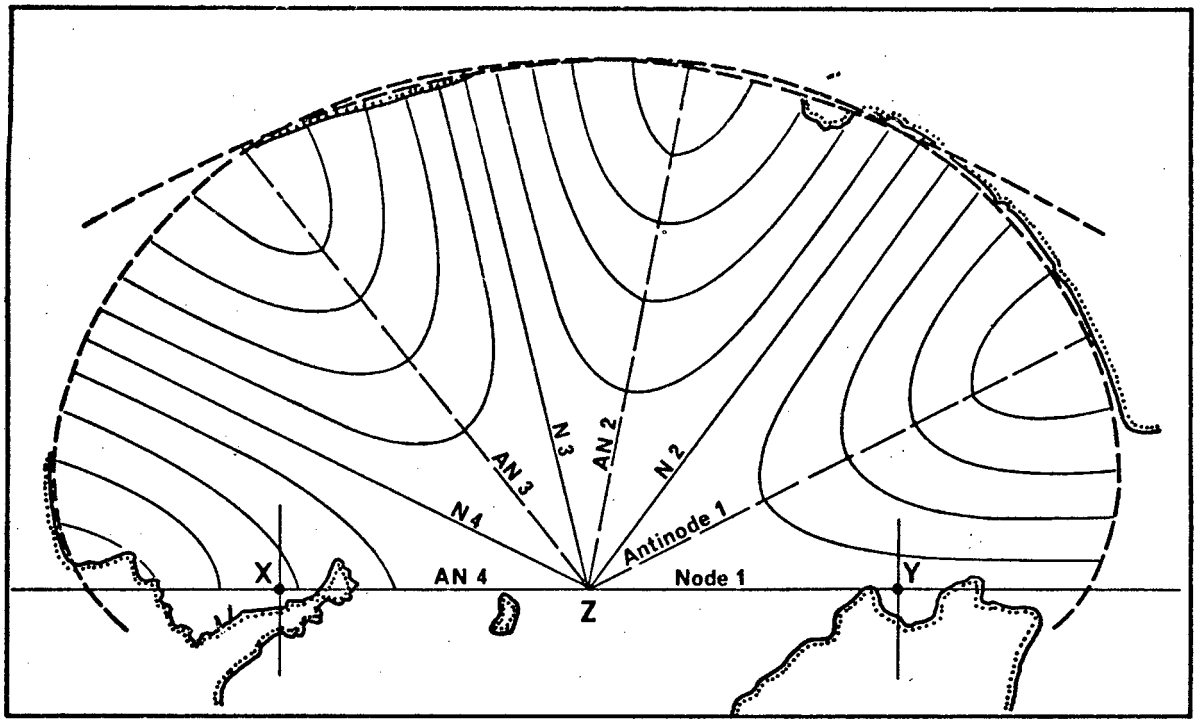

Fig. 60-A. Expected modal oscillation in Saldanha Bay.

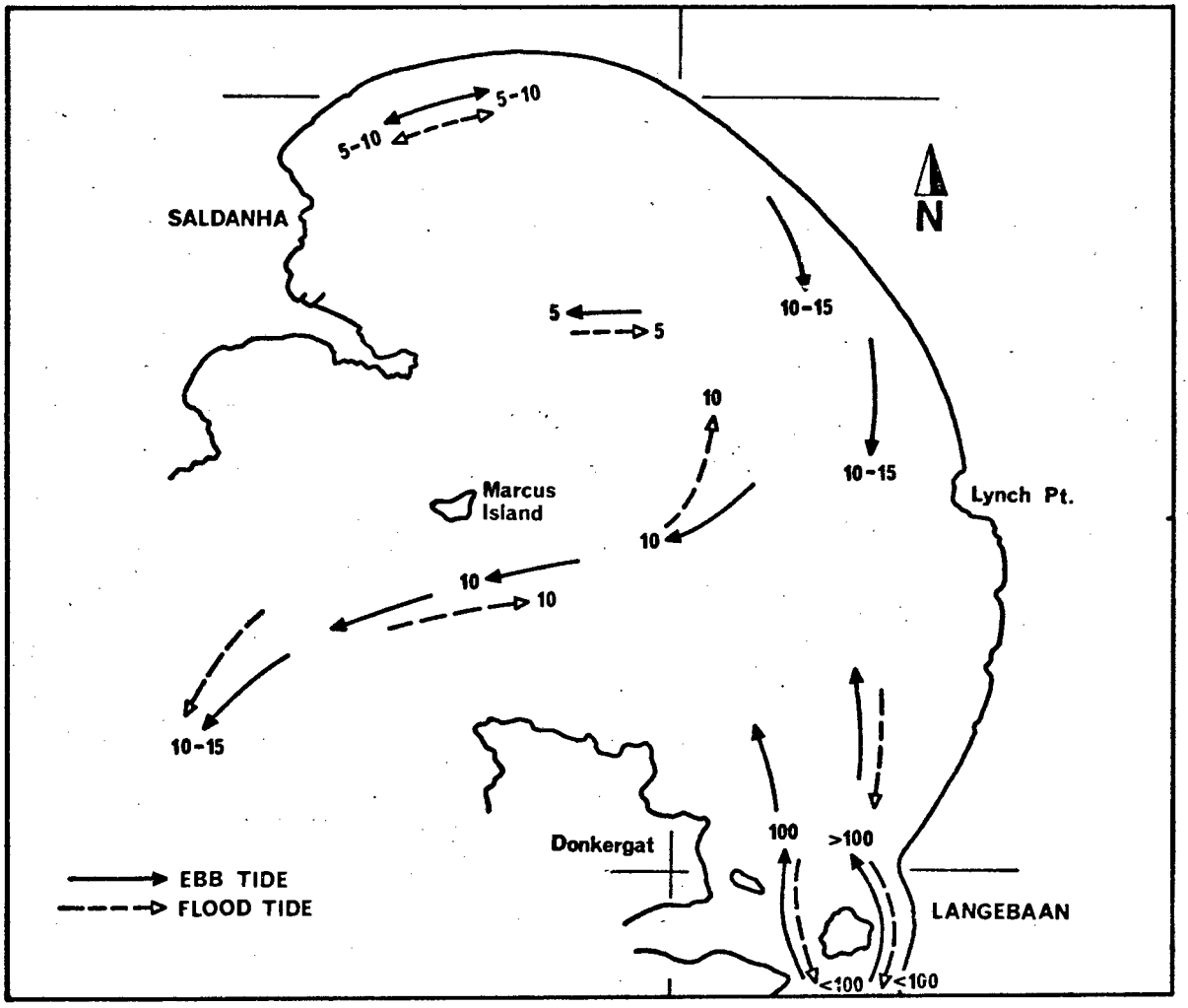

Fig. 60-B. Tidal currents 5 m below the surface (after Shannon and Stander, 1977).

inferred from drogue movements at 5 m below sea level. Tidal currents do not seem to exceed 10 - 15 cm/sec along the sea-bed. However, the deflection of the Elandspunt fan (Fig. 57) indicates significant current influence in this section of the bay. In addition, it may be assumed that tidal currents can dampen, or enhance, residual wave motion at almost any point in Saldanha Bay. This effect could play an important role in areas where wave motion alone, would be marginally too small to induce sediment movement.

Utilizing the wave refraction diagram (Fig. 59), the positions of equal energy increments between each set of orthogonals were marked and later connected by a smooth line (Fig. 61). The resulting diagram defines the relative energy levels at the sea surface of Saldanha Bay. Equating the energy input of any wave to 100% at the entrance to the bay, this energy will decrease proportionally to the reduction of any particular energy level at any point in the bay. Thus, at the most sheltered point in Saldanha Bay, i.e. in the northwestern corner, the energy entering the system will have reduced to 1/100 of the original value.

Comparing the trends of the wave refraction pattern with that of the relative energy levels, it is clear that the energy changes progressively along the crest of any individual wave. As a result, there must be an energy transfer along the wave crest away from the higher levels and towards the lower levels. The energy gradient is reflected by a progressively reducing wave height, and energy transfer is accomplished by mass movement of water down the gradient. Since, at the same time, there is a net mass movement in the direction of wave propagation, the resultant vector must form an angle between the two components. This vector is equivalent to the orthogonal joining successive lines of equal energy at any two points. Fig. 62 gives an impression of the expected mass transfer pattern at the sea surface in Saldanha Bay, based on wave energy alone. Significant modifications are only expected in the southern bay, where lagoonal ebb currents appear to reverse the pattern. The mass transfer pattern will apply particularly to sediments transported in suspension, and it is interesting to observe that the pattern predicts the transport of suspended material away from the abrasion platform and towards the low energy regions of the system. This feature is consistent with the observations discussed in the previous section. It should be noted,

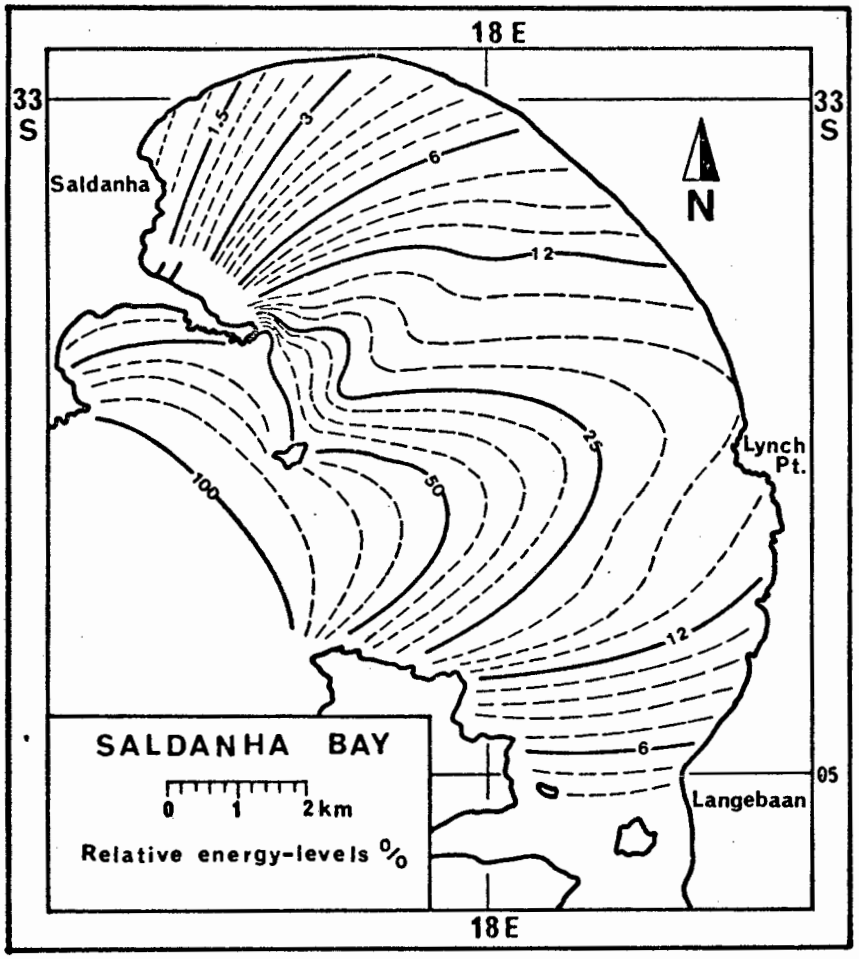

Fig. 61. Relative energy levels.

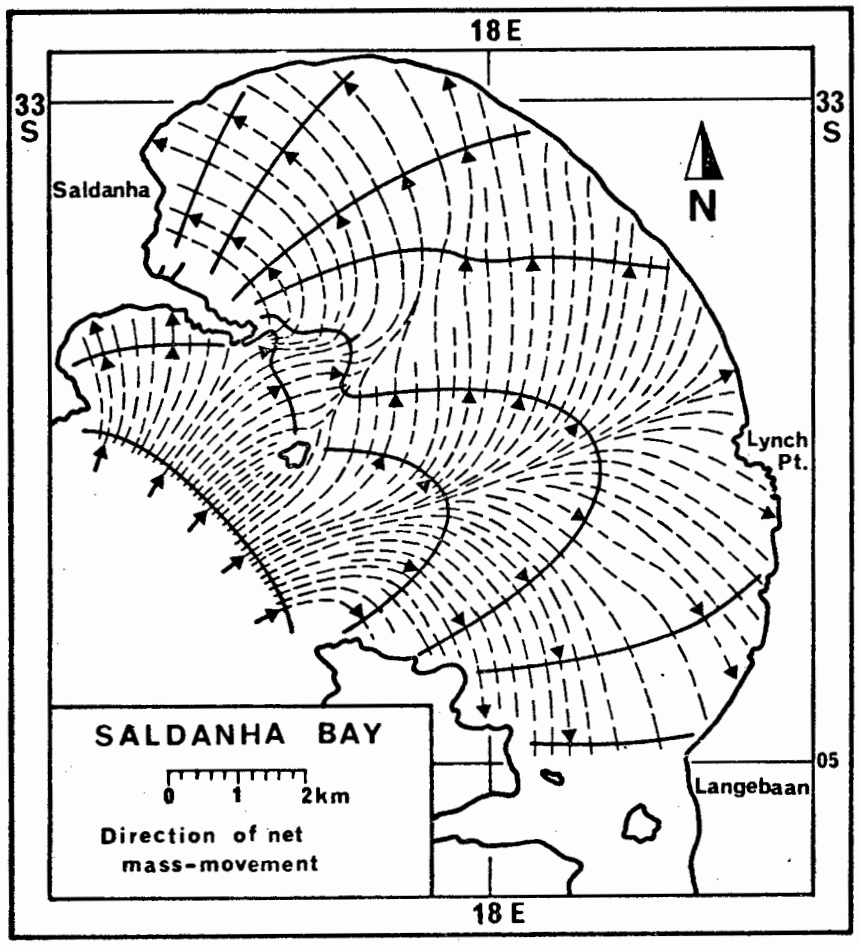

Fig. 62. Direction of net mass movement.

however, that the model does not necessarily apply to the surf zone.

The relative energy model discussed above provides a good theoretical basis from which the dissipation of orbital velocities with increasing water depth can be calculated at any point, and for any given wave parameters. It was pointed out in Section 2.3. that the wave regime in Saldanha Bay is exceptionally constant throughout the year. For this reason, it is unrealistic to assume that significantly higher or longer waves should have a lasting effect on sediment dispersal in the bay; e.g. 5 m waves occur for less than 6 cumulative days per year.

In Fig. 63 estimated peak velocities of the onshore component of the oscillatory currents generated by a 3 m/14 sec wave are shown. The situation reflects the conditions near the sea-bed immediately above the boundary layer. Velocities in the vicinity of the sediment grains should be lower than the velocities indicated in the diagram. Irrespective of the accuracy of the true velocities, the picture will provide an accurate relative impression. The areas of highest near-bottom energy correspond well with the areas defined as high energy zones in Fig. 55. The abrasion platform is distinctly outlined.

Assuming that a minimum velocity of 10 cm/sec is required to initiate sediment movement of very fine sand, ripple marks should be observed in the entire area enclosed by the 10 cm/sec contour. This leaves a relatively large area without sediment motion in the northern section of the bay. In fact, ripple marks were observed up to the undulating line in Fig. 63. The discrepancy between observed and predicted wave action is marginal, being below 5 cm/sec. This value can easily be increased by tidal currents and wind-stress currents, and it will be demonstrated later that, in some places, return flow currents are indicated by sedimentary patterns. An important aspect of the near-bottom velocity pattern is the overall low level of energy. In most cases, the velocity will not be sufficient to cause significant erosion. Only on the abrasion platform are velocities encountered that would result in mass erosion.

The effect of storm waves was tested in similar manner with a 3 m/8 sec wave (Fig. 64). It is immediately clear that shorter waves dissipate their energy far too rapidly with water depth to have any lasting effect

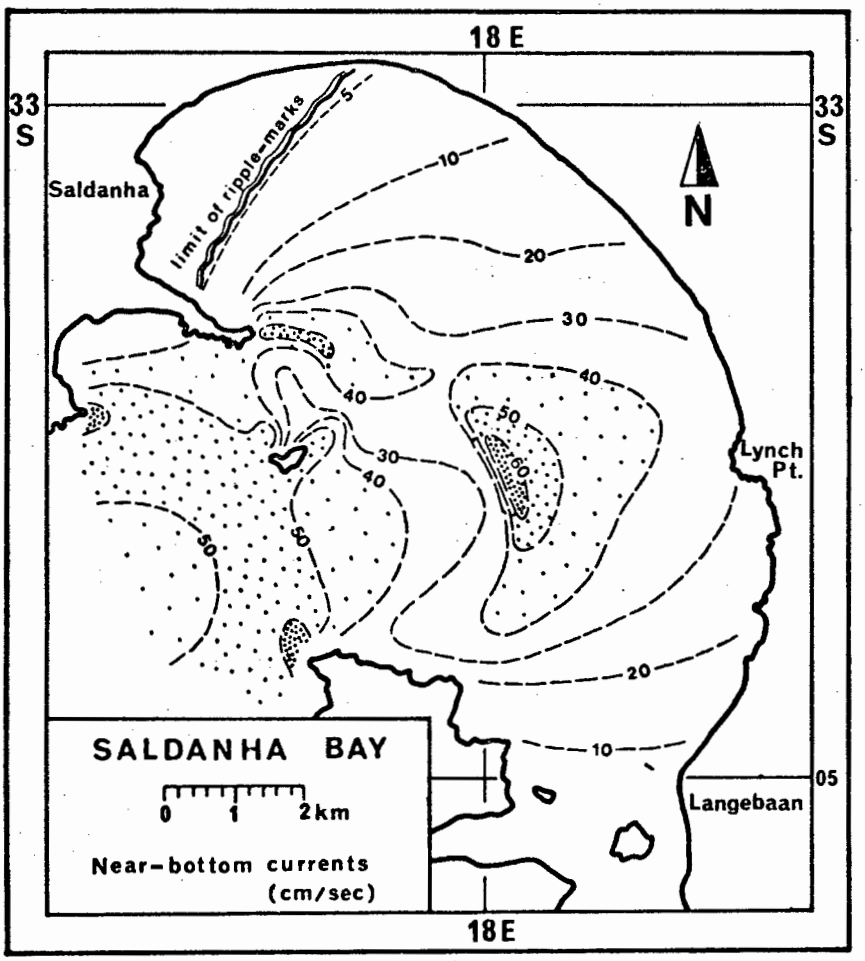
18 E
33 S
33 S
Saldanha
limit of ripple-marks
5
10
20
30
40
40
50
60
30
40
50
50
N
Lynch Pt.
20
10
SALDANHA BAY
0 1 2km
Near-bottom currents
(cm/sec)
Langebaan
05
18E

Fig. 63

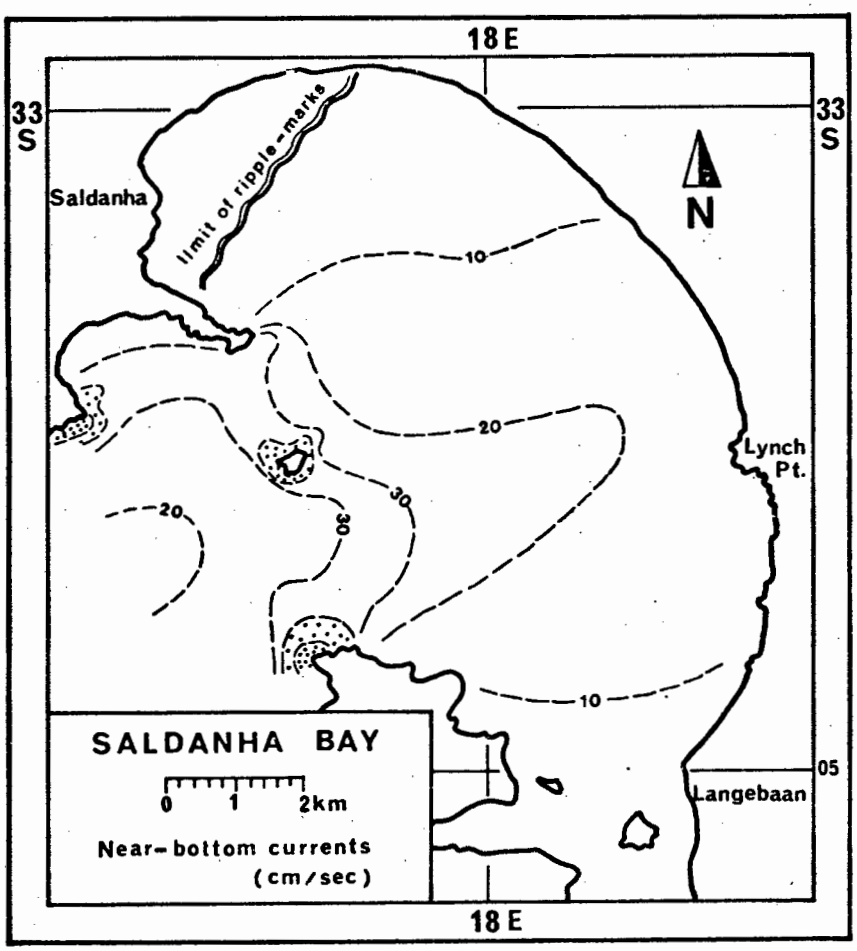
18 E
33 S
33 S
Saldanha
limit of ripple-marks
10
20
30
20
30
N
Lynch Pt.
10
SALDANHA BAY
0 1 2km
Near-bottom currents
(cm/sec)
Langebaan
05
18E

Fig. 64

on sedimentation. The energy model based on the most frequently occurring waves, with heights of about 3 m and periods around 14 sec, would thus appear to provide the most likely energy conditions that control the depositional processes in Saldanha Bay.

4.3. SOME GEOCHEMICAL PARAMETERS

The present study concentrates on the physical aspects of sedimentation and the geochemical parameters discussed below are complementary information. The geochemistry of the study area is subject to a separate study, parts of which have been published recently by Willis et al. (1977).

4.3.1. Carbonate Content ($CaCO_3$)

By far the most important geochemical parameter in the context of this study is the $CaCO_3$-content of the sediment. Carbonates occur entirely in form of bioclastic particles which are predominantly composed of mollusc, cirriped and bryozoan fragments. Echinoid spines and plates and benthic foraminifera contribute minor proportions. In this respect, the area conforms to the general situation along the south-western coastal areas of the Cape Province (Siesser, 1972; Flemming, 1976b). The association of these carbonate-producing organisms places the area within the "foramol" zone which is characteristic of temperate water conditions, as opposed to the tropical "chlorozoan" assemblage (Lees and Buller, 1972; Lees, 1974; Ginsburg and James, 1974).

The distribution pattern of the carbonates shows some very significant features (Fig. 65). There is a marked decrease of carbonate content towards the lower energy environments within each exposure zone. The whole outer bay has high carbonate concentrations, often reaching over 80%. The South Channel sediments consist of 50 - 60% $CaCo_3$, whereas the North Channel sediments contain 60%, reaching 80% in the vicinity of the exposed rocky shores. This feature would suggest that, in this area, the carbonates are most probably a modern sedimentary component, which is produced by mechanical breakdown of shell material in the high energy zones.

The entire abrasion platform in the centrally exposed section of the inner bay is rich in carbonate sediments. Values, in general, exceed 50%

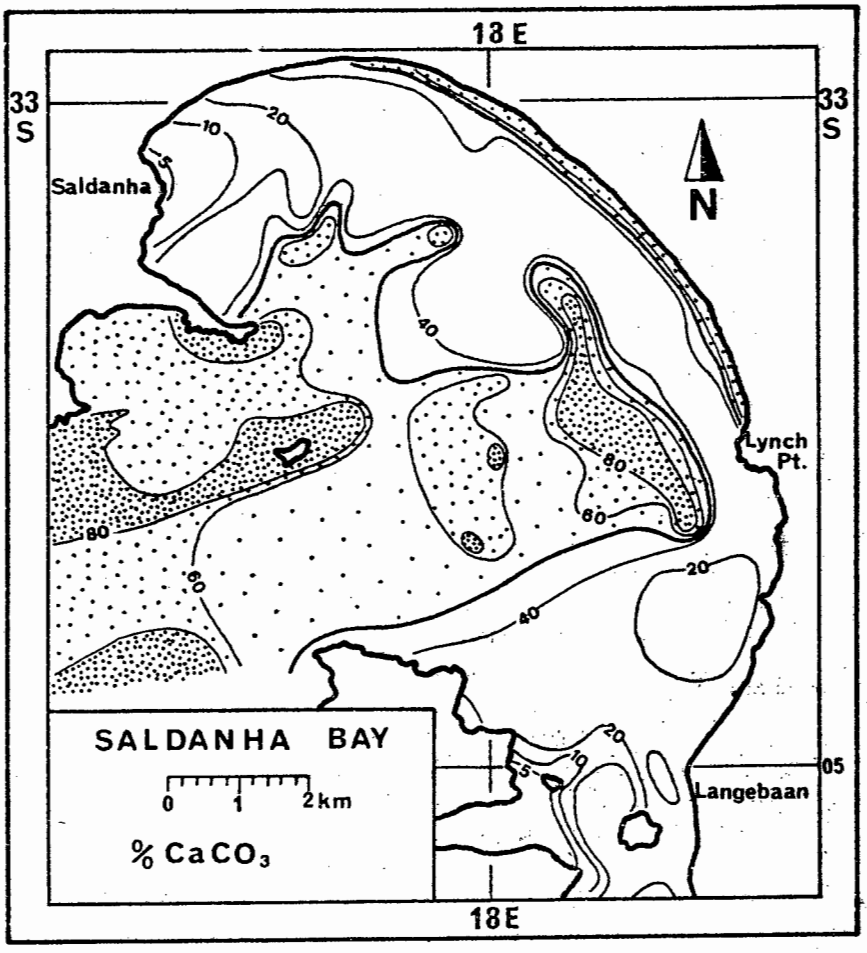
18 E
33 S
Saldanha
N
Lynch Pt.
Langebaan
05
SALDANHA BAY
0 1 2km
% CaCO3
18E

Fig. 65

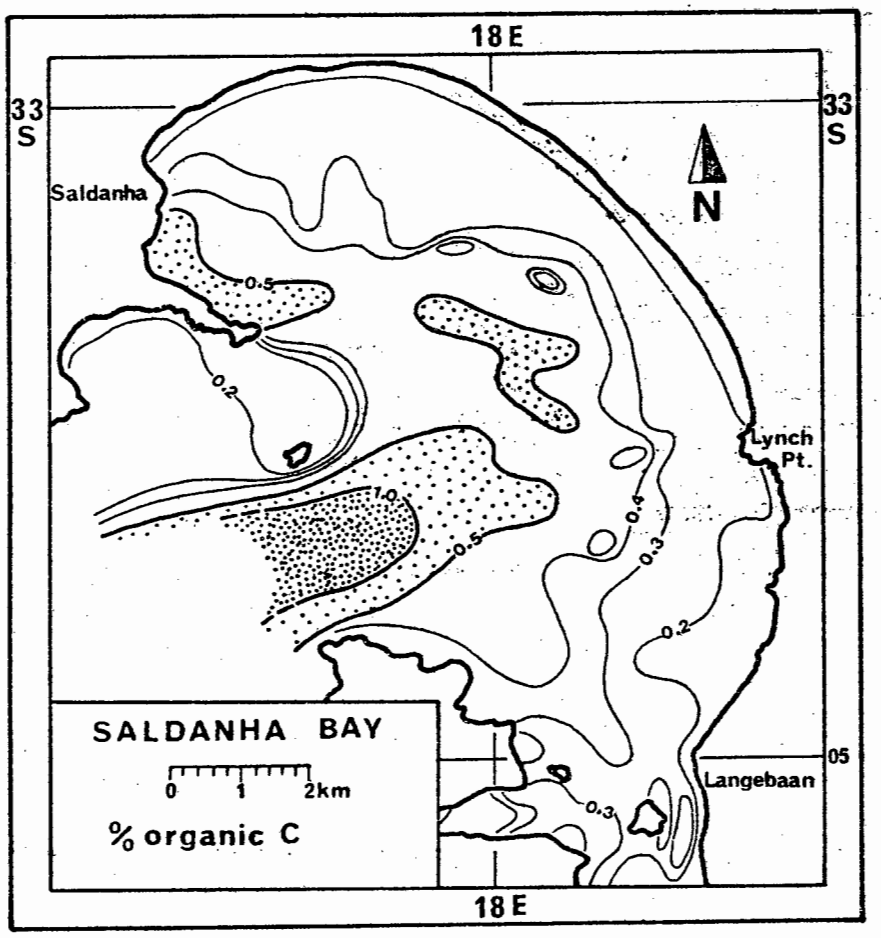
18 E
33 S
Saldanha
N
Lynch Pt.
Langebaan
05
SALDANHA BAY
0 1 2km
% organic C
18 E

Fig. 66

and reach over 90% on the inshore section of the platform where large patches of shell gravels have accumulated as lag deposits. This residual sediment is probably relict in nature, having been reworked from underlying calcrete layers by a mechanism discussed in a previous section. The inshore sand prism of the exposed zone, on the other hand, contains less than 40% $CaCO_3$.

The semi-exposed zone and the transitional zone in the southern bay are dominated by terrigenous sediments containing under 40% $CaCO_3$ in general and under 20% locally. The semi-exposed zone in the north, on the other hand, can be divided into an offshore sector in which carbonate contents exceed 50%, and an inshore sector in which 40% $CaCO_3$-contents are rarely achieved. The sheltered zone in the north shows a progressive decrease in carbonate contents from 40% to under 5% in the most sheltered part.

The carbonate content of beach sediments varies markedly. Highest values are observed along the northeastern shoreline where over 60% $CaCO_3$ occurs. Towards the sheltered zone it progressively decreases to below 5%. Relatively low values (20 - 40%) are also observed along the southeastern beaches between Lynch Point and Langebaan.

Saldanha Bay can thus be divided into twodistinct carbonate provinces: an inshore belt consisting of slightly calcareous to calcareous quartzarenites and an offshore area, comprising quartzose to slightly quartzose calcarenites. The carbonates consist predominantly of fragmented shell material, which is partly supplied from modern sources and partly from reworked relict deposits.

4.3.2. Organic Carbon Content

The organic carbon content of Saldanha Bay sediments follows a clear pattern (Fig. 66). The beaches contain less than 0.2% organic carbon, while the whole inshore sand prism, from north to south, does not exceed 0.3%. The sheltered zone in the north reaches $>0.7\%$ in its deeper parts, but values decrease progressively to less than 0.2% in the north. The bay-lagoon transitional zone in the south contains under 0.3% organic carbon in its shallowest parts near the outflow channels, but decreases gradually seawards to $<0.4\%$ in the distal tidal delta.

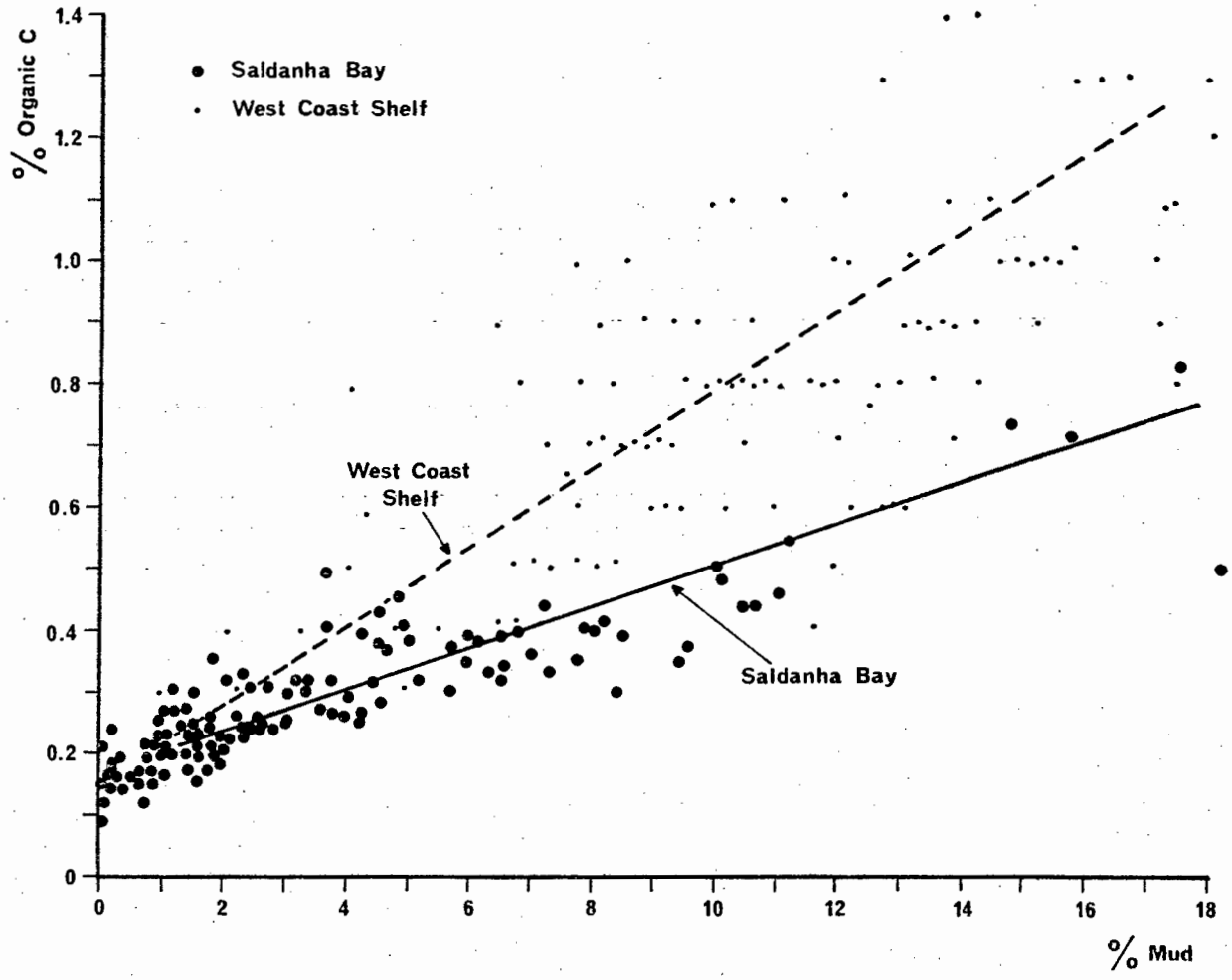

Fig. 67-A. The relationship between organic carbon and mud content of Saldanha Bay sediments.

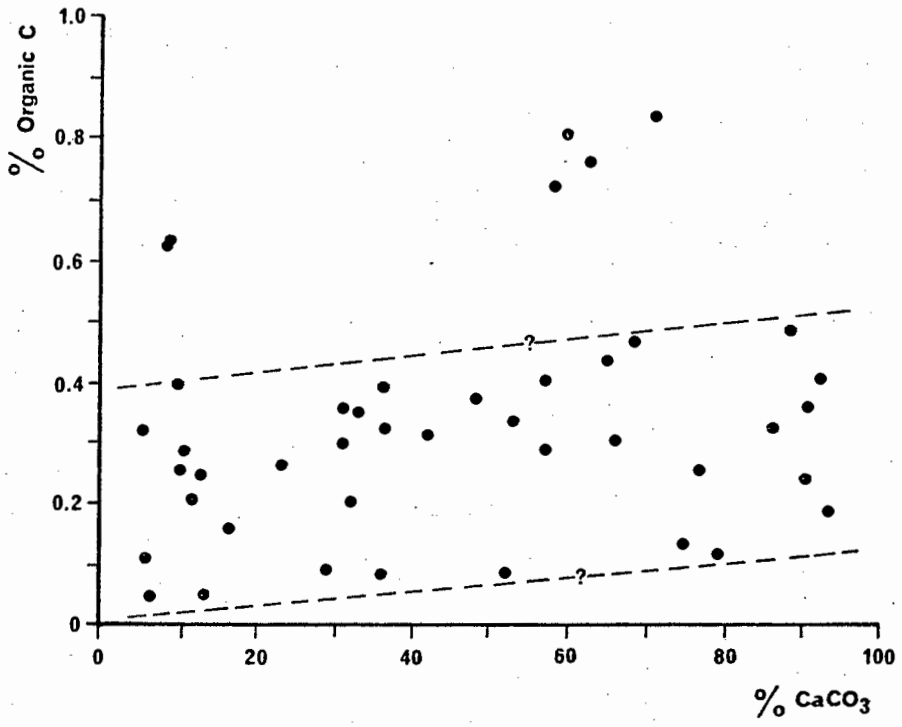

Fig. 67-B. The relationship between organic carbon and carbonate content of Saldanha Bay sediments.

On the abrasion platform organic carbon contents vary significantly between 0.3% and 0.7%, whereas the North Channel and North Bay sediments contain under 0.2% and 0.3%, respectively. The highest organic carbon contents are observed in the deeper parts of the South Channel, where values over 1.0% were recorded.

There is a good correlation between organic carbon and mud content of the sediment (Fig. 67-A). This appears to be a common feature and was observed, amongst others, by Birch (1977) along the west coast of South Africa, and by Van Andel and Veevers (1967) on the Sahul Shelf off northwestern Australia. Each area seems to have a very characteristic trend, indicating that org.-C / mud ratios could serve as environmental indicators. In Fig. 67-A the Saldanha Bay trend has been contrasted with that of the open west coast shelf as recorded by Birch (1977). The diagram reveals a distinctly different trend in each case. While the ratio is similar at very low concentration levels, the rate of increase of organic carbon in the open shelf sediments is about twice as high as that in Saldanha Bay. With each percent of increase in mud, the organic carbon increases by 0.035% in Saldanha Bay but by 0.075% on the open shelf. At the one percent mud level both contain about 0.2% organic carbon. In addition, the grouping of the point cluster demonstrates the considerable difference in the average mud contents of both areas.

No significant correlation was observed between organic carbon concentrations and carbonate contents of the sediment (Fig. 67-B). One might infer a slight increase of organic carbon content with increasing carbonate concentration levels, but the point cluster is very wide and ill-defined. Gaudette *et al.* (1974) have drawn attention to a possible influence of carbonate contents on organic carbon values, but this does not appear to be significant in the study area.

4.3.3. Potash (K_2O)

The potash content of the sediments in Saldanha Bay were determined with the phosphates by the Phosphate Development Corporation, Phalaborwa. Since most of the bedrock exposed in various parts of the bay consists of granite, it was expected that K_2O-values might give an indication of the

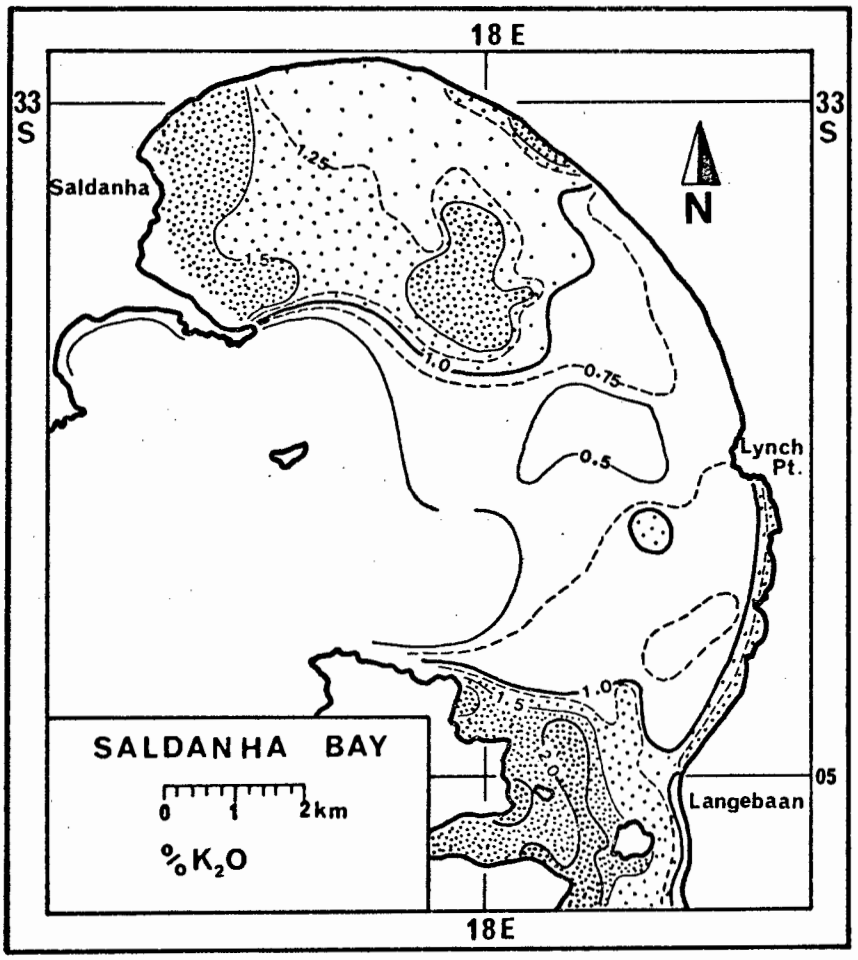
18 E
33 S
33 S
Saldanha
N
1.25
1.5
1.0
0.75
0.5
Lynch Pt.
1.0
1.5
2.0
05
Langebaan
SALDANHA BAY
0 1 2km
%K2O
18 E

Fig. 68

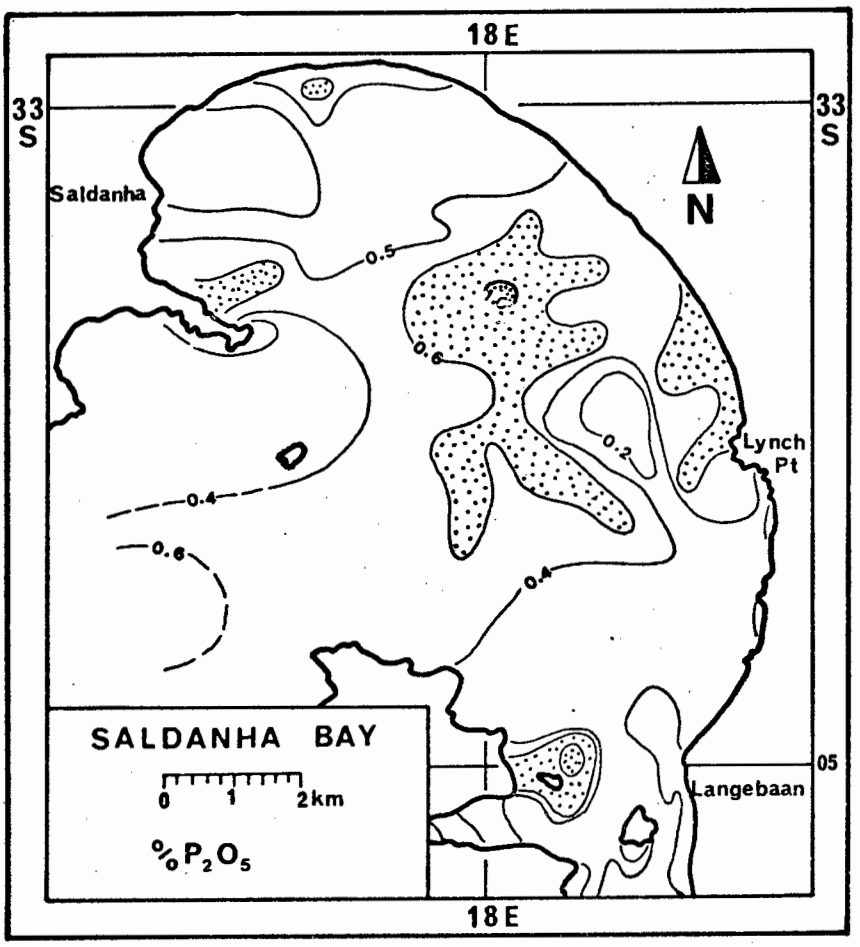
18 E
33 S
33 S
Saldanha
N
0.5
0.6
0.2
Lynch Pt
0.4
0.6
0.4
05
Langebaan
SALDANHA BAY
0 1 2km
%P2O5
18 E

Fig. 69

feldspar component in the terrigenous sediments. The results are in good agreement with those reported by Willis et al. (1977).

Concentrations of K_2O increase towards the semi-exposed and sheltered areas of the bay. Values are low in the whole outer bay and on the abrasion platform (Fig. 68). Correlation with mud content is poor and it is thus concluded that K_2O-values are probably related to breakdown of granitic material, as implied by Willis et al. (1977). The contribution of potassium feldspar would therefore not exceed 1.5% of the total sediment.

4.3.4. Phosphate (P_2O_5)

The main objective in analyzing the sediments of Saldanha Bay for P_2O_5 was to determine whether significant amounts of pelletal phosphates were supplied to the area. This possibility had to be considered because of the large phosphate deposits recorded onland in the vicinity of Saldanha Bay. These deposits are presently being mined for commercial use (Visser and Schoch, 1973).

Large concentrations of pelletal phosphates have been reported on the outer shelf northwest and southwest of Saldanha Bay (Birch, 1977b). The phosphate-rich sediments on the shelf contain at least 5% P_2O_5. The sediments of Saldanha Bay, on the other hand, rarely contain more than 0.7% (Fig. 69).

4.4. SEDIMENT DISTRIBUTION PATTERNS

This section deals with the major sediment distribution patterns, whereby the characteristic features of the total sediment are contrasted with those of the terrigenous and the bioclastic components. Differences between the latter two were investigated with particular care, as it was hoped that this might shed some light on the differential response of the two individual components to the depositional processes.

4.4.1. Total Sediment

The total sediment in Saldanha Bay consists predominantly of sand-sized

material. Muds and gravels both form subordinate size groups. The muds were probably added independently, and possibly after the redistribution of sediments in the bay. This is concluded from the poor correlation of mud contents with any of the other size classes constituting the total sediment.

A belt of muddy sediments, reaching up to 10% in some places, stretches from the sheltered zone in the north, across the deeper part of the inner bay, towards the Donkergat peninsula in the south (Fig. 70). Patches of high mud concentrations were recorded on the abrasion platform, i.e. in the most exposed part of the bay. Re-examination of original sample material indicates that this abnormally high mud content could be related to biological activity. All the samples from this area contain a substantial amount of broken tube sections of the polychaete Diapatra, which was observed to form fairly extensive mats on many calcrete outcrops. The walls of these tubes contain a high proportion of muddy sediment. Since the sediment was treated with H_2O_2 in order to separate the muds, most of the tubes would have been destroyed in the process, thus adding a fair proportion of muddy material to the total sediment. The mud on the abrasion platform was therefore originally part of an hydraulically coarser particle group.

Towards the shore, the mud content decreases rapidly and the beaches are virtually mudfree. Muds are also absent in the North Channel and in North Bay. The South Channel again presents a peculiar phenomenon. Muds are here concentrated in numerous lenses, each 2 - 3 cm in diameter. The surrounding very fine sand is almost free of mud. The mode by which these mud lenses are formed is not known. The phenomenon is not restricted to the South Channel. In lesser density, mud lenses were also observed in sediments from the inshore sand prism along the shoreface of the open coast off Langebaan Lagoon. It would appear that, here too, the concentration of almost pure mud is achieved by polychaetes which deplete the surrounding sediment of any "free mud". Alternatively, the mud lenses could represent an incipient form of flaser bedding, as described by Reineck and Wunderlich (1968). A foreign source for the mud lenses can be excluded under the present hydrodynamic conditions, although this may not always have been the case. Mud pebbles are at present being formed in Langebaan Lagoon by reworking of marsh deposits.

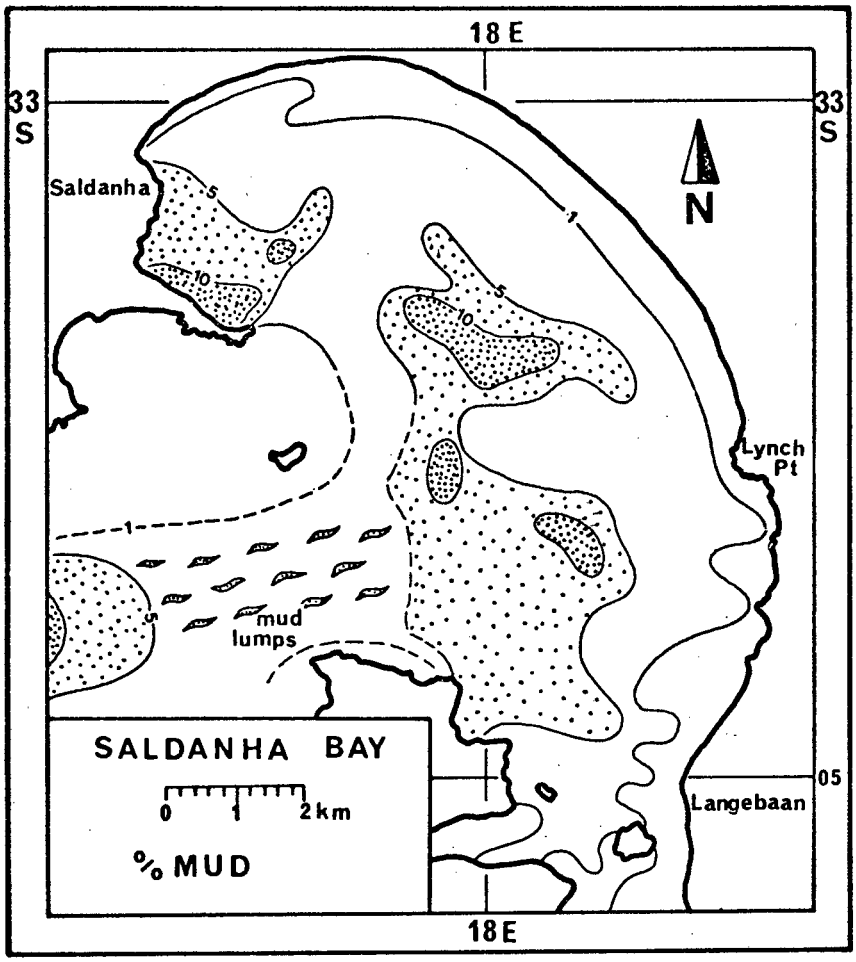
18 E
33 S
Saldanha
N
Lynch Pt
mud lumps
SALDANHA BAY
0 1 2km
% MUD
Langebaan
05
18 E

Fig. 70

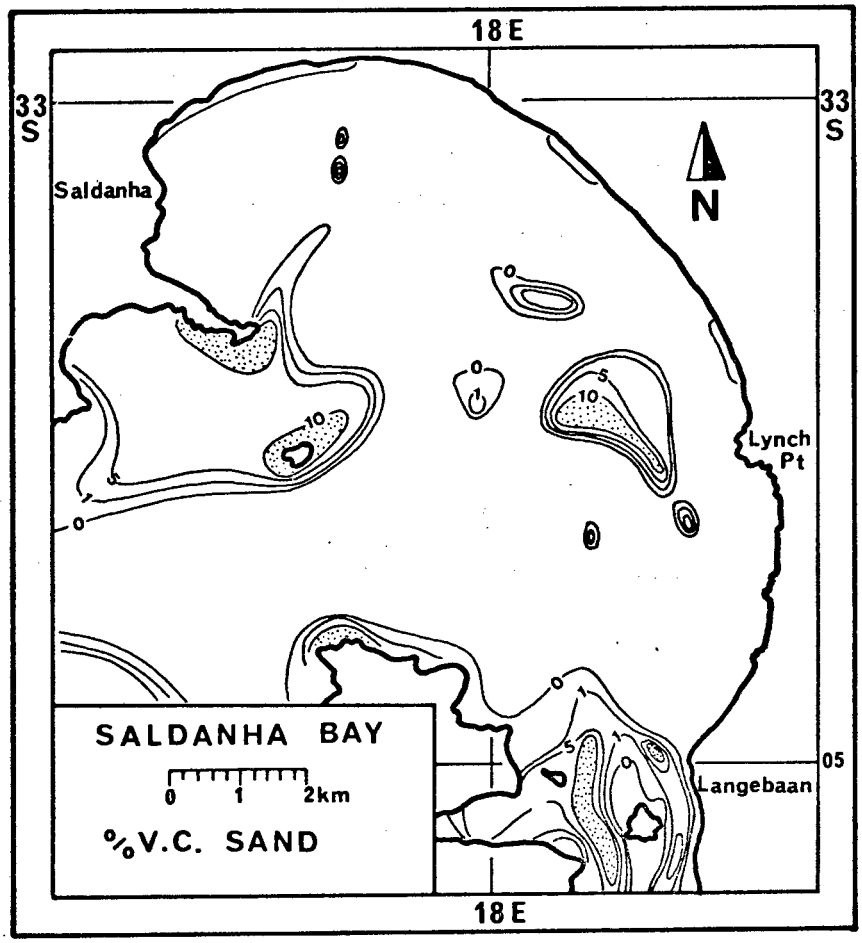
18 E
33 S
Saldanha
N
Lynch Pt
SALDANHA BAY
0 1 2km
%V.C. SAND
Langebaan
05
18 E

Fig. 71

However, there is no evidence that mud pebbles are actually being transported into the bay.

Gravels are not very common in Saldanha Bay, with the exception of some very localized accumulations of larger shell fragments. The shell gravels along the inner abrasion platform were recorded as gravels by side-scan sonar due to their acoustic properties. Their back-scattering potential is higher than that of sand although, hydraulically, most of the material is a coarse to very coarse sand, rather than a true gravel in the strict sense of the word.

Very coarse sands are restricted to well defined localities (Fig. 71). They are associated with the high energy zones of the bay. Relatively high values are encountered in North Bay, the North Channel, and on the inner abrasion platform. Coarse sand follows the same general pattern, although it is spread over slightly larger areas (Fig. 72). It forms the coarsest size fraction that achieves local concentration levels in excess of 50%.; significantly these areas all have carbonate contents of over 80%, indicating a definite size control by an individual sedimentary component. This feature would be related to the mechanical breakdown of originally larger, bioclastic material.

The distribution of medium sand is clearly related to the pattern of the two coarser size fractions (Fig. 73). Together, they appear to form a genetic suite, being grouped around the same spreading centres, whereby each successively smaller size-class occupies a larger overall area. Whereas large areas in Saldanha Bay lack very coarse material, areas without medium sand are more localized, the most important one being the South Channel. In North Bay the medium sand fraction forms a distinct depositional unit with concentration levels well above 50%. It is the only real medium sand facies in the whole inner and outer bay. Medium sand distribution correlates well with the 60% $CaCo_3$ boundary.

The medium sand and the coarse sand distribution patterns both clearly separate the two main source areas. There does not appear to be significant mixing between the sediments originating from the abrasion platform, on the one hand, and the North Channel area, on the other. As a result, there should be an equally clear separation between the depositional

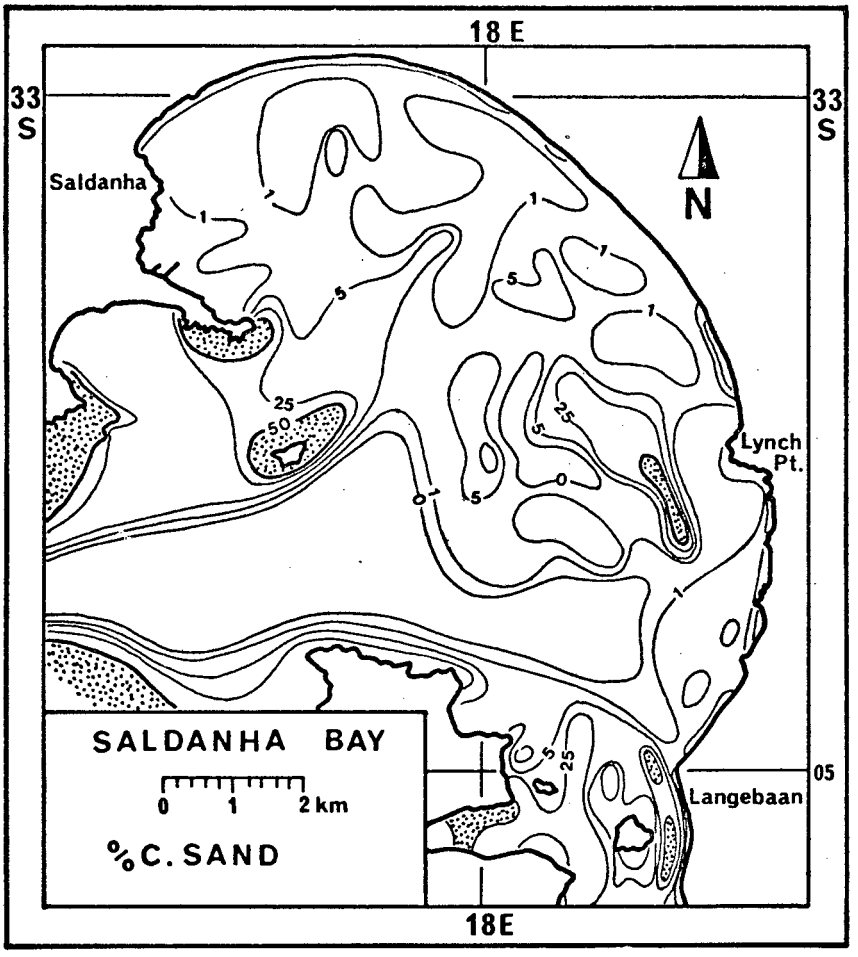
18 E
33 S
33 S
Saldanha
N
Lynch Pt.
SALDANHA BAY
0 1 2 km
%C. SAND
Langebaan
05
18E

Fig. 72

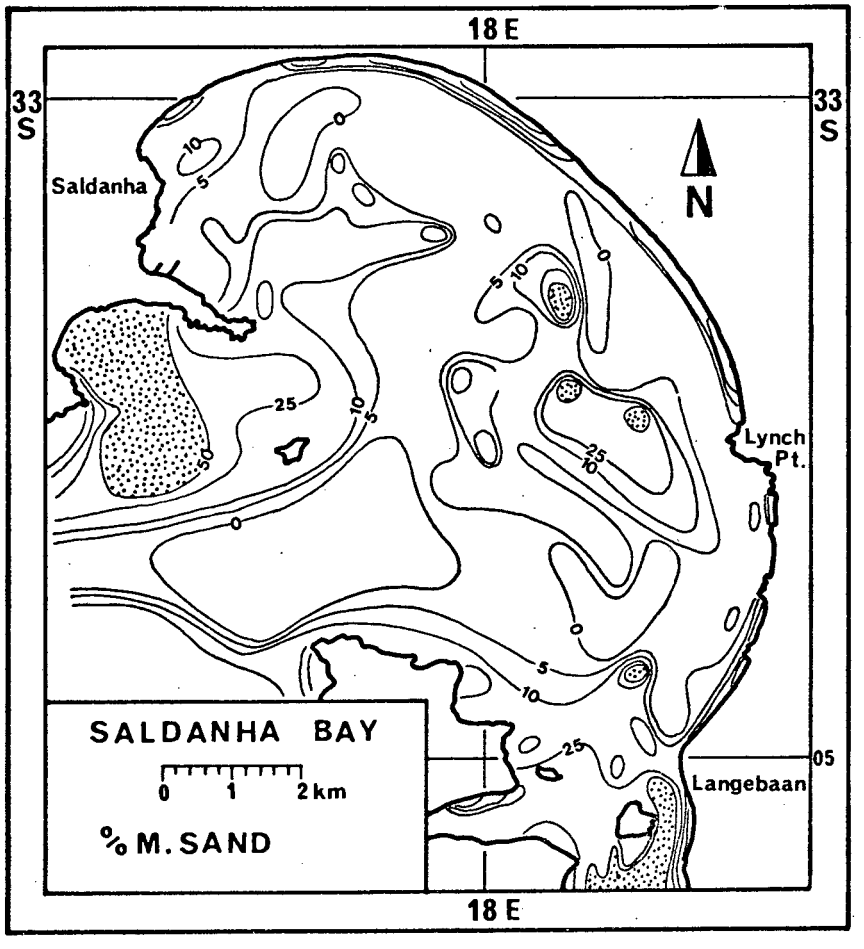
18 E
33 S
33 S
Saldanha
N
Lynch Pt.
SALDANHA BAY
0 1 2 km
% M. SAND
Langebaan
05
18 E

Fig. 73

areas of relict carbonates and modern carbonates. Although radiocarbon dates are not available to prove this assumption, their macroscopic appearance would suggest that the deduction is correct. In a recent study along the coast of Mauritania, Koopmann (1975) has separated relict and modern carbonates on the basis of their macroscopic appearance. His hypothesis was subsequently confirmed by radiometric dating. The distribution of carbonates in Saldanha Bay (Fig. 65) also reflects the separation of the two areas.

With the finer sand fractions there is a complete change in the general trend of the distribution pattern. Finesand is concentrated in the tidaldelta of the bay-lagoon transitional zone (Fig. 74). Here over 50% of the total sediment consists of fine sand. Other areas with more than 50% of this size fraction are very small, being situated in the central part of the northern bay and in a narrow belt north of Lynch Point.

Most of the fine sand in the bay appears to be associated with the tidal delta. As will be seen in a later section, this sediment forms part of the extended fine sand sheet mantling almost the entire lagoon. The tidal delta therefore acts as a reservoir from which fine sand is supplied to the remainder of the bay. This is clearly reflected in the distribution pattern. A belt of fine sand stretches from the tidal delta across the entire bay into the sheltered zone of the northern bay, and a tongue of fine sand reaches into the South Channel. It is interesting to observe that the fine sand in the South Channel is concentrated more towards the southern margin, where ebb current dominance was concluded from the orientation of the sediment fan near Elandspunt.

Very low concentration levels of fine sand are observed on the inner abrasion platform and along the inshore section of the whole northern bay. The North Channel and the North Bay form another area of low fine sand content. Higher contents are again observed along the northeastern shoreline. This area appears to be fed from a separate source, which is probably related to cliff erosion observed along this part of the coast. The distribution pattern in this inshore zone suggests a southerly longshore current in the surf zone. A current of this nature can, in fact, be inferred as part of a return flow system generated by the instability of water masses piled up in the northern bay by the persistent southwesterly winds.

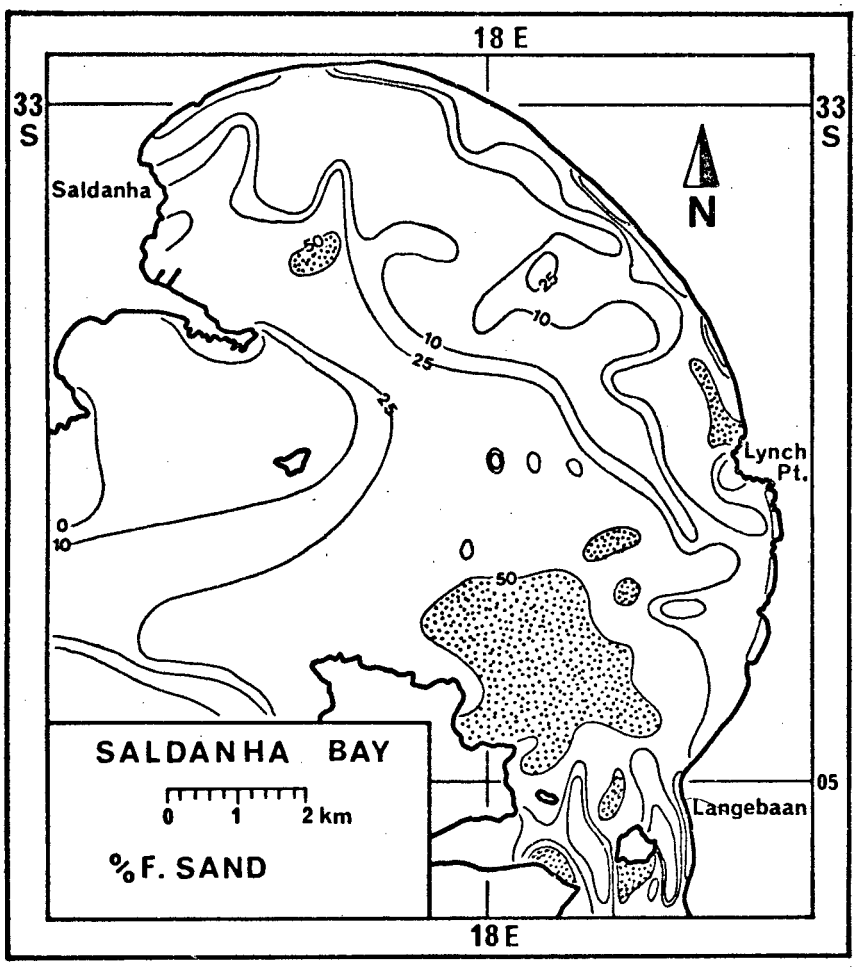
18 E
33 S
33 S
Saldanha
N
50
25
10
10
25
25
0
10
0
0
0
50
Lynch Pt.
SALDANHA BAY
0 1 2 km
%F. SAND
05
Langebaan
18 E

Fig. 74

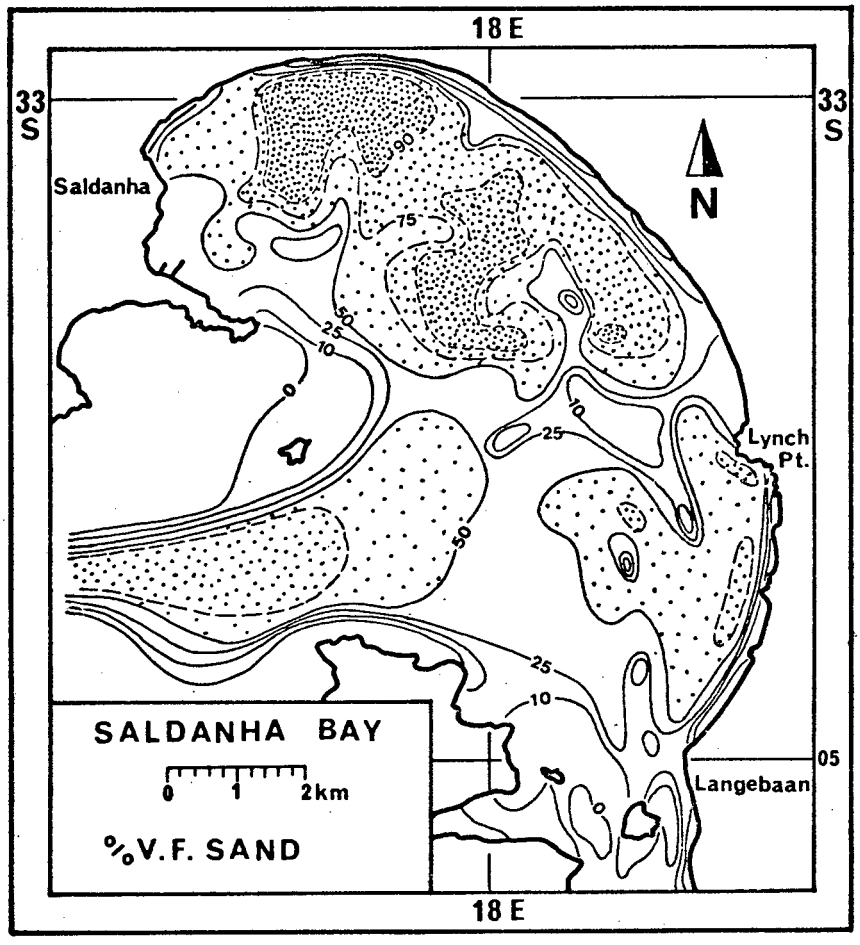
18 E
33 S
33 S
Saldanha
N
90
75
50
25
10
0
10
25
50
25
10
0
Lynch Pt.
SALDANHA BAY
0 1 2km
%V.F. SAND
05
Langebaan
18 E

Fig. 75

By far the largest area in Saldanha Bay is occupied by very fine sand (Fig. 75). With the exception of a narrow gap near Lynch Point, the entire nearshore sand prism consists of very fine sand. Both semi-exposed zones and most of the sheltered zone in the north contain over 50% of this size fraction, while large areas in the northern and northeastern bay reach concentration levels over 75%. Individual samples from this area were recorded to consist 100% of very fine sand.

Very fine sand is totally absent in North Bay and in the North Channel. Low concentrations are found on the inner abrasion platform and on the proxima tidal delta. Most beaches contain little very fine sand. In the South Channel, on the other hand, it again reaches values over 75%. Its boundary to the abrasion platform is relatively sharp, although very fine sand can be found in many places on the outer platform. This widespread blanket of very fine sand in Saldanha Bay strongly supports the equilibrium concept formulated in an earlier section.

The sediment distribution patterns in Saldanha Bay suggest the presence of two overlapping, hydraulic populations. The coarser population consists of medium and coarser-grained sediments and is supplied from sources within Saldanha Bay. The finer population comprises fine and very fine sands and appears to have been supplied from a source outside Saldanha Bay. Its affiliation to the tidal delta at the mouth of Langebaan Lagoon, and its overall spreading pattern, suggest a lagoonal origin for this sediment. The overlapping nature of the distribution patterns of the two hydraulic populations indicate that these have been mixed in various proportions in different parts of the system.

The mean diameter map summarizes the dominant size-controlled features of sediment distribution (Fig. 76). The abrasion platform is clearly outlined, although conventional contouring fails to reproduce the extreme patchiness of sediment distribution in this area. This feature is particularly evident from the micro-topography of the abrasion platform as recorded by side-scan sonar (viz. Fig. 55 and Plate 2). The high energy zones in the North Channel and in North Bay are appropriately represented, and the widespread very fine sand blanket adequately outlines the South Channel, the sheltered zone in the north, and the two semi-exposed zones bordering on the abrasion platform.

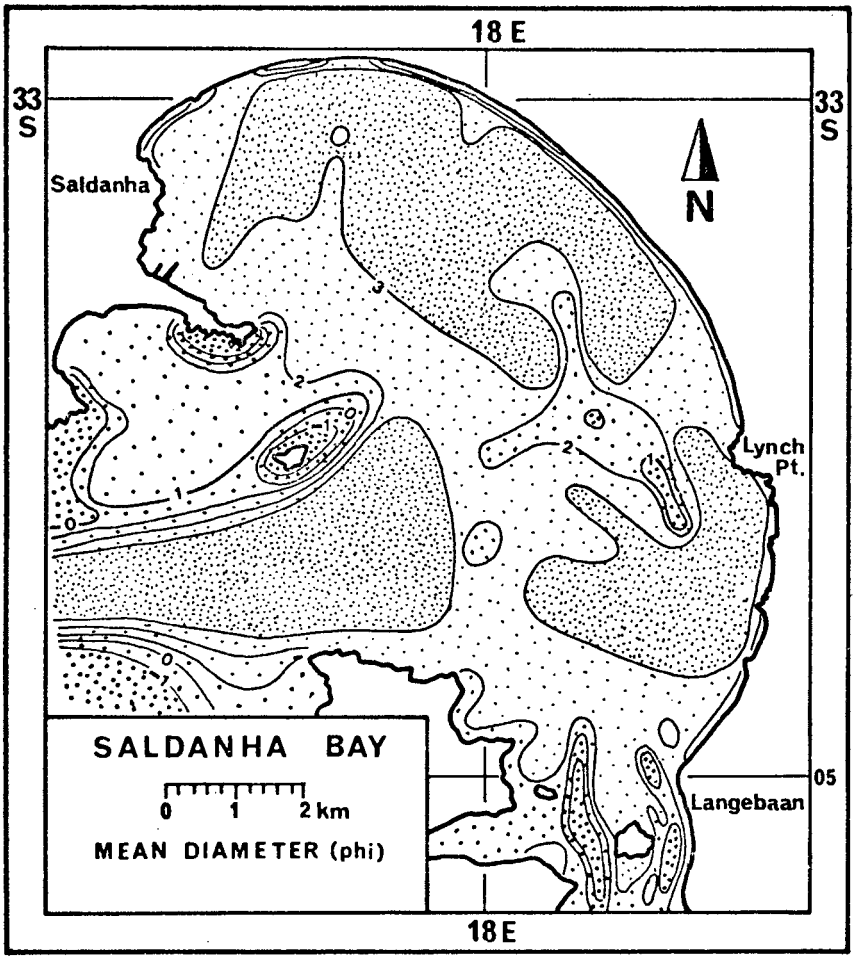
18 E
33 S
33 S
Saldanha
N
Lynch Pt.
SALDANHA BAY
0 1 2 km
MEAN DIAMETER (phi)
Langebaan
05
18 E

Fig. 76

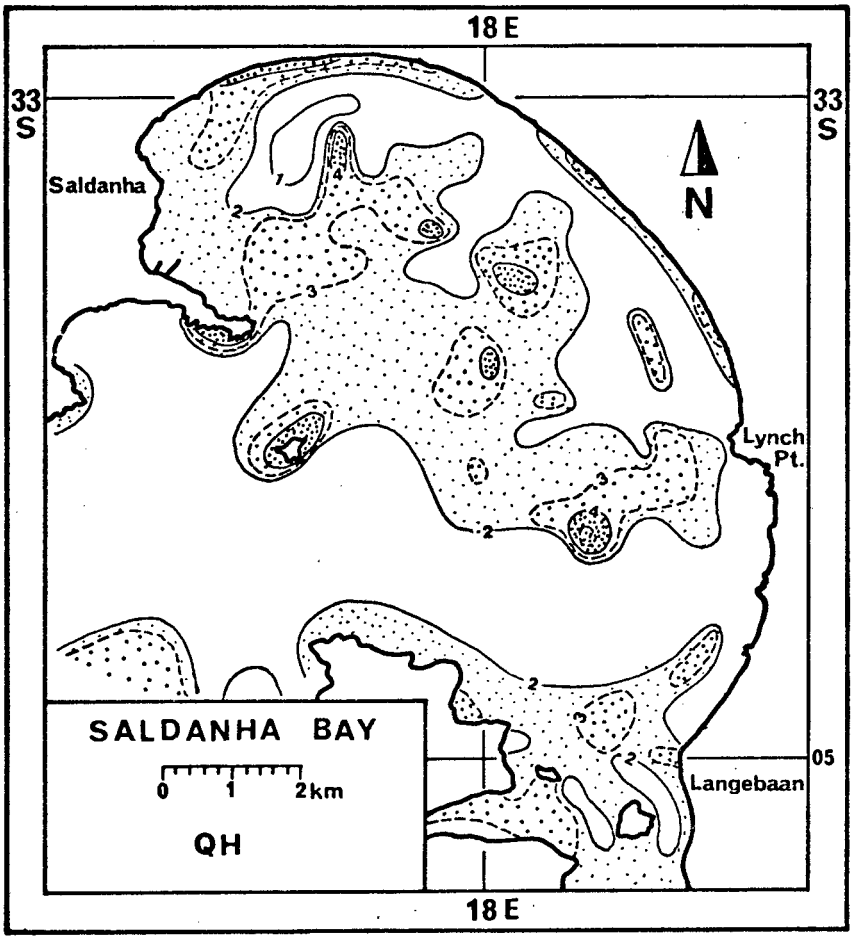
18 E
33 S
33 S
Saldanha
N
Lynch Pt.
SALDANHA BAY
0 1 2km
QH
Langebaan
05
18 E

Fig. 77

The sediment is generally well to very well sorted, moderate sorting being restricted to a number of small isolated patches (Fig. 77). In accordance with the model of progressively mixing sediments discussed in Section 3.6.2., the poorest sorting is, in most cases, associated with areas of strongest mixing. An exception is formed by the modern bioclastic source along the North Channel margins. Here, sorting is moderate because the whole suite of grain sizes is produced in the same zone. Sorting then increases rapidly as the finer sizes are progressively eliminated. On the inner abrasion platform, on the other hand, sorting is very good because the source material was already well sorted when originally deposited.

The sediments of Saldanha Bay are divided into two skewness provinces. The general trend is from positive skewness in deeper water to negative skewness in shallow water (Fig. 78). Large parts of the inshore sand prism are very negatively skewed. The North Bay, the North Channel, the South Channel and the tidal delta form a continuous positively skewed unit. Another positively skewed area is defined on the inner abrasion platform, and a third positively skewed deposit occurs in the centre of the sheltered zone in the northern bay.

The positive skewness of the predominantly bioclastic sediment in the North Channel source area is not unexpected, since progressive breakdown of the original shell material will continuously add a finer tail to the sediment. With increasing distance from the source area the sediment gets finer and less skewed at first. The finer the sediment becomes, the stronger it is dominated by the fine population; the subordinate coarse population now induces a negatively skewed size distribution. In most parts of the bay, skewness is therefore largely a function of proportion between the coarser and the finer hydraulic populations. Both populations appear to have been slightly positively skewed, but proportional mixing has resulted in the skewness pattern observed today.

The above interpretation of sediment distribution patterns in terms of depositional processes has relied entirely on the spatial relationships between individual size parameters. Below it will be shown that these interpretations are supported when viewed graphically in form of scatter plots.

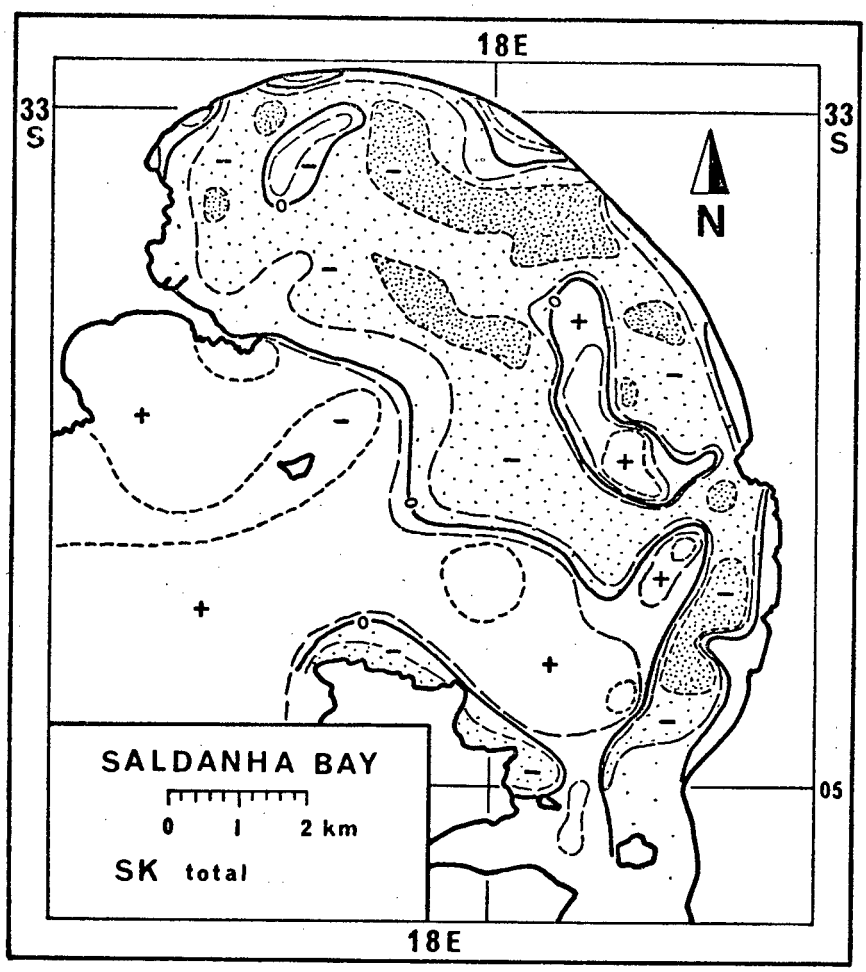

Fig. 78

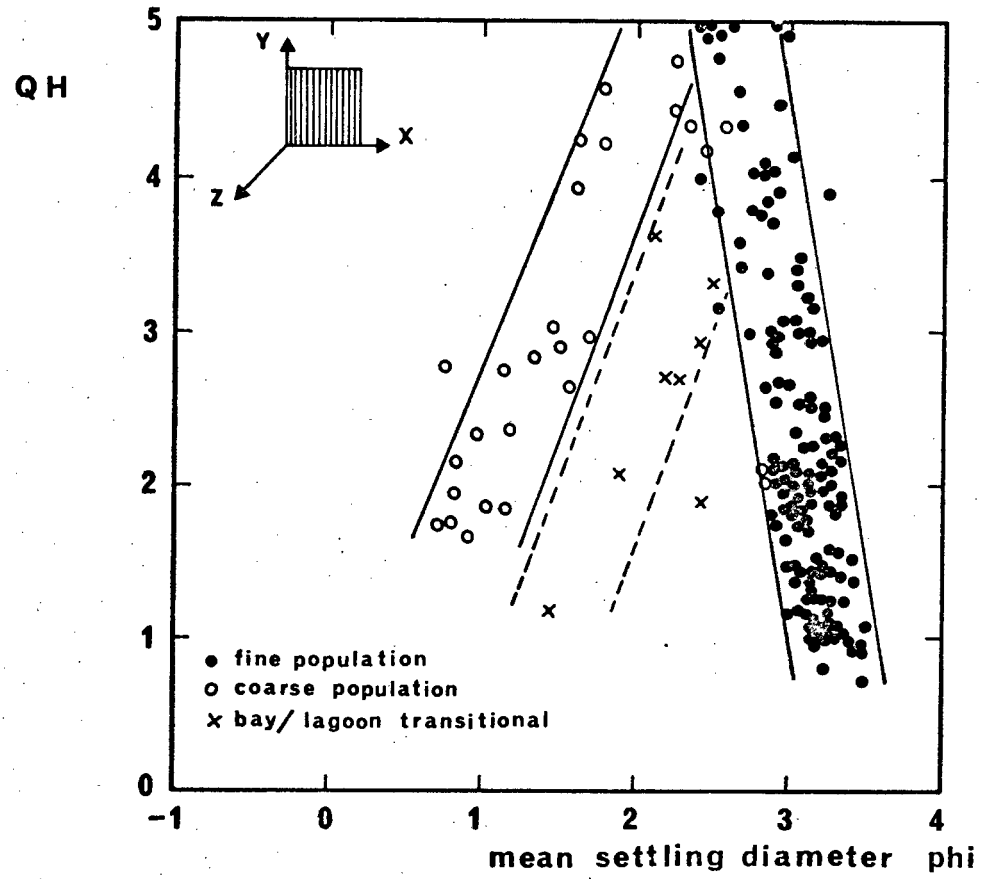

Fig. 79. The relationship between mean diameter and sorting of Saldanha Bay sediments

In Fig. 79 the relationship between mean settling diameters and relative sorting coefficients are investigated. The diagram clearly separates the two hydraulic populations recognized in the size distribution patterns. The process of progressive mixing is illustrated by the two upward converging arms of the two point clusters. The fine population decreases rapidly in sorting, while gradually becoming coarser. In analogy the coarse population becomes less well sorted as it gets finer. A second coarse population is indicated below the first one. It consists of sediment samples originating from the proximal tidal delta channels which are more closely related to the lagoonal sediments.

The further a sample is situated upwards in each converging arm, the more it loses the size characteristics of its parent population. Where the two populations overlap, i.e. at the apex of the three-dimensional helix described by the mixing sediments, both have reached a degree of mixing at which their original size characteristics are totally obscured.

The relationship between the mean diameter and skewness is illustrated in Fig. 80. It represents the two-dimensional projection of the data points plotted in Fig. 79 onto the XZ-plane of the coordinate system. The lower portion of the points cluster, where the samples show strong negative skewness, represents the inshore sand prism. The abrasion platform is represented at the upper left, being medium to coarse-grained and positively skewed. At the upper right of Fig. 80 an isolated cluster of almost symmetrical very fine sands is observed. These sediments originate from the near-symmetrical to positively skewed very fine sand deposits, situated in thecentral part of the sheltered zone in the north, and the semi-exposed zone in the south, where it forms an appendix to the positively skewed tidal delta (Fig. 78). These samples form the fine endpoint of the helical point cluster and should, therefore, reflect the size distribution characteristics of the parent population at the time it entered the system. If this interpretation is correct, then they should not show any sign of mixing with the coarser population in the bay. A re-examination of the distribution patterns of the medium, coarse and very coarse sands indeed confirms that these grain sizes do not occur at the localities of the positively skewed very fine sands. The same applies to the very fine sands in the South Channel.

The relationship between relative sorting and skewness (YZ-plane)

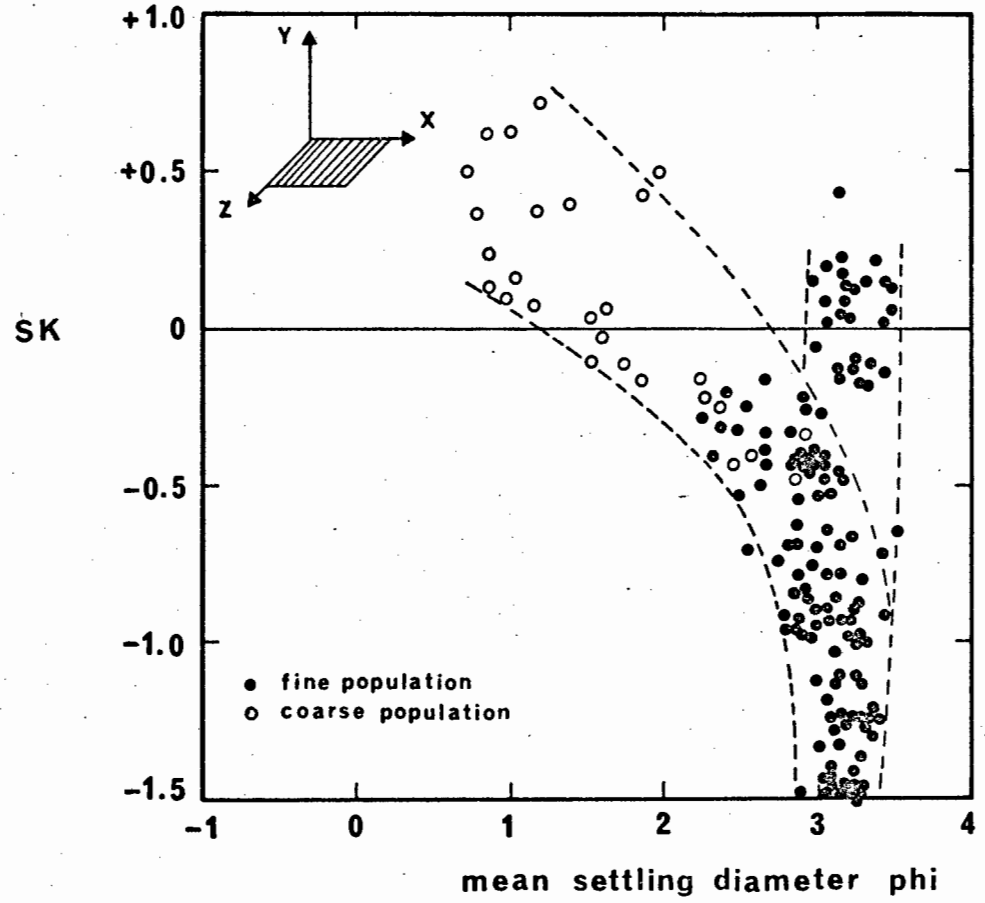

Fig. 80. The relationship between mean diameter and skewness of Saldanha Bay sediments

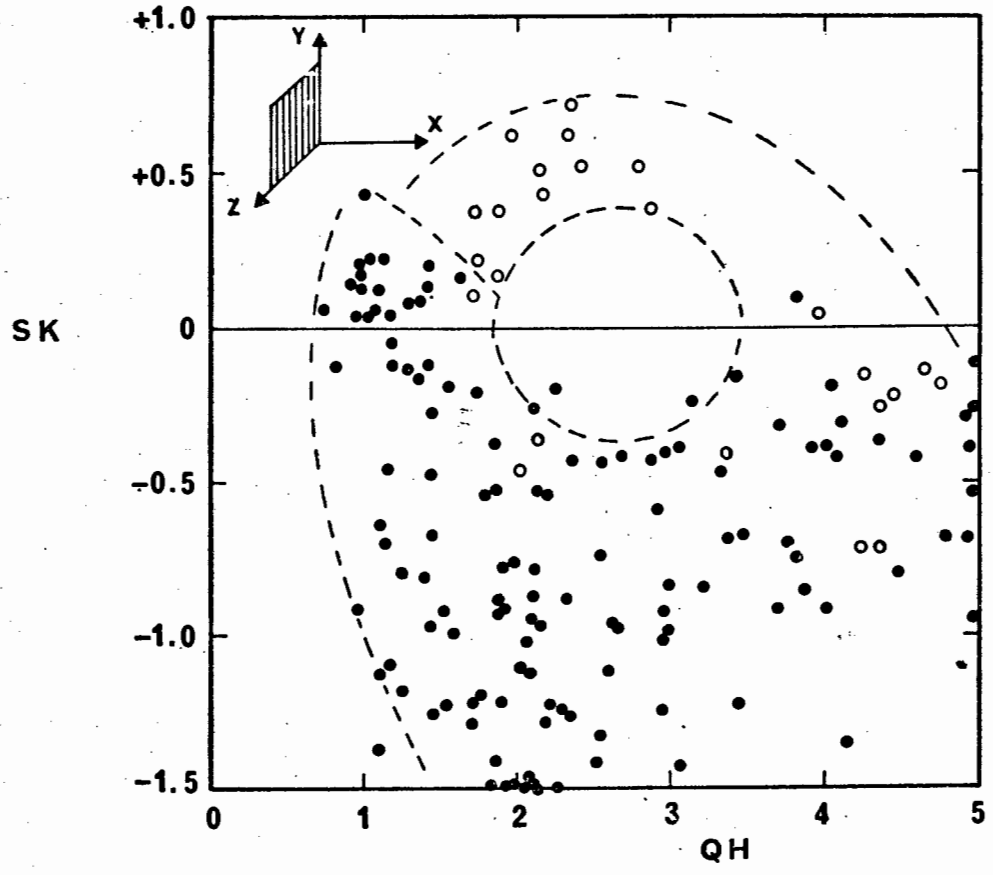

Fig. 81. The relationship between skewness and sorting of Saldanha Bay sediments

is illustrated in Fig. 81. It represents the two-dimensional image of the point cluster viewed at right angles to the other two planes. The helical model of Folk and Ward (1957) predicts a circular arrangement of data points, which leave an empty space in the centre. The point cluster in Fig. 81 is more or less circular but the empty space is displaced from the centre to the upper edge. This indicates that the axis of the helix is not facing perpendicular to the sorting/skewness plane. As a result the points from successive helical levels begin to overlap thereby obscuring the overall trend.

The approximate position and orientation of the idealized helix is presented in Fig. 82. For comparative purposes the helix of Folk and Ward (1957) is also shown (dotted line). It should be pointed out that the coarse arm of the helix is not very well defined because the mixing process on the abrasion platform and adjacent to the North Channel takes place over such short distances that the sample pattern, in spite of its overall density, has not adequately covered this transitional zone. As a result, the individual scatter plots are dominated by the omnipresence of samples belonging to the fine hydraulic population. The apparent gaps in the inferred helix, therefore, do not indicate the absence of such material but simply reflect inefficient sampling in areas where this sediment is spread over very small distances.

The previous discussion has indicated that the coarse population is predominantly composed of bioclastic sediments, and that grain size appeared to be dependent on the carbonate content. This interpretation is confirmed by plotting mean diameters against carbonate contents (Fig. 83). The diagram demonstrates that the size control varies between different carbonate concentration levels, i.e. size control increases stepwise as carbonate content increases. Up to the 30% $CaCO_3$-level there is no distinct influence. Between 30% and 70% there is an overall increase in size by about 0.7 phi-intervals, and from 70% to 95% $CaCO_3$-content the mean diameter increases by 1.8 phi-intervals. The region between 30% and 70% would thus represent the areas of strongest mixing.

The apparent size control of the coarse hydraulic population by the $CaCO_3$-content of the sediment is readily explained by the far-reaching separation of bioclastic and terrigenous particles into the two hydraulic

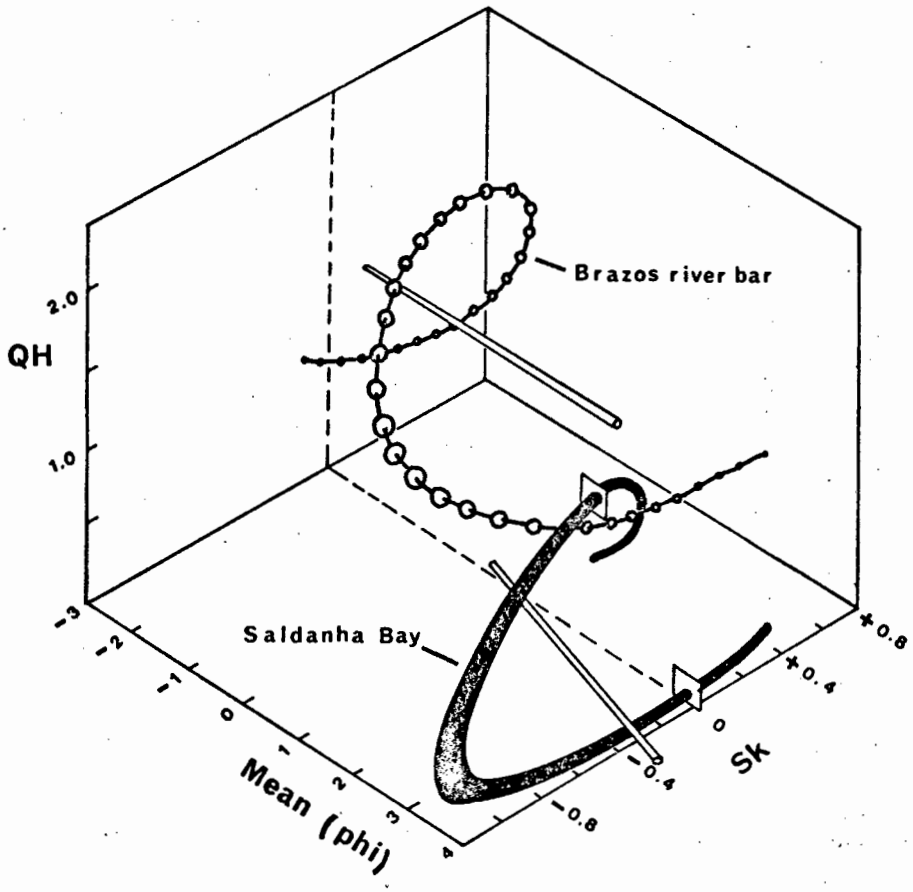

Fig. 82. The three-dimensional relationship between mean diameter, sorting, and skewness

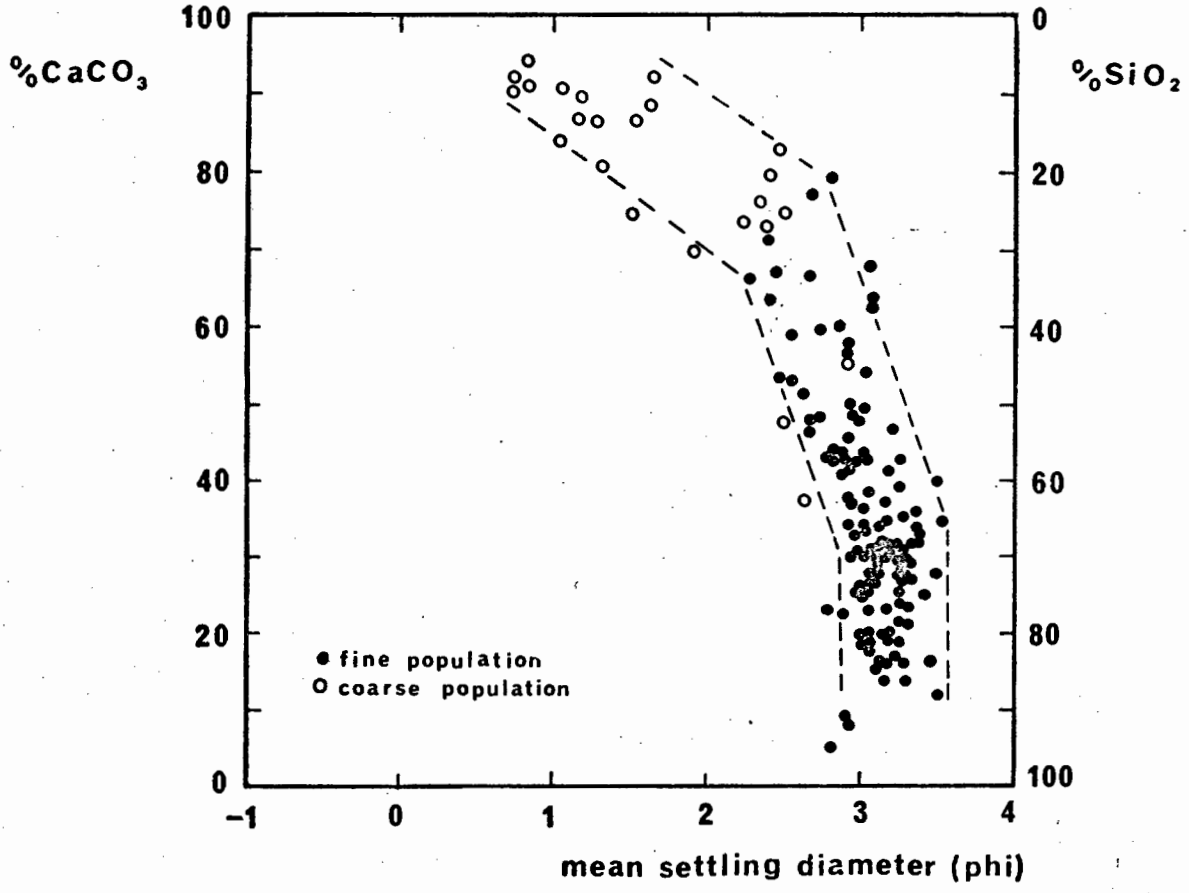

Fig. 83. The relationship between mean diameter and carbonate content

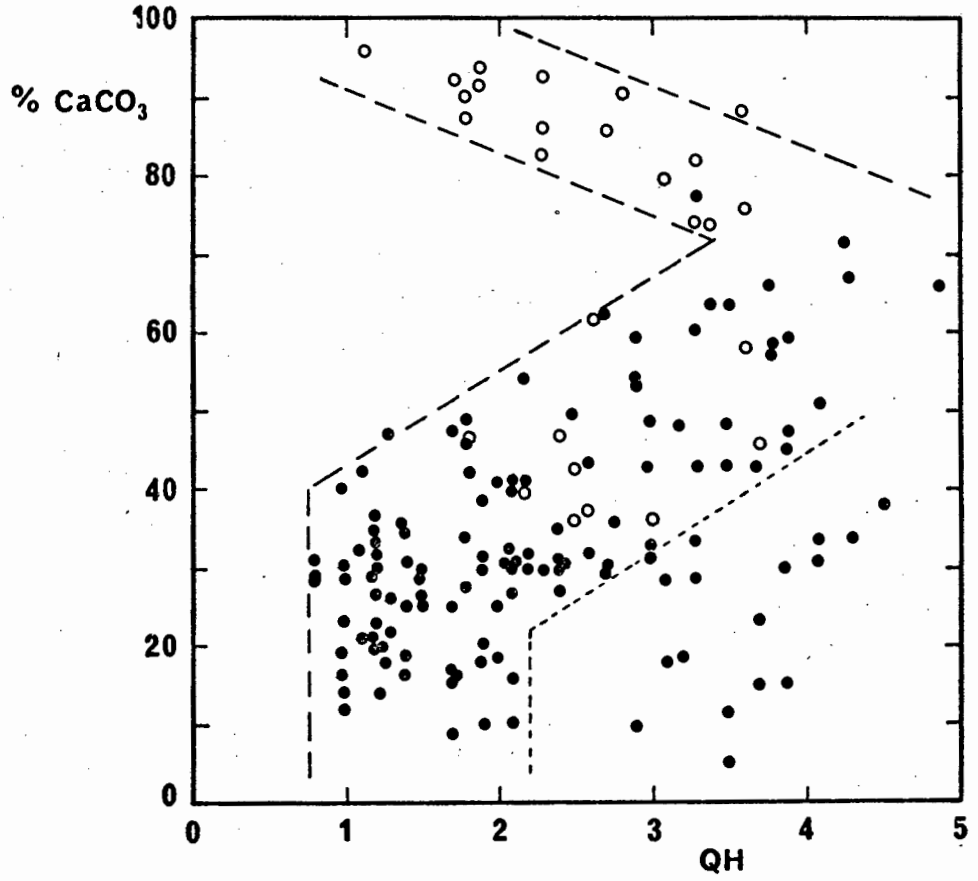

Fig. 84. The relationship between sorting and carbonate content of Saldanha Bay sediments

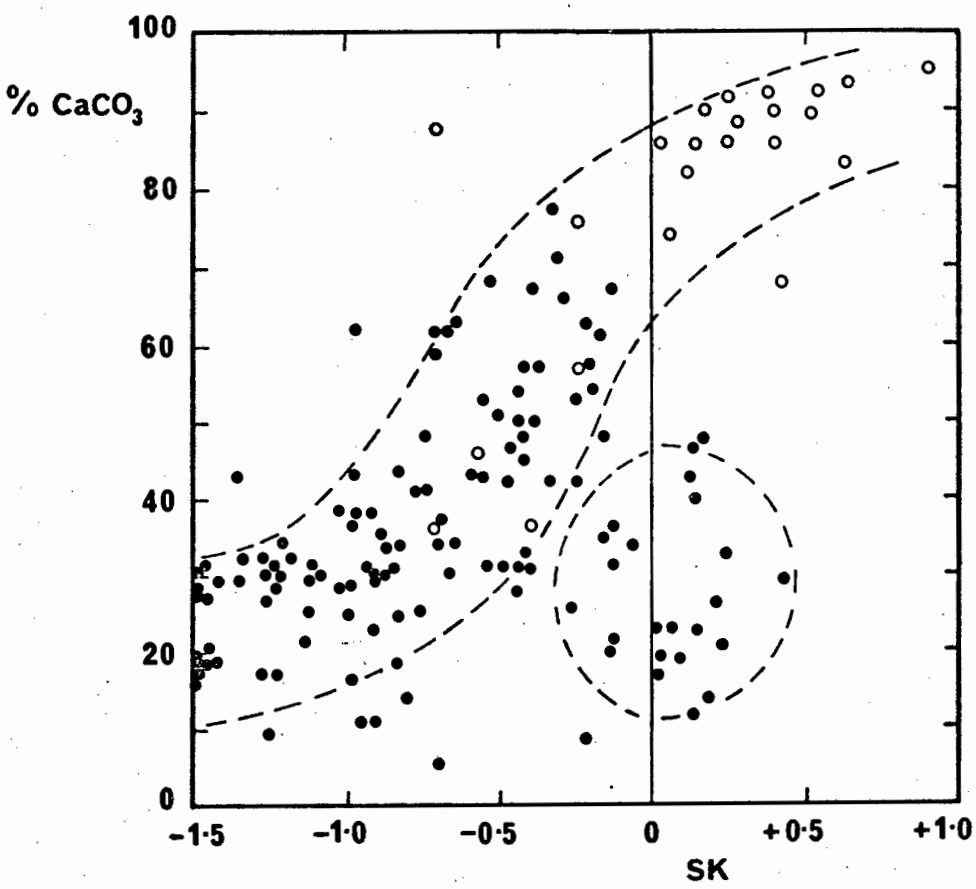

Fig. 85. The relationship between skewness and carbonate content

populations. A similar size dependence of the terrigenous component on SiO_2-contents, however, is not observed. This feature is a strong argument in support of the deduction that the finer population has been supplied from a foreign source. The sediment had already undergone a process of efficient size sorting by the time it entered into the sedimentary system of Saldanha Bay. This is reflected by the progressive decrease in grain size from the proximal tidal delta to the distal tidal delta which has retained most of the fine sand, allowing only very fine sand to bypass for redistribution in Saldanha Bay.

The dependence of mean size on $CaCO_3$-contents suggests that the two parameters should be interchangeable without obscuring previously defined trends, e.g. in Fig. 79 (mean vs. sorting) and Fig. 80 (mean vs. skewness). That this holds true is illustrated in Fig. 84 and Fig. 85, respectively. Fig. 84 in addition demonstrates that the coarsest bioclastic parent population is not as well sorted (QH = 1.7) as its very fine terrigenous counterpart (QH = 0.8), in spite of it being a residual sediment. This phenomenon appears to provide further evidence for the effect of particle shape on relative sorting discussed in Section 3.4.

The evident difference in composition between the two hydraulic populations, and the differential response of each individual sedimentary component to the depositional processes inferred from their respective distribution patterns, certainly warranted further inspection of these features. Thus, in order to establish the exact effects of each component on the size characteristics of the total sediment, both components were subjected to a detailed investigation. The results of this investigation are discussed in the following two sections.

4.4.2. Terrigenous Component

The discussion of the terrigenous component is based on the results of the complete hydraulic size analysis of the acid-insoluble residue of the total sediment. All available samples were processed in this manner (viz. Section 3.2.).

The distribution patterns of very coarse sand (Fig. 86), coarse sand (Fig.87) and medium sand (Fig.88) are not much different from the total sediment

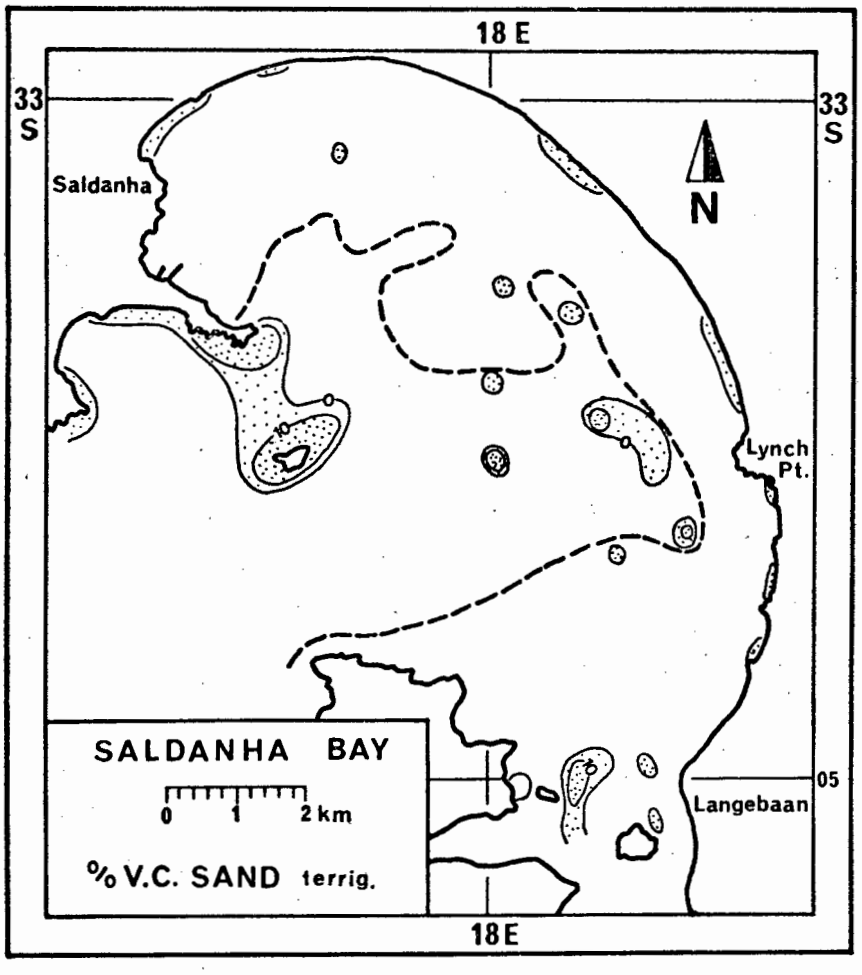
18 E
33 S
33 S
Saldanha
N
Lynch Pt.
SALDANHA BAY
0 1 2 km
% V.C. SAND terrig.
05
Langebaan
18E

Fig. 86

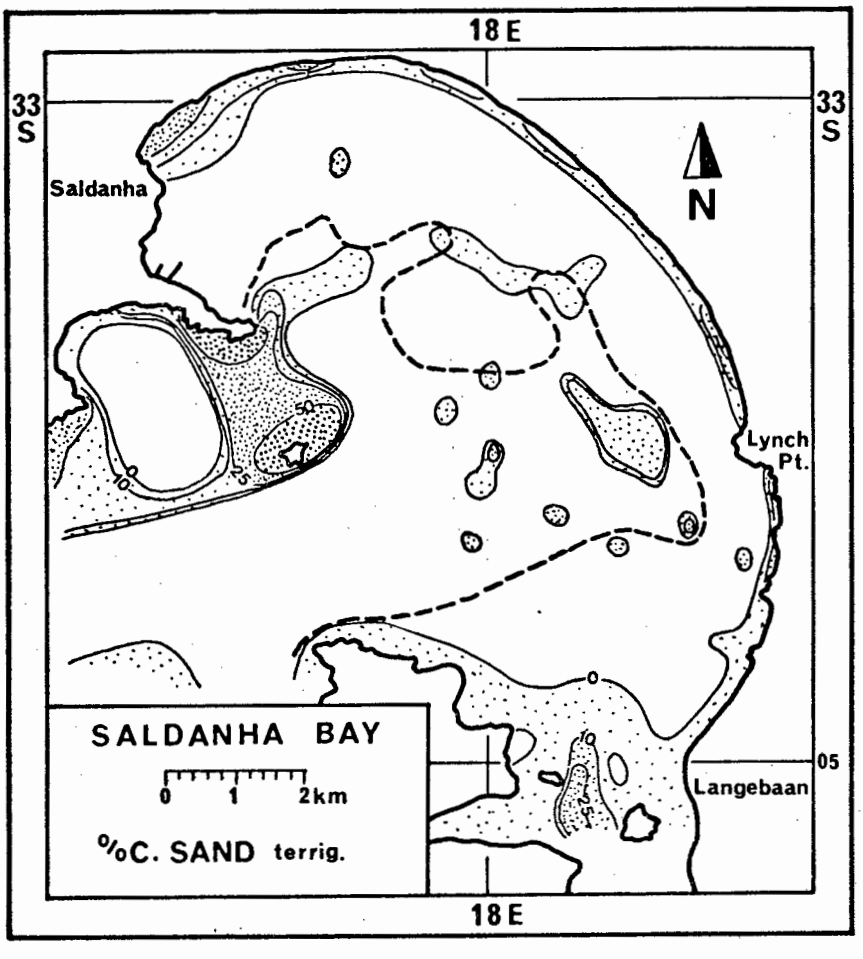
18 E
33 S
33 S
Saldanha
N
Lynch Pt.
SALDANHA BAY
0 1 2km
%C. SAND terrig.
05
Langebaan
18E

Fig. 87

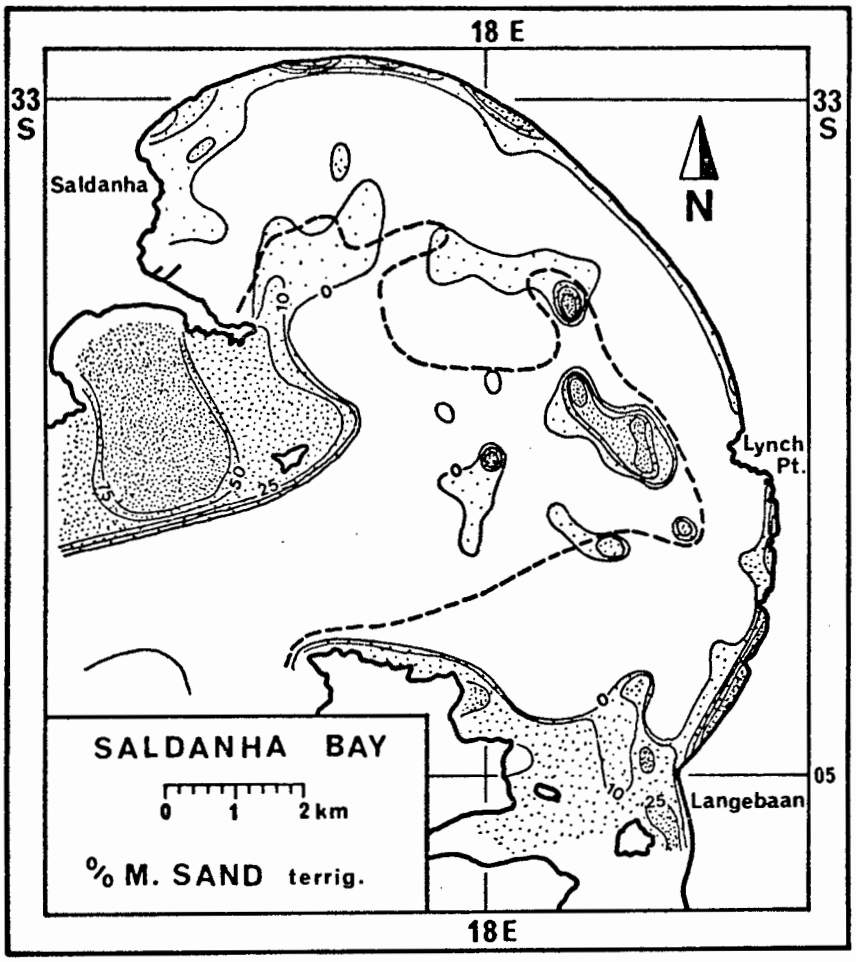
18 E
33 S
33 S
Saldanha
N
Lynch Pt.
SALDANHA BAY
0 1 2km
% M. SAND terrig.
Langebaan
05
18 E
0
10
25
50
75

Fig. 88

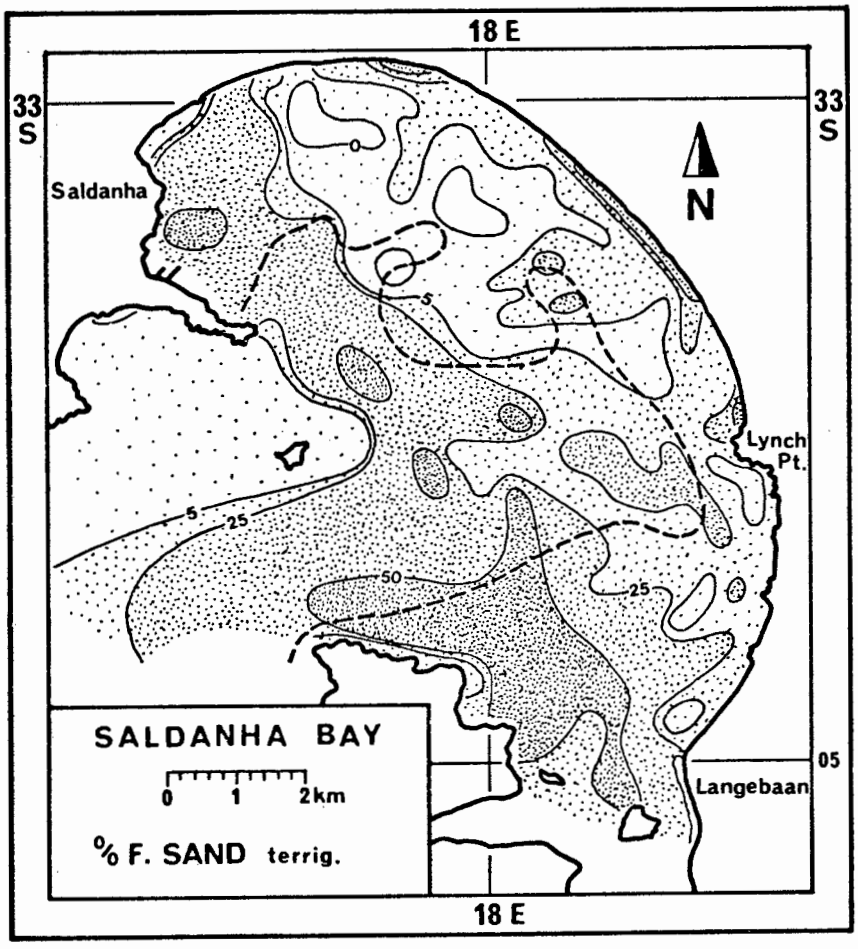
18 E
33 S
33 S
Saldanha
N
Lynch Pt.
SALDANHA BAY
0 1 2km
% F. SAND terrig.
Langebaan
05
18 E
0
5
25
50

Fig. 89

(viz. Fig. 71, 72 and 73). The areas of highest concentration coincide in both cases, but overall spreading is considerably more restricted. In addition, the high carbonate content of the total sediment indicates that the combined contribution of medium, coarse and very coarse terrigenous sediment to the total sediment is extremely small. The highest proportion of the total terrigenous sand fraction achieved by these three size classes combined is about 70%. However, the terrigenous component, as a whole, only contributes about 10% to the total sediment in these areas, and as a result the overall contribution of the terrigenous coarse population does not exceed 7%. In order to allow a quick assessment of relative concentration levels, the 50% $CaCO_3$-level has been contoured on all the maps (heavy broken line).

The coarse and the medium sand patterns both penetrate into the most sheltered part of the northern bay, in a gradient that decreases from the beach towards the harbour along the inner margin of the bay. The direction of this size gradient would suggest an influx of coarser material into this area from the northern beach, or winnowing of the fine material. Since wave action is far too weak for any such sediment transport, besides being oriented in the opposite direction, the only solution would seem to be an inshore return flow generated by the instability of water masses piled up by wind stress, similar to that observed in the northeastern section of the bay.

The sheltered zone of the bay is thus controlled by two depositional processes. Oblique wave incidence along the northern shoreline (Fig. 59) results in the winnowing of fine sediment from the beach; subsequent transport by littoral drift in the intertidal zone of the beach removes this sediment towards the northeastern shoreline, thereby accounting for the lack of fine sediment on the beach of the most sheltered parts of the bay. In the shallow sublittoral zone, on the other hand, exactly the opposite happens. Longshore drift fed from a return-flow current carries coarser grain sizes into the shallow water along the northwestern shoreline and, effectively prevents the deposition of very fine sands in a narrow belt along the northwestern shoreline (Fig. 90).

A major change, similar to the one observed in the total sediment patterns, is evident in the distribution patterns of the fine and very fine terrigenous sands (Fig. 89 and 90). An interesting difference is

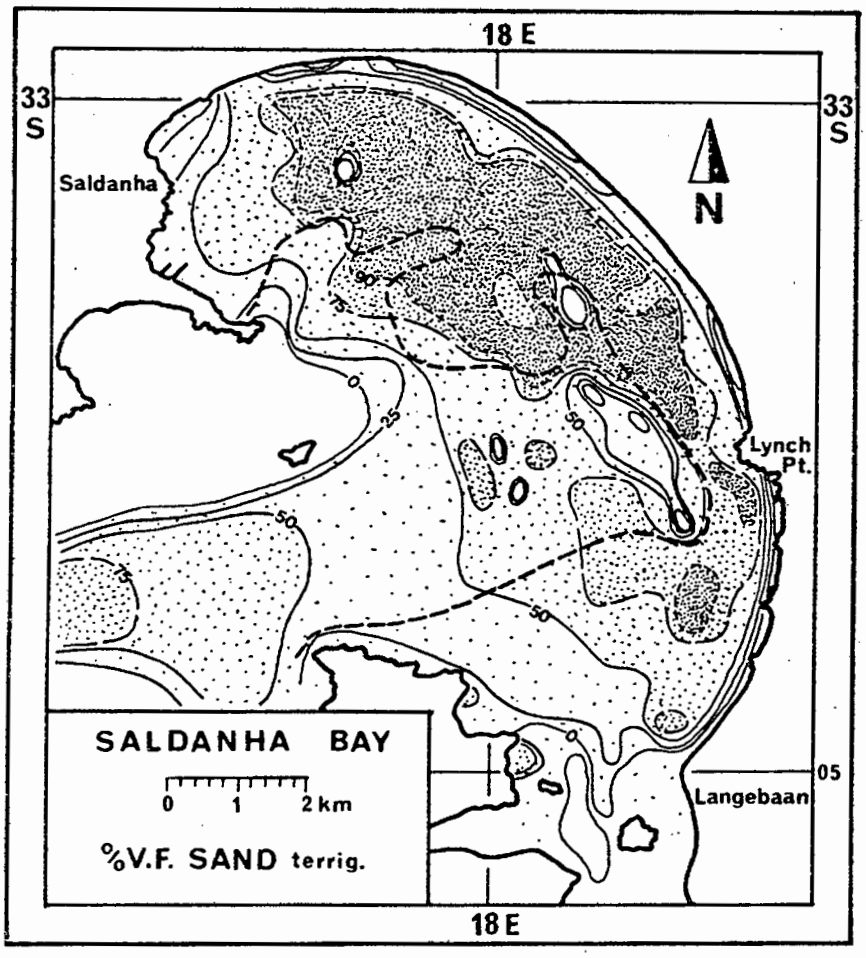
18 E
33 S
33 S
Saldanha
N
Lynch Pt.
SALDANHA BAY
0 1 2 km
%V.F. SAND terrig.
Langebaan
05
18 E

Fig. 90

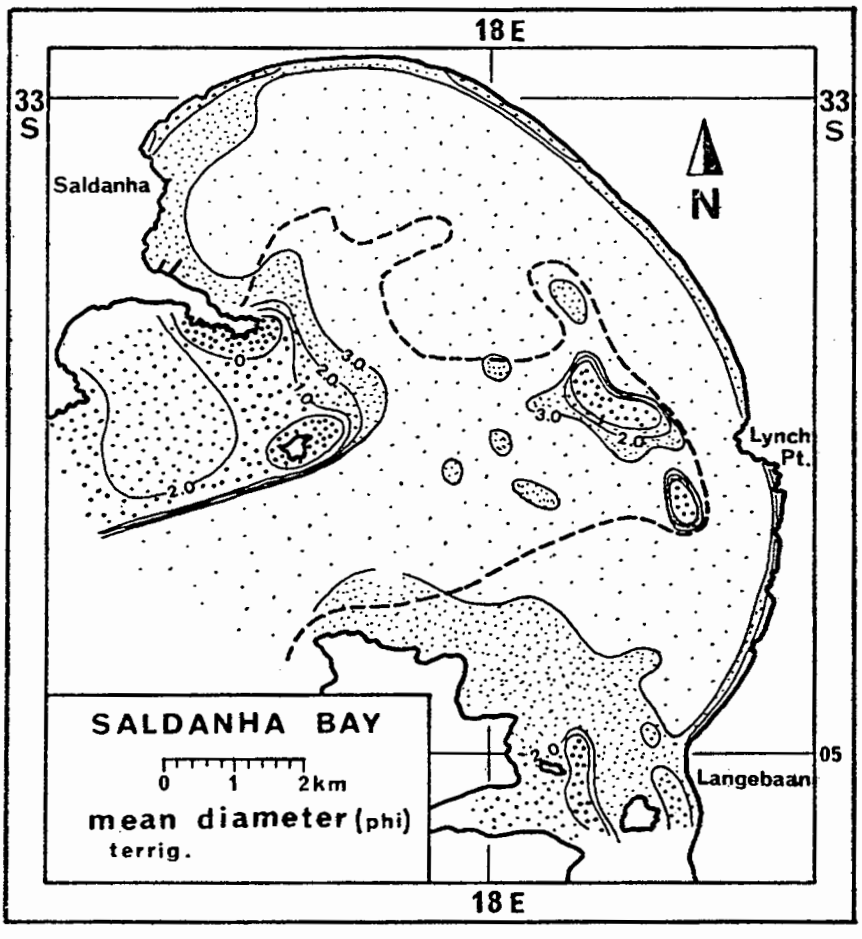
18 E
33 S
33 S
Saldanha
N
Lynch Pt.
SALDANHA BAY
0 1 2km
mean diameter (phi)
terrig.
Langebaan
05
18 E

Fig. 91

that larger proportions of fine sand penetrate into the South Channel from the tidal delta in the southern bay. As a result, the 50% very fine sand boundary for terrigenous sediments lies considerably deeper in the South Channel (at about -24 m) than that of the total sediment (at about -16 m). Again the influence of the ebb current along the southern margin of the South Channel is well recorded. Some fine terrigenous sand is also supplied from the northeastern beaches, accumulating southwest of Lynch Point.

The very fine terrigenous sand covers a considerably larger area than the total sediment would have suggested. This feature clearly indicates the lack of locally supplied coarse terrigenous sediment, which would normally have caused considerable dilution in the vicinity of the abrasion platform and the North Channel. This aspect is also well illustrated in the mean diameter map (Fig. 91). The only areas in the inner bay that are not occupied by very fine terrigenous sand are the inner abrasion platform, the tidal delta, and the return flow region in the northwestern bay. This feature is particularly relevant as it demonstrates, beyond doubt, that most of the bay has achieved a dynamic equilibrium between wave energy and sediment distribution.

On the basis of this observation, the abrasion platform can be divided into a marginally active inshore section, stretching between -11 m and -13 m, and an offshore inactive section that terminates at approximately -15 m. In this area, water movement appears to be strong enough to prevent very fine sand from mantling the calcrete outcrops. Below -15 m, however, very fine sand forms a continuous sheet which is occasionally penetrated by low calcrete pinnacles down to a depth of about -18 m.

Sorting trends differ from those of the total sediment only as far as the general sorting levels are concerned (Fig. 92). On average, the sorting of the terrigenous sediment is better than that of the total, and considerably better than that of the bioclastic sediment. This is particularly well illustrated in the mean diameter versus relative sorting diagram (Fig. 93). The two populations remain defined, although 77% of the samples constituting the fine hydraulic population are grouped in the extremely well sorted category (QH = 0.5 - 1.0). Over 90% of these samples are either extremely well, or very well, sorted, leaving less than 10% which are mixed with sediments from the coarser population.

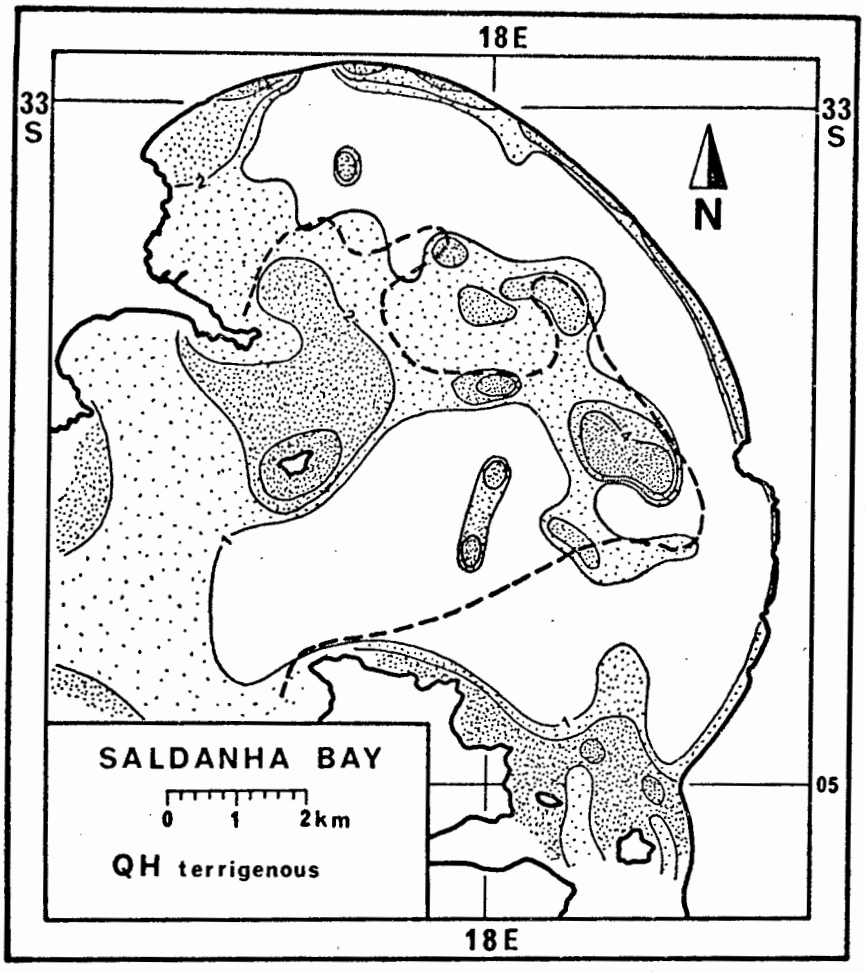

Fig. 92

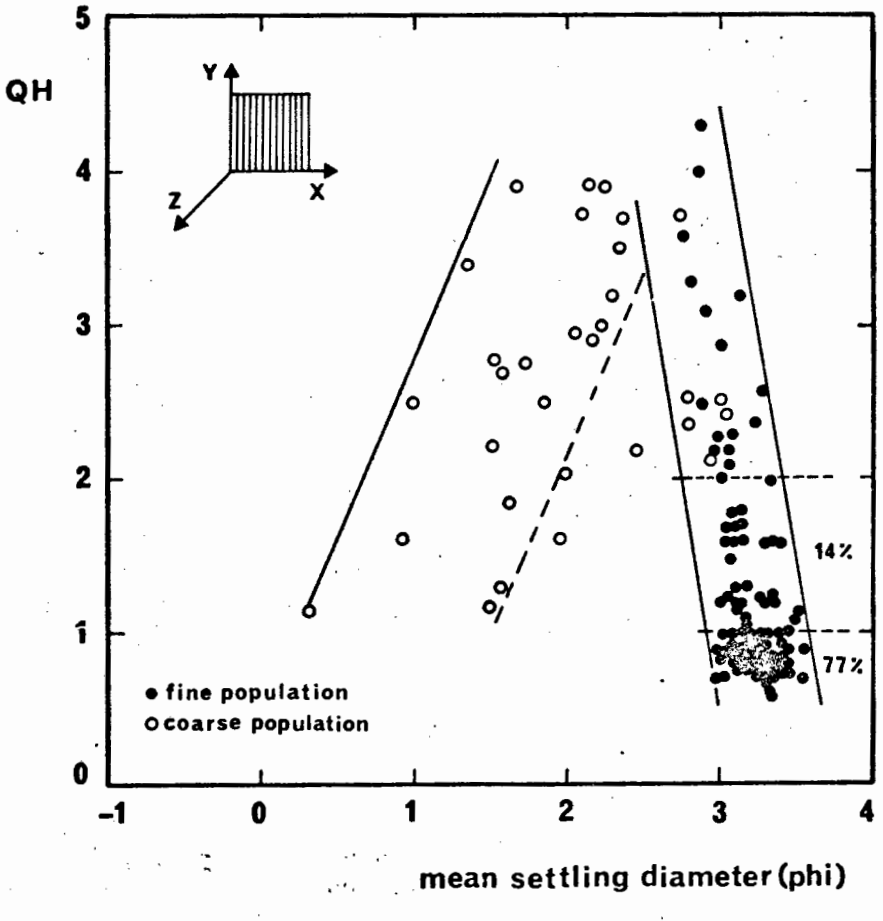

Fig. 93. The relationship between mean diameter and sorting of the terrigenous component

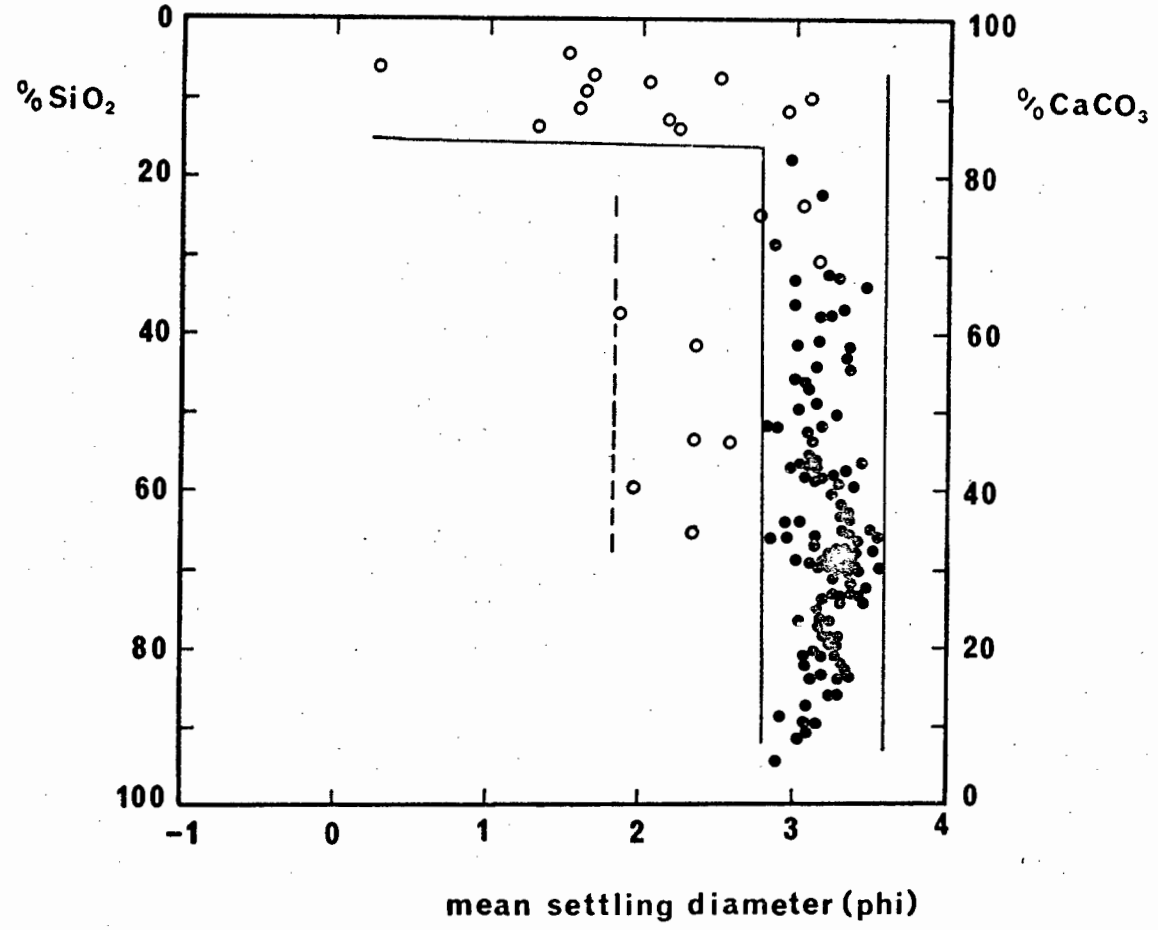

Fig. 94. The relationship between the mean diameter and the quartz content of the terrigenous component

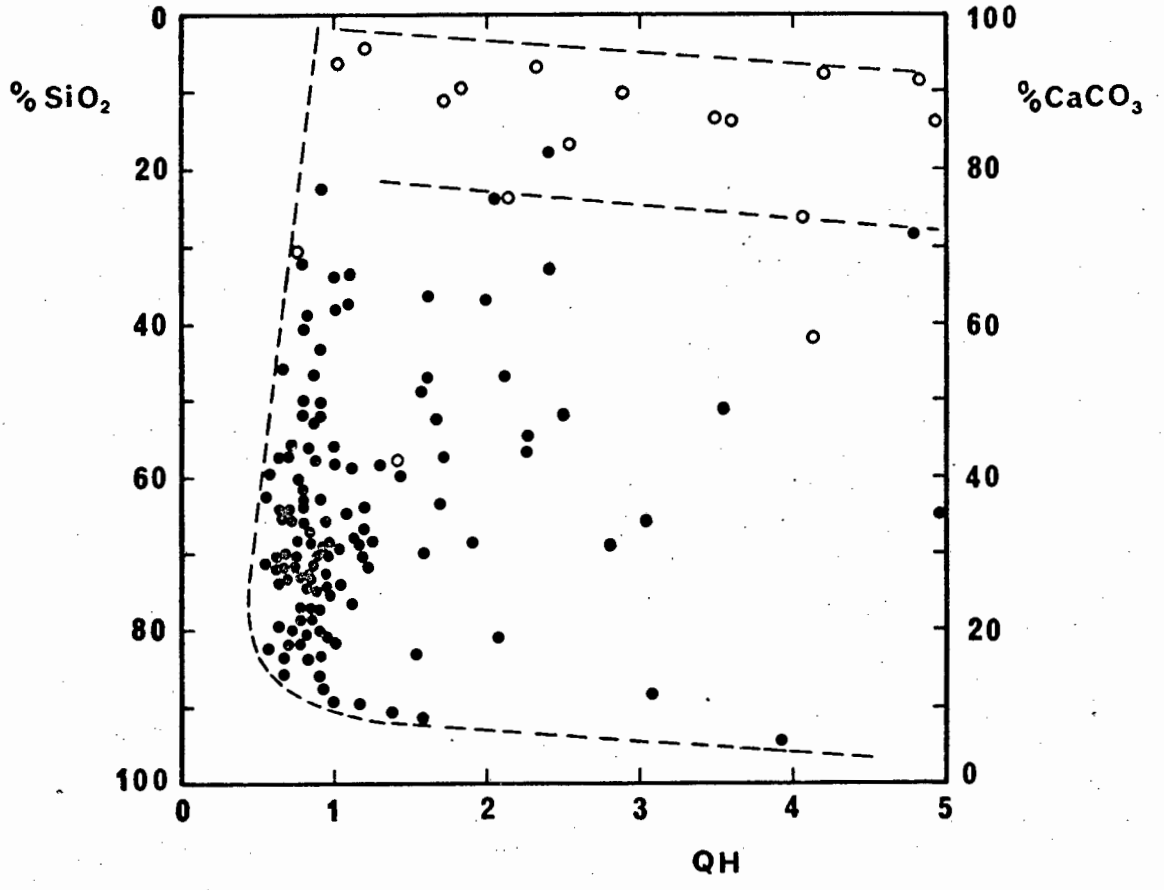

Fig. 95. The relationship between sorting and the quartz content of the terrigenous component

These samples are grouped very closely around the actively abrading zones in Saldanha Bay, which were localized on the inner abrasion platform and the North Channel margins. In these areas the total terrigenous sediment contributes less than 10% to the total sediment.

The local supply of coarser terrigenous sediment is so low that it has virtually no influence on the overall size characteristics of the terrigenous sediments. This is well illustrated in Fig. 94, where mean diameters were plotted against the total quartz content of the sediment. The size control over the total sediment by the carbonate content must, therefore, be a feature of the bioclastic component. This aspect is also demonstrated when plotting relative sorting of the terrigenous component against the relative concentration of each component (Fig. 95). Almost the entire fine population is grouped around QH = 1, irrespective of the contribution of any one of the two components. Only the coarse population appears to decrease rapidly in sorting as the quartz content increases.

Perhaps the most striking difference between the terrigenous component and the total sediment is recorded in their respective skewness patterns. Whereas the total sediment in the inner bay is predominantly negatively skewed (viz. Fig. 78), this trend is completely reversed in the terrigenous skewness pattern (Fig. 96). Over large areas the terrigenous sediments are positively skewed. A number of small areas where sediments are negatively skewed appear to outline the localities at which mixing has taken place. This feature is perfectly reflected in the mean diameter vs. skewness diagram (Fig. 97). About 83% of all samples belonging to the fine population are now concentrated in the upper right corner of the diagram. It will be recalled that a similar, but smaller grouping was observed in the respective plot of the total sediment (viz. Fig. 80) and that this was interpreted as reflecting the inherited size characteristics of the parent population. This conclusion is now confirmed. An interesting feature of this sample group is their overall low $CaCO_3$-content which rarely exceeds 40%.

In the section on the total sediment, it was shown that the two converging arms of the point cluster in Fig. 79 reflect the typical image of two progressively mixing hydraulic pupulations. The terrigenous component shows some significant deviations from this trend. Although

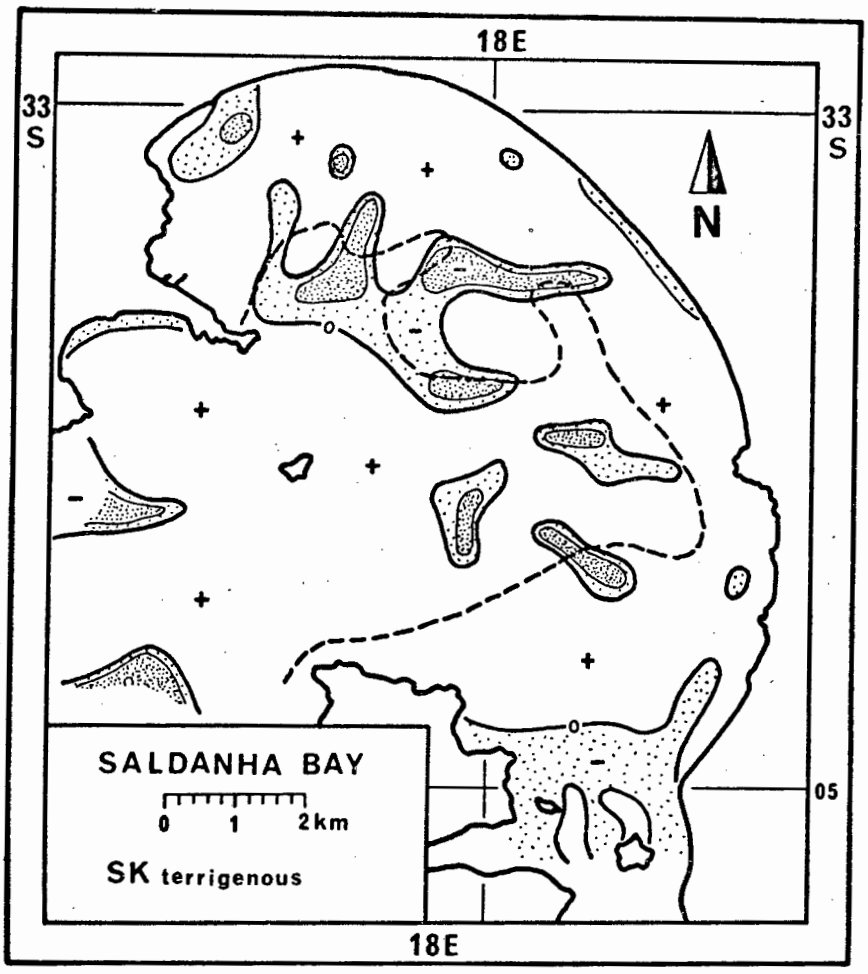

Fig. 96

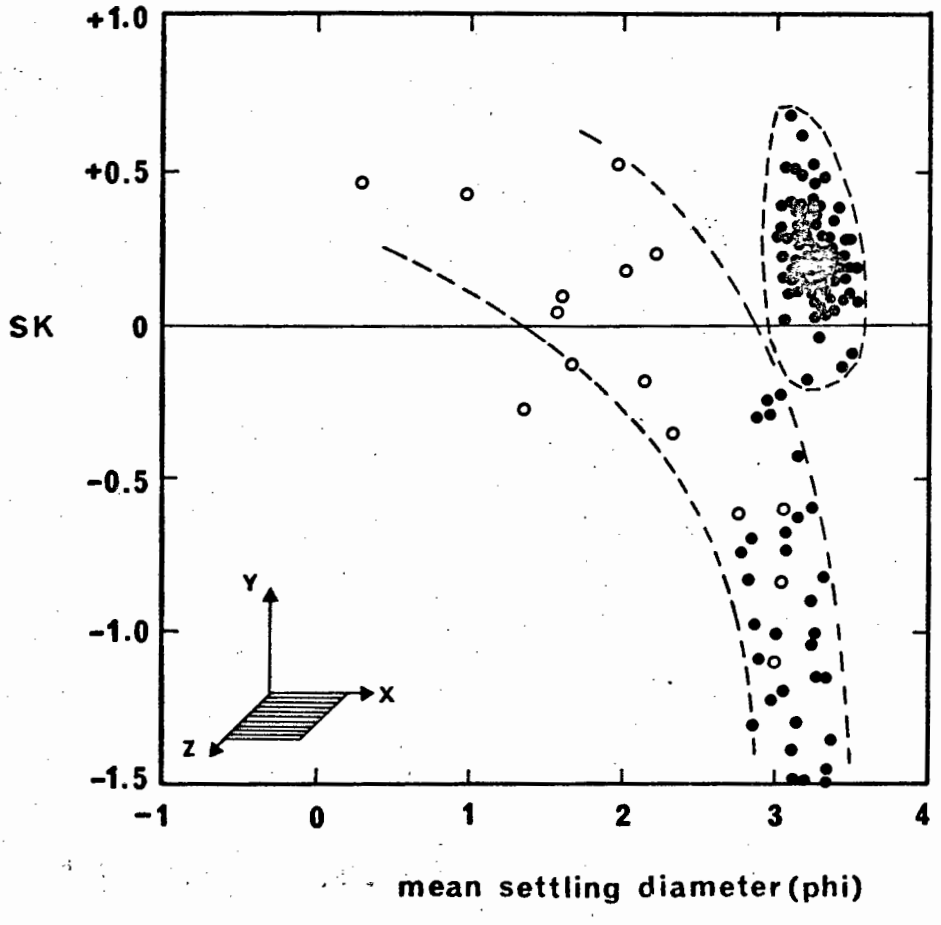

Fig. 97. The relationship between mean diameter and skewness of the terrigenous component

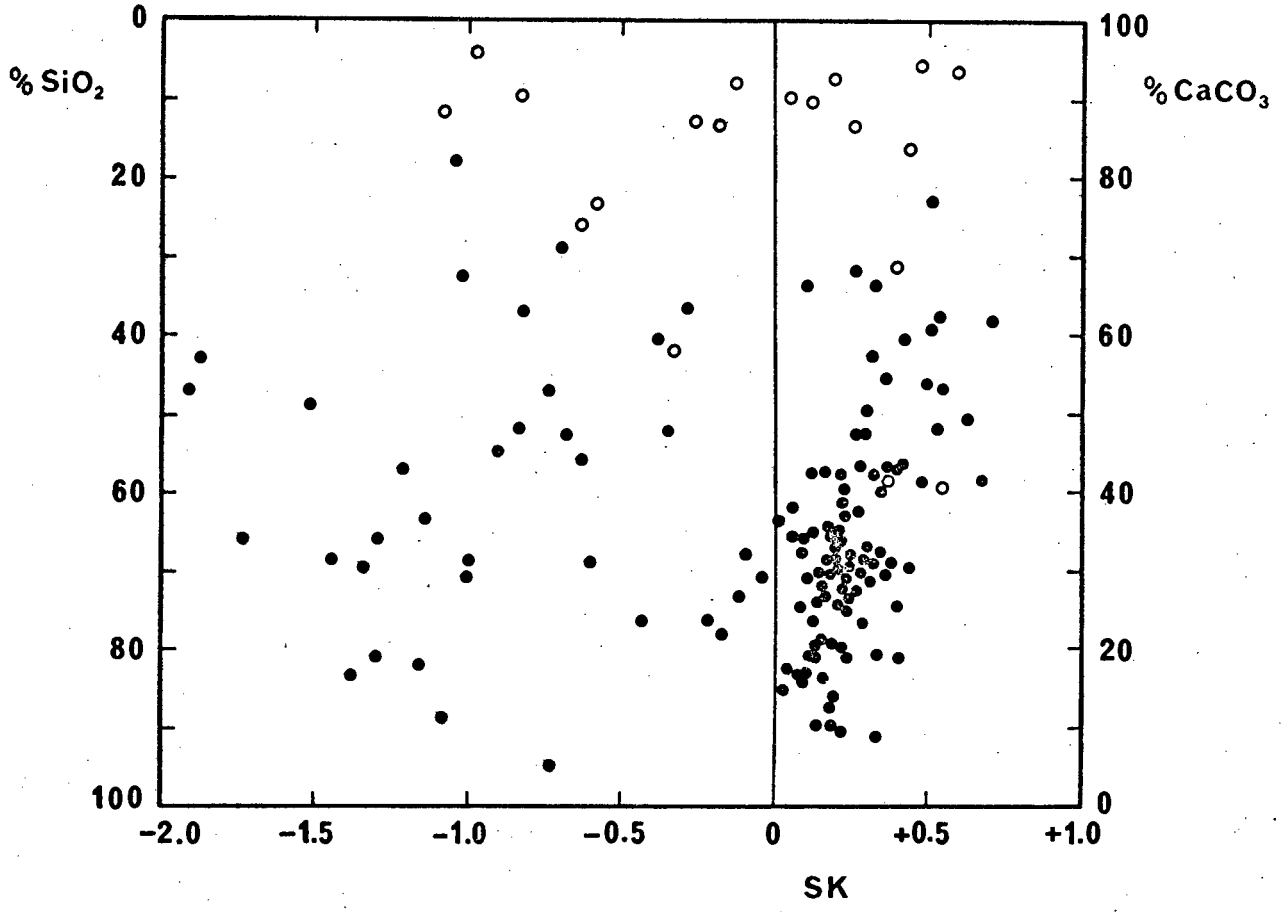

Fig. 98. The relationship between skewness and quartz content of the terrigenous component

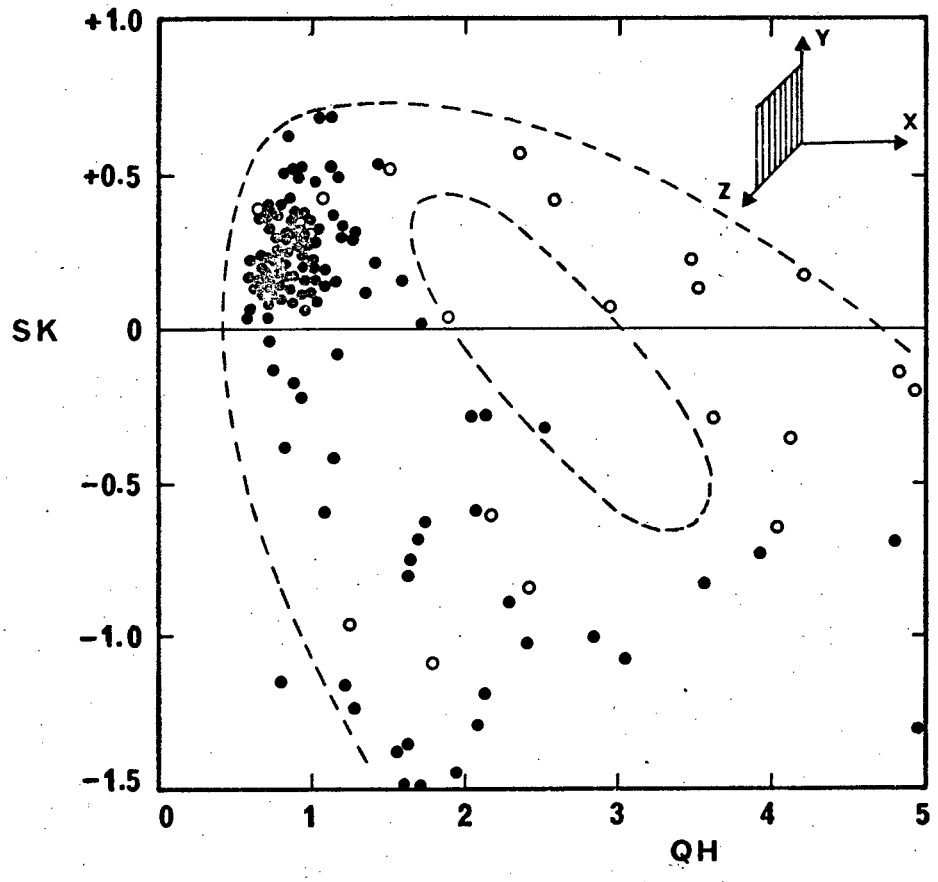

Fig. 99. The relationship between sorting and skewness of the terrigenous component

mixing is observed in about 15% of the samples, the remaining 85% appear to be completely separate. This is attributed to the fact that the coarse terrigenous population, i.e. medium, coarse and very coarse sands, is extremely scarce in Saldanha Bay. The effect of mixing is, therefore, restricted to the immediate vicinity of the local production zones. Since the total sediment shows considerably stronger mixing, it is concluded that this is caused by the bioclastic component which appears to be predominantly supplied from local sources. This feature is investigated in the following section.

4.4.3. Bioclastic Component

The size parameters of the bioclastic component were not directly measured by settling tube analysis, but were calculated by subtracting the terrigenous size distribution from that of the total sediment. The results obtained in this manner should, therefore, be regarded as approximations only.

The size distribution patterns of very coarse sand (Fig. 100), coarse sand (Fig. 101) and medium sand (Fig. 102) conform, in most respects, to the general situation observed in both the total sediment and the terrigenous component. In contrast to the terrigenous patterns, each respective size fraction of the bioclastic component is spread over considerably larger areas. The spreading patterns centre around the abrasion platform and the rocky shorelines which border on the North Channel. There is no evidence that any sediment of this size group is supplied from outside the system. Some coarse bioclastic sediment occurs on the proximal tidal delta, where the coarse bedload of the tidal channels is deposited as a lag from the progressively decreasing tidal currents. This area actually forms an integral part of the lagoonal system, although physiographically it is part of Saldanha Bay.

Small amounts of this coarser channel sediment has found its way into the southeastern part of the bay. In this respect it does not differ from the terrigenous component and, as a result, this feature is also reflected by the total sediment. An interesting feature of the distribution pattern of the medium bioclastic sand fraction is the faithful manner in which its inshore 10% concentration limit is contoured by the 50% $CaCO_3$ contour.

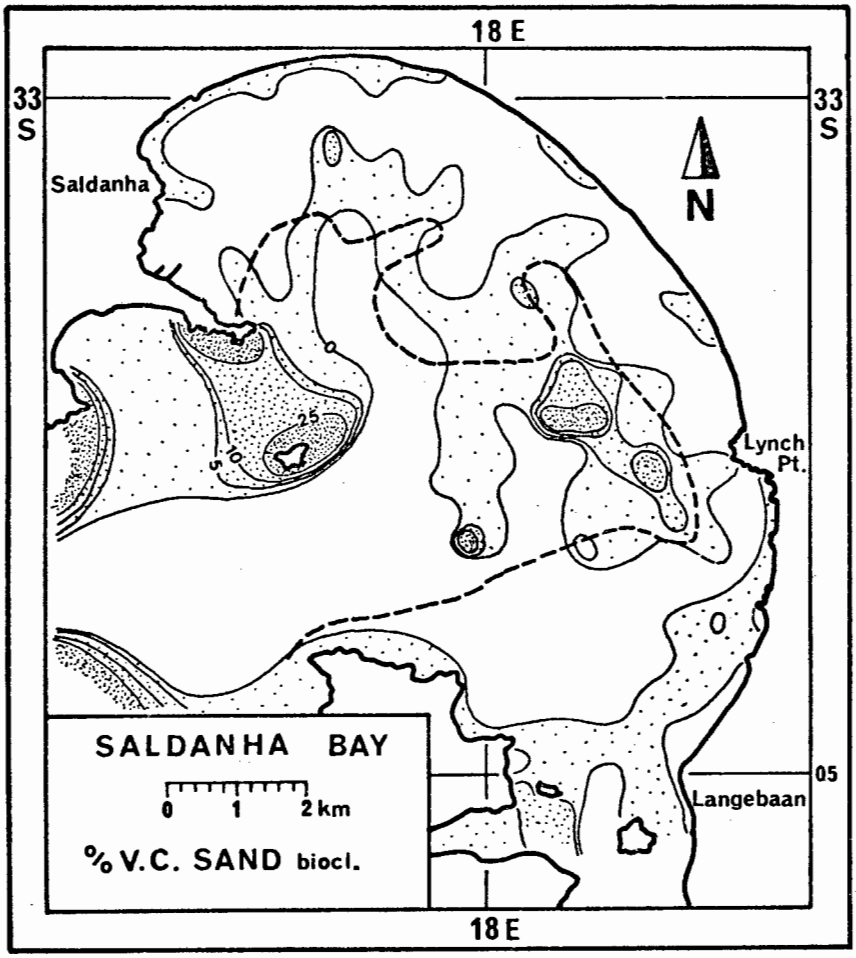

Fig. 100

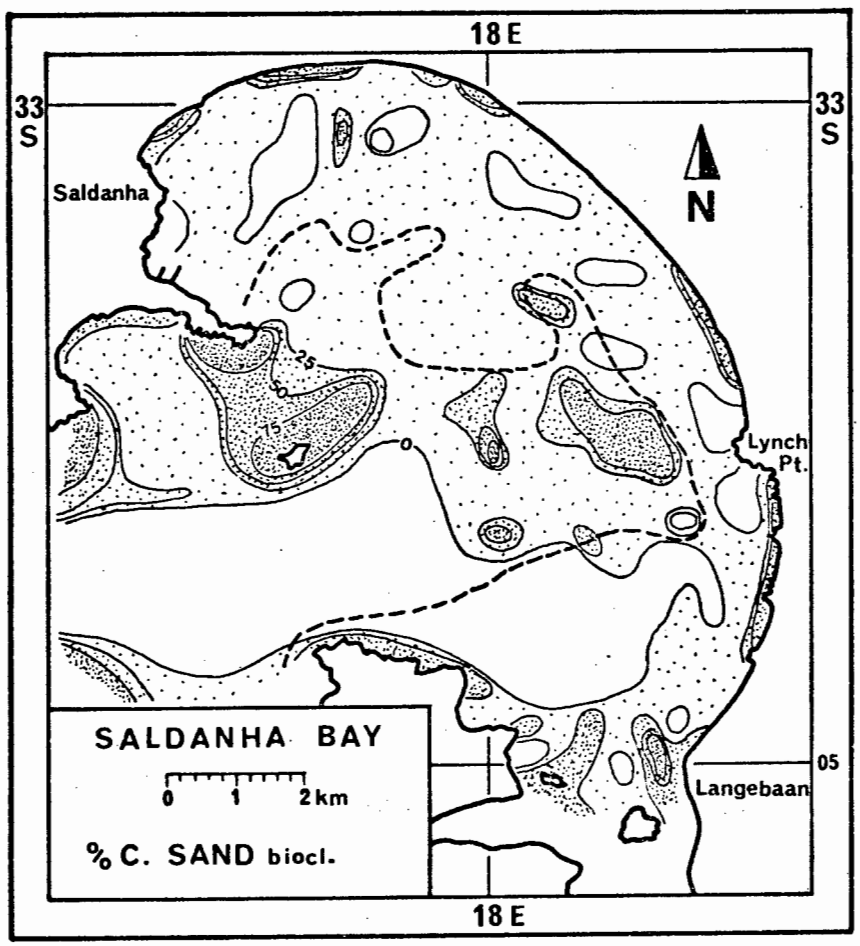

Fig. 101

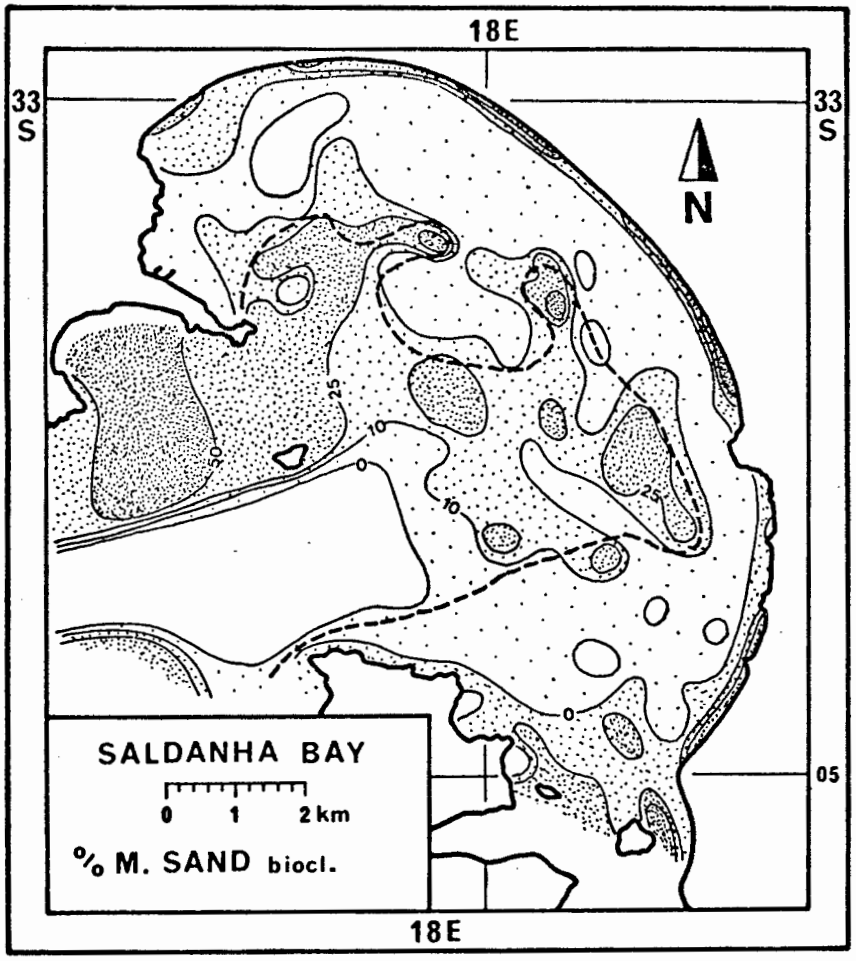

Fig. 102

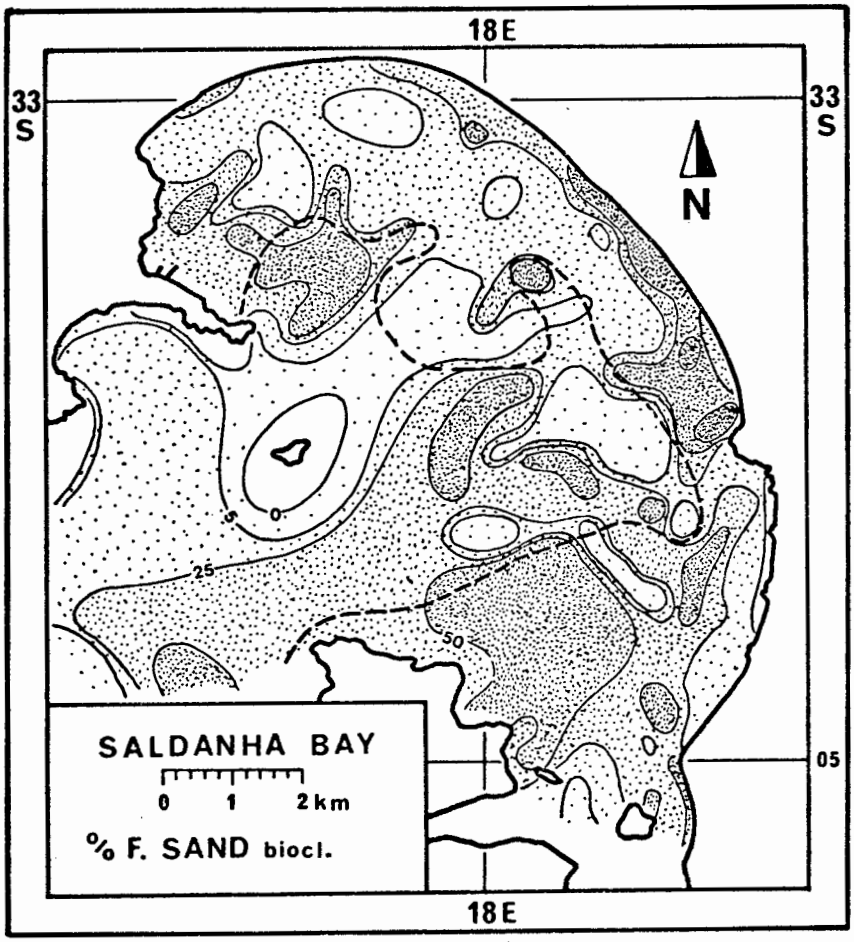

Fig. 103

A significantly different trend is observed when comparing the distribution of fine bioclastic sand with that of fine terrigenous sand. Whereas the terrigenous fine sand fraction has a single dominant spreading centre located in the tidal delta, at least four independent depositional areas of fine bioclastic sand are outlined in Fig. 103. The largest of these is situated in the tidal delta, thus conforming to the terrigenous spreading centre. However, unlike the terrigenous pattern, the tidal delta deposit is sharply separated from the central exposed part of the bay by a narrow belt of very low fine sand concentration.

A second depositional unit is located on the lower abrasion platform. The origin of this sediment is not clear, but its relative isolation suggests that it was probably eroded on the inner abrasion platform and, subsequently, transported offshore until energy levels became too low to uphold further transport. Inshore of this deposit, a third depositional unit of fine bioclastic sand is encountered. Highest concentrations occur just north of Lynch Point. This sediment is quite obviously derived from the northeastern beach where some cliff erosion is still supplying material to the beach today. From there it stretches south in a tongue which ends just southwest of Lynch Point. This feature probably provides the greatest support for a southerly longshore current in this area. Near Lynch Point, i.e. in the most exposed part of the bay, this return flow appears to develop into a strong rip current which seems to lose its power at the -10 m level. The influx of sediment consists predominantly of bioclastic material since a similarly clear trend is not observed in the terrigenous fine sand pattern. Two return flow cells are, therefore, clearly established which counteract the general wave dominated regime in the bay, producing some well defined depositional features.

A fourth and final depositional area of fine bioclastic sand is located in the northern offshore part of Saldanha Bay. It is completely separated from the other three areas. Its source is without doubt the North Channel production zone, as it neatly links up with the size sequence of bioclastic sediments, beginning with the very coarse sands in North Channel itself. From here the sediment is gradually separated into sequentially overlapping size fractions, each of which is deposited at its respective stable position in the course of the decreasing energy front defined by the wave refraction pattern.

This pattern of fine sand distribution indicates that only the very coarse and the coarse sands have remained in the immediate vicinity of the source areas. Medium sand follows close by, whereas fine sand occupies areas which are clearly separated from the actual source areas. A substantial proportion of fine bioclastic sediment is, therefore, supplied from the local production zones. This is a significant contrast to the fine terrigenous sand which is predominantly supplied from outside the bay. However, this feature is not unexpected, because the material supplied locally consists predominantly of bioclastic sediment.

The distribution of very fine bioclastic sand is again similar to the pattern of the terrigenous counterpart. It covers a smaller overall area (Fig. 104), and is concentrated shoreward of the 50% $CaCO_3$ limit. As a result, it contributes less than about 30% on average to the total sediment, if the smaller amounts of coarse and medium sands are not included. Very fine bioclastic sediment forms a subordinate component in the tidal delta, and is practically absent in the North Channel and in the North Bay. As in the case of the terrigenous fine and very fine sediment, the South Channel also acts as a deep-water sink for the bioclastic very fine sand fraction. An interesting aspect is the shallower position of the 50% concentration limit mentioned in the previous section.

The distribution patterns of the mean diameters of the bioclastic and the terrigenous components differ substantially with respect to the total area occupied by fine and very fine sand respectively. As shown above, the bioclastic sediment contains a far larger fine sand proportion than the terrigenous sediment. As a result, the mean diameter map of the bioclastic component displays large areas which are occupied by fine sand (Fig. 105). Very fine bioclastic sediments are evidently far less abundant than very fine terrigenous sediments.

The relative sorting pattern of the bioclastic sediment differs in two important aspects from that of the terrigenous sediment. Firstly, it is considerably less well sorted and secondly, the areas of poorest sorting do not coincide in every respect (Fig. 106). Especially in the northern bay, the mixing zone extends considerably further inshore, thereby constricting the better sorted inshore sand prism into a narrow belt. This feature is ascribed to the much larger supply of fine bioclastic sand which, as a result, has penetrated much further into the very fine sand domain. Whereas almost

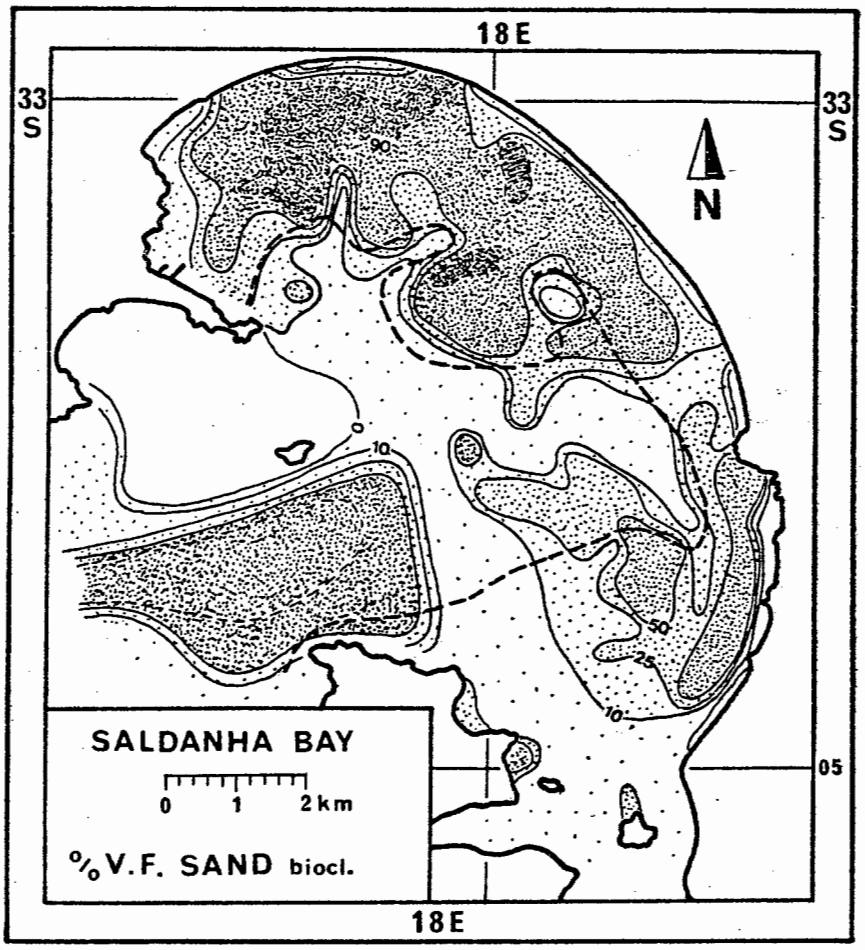

Fig. 104

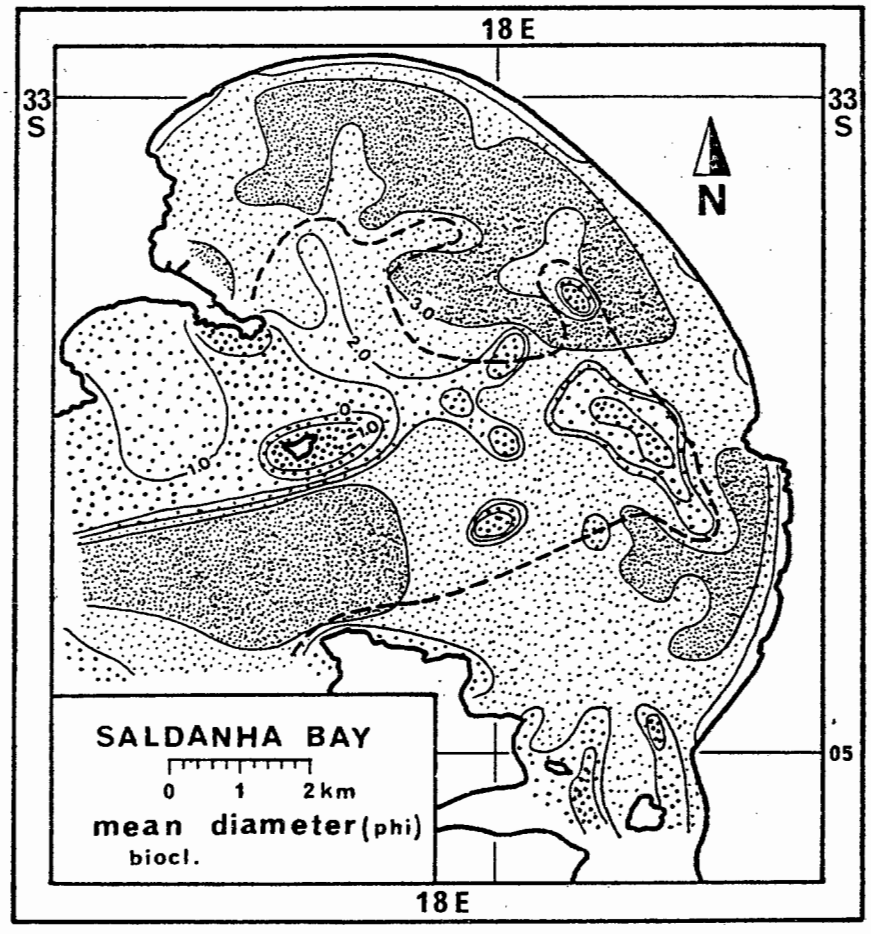

Fig. 105

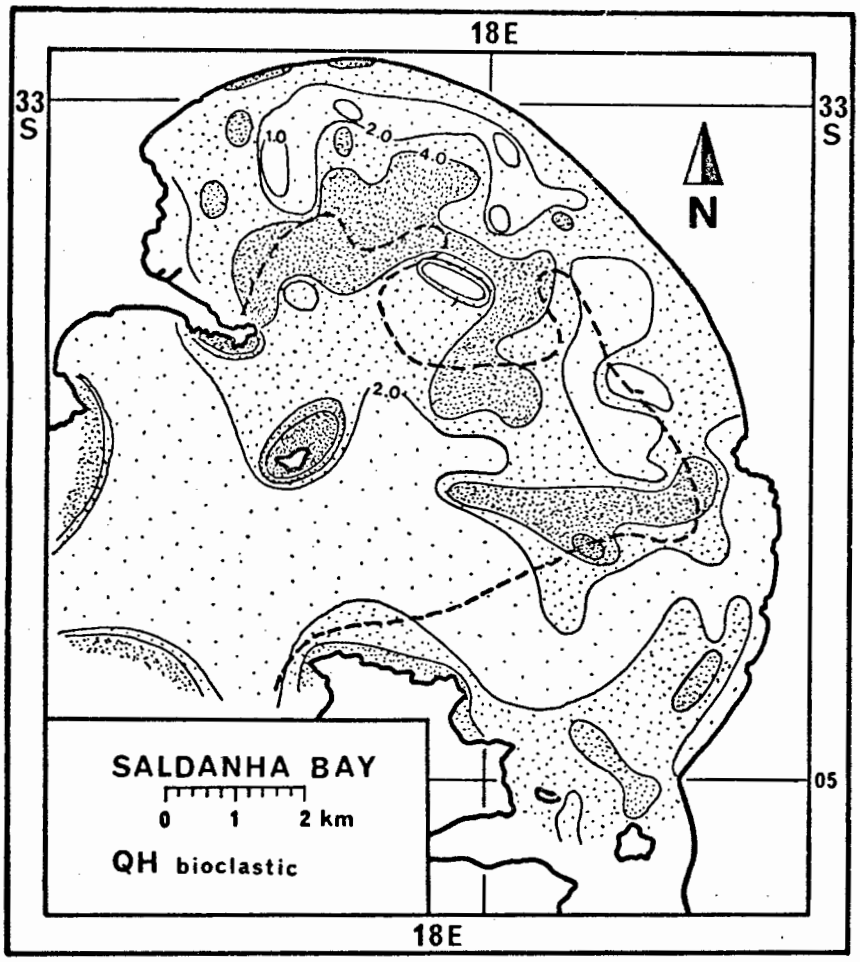

Fig. 106

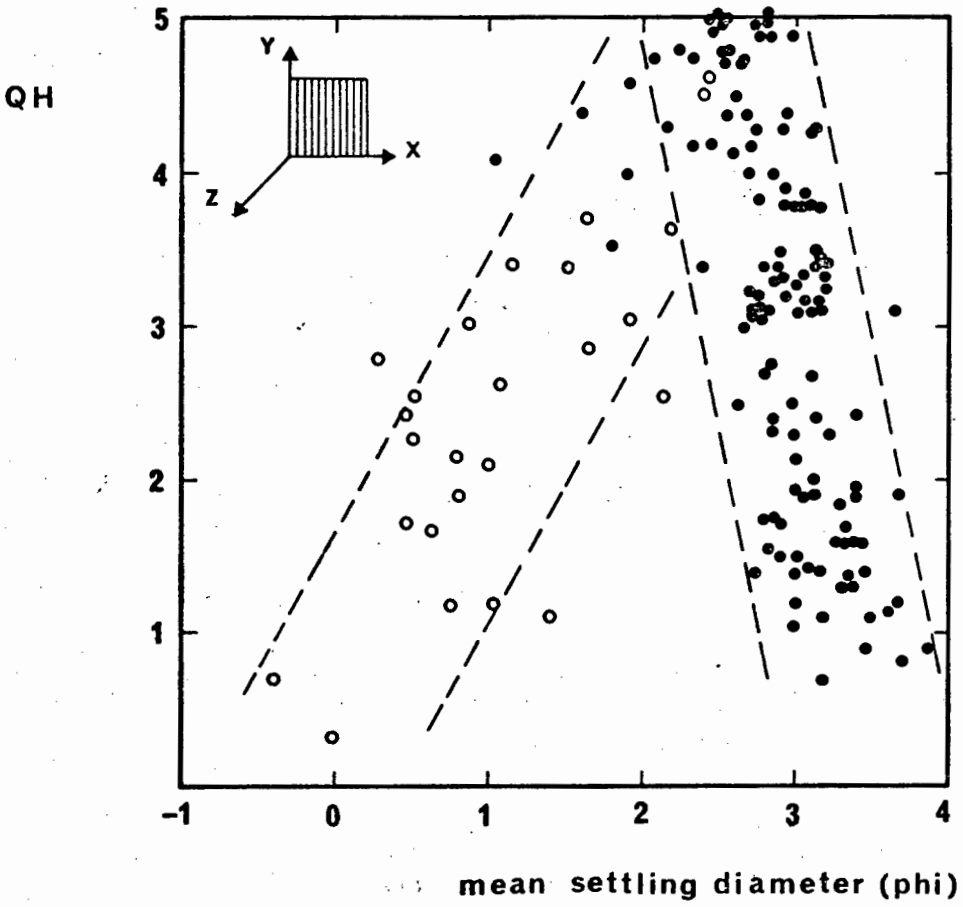

Fig. 107. The relationship between mean diameter and sorting of the bioclastic component

the total fine and very fine sand component of the terrigenous sediment formed part of the fine hydraulic population, a large proportion of the fine bioclastic sand, and probably also a minor proportion of the very fine bioclastic sand, actually represents the fine end-member of the coarser hydraulic population. This inequality between the proportional constitution of each bioclastic and terrigenous hydraulic population has resulted in a rather complex relationship between the individual components of the total sediment.

The difference in sorting between the bioclastic and the terrigenous sediments is parhaps best illustrated when comparing the respective mean diameter vs. sorting pattern of the former (Fig. 107) with that of the latter component (viz. Fig. 93). Whereas 77% of the terrigenous sediment was found to be extremely well sorted, only 2% of the bioclastic component reach this optimal level. In Section 3.5. it was demonstrated that, in hydraulically equilibrated sediments, the bioclastic component should reach an average optimal degree of relative sorting of around 1.5. In this context only about 20% of the bioclastic samples appear to be hydraulically equivalent to the extremely well sorted terrigenous sands. This feature, in fact, supports the previous conclusion that only a small proportion of the fine bioclastic sediments were carried into the bay in conjunction with the terrigenous sediment. This is further corroborated by the observation that the very fine sands in Langebaan Lagoon are very low in carbonate.

The effects of relative concentration levels on the mean diameters and the sorting levels of the bioclastic component are investigated in Fig. 108 and Fig. 109, respectively. It will be remembered that no such influence was observed on the corresponding terrigenous parameters. Both bioclastic size parameters, on the other hand, are clearly dependent on relative concentration levels, especially between the 30% and the 80% $CaCO_3$ levels. This feature further supports the conclusion that most of the bioclastic sediment in Saldanha Bay forms a successive, size-sorting sequence of a single hydraulic parent population, related to source areas within the system. In both cases it is the bioclastic trend that controls the overall trend observed in the total sediment (viz. Fig. 83 and Fig. 84).

The striking difference between the skewness patterns of the terrigenous and the total sediment was pointed out previously. Since terrigenous and

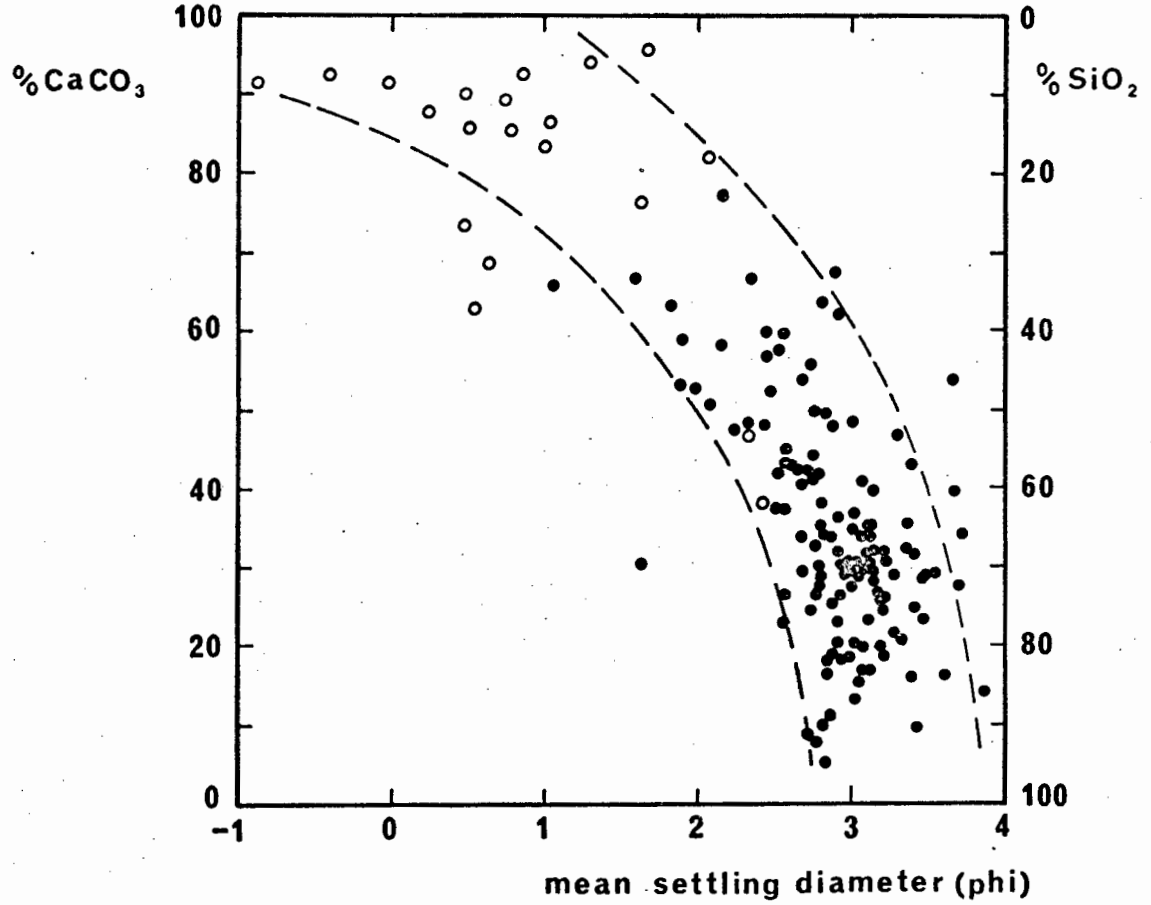

Fig. 108. The relationship between mean diameter and carbonate content of the bioclastic component

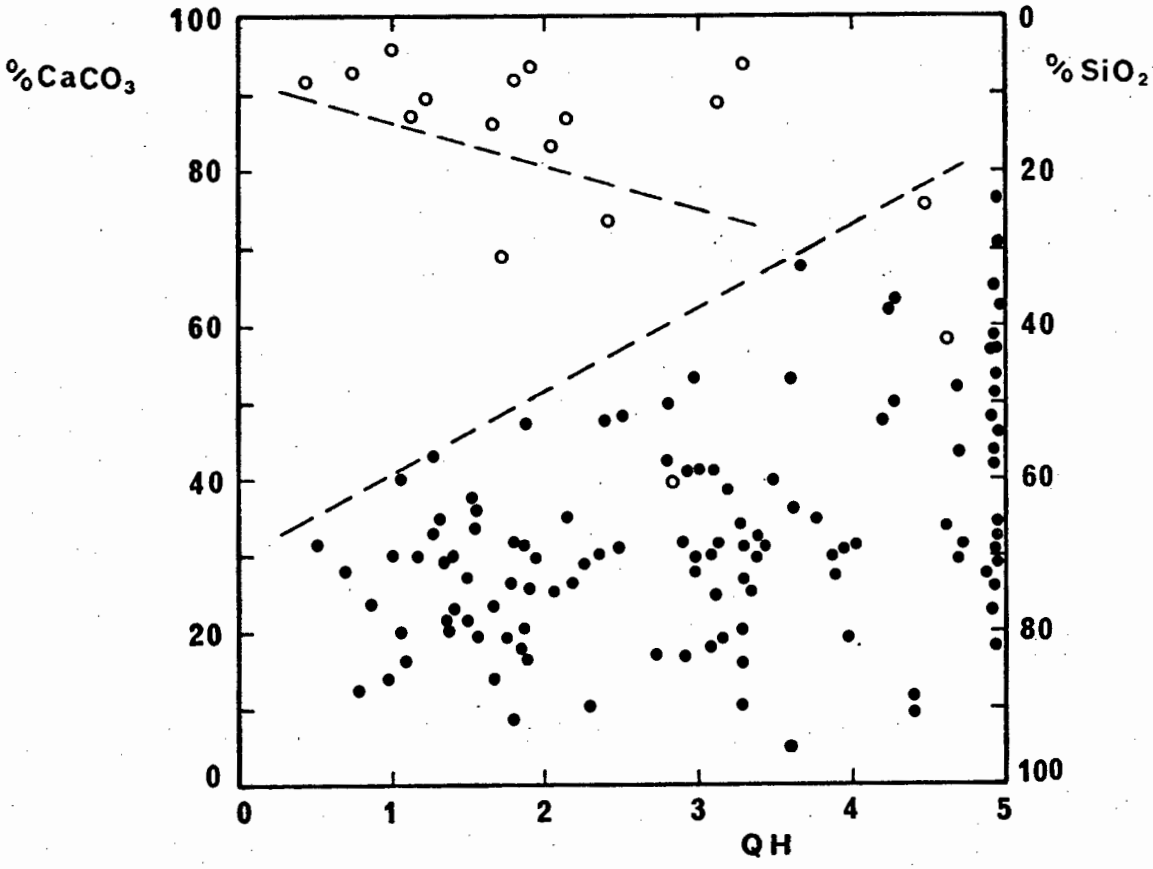

Fig. 109. The relationship between sorting and carbonate content of the bioclastic component

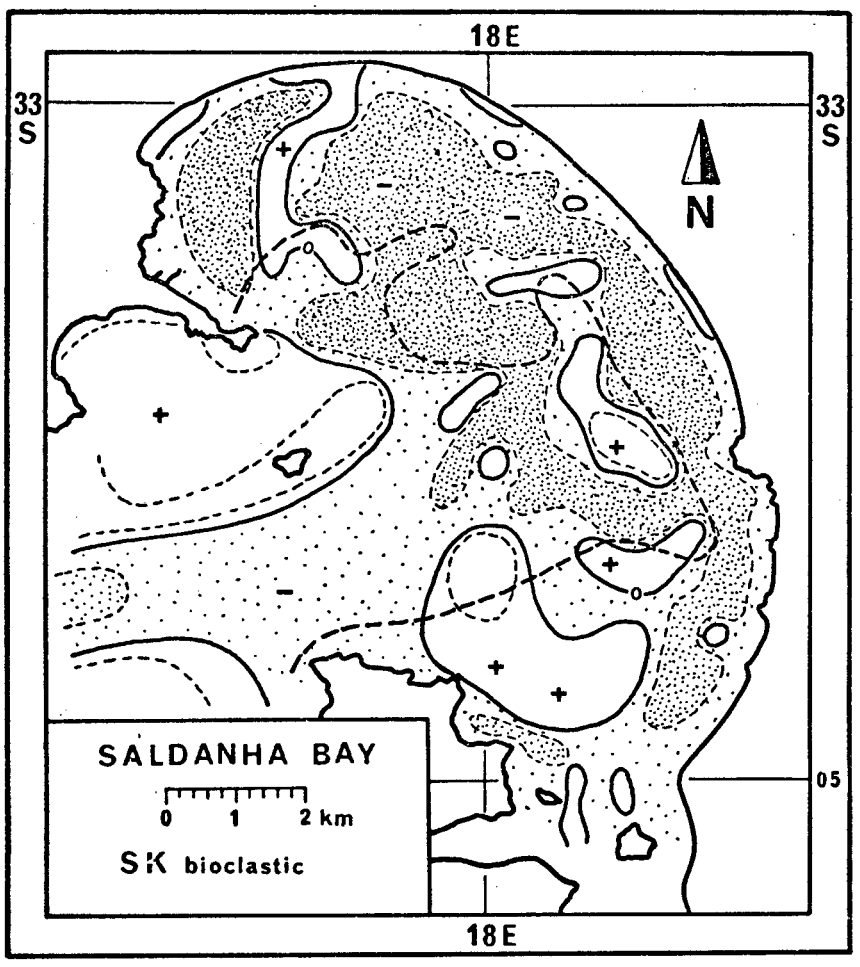

Fig. 110

bioclastic skewness in combination are responsible for the total picture, one might expect a significantly different skewness pattern between the two components. This is indeed reflected in Fig. 110, where the situation is almost entirely reversed. Most of the bioclastic sediment in the inner bay is very to extremely negatively skewed, whereas the terrigenous sediment was predominantly positively skewed (voz. Fig. 96). The total sediment, in which both are combined, presents a negatively skewed picture. Only the tidal delta and the major source areas are positively skewed in both cases.

This aspect is perhaps the most convincing evidence in favour of the interpretation about origin and mixing process of the two hydraulic populations as outlined above. Even if the total fine population were slightly negatively skewed when it entered the bay, it would have to be mixed, either with a substantial proportion of strongly negatively skewed fine sediment supplied from local sources, or a proportionally smaller but coarser population, in order to produce the overall skewness pattern of the total sediment. The evidence, as outlined above, strongly favours the second situation.

Further evidence in support of this conclusion is supplied by the mean diameter vs. skewness plot (Fig. 111). The trend which was already indicated in the mean diameter vs. sorting relationship is even more clearly defined. Only 11% of the fine bioclastic population corresponds to the position defined by the terrigenous sediment as reflecting the parent population.

In the mean diameter map, it was demonstrated that, on average, the bioclastic sediments were coarser than the terrigenous ones, especially in the fine sand category. This feature is illustrated quantitatively in Fig. 112, where the mean diameters of the two components are directly compared. The diagram illustrates the hydraulic equivalence of the two components. The closer they lie to the central diagonal line, the better they are equilibrated. It is quite evident that the least equilibration is observed in the fine sand size. This region would thus represent the samples in which mixing between two independent hydraulic populations has its strongest effect. The observation is in full agreement with the conclusions reached earlier.

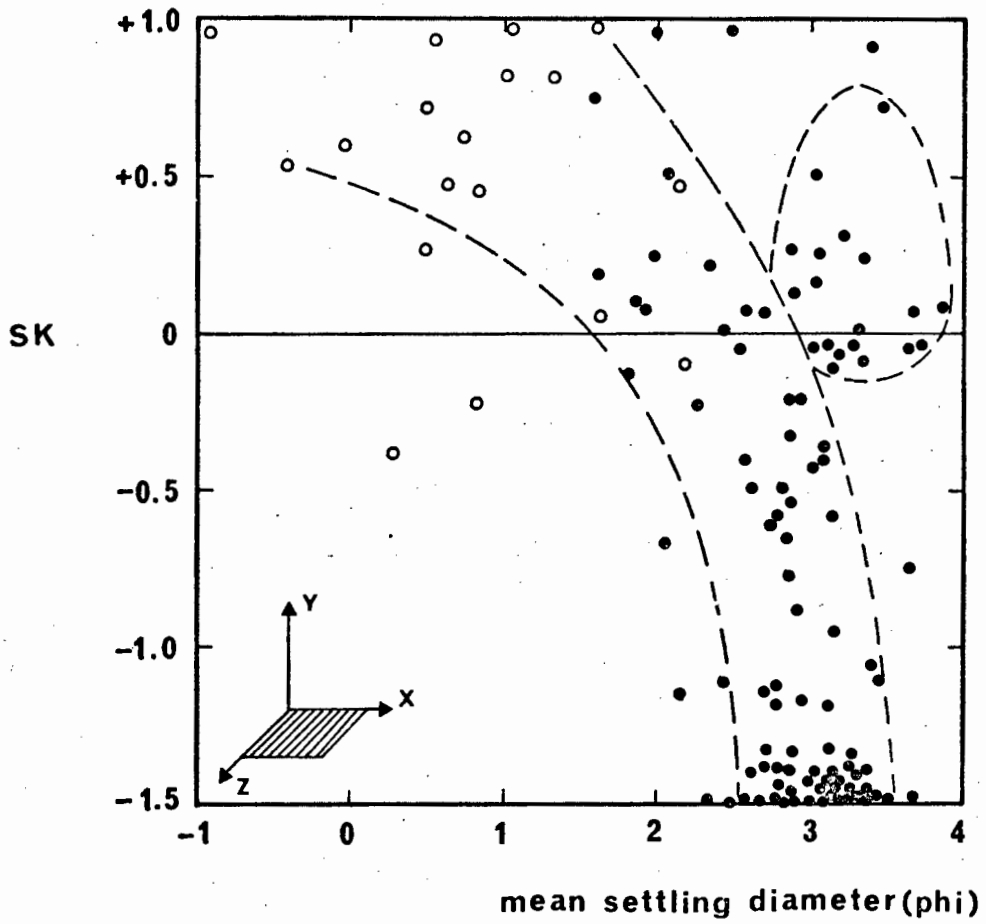

Fig. 111. The relationship between the mean diameter and skewness of the bioclastic component

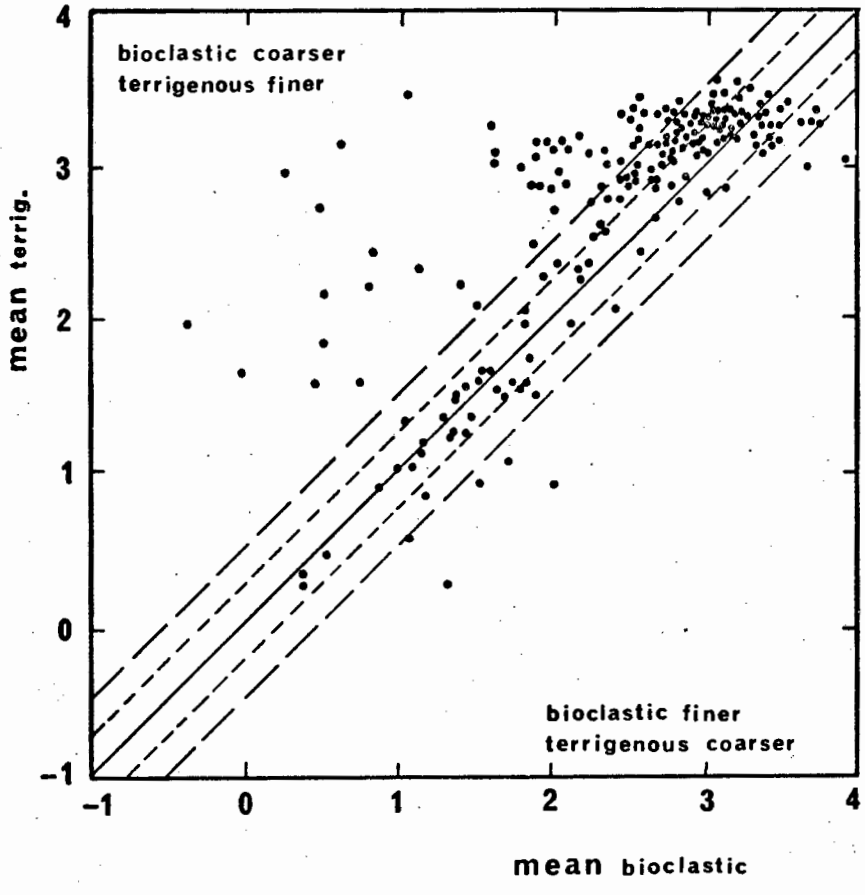

Fig. 112. The hydraulic relationship between the terrigenous and the bioclastic component in Saldanha Bay

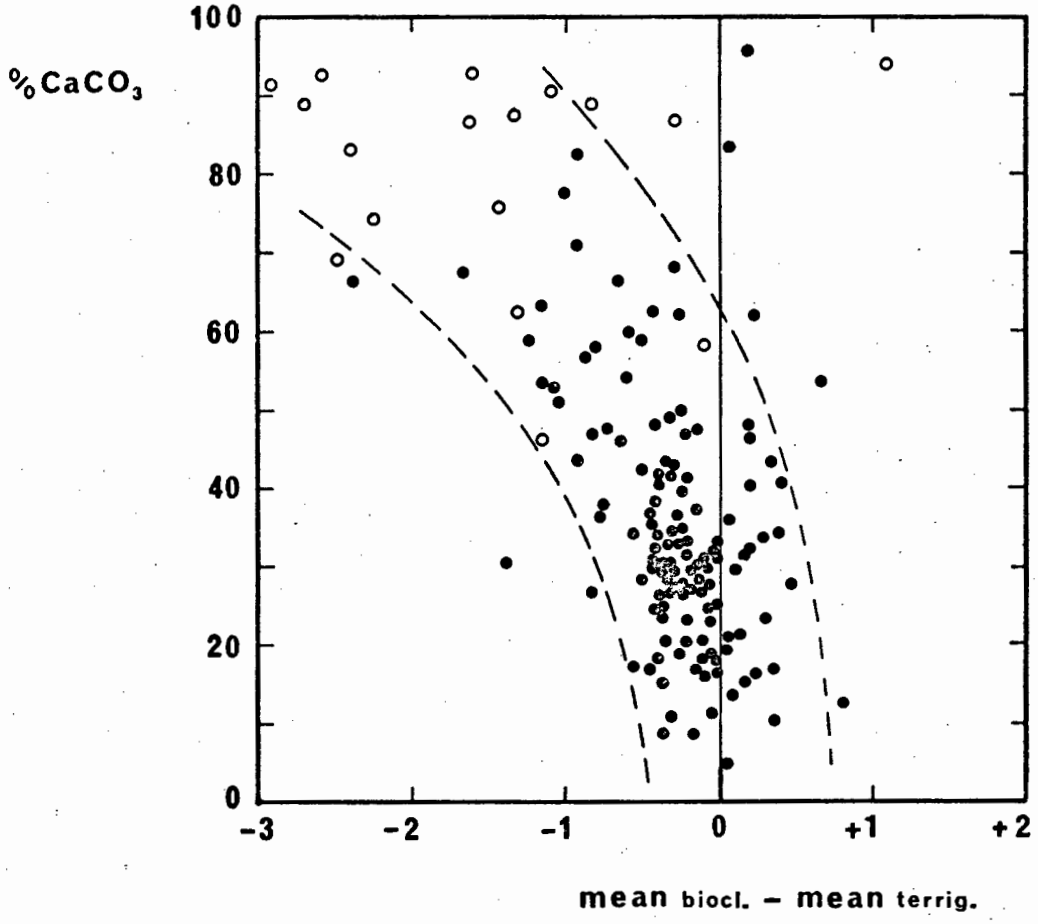

Fig. 113. The deviation from hydraulic equilibrium between the two sediment components in relationship to the carbonate content of the sediment

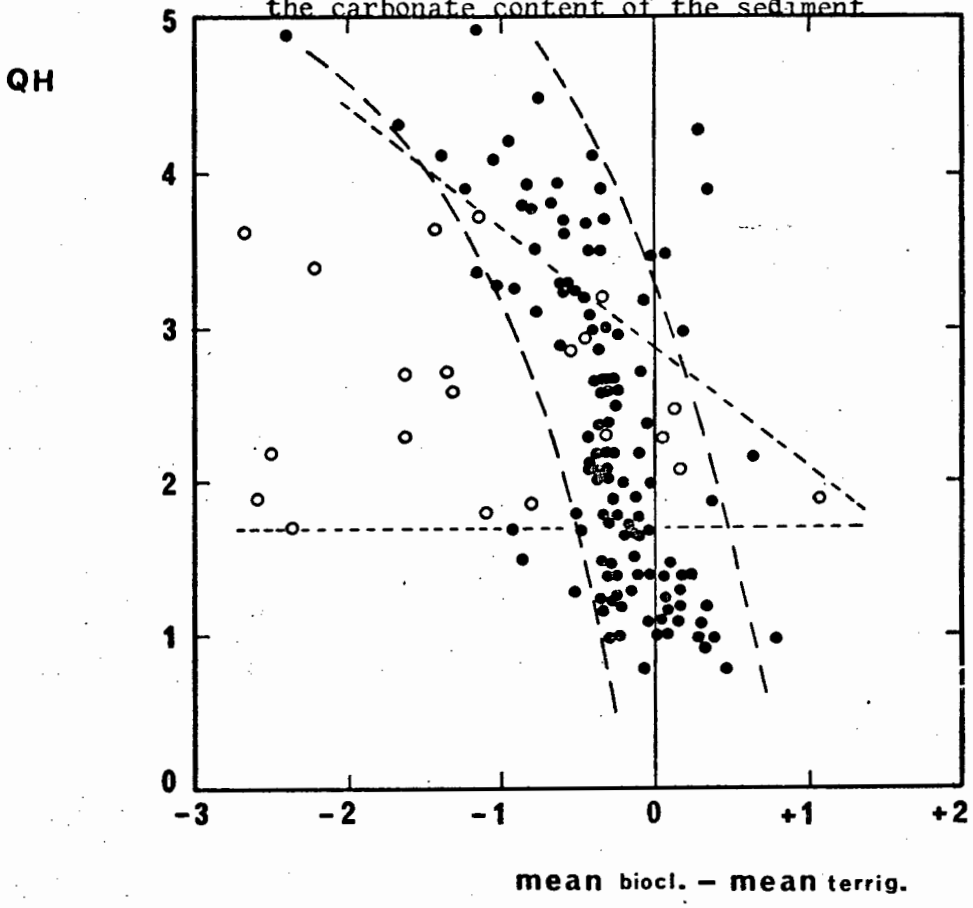

Fig. 114. The deviation from hydraulic equilibrium between the two sediment components in relationship to the sorting of the total sediment

This hydraulic relationship between the two components should also be reflected in their relationship to the carbonate content. In Fig. 113 the deviation from complete hydraulic equilibrium between the two populations is plotted against the carbonate content. Clearly the deviation increases with increasing carbonate content. It can thus be concluded that most of the bioclastic material does, in fact, form part of the coarser hydraulic population, whereas most of the terrigenous sediment forms the fine hydraulic population. In each case the other component group constitutes only a minor proportion of the respective hydraulic population. In accordance, the relative sorting levels progressively decrease the stronger the deviation between hydraulic equivalence becomes (Fig. 114).

4.5. MODES OF SEDIMENT TRANSPORT AND DEPOSITION

In previous sections, it was demonstrated that the size characteristics of the total sediment are a complex function of the combined features of the two hydraulic populations, each of which consists almost entirely of a single sedimentary component. As a result, the grain size patterns of the total sediment tend to obscure, and even obliterate, the more subtle characteristics of the individual hydraulic populations. On the basis of the total sediment alone, it was possible to detect a foreign fine sediment component in the system and to locate its source with high probability in Langebaan Lagoon. However, the trends of the total sediment did not reveal with certainty the proportions of coarse or fine sediment supplied from local or foreign sources.

By investigating the size characteristics of the two main sediment components separately, it was possible to assess semi-quantitatively the relative proportions contributed by the bioclastic component and the terrigenous component in each size fraction. Furthermore, the specific spreading patterns of successive size classes of each component revealed that by far the largest proportion of bioclastic material was actually supplied from sources within Saldanha Bay, whereas most of the terrigenous sediment was carried in from outside. The two hydraulic populations in Saldanha Bay, therefore, consist essentially of a locally supplied, coarser bioclastic one with a small terrigenous component, and of a finer, predominantly terrigenous population containing a small bioclastic component originating from outside the bay.

The two component groups also indicated a differential response to the mechanism of sediment transport, although it has not become clear in which manner this might be happening. In this section specific modes of the depositional process are investigated in order to gain a better understanding of this behaviour. To achieve this, the empirical model of Passega (1957), as outlined in Section 3.6.3., was utilized.

The relationship between the first percentile and the mean diameter of the total sediment is illustrated in Fig. 115. In terms of the model, the fine population is predominantly transported in the upper bottom suspension (Saltation 2), graded suspension and uniform suspension (together 79% of all samples), whereas the coarser population is mainly transported in form of a traction carpet and in lower bottom suspension (together 78% of all samples). The spatial relationship between the individual modes is presented in Fig. 116. The pattern is surprisingly similar to the mean diameter map, and almost identical in design to the combination of the dominant size fractions into a single map. This striking correlation in itself strongly supports the approach by this depositional model. It demonstrates its usefulness in recognizing depositional processes in relation to depositional environments.

An important aspect in the interpretation of the above pattern is the "rule of irreversibility" of the size-dependent transport mechanisms. In this rule it is stated that sediments transported at a lower hydraulic level (e.g. as bedload) can, under constant hydrodynamic conditions, not bypass an area in which sediments were deposited from a higher hydraulic level (e.g. suspension). Deposition from successive hydraulic levels indicates the direction of the energy gradient. On the other hand, sediments carried at a higher level can, without difficulty, bypass areas deposited from lower levels. This rule does not apply in the narrow velocity range separating the thresholds of erosion and deposition (viz. Fig. 41). Exceptions of this rule usually relate to extreme weather conditions, such as storm surges, in which case coarser material can find its way into predominantly finer depositional units. Cases of this nature have been reported by Reineck and Singh (1972). In Saldanha Bay this situation appears to be rare, although not entirely absent. The ribbon-like patterns of shell deposits along the inner margin of the abrasion platform seem to reflect storm surge activity.

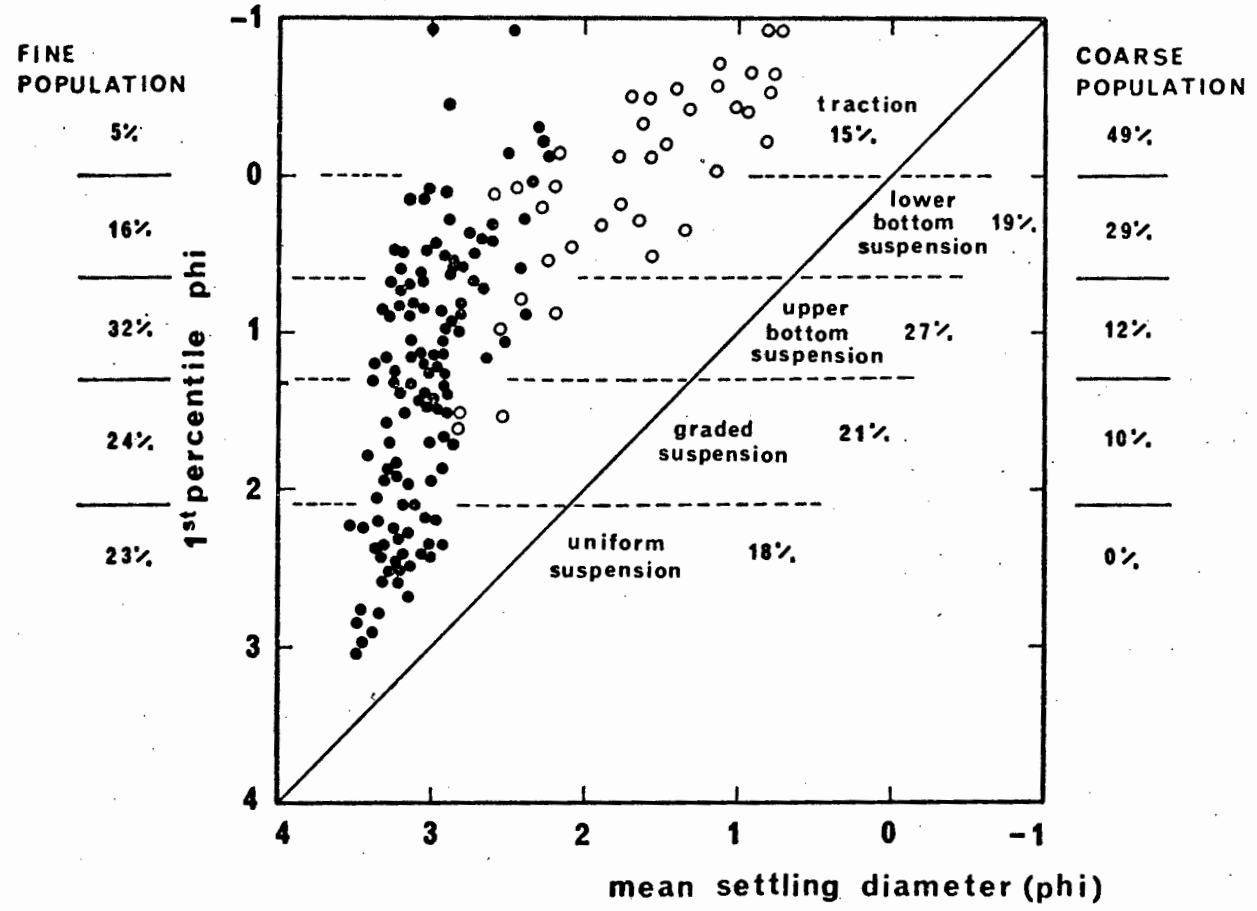

Fig. 115. Modes of sediment transport (Total Sediment)

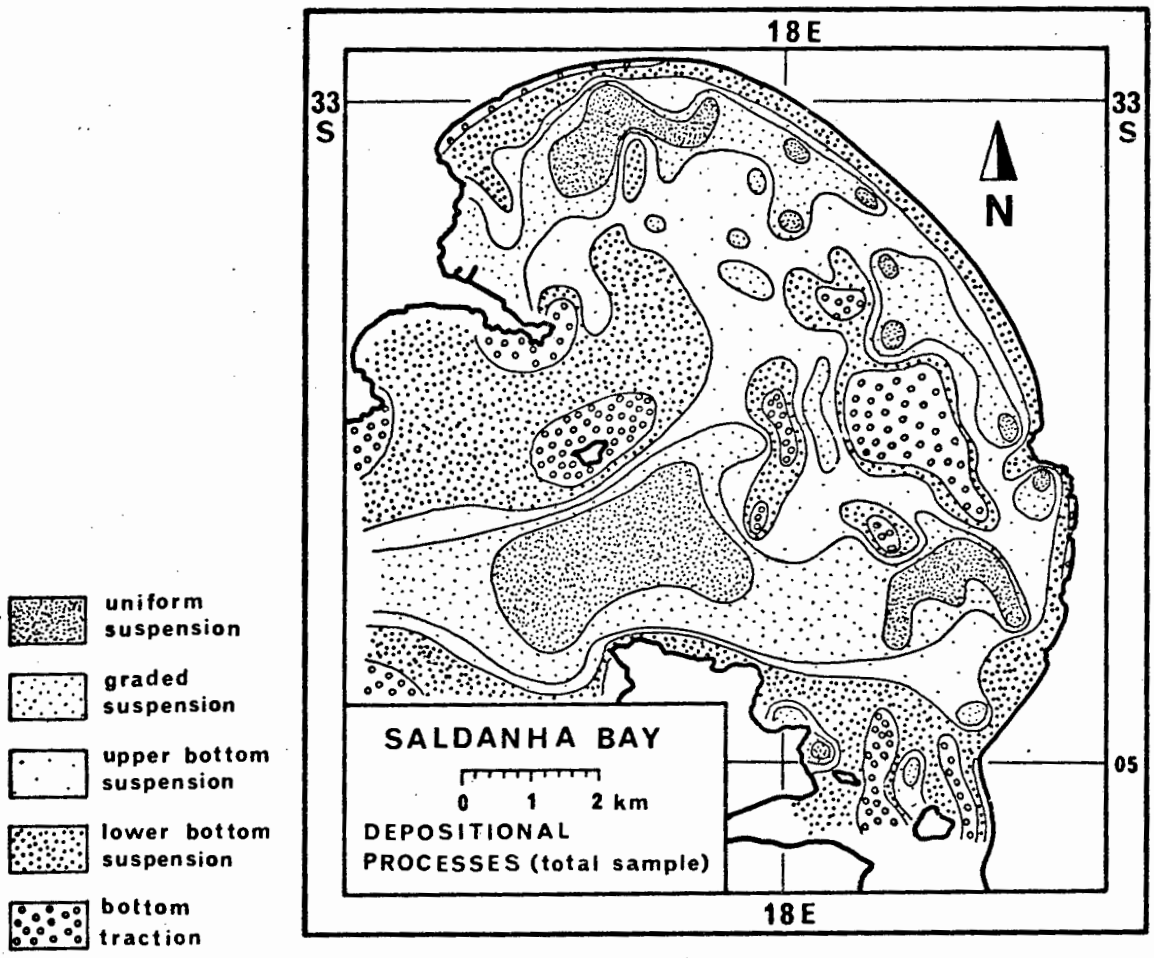

Fig. 116. Sediment transport patterns in Saldanha Bay

The depositional pattern of the total sediment in Saldanha Bay clearly excludes foreign sediment influx that would require transport in bedload, i.e. transport as a traction carpet, lower bottom suspension and upper bottom suspension. As a result, only the fine hydraulic population could possibly have originated from a foreign source. This conclusion is in full agreement with earlier observations based on the spreading patterns defined by successive size fractions.

Since the depositional patterns of the total sediment do not provide any information on the relative proportion that local or foreign sources might have contributed to the fine sediment of the total pattern, this aspect was again investigated by observing the depositional patterns of the terrigenous and the bioclastic components separately. In Fig. 117 and Fig. 118 the CM-diagrams of the two components are contrasted. It is immediately clear that both components follow entirely different depositional modes. Whereas 86% of the samples belonging to the fine terrigenous component are transported in uniform suspension, only 6.4% of the bioclastic samples fall into this category. Alternatively, 64% of the bioclastic samples are transported in a traction carpet, whereas only 1.6% of the terrigenous samples fall into this category.

The areal relationships of the different depositional modes as illustrated in Fig. 117 and Fig. 118 are presented in Fig. 119 and Fig. 120, respectively. The two patterns appear to solve the problem of provenance and dispersal of the individual sedimentary components. The medium, coarse and very coarse terrigenous sands, which are deposited from lower bottom suspension and traction, must originate entirely from sources within Saldanha Bay. The source areas are closely related to the inner abrasion platform and the North Channel/North Bay area. The fine terrigenous sands, which were deposited from upper bottom suspension, were supplied both from local and from foreign sources.

The size-velocity relationship of fine sands (viz. Fig. 41) divides this size class into a bedload phase and a suspension phase. The division line is drawn approximately at the 150 micron size level. From this relationship it is concluded that any foreign fine sand that was coarser than 150 microns will have been left behind in the tidal delta, whereas the fraction finer than this limit may have bypassed this area, penetrating further into the bay.

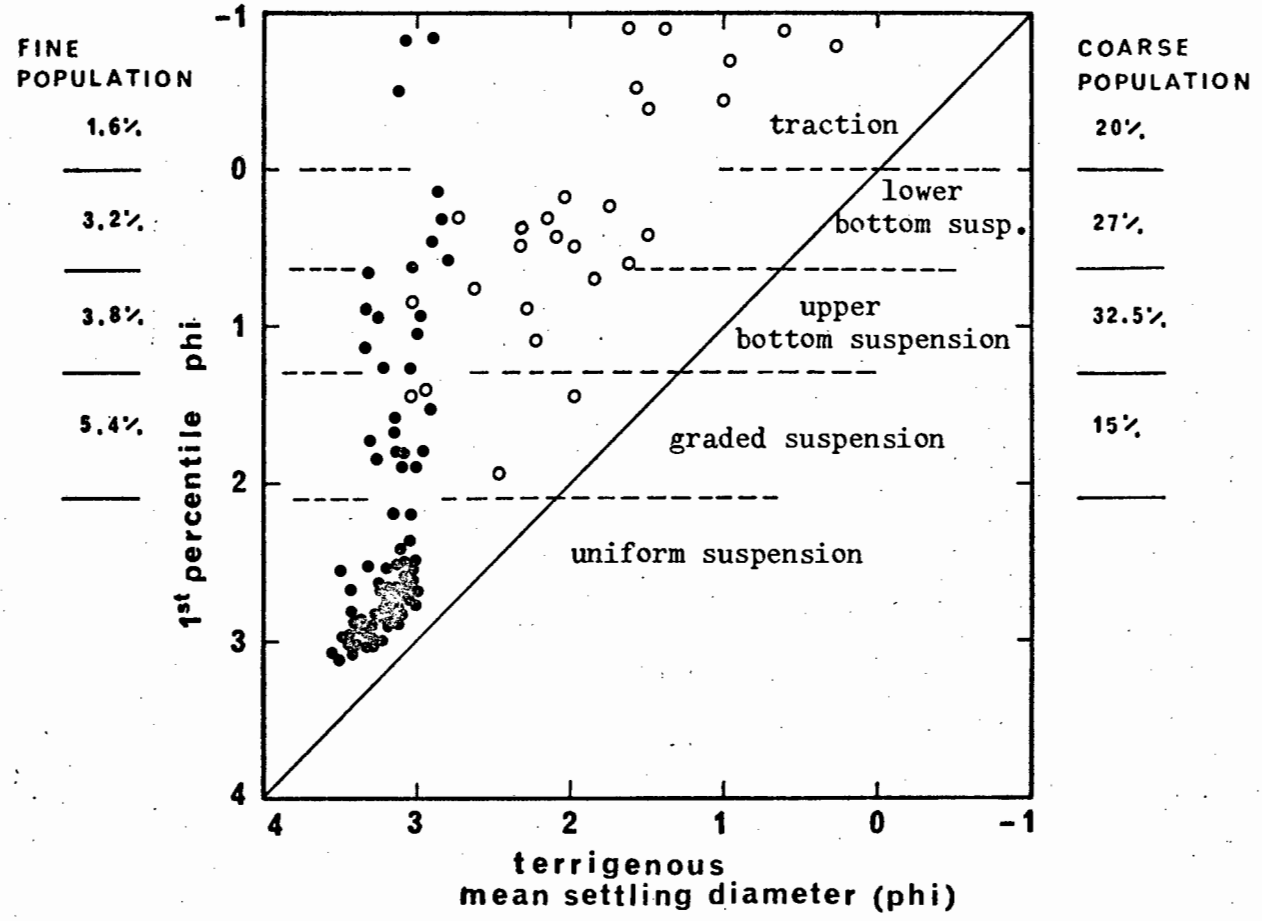

Fig. 117. Modes of sediment transport (terrig.comp.)

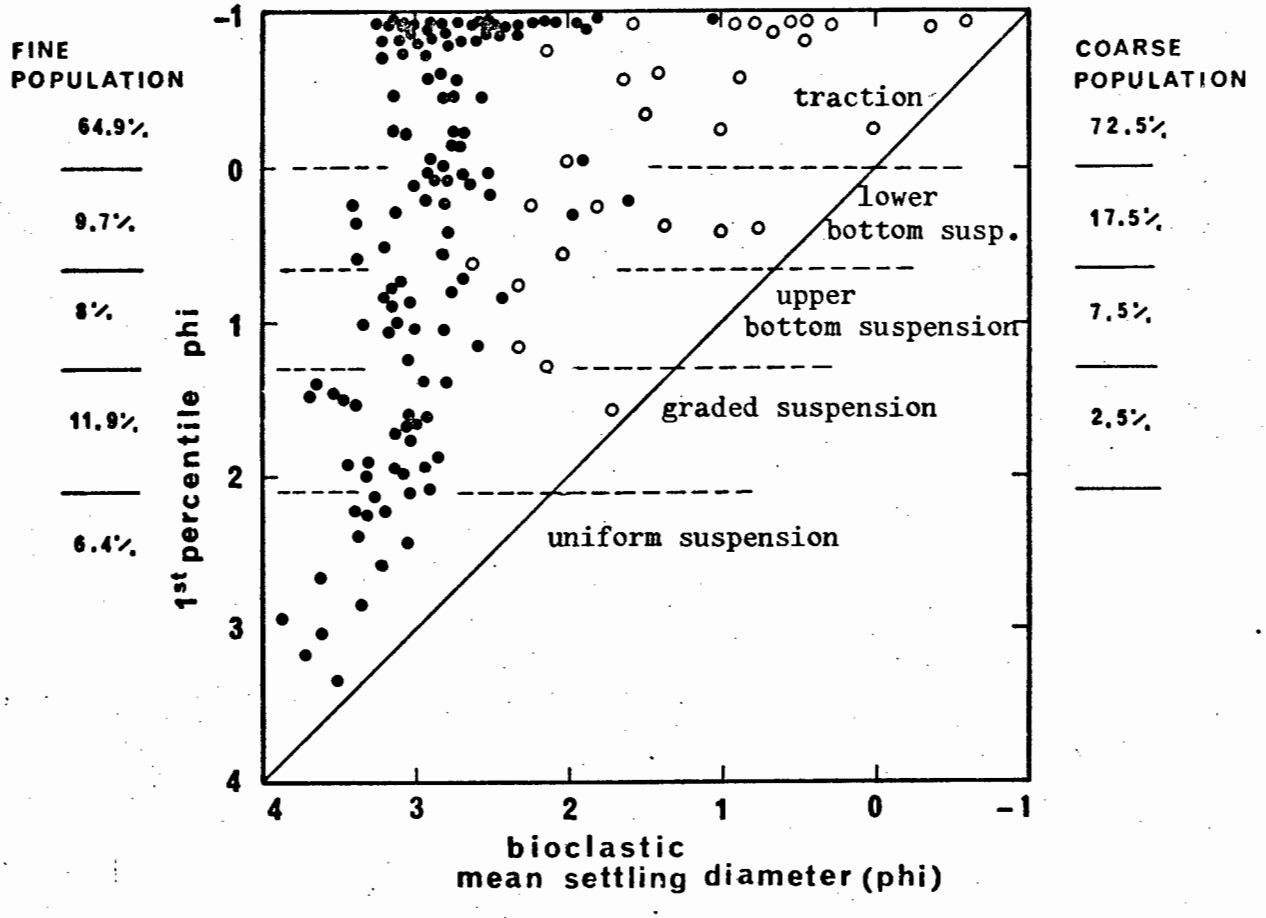

Fig. 118. Modes of sediment transport (bioclastic component)

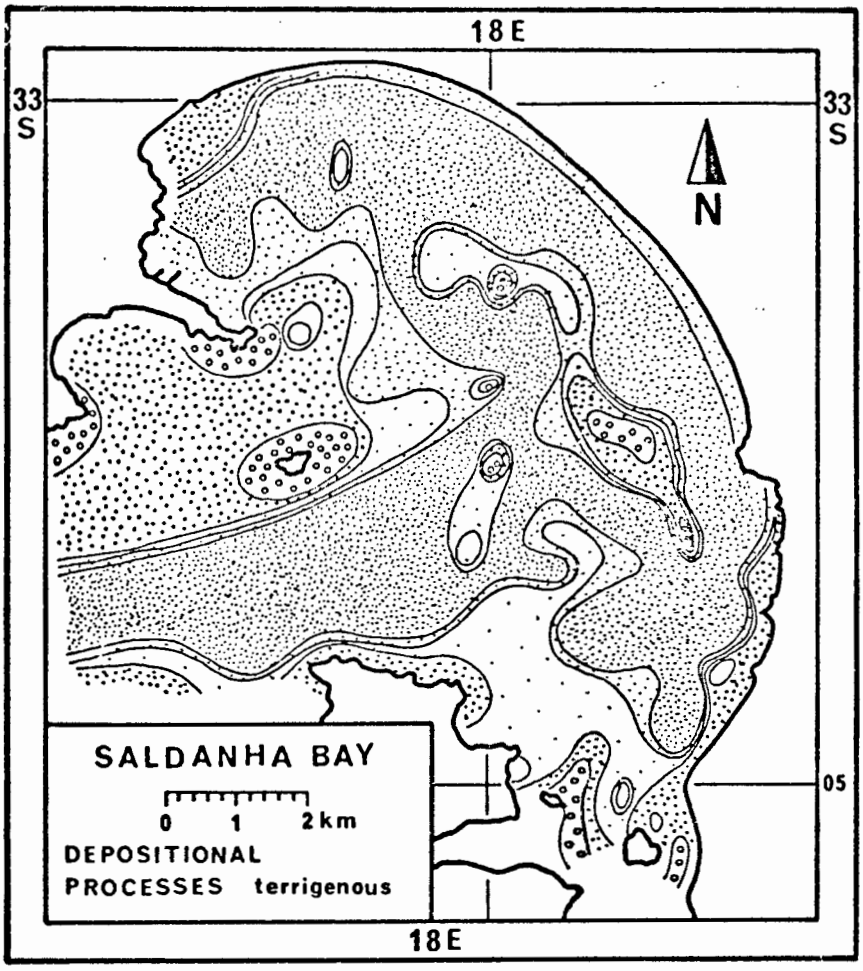

Fig. 119

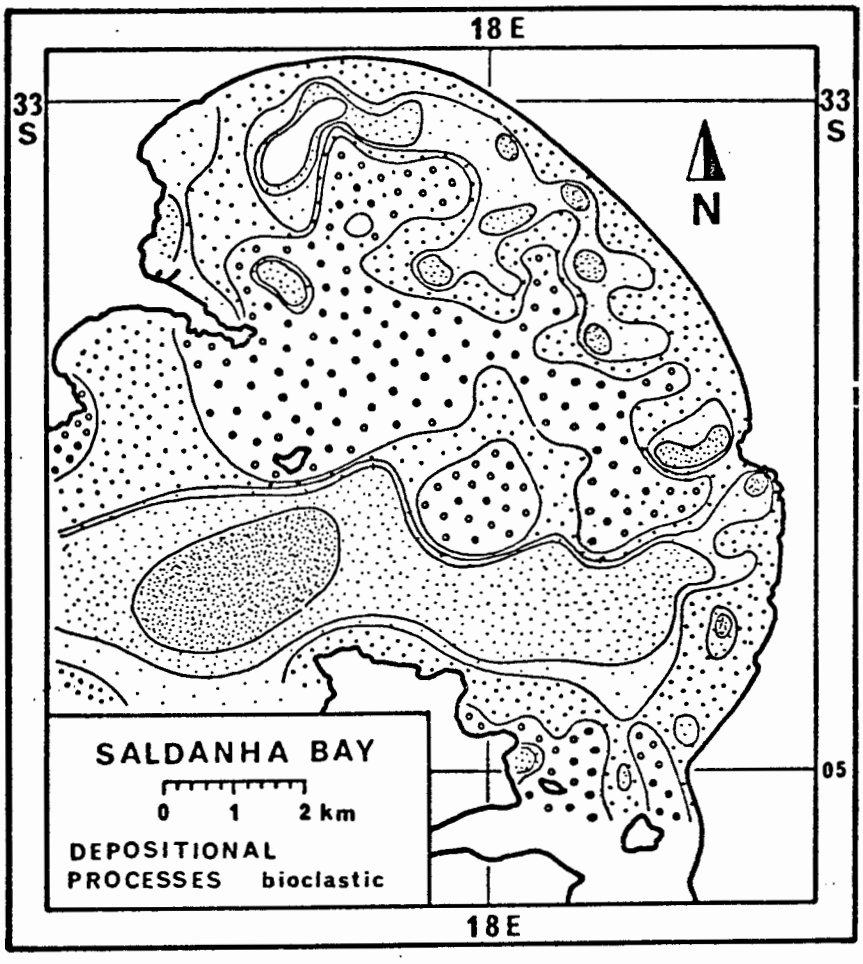

Fig. 120

The very fine sand, on the other hand, has unrestricted access to any part of the system, and will deposit at any place at which the energy conditions are favourable.

An unexpected piece of evidence supporting the lagoonal origin of the very fine terrigenous sands was obtained from stereo-scanning electron microscopy (SEM). In Plate 2 a number of selected micrographs are presented which illustrate a feature that relates the very fine sands of Saldanha Bay to those of Langebaan Lagoon. It was observed that sediment grains in Langebaan Lagoon very frequently had juvenile diatom frustules attached to them. From the nature of attachment it would appear that the frustules are actually welded to the quartz grains (Plate 2-A, -B, -C and -D). The phenomenon requires localized dissolution and reprecipitation of silica. It would appear that the special pH conditions in the low energy regions of the lagoon favour the formation of the chemical environment required for the reprecipitation of silica. Sediment grains from the open coast, on the other hand, are clean and polished showing no trace of contemporary diagenetic effects (Plate 3: G and H). However, the fine sediments of Saldanha Bay clearly resemble their lagoonal counterparts (Plate 3: E and F). Here too, attached diatom frustules can be observed, although not as frequently and not as well preserved, as in lagoonal sediments. More common are the remains of circular plates which possibly indicate the abrasional effects of sediment transport. On the basis of this evidence, the very fine sands cannot have originated from the open shelf. This conclusion favours a lagoonal origin of this sediment.

In contrast, the bioclastic component presents a totally different picture. A distinct physical barrier is observed at the mouth of the lagoon for any bioclastic material too coarse to be transported in graded or uniform suspension. Deposition from graded suspension, however, is almost entirely restricted to the southern semi-exposed zone and the South Channel. Very small areas in the inner bay represent sediments deposited from graded suspension and it is, therefore, concluded that only minor quantities of fine or very fine sediments appear to have reached the northern parts of Saldanha Bay.

Significantly, there is only one area in the inner bay where deposition from uniform suspension has been recorded. The area is identical to the one that was earlier recognized as containing sediments with similar size characteristics as the parent population when it entered the system. The

PLATE 2.

A. SEM micrograph of fine-sand quartz grain from Langebaan Lagoon with attached juvenile diatom frustules.

B. Detail of 2-A. The frustule appears to be welded to the grain surface.

C. The welding seam remains intact even after the frustules have been destroyed.

D. Remains of juvenile diatom frustule only 5 microns in diameter (Saldanha Bay).

E. Quartz grain from Saldanha Bay with diatom frustule still intact.

F. Quartz grain with diatom frustule from the South Channel of Saldanha Bay.

G. Quartz grain from the exposed shoreface off Langebaan Lagoon. Note the clean and polished surface.

H. Quartz grain from the exposed shoreface off Langebaan Lagoon. Note the clean and polished surface.

Plate 3

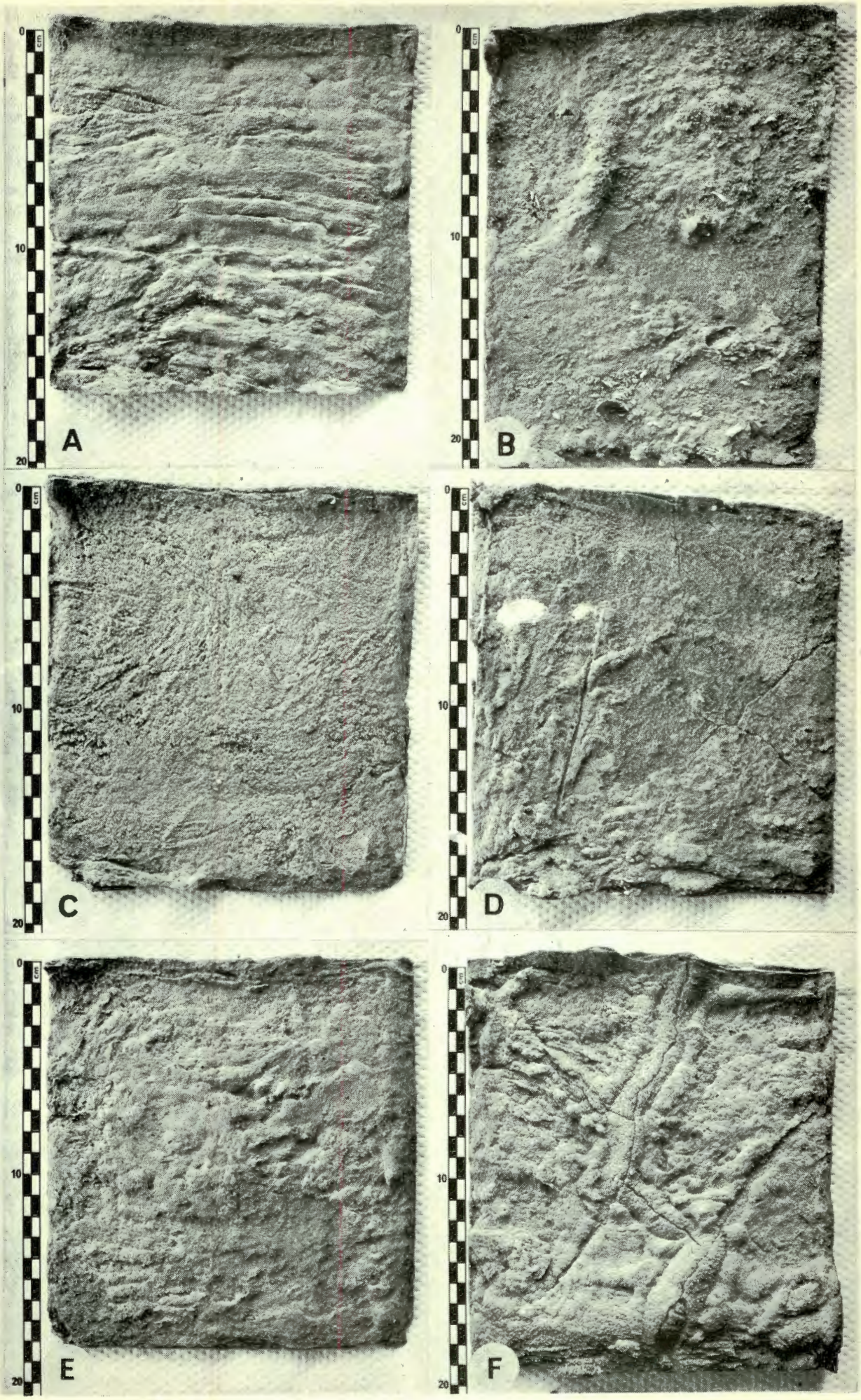

The present finding, based on an independent line of evidence, thus leads to the same conclusion. The carbonate content of the sediments in this area should, therefore, reflect the highest possible percentage of very fine bioclastic material that can have been supplied to this area from outside. This proportion does not exceed an average of about 20%. Since this area is very restricted in size, it is further concluded that, in most other inshore areas, the true foreign carbonate proportion should be considerably lower. The bioclastic material in most parts of Saldanha Bay, whether fine or coarse, was supplied from local sources.

Depositional processes in Saldanha Bay are, therefore, characterized by two progressively mixing hydraulic populations; a coarser, predominantly bioclastic population that was entirely supplied from sources within the bay and which contains not more than about 10% terrigenous sediment, and a finer, predominantly terrigenous population, containing less than 20% bioclastic material, which was supplied from a source located in Langebaan Lagoon.

Under present hydrodynamic conditions the bay has reached a dynamic equilibrium. This feature is reflected by the symmetry of its coastline, the bathymetry and the relationship between relative energy levels and sediment distribution patterns. Equilibrium conditions are particularly well reflected by the abundance of very fine sand. The only areas where equilibrium has not entirely been achieved are located on the inner abrasion platform, and along a short stretch of shoreline in the most exposed parts of the bay where some cliff erosion is still in progress.

4.6. LITHOFACIES OF SALDANHA BAY SEDIMENTS

Energy dispersal in Saldanha Bay is predominantly controlled by wave refraction and is modified locally by tidal currents and wind stress currents. As a result, different parts of Saldanha Bay are exposed to different energy spectra and sediment distribution is clearly related to various energy zones. Fig. 121 illustrates the energy zonation based on the wave refraction pattern.

In terms of the energy concept, each zone represents a distinct depositional unit, although the sharp boundaries are rather arbitrary as energy dispersion is always a more or less gradual process. However,

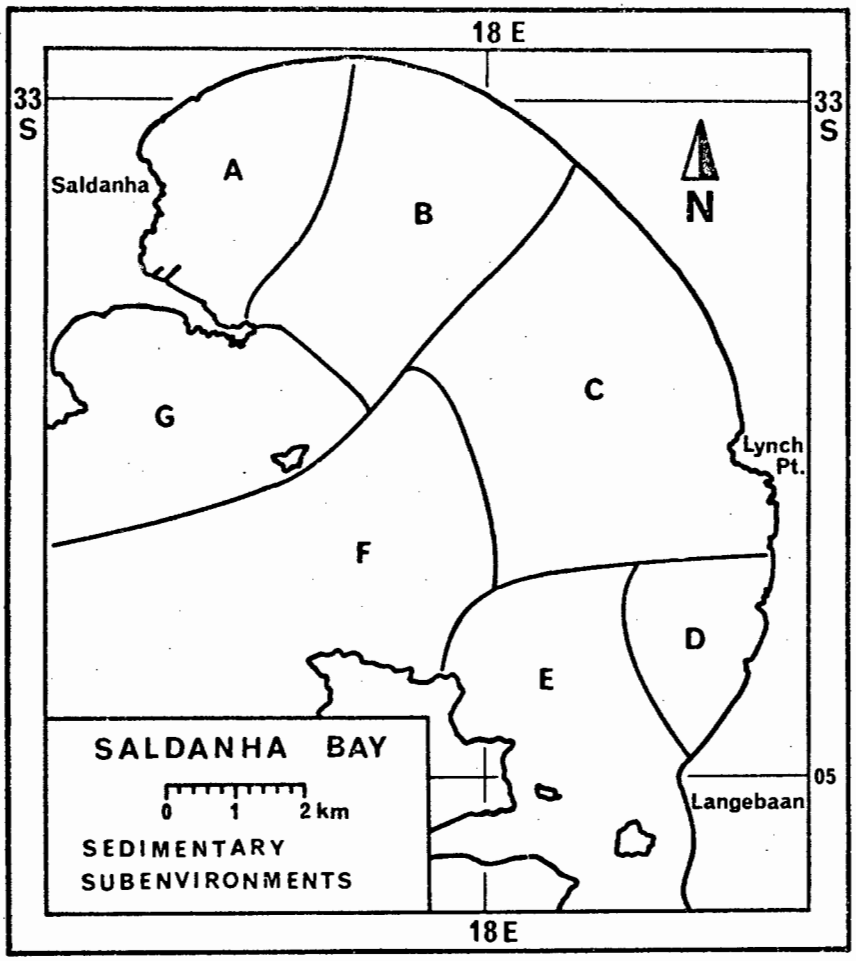

Fig. 121

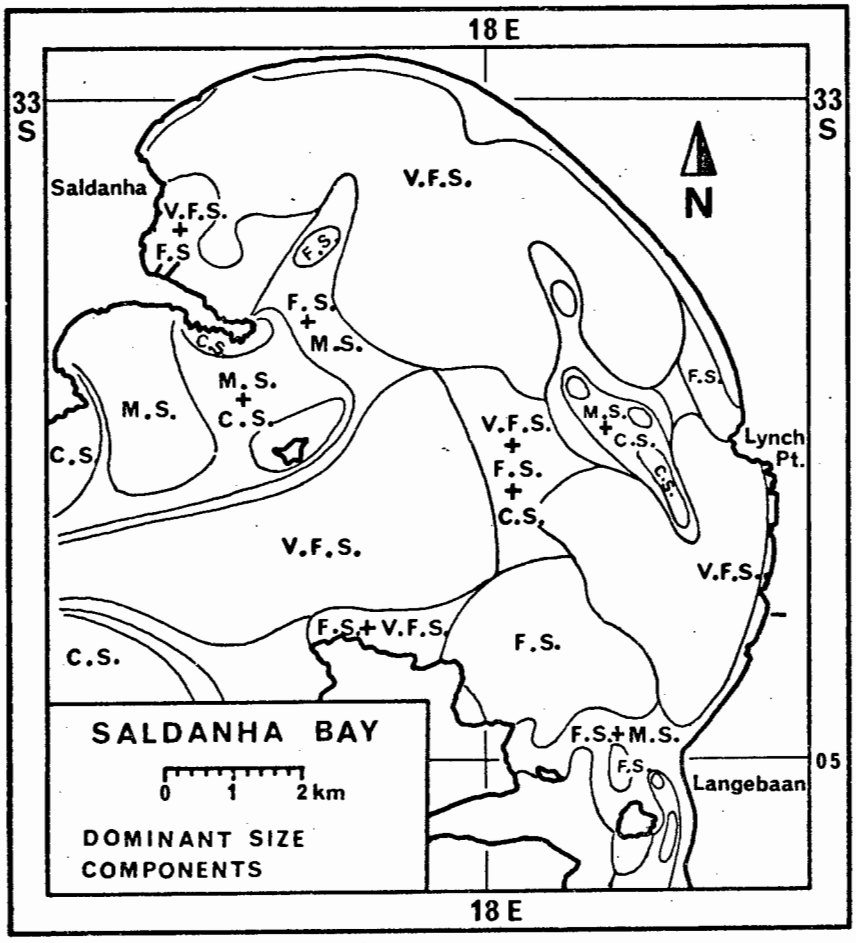

Fig. 122

PLATE 3.

A. Relief-cast of box-core from the sheltered zone in the northern part of Saldanha Bay.
Note slight lamination and ripple structure at centre and bottom (water depth 5m).

B. Relief-cast of box-core from the northern semi-exposed part of Saldanha Bay (water depth 7m).

C. Relief-cast of box-core from the inshore sand prism of the exposed part of Saldanha Bay (water depth 7m).

D. Relief-cast of box-core from the inshore sand prism of the exposed part of Saldanha Bay.

E. Relief-cast of box-core from the inshore sand prism of the southern semi-exposed zone (water depth 5m).

F. Relief-cast of box-core from the tidal delta in the southern part of Saldanha Bay (water depth 5m).
N.B. The tube-like structures are not primary structures but crack fillings during preparation.

Plate 2

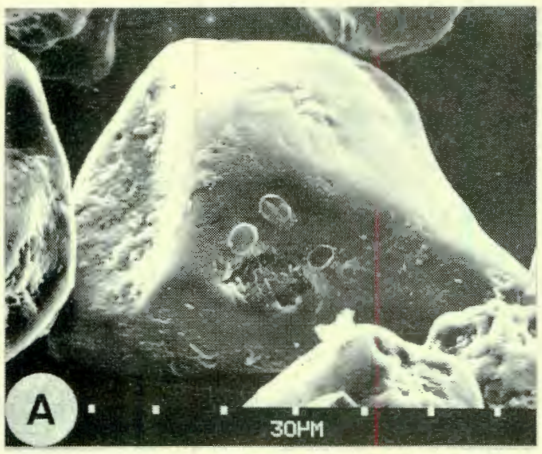

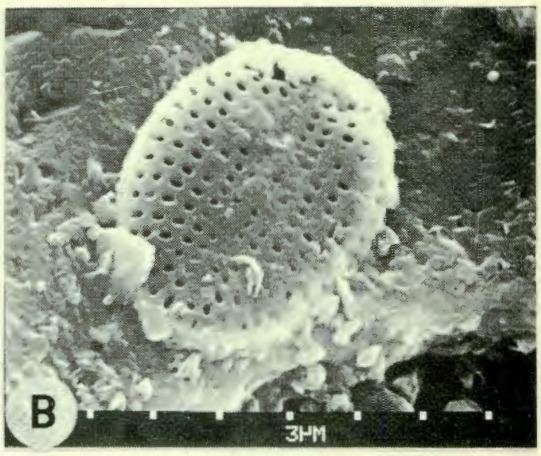

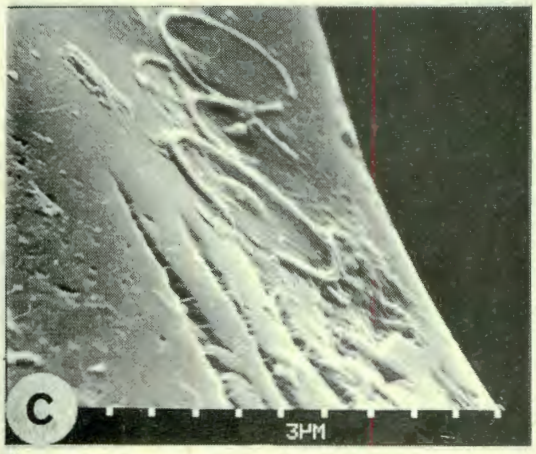

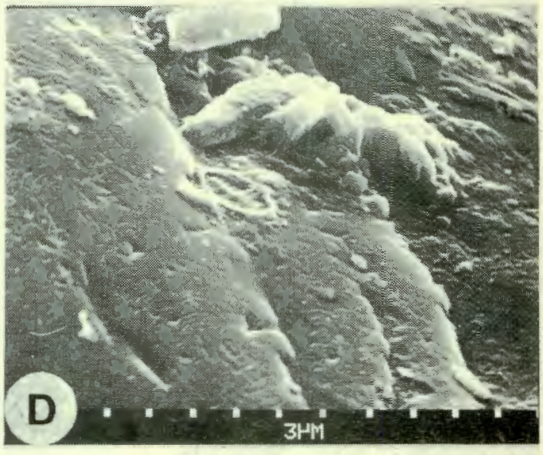

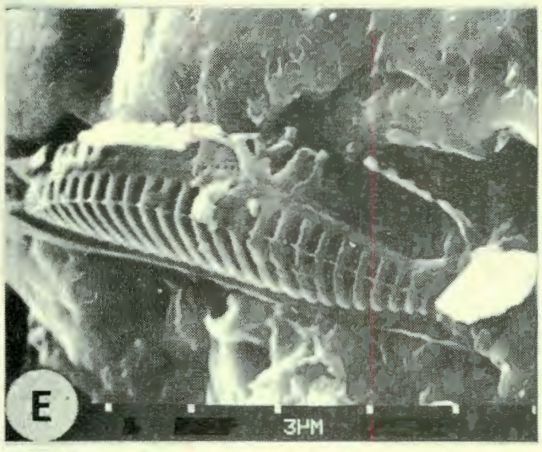

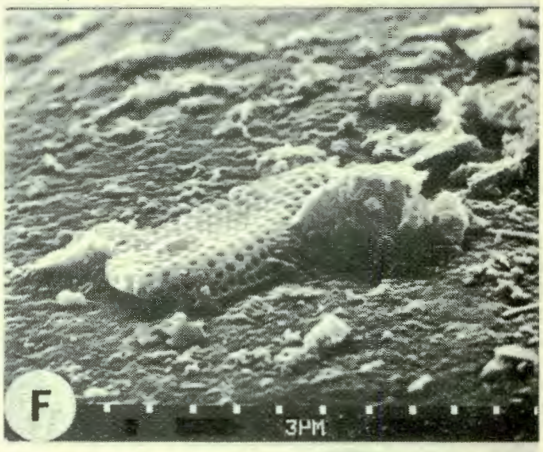

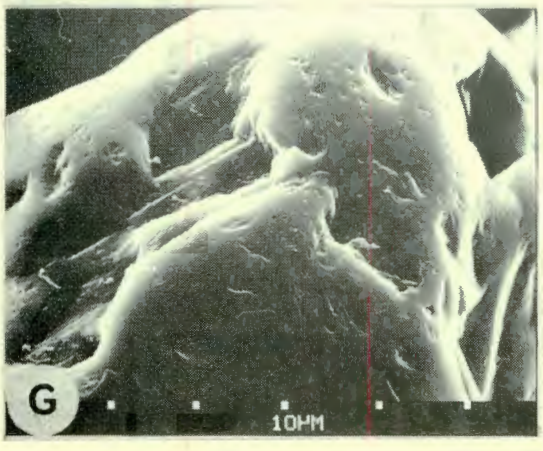

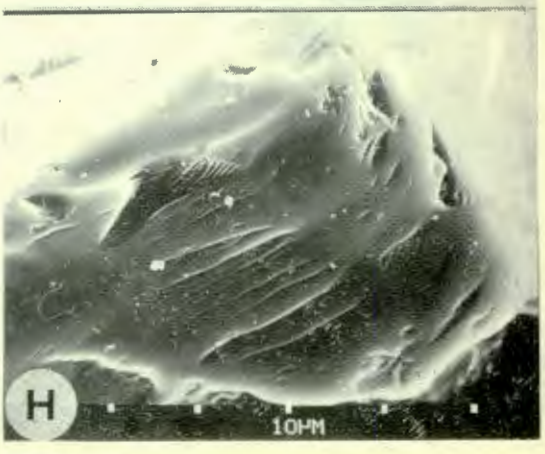

Fig. 55 clearly demonstrates that each zone has quite characteristic depositional features which were expressed in physiographical terms. This aspect received further support by the modes of sediment transport and deposition discussed in Section 4.5., where it was demonstrated that the areal zonation of individual modes (viz. Fig. 116) was very similar to the mean diameter map and almost identical in design to the combination of the dominant size fractions (i.e. areas in which a particular size fraction contributes over 50% to the total sediment).

In order to illustrate this feature, dominant size fractions were combined in a single map (Fig. 122). The agreement with the energy zonation is indeed striking. Physiographically these areas have been defined as depositional subenvironments of the bay. They provide a useful framework for a comprehensive facies approach. Fig. 123 demonstrates that each subenvironment has a characteristic grain size image as defined in Section 3.5.5. Since most of the sediments are composed of very fine sands, internal structures have been of limited use for environmental recognition. This is illustrated by the very similar appearance of relief casts prepared from square-box cores recovered from the various inshore subenvironments (Plate 3).

The individual subenvironments are characterized by a complex association of textural and mineralogical parameters. Since the textural characteristics were shown to be directly controlled by the mixing of the two hydraulic populations, each of which was predominantly composed of a mineralogically distinct component, lithology was given preference over texture for the definition of sedimentary facies. Textural parameters were subsequently utilized for the definition of subfacies within each facies unit.

The lithological classification of sediments in Saldanha Bay is illustrated in Fig. 123. The scheme is based on the triangular subdivisions discussed in Section 3.6.6. (Fig. 50). The whole area can be subdivided into two major lithological provinces, which are clearly arranged with respect to relative energy levels and water depth (Fig. 124). Thus, the entire nearshore zone consists of quartzarenites. This belt widens progressively as it develops towards the semi-exposed and sheltered sections of the bay. In fact, the semi-exposed and bay/lagoon transitional subenvironments in the southern bay and the sheltered subenvironment in

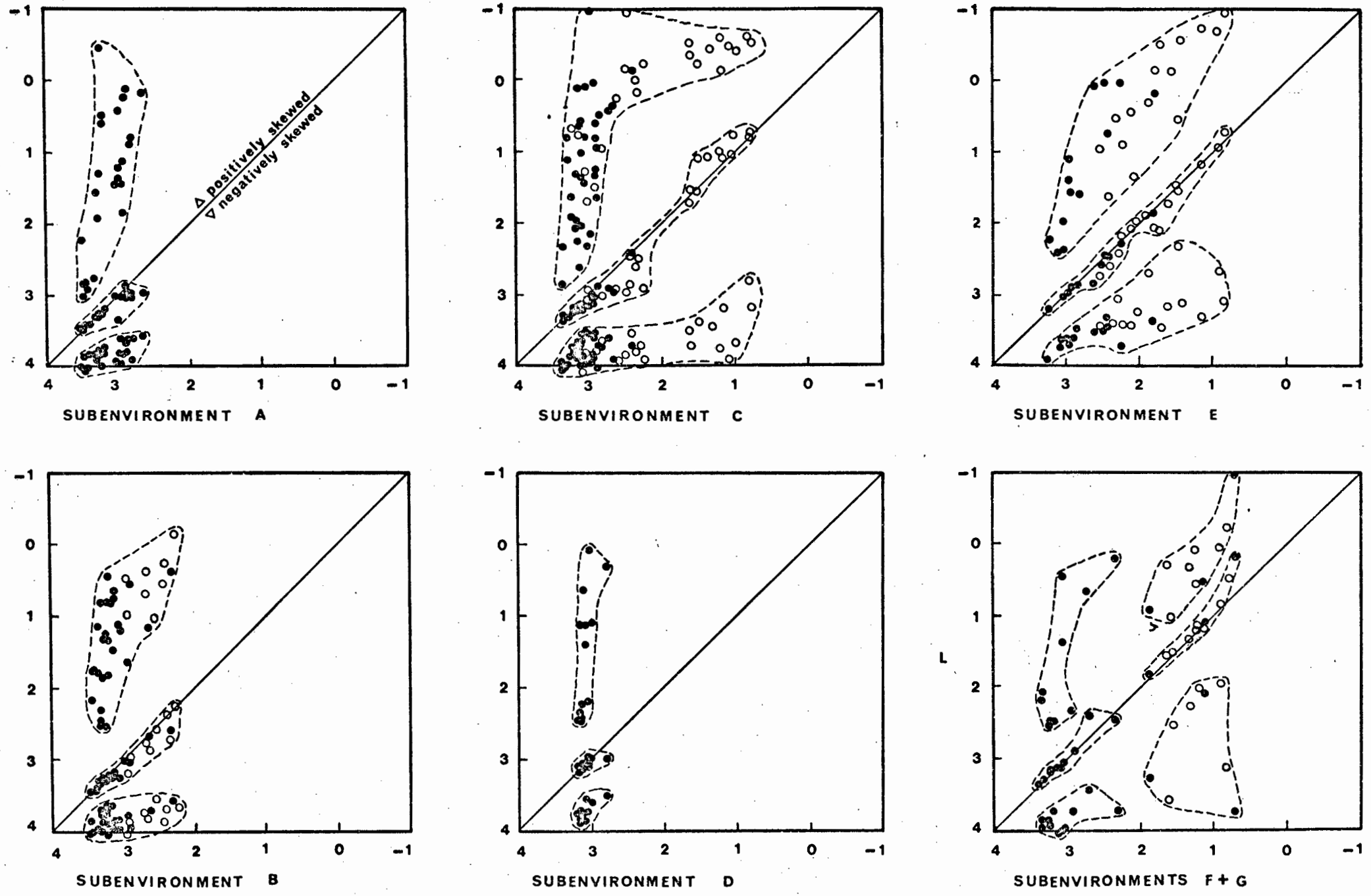

Fig. 123. Grain-size images of individual subenvironments in Saldanha Bay

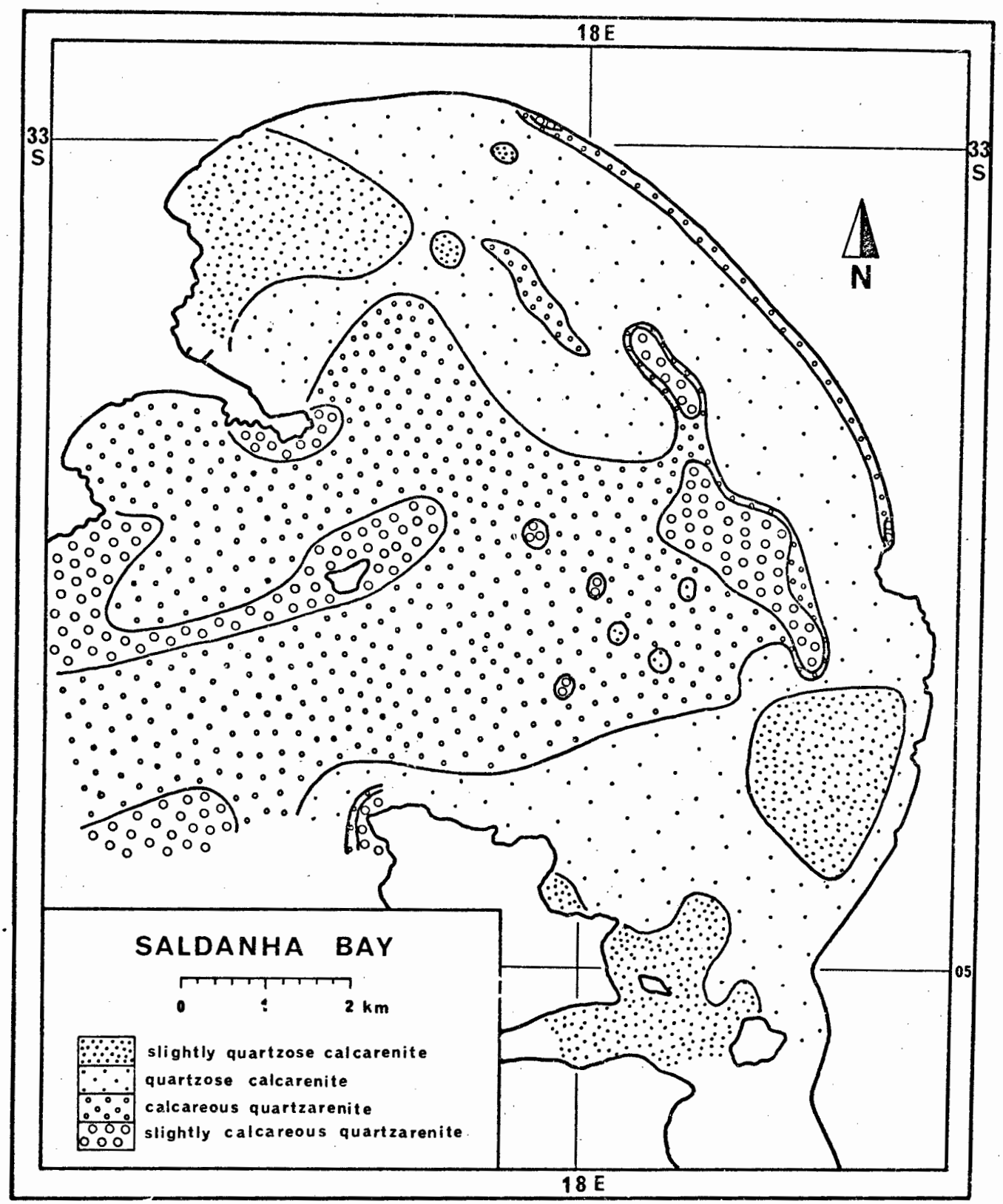

Fig. 124. Lithology

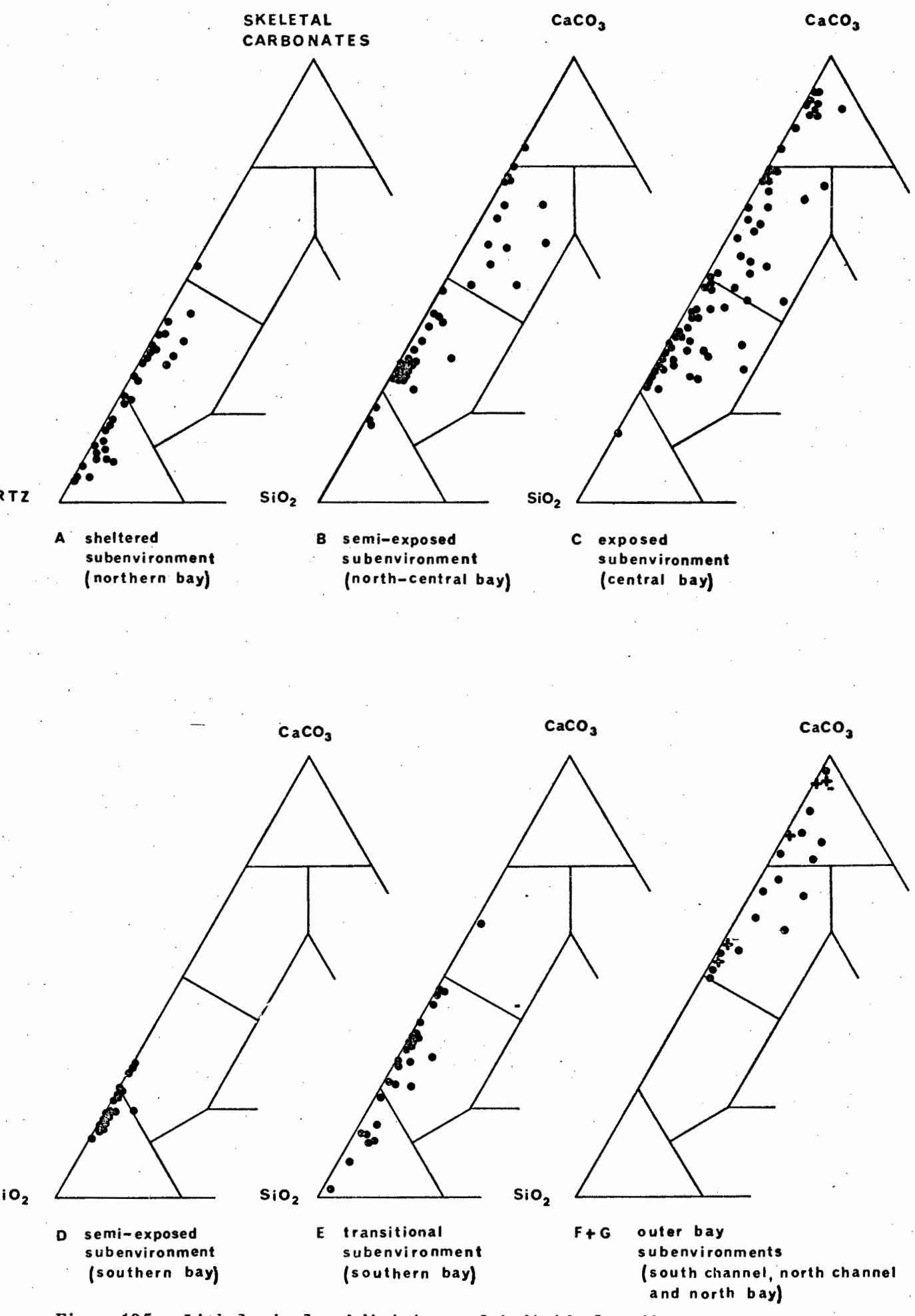

Fig. 125. Lithological subdivisions of individual sedimentary subenvironments in Saldanha Bay

the north, belong exclusively to this lithological province. The more exposed parts of the bay, on the other hand, consist entirely of calcerenites. Both provinces can be further subdivided into units in which each component group contributes either more than 75% to the total sediment, or less. It is interesting to note that slightly calcereous quartzarenites, for example, occur only in the northern, sheltered subenvironment and the southern, semi-exposed and transitional subenvironments. Slightly quartzose calcarenites, on the other hand, are invariably associated with bioclastic production zones. This feature appears to reflect the different transport potential of each component group.

The zonation pattern of depositional subenvironments was then superimposed on the lithological pattern and each lithological unit within each subenvironment was defined as a lithofacies of the system. The characteristic point clusters of lithofacies in relationship to their subenvironments are illustrated in the respective diagrams of Fig. 125. That energy dispersion is a progressive process is demonstrated by the fact that individual facies are represented in more than one subenvironment. The overall pattern, however, is quite distinct in each case.

Each lithofacies, in its above defined form, now provides information about the depositional area within the coastal environment, and the major components constituting the sediment. Textural information is, thus far, still restricted to the term "arenite" which means simply "composed of sand-sized particles". Since these sands are extremely variable with respect to their textural characteristics, each lithofacies can be described in terms of its textural attributes. In this manner textural subfacies can be distinguished. Grain-size characteristics are summarized in Fig. 122, whereas sorting and skewness are illustrated in Fig. 77 and Fig. 78, respectively.

CHAPTER 5. LANGEBAAN LAGOON

5.1. PHYSIOGRAPHIC SETTING

5.1.1. General Features

Langebaan Lagoon forms a southern appendix to Saldanha Bay, stretching for about 15 km parallel to the coast. The lagoon is separated from the open sea by a stratigraphically compound barrier. The central and southern parts of the barrier consist of semi-consolidated and unconsolidated late Pleistocene and Holocene coastal-marine sediments. This section is 1.5 - 2 km wide. To the north, the sedimentary barrier is linked to a granite peninsula, which is on average 4 km wide and forms the southern headland of Saldanha Bay (Fig. 8).

The mouth of the lagoon opens to the wave-sheltered southern part of Saldanha Bay and is controlled by granite outcrops that divide the outlets into two separate channels. The western channel is constricted by a submerged granite bar reaching up to 6 m below lea level. The eastern channel, on the other hand, has been scoured to a maximum depth of about 17 m; both channels are about 400 m wide. The northern section of the lagoon, which is lined by high granite ridges, averages about 2 km in width, whereas the central and southern sections are 3.5 - 4 km wide. The total wet surface area of the modern lagoon amounts to at least 40 km^2.

According to Emery and Stevenson (1957), Hoyt (1967), and Phleger (1969), coastal lagoons normally develop behind sediment barriers formed during gradual submergence of the coast. Although Langebaan Lagoon is also related to a rising sea-level it did not, however, form in the shelter of a modern barrier or prograding sand spit, as suggested by Birch (1977b), but owes its existence to selective scouring of a drowned dune landscape in the course of the Flandrian transgression, as indicated by Tankard (1976). The modern barrier, therefore, consists of a remnant Pleistocene core that has weathered marine erosion during the early Holocene, and was subsequently modified by coastline progradation. Langebaan Lagoon is, therefore, the result of selective erosion acting in a unique geological environment, rather than the outcome of lagoonal evolution in terms of the conventional model.

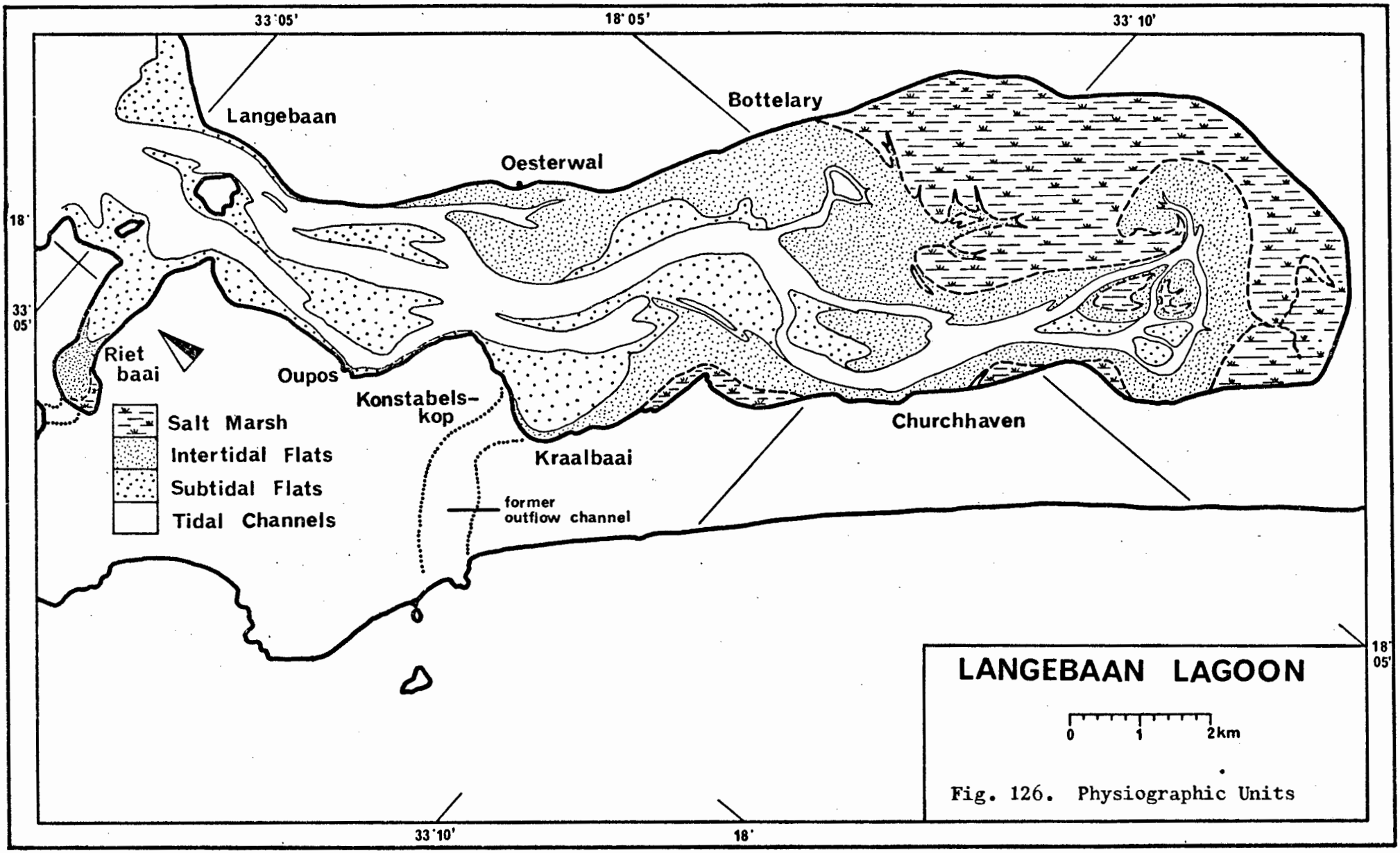

Fig. 126. Physiographic Units

The lagoon can be divided into a number of well defined, physiographic units, which are controlled by the strong energy gradient of the tidal flow. In this respect, the lagoon differs from Saldanha Bay, where the relationship between physiography and wave energy is not as easily recognized. Four major units, illustrated in Fig. 126, are distinguished: 1) tidal channels, 2) subtidal flats and channel bars, 3) intertidal flats, and 4) salt marshes.

The physiographic sequence of these units indicates a prevailing north-south energy gradient. This aspect is illustrated by the absence of intertidal flats and salt marshes in the northern lagoon, the dominance of intertidal flats in thecentral lagoon and the dominance of salt marshes in the southern lagoon. Most of the intertidal flats, and almost all of the salt marshes, occur along the southeastern and southern margins of the lagoon, thus indicating a secondary energy gradient from west to east.

The north-south energy gradient of Langebaan Lagoon is also reflected by the bathymetry of the channel systems (Fig. 127). The greatest channel depth, reaching almost -17 m, is observed along the narrowest channel section between Langebaan village and Skaapeiland. Towards the south, the channel depth decreases progressively, although a number of additional troughs, reaching 9.5 m in the central lagoon and 5.5 m near Churchhaven, can be observed.

Each physiographic unit is characterized by a typical association of large-scale sedimentary structures, produced by dynamic response of the sediment surface to tidal currents, wind driven currents, and surface waves; the latter two are strongly seasonal in their effects. A schematic map illustrates the distribution of major bedforms and sediment surface structures observed in the various units (Fig. 128). An interesting feature of these large bedforms is their preferred orientation with respect to the energy levels of the flow system. Thus, on the intertidal flats, where energy levels are relatively low, the majority of bedforms are oriented parallel to the direction of flow, whereas channel bedforms are almost exclusively transversely oriented. A selection of large intertidal bedforms are presented in Plate 4. These bedforms should not be confused with small current and wave-generated ripple marks, which occur throughout the entire system. Major bedforms are conspicuously absent on most subtidal flats and channel bars.

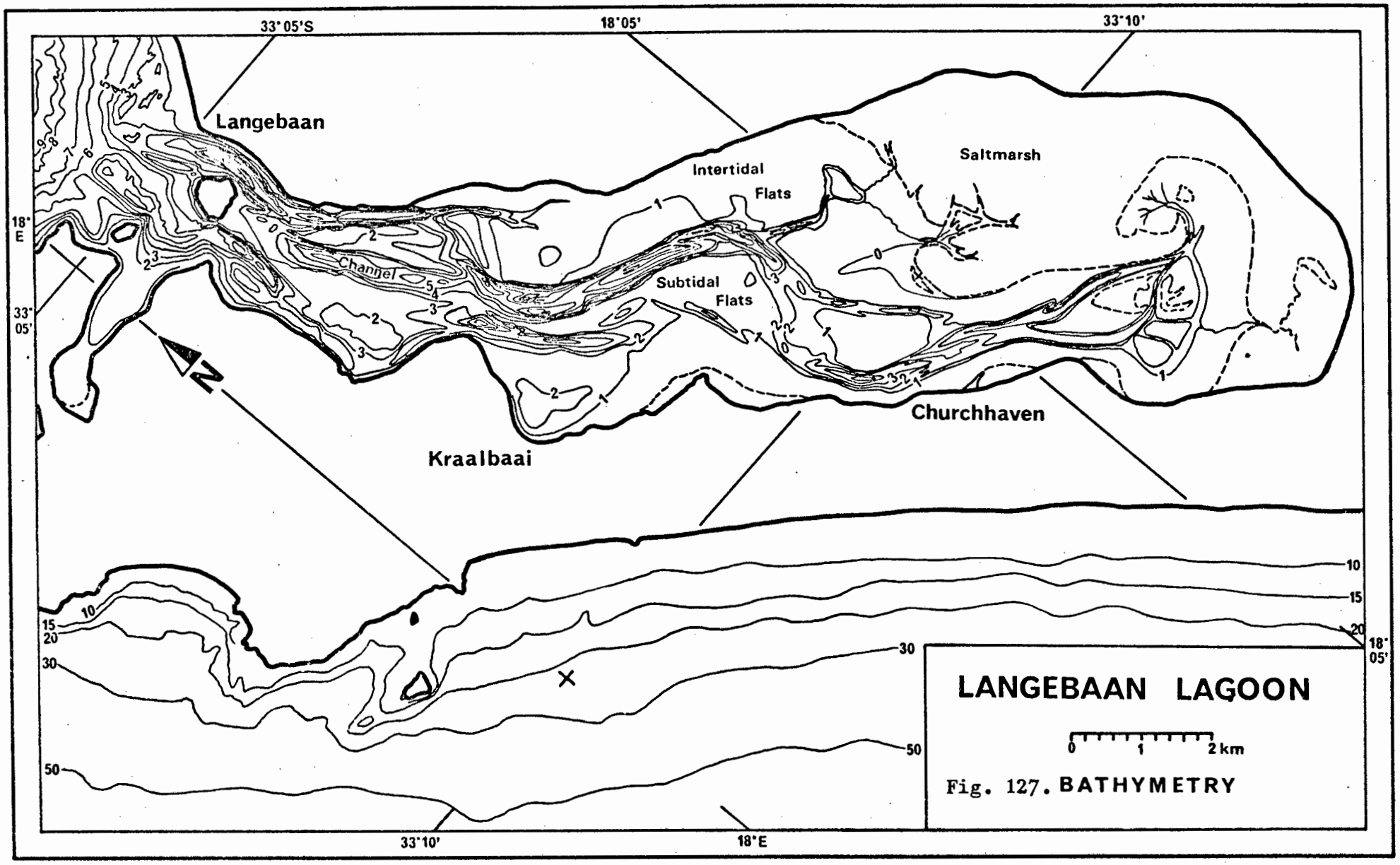

Fig. 127. BATHYMETRY

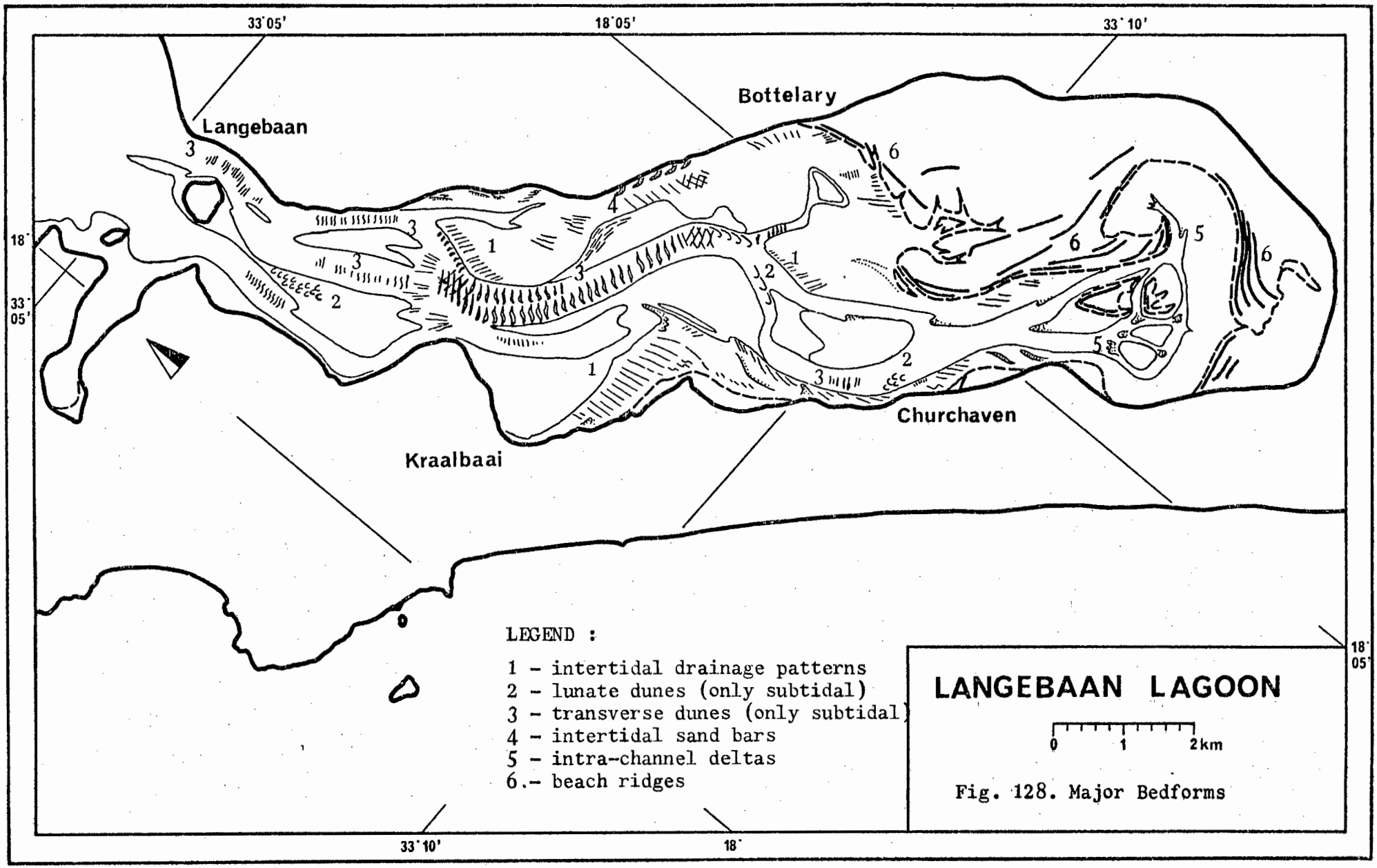

Fig. 128. Major Bedforms

Plate 4

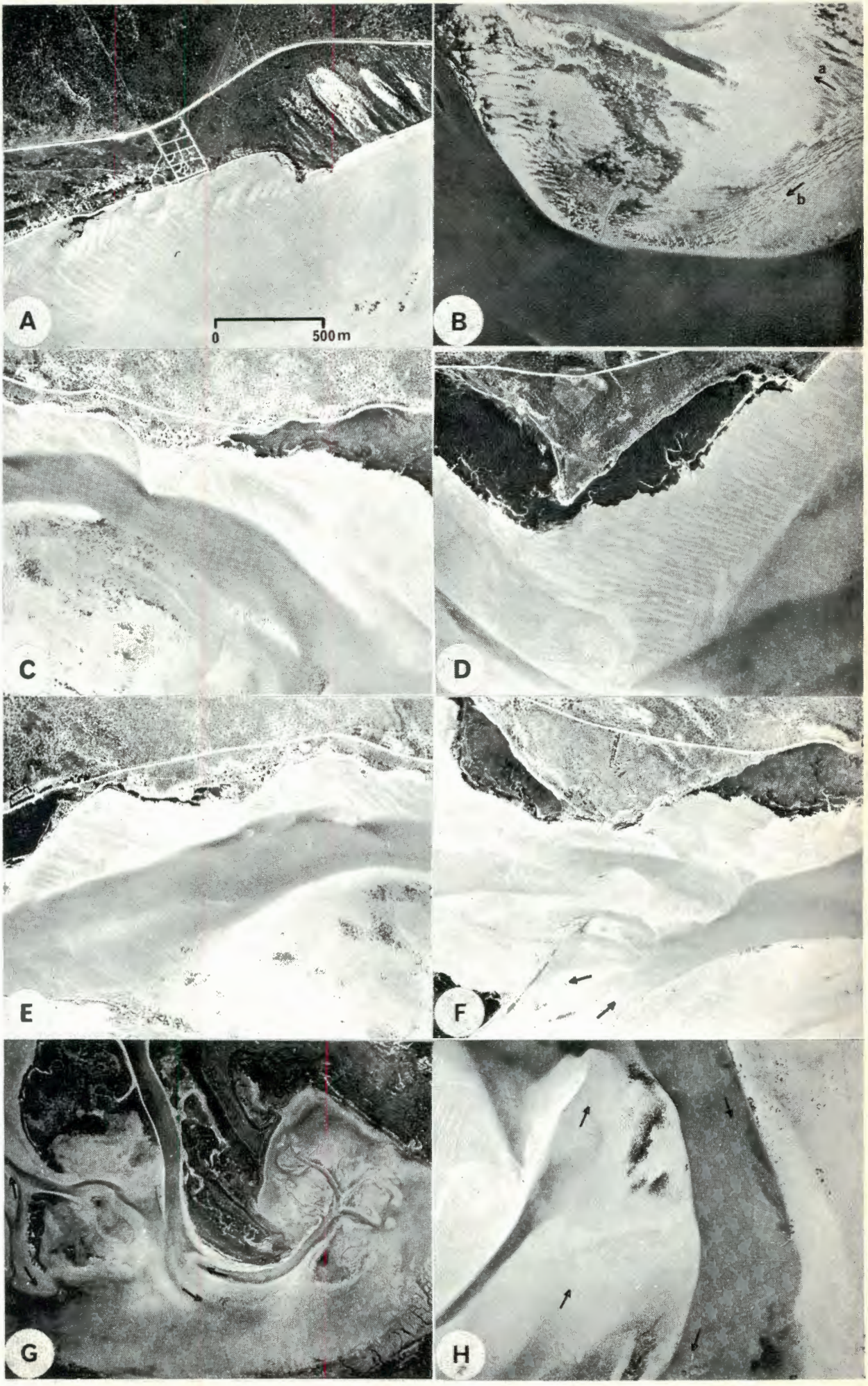

PLATE 4.

A. Multiple inshore sand bars and run-off structures along the eastern shore-line of the central lagoon.

B. Current-aligned marine vegetation on the intertidal flats of the north-central lagoon.
a. current direction just after high tide.
b. current direction after(a)has fallen dry.

C. Sand bars along the southwestern margin of the lagoon.

D. Large tide and wind controlled run-off structures near Kraalbaai (see also Plate 7-E).

E. Sand bars and run-off structures along the southwestern margin of the lagoon.

F. Evidence for ebb and flood-current flow separation in the southern lagoon.
Note the intra-channel deltas.

G. Intra-channel deltas in combination with ebb and flood-current dominated channels.

H. Large intertidal sand spit facing in the direction of the ebb current.

A comparison of aerial photographs dating back to 1937 has revealed very little change in the position of major channel margins and sandbanks. The only major change was observed in the proximal tidal delta region at the seaward extension of the eastern outflow channel, just north of Skaapeiland and Langebaan village (Fig. 129). At the point where the eastern channel bank meets the wave controlled beach-front of the southeastern bay, sediment accretion has led to progradation of the point by about 150 m over the past 40 years. In the course of progradation, the beachline has remained aligned with the log.spiral trend defined by the southeastern shoreline of the bay.

Similarly, there has been a westward displacement of a submerged sandbank north of Skaapeiland by about 200 m over the same period of time. In both cases, there has been little change since 1968, whereas the period between 1960 and 1968 appears to have been the most active one, with an average rate of 5.3 m and 8.7 m/year, respectively. The actual gain in sediment at the Langebaan beach point is not really large, amounting to not more than about 150 000 m^3 spread over an area of only 0.075 km^2. The submerged bar, on the other hand, does not appear to have gained any sediment at all, but seems to have been simply displaced as a whole. Since there is no visible change at all inside the lagoon, the writer believes that this feature has resulted from minor human interference with the marginal flow pattern along the eastern banks of the outflow channel at Langebaan. An example of this effect is the construction of a naval jetty and the subsequent operation of crashboats along the shallow channel banks just inside the lagoon.

In the central section of the lagoon, east of Kraalbaai, a large intertidal sand spit would provide a sensitive control feature for any changes within the system. The spit is oriented in the ebb current direction and if any significant change in the sediment budget of Langebaan Lagoon had taken place during the last 40 years, this would surely have been recorded in the response pattern of the sand spit. Comparing the respective aerial photographs of the area does not, however, reveal any major alteration in position or overall size of the spit. The only visible effect is a quasi-stable oscillation about its NW/SE axis (Fig. 130). This oscillatory movement probably reflects a seasonal effect of the changing wind pattern.

A striking physiographic feature of the lagoon is presented by the

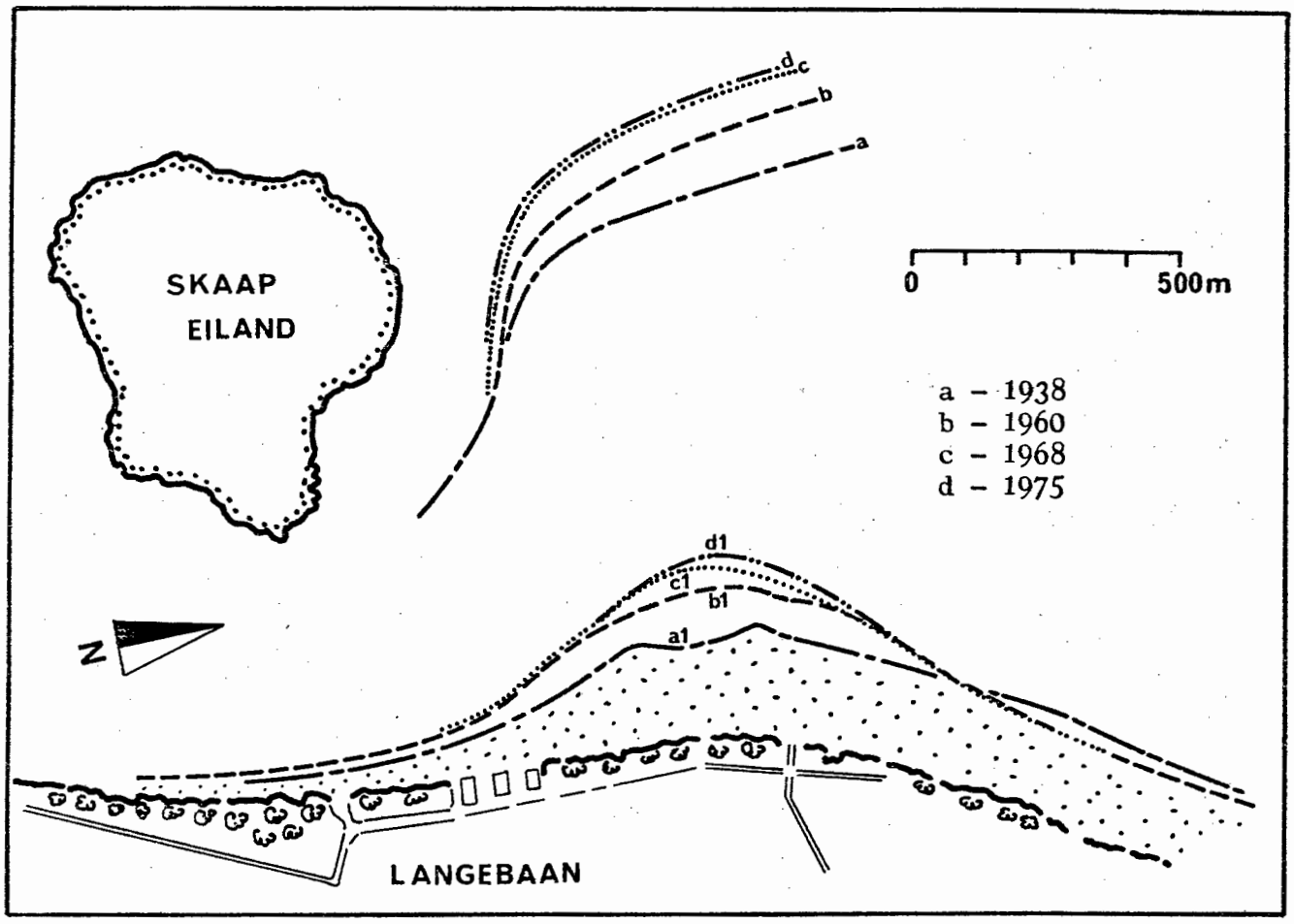

Fig. 129. Beach progradation and sandbar displacement along the eastern outflow channel

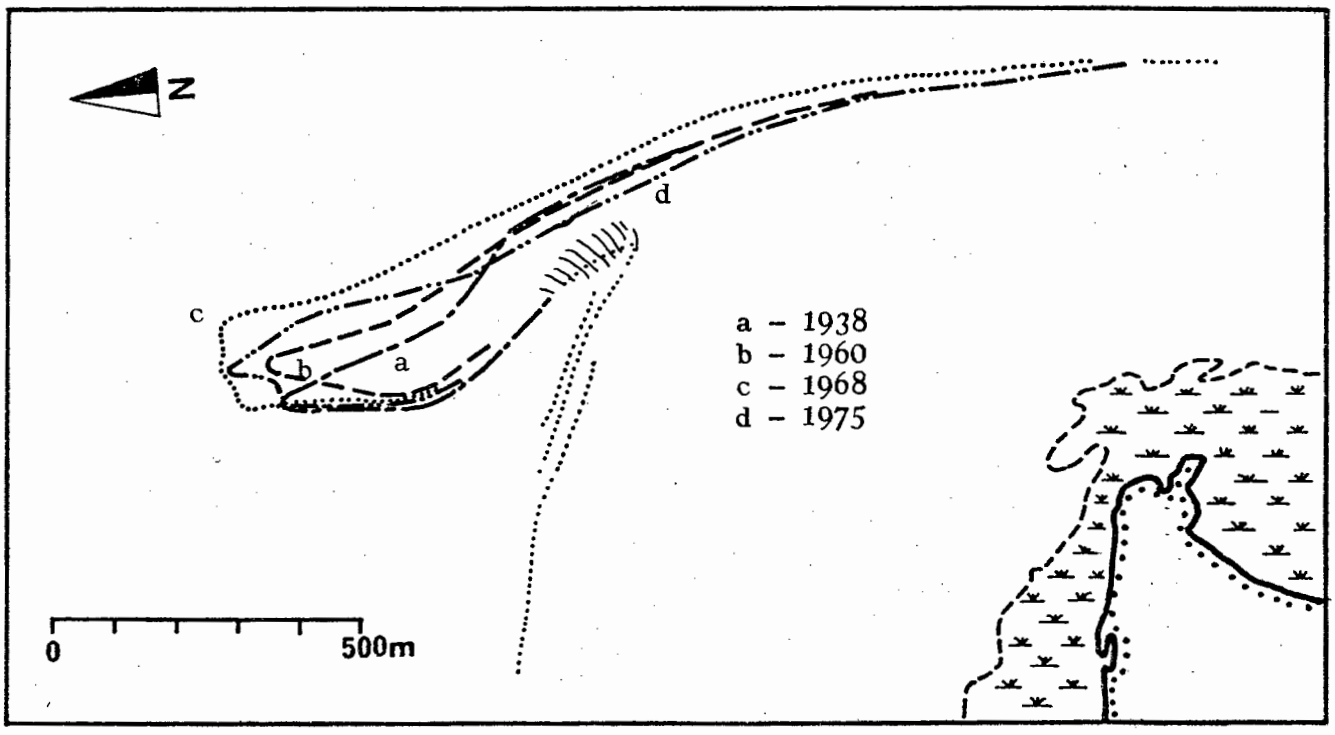

Fig. 130. Intertidal sand spit in the central lagoon

steep and sometimes cliffed, margins of the semi-consolidated dune barrier along the southwestern shoreline of Langebaan Lagoon, stretching between Kraalbaai en the south. In many places the cliff reaches a height of over 15 m and frequently the upper edge is formed by a truncated calcrete horizon. Large slabs of collapsed dune rock line many beaches, especially at Kraalbaai. Here a single isolated stack, some 5 - 6 m high, leaves no doubt about the considerable erosional activity that must have prevailed some time in the past. Erosion on this scale is not conceivable under the present hydrodynamic conditions.

Perhaps the most convincing evidence for low contemporaneous erosion is presented by the presence of narrow belts of salt marshes that fringe over 60% of the shoreline, adjacent to the fossil dune cliffs. Other evidence is provided by the position of the present cliff in relation to the shoreline. In many instances, especially near Churchhaven, the cliff follows the outline of former coves which today are partially infilled and completely isolated from the open lagoon. Similar features were observed along the northeastern shoreline just south of Langebaan village. The relict nature of these cliffs is unmistakable (Plate 5-A to 5-E).

The fossil dune barrier must once have extended considerably farther into the modern lagoon. This is particularly well documented by a large slab of dune rock that was found in a tidal creek about 200 m away from the present dune margin. It weighs at least several tons and, therefore, could not have been transported beyond the edge of a former undercut cliff. This boulder is resting on a relict terrace which extends at least up to the spring low tide level, reaching a maximum distance of about 1 km away from the modern shoreline. The terrace forms the basis of the entire western tidal flat system and is usually covered by at least 50 cm of younger unconsolidated sediments. A similar terrace is partially exposed near Oesterwal along the eastern shoreline of the lagoon.

The physiographic features discussed above clearly indicate that the lagoon must have been exposed, at some stage of its Holocene history, to considerably higher erosional activity. Since the modern hydrodynamic regime of the lagoon prohibits erosion on this scale at the localities described above, it is concluded that the flow pattern of the lagoon must have been different during that period. Further investigations into this phenomenon have produced strong evidence in support for a high stand of

PLATE 5.

A. Relict cliffs and channel alignment along the northeastern shoreline of Langebaan Lagoon.

B. Kraalbaai and the lagoonal side of the former outflow channel (arrow).

C. The relict calcrete cliff (arrows) marks the position of the coastline at the peak of the Flandrian transgression some 5500 years B.C.

D. Relict cliffs along the tombolo separating Rietbaai from the open sea.

E. Salt marshes in the southern lagoon.
a. high-lying marshlands (about + 2.5m).
b. modern marsh.

F. The truncated fossil dune barrier along the southwestern shoreline of Langebaan Lagoon.

G. Sand fans along the fossil dune margin form the only modern sediment source in the central and southern parts of Langebaan Lagoon.

H. Sand flow generated by a sporadic rush-flood during the rainy winter season.

Plate 5

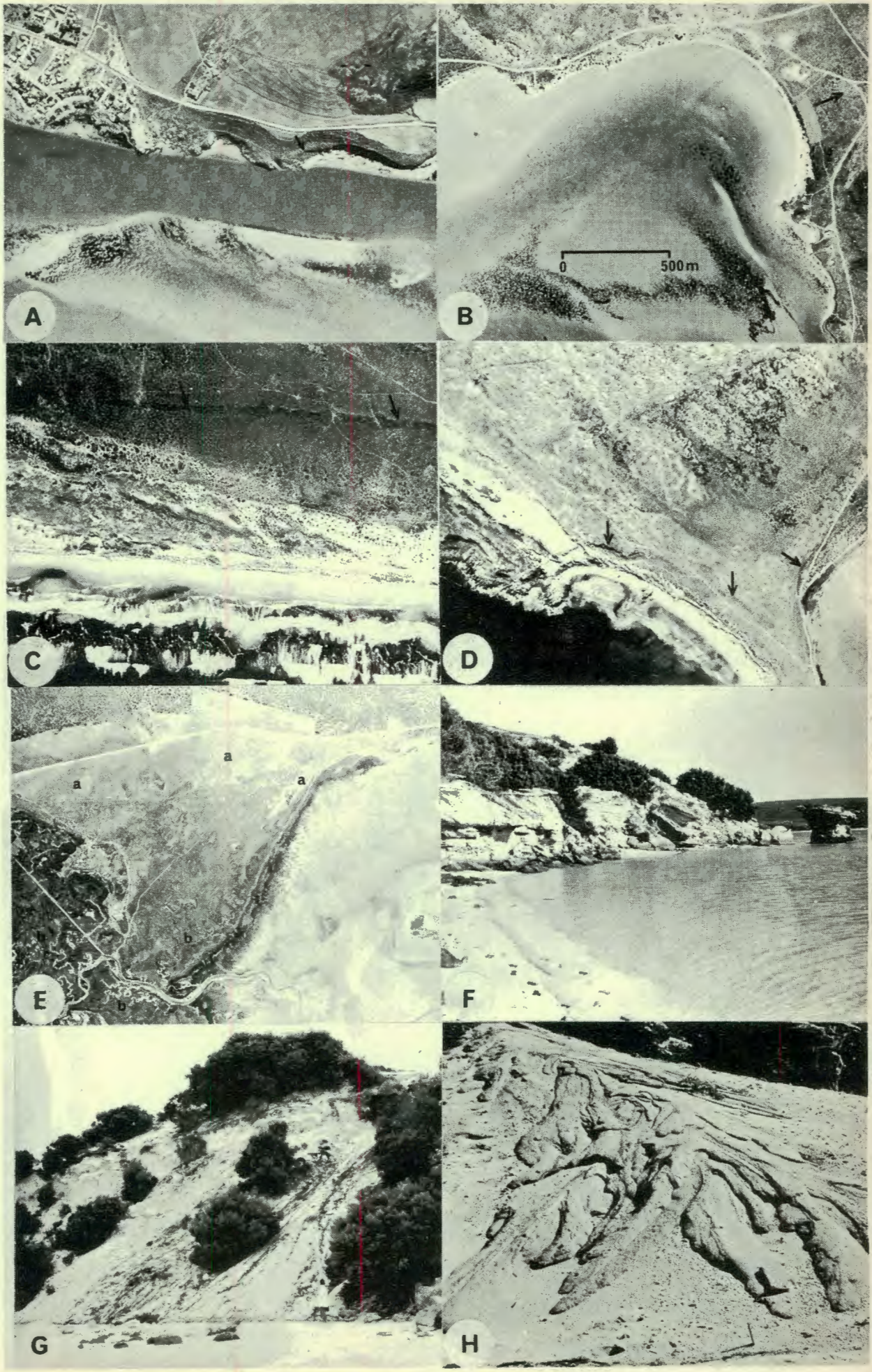

the Holocene sea-level.

5.1.2. Specific Features relating to a Holocene High Stand of the Sea

An important aspect regarding the lagoonal history is the presence of large fossil oyster reefs below most intertidal flat sediments east of the central channel, and below many shallow channel bars. The total mass has been estimated at several million metric tons (Tankard, 1975). Fossil oysters have also been found below the salt marshes and marshlands near Geelbek in the south. The base levels of individual reefs are situated at least 5 m below the modern sea level. Tankard (1976) has correlated the oyster reefs with the last interglacial transgression which reached its peak level some 120 ka B.P. However, radiocarbon dates from the bottom and the top of a reef have produced ages of only 6410 ± 45 years B.P. (GrN - 5878) and 1740 ± 50 years B.P. (Pta - 1667), respectively. The oysters (mainly Ostrea atherstonei) are, therefore, Holocene in age.

The young age of these shells also excludes the possibility of contamination by C^{14}-isotopes of different age. This problem was found to be critical in marine shell material older than 15 - 20 ka (Mörner, 1971; Fairbridge, 1971). In such cases the true age can not be reliably inferred and the recorded age would represent a minimum age only. The effects of partial recrystallization are well presented by Chappel and Polach (1972). In addition, the oyster shells from Langebaan Lagoon do not show any evidence of significant recrystallization. In fact, the voids between individual growth laminae of the shell have remained empty, or have been filled only partially with loose grit.

The presence of Holocene oyster reefs in Langebaan Lagoon requires that the postglacial sea-level reached its present position at least by 6400 B.P. It is inconceivable that the lagoonal basin could have been scoured at a sea-level below the present since the only connection to the sea lies in the southern, sheltered part of Saldanha Bay.

In this connection, two other physiographic features deserve closer attention. Between Kraalbaai and the open sea, a low valley separates the granite peninsula from the sediment barrier (viz. Fig. 127). This

valley appears to trace the course of a former outflow channel. Its lowest level today is just over 3 m above mean sea-level (Fig. 131). At the seaward end of this valley a beach ridge forms a low barrier across the whole width of the former channel. The crest of this beach ridge lies about 4 m above mean sea-level, in the shelter of a rocky promontory. Even storm waves do not reach the base of the deposit, which consists almost entirely of marine gastropod shells (Bullia sp.)

The age of the beach ridge has been dated at 2040 $\pm$ 60 years B.P. (Pta - 1601). In order to construct a beach ridge in this position, the sea must have stood at least 1-1.5 m above its present level. Its extension across the entire width of the channel would indicate a last-phase event in the closing of the channel. Considering the sea-level position inferred from the oldest oyster reefs and the base level of the relict channel, it is concluded that the Holocene sea must have stood some 3 - 4 m above its present level between 6400 and 2000 years B.P.

Another conspicuous feature in Langebaan Lagoon is presented by extensive areas of high-lying marsh deposits in the south and southeast. In Fig. 132 seven cross-sections through various parts of this marshland provide excellent evidence for the elevated position of their landward edges. The profiles are based on closely speced and photogrammetrically determined spot-heights with an accuracy of better than 20 cm. On average, these profiles would call for a sea-level of at least 2.5 m above its present level. Since marsh growth under the physiographic conditions in Langebaan Lagoon would be related to the emergence of intertidal flats, it is concluded that the original sea-level will have stood higher than the level inferred above.

Two additional radiocarbon dates from the Saldanha Bay area which indicate high lea-levels, are reported by Parker (1968) and Vogel (pers. comm., 1976). The former has dated shell material recovered from beach deposits 6 - 7 m above present sea-level at Jutten Point, near the South Head, at the entrance to Saldanha Bay. This material was dated at 2070 $\pm$ 50 years B.P. (Pta - 461). This date is almost identical to the one obtained for the beach ridge discussed above and is, most probably, related to the same event. The considerably higher elevation of the Jutten Point sample position simply reflects the local storm beach level at the more exposed parts of the coastline. Whereas the inference of a sea-level from the Jutten Point material is almost impossible, the

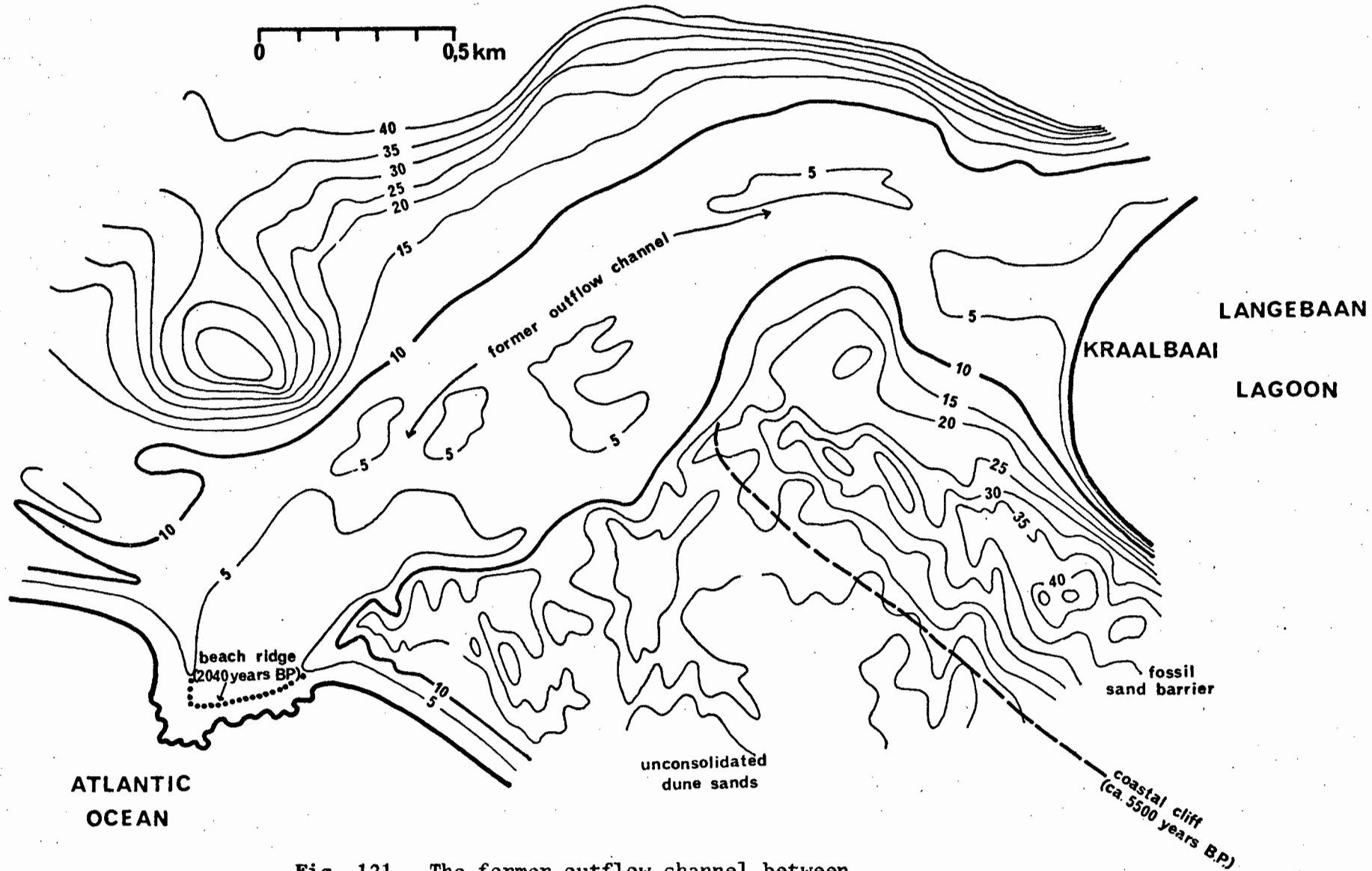

Fig. 131. The former outflow channel between Kraalbaai and the open sea

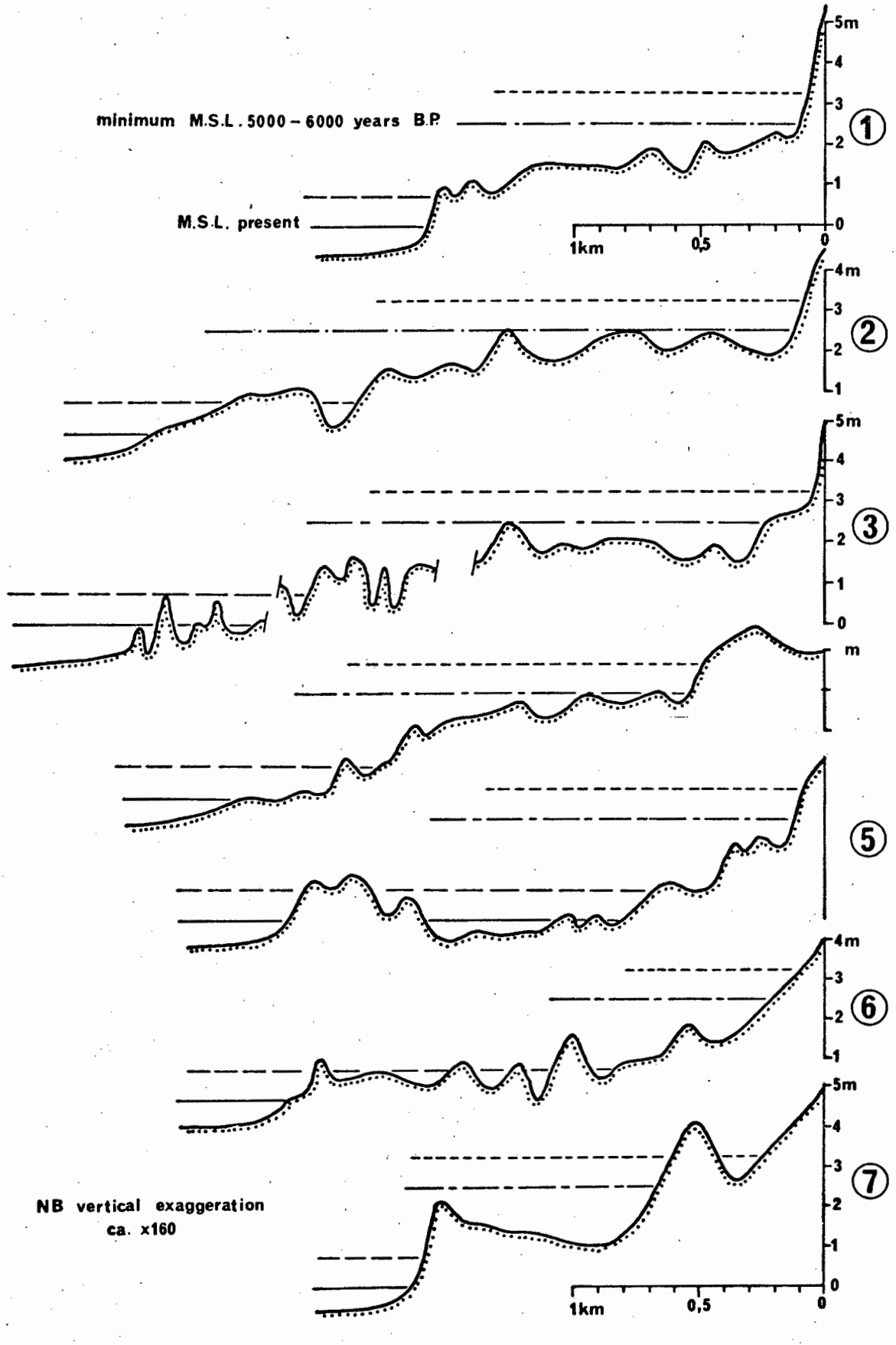

Fig. 132. Cross-sections through the marsh areas of Langebaan Lagoon

position of the beach ridge would appear to provide a reliable level.

Vogel (pers.comm., 1976) has dated shell material from the Bomgat cave on the Hoedjiespoint peninsula facing the North Bay. The interior of the cave, which lies at least 4 m above the present sea-level (Tankard, 1976), appears to have been awash sometime during the Holocene. At the back of the cave, beach cobbles and shelly sands form an undisturbed deposit. Shell material recovered from this site was dated at about 3500 years B.P. In order to reach the interior of the cave, the present sea-level would have to be raised by at least 1.5 - 2 m. A number of other studies, in which high stands of the Holocene sea level along the South African coast are indirectly inferred, are presented by Krige (1927), Martin (1962 and 1968), Tyson (1971), Butler and Helgren (1972) and Coetzee (1975).

From the above evidence, it is concluded that the Holocene sea-level must have crossed its present position about 6500 years ago, reaching a maximum level of at least +3 m between 6000 and 5000 years B.P. During this period the Kraalbaai channel and a smaller channel in Riet-baai were connected to the open sea, thus providing additional outlets for the lagoonal waters. The ebb current flowing through Kraalbaai was responsible for the undercutting and erosion of the lagoonal side of the fossil dune barrier, thereby cutting an extensive terrace into the under-lying calcretes. At the same time, oyster reefs flourished in abundance. In the course of the subsequent regression, salt marshes began to encroach upon former tidal flats and oyster reefs. At about 2000 years B.P. the Kraalbaai channel fell dry, and as a result, the flow pattern in Langebaan Lagoon orientated itself towards its present outflow channels. Along the southwestern shoreline of the lagoon, the former erosional activity was replaced by low-energy depositional processes, leading to the formation of intertidal flats and salt marshes. Thus, independent evidence has led to similar conclusions about the Holocene development of the lagoon. At this stage, it is not possible to resolve the exact course of the Holocene sea-level beyond the events directly inferred from the available radiocarbon dates.

The course of the Flandrian transgression has been a subject of considerable controversy in the past. It is beyond the scope of this study

to provide an exhaustive review on this topic; thus only some of the more relevant literature will be briefly discussed. Guilcher (1969) has presented a review summarizing the state of sea-level research up to that date. However, in the meantime, a number of important studies have added new information, and shorter reviews covering some of this data are presented by Bird (1972), King (1974) and Komar (1976). No generally accepted model for the postglacial sea-level recovery has emerged thus far and the subject remains controversial to this day. Tankard (1975), discussing local sea levels, could find no evidence for higher stands during the Holocene. On the other hand, strong evidence in support of this concept has been mounting in recent years. Well documented data is available especially from Australia (Fairbridge, 1961; Thom, 1972; Thom and Chappel, 1975; Hagan and Logan, 1975; Woods and Brown, 1975; Thom, pers. comm., 1977), New Zealand (Schofield, 1964 and 1973), Kamtchatka (Leont'yev and Nikiforov, 1965), and Mauritania (Elouard, 1968; Einsele et al., 1974). The general time period under consideration is identical in all these studies and agrees well with the findings in Langebaan Lagoon.

Consistently negative evidence is today almost exclusively restricted to the North American continent (Redfield and Rubin, 1962; Bloom and Stuiver, 1963; Stuiver and Dadario, 1963; Upson et al., 1964; Newman and Rusnak, 1965; Shepard and Curray, 1967; Scholl and Stuiver, 1967; Milliman and Emery, 1968). The relatively smooth rise of the inferred North American sea-level curve, reaching its present level some 2000 years B.P., stands in sharp contrast to the unsteadily oscillating curves observed on almost every other continent (Fig. 133-A).

Most of the North American dates originate from coastal and shallow marine boreholes along the Atlantic coast of the U.S.A. In a recent study, Winker and Howard (1977) have seriously questioned the applicability of the existing stratigraphic framework in this area, which is based on the assumption that the Atlantic coast of the U.S.A. has been stable during Pleistocene times. These authors have provided convincing evidence for substantial, non-uniform warping of the whole coastal plain during the Pleistocene. There is no evidence so far to suggest that this tectonic activity has ceased during the early Holocene and a re-evaluation of radiocarbon dates and their stratigraphic implications is urgently required in the light of this new information. It would appear that the stratigraphic

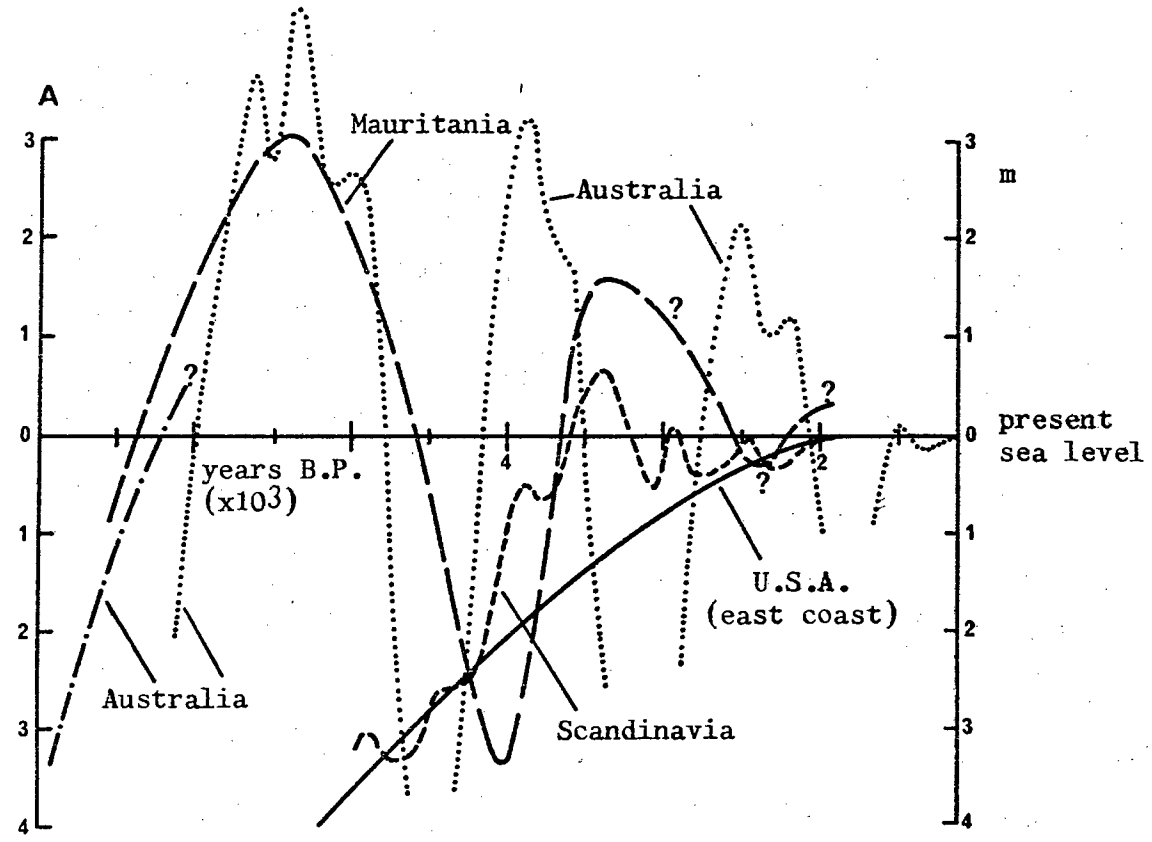

Fig. 133-A. The course of the Holocene sea level in various parts of the world

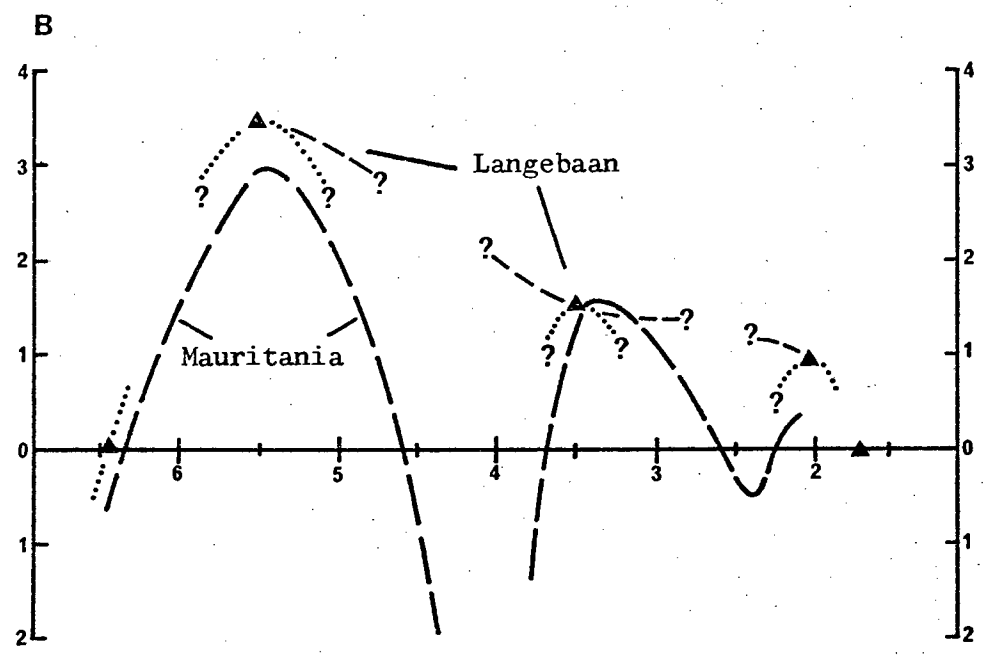

Fig. 133-B. Correlation between Langebaan sea level positions and those observed in Mauritania

record of the Holocene sea-level recovery along the Atlantic coast of the U.S.A. consistently lags behind, due to this warping effect.

Climatic fluctuations,inferred from oxygen isotope work on deep-sea cores, have been successfully correlated with well-documented sea-level data over the past 200,000 years or so (Emiliani, 1955; Shackleton and Opdyke, 1973; Mörner, 1973). Most of these studies have recorded a Holocene climatic optimum between 8000 and 4000 years B.P. This is particularly well documented in a recent study by Mörner (1973). On the basis of this evidence, the writer would prefer to relate the Holocene high stand of the sea observed in Langebaan Lagoon to a global eustatic event, although more regional tectonic effects cannot be entirely discounted. The data from Langebaan compare particularly well with that from North Africa, where a detailed reconstruction of the Holocene sea-level curve is based on field data discussed by Elouard (1968) and Einsele et al. (1974). The data from the two areas are compared in Fig. 133-B. The North African curve suggests that the regression that followed the initial high stand did not proceed smoothly but in a number of larger oscillations. Such repeated transgressive - regressive events have not been resolved in Langebaan; however, the conclusions reached about the general physiographic and sedimentary situation would remain essentially the same.

Langebaan Lagoon has thus experienced a rather eventful Holocene history. It will be demonstrated later that this has left strong imprints on the modern sediment distribution patterns. In fact, relevant aspects of the modern sedimentology can only be understood when considering the Holocene history of the lagoon as outlined above.

5.2. HYDRODYNAMIC CONSIDERATIONS

5.2.1. Current Patterns and Flow Velocities

Tidal flow in Langebaan Lagoon follows a semi-diurnal cycle and the area would be classified as a microtidal environment, i.e. with tidal ranges below 2 m (Davies, 1964 and 1972). Because of the elongation of Langebaan Lagoon and its relatively small outlets, the tidal range varies from place to place. An interesting feature is observed at the

outlets, where the spring tide range of 1.15 m is considerably less than the 1.50 m predicted for Saldanha Bay. Retief (1977) relates this phenomenon to a venturi draw-out effect through the narrow outflow channels. Thus spring tide and neap tide ranges are 1.15 m and 0.39 m, respectively, at the mouth of the lagoon and 1.35 m and 0.50 m, respectively, in the southern lagoon. Pertinent tide data are listed in Table 6.

It should be noted that any local tide level can vary strongly from its predicted mean value, due to the pronounced influence of prevailing winds. A strong seasonal effect can be observed in the southern and eastern lagoon, where strong southerly winds during summer depress both high tides and low tides, whereas during the winter months this effect is reversed with strong northerly winds increasing the high tide levels and causing a stow effect at low tide.

The flow pattern is rather complex but appears to be controlled by the ebb current. Fig. 134 gives an impression of the ebb current pattern of the surface water at spring tide in the northern section of the lagoon. The dominant flow paths indicate that most of the water appears to drain through the eastern channel. Flow rate calculations in fact demonstrate that the western channel, which is constricted by a submerged rock barrier, drains only a quarter to a third of the water volume flowing out of the lagoon in each ebb cycle. Table 7 gives an impression of the expected discharge per unit time for each channel. The total water volume entering and leaving the system in each tidal cycle amounts to 65 - 70 million m^3.

TABLE 7

Discharge rates at the mouth of Langebaan Lagoon

Outlet	average (m^3/sec)	maximum (m^3/sec)
Eastern Channel	2390	3744
Western Channel	900	1200

The asymmetry of the tidal ellipse produces peak ebb-current velocities that are about 20% higher than flood current velocities

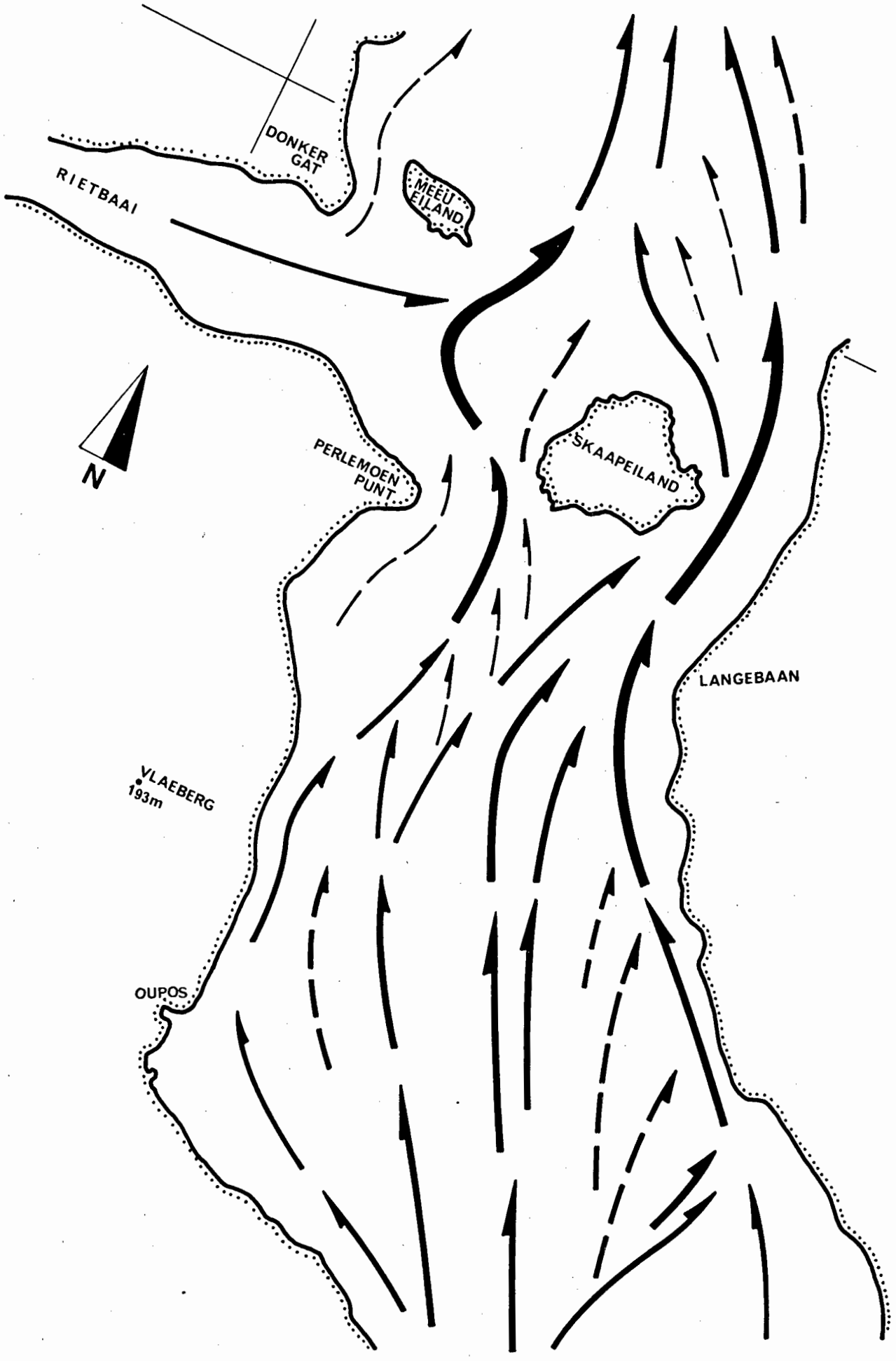

Fig. 134. The flow pattern of the ebb current

TABLE 6

A. Tide levels in Langebaan Lagoon (over 10 000 observations)

HEIGHTS	Lagoonal Mouth	Southern Lagoon
HATOY (1977)	2.01	2.20
MHWS	1.72	1.62
MHWN	1.29	1.24
ML	1.04	1.04
MLWN	0.79	0.85
MLWS	0.37	0.47
LATOY (1977)	0.23	0.07
RANGES		
SPRING TIDE	1.35	1.15
NEAP TIDE	0.50	0.39

B. Tidal delay between inlet and southern lagoon

MONTH	HIGH TIDE	TIME LAG	LOW TIDE	TIME LAG
	MEAN (min)	STD. DEV. (min)	MEAN (min)	STD. DEV. (min)
FEB	58.5	13.6	67.0	14.2
MAR	49.7	19.9	54.8	24.2
APR	35.4	37.9	36.3	42.0
MAY	28.6	29.8	45.5	27.0
JUN	41.5	29.2	59.3	27.9
JUL	26.9	37.2	37.0	40.6
AUG	29.5	37.2	50.2	27.5
SEP	36.2	27.4	49.2	34.7
OCT	28.7	32.8	54.2	31.3
NOV	41.1	30.6	99.0	14.9

(after Retief, 1977)

(Fig. 135-A). Current strength decreases progressively with distance from the mouth (Fig. 135-A: Inset A). In the eastern outlet, the maximum ebb current velocity that was recorded at the surface reached 130 cm/sec, whereas the western channel never exceeded 100 cm/sec. Flood current velocities are about 90 cm/sec for both channels. In the southern lagoon, ebb and flood currents drop to an average of 60 cm/sec and 45 cm/sec, respectively.

The elongate shape of the lagoon induces a considerable time lag between tidal events at various localities within the system. On average, there is a steady increase in the tidal delay with distance from the mouth, reaching an estimated maximum of ca. 80 min. for the turn of the current near high tide, and about 50 min. for the turn of the current near low tide, (Fig. 135-A: Inset B). An interesting phenomenon was observed in the relationship between the level of the tide and the reversal of the current. There appears to be a consistent time lag between the turn of the tide and the reversal of the current; e.g. at low tide near Churchhaven it was observed that the water was still flowing in the ebb direction, at a velocity of about 20 cm/sec, while the tide was already rising. This feature suggests a pronounced separation between inflow and outflow paths of the tidal currents. This phenomenon is well documented in the literature, e.g. van Straaten (1953), Jacobsen (1962), Schou (1967), Klein (1970). The distinct orientation of some intra-lagoonal channel deltas in fact confirms this interpretation.

Bottom currents are about 25% lower than surface currents, reflecting the effect of frictional drag near the channel beds. Since initiation of sediment movement is essentially a boundary layer phenomenon, near-bottom current velocities are a better indicator for the transport capacity of the flow. In Fig. 135-B the time-averaged velocity profiles, measured at about 1 m above the bottom at three localities in the lagoon, illustrate schematically the respective transport capacities of the ebb and the flood current at the different stations. The dominating position of the ebb current is immediately apparent. While the ebb current will generate underwater dunes in most parts of the channel system, the flood current reaches this capacity with certainty only in the northern parts of Langebaan Lagoon. As a result, major bedforms are expected to be predominantly oriented in the ebb current direction. A similar conclusion was reached when discussing the orientation of large surface structures on the intertidal flats (Section 5.1.1.)

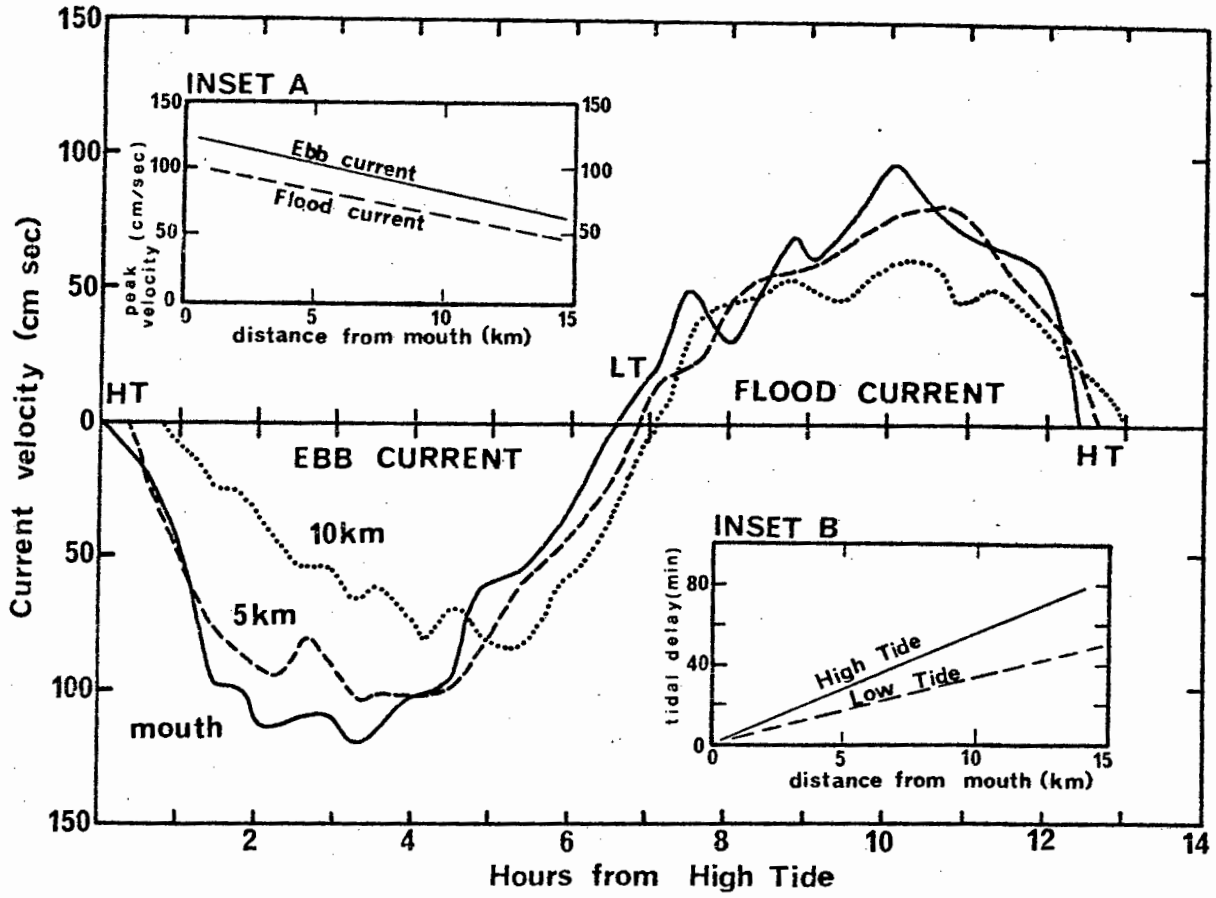

Fig. 135-A. Time-velocity diagram of the surface currents in Langebaan Lagoon measured at three stations

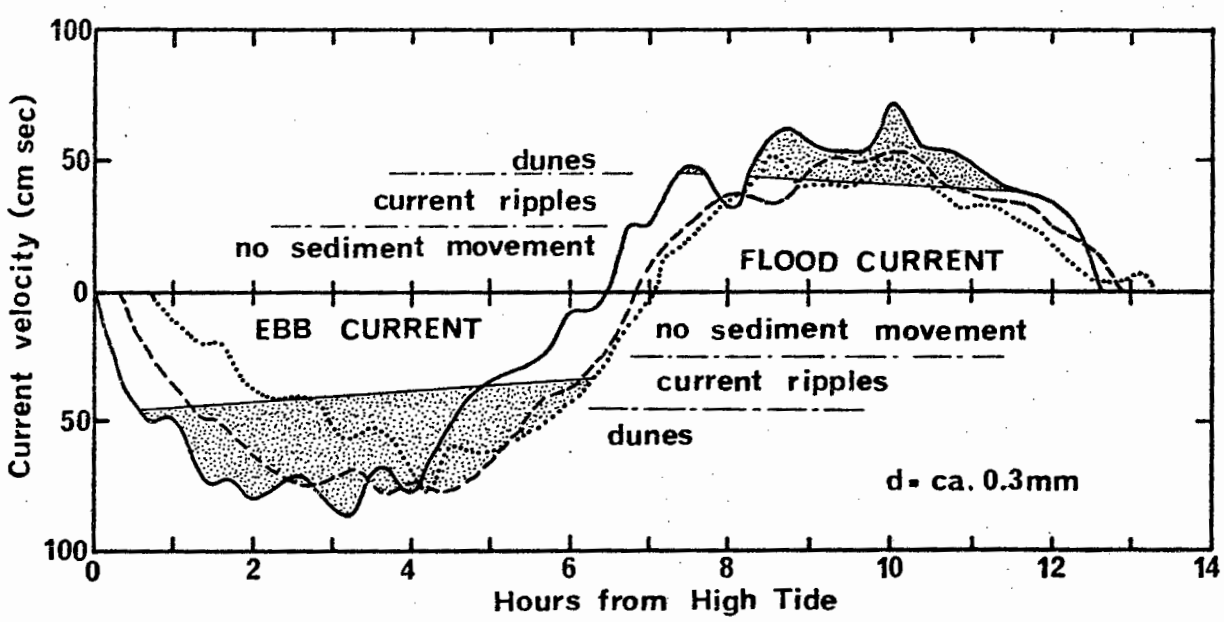

Fig. 135-B. Time-velocity diagram of the bottom currents in Langebaan Lagoon. Note the high potential for dune generation by the ebb current at all three stations

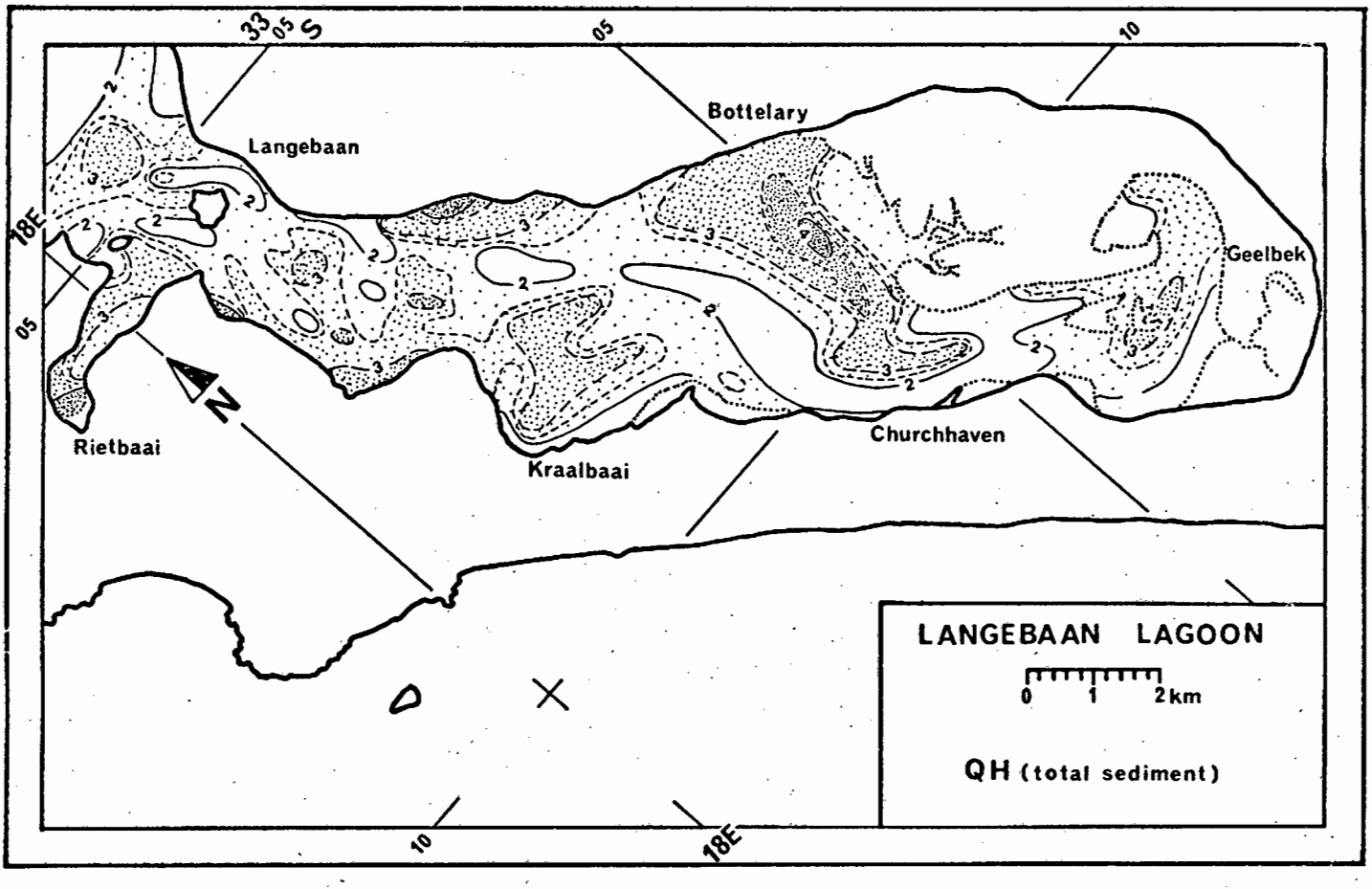

Fig. 153

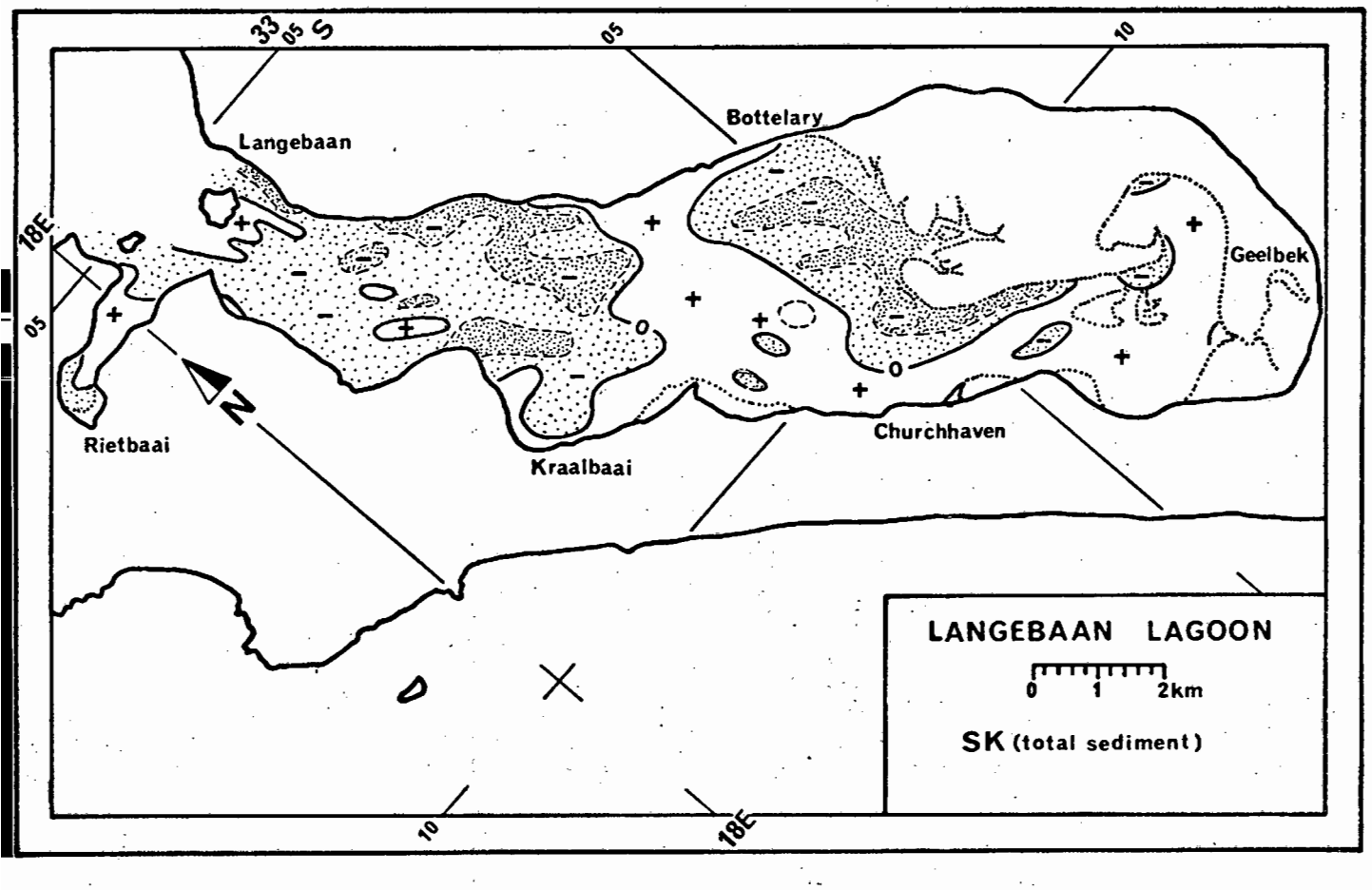

Fig. 154

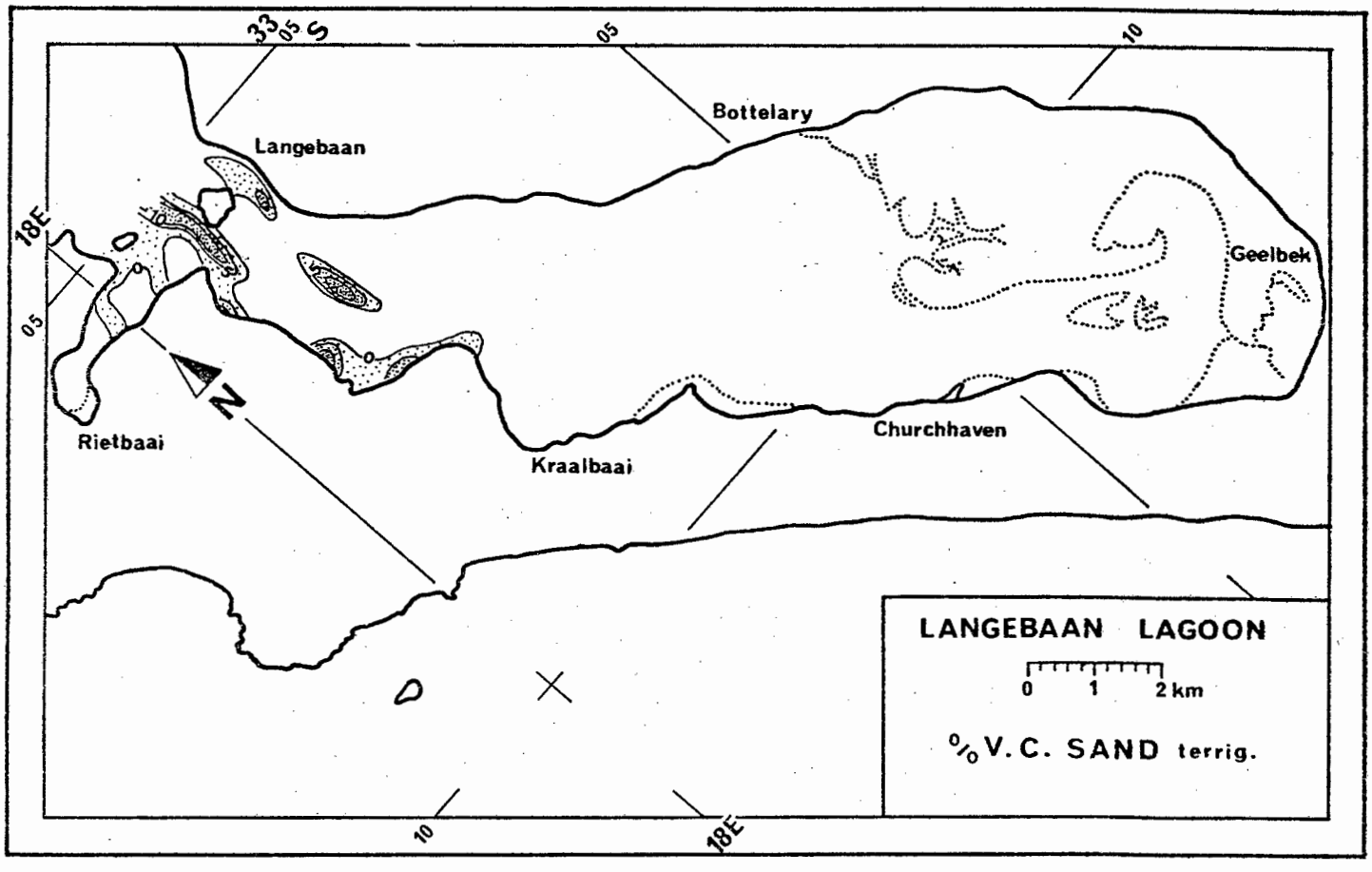

Fig. 158

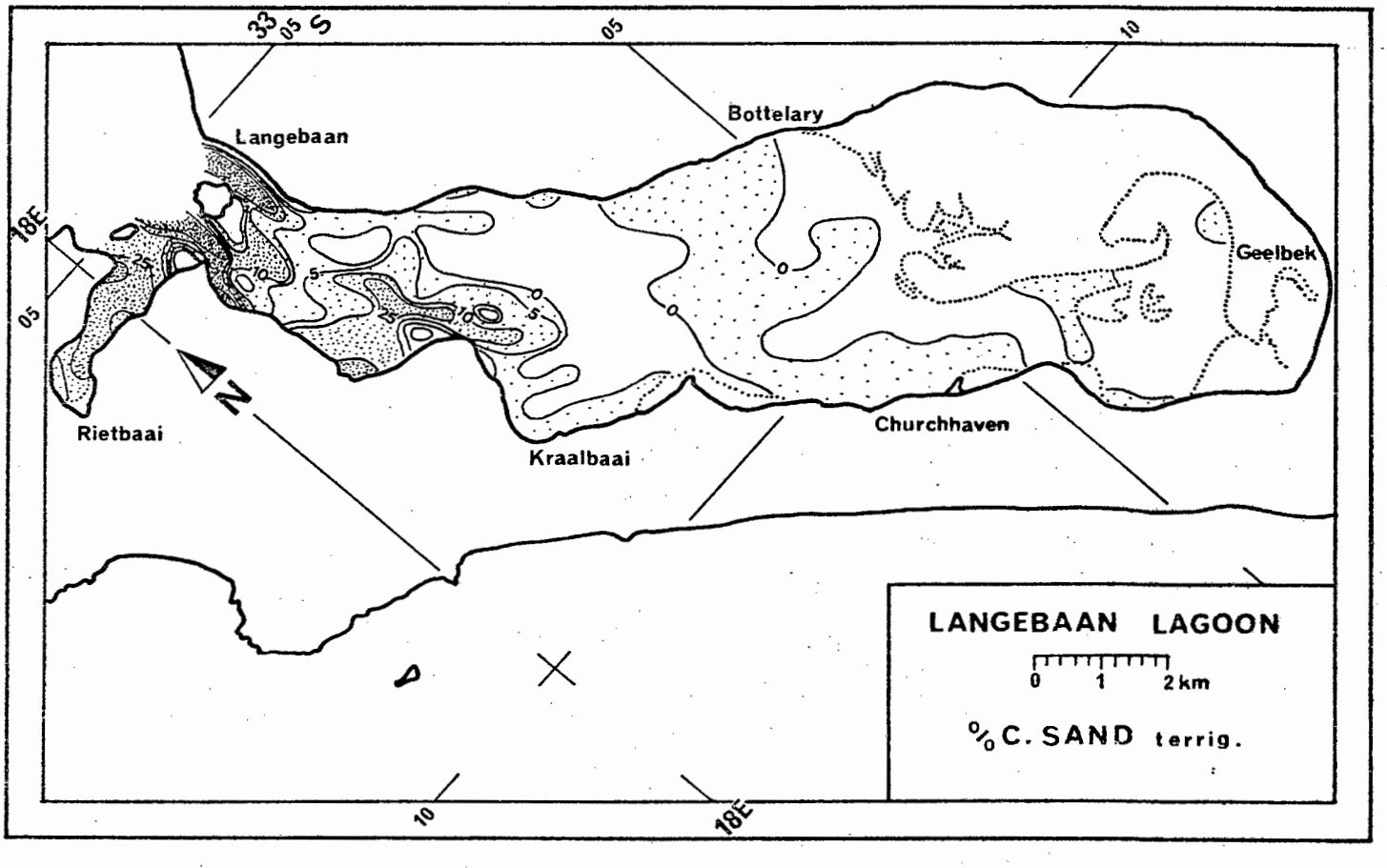

Fig. 159

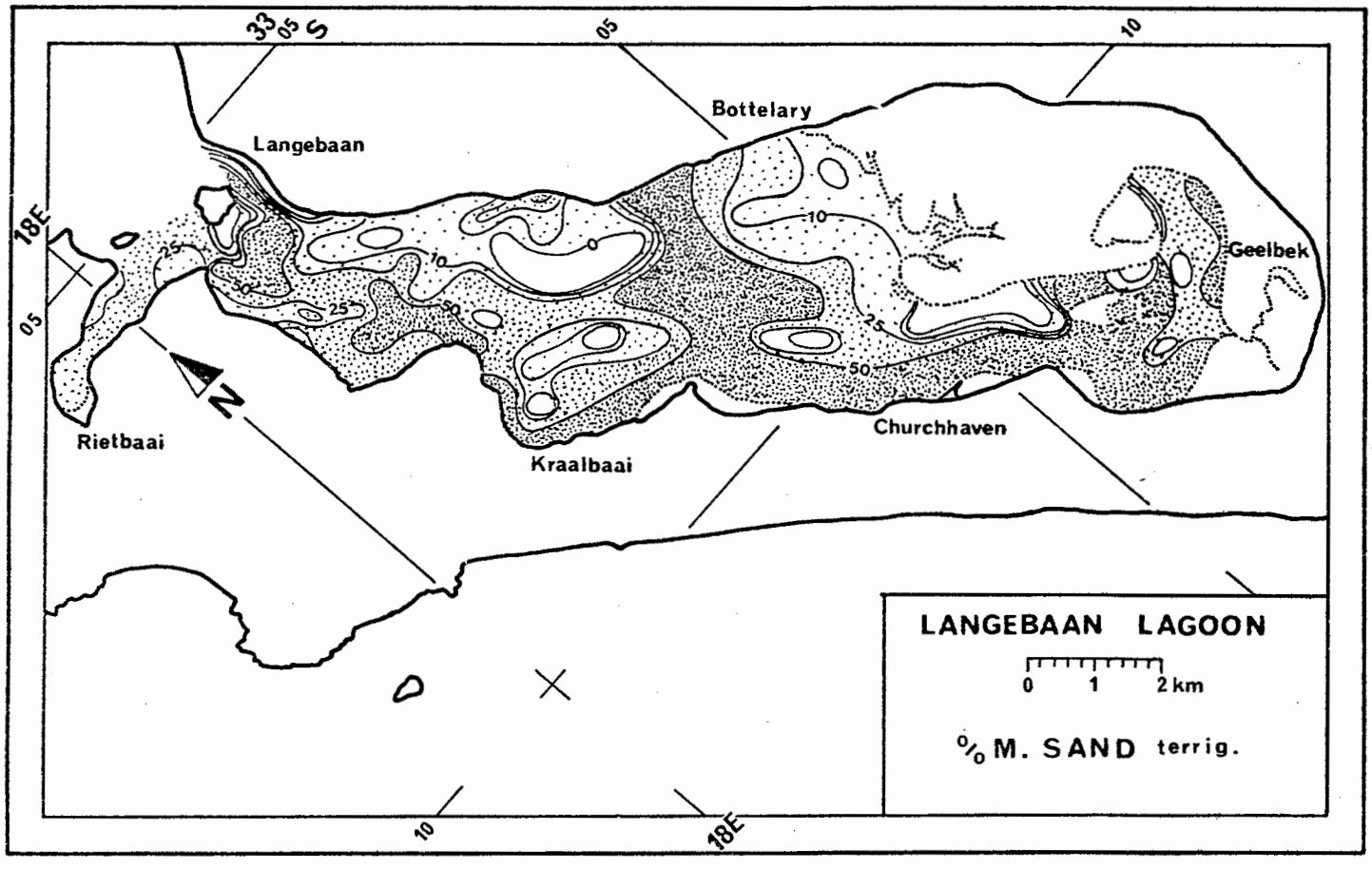

Fig. .160

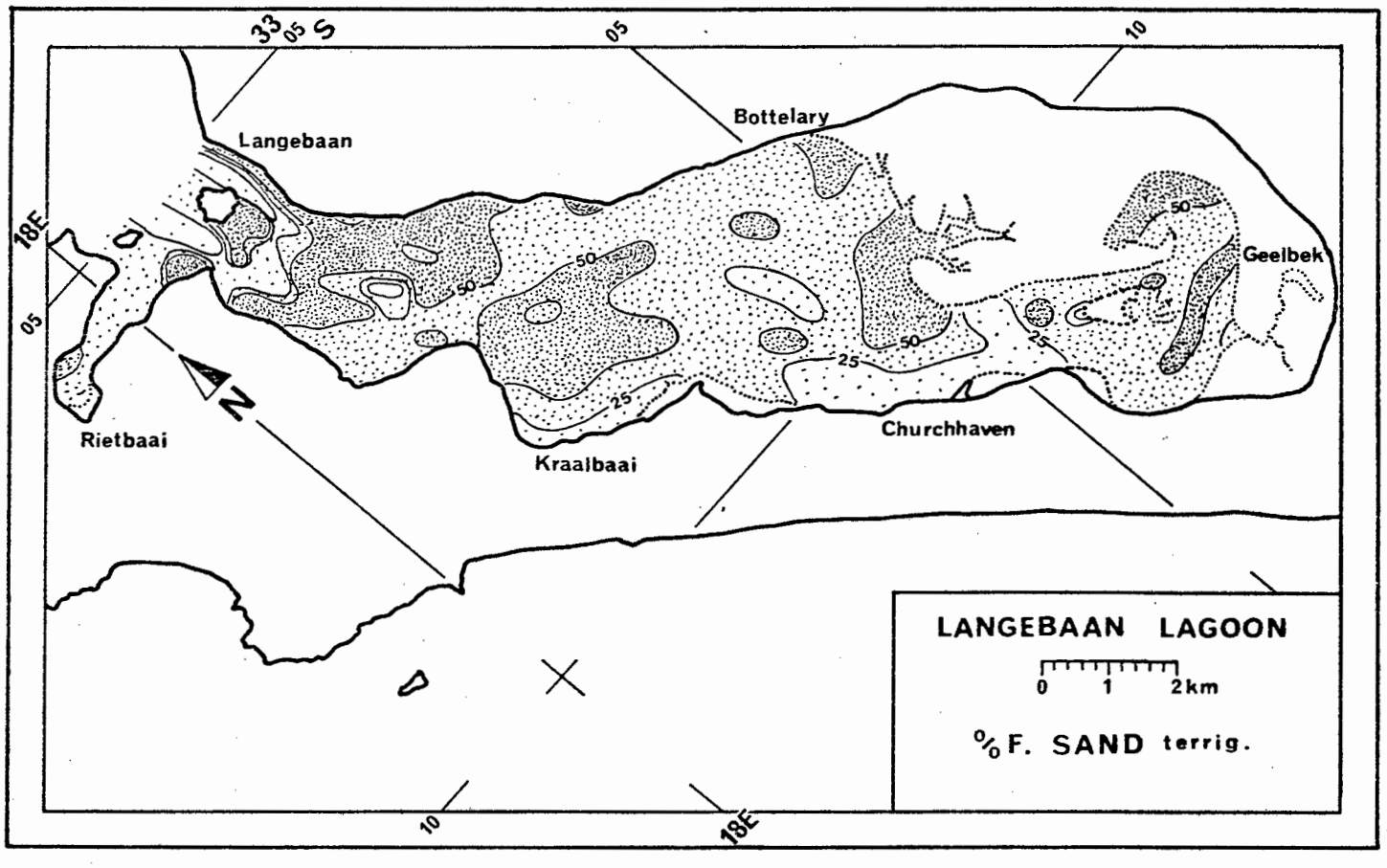

Fig. 161

It is spread over much smaller areas, being strictly confined to the outflow channels and the granitic fan deposits (Fig. 158). Even coarser terrigenous sands are not as widely spread as those of the total sediment, especially in the central and southern lagoon (Fig. 159). This indicates that most of the channel lag material is, in fact, composed of bioclastic sediment.

Medium sand (Fig. 160), fine sand (Fig. 161) and very fine sand (Fig. 162), on the other hand, have distribution patterns very similar to the respective size fractions of the total sediment. There is somewhat more fine, and very fine, terrigenous sand in the lagoon than might have been expected from the total sediment patterns, especially in the northern parts of the central lagoon and in the northern lagoon. The medium sand corridor, that was observed in the total sediment pattern, as cutting across the eastern tidal flat area between Oesterwal and Bottelary, is even better defined in the medium terrigenous sand pattern. The separation of an inner and an outer fine and very fine sand repository is thus well established. In general, the differences are small and very localized, simply emphasizing the trends already observed in the patterns of the total sediment. This is particularly well illustrated by the mean diameter map (Fig. 163), which is almost identical to that of the total sediment. In this respect, the lagoon differs substantially from Saldanha Bay, where the individual sedimentary components displayed considerably different mean diameter characteristics than the total sediment.

On the whole, the lagoon comprises very well to well sorted terrigenous sediments (Fig. 164). Extremely well sorted sediments ($QH<1$) are rare, and occur only in the eastern outflow channel and on the high levels of the north-eastern tidal flats. On the other hand, moderately sorted sediments are totally absent. The relative sorting of the terrigenous sediment is on average slightly better than that of the total, whereby this phenomenon appears to increase towards the better sorting categories.

In conformity with the total sediment, the medium sized terrigenous sediment is positively skewed, whereas the finer sediments are negatively skewed (Fig. 165). The division line between the two skewness groups is almost identical in the southern and the south-central lagoon, but differs slightly more in the northern and north-central regions. An important aspect is presented by the degree of skewness. The terrigenous skewness spectrum is displaced as a whole towards the positive side, i.e. the negatively skewed

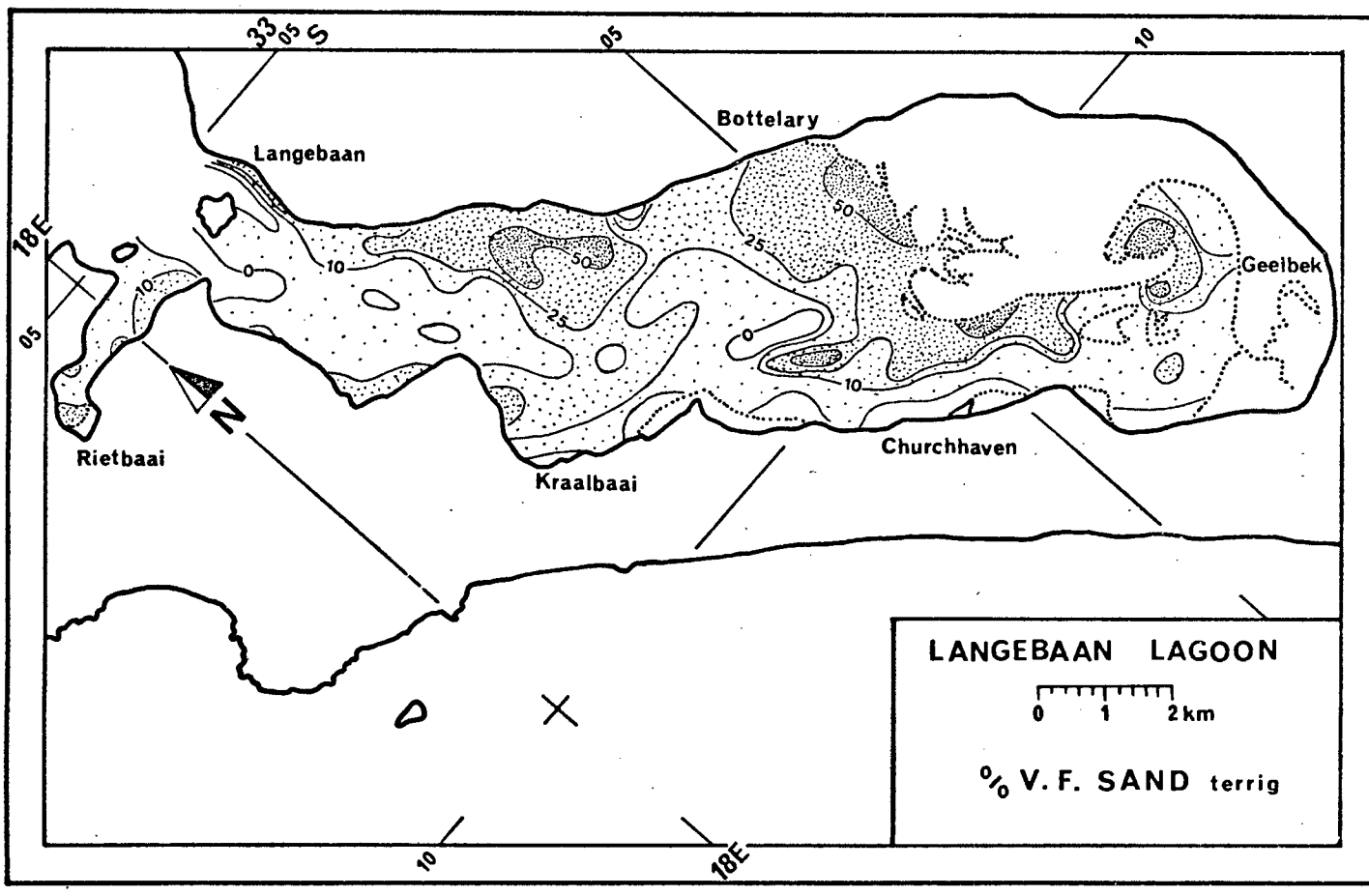

Fig. 162

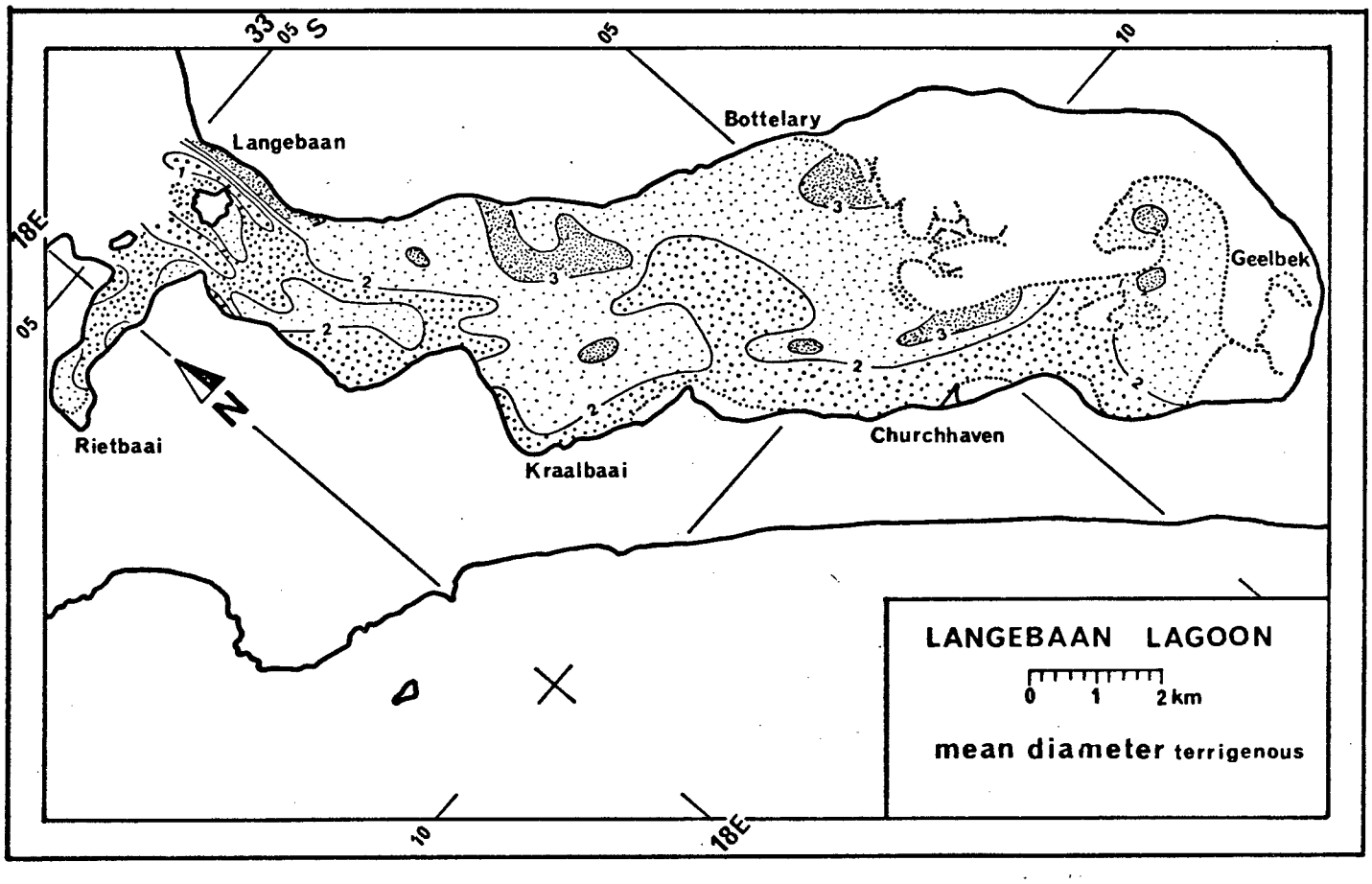

Fig. 163

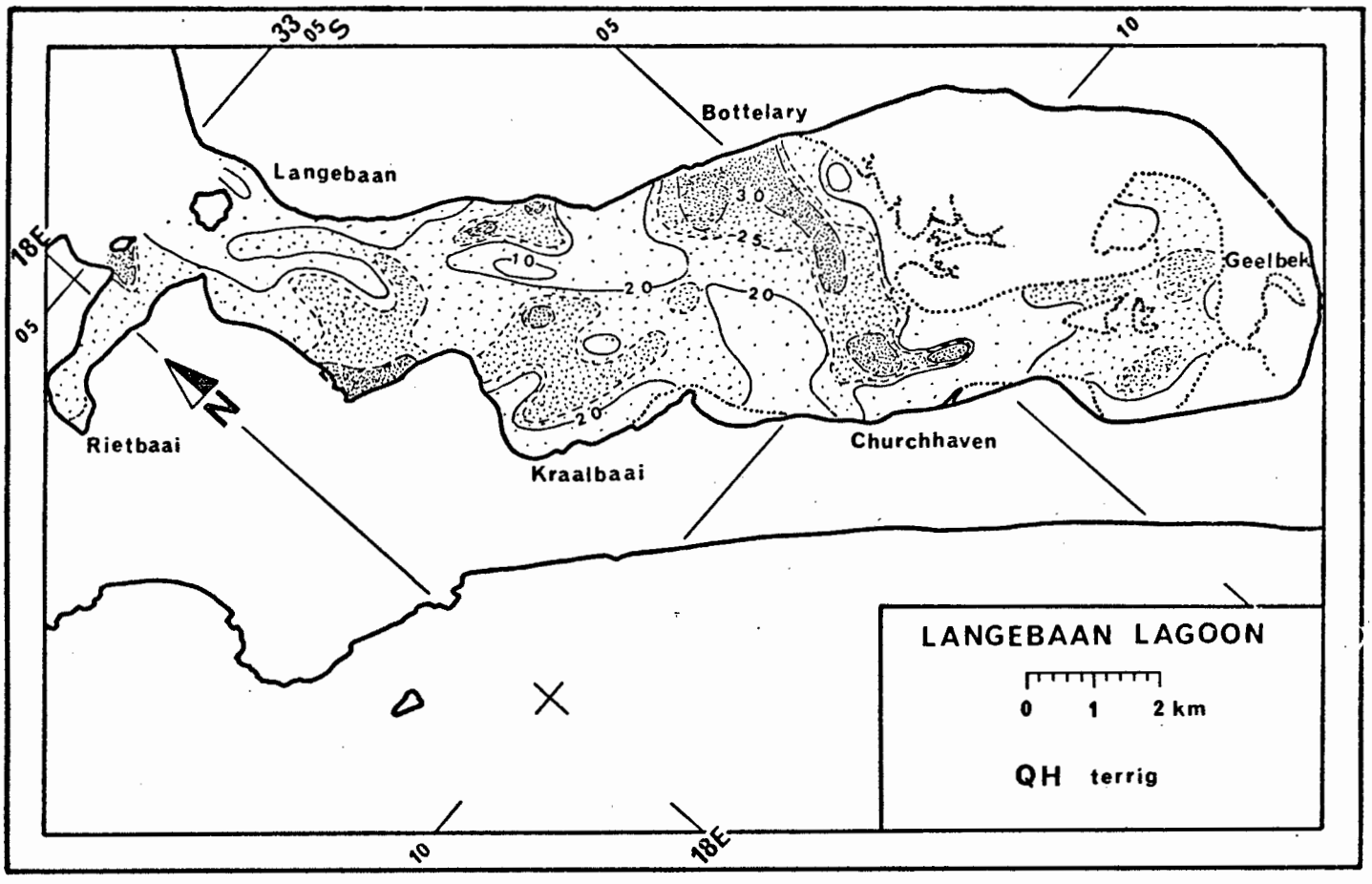

Fig. 164

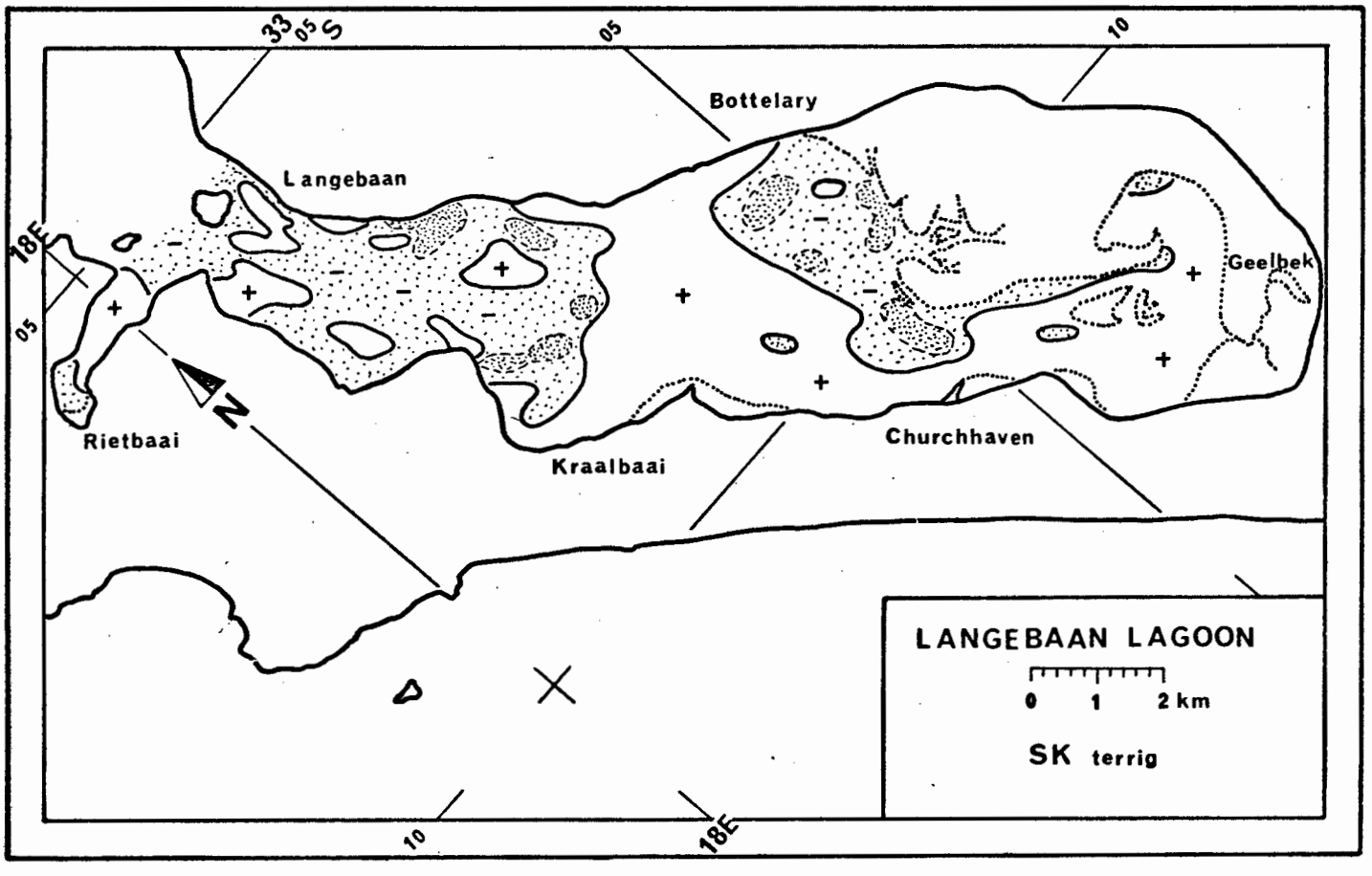

Fig. 165

terrigenous sands have, on average lower negative skewness values, whereas the positively skewed sands are, on average, stronger positively skewed. In the northern lagoon, there are larger areas with positively skewed sediments than in the total sediment pattern, and, in some places, there are positively skewed terrigenous sediments where the total sediment is negatively skewed. It appears that this phenomenon is related to the size distribution characteristics of the bioclastic component. On the whole, therefore, the terrigenous skewness spectrum is centered around the near-symmetrical level, whereas the total sediment leans more to the negatively skewed side.

The three-dimensional relationship between mean diameter, relative sorting and skewness of the terrigenous component is similar to that of the total sediment, although the point clusters are more cohesive and slightly displaced, in accordance with the skewness characteristics observed above. While the difference in the mean diameters is minimal, the whole point cluster in Fig. 166 (XY-plane) is displaced downward towards better sorting. As observed above, the displacement of individual points increases as the general level of sorting increases. Fig. 167 (XZ-plane) illustrates the manner in which terrigenous skewness characteristics have displaced the whole helix towards a more central position. The magnitude of this displacement amounts to at least 0.2 skewness intervals. The total modification of the position of the point cluster is illustrated in Fig. 168, which displays the skewness-sorting relationship (YZ-plane).

In summary, it can be concluded that the terrigenous component presents a very similar picture to that of the total sediment. The statistical size parameters of the terrigenous sediment in various parts of Langebaan Lagoon are controlled, in similar manner, by the mixing of a coarser and a finer hydraulic population. The three-dimensional relationship between the main size parameters describes a helical trend that is very similar, but not identical, to that of the total sediment. The deviation is not localized in isolated samples but systematic throughout the whole helical structure, whereby the displacement relative to the helix described by the total sediment amounts to at least 0.2 skewness intervals and between 0.2 and 0.4 QH-values.

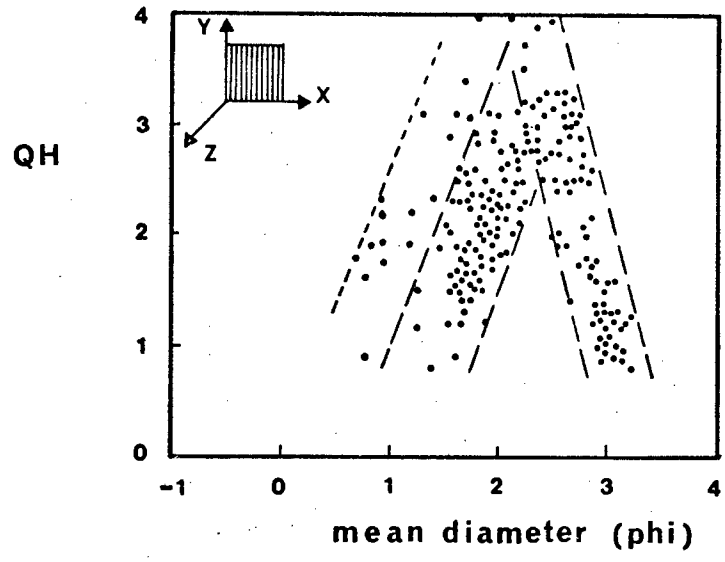

Fig. 166. The relationship between mean diameter and sorting of the terrigenous component

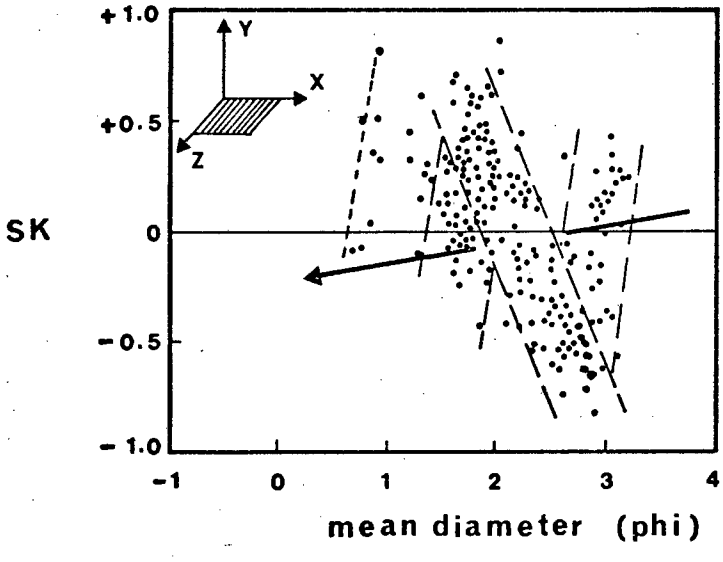

Fig. 167. The relationship between mean diameter and skewness of the terrigenous component

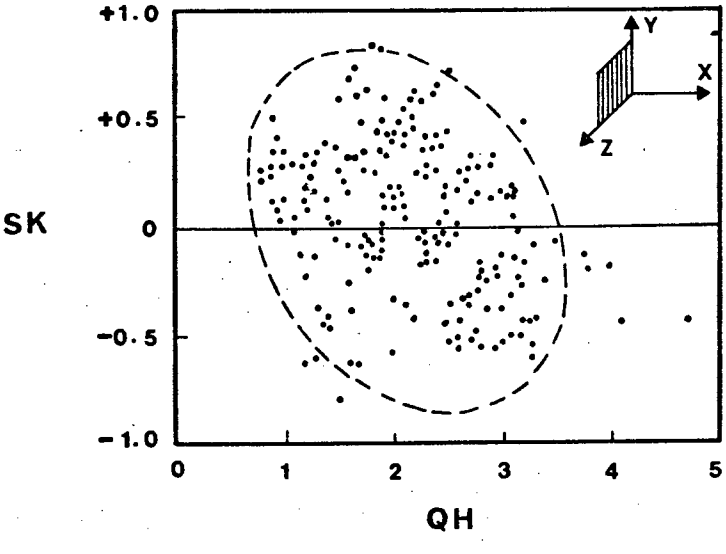

Fig. 168. The relationship between sorting and skewness of the terrigenous component

5.4.3. Bioclastic Component

In the previous section, it was shown that the distribution patterns of all the individual size fractions of the terrigenous component remained very similar to those of the total sediment. Since the bioclastic component forms the complementary element to the terrigenous component in the total sediment, it is not expected to differ significantly either. However, even subtle differences could shed some light on the relationship between the two components, with respect to their provenance and hydraulic response within the lagoonal system. A point to be born in mind is the overall, small contribution to the total sediment by the bioclastic component in the central and southern sections of the lagoon. Deviations between the two components in these areas will, therefore, not have the same effect on the total sediment as in the northern parts of the lagoon.

Gravels and very coarse sands are spread over larger areas than in the terrigenous sediments, although they also remain strictly confined to the northern lagoon (Fig. 169). The coarse bioclastic sand distribution is very similar to that of its terrigenous counterpart in the northern lagoon, but differs slightly more in the central and southern parts (Fig. 170). In general, areas without coarse sediment are smaller. Relative concentration levels are throughout slightly higher than in the respective terrigenous size fraction. The overall contribution to the total sediment, on the other hand, is considerably smaller because of the low contribution of bioclastic sediments to the total.

The medium sand pattern differs in two aspects. With the exception of a few small areas in the southern lagoon, there is virtually no locality in the lagoon that does not have at least a small proportion of bioclastic medium-sized sand (Fig. 171). In contrast, there are considerably larger areas lacking terrigenous medium sands, especially in the north-central parts of the eastern tidal flats. It would thus appear that the process of size sorting is more efficient in the terrigenous sediments. A second deviation is observed in the central section of the lagoon north of Churchhaven, where a lobe of medium sand extends across the channel onto the eastern intertidal flats. Unlike the terrigenous medium sands, the 50% concentration level of medium bioclastic sand does not reach the opposite shoreline of the lagoon. This feature may indicate that the bioclastic material does not have the same hydraulic response as the terrigenous sediment - a feature that appears to be

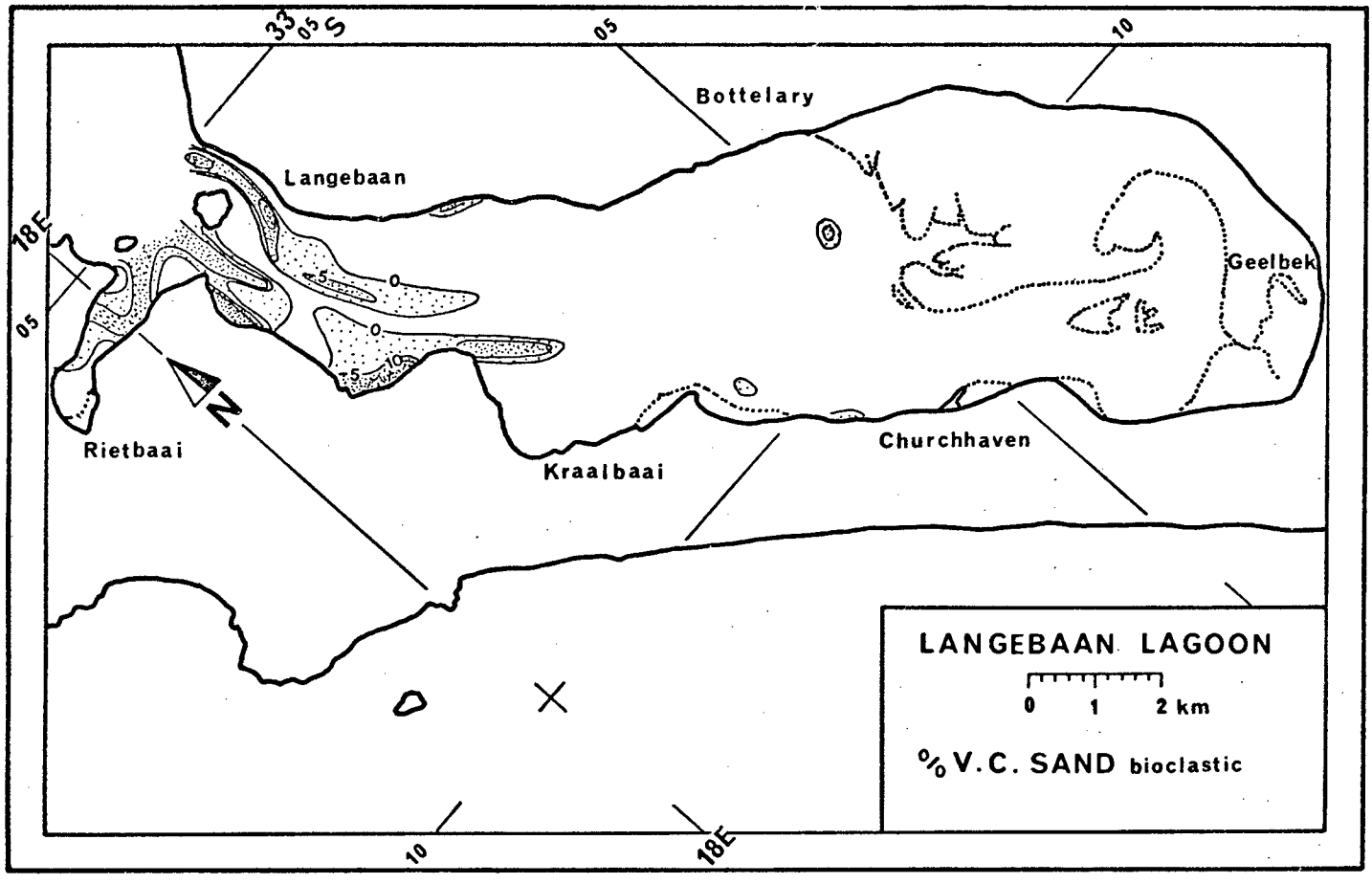

Fig. 169

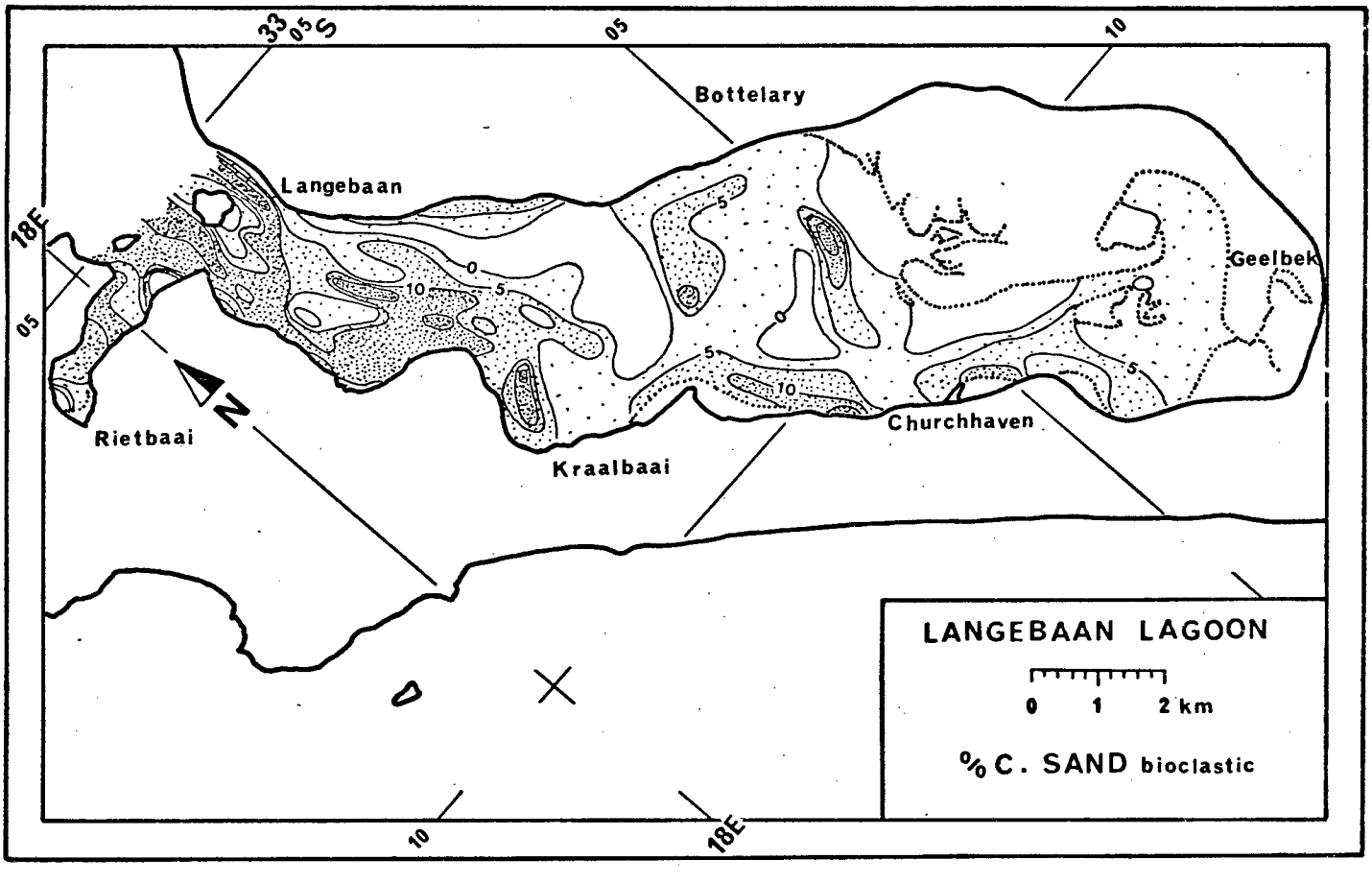

Fig. 170

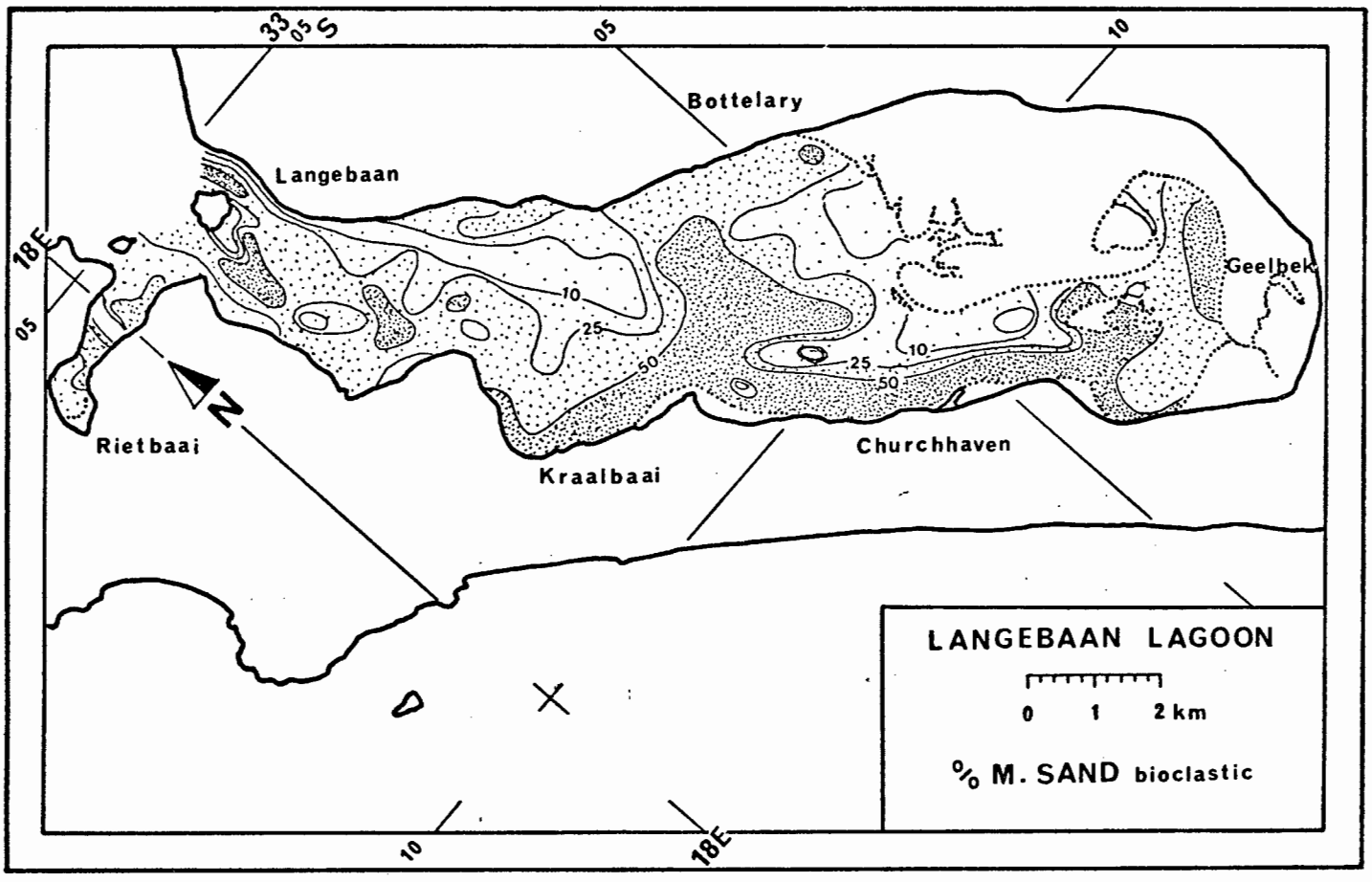

Fig. 171

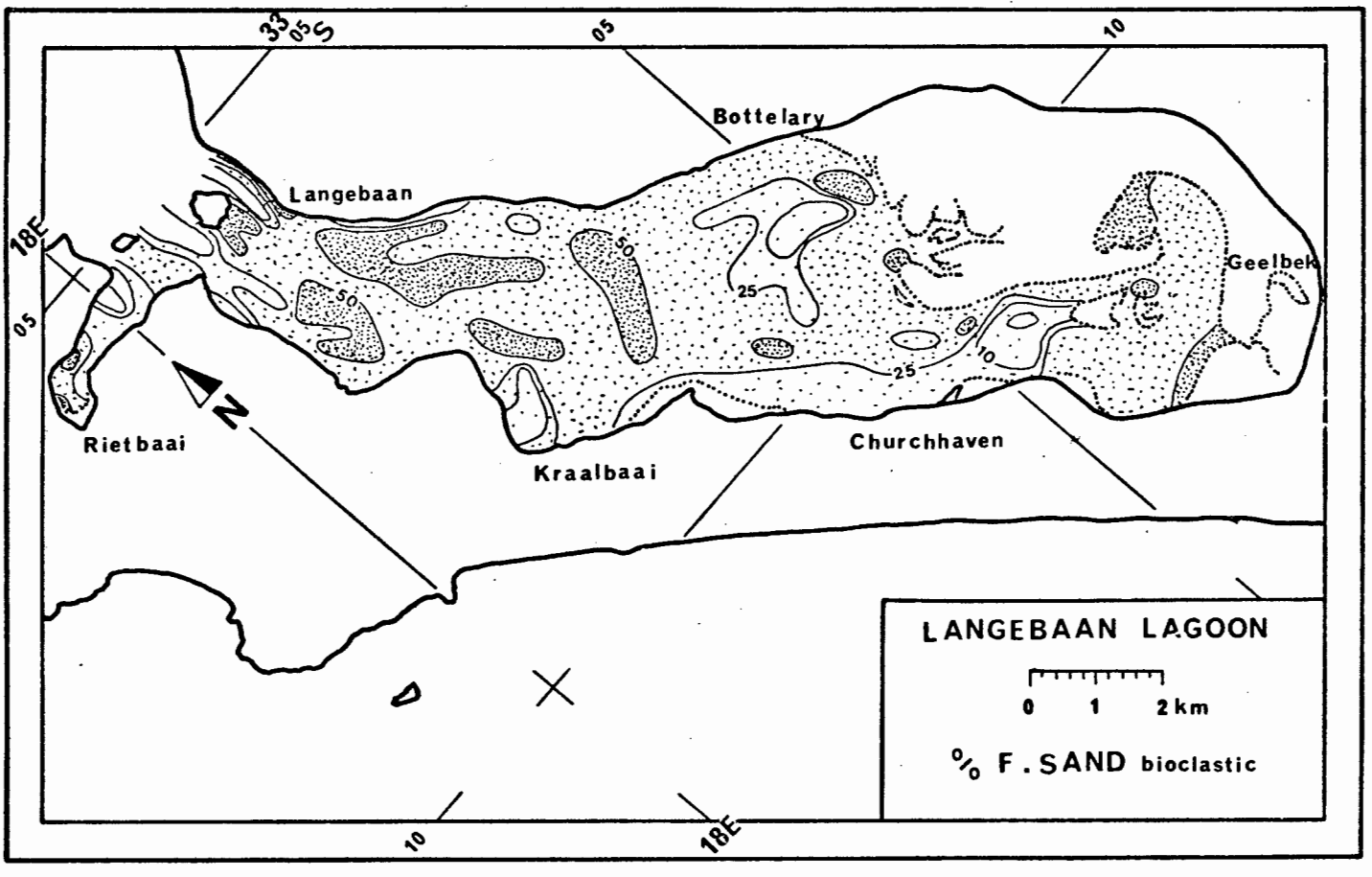

Fig. 172

particularly well recorded in areas close to threshold conditions. Although the sand belongs to the same size fraction, it is not transported as far into the low energy domain as the terrigenous sediment.

The distribution pattern of fine bioclastic sands shows the same general, blanketing effect as in the case of the terrigenous fine sand (Fig. 172). However, overall concentration levels are a little lower, and the areas containing over 50% fine bioclastic sands are smaller than their terrigenous counterparts. A common feature is the low concentration of fine sand adjacent to the fossil dune barrier. As in the case of the terrigenous fine sand, the fossil dune belt does not appear as a likely source for fine sediments. In fact, the fine sand content of the dune sediments is extremely low.

The distribution of very fine bioclastic sand, as with its terrigenous counterpart, forms the complementary pattern to that of the medium sands (Fig. 173). The bioclastic and the terrigenous patterns are very similar, with only one major deviation occurring along the salt marsh boundary south-west of Bottelary. The highest very fine bioclastic content occurs towards the centre of the eastern intertidal flat area, dropping off both towards the channels and towards the salt marshes. Very fine sand content of the terrigenous sediments, on the other hand, increases steadily right up to the salt marsh boundary. The overall contribution of very fine bioclastic sediment is proportionally very small in this area, and it would appear that some material is being mixed into the surface sediments from the underlying carbonate reservoir. Sediment thickness in this area is very low, often less than 10 cm. Towards the salt marshes, on the other hand, the sand cover reac hes 1 m and more.

The effect of minor differences in the individual distribution patterns between terrigenous and bioclastic sediments is best illustrated in their mean diameter maps. The overall pattern of the bioclastic sediment (Fig. 174) is almost identical to that of the terrigenous sediment (viz. Fig. 163). There is somewhat less fine and very fine sediment in the bioclastic component, and as a result, fine and very fine sediments occupy smaller overall areas, which is to the advantage of the medium sands. Since both components are so similar with respect to their mean diameters, the total sediment pattern will obviously not deviate substantially (viz. Fig. 152). As far as mean diameters are concerned, the two sedimentary components thus appear to be in hydraulic equilibrium.

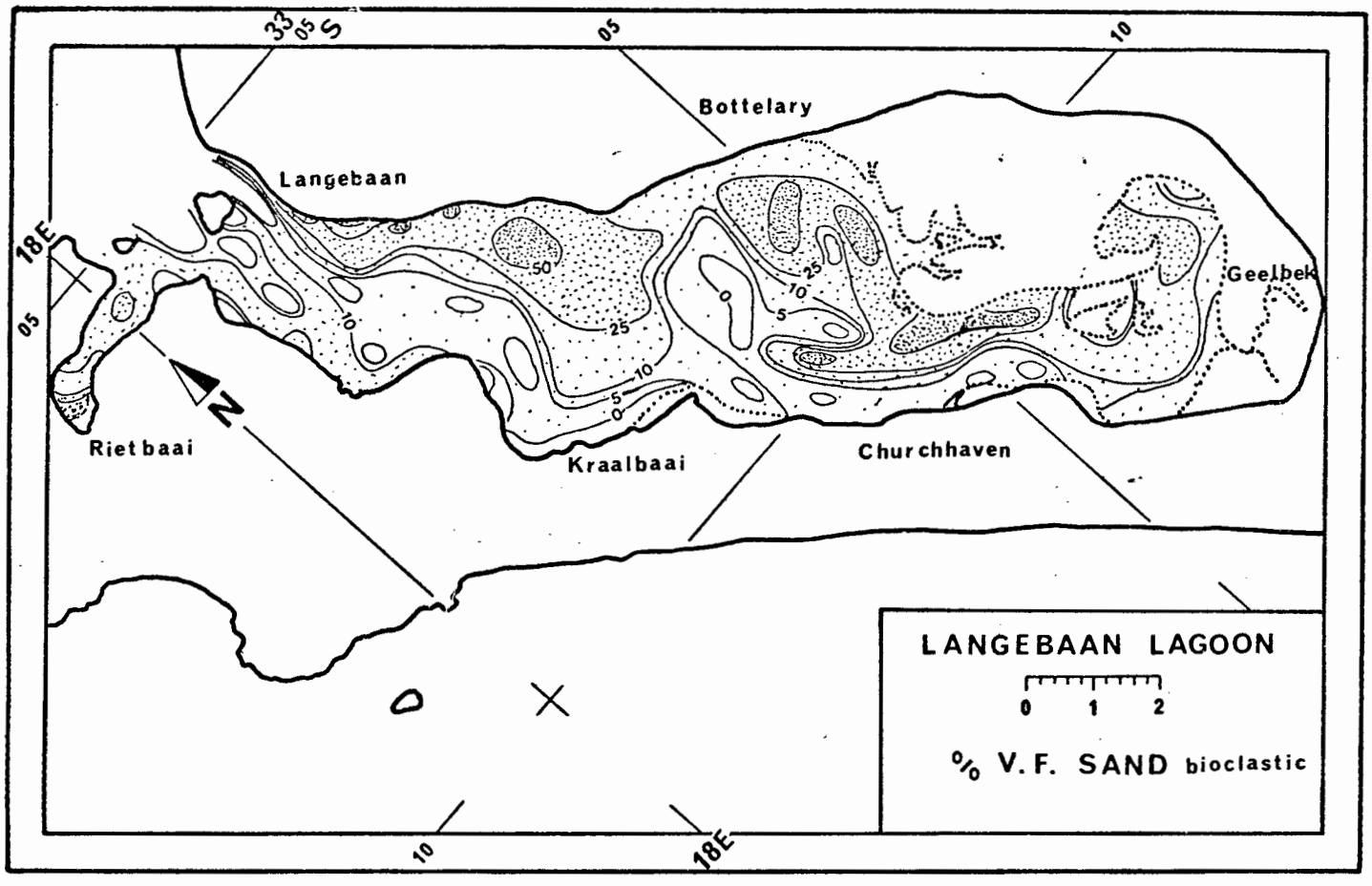

Fig. 173

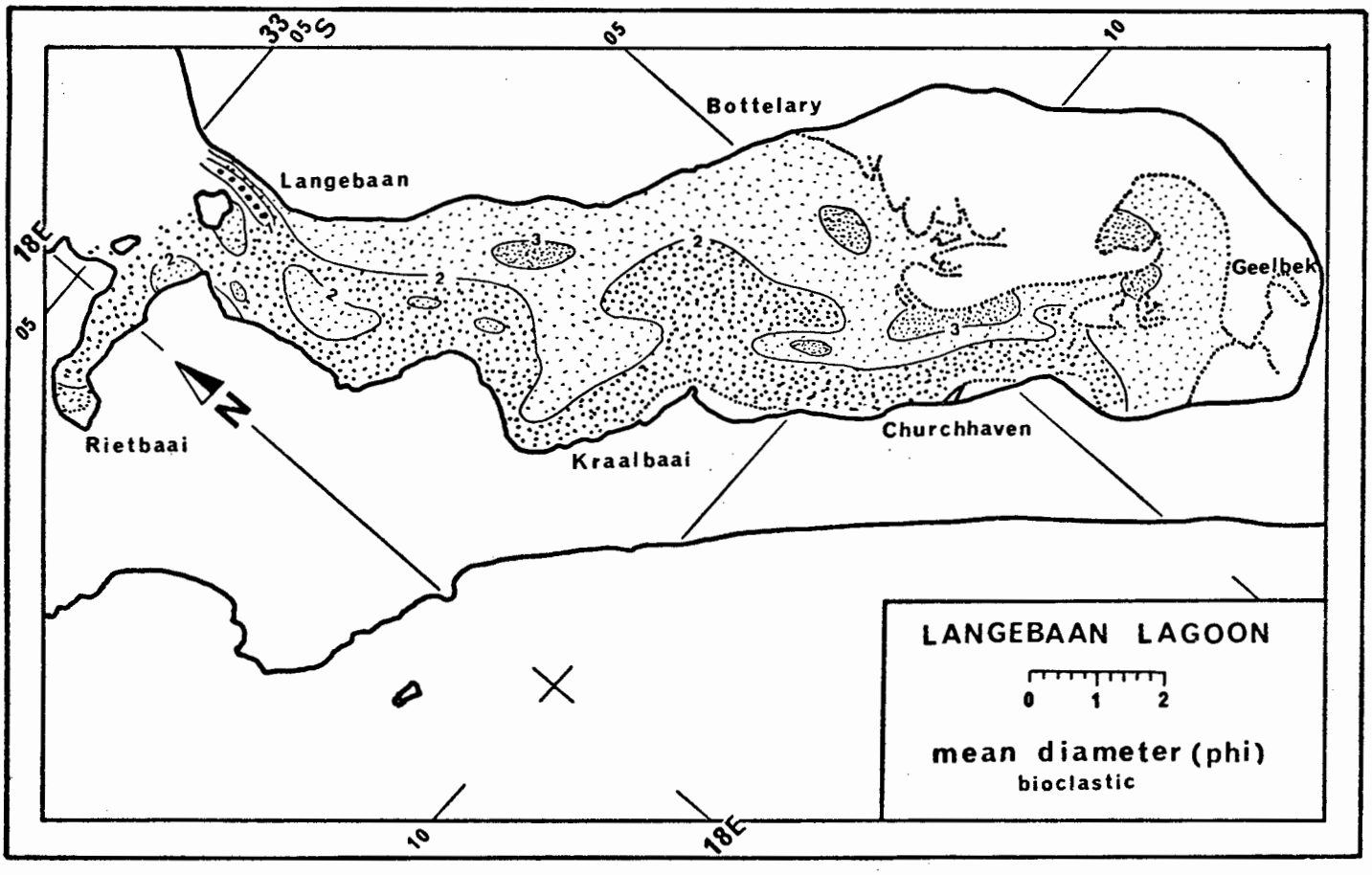

Fig. 174

Although the mean diameters of the two component groups are practically identical, the difference between their size-frequency distributions are more significant. This is particularly well illustrated by their respective sorting and skewness patterns. The bioclastic component is on average less well sorted, whereby the deviation increases towards the better sorting categories (Fig. 175). There is considerably less very well sorted bioclastic sediment in the lagoon, whereas moderate sorting, which was not observed in the terrigenous sediments, occurs much more frequently.

A similar observation is made in the skewness patterns. In each case, the bioclastic sediment is either less positively skewed, or considerably more negatively skewed, than the terrigenous sediment (Fig. 176). Since both components have been subjected to essentially the same hydrodynamic conditions, it would appear that each component group responds rather independently to the hydraulic size-sorting mechanism. This feature will be investigated in a special section, as it appears to form an important element in the depositional processes of the study area.

The relationship between mean diameter, relative sorting, and skewness of the bioclastic sediment is illustrated, in the same manner as before, by the two-dimensional projection of three-dimensional data points. The relationship between mean diameter and relative sorting in the XY-plane clearly reflects the characteristics observed in their areal distribution (Fig. 177). While mean diameters remain almost constant with respect to their terrigenous counterparts (viz. Fig. 166), the relative sorting levels of the bioclastic sediment are, in the majority of cases, strongly displaced in the direction of lesser sorting. In addition, the whole point cluster appears more stretched than that of the terrigenous sediment. The modification is particularly strong in the fine arm of the inverted V-shaped cluster. This feature is particularly well illustrated in the mean-skewness relationship (Fig. 178). The central axis of the helix is displaced sideways by at least 0.4 skewness intervals, and it would appear as though the majority of data points of the two components are, in addition, somewhat out of phase with respect to their position on the helix. This feature most probably reflects the difference in proportion supplied by each hydraulic population. Thus, the coarser population, which comprises mainly medium sands, contributes a proportionally much larger bioclastic component to the total sediments of Langebaan Lagoon than the fine to very fine-grained population.

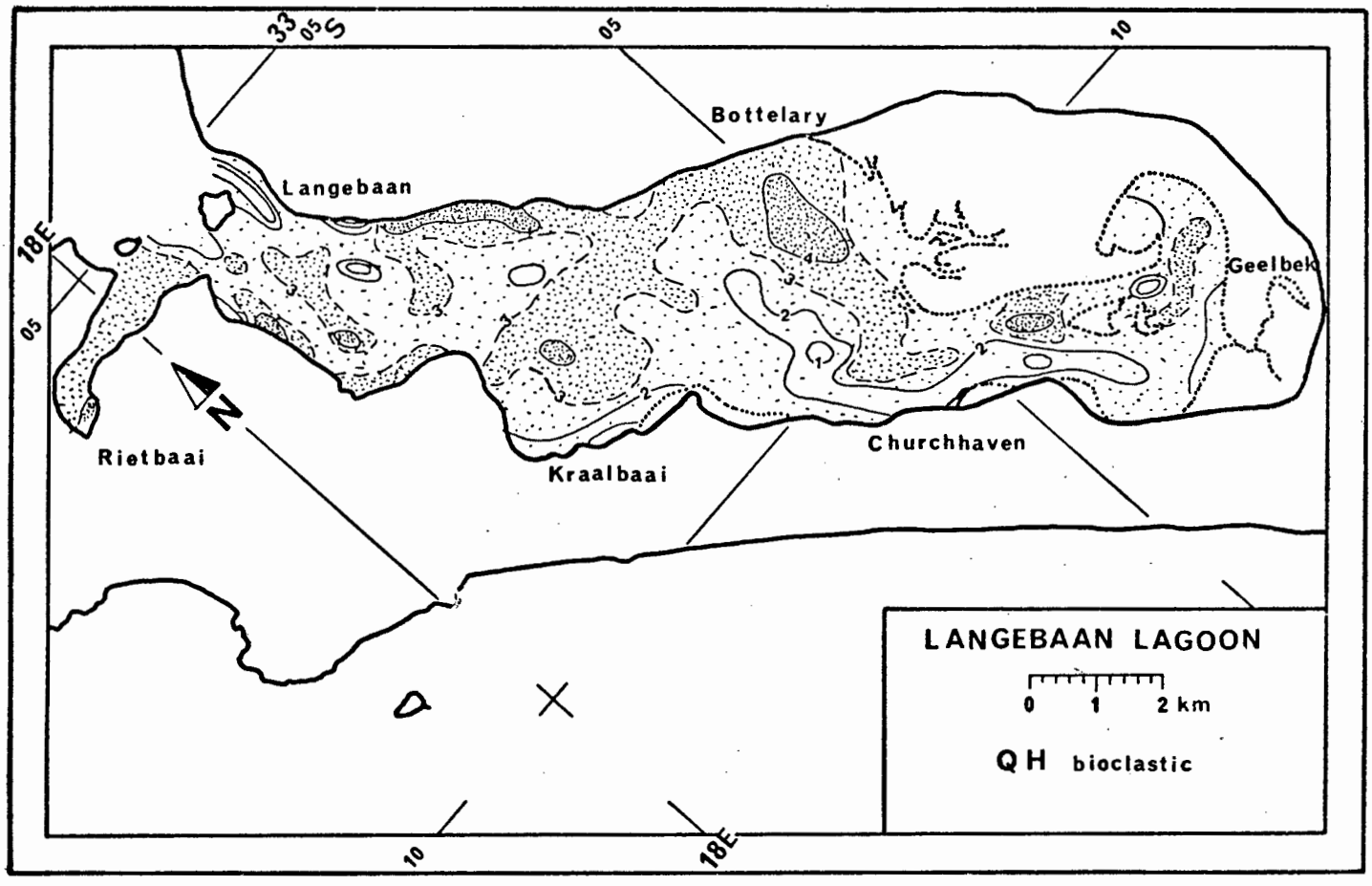

Fig. 175

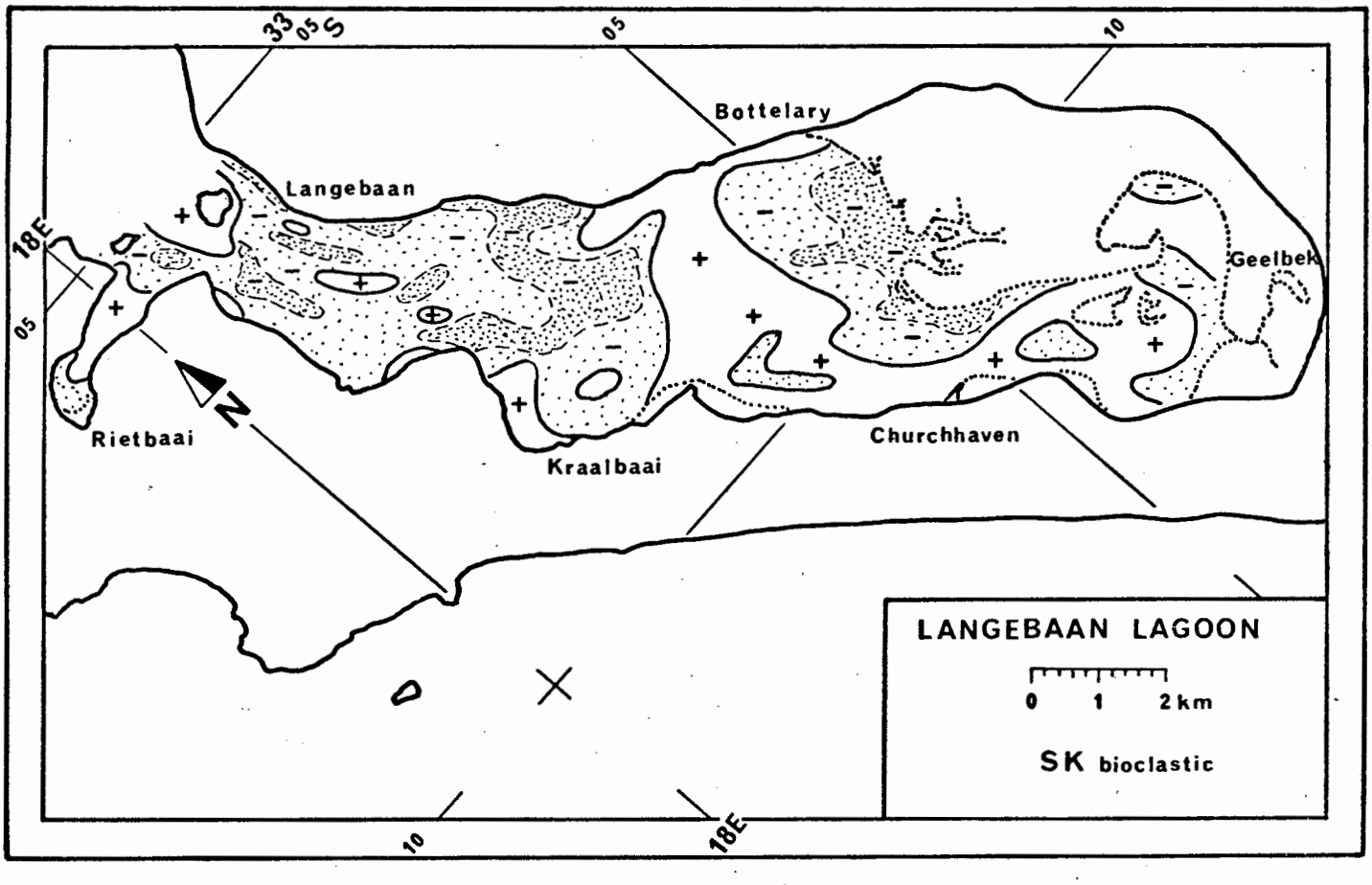

Fig. 176

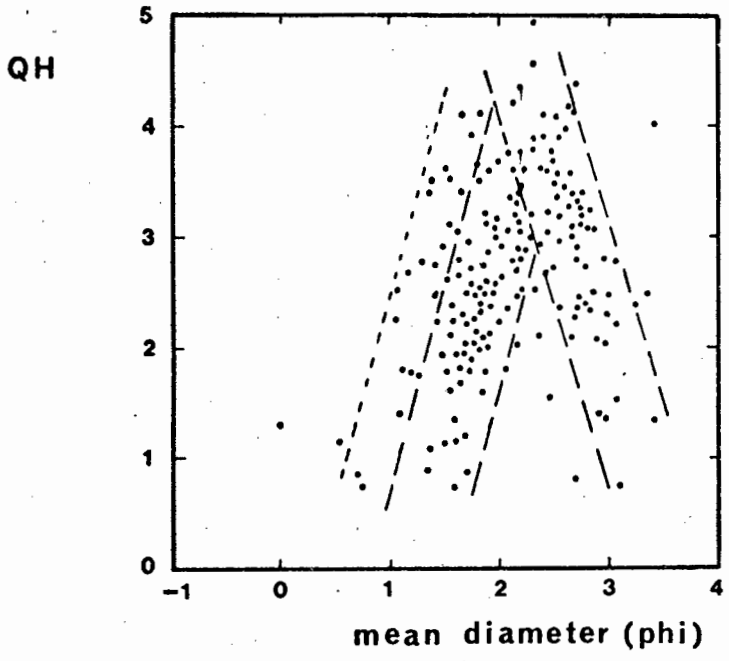

Fig. 177. The relationship between mean diameter and sorting of the bioclastic component

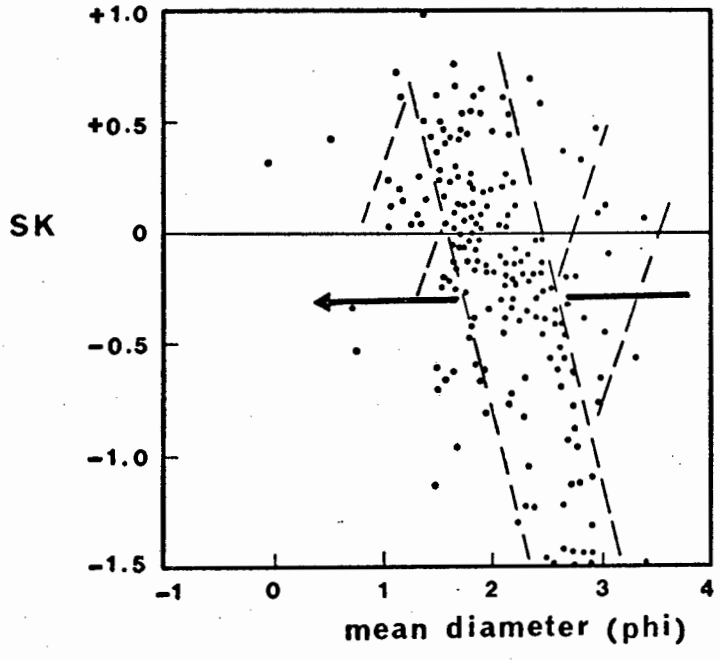

Fig. 178. The relationship between mean diameter and skewness of the bioclastic component

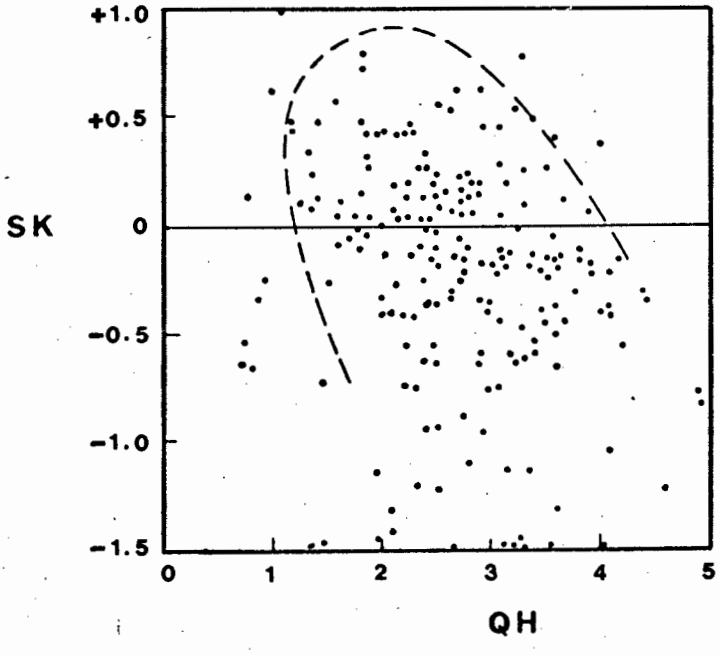

Fig. 179. The relationship between sorting and skewness of the bioclastic component

5.2.2. Current - Sediment Interaction

Over several decades there has been no major change in position or shape of the larger sedimentary bodies in Langebaan Lagoon. Although in the central and southern lagoon this may be due to structural constraints, such as the position of fossil oyster reefs, it also holds true for the large sandbanks of the northern lagoon, which are not stabilized by solid core structures (Fig. 136). Under present hydrodynamic conditions, there does not appear to be any net loss or gain of sediment in Langebaan Lagoon. The general stability of the major physiographic units in the lagoon suggests that sediment transport is in dynamic equilibrium with the hydraulic regime of the two-directional tidal flow. This stability should be reflected in the geometry of channel cross-sections - a feature that is well documented from alluvial channels (viz. Leopold and Maddock, 1953; Schumm and Lichty, 1965; Gessler, 1970; Graf, 1971; Ferguson, 1973; Allen, 1974; Bennett, 1976). In Langebaan Lagoon this phenomenon is well developed, especially in the eastern outflow channel. A strong velocity gradient is observed in either direction, depending on the tidal flow direction. The relationship between channel width and channel depth appears to be a strict function of the flow velocity in combination with the total cross-sectional area. The more the channel width is constricted, the deeper the channel becomes. A selection of eight more or less evenly spaced cross-sections illustrate this relationship (Fig. 137). At the same time, it is observed that the flow velocities increase with increasing channel depth and decreasing channel width (Fig. 138).

It would thus appear that the channel system adapts its geometry, in relationship to the prevailing flow conditions, by redistributing the available sediment until a dynamic equilibrium is established. Once equilibrium is achieved, there is no more sediment movement, unless the equilibrium is disturbed, either by addition of new sediment, or by a change in the flow conditions. In Langebaan Lagoon, there is virtually no addition of sediment, but the flow conditions are constant only as far as the periodicity of tidal cycles are concerned. Within each tidal cycle, current velocities and water depths constantly change, even though in a relatively steady and progressive manner. Thus, there is a continual short-term de-stabilization active in the system; this feature should produce continuous sediment instability on a small scale.

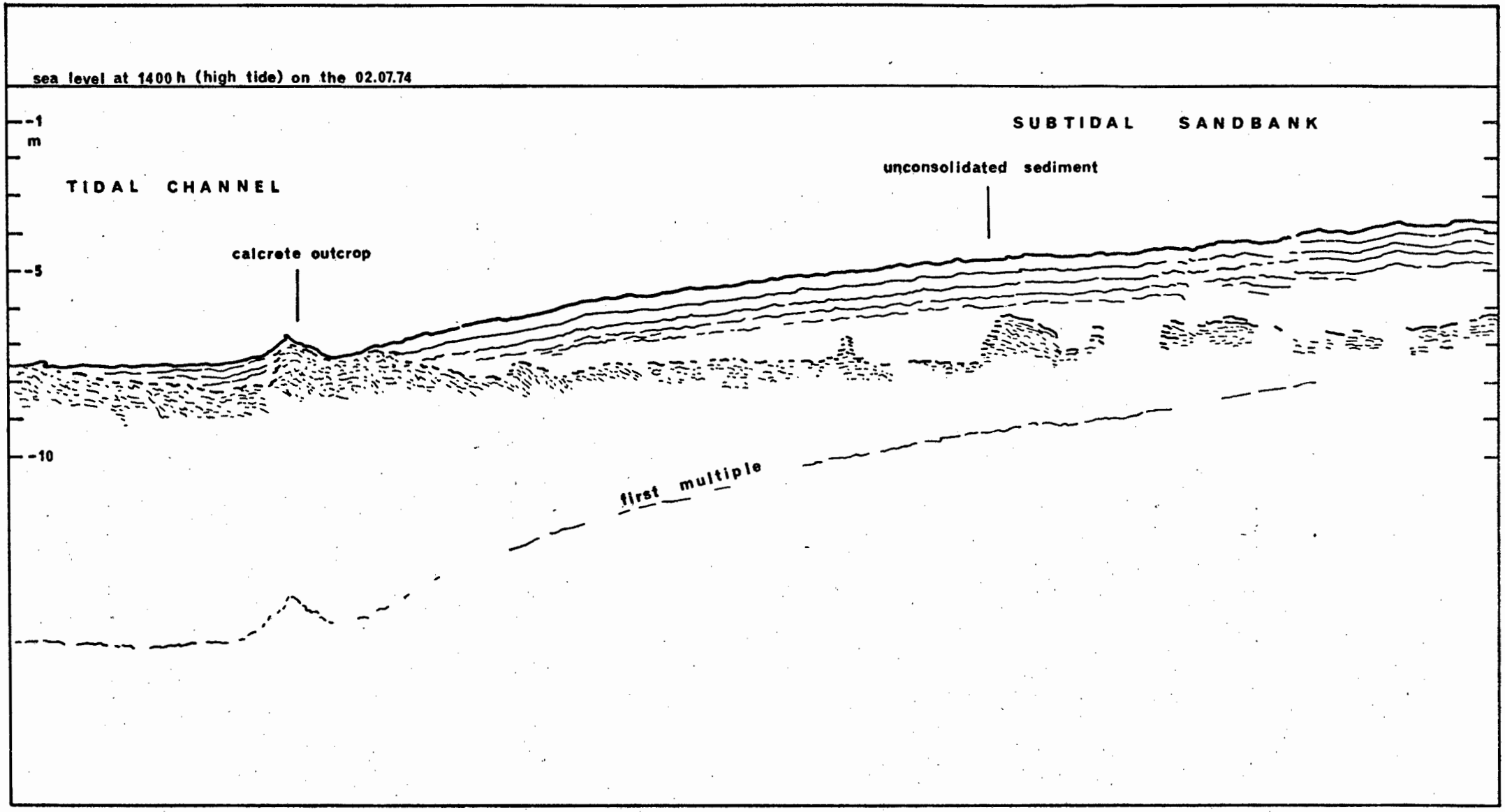

Fig. 136. Shallow seismic profile through a submerged sandbank

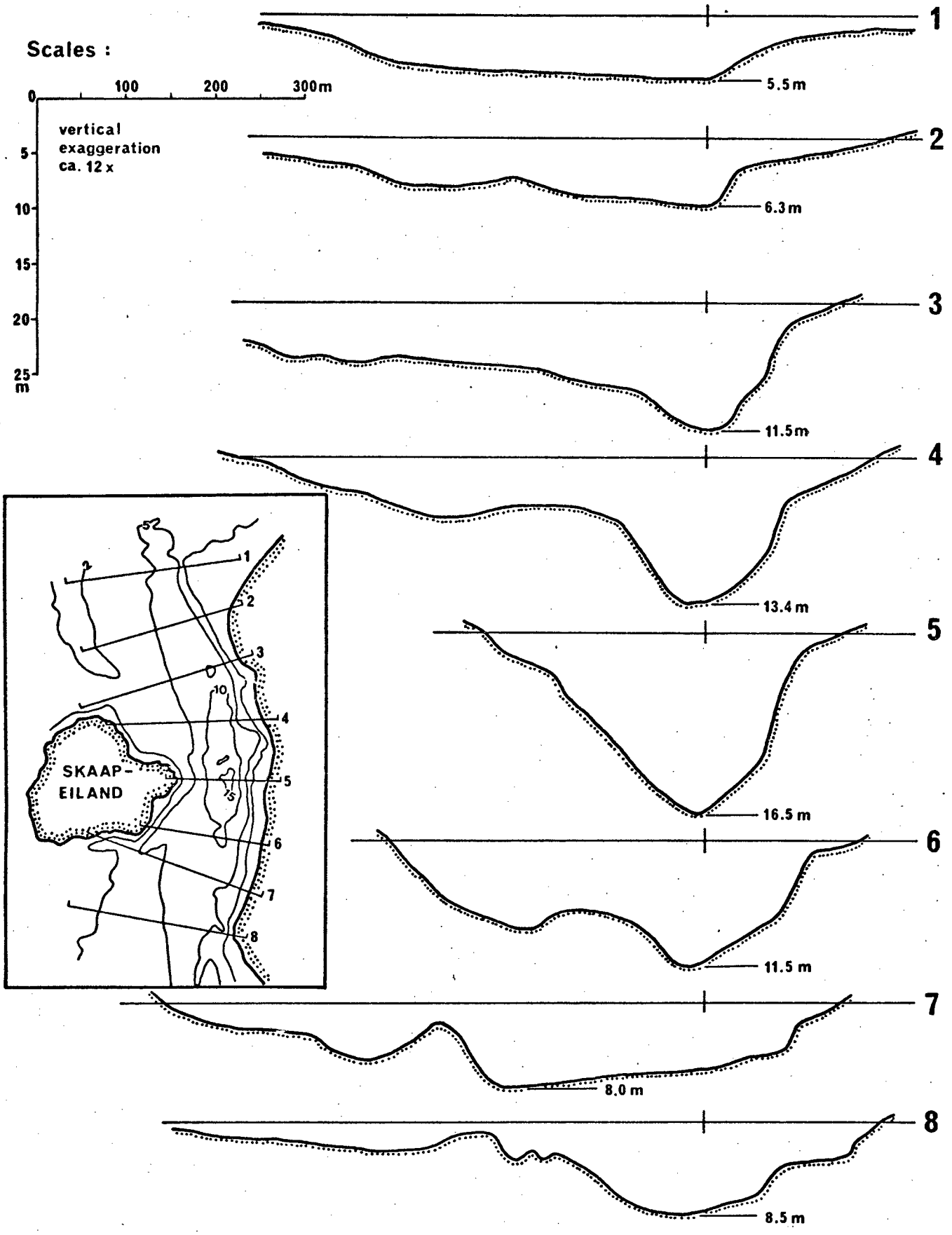

Fig. 137. Geometry of the eastern outflow channel

Side-scan sonar recordings in the channel systems have indeed revealed a variety of large bedforms, which are here interpreted as sediment response patterns to the de-stabilizing processes of the tidal regime. Plate 6 illustrates some of the more dramatic bedforms observed in Langebaan Lagoon. Whereas channel beds are clearly unstable under the prevailing peak flow conditions, channel banks appear to remain stable throughout the entire tidal cycle. Thus, in the process of self-stabilizing adjustment of channel geometry, the velocity profile in the channel cross-section has been modified, such that the effects of de-stabilizing forces are concentrated near the channel beds. In this manner, stable banks are maintained. In Langebaan Lagoon, this phenomenon is reflected in the grain size gradient along the cross-sectional profile of the channels.

The process-response phenomena resulting from the interaction between sediments in one-directional flow systems have been conveniently expressed in a number of empirical flow regime concepts (e.g. Sundborg, 1956; Bagnold, 1956; Simons and Richardson, 1962). Although the tidal flow regime is normally two-directional, each cycle is sufficiently long to be regarded as a one-directional component. In fact, the orientation of larger bedforms and other sand bodies, such as intra-channel deltas and marginal sand-tongues, clearly indicate that the major current vectors of the periodically opposing flow components follow separate, well defined flow paths (Plate 8).

One flow regime concept relates current velocity and flow depth to Reynolds Numbers (e.g. Sundborm, 1956). The Reynolds Number is defined as

$$Re = Vd / \mu \qquad (3)$$

where V is the mean current velocity, d is the hydraulic radius and μ is the kinematic viscosity. It was experimentally determined that, at $Re \leq 500$, flow is laminar, i.e. streamlines and particle trajectories remain essentially parallel to each other without lateral exchange. At $Re \geq 2000$, on the other hand, flow is turbulent, i.e. streamlines and particle trajectories are no longer parallel to each other, but are involved in vigorous lateral exchange due to random eddy diffusion. Between $Re = 500$ and $Re = 2000$ there is a transitional zone, in which progressive development from laminar to turbulent flow conditions are observed.

PLATE 6.

A. Small dunes in coarse sand along the channel bed of the eastern outflow channel (scale on 6-E).

B. Interference patterns in underwater dunes caused by a change in the current direction during the ebb cycle.

C. Converging dune fields of an ebb and flood-dominated section of the central channel.

D. Transverse dunes in the central channel of Langebaan Lagoon. Note the progressive decrease in wavelength parallel to the dune crests (a and b) as the water depth decreases.

E. Transverse dunes in the central channel of the lagoon. Note superimposed smaller dunes (a).

F. "Crowding" of dunes along a steep embankment of the central channel.

G. Interference patterns of dunes with different orientations produces a reticulate pattern.

H. Lunate-shaped dunes in the northern lagoon.

Plate 6

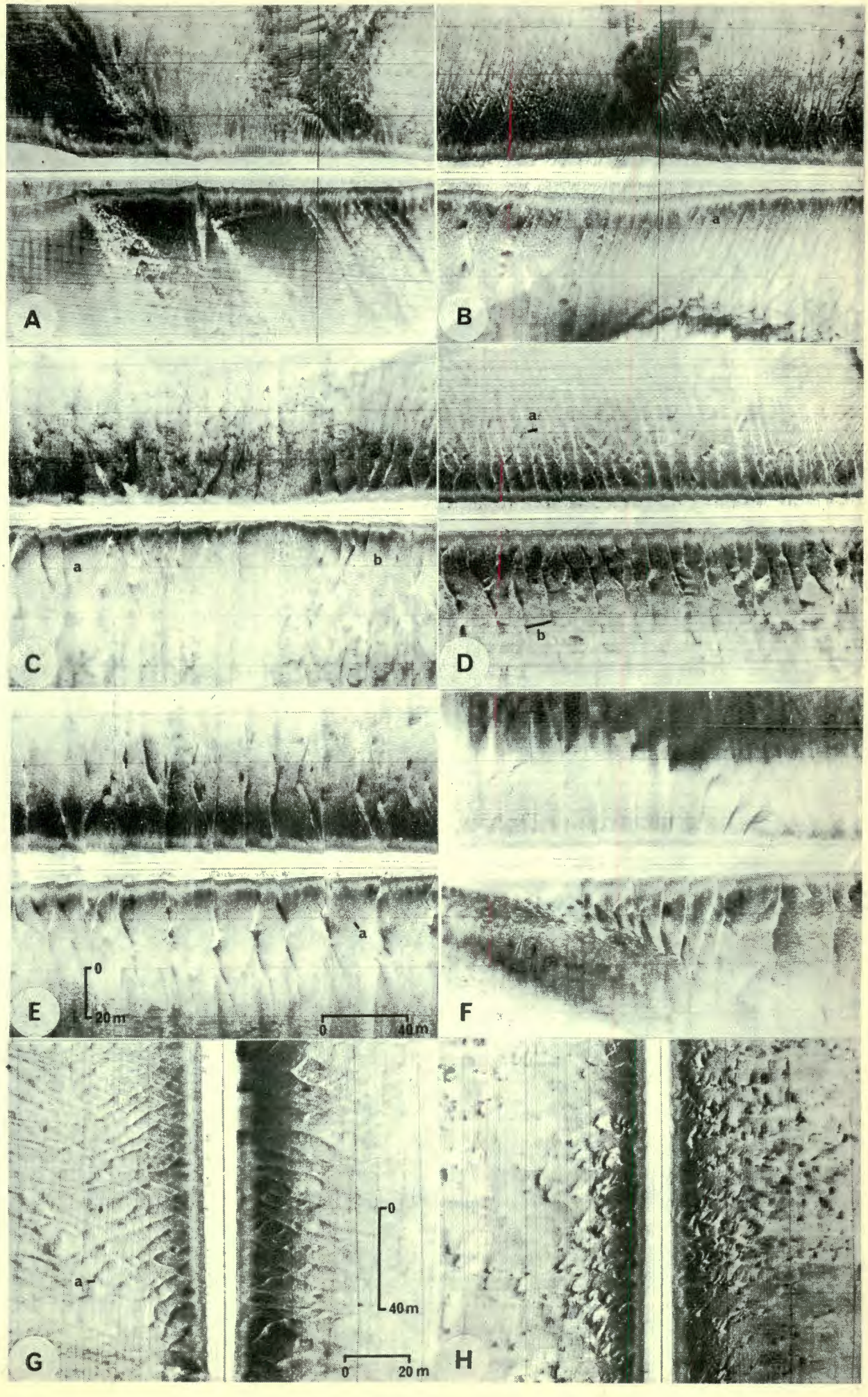

According to this concept, flow in the lagoonal channels will, at peak conditions, normally be turbulent, although there are extended periods during which flow will be either laminar, e.g. near slack tide, or transitional, e.g. in the early accelerating phase and the late decelerating phase of each tidal cycle. The relationship between Reynolds Numbers, initiation of sediment movement, and the generation and control of bedforms is, in addition, a function of particle size. In Fig. 139-A the various interacting flow parameters are related in a single diagram, and in Fig. 139-B the size dependency of initiation of sediment transport, and the boundaries of bedform stability, are illustrated. The latter diagram combines information from Sundborg (1956), Allen (1965) and Southard (1975). It allows a quick assessment of the expected sediment transport situation at various parts of the lagoonal channel system, as a function of the local grain size and velocity conditions.

The above concept does not specifically include the water depth or flow depth as important parameters, although a direct relationship between water depth, current velocity and sediment response has been observed in experimental studies (e.g. Simons and Richardson, 1962). It was found that bedform development, in relation to current velocity and water depth, could be expressed in terms of Froude Numbers, which are derived from the empirical equation.

$$F = V / \sqrt{gh} \qquad (4)$$

in which F is the Froude Number, V is the mean current velocity, g is the acceleration due to gravity, and h is the water depth. This relationship was verified in small open channels, but accurate information from wide and deep channels is still lacking.

Good general agreement exists between the Froude Number concept and the Reynolds Number concept (viz. Fig. 139-A). The upper flow regime coincides more or less with the rapid flow phase, and the lower flow regime with the tranquil flow phase (viz. Allen, 1965; Southard, 1975). Flow in Langebaan Lagoon is, therefore, predominantly tranquil-turbulent. Only at slack tide will there be tranquil-laminar flow. Rapid-turbulent flow conditions were not observed in the lagoon.

A curvi-linear relationship between peak velocities at the surface,

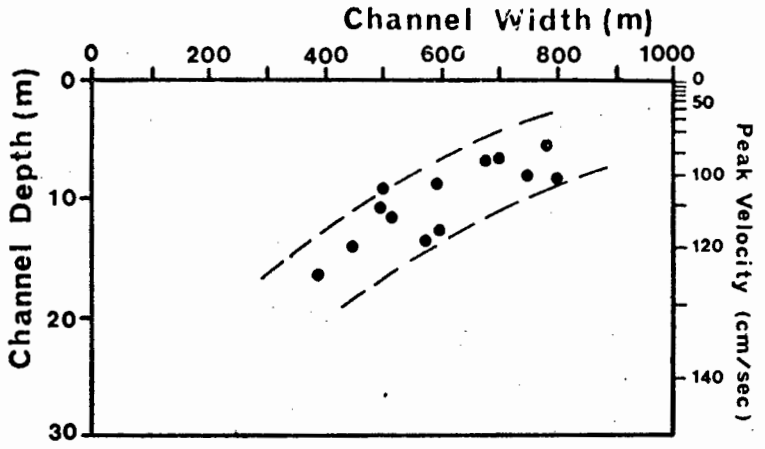

Fig. 138. The relationship between channel width, channel depth and peak current velocity in Langebaan Lagoon

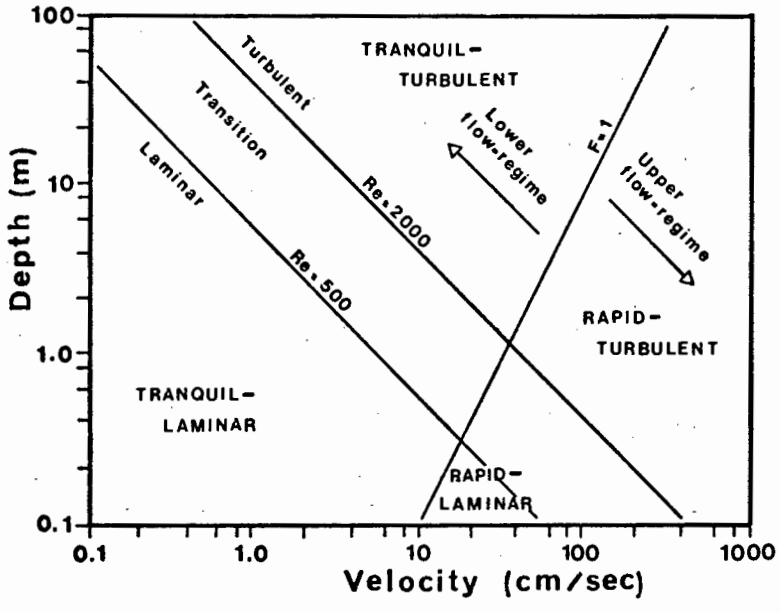

Fig. 139-A. The relationship between current velocity, flow depth and flow regime (after Allen, 1965)

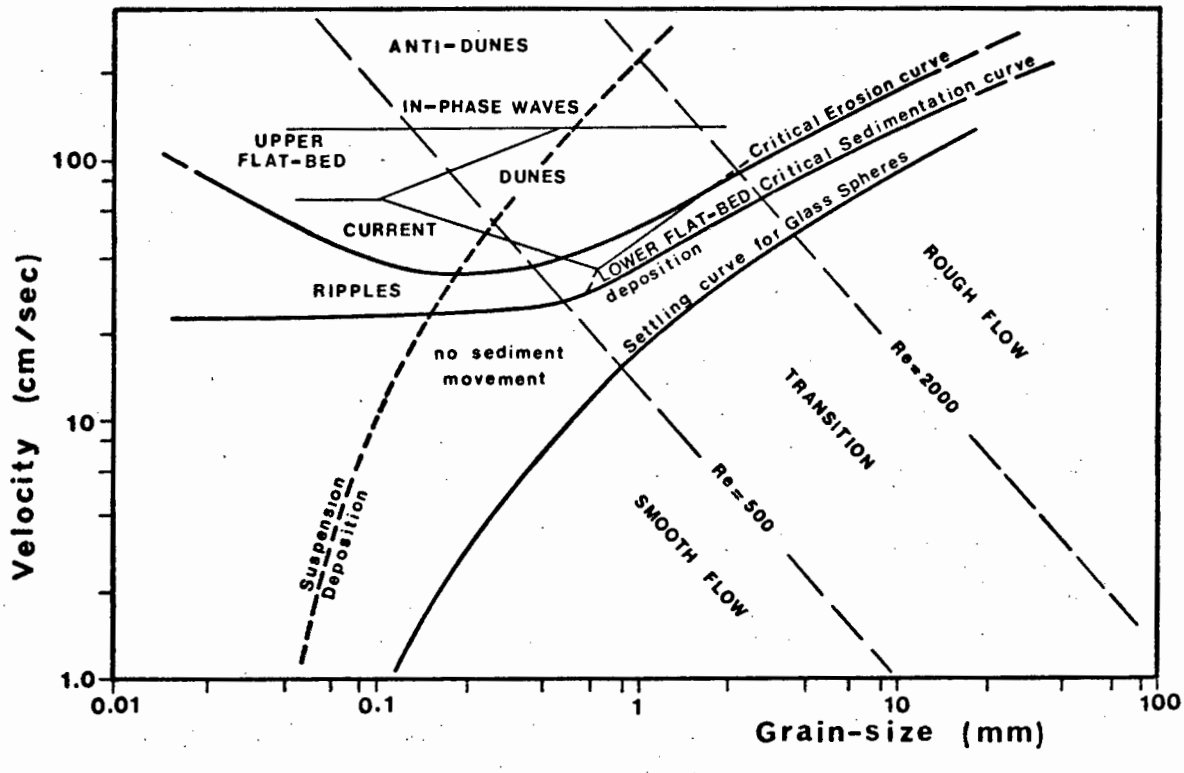

Fig. 139-B. Size-velocity diagram illustrating current-sediment interaction (compiled from various authors)

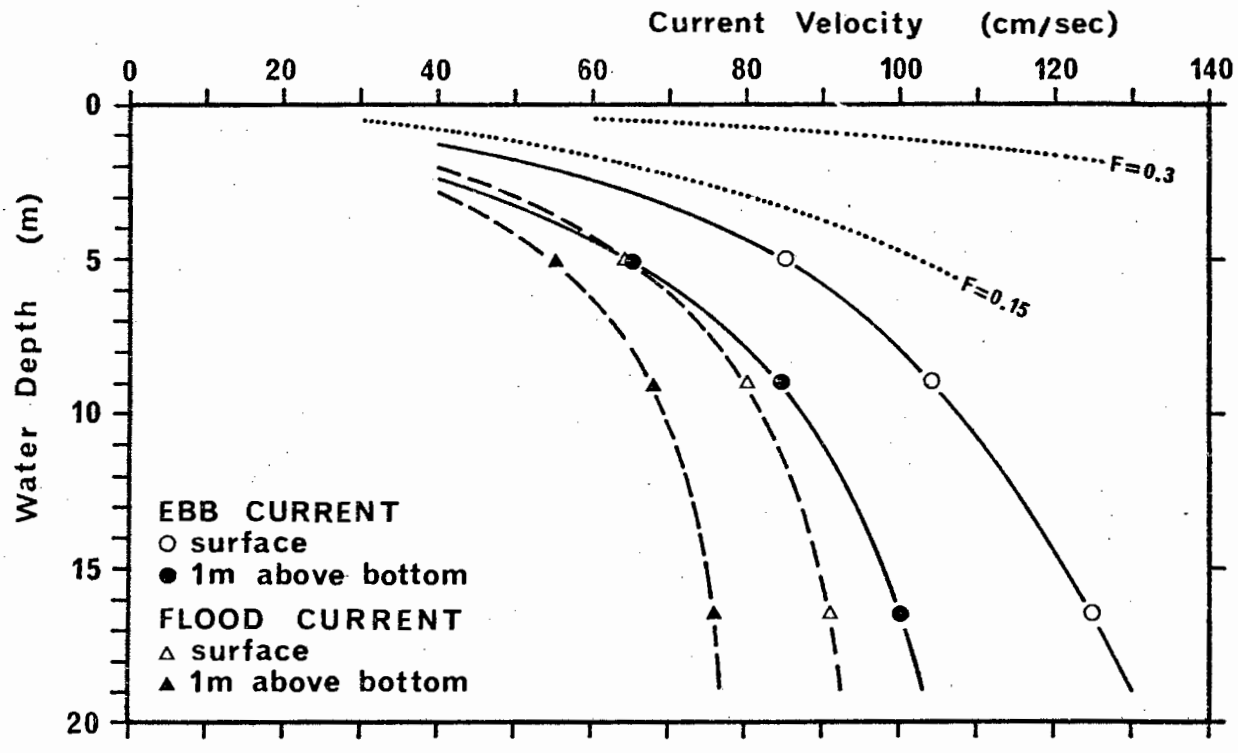

Fig. 140-A. The relationship between water depth and current velocity in Langebaan Lagoon.

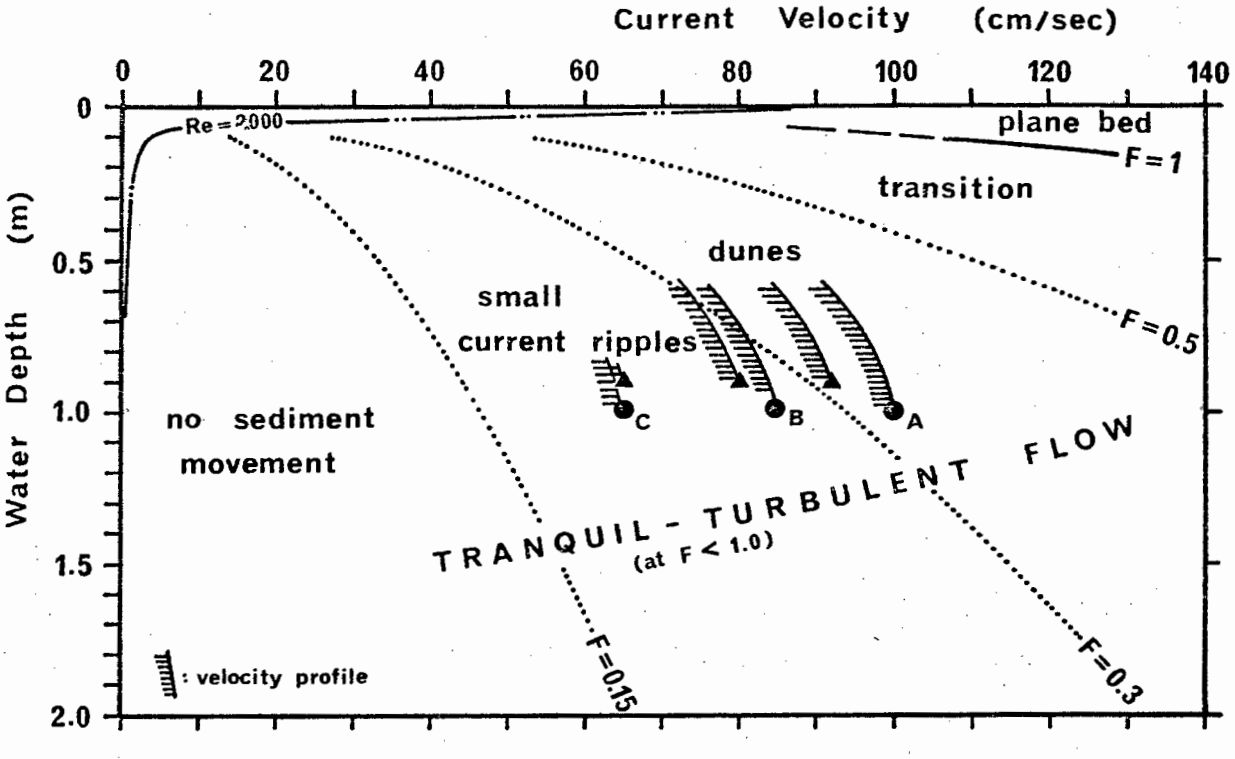

Fig. 140-B. The relationship between near-bottom velocity profiles and Froude Numbers calculated on the basis of an arbitrary flow depth of 2 m.

as well as at the bottom, was observed at various channel depths in Langebaan Lagoon (Fig. 140-A). Their overall relationship to the predicted transport pattern of the Froude Number, however, does not agree with the observed patterns. When calculating the Froude Number on the basis of the total water depth, it reaches a maximum of only 0.1, irrespective of the observed water depth. At this level, however, there should be no sediment transport at all. Even if certain allowances are made for local fluctuations of current velocities, grain size, and other irregularities, the situation does not improve substantially. The generalized diagram in Fig. 139-B, on the other hand, provides a reasonably good reflection of the observed situation.

In an attempt to resolve the problem, Froude Numbers were calculated, not on the basis of the true water depth, but by an arbitrary flow depth of 2 m (Fig. 140-B). The flow velocities measured at 1 m above the channel beds are now shifted into a feasible relationship to the predicted sediment transport patterns. It would appear that, in the case of Langebaan Lagoon, the true water depth is not relevant to the generation and control of dune bedforms. It is suggested that bedform development is controlled by a turbulent boundary layer that reaches a thickness of about 2 m at peak flow velocities. The true water depth can, therefore, be equated to the true flow depth only in those cases where the turbulent boundary layer has developed throughout the whole water column. This is normally the case in small channels, where a submerged turbulent boundary layer is maintained only for a short period before it expands through the whole water column. A recent study in which this phenomenon has received attention is presented by Yalin and Price (1974), who propose that the "scale of turbulence" is related to the size of dune bedforms, whereby the maximum height of the largest eddies would define the relevant flow depth of the system. A similar conclusion was reached by the writer (Flemming, 1977), when attempting to explain dune height/water depth discrepancies observed in the Agulhas Current flow system.

Considering the above discussion, major bedforms in the channel system of Langebaan Lagoon reflect the hydraulic response of the sediment to the shear velocity and thickness of a turbulent boundary layer. In correspondence to observations, dune bedforms do not occur on a large scale in the southern and south-central lagoon, because shear velocities are not sufficiently high to generate these large bedforms. Sediments transport is here controlled by

small current ripples and small dunes at best. In the central section of the main channel, on the other hand, large dunes are observed in response to high near-bottom current velocities. It will be noted that, between Konstabelskop and Oesterwal, the tidal flow is constricted by a large tidal flat area. Since there is no erosion of channel banks, it is concluded that this tidal flat area probably overlies a hard core structure of calcrete or a fossil oyster reef. In this constricted section of the main channel the largest dunes of the entire system are recorded, with heights up to 2 m and wavelengths up to 30 m. Most of these face permanently in the ebb current direction, although in some parts of the channel flood oriented dunes appear to occur. All of the larger dunes are complex structures, formed by smaller super-imposed dunes migrating in alternate directions with the changing tidal regime (Reineck, 1963). Since the ebb current dominates depositional processes, the larger bedforms are permanently aligned in this direction.

In the northern section of the lagoon, and particularly in the outflow channels, dune bedforms are considerably smaller, in spite of higher flow velocities. This phenomenon is a good example of the effect of grain size on bedform development. Very coarse sediments predominate in the outflow channels, and, as a result, dune bedforms are smaller at comparable flow velocities. Thus, a very coarse sand will just begin to form dunes at velocities where this bedform is already well developed in medium-sized sands (viz. Fig. 44 and Fig. 139-B).

Channel banks and slopes consist predominantly of fine sediments. The marginal velocity gradient appears to reduce at such a rate that individual grains remain totally immersed in a laminar sublayer. As a result, the transport potential in this region is very small, thus accounting for the relative stability of channel banks in Langebaan Lagoon. On the intertidal flats, current velocities are so low that dune bedforms are unable to develop. It is suggested that this phenomenon is indicative for tidal flat areas in microtidal environments. In meso- and macrotidal environments, on the other hand, intertidally exposed dune bedforms are the norm rather than the exception (viz. Evans, 1965; Reineck, 1970; Klein, 1970).

5.3. SOME GEOCHEMICAL PARAMETERS

As in the case of Saldanha Bay, geochemical parameters are of subordinate

importance within the context of this study. The only significant parameter is the carbonate content of the sediments, which is used as a measure of the relative proportion of bioclastic and terrigenous material, in the essentially two-component sedimentary system of the study area.

5.3.1. Carbonate Content

The relative concentration of skeletal carbonates in lagoonal sediments is almost directly proportional to the energy gradient of the tidal flow. The highest $CaCO_3$-levels, reaching 40 - 50%, are found in the northern section of the lagoon (Fig. 141). It rapidly decreases towards the south. The 10% concentration level runs almost due south through the central section of the lagoon, whereas the sediments in the southern lagoon do not even achieve 5%. The eastern intertidal flats contain 5 - 10% $CaCO_3$.

Carbonate contents increase from 10% to 20% immediately adjacent to the fossil dune barrier. This feature indicates that the main source area for the sediments in Langebaan Lagoon has supplied not more than about 20% of bioclastic material to the lagoonal sediments. The high carbonate content in the northern lagoon thus appears to be the result of selective concentration in the course of sediment transport. A similar conclusion was reached when discussing carbonate distribution patterns in Saldanha Bay. The depositional processes of bioclastic sediments in Langebaan Lagoon have received particular attention in this study, because of the clear trend and strong gradient observed in their distribution. A specific model relating carbonate concentration to the hydraulic behaviour of this particle group is discussed in a later section.

5.3.2. Organic Carbon Content

The organic carbon content of the lagoonal sediments is surprisingly low. On the open flats a maximum of 0.5% is reached near Geelbek in the very south (Fig. 142). The salt marshes, on the other hand, have a very high biological productivity and, as a result, organic carbon values are considerably higher, reaching over 2% in most places.

As before, organic carbon concentration is strongly correlated with the mud content of the sediments, whereby the overall trend is only

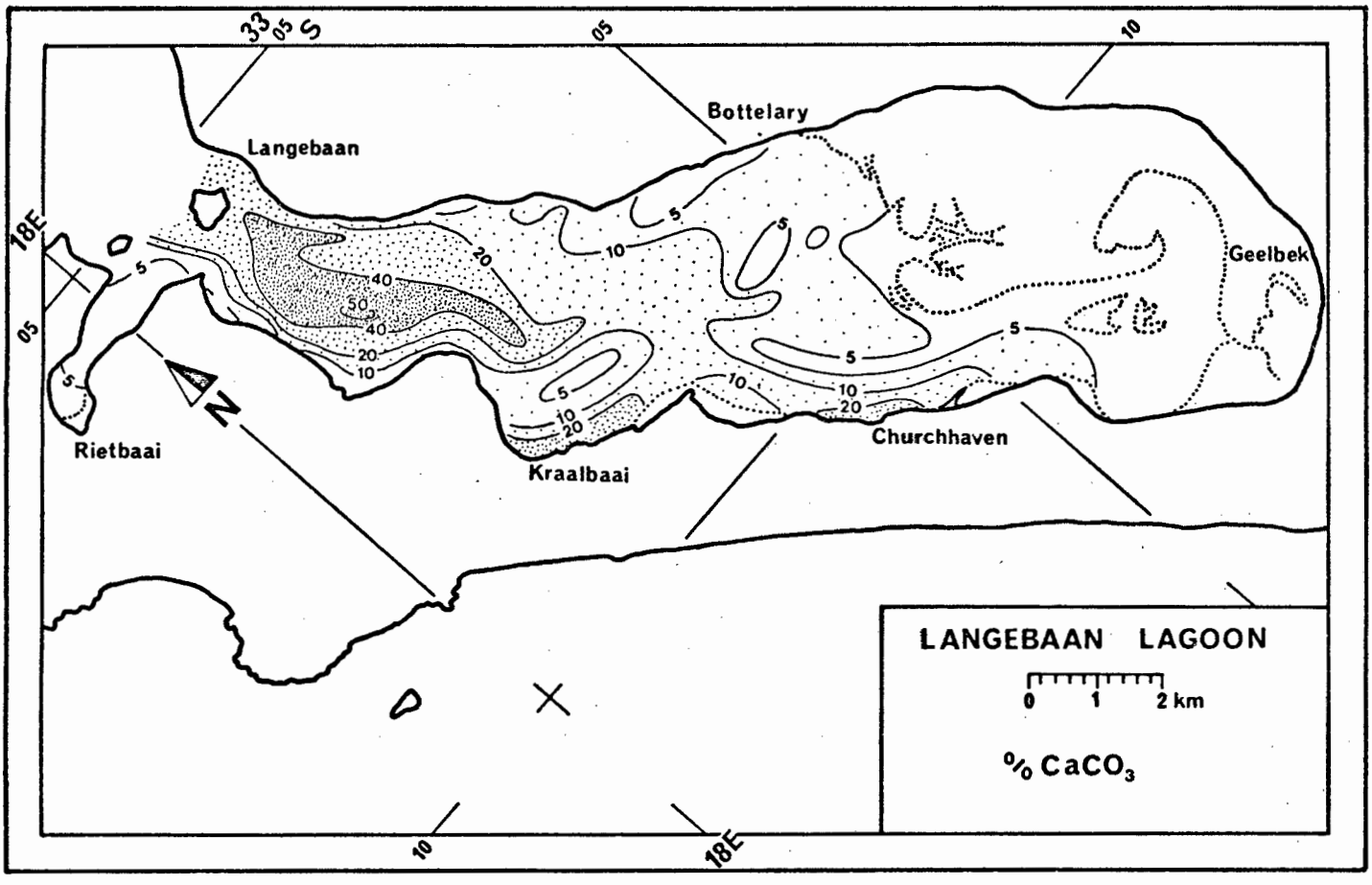

Fig. 141

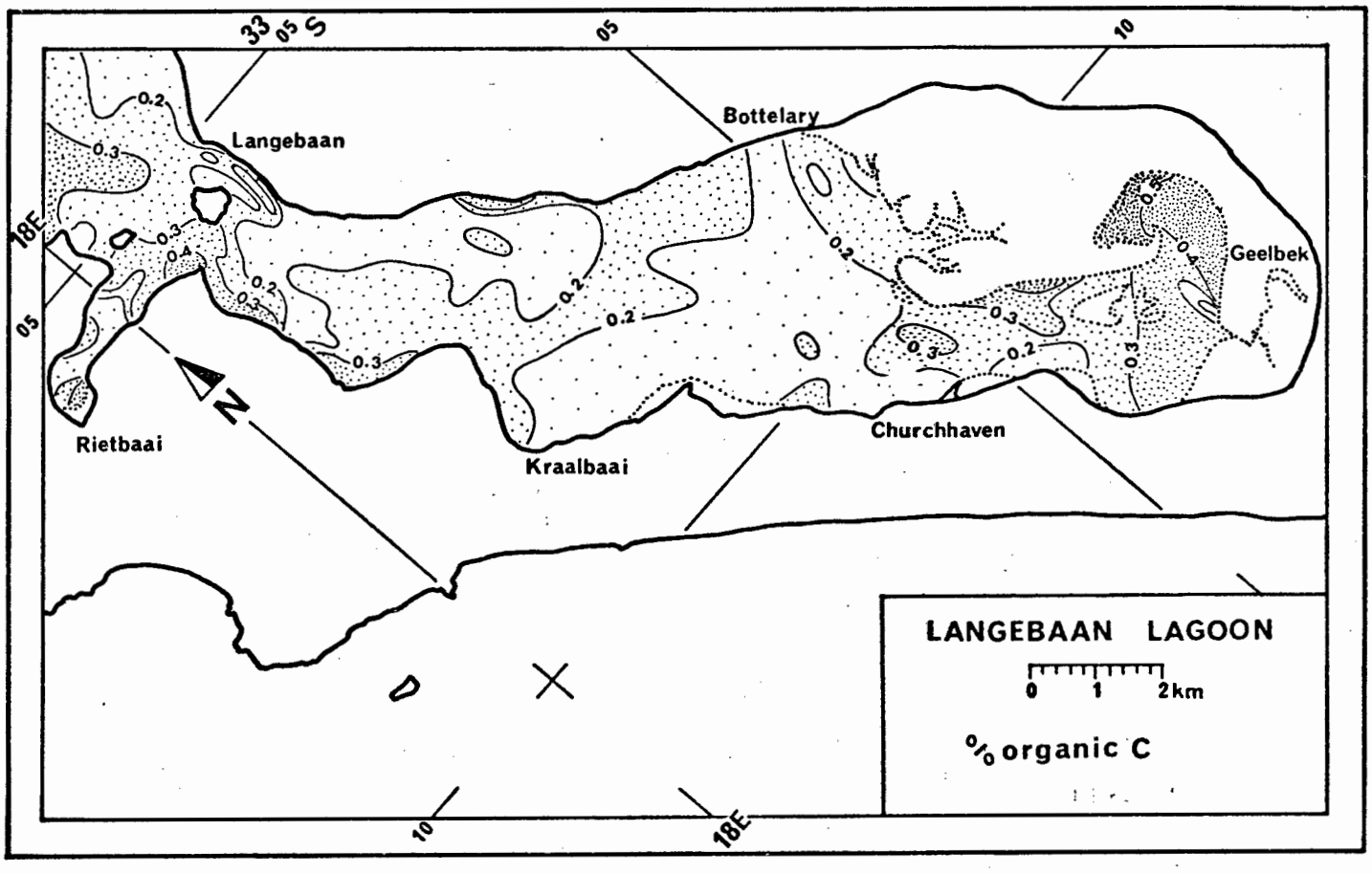

Fig. 142

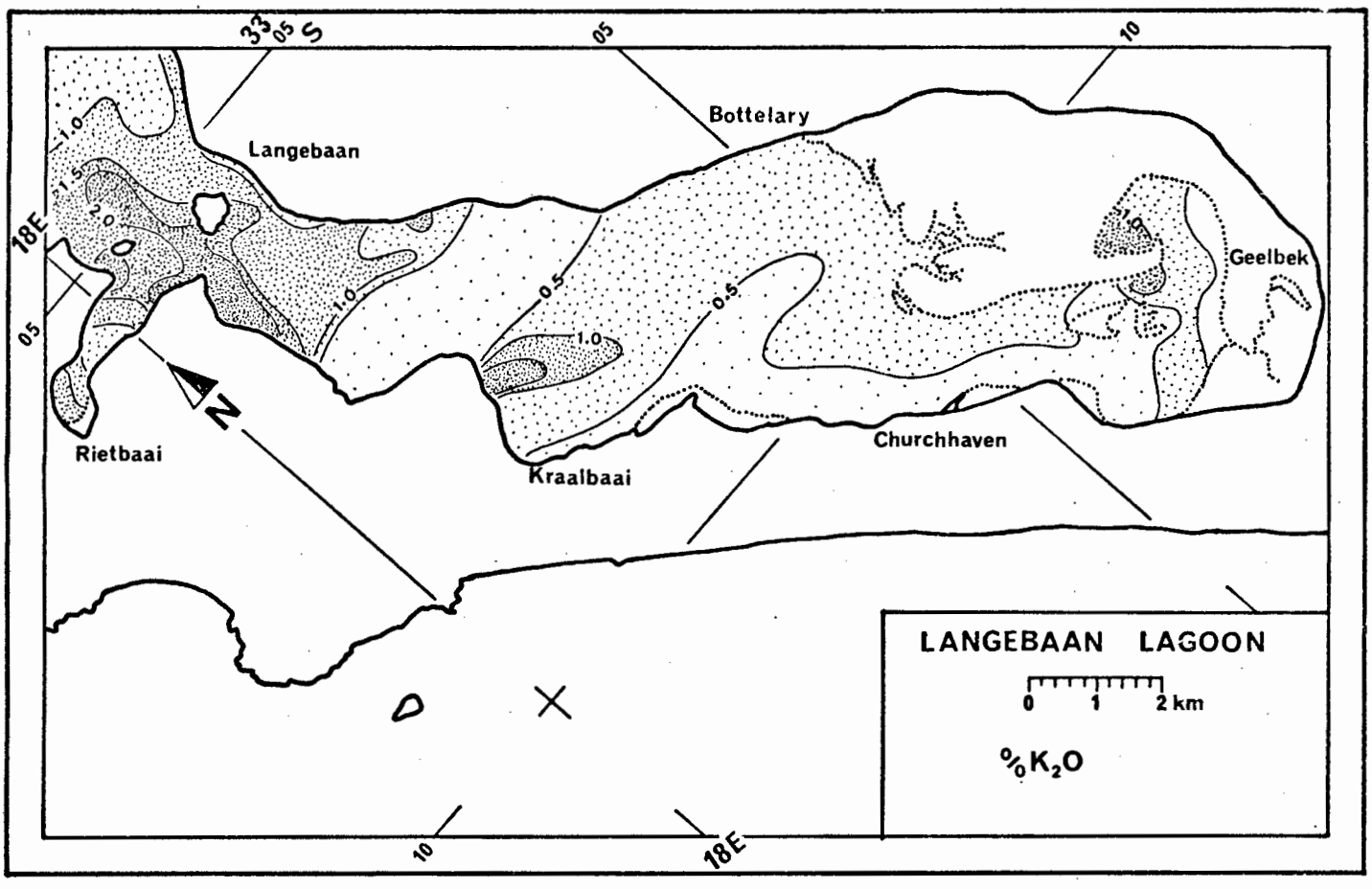

Fig. 143

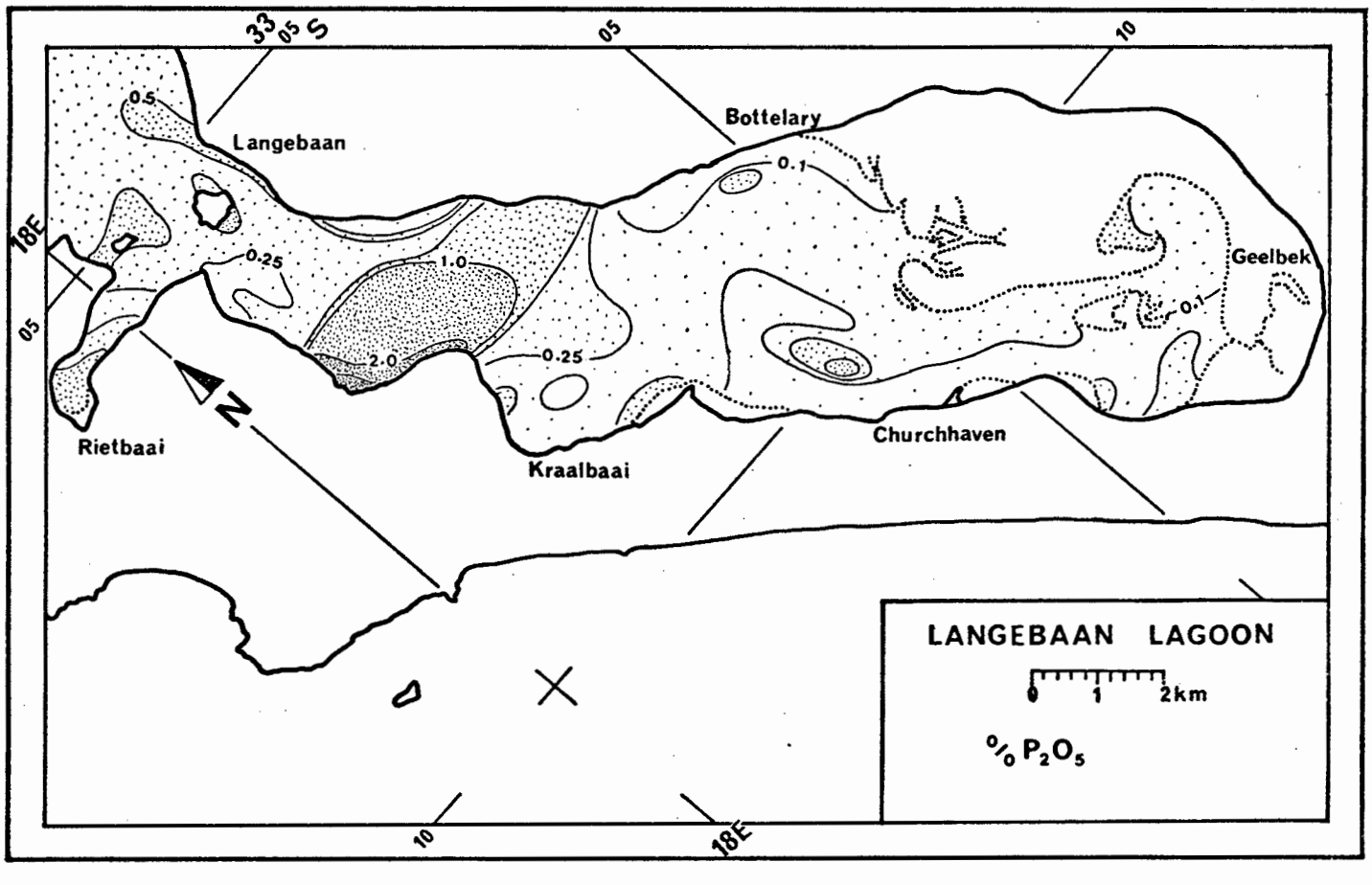

Fig. 144

marginally smaller to that observed in Saldanha Bay. Another noteworthy aspect is the relationship between the organic carbon content and the total organic matter in the lagoonal sediments (Carr, 1976). Organic carbon values are consistently smaller by a factor of about 0.05.

5.3.3. Potash Content

The distribution pattern of potash (K_2O) shows a twofold affinity, one to the areas where granitic rock fragments are common, e.g. in the western outflow channel and along the northwestern shoreline, and the other to areas of high mud content, such as the marsh areas in Riethaai and in the very south of Langebaan Lagoon (Fig. 143). Particularly high contents are observed where the sediment is in direct contact with granite bedrock, e.g. in the northwestern lagoon, where values reach 2.7% K_2O. It would thus appear that, in these latter sediments, some feldspar has survived the erosional processes, whereas in the former areas K_2O is derived from the clay fraction.

5.3.4. Phosphate Content

The phosphate content (P_2O_5) of lagoonal sediments is, with the exception of a small area near Cupos, very low. In general, the concentration level rarely exceeds 0.3%. Near Cupos, however, values of over 3% were recorded (Fig. 144). This enrichment in phosphate is without doubt related to the mining activity of phosphatic mineralizations on the upper slopes of Konstabelskop (Tankard, 1975b).

The low phosphate content in most of the lagoon indicates that a primary source of phosphatic sediments has not been tapped in the lagoon itself. In this respect, it conforms to the findings in Saldanha Bay. It appears that most of the economically viable deposits of phosphatic rocks in the vicinity of Saldanha Bay are, in fact, located at substantially higher topographic levels (viz. Visser and Schoch, 1973; Tankard, 1974; Brich, 1977).

5.4. SEDIMENT DISTRIBUTION PATTERNS

In this section, distribution patterns of individual size fractions

will be contrasted and compared to the general trends of the size parameters of the total sediment, as well as of individual sedimentary components. Particular attention is given to the terrigenous and the bioclastic sedimentary components, because their distribution trends are almost diametrically opposed, thereby indicating their apparent independent response to the depositional mechanisms. This feature, which was also observed in Saldanha Bay, is exceptionally prominent in Langebaan Lagoon.

5.4.1. Total Sediment

The overall size spectrum of lagoonal sediments is very similar to that of Saldanha Bay, although the contribution of individual size fractions is considerably different.

Gravels are very localized and mainly occur in the western outflow channel. Here the tidal current was unable to establish an equilibrium profile by adjusting the channel geometry, as observed in the eastern outflow channel, because of bedrock obstruction. As a result, the flow becomes turbulent throughout its depth; the same velocity was measured near the bottom and at the surface.

Other localized, but nevertheless important, gravel deposits occur along the northwestern margin of the lagoon between Kraalbaai and the lagoonal mouth. These deposits represent terminal fan material consisting of coarse granitic outwash. In contrast to the channel lag deposits, this fan material is poorly sorted, containing a substantial mud content. They form an easily recognizeable facies within the lagoon owing to their depositional isolation. The northwestern margin of the lagoon is exposed to rather low current activity; as a result, the coarse fan material has not been reworked and redistributed like most other sediments of the lagoon.

The mud content of lagoonal sediments reflects the northsouth energy gradient inferred from the physiographic subdivisions of the system (Fig. 145). In the northern lagoon, the mud content is generally below 0.5%, reaching over 1% only along the western margin in proximity to the gravel fan deposits discussed above. The mud content increases initially very slowly, reaching just over 1% in the central lagoon. Large parts of the eastern tidal flats are almost mudfree, due to the winnowing effect of waves and tidal currents

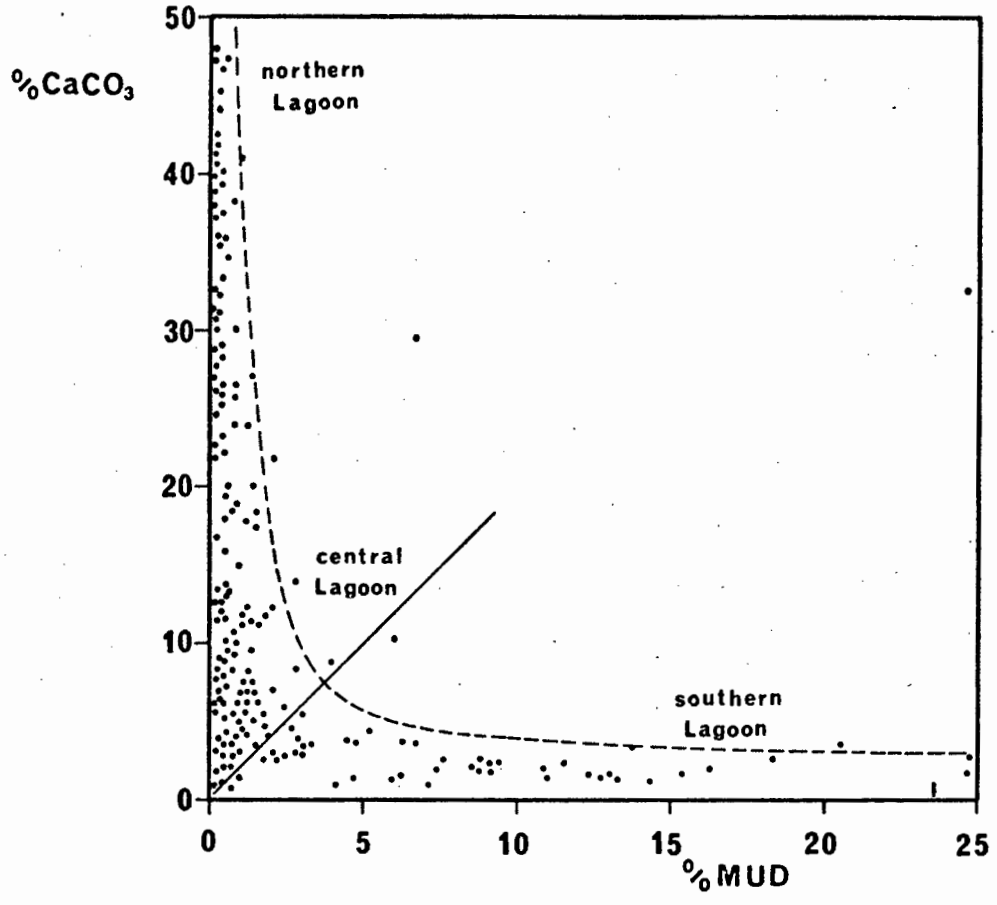

Fig. 146. The relationship between the mud content and the carbonate content in Langebaan Lagoon

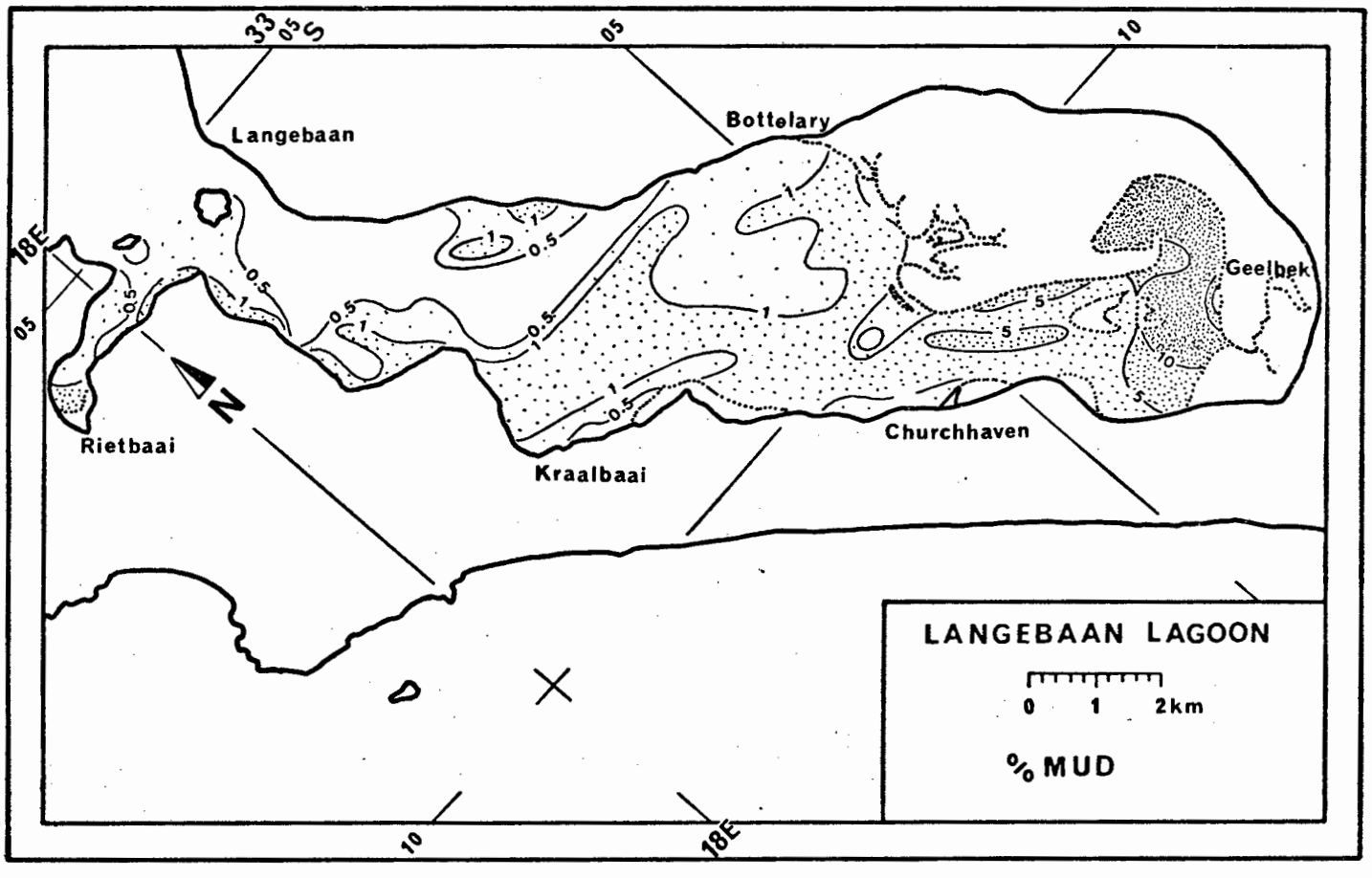

Fig. 145

acting in combination. In the southern lagoon, the mud content increases more rapidly, reaching 10% and more in the entire southeastern section near Geelbek. In most parts of the modern salt marshes mud values exceed 50%.

There is a peculiar inverse relationship between mud contents and carbonate contents in the lagoonal sediments. In Fig. 146 this relationship is illustrated in form of a hyperbolic trend producing a mirror image along the diagonal plane. A similar observation was made by Rusnack (1960) in a study of the Laguna Madre sediments along the south Texas coast. It would appear that this feature reflects the hydraulic relationship between two size endmembers within a size-velocity system. The bioclastic component would thus form the high energy endmember, while the mud would represent the low energy endmember. This interpretation does, in fact, correspond to the hydraulic model of shape sorting to be discussed later.

An important feature of Langebaan Lagoon is the total absence of open mud flats, which are so characteristic of many tidal flat areas in other parts of the world (e.g. Reineck, 1970; Ginsburg, 1975; Klein, 1976). This paucity of muds appears to be particularly characteristic of clastic tidal environments in arid and semi-arid regions. Similar observations were made in coastal lagoons of Baja California by Walton (1955), Redfield (1950) and Phleger and Ewing (1962). An important additional precondition is the absence of river drainage into the lagoonal system. This is demonstrated by the occurence of some mud flats in lagoons along the South Texas coast, such as Laguna Madre (Shephard and Moore, 1955 ; Rusnack, 1960), which are linked to a number of intermittent rivers that drain extensive catchment areas in the hinterland.

Very coarse sand is entirely restricted to the northern lagoon. Again the highest levels are observed in the western outflow channel (Fig. 147). Relatively high values are recorded along the northwestern margin in association with the gravel fan deposits. Another area with coarse sand is the subtidal flats in Rietbaai. This feature indicates that Rietbaai does not conform to the general trends observed in the remainder of the lagoon.

Coarse sand distribution is closely related to that of very coarse sand, although it is slightly more widely spread. In fact, small amounts of coarse sand are found in almost allparts of the lagoon (Fig. 148). It is the coarsest size fraction that achieves local concentration levels over 50%. The deepest parts of the eastern outflow channel, the central section

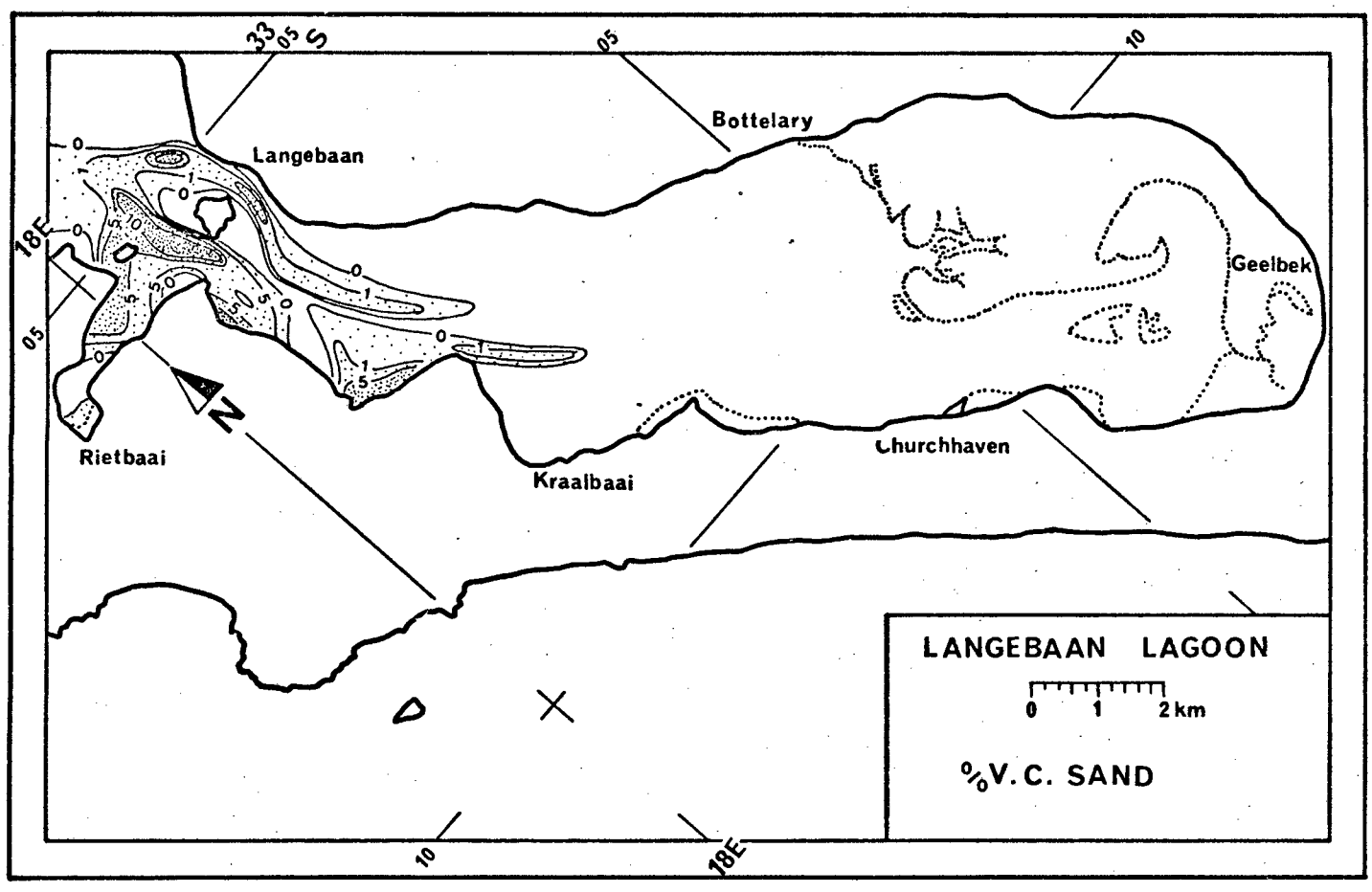

Fig. 147

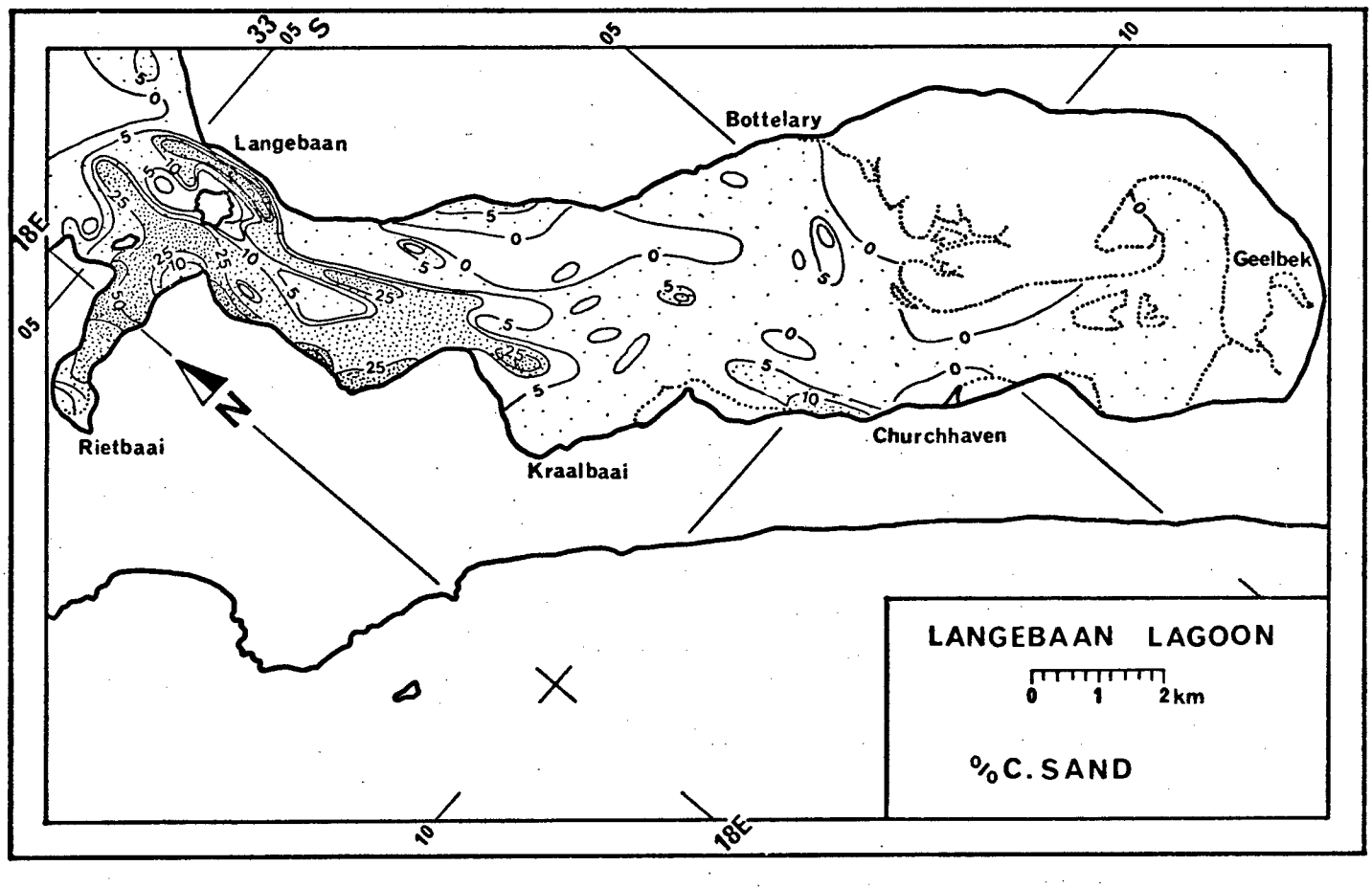

Fig. 148

of Rietbaai and some of the terminal fan deposits consist predominantly of coarse sand.

Most of the gravels, very coarse sand, and coarse sand represent channel lag material which is confined to the northern high energy section of the lagoon. They appear to form the exposed part of an extensive, predominantly bioclastic, gravel sheet that is encountered below a thin, unconsolidated sediment cover in most parts of the system. Material recovered from this layer was dated at 4260 $\pm$ 60 years B.P. (Pta - 1598), thus indicating its relict nature and probable association with the oyster reef biotope existing at that time.

Unlike Saldanha Bay, where the medium sands are closely related to the coarse population, they appear to represent an independent hydraulic population in Langebaan Lagoon. Medium sand predominantly occurs in the western half of the lagoon, being separated from the eastern section by the central channel. It would almost appear that the central channel acts as a physical barrier to the spreading tendency of medium sand. Only in the central lagoon does the hydraulic regime seem favourable to allow smaller amounts of this size fraction to reach the eastern tidal flats, where they form a narrow corridor at concentration levels over 25%. Very high concentrations, reaching over 75% in places, occur only in the southwestern part of the lagoon, adjacent to the fossil dune barrier. The paucity of other size fractions in this area and the fact that the fossil dune sediments themselves consist almost exclusively of medium-grained sediments, suggest that the eroded cliffs actually form the source for medium sands in Langebaan Lagoon. Since active erosion along this shoreline is grea tly reduced, it is concluded that the medium sand pattern most probably represents a relict feature.

Fine sand is almost as abundant as medium sand. It is spread over considerably larger areas and forms a more or less continuous blanket over most parts of the lagoon (Fig. 150). It is conspicuously absent only in the northern outflow channels and along the fossil dune barrier in the southwestern lagoon. The areas of high fine sand concentration indicate a depositional gradient that is directed towards the mouth of the lagoon and culminates in the tidal delta that is situated in the southern part of Saldanha Bay. The medium-sand corridor in the central section of the eastern tidal flats forms a division line between ebb and flood-current

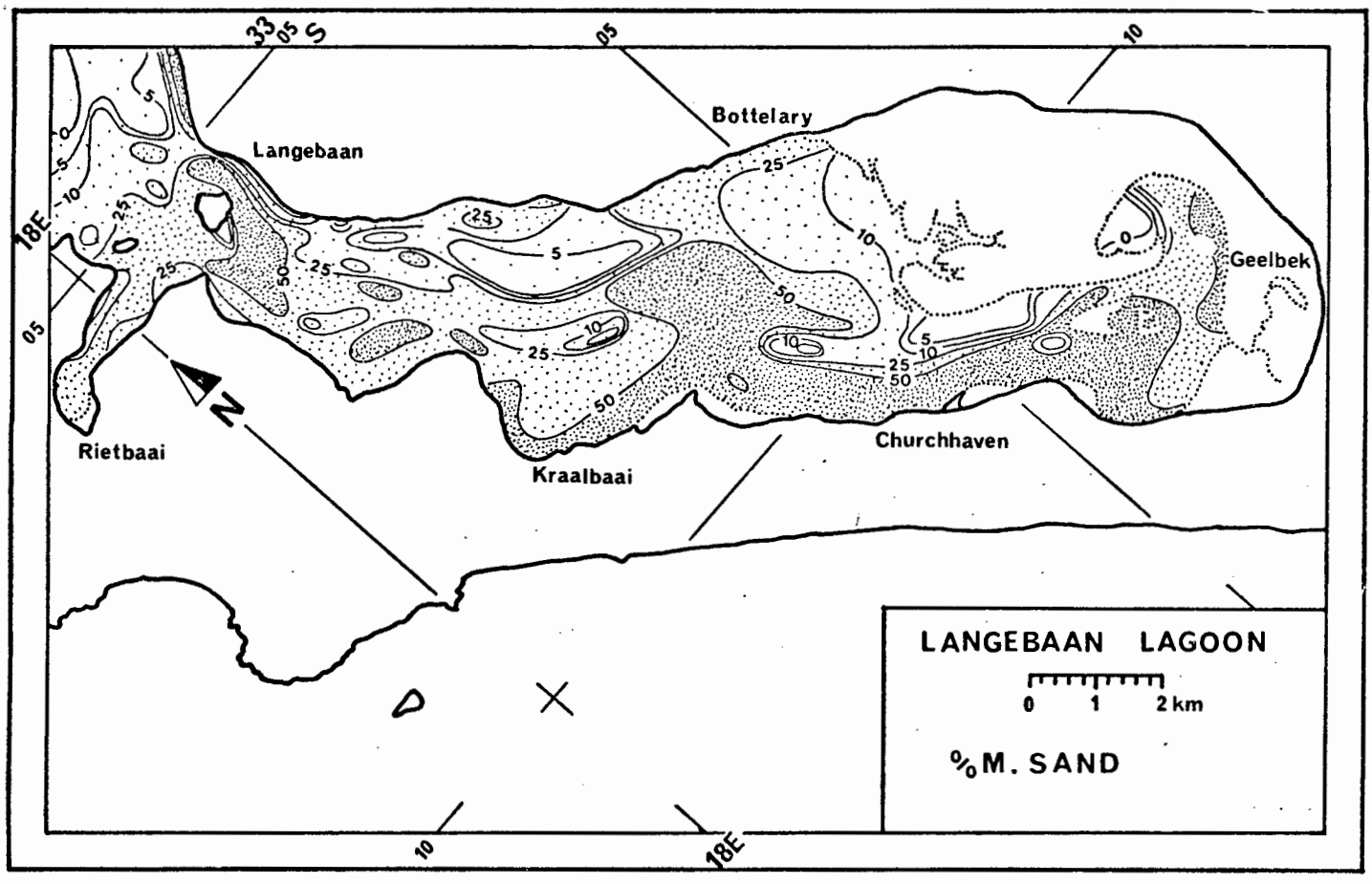

Fig. 149

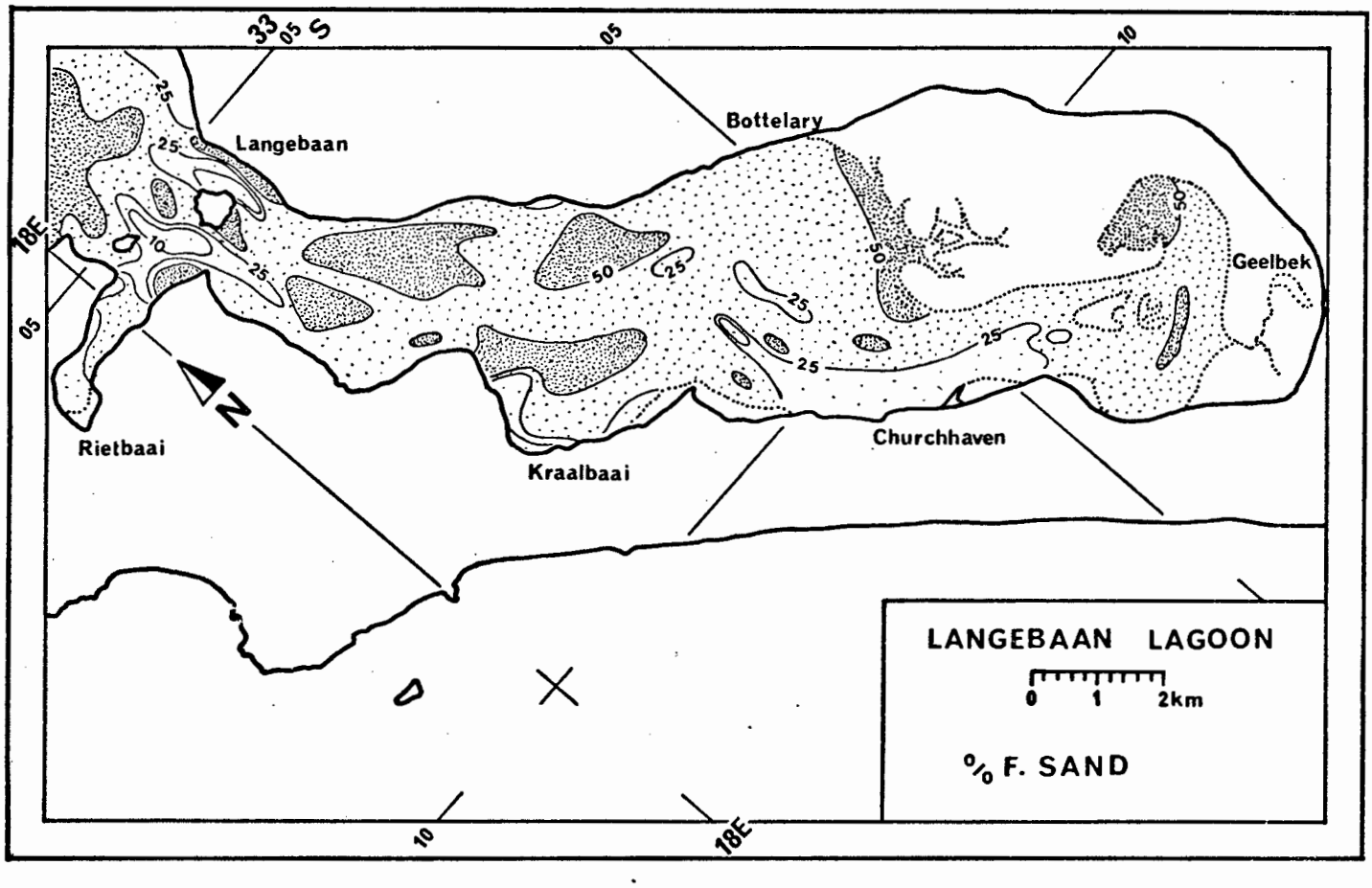

Fig. 150

dominated depositional processes. Fine sand is accumulated in fringing belts along large stretches of the southeastern salt marshes. This trend of fine sand deposition would further support the conclusion reached for the source of medium sand in Langebaan Lagoon. The ebb current control of depositional processes would discount an outside source for this sediment. It will be remembered that the depositional patterns in Saldanha Bay also favoured a lagoonal origin for most of its fine and very fine sediments.

The abundance of very fine sand in Saldanha Bay is contrasted with a strange deficiency of this size fraction in Langebaan Lagoon (Fig. 151). It forms a complementary pattern to the medium sand distribution and, with the exception of Kraalbaai, there is virtually no very fine sand on the western side of the central channel. Larger areas containing over 25% very fine sand are confined to the eastern tidal flats whereby the ebb-flood separation is particularly prominent. Areas with more than 50% very fine sand are confined to a narrow belt along the southeastern marshlands and to a few, very small and isolated patches on the highest parts of the eastern tidal flats. The abundance of very fine sand in Saldanha Bay indeed suggests that most of this size fraction was removed from the lagoon by ebb current activity. This feature strongly supports the conclusion that relative energy levels must have changed from place to place in Langebaan Lagoon at some stage during Holocene evolution.

The mean diameter map illustrates the dominating effect of the medium sand fraction on the overall distribution of the total sediment in Langebaan Lagoon (Fig. 152). The north-south division is faithfully recorded and the 2.5 phi contour line almost perfectly traces the 25% concentration limit of medium sand on the eastern tidal flats (viz. Fig. 149). Since this overall distribution pattern is so obviously related to depositional processes that have taken place during an earlier phase of the lagoonal history, it is concluded that modern sedimentary processes in the system have been so insignificant that these have been unable to substantially modify the inhereted relict distribution patterns. The modern trend is, therefore, reflected almost exclusively by the manner in which muds have accumulated in the lagoon. Modern sand supply is confined to minor sand flows generated along the fossil dune barrier by occasional heavy rainfall during the winter months (Plate 5 - G and 5 - H).

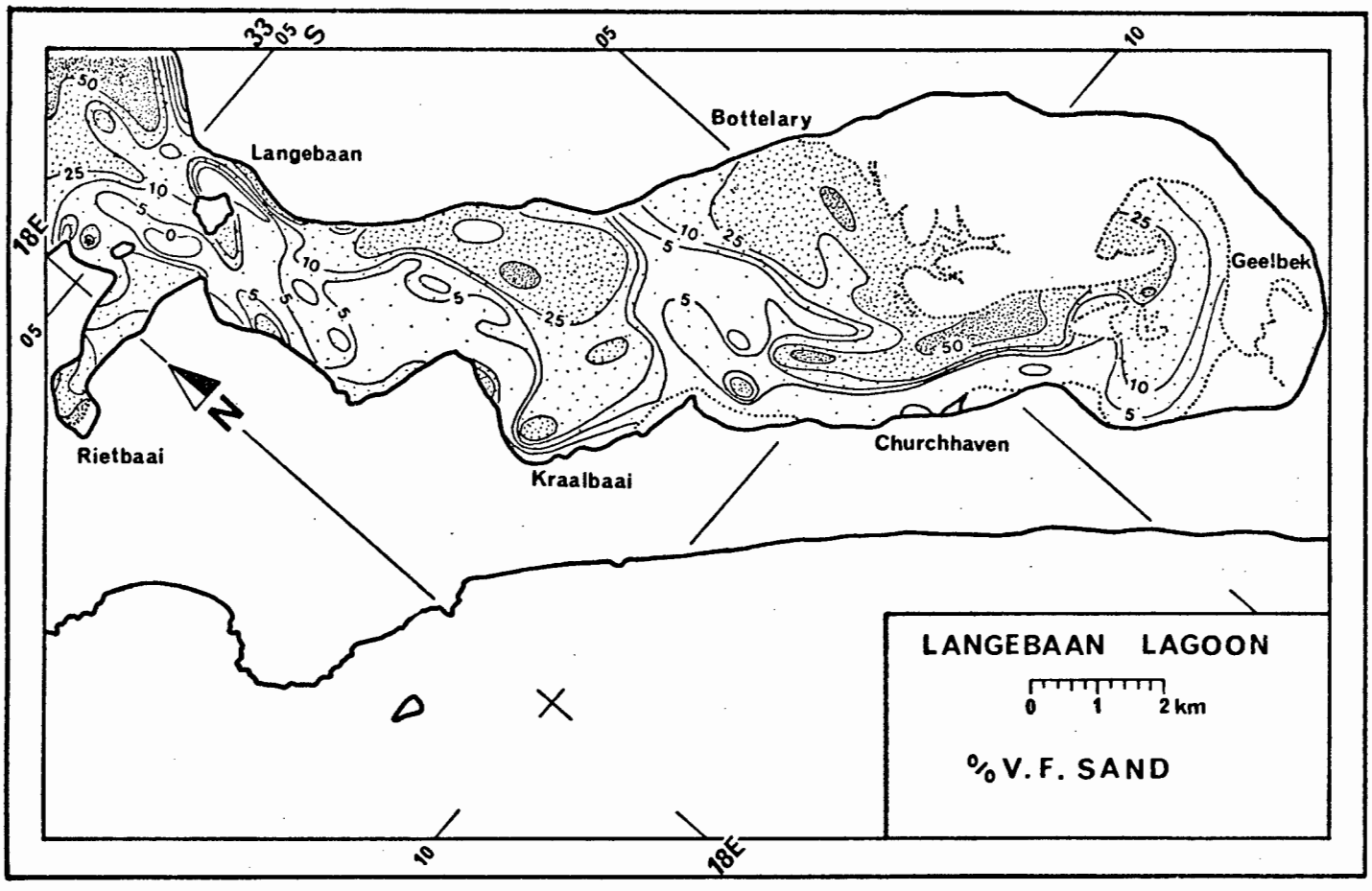

Fig. 151

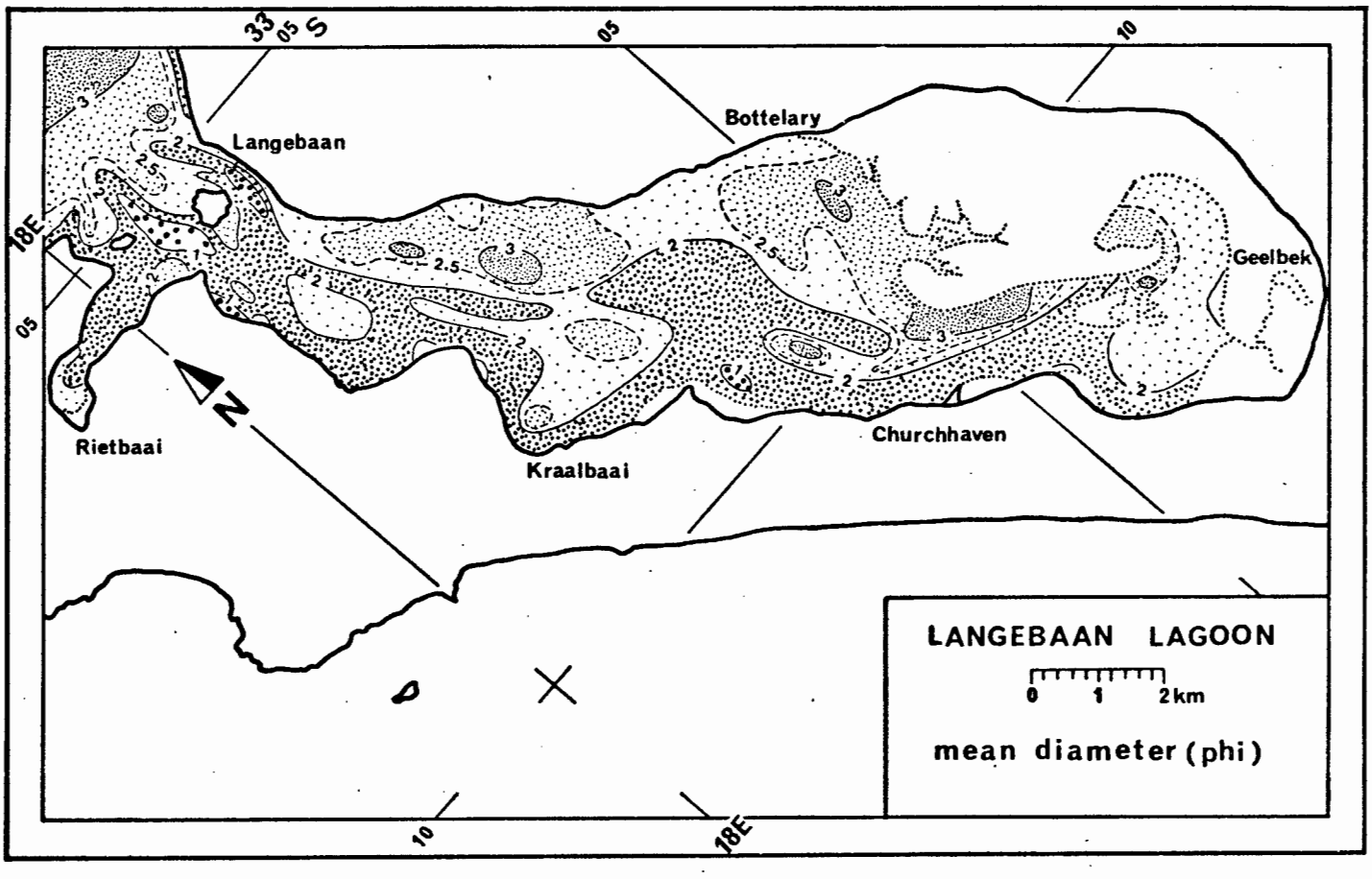

Fig. 152

The sediments of Langebaan Lagoon are relatively well sorted with QH values ranging from 0.8 (extremely well sorted) in the eastern outflow channel, to 4.2 (moderately sorted) along the granite margins in the northern lagoon and a single spot on the eastern tidal flats where a fossil oyster reef is exposed at the surface (Fig. 153). By far the majority of sediments are well sorted, with QH values between 2 and 4. In this situation, it is useful to contour further subdivisions, e.g. QH = 3, in order to define the sorting trends more clearly. Very well sorted sediments (QH = 1 - 2) occur in the northern outflow channels, along the fossil dune barrier from where a tongue reaches across to the northern section of the eastern tidal flats and in a belt lining the salt marshes in the southeastern lagoon. Thus both the medium-grained and the fine to very fine-grained sediments are very well sorted in close proximity to their respective source areas, suggesting that the lagoonal sediments most probably represent a mixture of these two well defined populations. Sorting would then simply be a function of this mixing process.

This interpretation is further corroborated by the skewness pattern of the sediments (Fig. 154). In the central and southern lagoon, the two size classes are clearly separated on the basis of their respective skewness properties. The medium-sized sediments in the central and southern lagoon are exclusively positively skewed, whereas the fine and very fine sands bordering on the marshlands are very negatively skewed. In the northern lagoon, progressive mixing and inclusion of coarser channel-lag sediments has modified the skewness character of the two populations according to the proportion that each contributes to the total sediment.

Thus, the relationship between mean grain size, sorting and skewness observed in Langebaan Lagoon is typical for two progressively mixing, hydraulic populations. This is clearly evident from the scatter diagrams representing the two-dimensional projections of their three-dimensional relationship. A model diagram, based on the work of Folk and Ward (1957) and Folk and Robles (1964), is discussed in Section 3.6.2. The mixing process between a very fine to fine population and a medium-sized population is illustrated in Fig. 155 by the relationship between mean diameter and sorting of the total sediment. The two upward converging arms of the point cluster reveal the size-sorting characteristics of the progressively mixing sediments.

The skewness-sorting relationship of the bioclastic component demonstrates its greater affinity towards negative skewness (Fig. 179). A far greater number of bioclastic size distributions are negatively skewed. At the same time, the axis of the bioclastic helix appears to dip more strongly than the axis of the terrigenous helic. This is concluded from the more pronounced elliptical outline of the bioclastic point cluster in Fig. 179.

In summary, it is concluded that, while the size characteristics of both sedimentary components are very similar and thereby reflect the major trends of the total sediment, each component nevertheless retains a certain characteristic image which is not evident from the total sediment. It would thus appear that the total sediment simply presents the average picture of its individual component groups. Each component group should, therefore, be treated as an independent hydraulic subpopulation of the total sediment and its major hydraulic populations.

5.5. DEPOSITIONAL PROCESSES

5.5.1. Sediment Sources

When discussing the sediments of Saldanha Bay, it was demonstrated that most of the fine and very fine sands originated from Langebaan Lagoon. The general distribution pattern of fine sediments, and especially the unusual deficiency of very fine sand in the lagoon, strongly support this conclusion. The depositional gradient of the two fine fractions is clearly controlled by the ebb current.

Since the fossil dune barrier consists almost entirely of medium sized sands, it can be discounted as a major source for fine sediments. It would thus appear that the fine sediment source is in some manner linked to the formation and destruction of salt marshes in the southeastern parts of Langebaan Lagoon. Undercutting and subsequent erosion of salt marsh was observed in slowly migrating marsh creeks and along some marsh boundaries, where wave action at high tide has led to extensive truncation of the seaward-facing edges (Plate 7-A and 7-B). This has led to the development of extensive mud pebble pavements along some beaches of the lagoon (Plate 7-C).

It is difficult to determine the original source of the fine sediment. A plausible explanation might be found when considering the former outflow channel at Kraalbaai. The shore-face and nearshore zone seaward of the

barrier consists of fine to very fine sands; it is possible that during each flood cycle some fine suspended sediment entered the lagoon. Although most of this would subsequently have been flushed from the system by the ebb current, a small portion may have been retained in the low energy regions of the lagoon, thereby slowly building up a fine sediment reservoir, which then formed the core zone of marsh development at the onset of the regression subsequent to the highest stand of the Holocene sea-level. After the Kraalbaai channel had fallen dry, the readjustment of the tidal flow pattern reworked some of this older marsh, thereby removing the finer grain sizes and gradually transporting them towards the outlets at Langebaan village. The very fine sand, being hydraulically less stable was almost completely removed, while the fine sand fraction contributed substantial amounts towards a new equilibrium in Langebaan Lagoon. This readjustment was completed some 200 years later, coinciding with the death of the last oyster bioherms in the lagoon (ca. 1800 years B.P.)

The medium sand, on the other hand, is related to the fossil dune belt. Since relative energy levels shifted away from the southwestern shoreline, most of the reworked dune sediment simply remained where it was. This is evident from the medium sand pattern. In the course of this readjustment, most channel beds, originally covered with a coarse shelly lag comprising material from marine organisms that were associated with the reef habitat (e.g. large bryozoan colonies), were covered by a thin layer of finer sediment. The only exception to this rule is observed in the northern lagoon, where this shelly lag deposit is still exposed in the areas where finer sediments have remained hydraulically unstable.

The marine origin of the finer sediments, and the aeolian origin of the medium sands, was confirmed by applying the model developed by Friedman (1961). As was pointed out in Section 3.5.4., this model does not predict environments, but simply the relationship of sediments to certain environments. On the basis of this model, the sediments of Langebaan Lagoon can be divided into two distinct groups: a dune related group and a shallow-marine related group (Fig. 180-A). Both groups actually consist of intertidal, subtidal, and channel sediments (Fig. 180-B). Both, however, have been correctly related to sediments originating from environments predicted in the model.

When plotting the areal distribution of samples categorized in the model, it was found that each group consistently traces the depositional areas

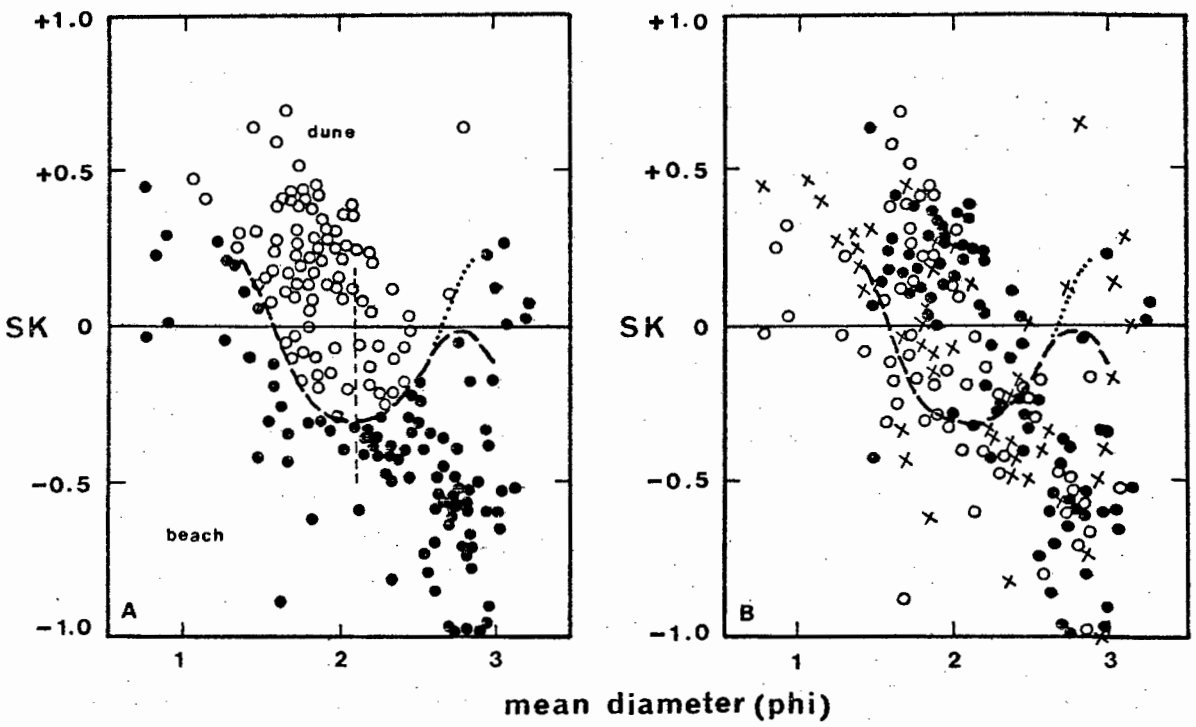

Fig. 180. The distinction between beach and dune sediments.

A. The sediments appear to consist of a dune and a beach population

B. All samples consist of modern lagoonal sediments

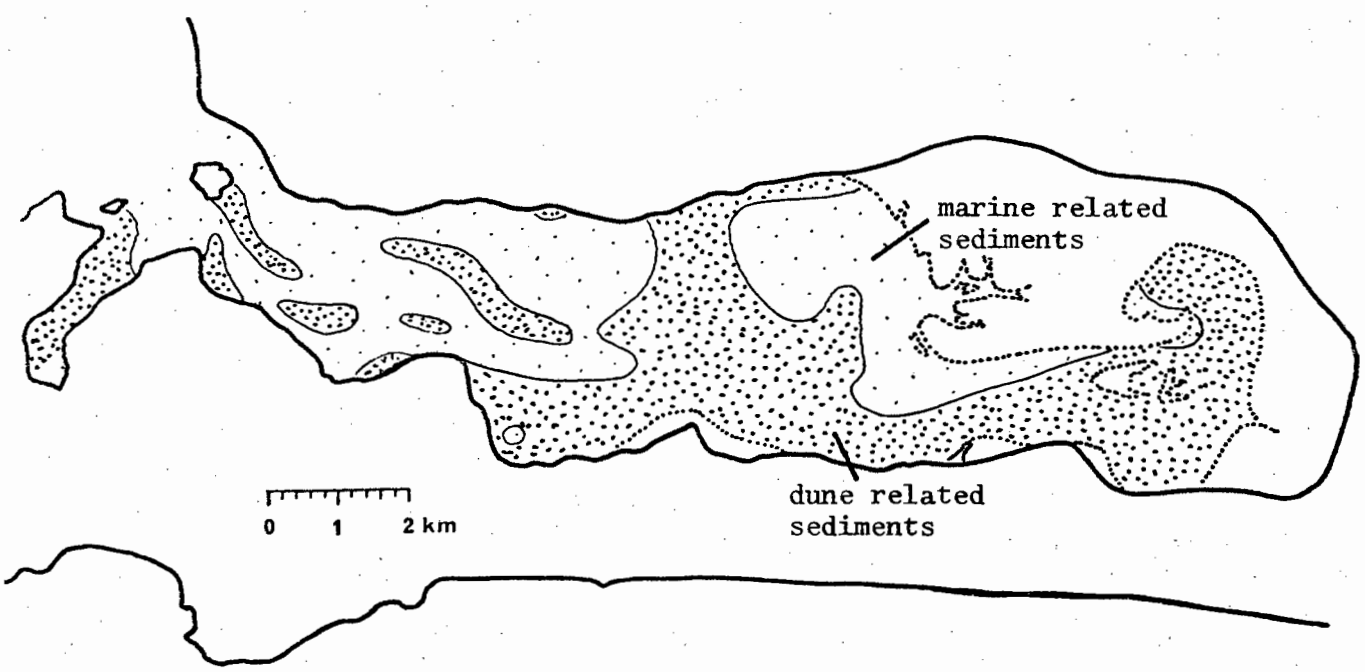

Fig. 181. The sediments of Langebaan Lagoon can be divided into a dune related and a shallow-marine related group.

dominated by either the fine population or the medium-grained population (Fig. 181). In addition, the pattern is amazingly similar to the skewness pattern of the total sediment. The consistency of the patterns excludes a purely coincidental agreement.

The data from Langebaan Lagoon in addition suggest a slight modification of the division line, on the basis of which the two groups are distinguished. In the original model of Friedman (1961), the division line drops into the negative skewness field and turns back towards Sk = 0 at a skewness level of about -0.3 and a mean diameter level of about 2.1. When it almost reaches Sk = 0 at a mean diameter level of 2.75, it again swings back towards negative skewness. The Langebaan data, on the other hand, suggest that the curve has a mirror plane through the mean diameter level of 2.1 (Fig. 180-A). A re-examination of Friedman's originally published data indicates that, at the finer end of his inferred curve, sample densities are rather low and do not warrant an accurate definition of the division line.

It remains to be investigated in which manner this model, in its modified form, relates to the three-dimensional relationship of the main size parameters. Its ultimate acceptance will depend on whether it can be defined within a three-dimensional co-ordinate system in form of an exclusive point cluster.

5.5.2. Textural Response to Sediment Mixing

In Section 5.4. it was demonstrated that the main size parameters of the whole sediment in Langebaan Lagoon can be described in terms of a three-dimensional point cluster, which is arranged in a quasi-helical structure. The idealized model of Folk and Ward (1957) predicts the relationship between the individual size parameters in the course of the mixing process.

In this section it will be demonstrated that each major, depositional environment in Langebaan Lagoon can be defined by its own characteristic helical relationship and that the helix described by the whole sediment simply reflects the combination of its individual members. The stronger its members deviate from each other, the more obscure will the whole structure become. Recognizing individual, clearly arranged sample associations could lead to a method of defining depositional members in situations where this is not obvious on the basis of other criteria, e.g. ancient environments. In

Langebaan Lagoon three units have been recognized: 1) intertidal flats, 2) subtidal flats, and 3) tidal channels.

5.5.2.1. Intertidal Flats

The helical structure produced by the three-dimensional relationship of size parameters of the intertidal sediments is better defined than in any of the other units (Fig. 182). The lateral scatter of data points is very small, and the whole point cluster is symmetrical. In the mean diameter-sorting diagram (Fig. 182-A), the two endpoints of the inverted V-shaped point cluster (which represents one whole revolution of the helix) represent the two respective, parent populations involved in the mixing process. In each case, their respective sorting levels are practically identical, approaching QH = 1. Their respective mean diameters are about 1.6 phi and 3.1 phi.

In the process of mixing, the sorting characteristics of each population rapidly decreases until a maximum is achieved, which in this case lies at the level of QH = 4.2. If the two populations are lognormal, the point of equal mixing will lie at the apex of the point cluster. From Fig. 182-A it can be seen that, for the intertidal sediments, this is not quite the case. Equal mixing occurs at a mean diameter of about 2.15 and a sorting level of about 3.0, whereas poorest sorting is achieved at a mean diameter of about 2.4 phi and a sorting level of 4.2.

The discrepancy between these two levels is explained by the fact that the two parent populations were not lognormally distributed when the process of mixing occurred. Fig. 182-B clearly demonstrates this feature. The coarse endmember is slightly positively skewed (Sk = +0.1), while the fine endmember is strongly negatively skewed (Sk = -0.4). At the point of equal mixing, i.e. where skewness is zero, relative sorting has reached 3.0 along the coarse arm of the cluster. It is interesting to observe that, in Langebaan Lagoon, the apex-point coincides with the line separating the dune derived sediment and the shallow-marine derived sediment as predicted by the model of Friedman (1961). The separation line contoured in Fig. 181, therefore, traces those localities on the intertidal flats at which poorest sorting is achieved.

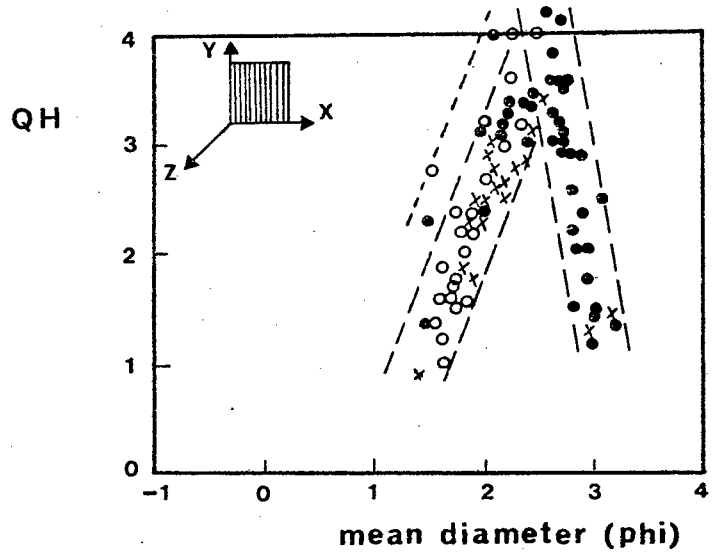

Fig. 182-A.

The relationship between mean diameter and sorting of intertidal sediments

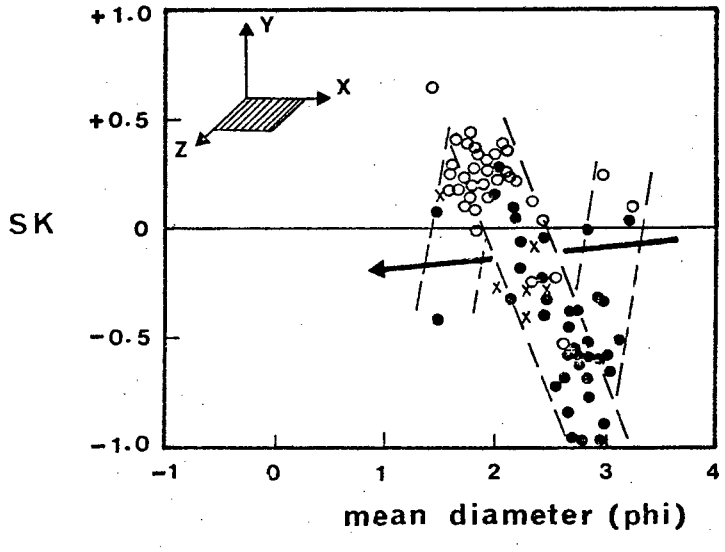

Fig. 182-B.

The relationship between mean diameter and skewness of intertidal sediments

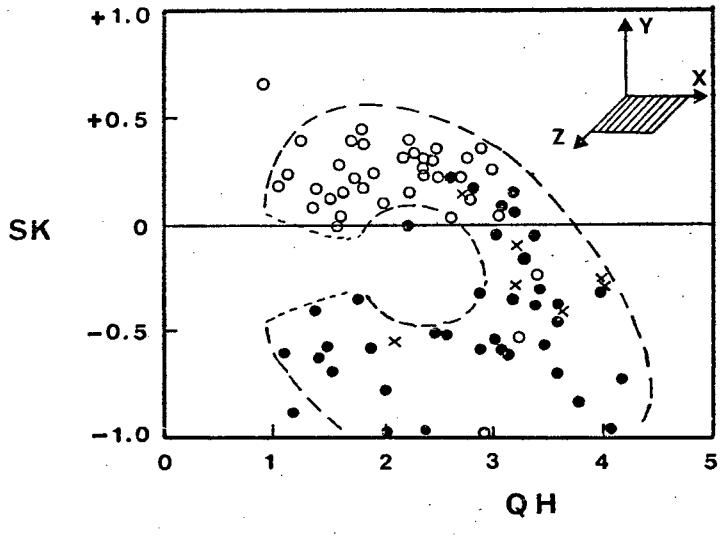

Fig. 182-C.

The relationship between sorting and skewness of intertidal sediments

The skewness-sorting relationship of intertidal sediments (Fig. 182-C) demonstrates that the central axis of the helix runs more or less parallel to the mean diameter co-ordinate (X-axis). This is concluded from the circular arrangement of the point cluster. The inner, empty circle indicates the good grouping of points close to the centre line of the helical progression. The central axis follows a skewness level of about Sk = -0.25 and a sorting level of about QH = 2.5. Together with the mean diameter of the apex of the helix (X = 2.4), these values represent the average size parameters of the intertidal sediments. The maximum diameter of the helix amounts to about 1.5 Sk-values and about 3.0 QH-values. The average degree of point scatter, i.e. deviation from the centre line of helical progression, amounts to about 0.5 mean diameter values, 0.8 QH-values, and 0.4 Sk-values.

5.5.2.2. Subtidal Flats

The relationship between the individual size parameters of subtidal sediments are illustrated in Fig. 183. From the mean diameter-sorting diagram (Fig. 183-A) it is clear that Rietbaai sediments do not fit into the general lagoonal pattern, and should strictly be treated as a separate depositional unit altogether. This is also justified by its geographic position at the mouth of the lagoon, where it forms a blind arm. Depositional processes in this area are not in direct contact with those in the remainder of the lagoon.

The point cluster (Fig. 183-A) differs significantly from that of the intertidal sediments. Although the mean diameters of the best sorted samples of each population have remained at about the same positions, their respective sorting values are no longer identical. The best sorted samples of the coarse population now reach a QH-value of only 2.0. This feature implies that the coarser sediments have undergone a certain degree of mixing before they have reached any subtidal flat locality. There is no original, unaltered sediment of the parent population on any of the subtidal flats. Very fine sediment that has retained its inhereted size characteristics, on the other hand, can still be found on some intertidal flats. The samples in question originate, without exception, from the very south of Langebaan Lagoon, i.e.from localities in close proximity to their original source areas.

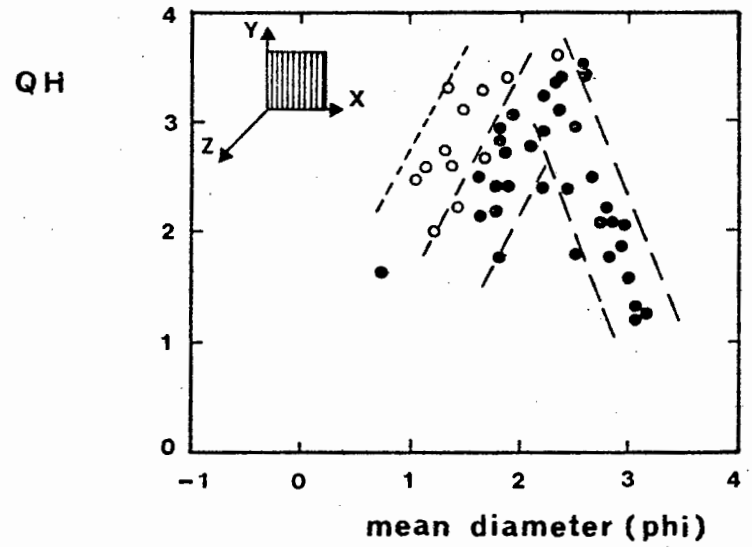

Fig. 183-A.

The relationship between mean diameter and sorting of subtidal sediments

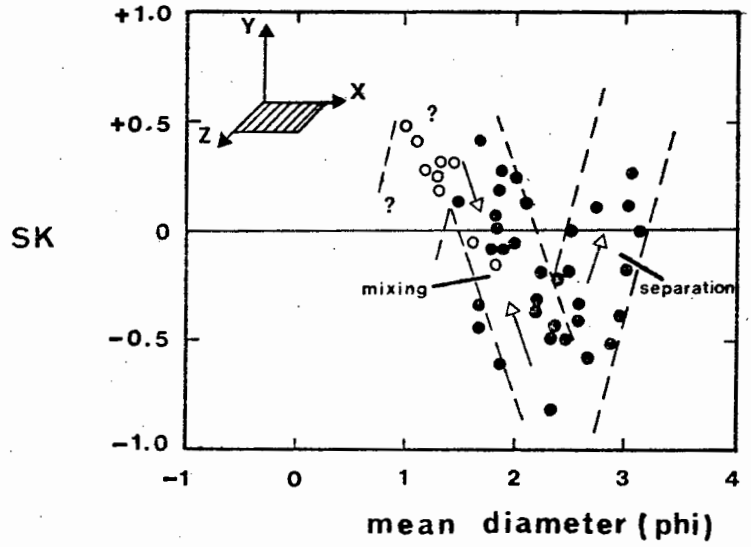

Fig. 183-B.

The relationship between mean diameter and skewness of subtidal sediments

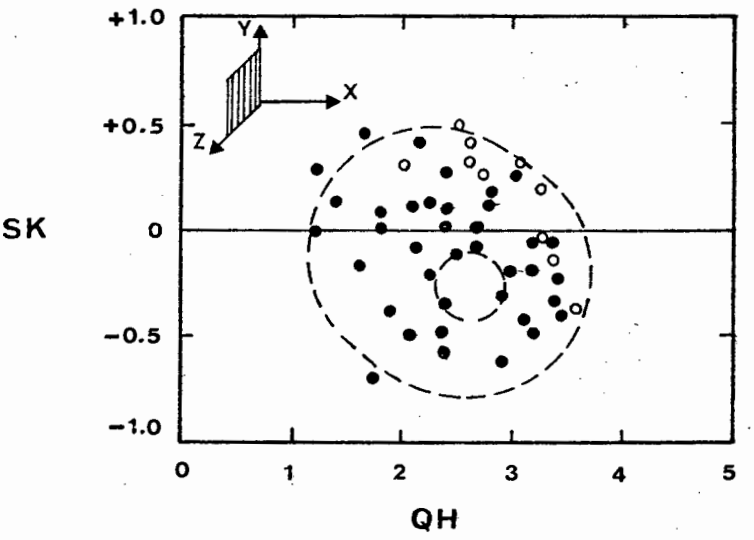

Fig. 183-C.

The relationship between sorting and skewness of subtidal sediments

The mean diameter - skewness relationship (Fig. 183-B) underlines the previous observations. In addition to the reduced sorting range, the whole point cluster of the helix appears to be slightly out of phase with that described by the intertidal sediments. This is indicated in Fig. 183-B by the extension of the fine arm towards positive skewness. These samples coincide with those that have retained their mean diameter and sorting characteristics. Their skewness, however,has changed from a strongly negative one to a positive one. It would thus appear that on the intertidal flats two processes counteract each other. In some cases mixing between the two populations is proceeding in the normal manner, while in other cases separation (i.e. unmixing) is observed. The size characteristics of this very fine sediment is practically identical to that found in Saldanha Bay; it will be recalled that in that case it was concluded that this size characteristic was indicative of the fine population at the time it entered the depositional system of the bay. The writer regards this feature as the most powerful evidence in support of a lagoonal origin of the very fine sands in Saldanha Bay.

In Fig. 183-C skewness and sorting are contrasted. The diagram demonstrates that the diameter of the helix described by intertidal sediments is considerably tighter, reaching a maximum diameter of only 1.2 Sk-values and 2.5 QH-values. In accordance, the diameter of the inner circle has reduced by almost 50%. The position of the central axis has remained at its original position.

On the whole, the subtidal sediments produce a similar picture to the one observed on the intertidal flats. The helix has become tighter, and includes an extension in which separation of previously mixed sediment is observed.

5.5.2.3. Tidal Channels

As in the case of subtidal sediments, a secondary component running parallel to the coarse population can be observed. This arm, illustrated in Fig. 184-A, represents samples from those areas in the northern channel system in which lag sediments were recorded. Thus, a third coarse population is locally mixed into the sediment from the other two populations. Since the lagoon is ebb current dominated, this additional mixing process is very

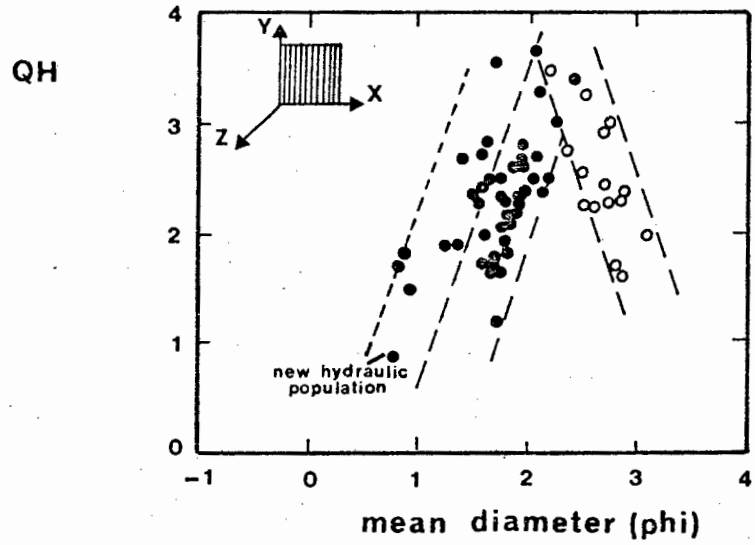

Fig. 184-A.

The relationship between mean diameter and sorting of channel sediments

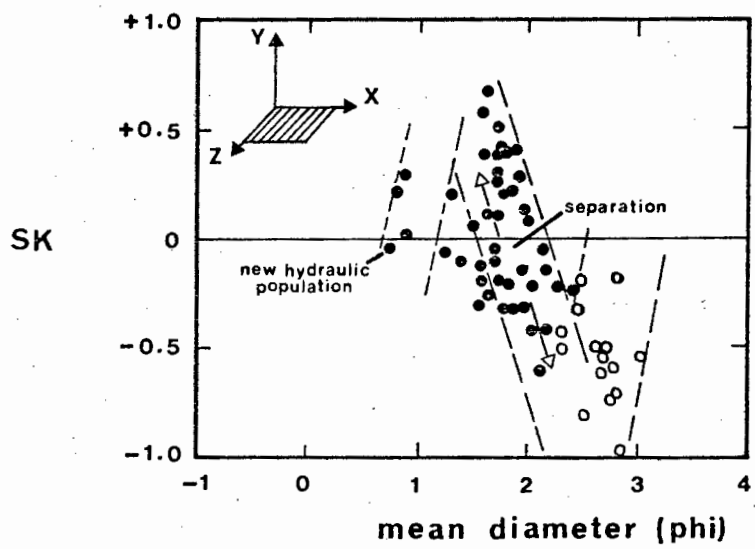

Fig. 184-B.

The relationship between mean diameter and skewness of channel sediments

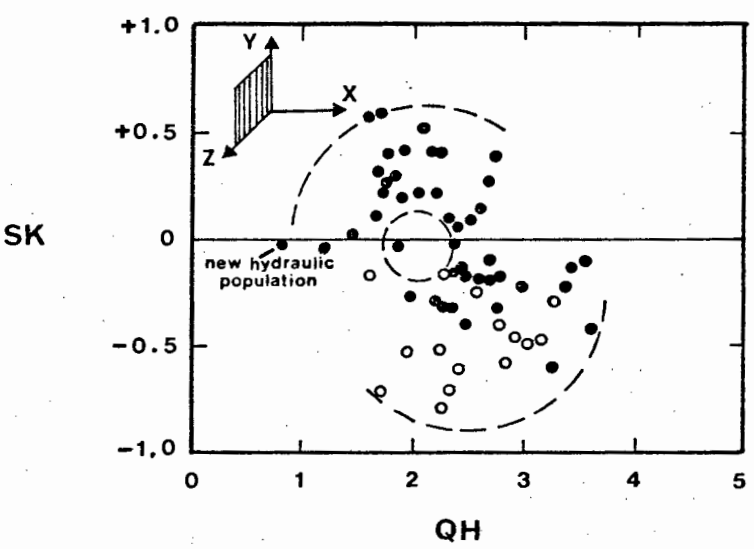

Fig. 184-C.

The relationship between sorting and skewness of channel sediments

localized and has not affected the sediments further south.

The fine population of the point cluster in Fig. 184-A is exclusively composed of channel slope samples. Since this material has been eliminated from the channel bed material, it is concluded that the helix described by the channel sediments represents a separation process rathern than a mixing process. Together with the samples representing channel lag sediments, this feature has resulted in a greatly distorted helix. This is quite evident from the poorly defined images in Fig. 184-B and Fig. 184-C.

The reversed trend is demonstrated by the fact that, in the direction of increasing energy, the sorting characteristics of both populations increase. The channel bed sediment is, in fact, transformed into a completely new hydraulic population, as indicated by the extremely well sorted and lognormal character of the sample material recovered from the eastern outflow channel. This sample point has been specifically marked in all three diagrams.

In summary, it is concluded that the mixing process of the two hydraulic populations is predominantly confined to the southern and central lagoon. This process is reversed in the channels of the northern lagoon, where progressive size-sortinghas eliminated the finer grain sizes. Fine sediment is unstable under the flow conditions observed in the northern channels. Instead, it forms the channel slopes and banks where the energy gradient is greatly reduced. In this manner, a completely new hydraulic population gradually evolves from the sediments of the channel beds. The basic size distribution characteristics of this population are defined by the sediment in the eastern outflow channel.

5.5.3. A Model Approach to Sediment Mixing in Langebaan Lagoon

The previous discussion has repeatedly indicated that the strict helical relationship between progressively mixing, hydraulic populations enables the approximate prediction of the mixing stage achieved at any point in the system, on the basis of the main size parameters of the sediment. In this section it will be demonstrated that the degree of mixing can be accurately predicted from the relationship among the individual size parameters. To achieve this, all three size parameters discussed in this study,

plus kurtosis, were averaged over discrete mean size intervals (0.2 phi-intervals), and subsequently superimposed in two-dimensional diagrams.

In Fig. 186-A the average size characteristics of each population have been co-plotted for all 220 samples from Langebaan Lagoon. The discussion in the previous section, however, has indicated that the process of mixing is not identical in each physiographic unit of the system and, in order to avoid oversimplification, the exercise was repeated for each case separately. Thus, Fig. 186-B represents intertidal flats, Fig. 186-C subtidal flats, and Fig. 186-D the tidal channels.

Corresponding trends of the two populations were then synthesized into a single interpolated curve and, subsequently, presented in individual co-ordinated diagrams (Fig. 187). Each graphic model, representing the three depositional units, relates sorting (QH), skewness (Sk) and kurtosis (K), as a function of mean diameter (X). In this form, the difficulty of comprehending three-dimensional relationships is overcome.

It will be noted that, in correspondence to the findings in the text, each model presents a different image. Although certain similarities exist in the finer size classes, there is little agreement in the coarser size categories. For this reason it was decided that a single comprehensive model for the whole lagoon would serve no purpose. In each case, the model accurately predicts the average characteristics of the size frequency distribution at any point in Langebaan Lagoon, on the basis of the mean diameter alone. At the same time, the degree of mixing between the two hydraulic populations can be assessed.

All three models clearly demonstrate that the populations involved in the mixing process in Langebaan Lagoon are not lognormally distributed. The greatest similarity to the ideal model presented by Folk and Ward (1957) is achieved by the intertidal flat sediments (Fig. 187-A). The only difference is a slight shift of the skewness curve by 0.3 phi values along the mean diameter scale, in the direction of the coarser size classes. This feature reflects the non-normality of the parent populations. This out-of-phase tendency increases in the subtidal model to0.8 phi intervals (Fig. 187-B) and to 0.9 phi intervals in the channel model (Fig. 187-C).

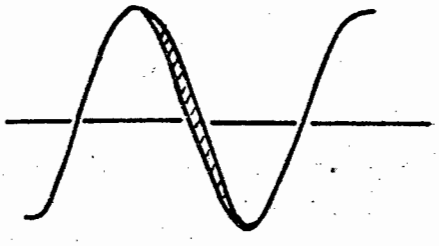

1. Point progression

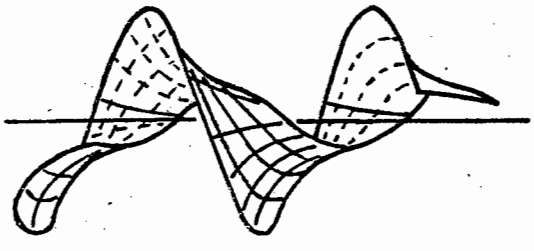

2. Line progression

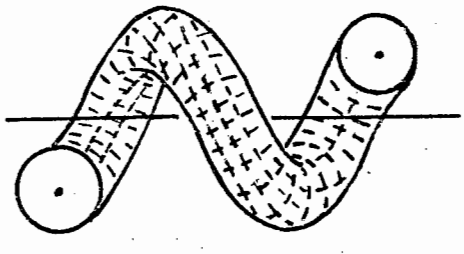

3. Plane progression

Fig. 185-A. Various types of helices (after Wunderlich, 1967).

1. point helix
2. line helix
3. plane helix

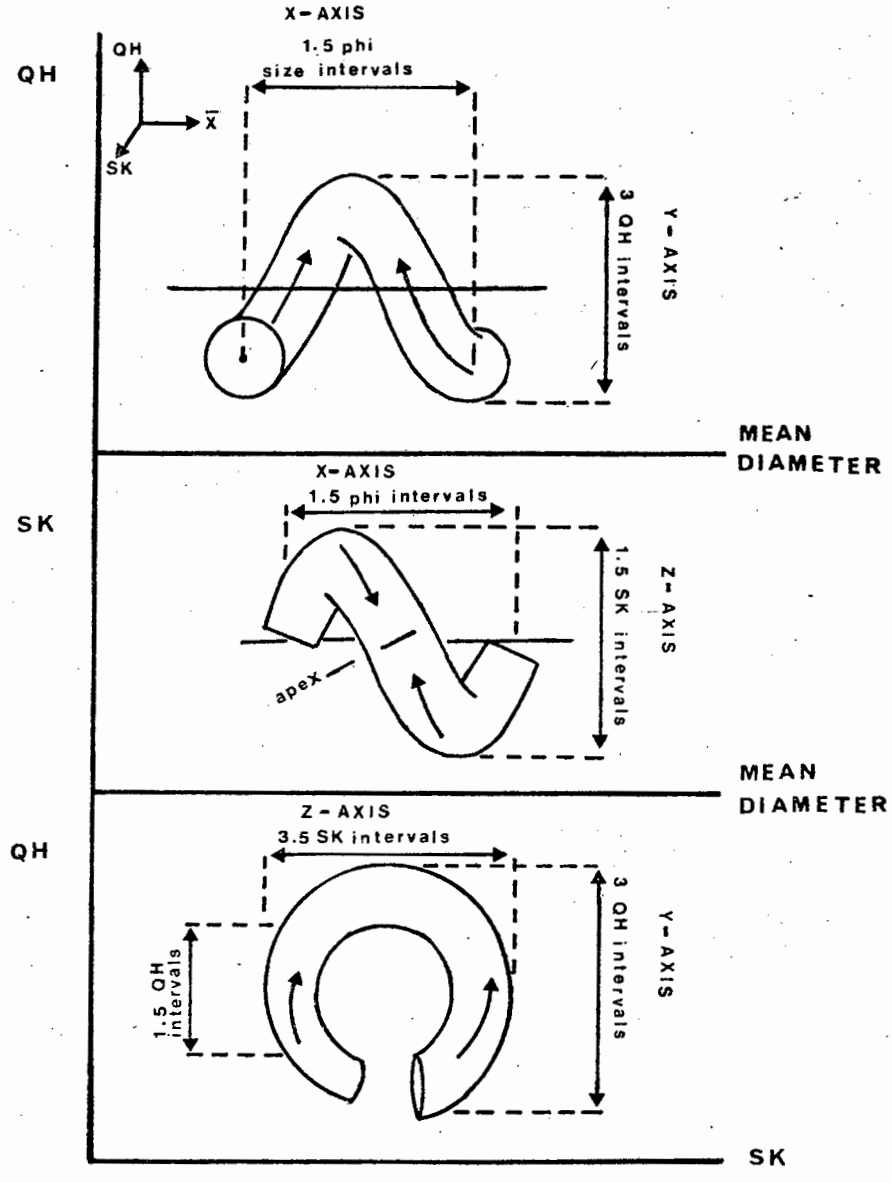

Fig.185-B. Quantitative expression of a helical progression.

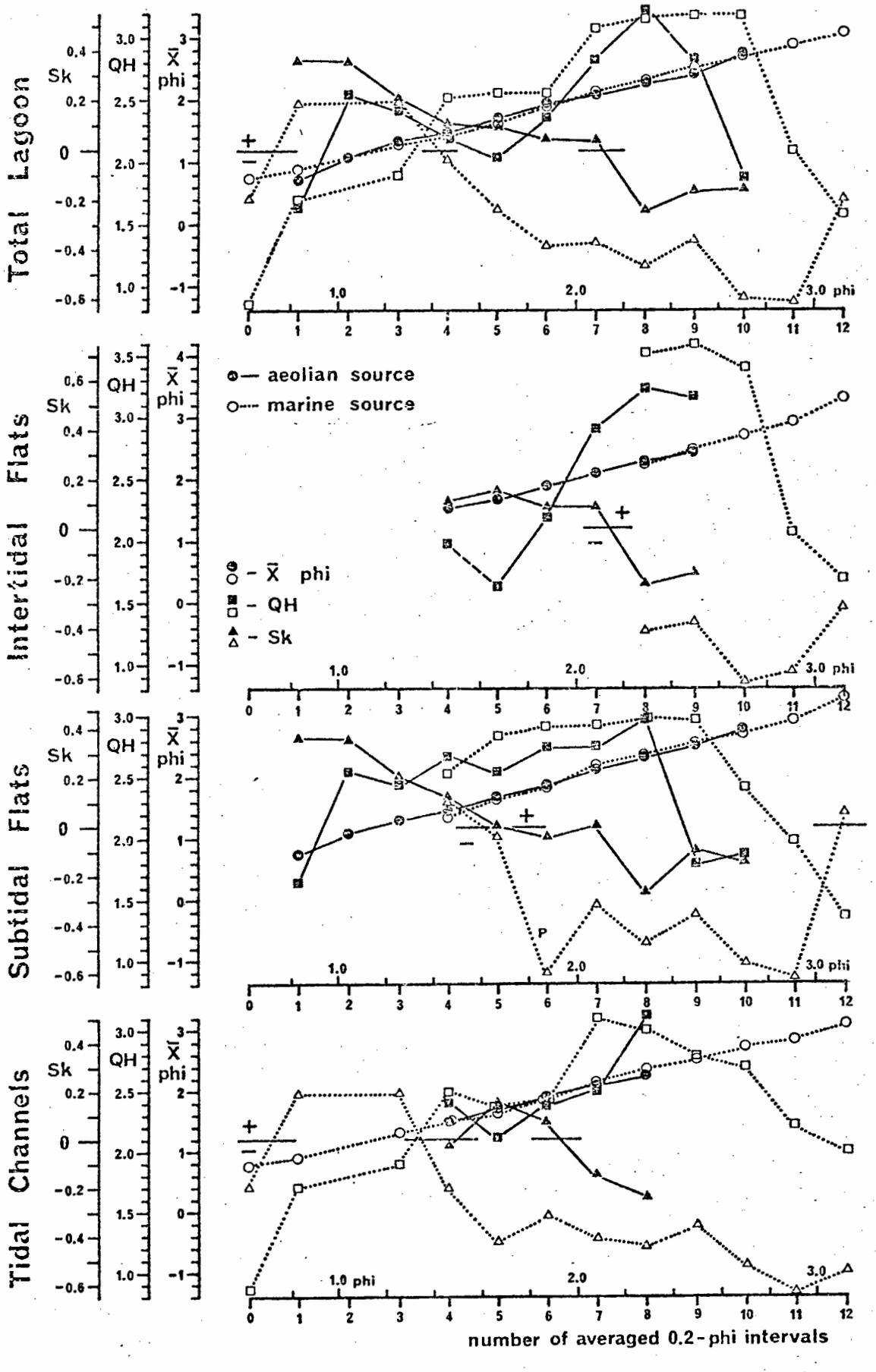

Fig. 186. Average size characteristics of various lagoonal sediments

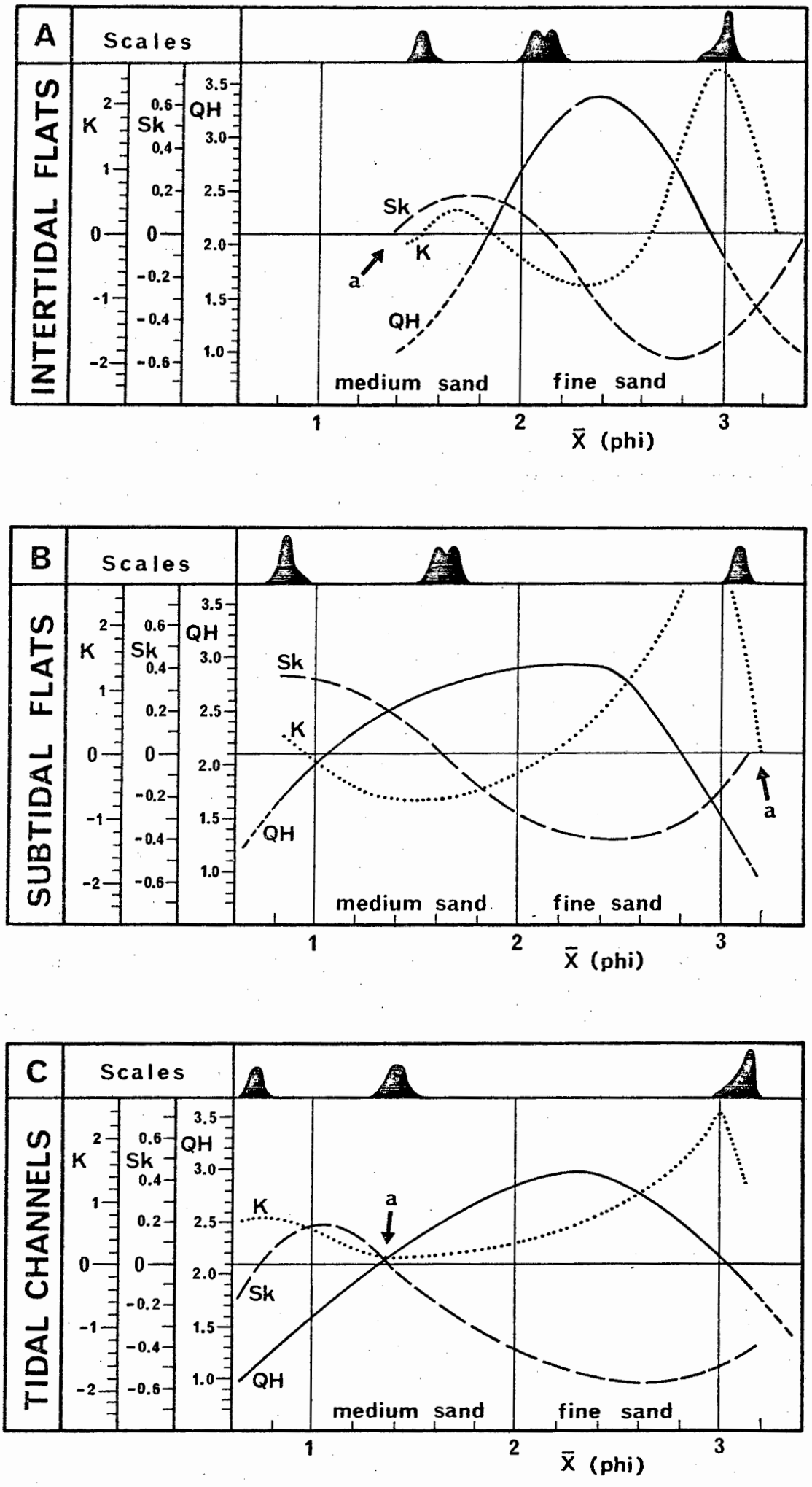

Fig. 187. Three graphic models by which the average size distribution characteristics at any point in the lagoon can be determined on the basis of the mean diameter alone.

In this study the point cluster was reduced to single line relationships similar to that discussed by Folk and Robles (1964). In reality, the data points scatter around this average value, and it cannot be excluded that this scatter may take on a significant shape which itself may be a characteristic feature of the environment. A number of possible helical structures are presented in Fig. 185-A. At this stage it cannot be decided whether averaging is justified on the sole assumption that the scatter of data points, around the helical centre line, simply reflects a certain inherent "background noise" produced on a local scale by the unsteady nature of complex sedimentary processes. It cannot be excluded that the scatter actually consists of a bunch of single line helices, each of which connects individual data points along a specific path of the depositional process.

A first attempt to quantify a helical structure is demonstrated in Fig. 185-B. The example represents the helical relationship of intertidal sediments. Characterization of helical trends in this manner could be useful for data processing by computer for the purpose of comparative studies. It should also be possible to express the helix in vectorial form since a three-dimensional co-ordinate system is used anyhow. To pursue this interesting aspect further is beyond the scope of this study.

5.5.4. Modes of Sediment Transport and Deposition

Having discussed sediment distribution patterns, the major sediment sources, and the strict control of textural relationships in the course of sediment mixing, this section deals with the modes of sediment transport in the course of which the sediment was deposited. To achieve this, a slightly modified version of the depositional model developed by Passega (1957) is utilized (Section 3.6.3.) By relating the 1st percentile and the mean diameter, a number of transportational modes are recognized that serve to explain the various depositional characteristics of Langebaan Lagoon. The mode by which a sediment of given size is transported is directly related to the energy level of the flow system.

Five modes of transport are distinguished on the basis of the point scatter in the CM-Diagram covering the whole lagoon (Fig. 188-A). By far the largest number of samples falls into the upper bottom suspension (saltation 2) category (46%); lower bottom suspension (saltation 1) is represented by 24%,

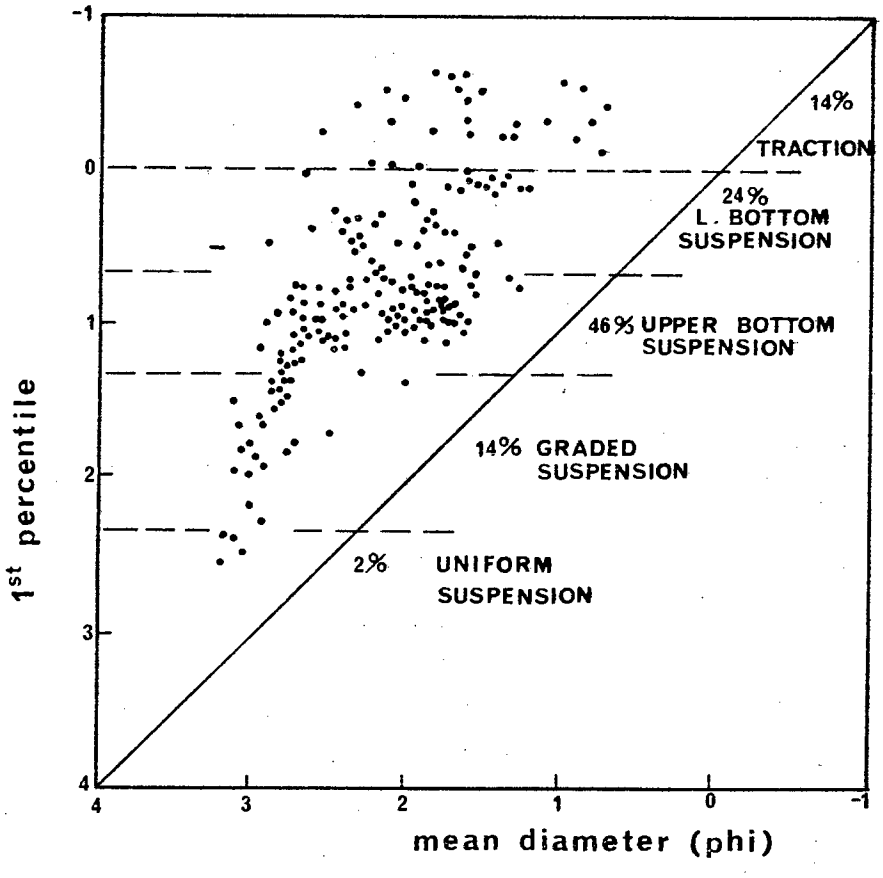

Fig. 188-A. Modes of sediment transport and deposition of the total sediment in Langebaan Lagoon

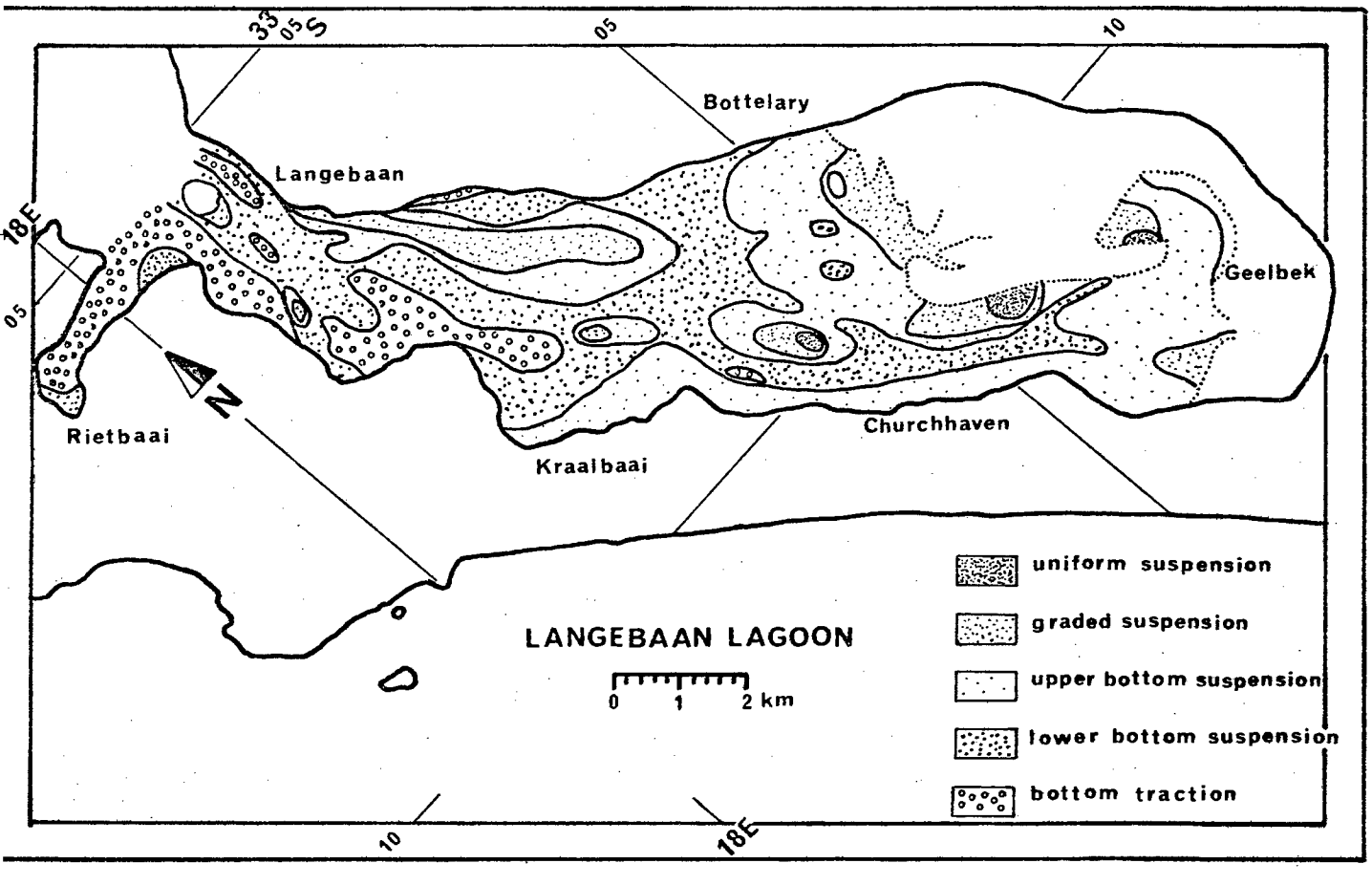

Fig. 188-B. The areal pattern of sediment transport and deposition in Langebaan Lagoon.

bottom traction and graded suspension both claim 14% and uniform suspension was recorded in 2% of all cases. The areal distribution of these modes is illustrated in Fig. 188-B. The overall pattern forms a coherent and meaningful picture that is related to a complex combination of different size parameters and it can be assumed that each zone reflects the stability conditions for sediments of specific size characteristics. In each case, the predominant mode by which the sediment was transported into the depositional environment appears to be recorded. Since this is a function of the velocity gradient in the transporting medium, hydraulically coarser sediment will normally not transgress over hydraulically finer sediment, as long as the hydrodynamic conditions remain unaltered. An exception to this rule can be observed in a number of depositional zones in which no individual size class predominates. In these areas, e.g. the fine - medium sand corridor on the eastern tidal flats, the velocity gradient fluctuates strongly enough in the course of a tidal cycle to allow influx of sediment of different hydraulic stability. It would appear that, once this sediment is deposited, it is mixed by burrowing organisms, thereby effectively preventing its subsequent remobilization and removal.

Upward-fining cycles of the type observed in Langebaan Lagoon may form under stable, hydrodynamic conditions with a continual supply of new sediment. However, substantial influx of new sediment is almost negligible and the depositional pattern is interpreted as being related to a general redistribution of sediments after the closing of the Kraalbaai channel, some 2000 years B.P. When this channel was still active, sedimentation in the lagoon appears to have been minimal, being confined to fine and very fine sand accumulation in the southeastern section of the system. Low sedimentation rates were the vital precondition for the survival of the oyster reefs.

After the emergence of the Kraalbaai channel, flow readjustment to the modern outflow channels resulted in a rapid change of relative energy levels from place to place in the lagoon. Sediment that had increasingly become trapped in the system, during the late phase of intermittent flow through the former channel, was now redistributed. Since the oyster reefs formed zones of relatively low energy, sediment began to stabilize on these elevated levels, thereby defining the position of the modern intertidal flats. In the course of this readjustment, very fine sand was almost entirely eliminated from the system. Even fine sand was initially

unstable; substantial quantities were removed and deposited in the tidal delta region at the mouth of Langebaan Lagoon. However, a new equilibrium was achieved before all of the fine sand could leave the system. This is indicated by the relatively high proportion of fine sand in most parts of the lagoon, especially in channel bank sediments of the northern lagoon.

The whole process appears to have been completed within 200 years after the Kraalbaai channel had fallen dry. This is documented by the age of fossil oysters recovered from the top of a barely exposed oyster reef. The date of 1780 ± 60 years B.P. records the time of final burial of the last remaining oyster reefs. Sedimentation within the lagoon since that event does not appear to have been significant. This is concluded from the fact that the modern sediment distribution still reflets the relict pattern established in the readjustment phase. Another important indicator for low sedimentation rates since that time is provided by Kraalbaai itself, which today is situated in a position where, under normal circumstances, an intertidal flat area would be expected. However, 2000 years of sedimentation have not been able to fill Kraalbaai.

Each physiographic unit within Langebaan Lagoon shows a characteristic association of depositional modes, whereby a clear trend from higher levels of transport to lower levels of transport is defined from intertidal flats to tidal channels (Fig. 189). The intertidal flat sediments produce a point scatter in which eastern, western and southern tidal flats are easily distinguished (Fig. 189-A). Western and southern tidal flat sediments are very uniform, with a coarsest percentile of about 1 phi and mean diameters between 1.5 and 2.0 phi in the former case and 1.8 to 2.3 phi in the latter case. Eastern tidal flat sediments, on the other hand, demonstrate their stronger degree of mixing by a progressive gradation from fine percentiles and very fine mean diameters, to coarse percentiles and fine to medium mean diameters. By far the most important mode of transport is upper bottom suspension (65% of all samples), followed by graded suspension, with 20% of all samples.

Subtidal flat sediments (Fig. 189-B) range from graded suspension (16%), through upper bottom suspension (29%), lower bottom suspension (34%), to traction transport (16%). The Rietbaai samples are not included in these figures. They are considerably coarser, being transported exclusively

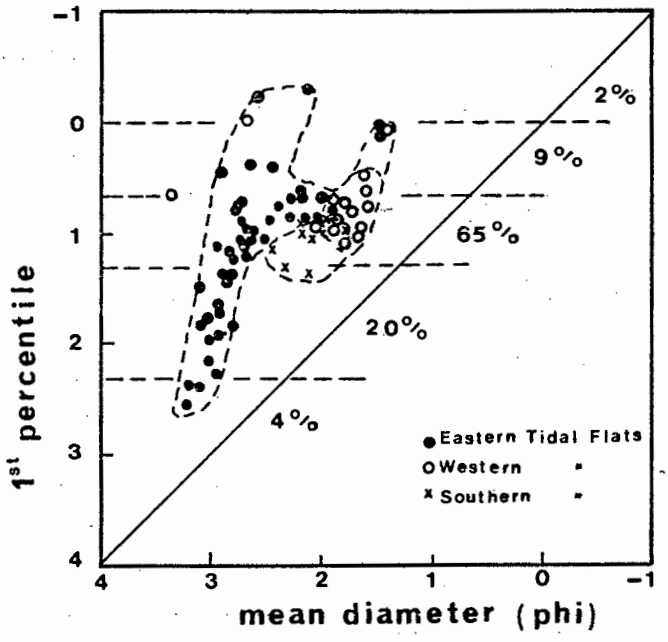

Fig. 189-A.

Modes of sediment transport on intertidal flats

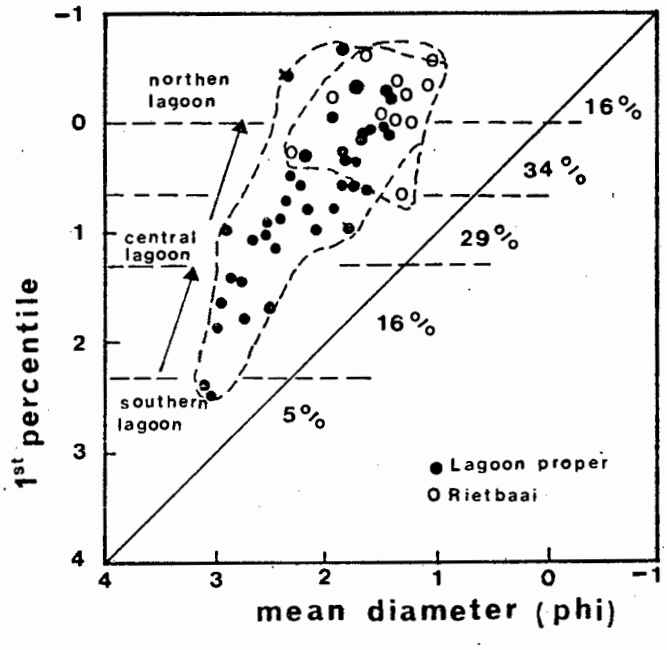

Fig. 189-B.

Modes of sediment transport on subtidal flats

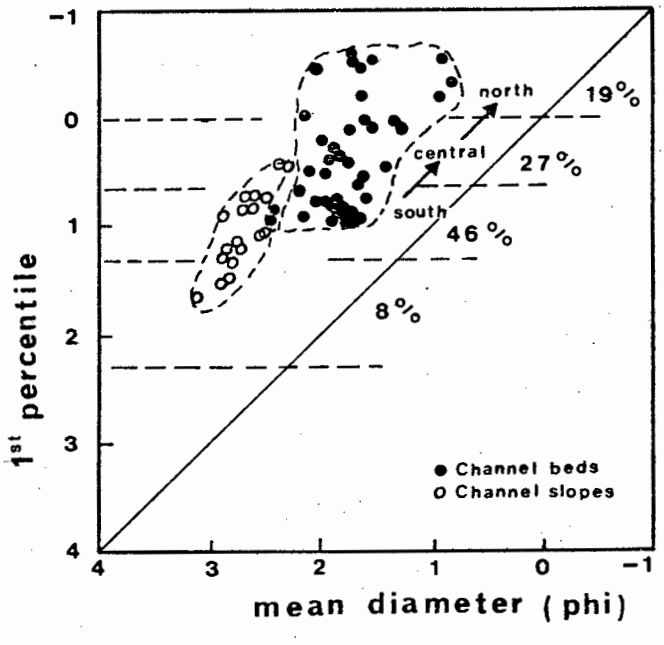

Fig. 189-C.

Modes of sediment transport in tidal channels

in traction carpets and lower bottom suspension.

The different hydraulic control of channel beds and channel slopes is well illustrated in Fig. 189-C. Channel bed sediments are deposited from upper bottom suspension in the southern lagoon, lower bottom suspension in the central sections and from traction transport in the northern lagoon. Channel slope sediments, on the other hand, have finer mean diameters and are predominantly transported in graded suspension and upper bottom suspension.

Each physiographic unit can, therefore, be characterized by very specific successions of different transport modes, in the course of which the various sediment types were deposited. When superimposed, the various patterns show considerable overlap, thus indicating the continuous nature of sedimentary processes in Langebaan Lagoon.

5.6. EFFECTS OF PARTICLE SHAPE ON SETTLING VELOCITY, SEDIMENT TEXTURE, AND DEPOSITIONAL PROCESSES

5.6.1. Introduction

The physical properties of sediments such as mean size, sorting, density and particle shape are, together with the dynamic forces of the fluid, the most important factors controlling depositional processes (viz. Blatt et al., 1972; Pettijohn et al., 1972). A number of studies have paid particular attention to such properties in depositional structures produced in the course of hydraulic transport. It was found that, in particular, the settling rates of particles contributed to the sorting characteristics of sediments (e.g. Brush, 1965; Jopling, 1965; Simons et al, 1965). It is a well known phenomenon that particle shape affects settling velocities (viz. Graf and Acaroglu, 1966) and thus, it can be concluded that particle shape must also affect sorting. Since natural sediments are often composed of multishaped particles, this feature requires special attention if depositional processes are to be fully understood. In Langebaan Lagoon this is particularly important, as local sediments consist of a mixture of siliciclastic and bioclastic particles.

In previous sections of this study, it was frequently observed that

the bioclastic component appeared to respond rather independently of the terrigenous component to the mechanisms controlling transport and deposition. As a result, the differential response of individual components will have to be considered when discussing the overall size distribution characteristics of the total sediment. The strongest indication of such effects is observed in the selective concentration of bioclastic material in the northern lagoon. Shape is the only obvious physical property in which the two components appear to differ substantially. Density differences were shown to be negligible, as indicated by the similarity of the various mean diameter maps. The terrigenous component consists of subrounded to well rounded quartz particles, whereas the bioclastic component is composed of platy to irregularly shaped skeletal carbonate particles.

By comparing the two shape groups it will be demonstrated that there appears to exist a functional relationship between particle shape, sediment texture and depositional processes.

5.6.2. Effect of Shape on Settling Velocity

The effect of shape on settling velocities of sedimentary particles have been a topic of interest for some time. Hydraulic engineers especially, have, for practical purposes, pursued a better understanding of the effects of particle shape in connection with sediment transport problems. Some studies concentrate mainly on the settling behaviour of well defined geometric objects such as spheres, cubes, rods, octahedrons, tetrahedrons, prisms and plates of various dimensions (viz. Schiller, 1932; Wadell, 1934; McNown and Malaika, 1950; McNown et al., 1951; Marchillon et al., 1964; Janke, 1966). Other studies have made use of natural grains or artificially produced particles with irregular shapes (e.g. Richards et al., 1907; Rubey, 1933; Krumbein, 1942; Pettyjohn and Christiansen, 1948; Albertson, 1953; Schultz et al., 1954; Berthois, 1962; Moreland, 1963; Graf and Acaroglu, 1966; Folk and Robles, 1964; Maiklem, 1968; Stringham et al., 1969; Braithwaite, 1973). A number of relevant features concerning particle shape and settling velocities in the context of this study were previously discussed in Section 3.4.

The definition of shape and the derivation of a classification in terms of shape factors has remained a difficult problem. Until the

introduction of the boundary-layer concept by Prandtl (Prandtl and Tietjens, 1934), the phenomenon of shape-induced drag lacked a sound physical basis. Prandtl (1956) demonstrated that the whole particle is involved in the drag phenomenon, i.e. both inertia and viscous forces act on the particle and experimental work has shown the existence of a functional relationship between these two forces. For convenience this relationship has been expressed in a non-dimensional form, as the ratio between inertia and viscous forces (Reynolds Numbers). From this it can be concluded that the drag effect on any particle must change with a change in the Reynolds Number (Re). Experiments have confirmed this deduction, which is illustrated in Fig. 190-A in which drag coefficients are plotted against Reynolds Numbers. The drag coefficient forms part of the general drag formula and is a factor of proportionality which is independent of the size and the settling velocity of a particle.

Thus, the drag force, i.e. the resistance to motion, of any object can easily be determined once its drag coefficient has been determined (viz. Graf, 1971). In accordance with Prandtl's boundary layer theory, shape is expressed as the ratio between the surface area of a sphere having the same volume as the particle and the actual surface area of the particle (Wadell, 1934; Pettyjohn and Christiansen, 1948). In the above definition of shape, a perfect sphere would have a shape factor of unity, whereas any deviations from a spherical shape will be expressed as fractions of one. This was experimentally tested for a number of well defined geometrical objects, the results of which are presented in Fig. 190-A.

Clearly, in practice it is impossible to measure the surface areas of irregularly shaped particles and, in order to overcome this problem, some researchers prefer the use of a more practical definition of shape, in which the shape factor is determined by the ratio between the smallest diameter of the particle and the square root of the product of the largest diameter and the intermediate diameter (Corey Shape Factors). For more details, the reader is referred to McNown and Malaika (1950), Albertson (1953) and Graf (1971). Although equivalent shape factors of both methods do not produce identical results, the general trend and magnitude of order are very similar in both cases. Drag coefficients in relationship to Reynolds Numbers for various shape factors determined by the latter method have been superimposed on those of the former approach in order to illustrate the difference (Fig. 190-B).

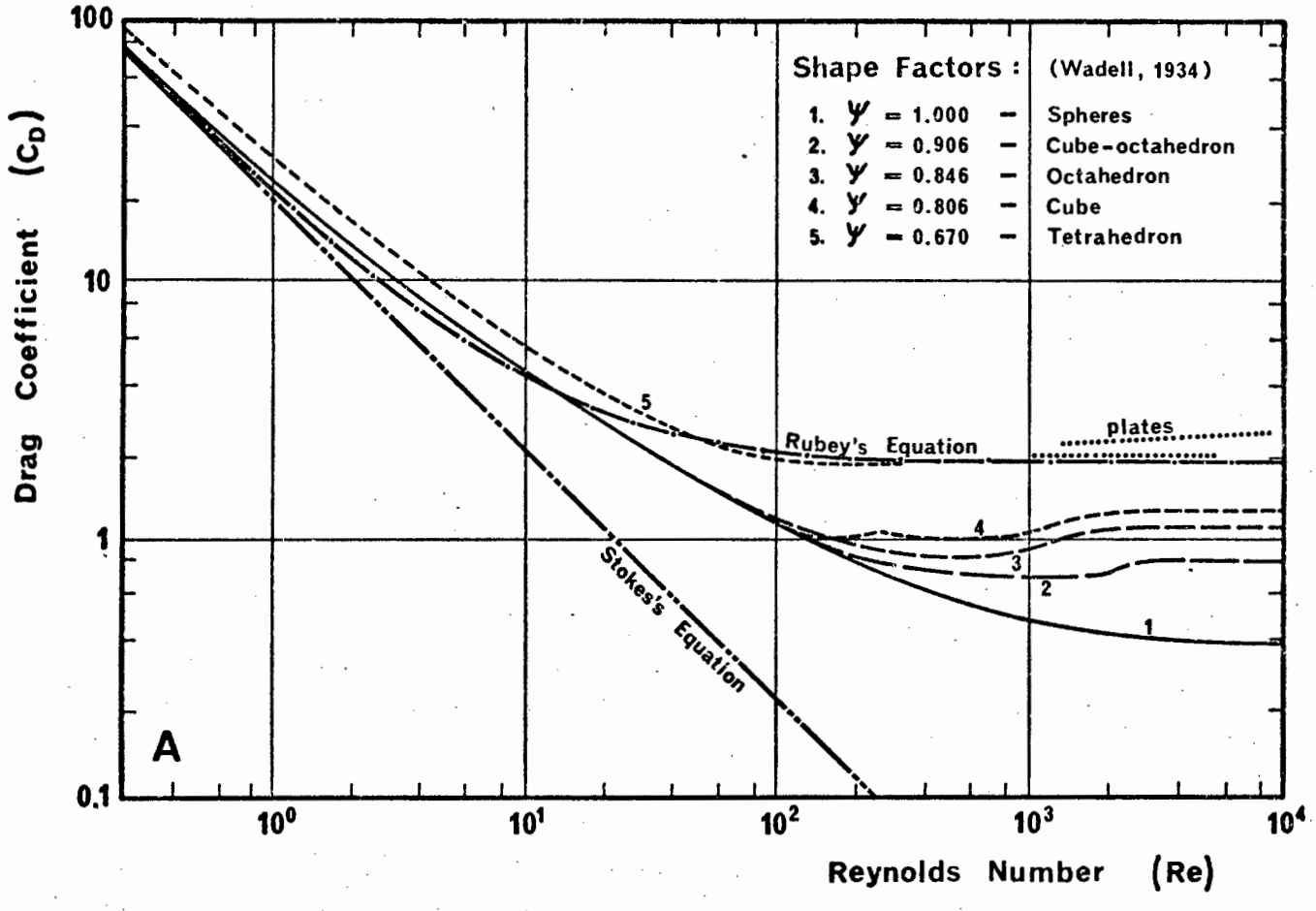

Fig. 190-A. Drag coefficients (Cd) as a function of Reynolds Numbers (Re) and particle shape (ψ).

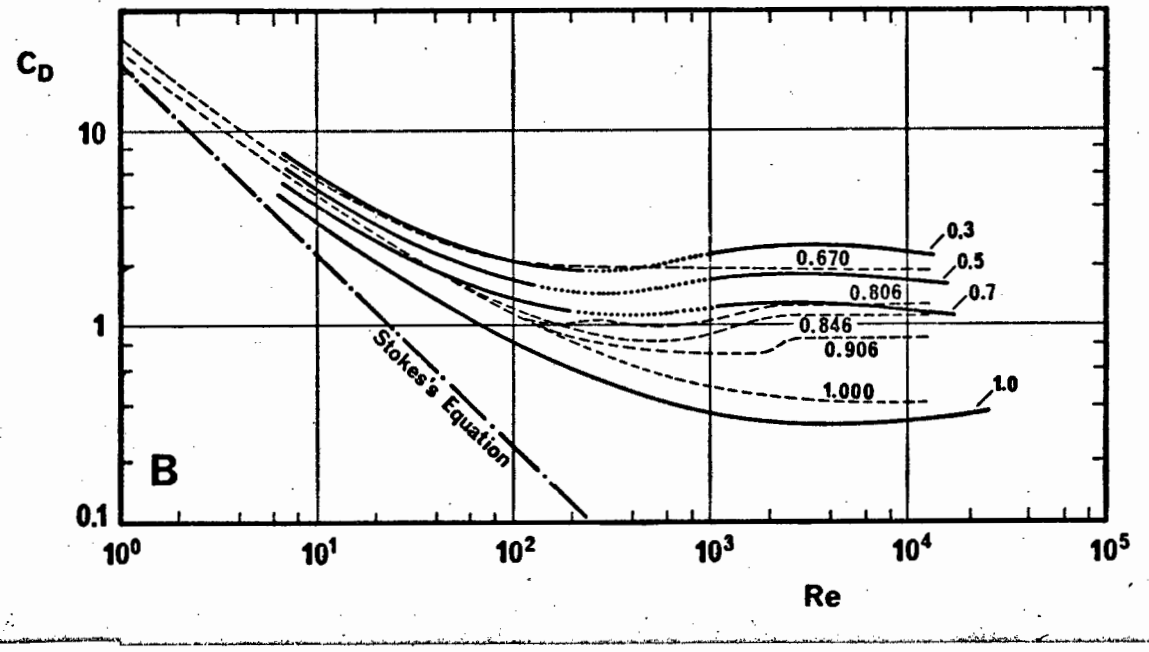

Fig. 190-B. Corey shape factors superimposed on hydraulic shape factors.

Maiklem (1968) and Braithwaite (1973) have demonstrated that, in addition to the drag phenomenon as such, particles belonging to defineable shape groups are characterized by specific fall modes; the major fall modes that were distinguished being: 1) straight fall, 2) spinning, 3) spiralling, and 4) erratic tumbling. Thus, the settling behaviour of sedimentary particles is a complex function of density, shape, drag force and settling mode. From Fig. 190-A it can be seen that at low Reynolds Numbers (Re - 1) the drag coefficient/Reynolds Number relationship follows Stokes's law of settling, irrespective of the shape of a particle. This region applies to particles moving in very viscous fluids such as heavy oil, mud flows, or certain magmas, or to particles smaller than about 0.1 mm moving in fluids of relatively low viscosities such as water. In both cases, the viscous forces dominate over the inertial forces, resulting in relatively large drag effects and hence low settling velocities. At Re - 1 the trend departs from that defined by Stokes's equation, whereby the rate of drag-decline progressively reduces with increasing Reynolds Numbers until, at about Re = 2000, the drag coefficient becomes almost constant for individual shape factors. A similar effect can be observed in the size-velocity diagram presented in Fig. 191.

It should be pointed out here that it has been extremely difficult to define the full drag curves in terms of a single empirical equation - even for spheres (viz. Graf and Acaroglu, 1966). For the full range, and especially at high Reynolds Numbers, the experimentally determined relationships defined in Fig. 190-A appear to provide the only reliable means of determining the drag coefficients at various Reynolds Numbers.

The sediments investigated in this study were recovered from depositional environments formed under tranquil-turbulent flow conditions, i.e. at Reynolds Numbers in excess of 2000 (viz. Allen, 1965). At this level, as was shown earlier, drag coefficients remain almost constant for individual shape factors. In effect this means that, although particles of different shapes may have identical settling velocities, their respective drag coefficients can differ considerably. It will be demonstrated later in this section that this feature seems to have a significant influence on depositional processes.

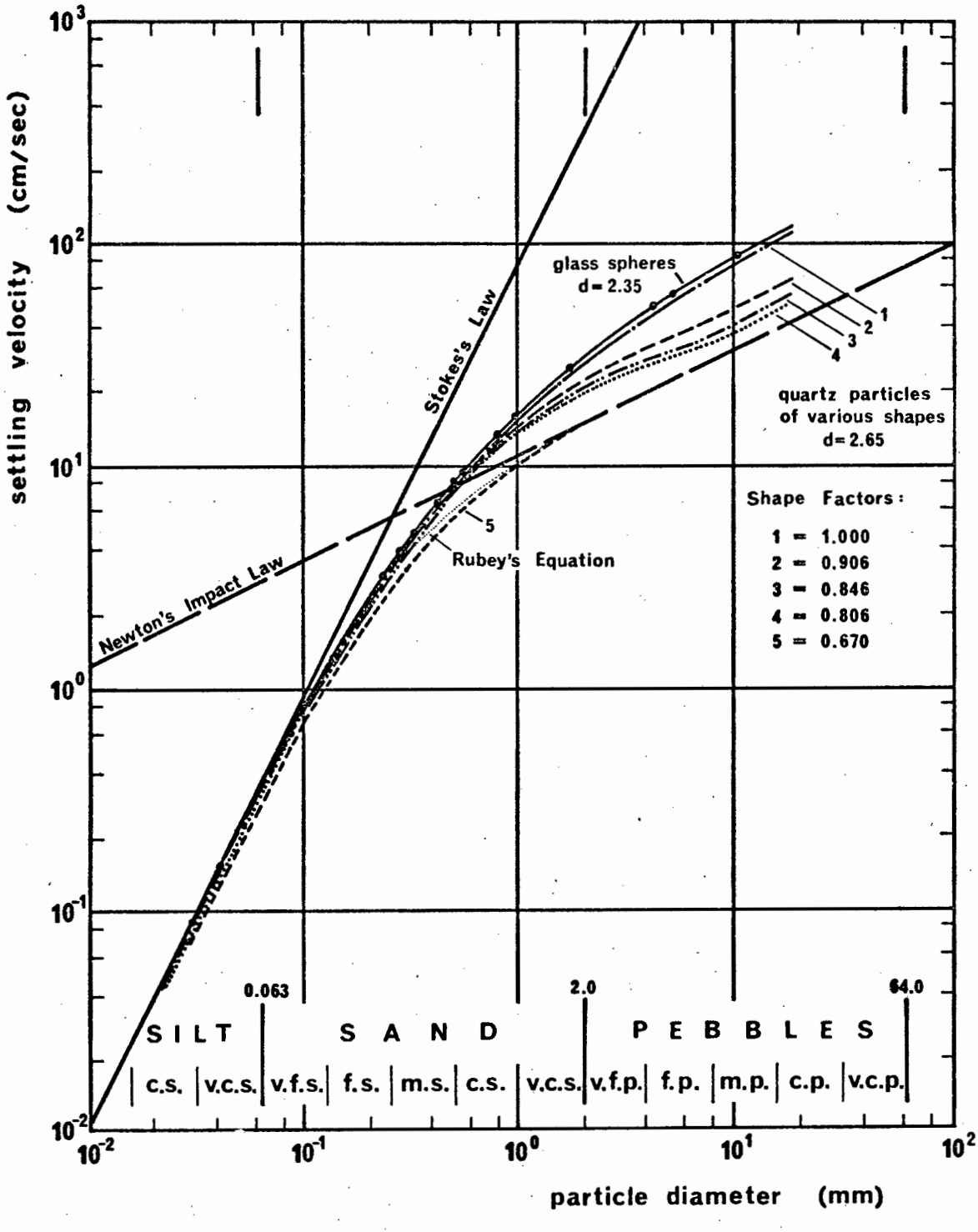

Fig. 191. The effect of shape on settling velocity.

5.6.3. Effect of Particle Shape on Sediment Texture

The effects of particle shape on textural parameters have received little attention in the literature, especially for settling tube data. This is largely due to the fact that it is difficult to study and compare individual shape grounds of a sediment, as there is no practical way of separating these in sufficient quantity to allow separate sieving. The settling method, on the other hand, does, under certain conditions, facilitate this approach.

The procedure adopted in this study is discussed at length in Section 3.2. Although a certain error must be anticipated in the calculation process of the bioclastic size parameters, the consistency of the results speak in their favour. Any trends observed in the comparison of the various size parameters of each group were constantly cross-checked against possible effects of relative concentration levels, in order to be sure that the observed trends were in fact a shape-inherent feature.

5.6.3.1. The Effect of Shape on Mean Diameter

In Fig. 192-A the mean settling diameter of the terrigenous and the bioclastic components are compared. The close grouping of values indicates that both components have very similar mean diameters, i.e. with few exceptions, the terrigenous and the bioclastic particle groups are close to hydraulic equilibrium. About 73% of all samples fall into a half-phi scatter range and 95% into a full phi scatter range, whereby almost 70% of all samples have a slightly coarser carbonate component.

An interesting feature is the apparent, systematic relationship between the two components at various grain size levels. The whole cluster follows a well defined, size-dependent trend which is revealed when averaging mean diameters over small size intervals (Fig. 192-B). In order to verify this trend, the mean diameters of both components were plotted individually against the mean diameters of the total sediment (Fig. 193). The general trends are confirmed. At an average mean diameter of about 1.7 phi (0.310 mm) both components have practically identical mean diameters. For coarser sediments the bioclastic component is on average finer, whereas for finer sediments it is on average coarser. Fig. 194 demonstrates that this trend is consistent at any concentration level. The observed feature is thus a

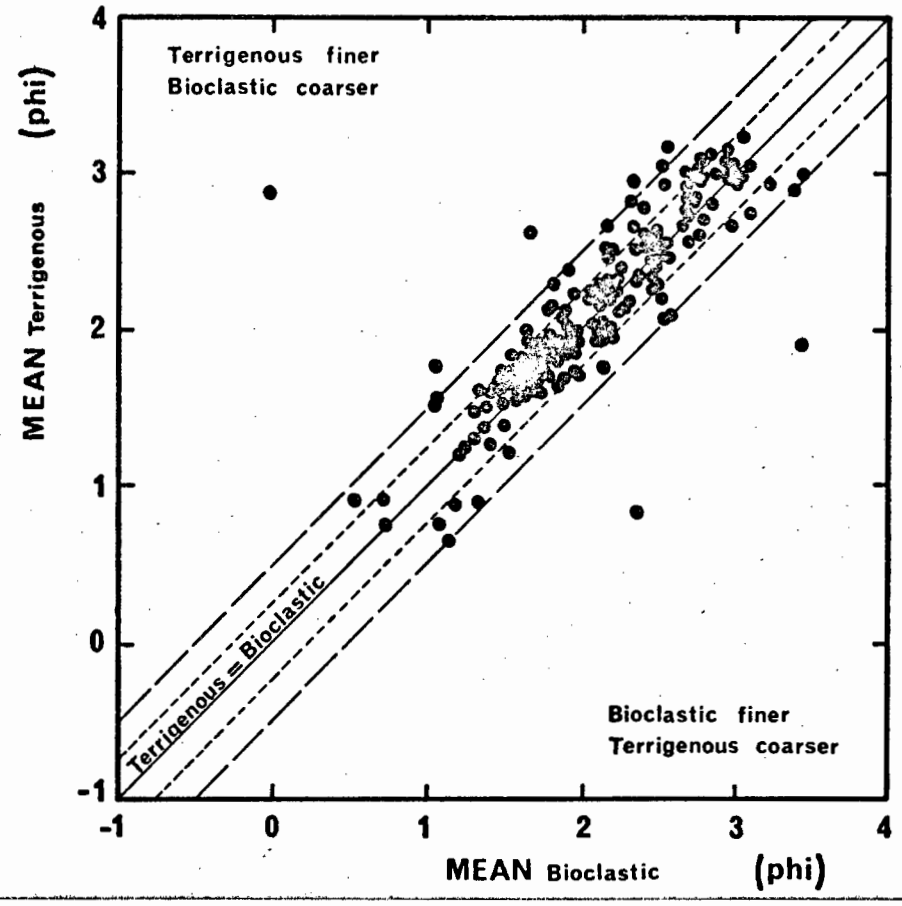

Fig. 192-A. A comparison of the mean diameters of the two shape groups. Both components approach hydraulic equilibrium.

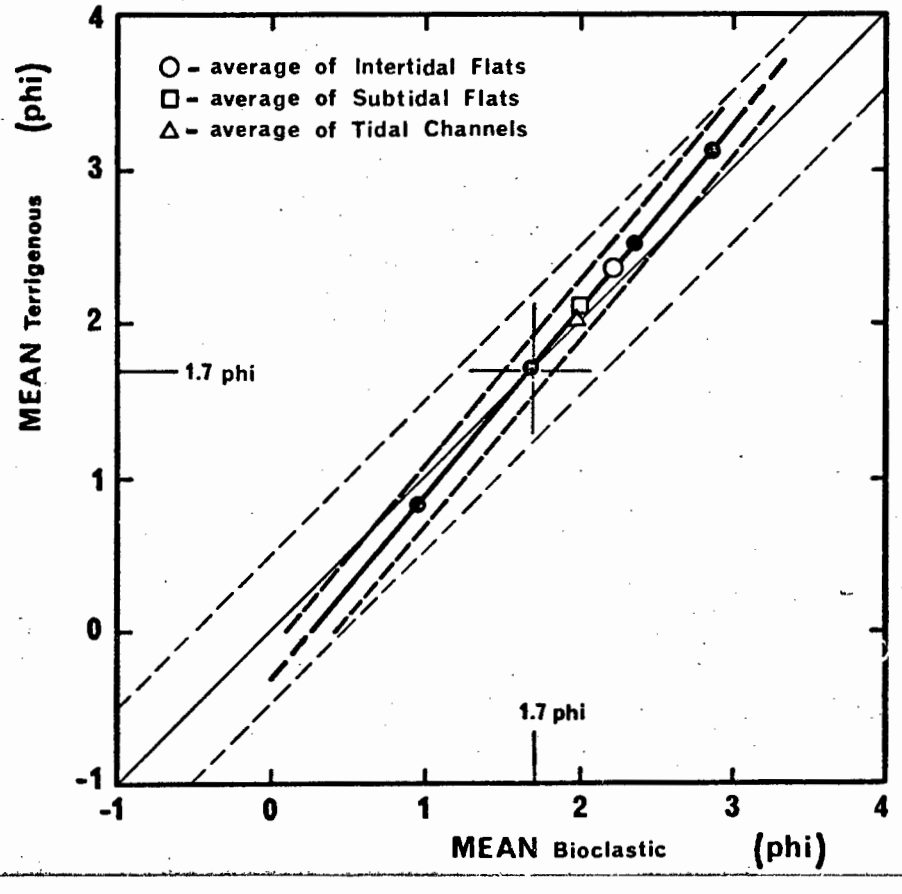

Fig. 192-B. Sediments coarser than 1.7 phi have on average a slightly coarser bioclastic component whereas sediments finer than 1.7 phi have on average a slightly finer bioclastic component.

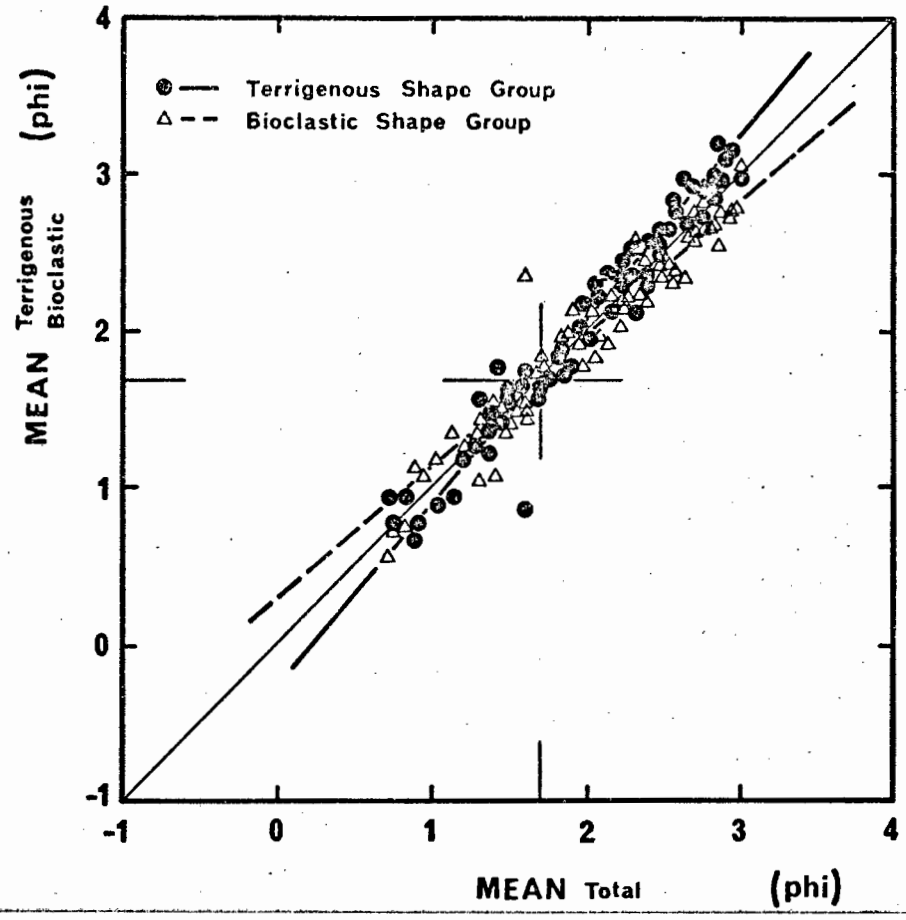

Fig. 193. Both shape components demonstrate their individual trends in relationship to the total sample.

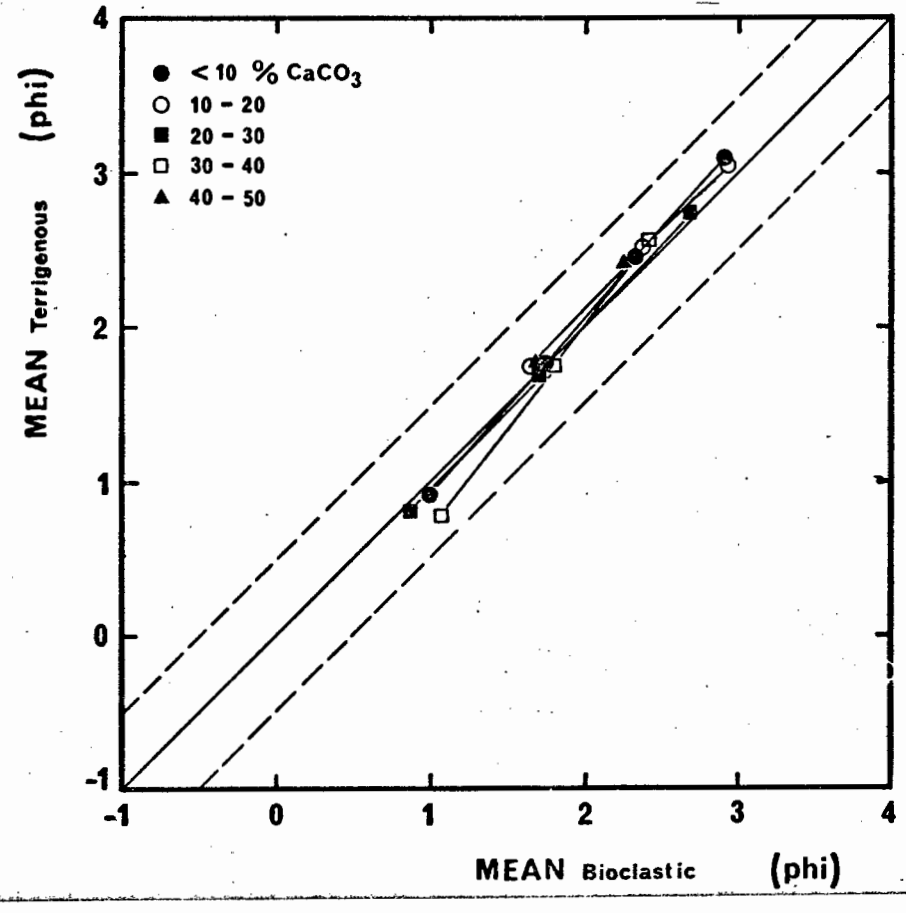

Fig. 194. Relative concentration levels of one component do not affect the observed mean diameter trend.

shape controlled phenomenon.

Due to the lack of comparative data in the literature, it is difficult to decide whether the observed relationship is a fundamental property of mixed sediments, or whether it is merely a feature reflecting the dynamic conditions under which the sediment was deposited in the study area. Furthermore, it cannot be excluded that the observed trend is, to some degree, an inhereted feature of the individual size distributions of each shape group. However, both components have been subjected to the same hydraulic size-sorting processes; it is, therefore, very likely that the relationship is a shape controlled feature.

5.6.3.2. Effect of Shape on Relative Sorting

The preference of relative sorting to standard sorting coefficients has been discussed in detail in a previous section of this study (Section 3.5.) It was demonstrated that relative sorting is a more useful parameter for the interpretation of depositional processes. At the same time, a new classification of relative sorting categories was proposed.

The sorting relationship between the two shape groups is very interesting. From Fig. 195 it can be seen that for 84% of all cases the terrigenous particle group is better sorted. When averaging values over small sorting intervals a linear relationship appears to emerge (Fig. 196). In less well sorted sediments (QH = 5), the difference seems insignificant. However, with improving sorting there is a progressively increasing lag in the sorting of the irregularly shaped particle group. Equivalent levels of average sorting for both particle groups are listed in Table 8.

The trend is independent of the relative concentration levels of each group, as indicated in Fig. 197 and again it is concluded that the feature is essentially a function of particle shape. It would thus appear that sediments with low bulk shape factors will not achieve the same level of relative sorting as sediments with high bulk shape factors, when exposed to the same hydrodynamic conditions. Sorting is, therefore, not only a function of particle size, but also of particle shape, whereby relative sorting patterns of differently shaped particle groups will be out of phase with each other, according to the general trend outlined in Fig. 196 and

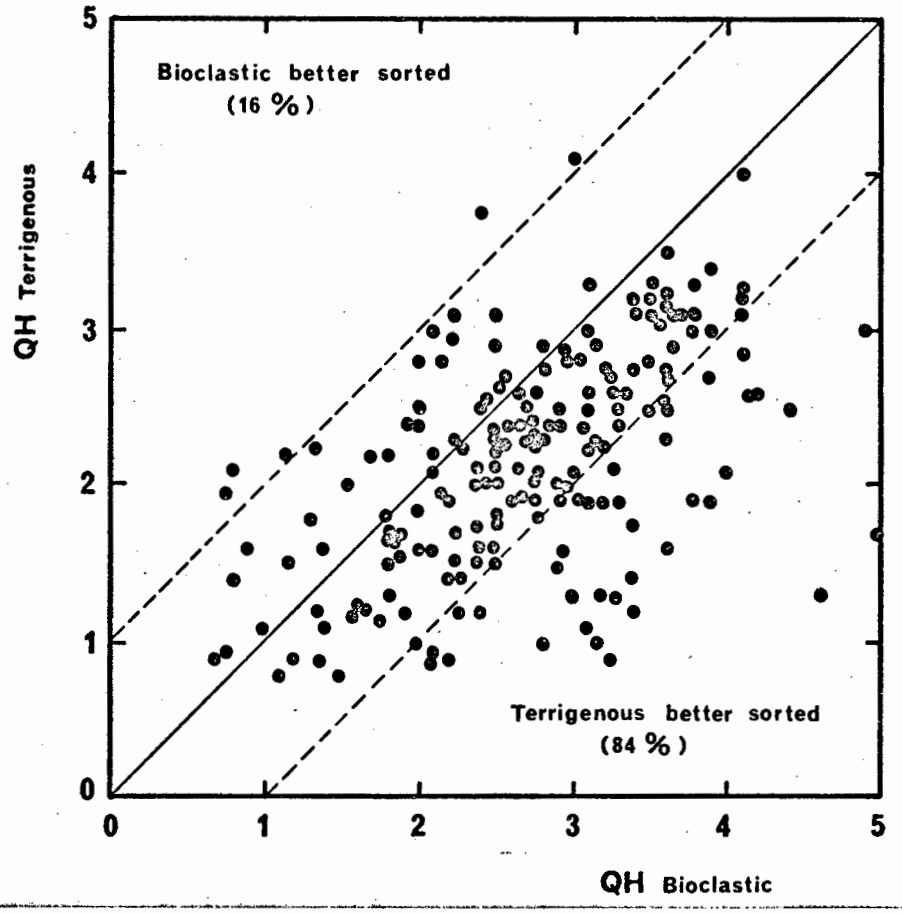

Fig. 195. The sorting relationships between the two shape groups.

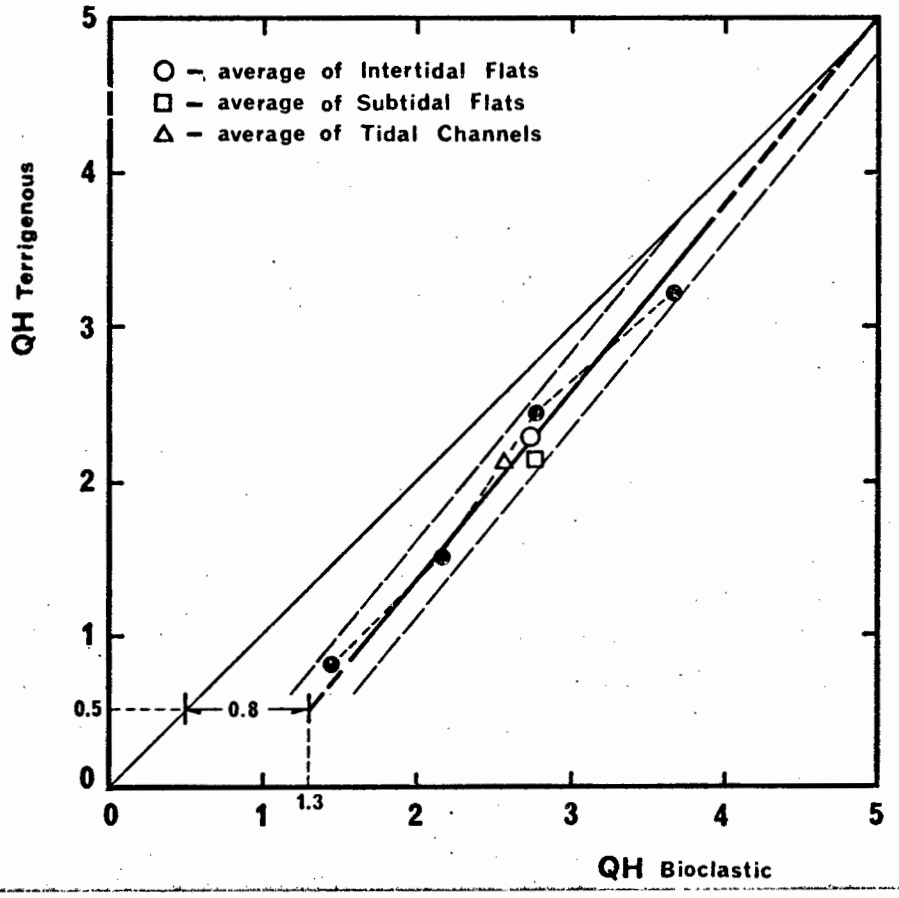

Fig. 196. On average the terrigenous component is better sorted than the bioclastic one. The difference increases systematically towards the elementary sorting level of QH = 0.5.

summarized in Table 8.

It is interesting to observe that differently shaped particle groups of the same sediment appear to retain their individual sorting characteristics, irrespective of the size-sorting process.

TABLE 8

Equivalent levels of average relative sorting (QH) for two differently shaped particle groups of the the same sediment.

QH subrounded to wellrounded quartz	QH irregularly shaped skeletal carbonates
0.5	1.3
1.0	1.7
1.5	2.1
2.0	2.5
2.5	2.9
3.0	3.3
3.5	3.75
4.0	4.15
4.5	4.55
5.0	5.0

5.6.3.3. Effect of Particle Shape on Skewness and Kurtosis

Skewness is a function of the third and second moments of a size frequency distribution, whereas kurtosis is a function of the fourth and second moment (viz. Blatt et al., 1972). Since sorting is the square root of the second moment, it will be clear that sorting must, to some degree, control the skewness and the kurtosis of sediment size distributions.

In Fig. 198 skewness values of the terrigenous particle group are plotted against those of the bioclastic one. By averaging values over small intervals an overall trend is once again observed (Fig. 199). The trend remains defined, although with somewhat lesser slope, if some of the

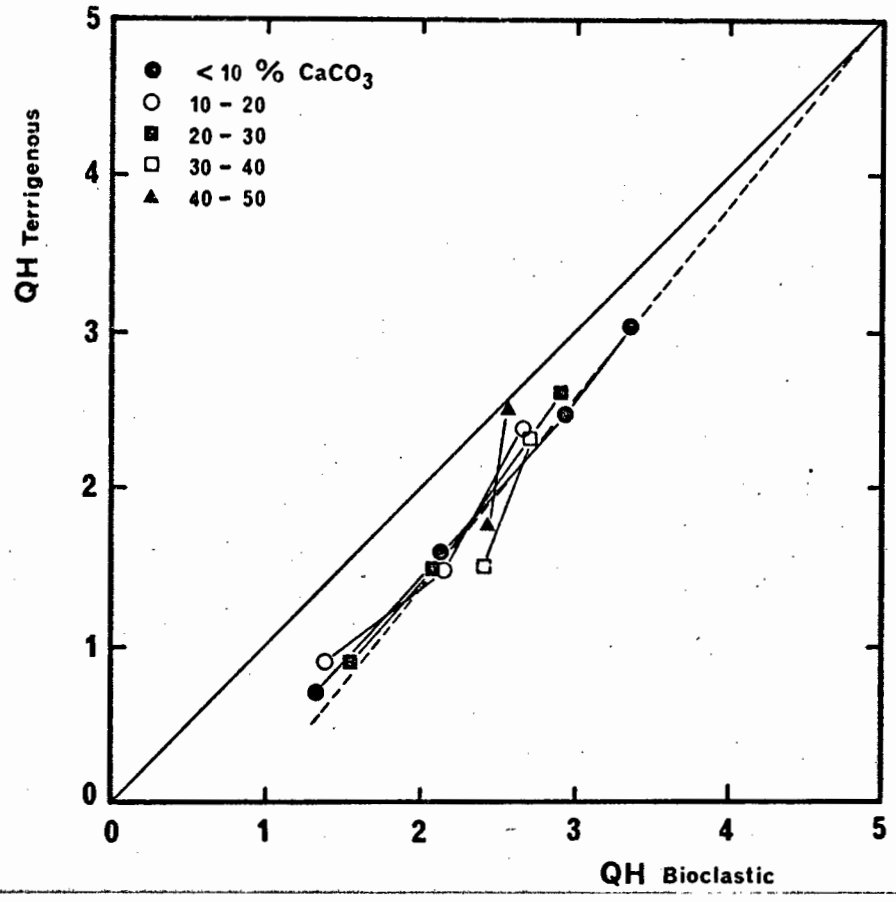

Fig. 197. Relative concentration levels of one component do not affect the observed sorting trend.

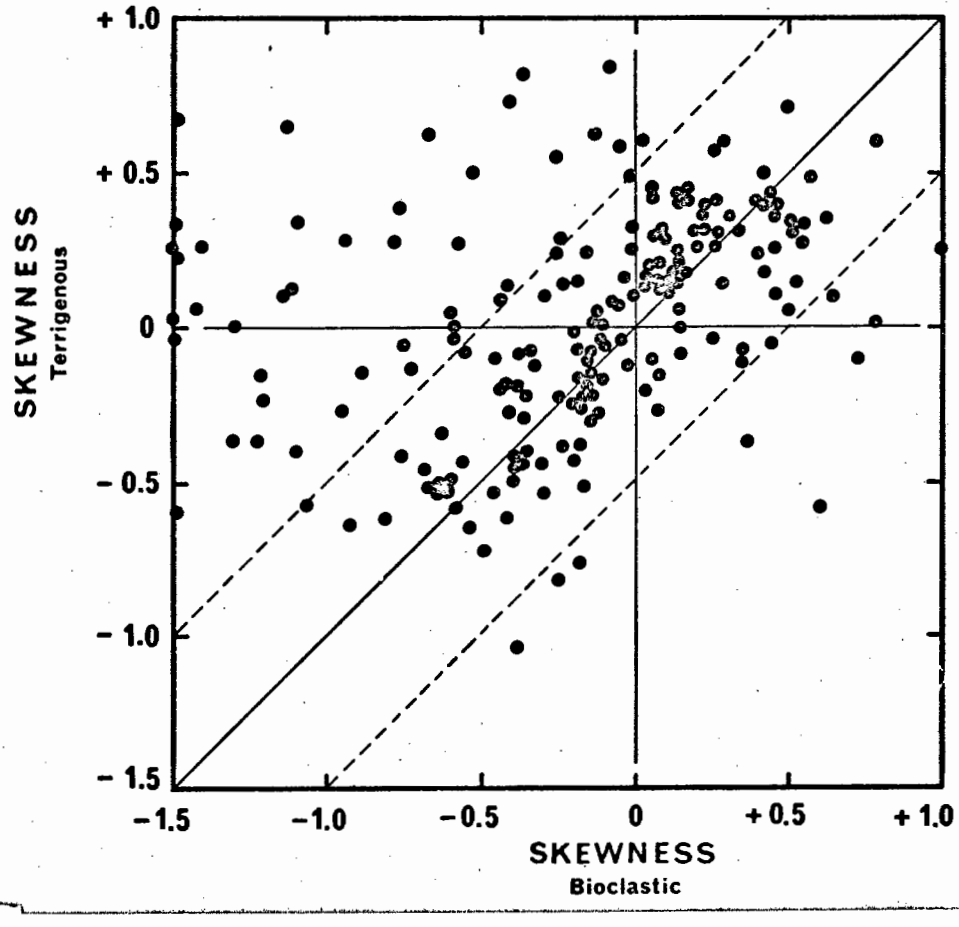

Fig. 198. The skewness relationships between the two shape groups.

more widely scattering values are eliminated. Fig. 200 demonstrates that here too the relative concentration of one shape group relative to the other does not affect the overall trend. Some of the more widely scattering trends are probably due to the small number of values available for averaging (see brackets).

In Fig. 199 four areas can be distinguished in which specific relationships between the two shape groups exist. In area A, the terrigenous component is positively skewed while the bioclastic one is negatively skewed (24% of all cases). In area B, both components are negatively skewed (38% of all cases), whereby in subarea B_1 the bioclastic component is stronger negatively skewed (22% of all cases) and in subarea B_2 the terrigenous group is more negatively skewed (16% of all cases). In area C, the terrigenous group is negatively skewed (6% of all cases). In area D, both groups are positively skewed (32% of all cases), whereby in subarea D_1 the terrigenous group is stronger positively skewed (20% of all cases) and in subarea D_2 the bioclastic group is stronger positively skewed (12% of all cases).

Thus, the bioclastic particle group is, in 64% of all cases, either more strongly negatively skewed or less positively skewed than the terrigenous group. On average the terrigenous group is near symmetrical whereas the bioclastic group is clearly negatively skewed (Fig. 199). It will be recalled that in addition the bioclastic group is on average slightly coarser and less well sorted than the terrigenous one.

Kurtosis has not been specifically investigated in this study but, as can also be inferred from their sorting relationships, it was observed that the irregularly shaped bioclastic particle group tended to be less peaked, i.e. more platykurtic, than the better rounded terrigenous one.

Summarizing the textural characteristics of individual particle shape groups within the same sediment, it is concluded that distinctly different shape groups respond independently of each other to the process of hydraulic transport. In each case they retain the textural characteristics inherent in their respective shape group. The total sediment, therefore, simply reflects the sum average of the textural characteristics contributed by its individual shape components.

At this stage it might be useful to recall the scatter of data points

PLATE 10.

A. The fragile tubes of *Euclymene* exposed by gentle wave action.

B. Faecal pellets of *Callianassa* filling ripple trough.

C. Crawling trace of *Diogenes*.

D. Bird tracks on intertidal sand bar.

E. Drag marks and burial pattern of marine algae.

F. The characteristic track of *Bullia*.

Plate 10

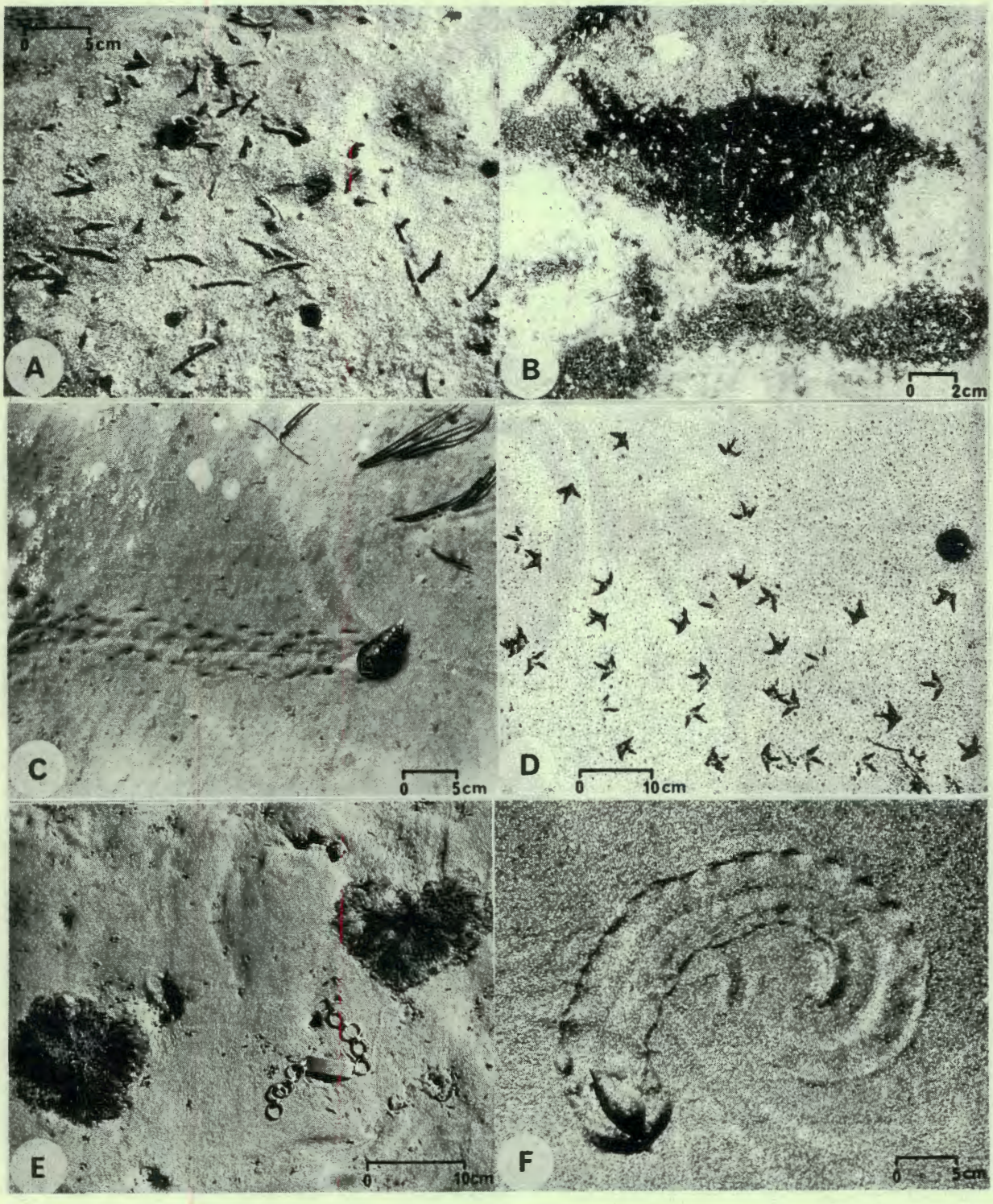

PLATE 11.

A. Well preserved lamination in the upper 5 cm of the sediment and complete bioturbation of the lower portion are characteristic of eastern tidal flat sediments.

B. Smallcup-and-fill structures and faintly preserved lamination in western tidal flat sediment.

C. Complete bioturbation of slightly muddy tidal flat sediments in the southern lagoon.
Note Callianassa burrows.

D. Cross-section through Spartina marsh.

E. Cross-section through Salicornia marsh.

F. Laminated sand of lagoonal beach ridge.
Note intercalated mud lenses.

The transition from upper intertidal flats into salt marshes is characterized by the same sequence of halophytes observed in most parts of the world. A fringing belt of Zostera is followed at mid-tide level by Spartina which in turn is progressively replaced towards the high-water line by Arthrocnemum and Salicornia. The latter extends well into the supratidal zone. The whole sequence, however, is not always represented. Thin algal mats are common in tidal pools of the salt marshes, but they are not very well developed and thus are not a characteristic feature in the lagoon.

Most tidal pools are poorly populated by marine organisms and biological surface structures rare. This is due mainly to the large seasonal variations in salinities, which fluctuate by up to 40 parts per thousand and thus lie well beyond the tolerance level of most marine organisms.

5.7.2.3. Internal Sedimentary Structures

In general, the entire intertidal flat subenvironment is strongly bioturbated. However, the degree of bioturbation decreases towards the spring high tide level and the lagoonal beaches. The eastern tidal flats often show well preserved lamination in the upper 5 cm of the sediment, whereas the lower portion is completely bioturbated (Plate 11-A). In areas where very fine sand predominates lamination is not always recognized macroscopically.

In the west, the lower tidal flats are strongly bioturbated throughout but the upper flats frequently show some lamination similar to the eastern flats. Small cut and fill structures resulting from runnel flow are common (Plate 11-B). In both units the mud content is low. Burrowing in the western flats is predominantly performed by Callianassa and a wide variety of polychaetes, whereas the finer sediments of the eastern flats locally provide favourable conditions for Upogebia and Assiminea. Both species are rare on the western tidal flats where medium sands predominate.

The sediments of the southern tidal flats are completely bioturbated, especially in area where mud contents are high (Plate 11-C). Here Upogebia is the most abundant burrowing crab. However, population densities decrease with the onset of marsh halophytes. Animal burrows are increasingly replaced by root casts whereby the root structures of the various marsh plants are easily distinguished (Plate 11-D and 11-E). The beach ridges which normally separate the intertidal flats from the marshlands are weakly bioturbated.

They consist of well sorted quartz sands interbedded with occasional mud lenses that increase in frequency towards the bottom where they merge with the underlying marsh muds (Plate 11-F).

The internal sedimentary structures of the salt marshes are very variable but in general follow the facies model discussed by Bouma (1963). An important feature of the local salt marshes is the sequence of recurring beach ridges which show the growth pattern of the salt marshes in the course of their Holocene development.

5.7.3. Subtidal Flats

5.7.3.1. Physical Surface Structures

Sedimentary bedforms are rare on the subtidal flats and channel bars. Biological processes dominate in sheltered areas whereas channel bars often have smooth surfaces. Wave-generated ripple marks are occasionally observed in the very shallow areas, but these have a low preservation potential. Larger current-generated bedforms are sometimes observed along the lower slopes of channel bars, but it is usually difficult to draw a sharp line between the channel beds and the lower extensions of submerged bars and sandbanks.

5.7.3.2. Biological Surface Structures

The subtidal flats comprise a current-sheltered unit and a more exposed channel-bar unit. The degree of surface bioturbation reflects the general energy conditions discussed in the physical section above. The current-sheltered unit is strongly modified by surface bioturbation, forming an uneven surface of scattered mounds and hollows produced by the combined effect of burrowing organisms and feeding habits of certain fish. In areas of fine sediment marine algae, notably Gracilaria, are abundant. The bivalve Mactra and the polychaete Pectinaria can be distinguished, respectively, by their siphon holes and chimney-like tubes protruding from the sediment. The burrowing activity of Pectinaria is well documented by Schäfer (1963). Callianassa holes are very frequently lined by a small sand brim - a feature that is not commonly observed on intertidal flats.

The coarser-grained surface of the granite outwash fans do not show many signs of bioturbations except for occasional Callianassa burrows. Usually they are densely covered with marine algae, notably Ulva and Gracilaria. The channel bar unit, on the other hand, consists generally of smooth sand surfaces without obvious traces of biological activity. In many places, however, channel bars are densely populated by Mactra. Their presence is rather concealed at the surface.

5.7.3.3. Internal Sedimentary Structures

The subtidal flats can be grouped into three distinct facies. One is formed by terminal fans that line the granite slopes of the northwestern shore. These consist of a poorly sorted granitic outwash into which some shell material has been mixed. The mud content is relatively high (> 5%) and although Callianassa burrows are quite frequent, these fan deposits are free of any physical structures (Plate 12-A).

Quite different in appearance are the sheltered subtidal flats which usually consist of fine sand. These are located in the northern part of the lagoon immediately south of the inlets in the shelter of Skaapeiland, along the highest parts of submerged sandbanks, and in Kraalbaai. The sediment is well sorted with a low mud content. This unit is completely bioturbated with no indications of inorganic structures (Plate 12-B). In some places the fronds of Gracilaria have been buried by burrowing organisms to form root-like structures in the sediment.

A third subtidal facies is defined by the more current-exposed channel bars which consist mainly of well sorted medium sands. The mud content is very low. Their exact boundaries are difficult to define because there is usually a gradual transition into either a true channel facies, or a more sheltered subtidal facies. Horizontal lamination and small-scale ripple cross-bedding can occur in the upper centimetres.

This unit is the preferred habitat of Mactra, several million individuals of which are estimated to populate the lagoon. In some cases several hundred individuals per square metre have been counted. Wherever population densities are high enough, physically controlled internal structures are effectively destroyed. An interesting point in connection with Mactra is their high

PLATE 12.

A. Cross-section through granitic outwash deposit in the northwestern lagoon.

B. Completely bioturbated , sheltered subtidal flat sediment

C. Weakly bioturbated, proximal tidal delta facies.
Note the shelly lag material.

D. Weakly bioturbated, coarse channel sediment.
Note herringbone cross-bedding on the upper right.

E. Weakly bioturbated, shell-rich channel deposit.

F. Weakly bioturbated channel sediment.
Note escape structure of Mactra and Callianassa tube on the right.

Plate 12

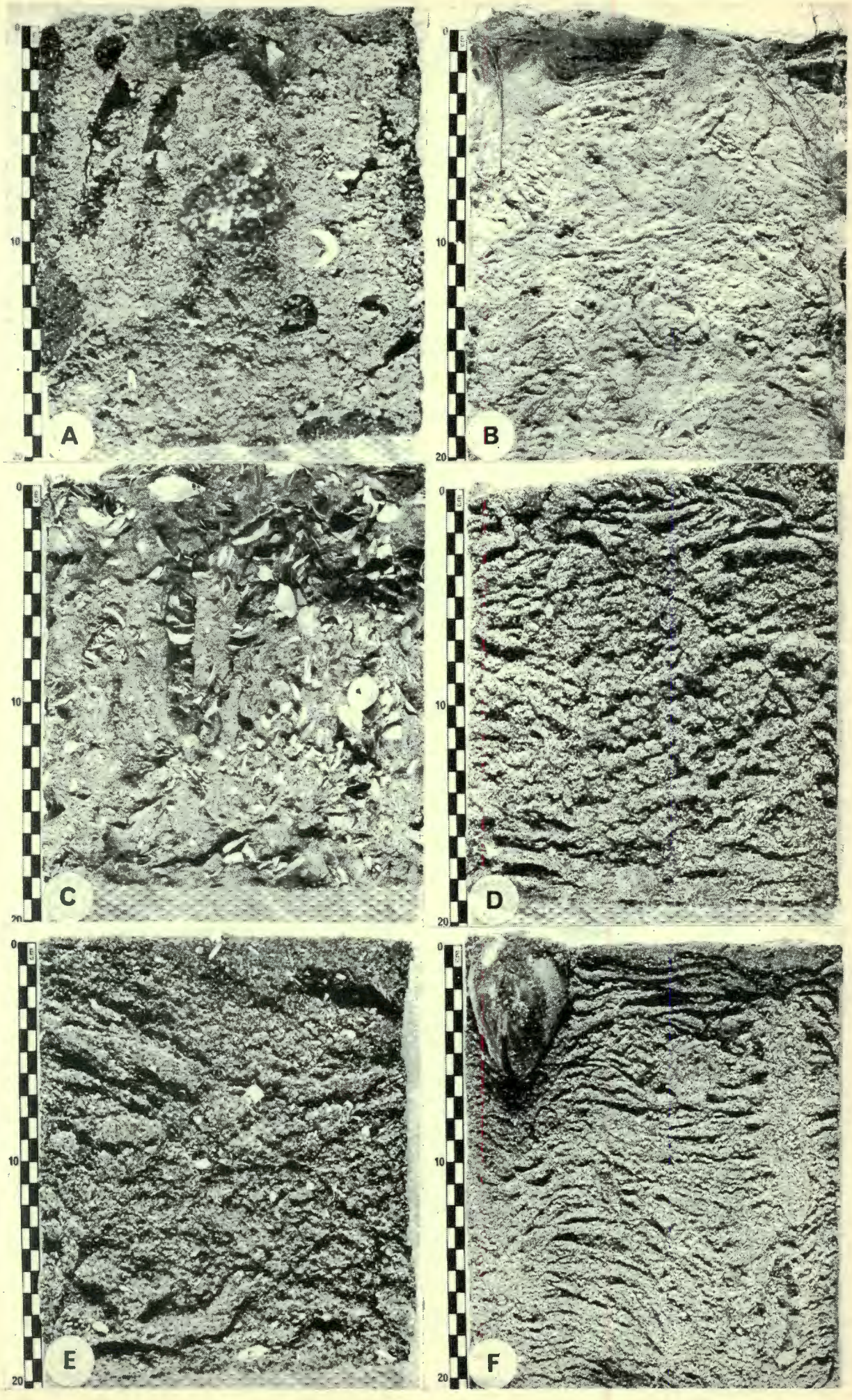

filtering rate (Field, pers. comm. 1975). Each adult mussel will filter about 1 l/min of sea water. Considering the overall population in Langebaan Lagoon, their combined filtering capacity in the course of a tidal cycle will amount to a fair proportion of the total water mass entering or leaving the system.

5.7.4. Tidal Channels

5.7.4.1. Physical Surface Structures

Channels are characterized by a wide range of current-controlled bedforms. Current ripples occur practically throughout the channel system; in many parts of the central and northern lagoon current velocities are high enough to generate underwater dunes (Plate 6). Side-scan sonar records indicate that most dune fields are controlled by the ebb current. Flow separation of the ebb and flood current is locally well documented by dunes facing in the opposite direction. Complete reversal of the large dune bedforms was not observed, although smaller superimposed dunes will normally change direction during each tidal cycle.

The most frequently observed dune bedforms are long, straight or sinuous crested transverse forms (Allen, 1968). These reach heights up to 2 m and wavelengths in excess of 30 m (e.g. Plate 6-E). Lunate dunes (Plate 6-H), of the type described by Häntzschel (1938) as D-shaped megaripples and by Harms and Fahnenstock (1965) as spoon-shaped scours, are common. Interference patterns within dune fields are occasionally observed (Plate 6-B and 6-G). These occur under two different conditions. In some places where the flow paths of ebb and flood currents cross at oblique angles, interference patterns of dunes facing in opposite directions were observed. In other cases interference patterns form where the flow changes its direction in the course of the same tidal cycle, e.g. at the onset of the ebb current, the flow frequently takes short cuts across intertidal flat areas and the upslope channel banks often respond by dune formation. When the tide has dropped sufficiently the current is forced back into its main channel and thereby generates dunes at different angles to the former ones.

5.7.4.2. Biological Surface Structures

Biological surface structures are of little importance in the channel systems because physical processes dominate to such an extent that biological surface activity has an extremely low preservation potential. Nevertheless, in some parts of the main channel current alignment of marine vegetation can be observed. In side channels of the eastern tidal flat areas the polychaete Diapatra occasionally forms extensive mats.

5.7.4.3. Internal Sedimentary Structures

The distal tidal delta consists of well sorted fine sand exposing a firm well-packed surface. There is no mud in the sediment and the internal lamination is barely visible although bioturbation is not obvious. Towards the inlets the mean diameter of the sediment increases rapidly. Sediment sorting, on the other hand, decreases initially as a shelly lag is incorporated. This shell-sand mixture forms a distinct facies on the inlet-facing, proximal tidal delta. It displays no obvious internal structures except occasional current-aligned shell fragments. Bioturbation traces are sporadic, consisting mainly of Callianassa burrows. Abandoned burrows are frequently filled with shell fragments that are neatly stacked in vertical columns (Plate 12-C).

In the narrowest parts of the inlets the sediment is again very well sorted and ripple cross-lamination is frequently preserved. In some cases even herringbone cross-bedding can be observed (Plate 12-D and 12-E). There is no mud content in this facies and bioturbation traces are very sporadic. Further into the lagoon the channel sediments become finer and bioturbation increases, although still not significantly. Mactra and Callianassa are the main burrowing organisms (Plate 12-F). Bioturbation by polychaetes is usually underestimated because they leave few distinct traces.

In areas where large underwater dunes occur, crossbedding is extremely well preserved, often in form of cosets (Plate 13-A). In general, bioturbation is very low on the crests of large dunes but increases towards the troughts (Plate 13-B). An interesting observation was made in a narrow belt along the lower leeward slopes of large flood-oriented dunes where a dense population of Mactra mussels appears to occupy an ecological niche. Their burrowing capability seems to cope efficiently with the sedimentation rates on the leeward slopes of these dunes. They have not been observed in the ebb-oriented dunes, where higher sedimentation rates seem to prevent the settlement of

PLATE 13.

A. Cosets of dune cross-bedding from dune crest of the central channel section.

B. Weakly bioturbated dune trough sediments.

C. Pebble layer of the late-Eemian +3m transgression near Churchhaven.

D. Dense Callianassa bed at the base of the fossil, aeolian dune barrier.

E. Shelly lag deposit formed by migrating tidal channels during the Eemian high stand of the sea.
Note the many articulated shells and the scour hole in underlying calcrete.

F. Detail of the sharp contact between the shell lag-deposit and the underlying calcrete.

Plate 13

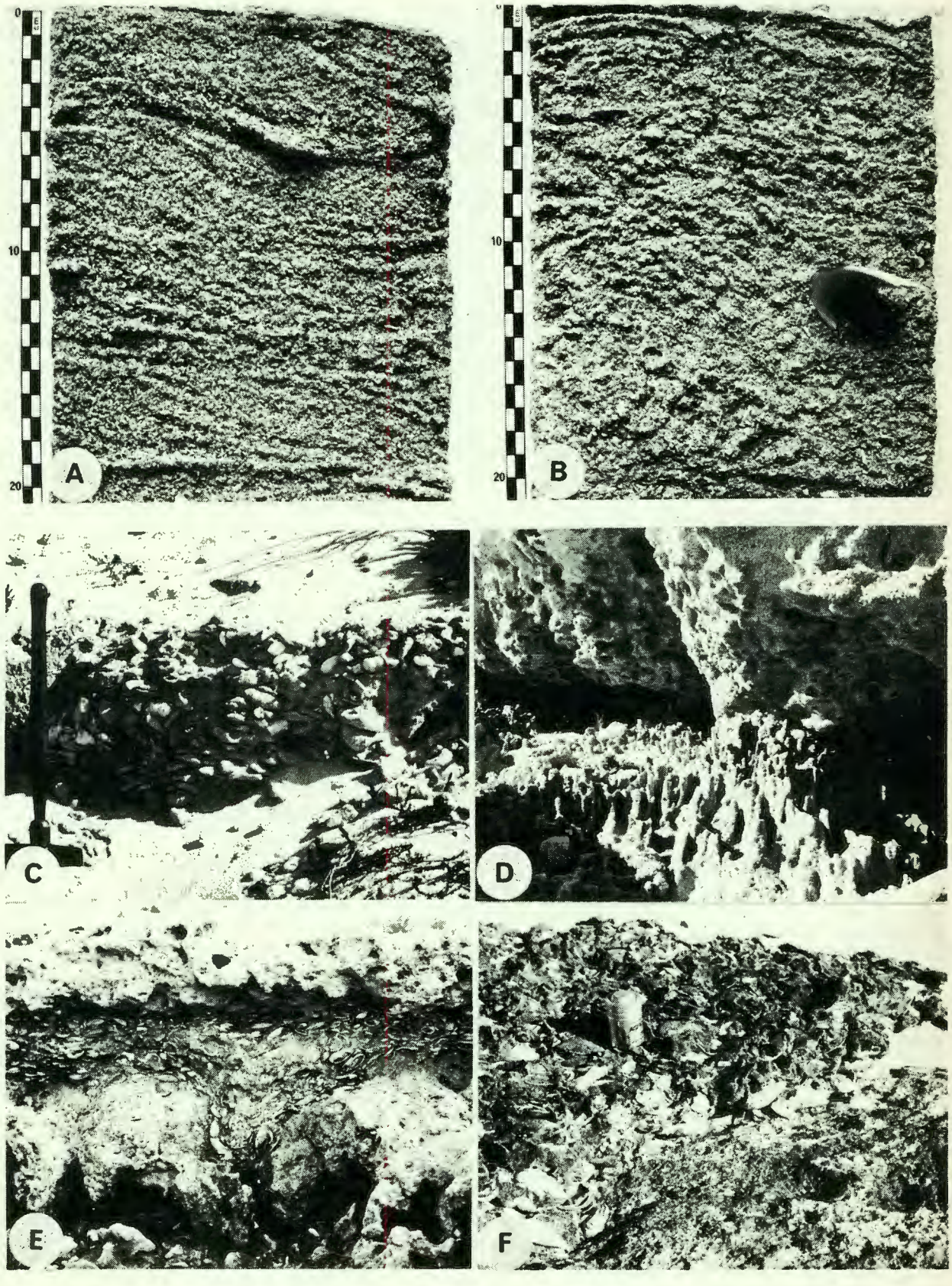

mussel larvae.

5.8. LITHOLOGICAL CHARACTERISTICS OF LANGEBAAN LAGOON

In contrast to Saldanha Bay, where energy zones were defined somewhat arbitrarily, Langebaan Lagoon allows a clear distinction of individual depositional subenvironments. Each depositional subenvironment coincides with one of the physiographic units discussed in Section 5.1.1. (see also Fig. 127). The different energy gradients are reflected in the grain size images of the intertidal flats (Fig. 206-A), subtidal flats (Fig. 206-B), and tidal channels (Fig. 206-C), respectively.

As outlined earlier, the depositional processes in Langebaan Lagoon are characterized by the mixing of two hydraulic populations. The degree of mixing is perhaps best illustrated by the relative proportion of individual size fractions in the total sediment. In Fig. 207 the dominant size fractions of the sediment, i.e. those fractions which, either individually or in combination of two or more, contribute over 50% to the total sediment, have been superimposed in a single map. Zones of low mixing are characterized by a single dominant size fraction, whereas stronger mixing is reflected by the combination of two or more size fractions. Their respective sorting and skewness characteristics were presented previously in Fig. 153 and Fig. 154.

Lithologically the lagoon is considerably less complex than Saldanha Bay. With the exception of a single sample, the sediments of the entire lagoon contain less than 50% $CaCO_3$ and thus qualify lithologically as quartzarenites (Fig. 208). On the basis of the carbonate content the sediments of the lagoon can be divided into two lithological provinces. Calcareous quartzarenites are confined to the northern lagoon; it is interesting to observe that the western margin, i.e. the nearshore belt where terminal fans of granitic outwash occur, has a relatively low carbonate content. This zone and the remainder of the lagoon comprise slightly calcareous quartzarenites. Because of the high mud content the salt marshes would be classified as slightly calcereous, arenaceous quartzlutites.

The lithological classification of the individual subenvironments is presented in triangular diagram form in Fig. 209. There is considerable

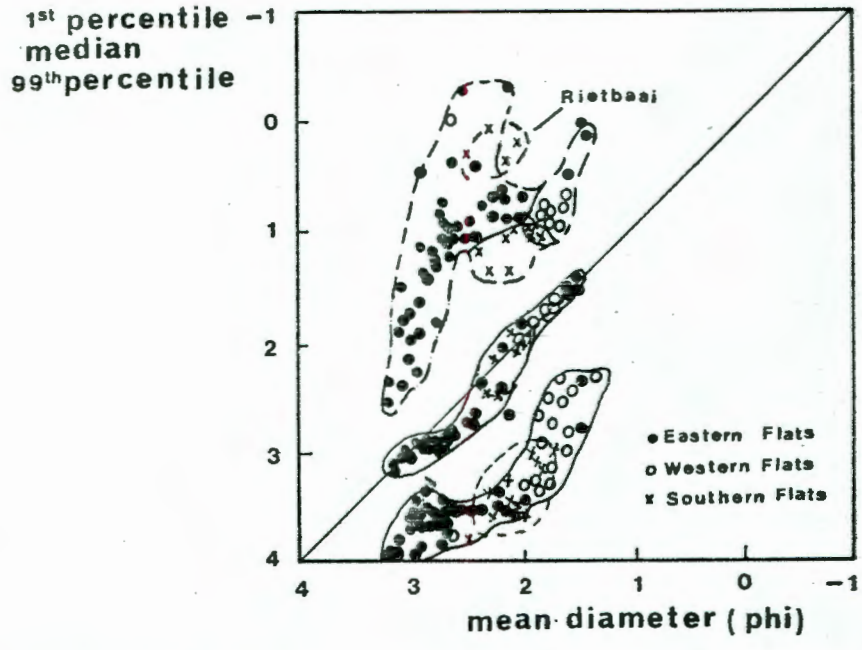

Fig. 206-A.

Grain-size image of intertidal flats

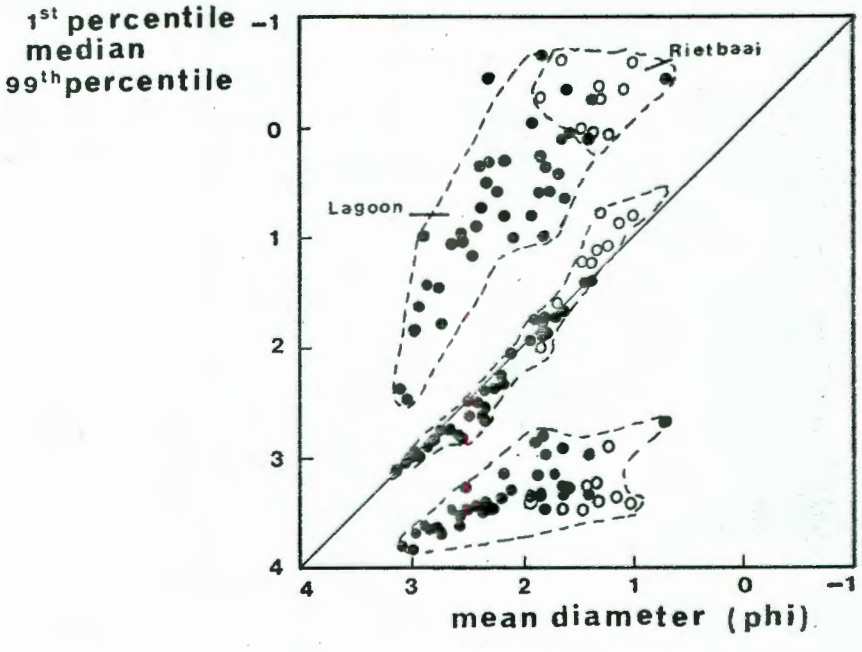

Fig. 206-B.

Grain-size image of subtidal flats

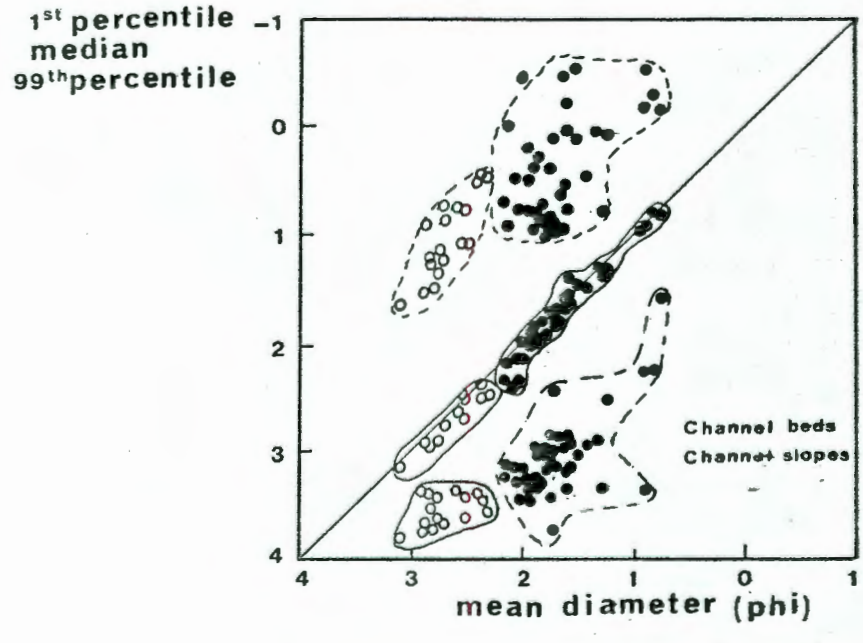

Fig. 206-C.

Grain-size image of tidal channels and channel slopes

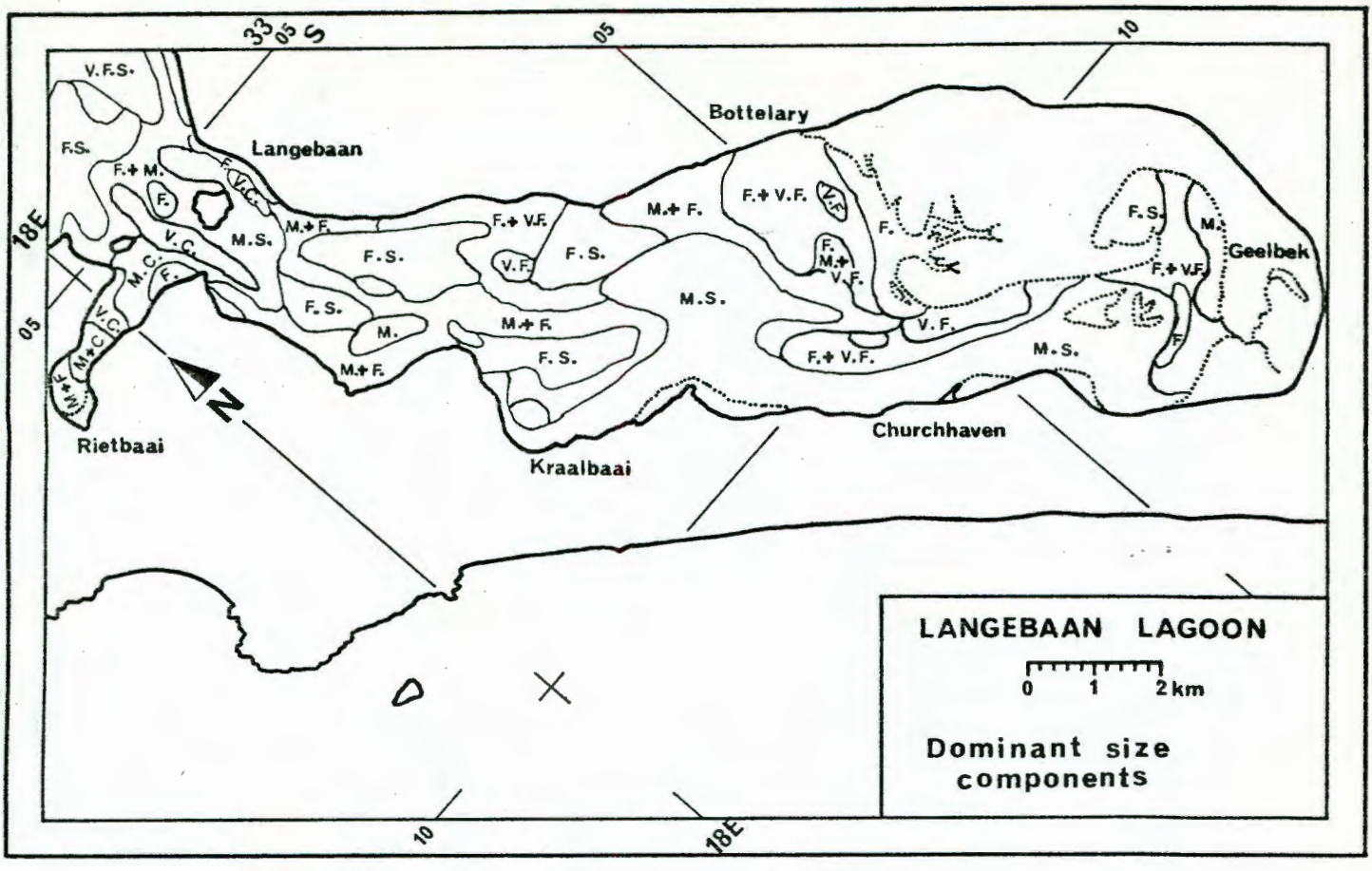

Fig. 207

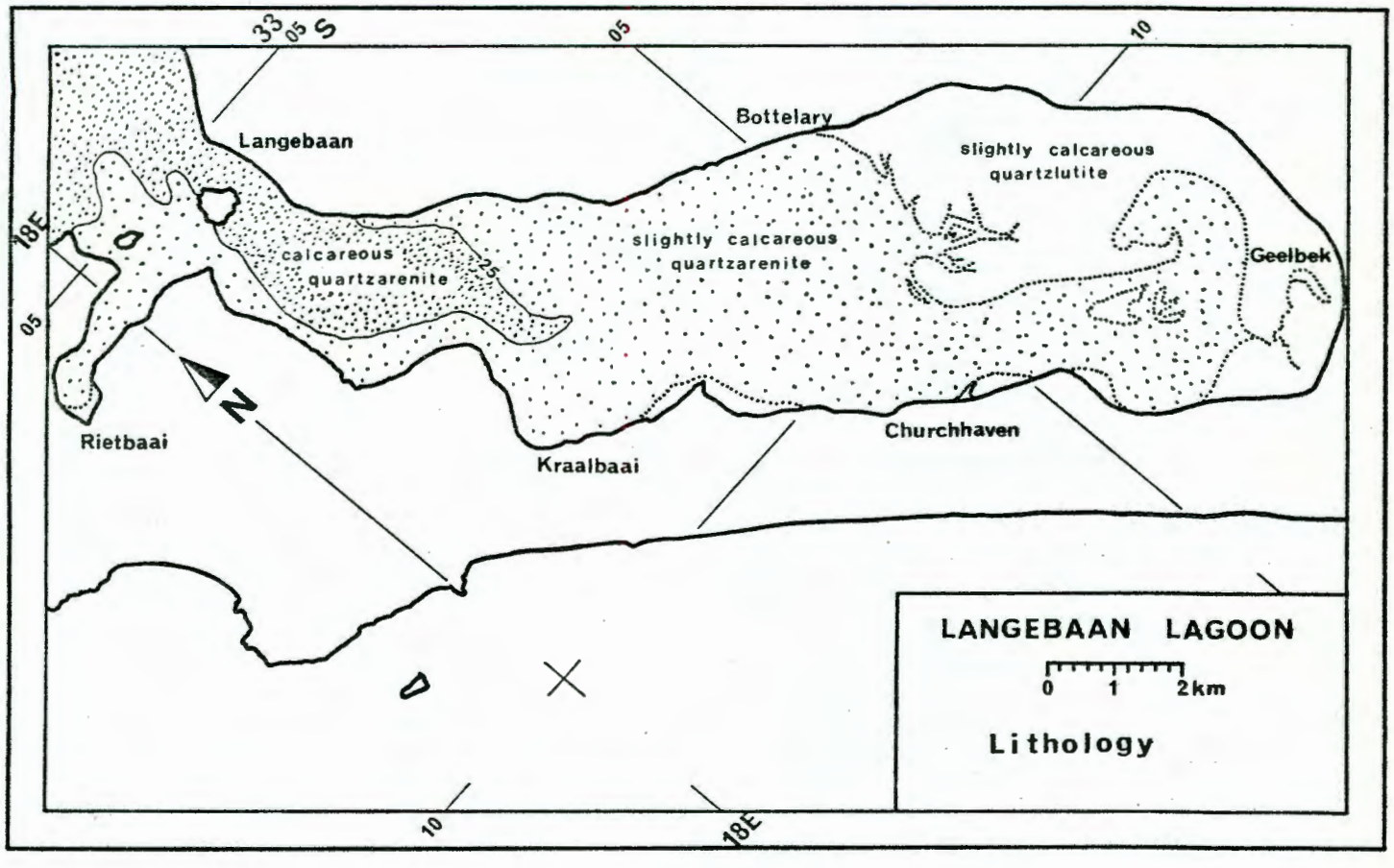

Fig. 208

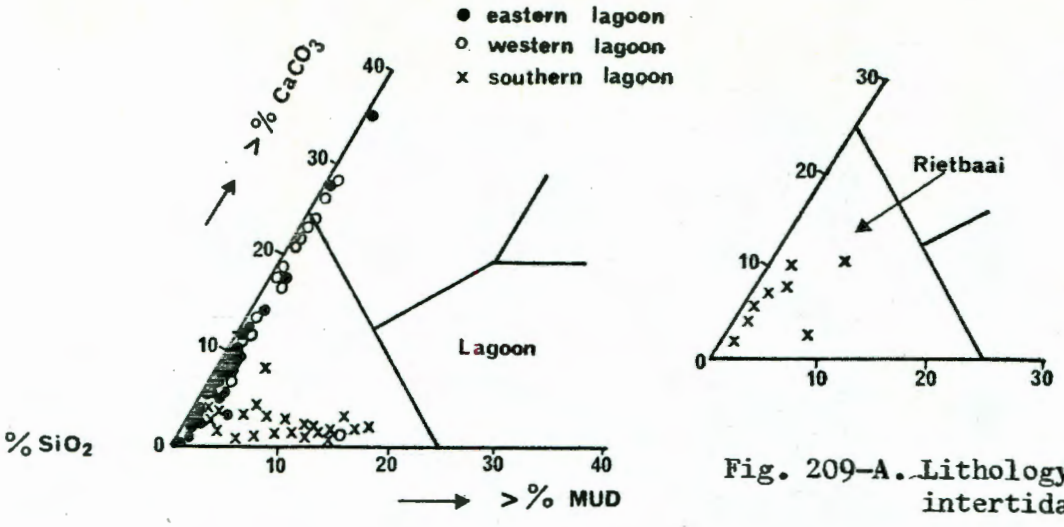

Fig. 209-A. Lithology of intertidal flats

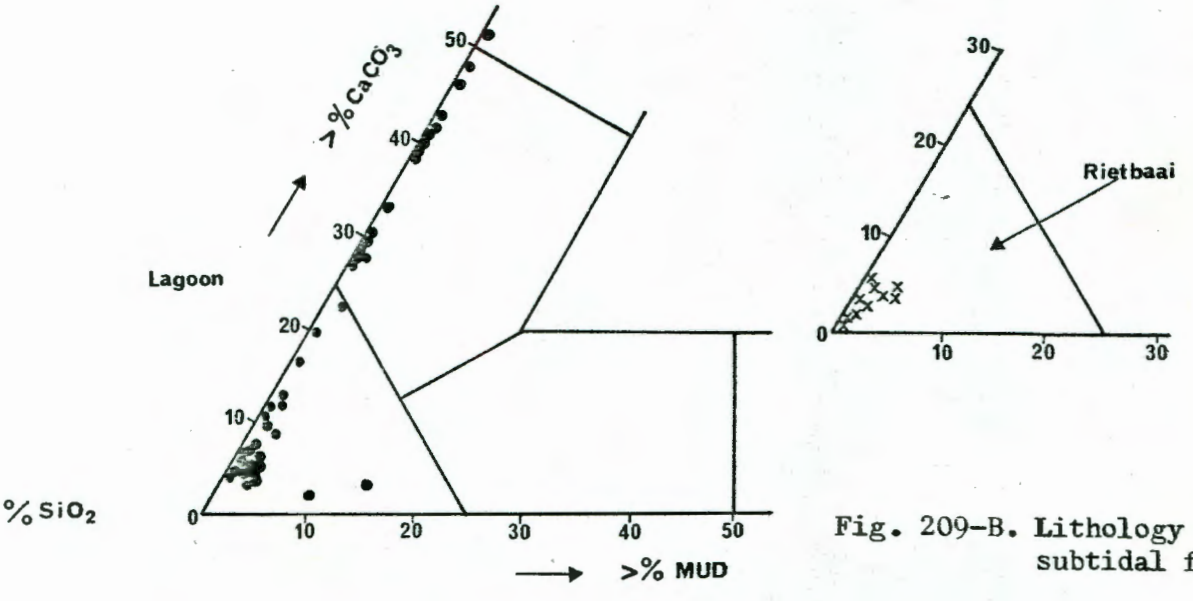

Fig. 209-B. Lithology of subtidal flats

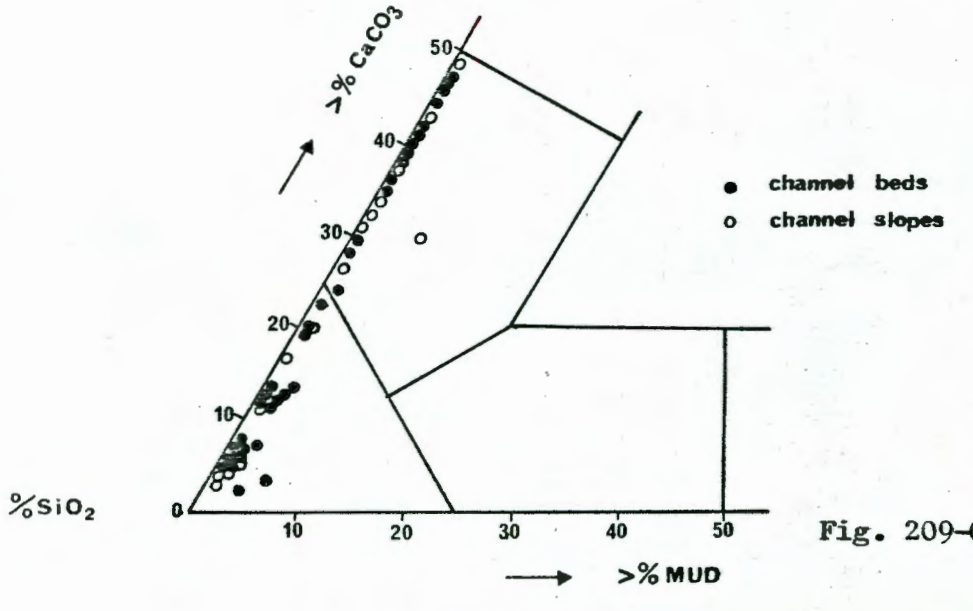

Fig. 209-C. Lithology of tidal channels

overlap between the three units, as one might expect from the progressive mixing process of the two hydraulic populations. The intertidal flat sediments consist almost exclusively of slightly calcareous quartzarenites whereby eastern, western, and southern tidal flats are each grouped in a distinct point cluster (Fig. 209-A). The eastern tidal flat sediments have on average a low carbonate content (under 10%) and also a low mud content (under 5%). The western tidal flats, on the other hand, are characterized by a low mud content (under 5%) but a higher carbonate content (10 - 30%). Southern tidal flat sediments in turn have a low carbonate content (under 10%) but a higher mud content (5 - 20%).

Subtidal flats (Fig. 209-B) and tidal channels (Fig. 209-C) both have practically the same lithological characteristics, ranging from almost pure quartzarenites (over 95% SiO_2) in the southern lagoon to calcareous quartzarenites (25 - 50% $CaCO_3$) in the northern lagoon. In thecentral and southern parts the lithological character of both subtidal flats and channels is identical to that of the intertidal flat sediments. These units can be distinguished from each other only on the basis of their characteristic primary sedimentary structures, as outlined in the previous section.

Only two units in Langebaan Lagoon would qualify as sandstones in the strict sense of the word (Pettijohn et al., 1972). These are the sediments of Rietbaai in the northwest of the lagoon and the eastern tidal flat sediments. Both contain under 5% mud and less than 5% $CaCO_3$.

CHAPTER 6. THE EVOLUTION OF SALDANHA BAY AND LANGEBAAN LAGOON

6.1. INTRODUCTION

The discussion of the evolution of Saldanha Bay and Langebaan Lagoon has been divided into two sections. The first section deals with the late Pleistocene history of the area. This elaboration is considered necessary in order to understand the stratigraphic framework within which the modern system has evolved. It forms a vital aspect when considering the merits of various hypotheses about the origin of the lagoon.

The second section deals in more detail with the Holocene evolution of Saldanha Bay and Langebaan Lagoon whereby the emphasis lies on the lagoon, as it provides most of the evidence concerning successive Holocene events.

6.2. LATE PLEISTOCENE HISTORY OF THE STUDY AREA

On all but one count, the writer agrees with the evolutionary concept developed by Tankard (1975 and 1976). The fossil oyster reefs, which Tankard (1975) has associated with the last interglacial period, are now firmly placed within the Holocene and will be discussed in the second section. On the basis of the stratigraphic evidence, two basic hypotheses for the development of an Eemian lagoonal complex have been proposed. The first proposes a barrier-beach system, stretching from False Bay in the south at least up to Elandsbaai in the north. The second suggests a northward prograding sand spit, which eventually linked Ysterfontein with the granite peninsula in the south of Saldanha Bay.

The stratigraphic sequence of the fossil barrier provides evidence in favour of the former model. A stratigraphic cross-section through the fossil core of the barrier is presented in Fig. 210. There is no direct field evidence that would support the sand spit concept. Moreover, it can be rejected on the basis of hydrodynamic considerations. The wave-climate and littoral sediment-transport directions are exposed to a strong seasonal effect along the open west coast of the southwestern Cape Province. It would appear that the moderately strong, southeasterly to southwesterly winds in summer are effectively counteracted by less frequent, but considerably

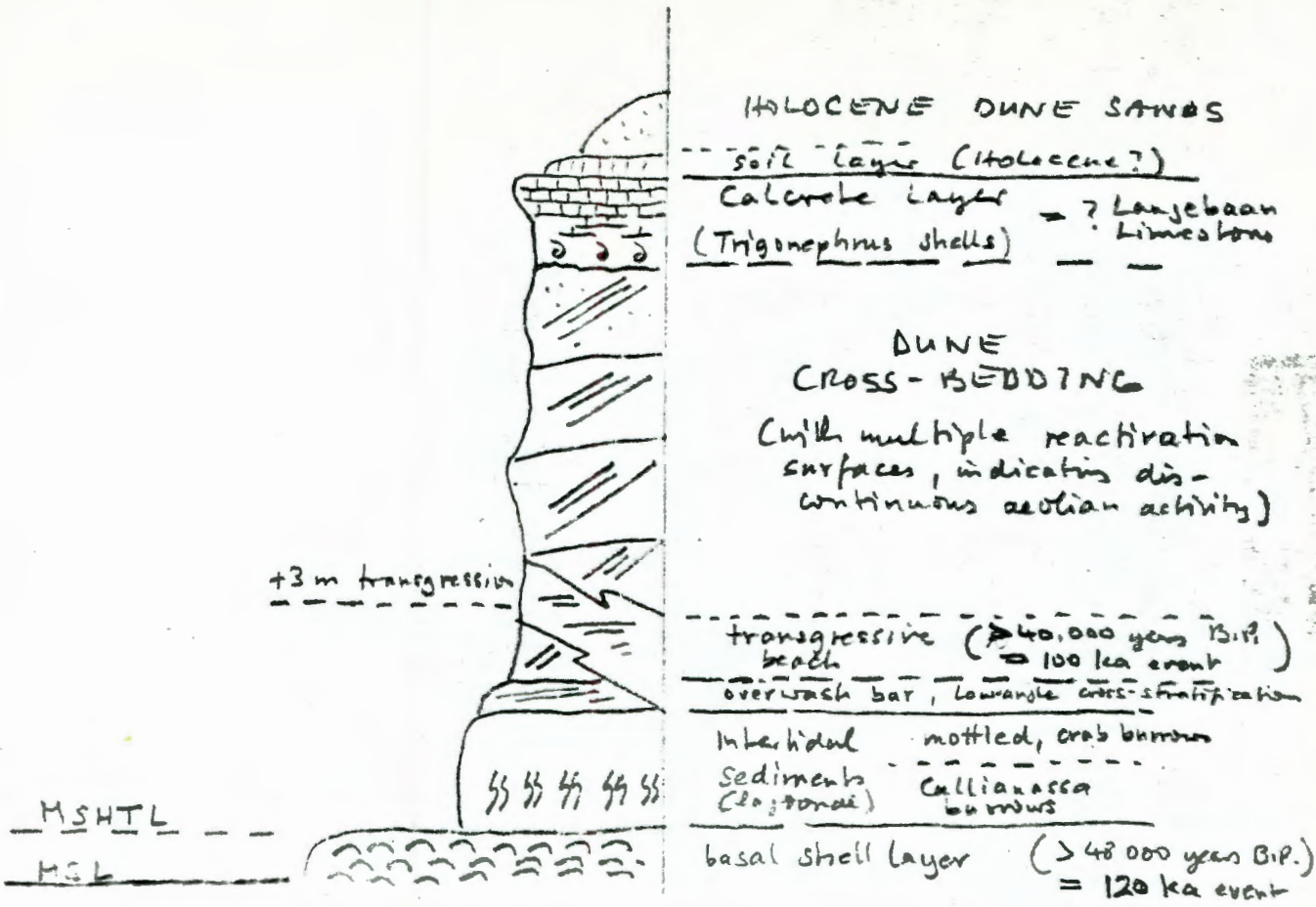

Fig. 210 Schematic Cross-section through the fossil dune barrier.

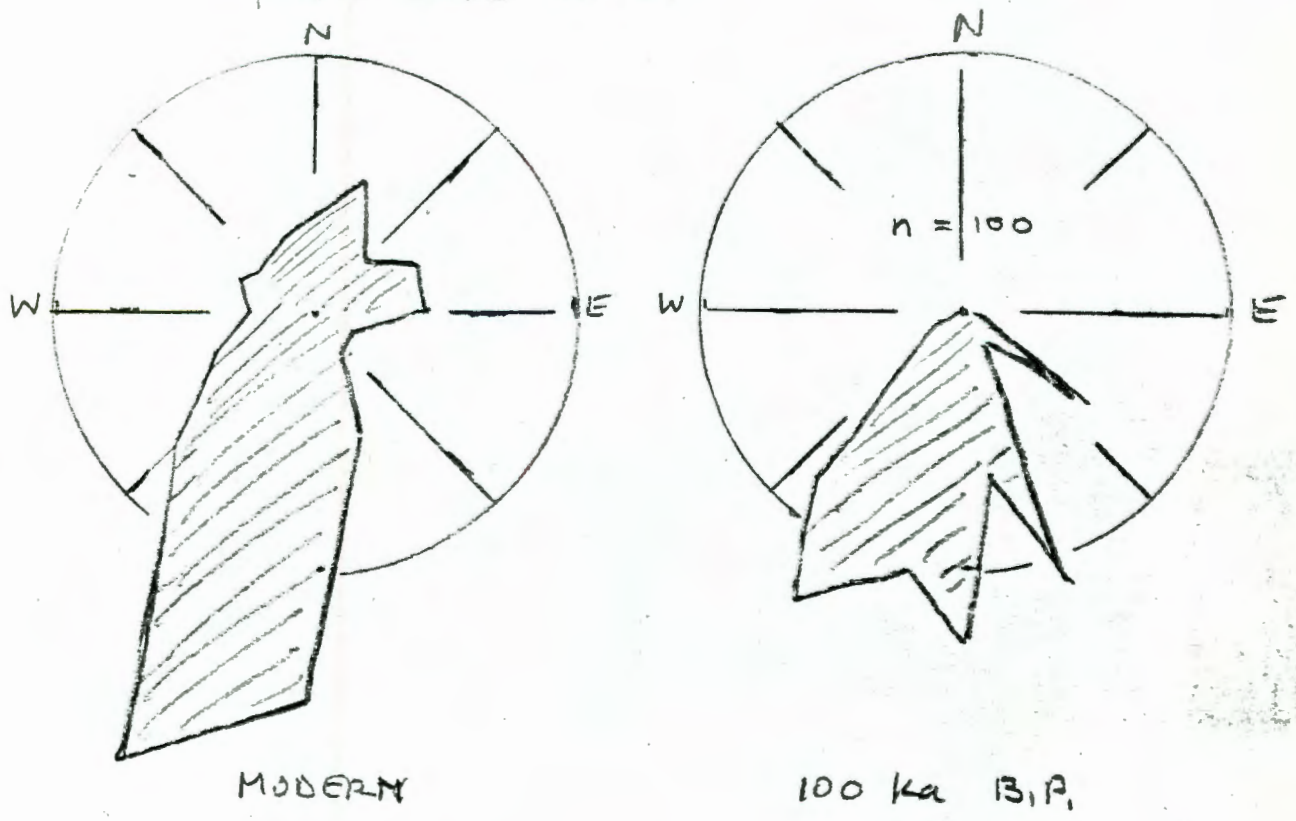

Fig. 211. Modern and palaeo-wind directions inferred from the orientation of dune slip-faces

more violent northerly storms during winter. As a result, there is no evidence for any net gain or loss of substantial quantities of sediment in any one direction. Palaeo-wind directions, inferred from the dip directions of the fossil dune slip-faces, indicate that during the Eemian the wind pattern was essentially identical to the modern pattern (Fig. 211). Under these conditions, however, a northward prograding sand spit is not considered feasible. In addition, there is no evidence in the exposed stratigraphic record. Not a single northward dipping beach deposit has been recorded, as would be required by successively developing sand hooks at the northern tip of the spit. Furthermore, a continuous basal lag deposit, as observed intermittently along the entire lagoonal shoreline, is not normally associated with sand spits developing in one direction.

The evidence for a barrier-beach situation is, on the other hand, overwhelming. The basal shell agglomeration is a typical feature of migrating tidal-channels behind and between barrier beaches (Plate 13-E and 13-F). The shell material itself suggests strong current control rather than wave domination. Many of the bivalves are still hinged; often both valves are slightly displaced or rotated around their hinge. The vast majority of shells are oriented with their convex sides facing upward. Most of the bi-valves belong to sand-dwelling, estuarine or lagoonal communities (Tankard, 1975).

The basal shell layer is usually overlain by intertidal sediments, although in some places seaward-dipping beach sediments are found. The intertidal sediments are strongly bioturbated, Callianassa tubes being particularly common (Plate 13-D). Tube densities of several hundred per square metre are found, thus indicating extremely sheltered conditions in localities where channel erosion had previously accumulated a basal shell-bed. The intertidal sediments become increasingly mottled towards the upper limits and gradually grade into aeolian sands. The dune sequence is frequently underlain by a thin sand body displaying landward dipping low-angle cross-stratification. This is a typical feature of overwash bar activity.

The general transition from marine into non-marine sediments occurs at about 1 - 1.5 m above present high water level, in what appears to have been a continuous depositional process. This lower unit is associated with the late-Eemian events, shortly after the onset of the regression that

followed the initial high stand of the sea at about 120 ka B.P. This conclusion is reached on the basis of radiocarbon dates, obtained on shell material recovered by Parker (1968) from the basal bed. This layer dates older than 48 500 $\pm \frac{3600}{2900}$ years B.P. (Pta - 096).

There appears to have been a second, minor transgression reaching about +3 m soon after the initial regressive phase. Evidence for this event is found along the fossil tombolo in Rietbaai and near Churchhaven where a calcrete pebble layer, containing marine shell material, is intercalated into the fossil dune sequence (Plate 13-C). This transgression seems to have breached the previous barrier in a number of places thereby reworking some previously indurated sediments. The shell material of this layer was dated at older than 40 000 years B.P. (Pta - 1675). The event must, therefore, still form part of the late Eemian regressive phase which appears to have been interrupted by minor transgressive phases. The feature is tentatively correlated with the 103 ka level recorded by Broecker et al. (1968) and the 100 ka event reported by Chappell (1974). Tankard (1976) has recognized similar events at other localities along the west coast of Southern Africa. Besides this feature there is no further evidence for late Pleistocene sea level oscillations in the vicinity of Langebaan Lagoon. On the basis of the above evidence, the indurated late Pleistocene dune sediments are most probably related to the late Eemian withdrawal of the sea.

The last pre-Holocene depositional activity is represented by an extensive calcrete sheet, which caps the entire fossil dune sequence in the immediate vicinity. Towards the modern coast this calcrete layer is turncated to form a continuous scarp that runs parallel to the modern shoreline (Plate 5-C). It is situated about 1 - 2 km inland. The age of this calcrete layer is not known although it obviously is younger than the 100 ka, inferred for the lower levels of the fossil sequence. The calcretized layer is characterized by the fossil land-snail Trigonephrus, suggesting its correlation with the Langebaan Limestone Member of the Bredasdorp Formation (Visser and Schoch, 1973; Tankard, 1976).

A high interstadial sea level has been inferred by Siesser (1974 and 1975) on the basis of a radiometric date obtained from intertidally exposed dolostone in the northwestern part of Saldanha Bay and False Bay. The age of this rock was dated at 20 300 $\pm \frac{600}{630}$ years B.P. Kensly (1976) reports a raised beach deposit at Milnerton, dated at 35 000 years B.P.,

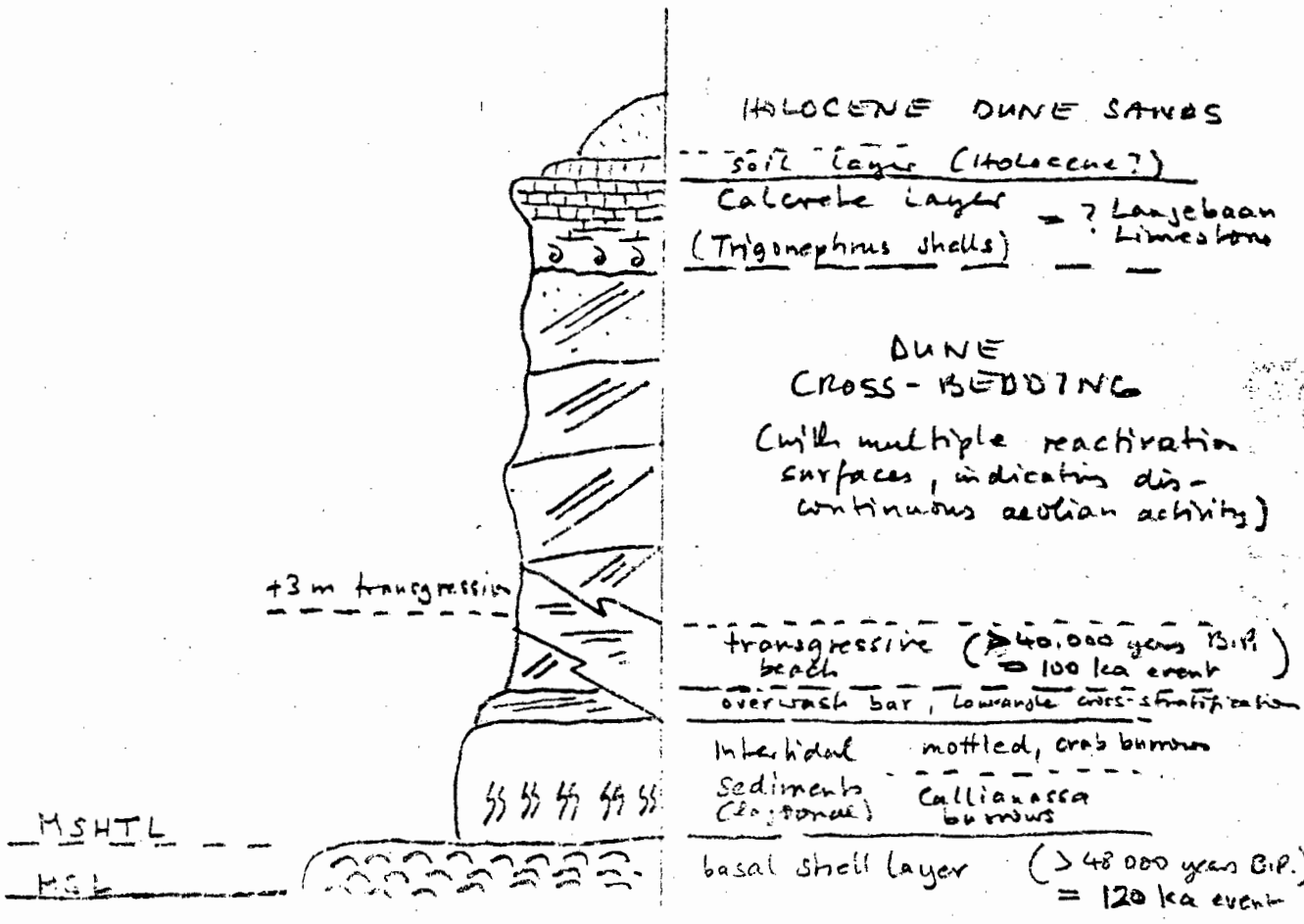

Fig. 21c Schematic Cross-section through the fossil dune barrier.

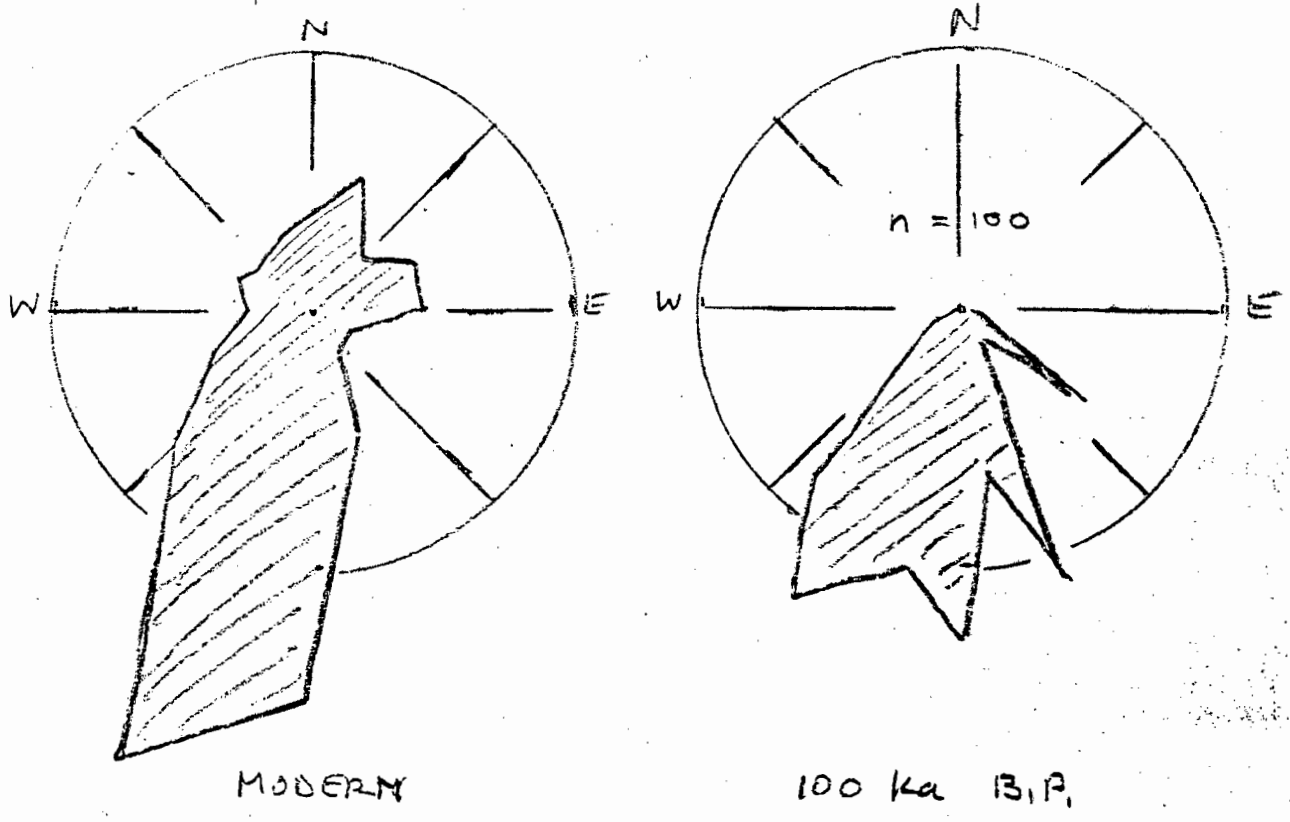

Fig. 21d. Modern and palaeo-wind directions inferred from the orientation of dune slip-faces

more violent northerly storms during winter. As a result, there is no evidence for any net gain or loss of substantial quantities of sediment in any one direction. Palaeo-wind directions, inferred from the dip directions of the fossil dune slip-faces, indicate that during the Eemian the wind pattern was essentially identical to the modern pattern (Fig. 211). Under these conditions, however, a northward prograding sand spit is not considered feasible. In addition, there is no evidence in the exposed stratigraphic record. Not a single northward dipping beach deposit has been recorded, as would be required by successively developing sand hooks at the northern tip of the spit. Furthermore, a continuous basal lag deposit, as observed intermittently along the entire lagoonal shoreline, is not normally associated with sand spits developing in one direction.

The evidence for a barrier-beach situation is, on the other hand, overwhelming. The basal shell agglomeration is a typical feature of migrating tidal-channels behind and between barrier beaches (Plate 13-E and 13-F). The shell material itself suggests strong current control rather than wave domination. Many of the bivalves are still hinged; often both valves are slightly displaced or rotated around their hinge. The vast majority of shells are oriented with their convex sides facing upward. Most of the bi-valves belong to sand-dwelling, estuarine or lagoonal communities (Tankard, 1975).

The basal shell layer is usually overlain by intertidal sediments, although in some places seaward-dipping beach sediments are found. The intertidal sediments are strongly bioturbated, Callianassa tubes being particularly common (Plate 13-D). Tube densities of several hundred per square metre are found, thus indicating extremely sheltered conditions in localities where channel erosion had previously accumulated a basal shell-bed. The intertidal sediments become increasingly mottled towards the upper limits and gradually grade into aeolian sands. The dune sequence is frequently underlain by a thin sand body displaying landward dipping low-angle cross-stratification. This is a typical feature of overwash bar activity.

The general transition from marine into non-marine sediments occurs at about 1 - 1.5 m above present high water level, in what appears to have been a continuous depositional process. This lower unit is associated with the late-Eemian events, shortly after the onset of the regression that

followed the initial high stand of the sea at about 120 ka B.P. This conclusion is reached on the basis of radiocarbon dates, obtained on shell material recovered by Parker (1968) from the basal bed. This layer dates older than 48 500 $\pm \frac{3600}{2900}$ years B.P. (Pta - 096).

There appears to have been a second, minor transgression reaching about +3 m soon after the initial regressive phase. Evidence for this event is found along the fossil tombolo in Rietbaai and near Churchhaven where a calcrete pebble layer, containing marine shell material, is intercalated into the fossil dune sequence (Plate 13-C). This transgression seems to have breached the previous barrier in a number of places thereby reworking some previously indurated sediments. The shell material of this layer was dated at older than 40 000 years B.P. (Pta - 1675). The event must, therefore, still form part of the late Eemian regressive phase which appears to have been interrupted by minor transgressive phases. The feature is tentatively correlated with the 103 ka level recorded by Broecker et al. (1968) and the 100 ka event reported by Chappell (1974). Tankard (1976) has recognized similar events at other localities along the west coast of Southern Africa. Besides this feature there is no further evidence for late Pleistocene sea level oscillations in the vicinity of Langebaan Lagoon. On the basis of the above evidence, the indurated late Pleistocene dune sediments are most probably related to the late Eemian withdrawal of the sea.

The last pre-Holocene depositional activity is represented by an extensive calcrete sheet, which caps the entire fossil dune sequence in the immediate vicinity. Towards the modern coast this calcrete layer is turncated to form a continuous scarp that runs parallel to the modern shoreline (Plate 5-C). It is situated about 1 - 2 km inland. The age of this calcrete layer is not known although it obviously is younger than the 100 ka, inferred for the lower levels of the fossil sequence. The calcretized layer is characterized by the fossil land-snail Trigonephrus, suggesting its correlation with the Langebaan Limestone Member of the Bredasdorp Formation (Visser and Schoch, 1973; Tankard, 1976).

A high interstadial sea level has been inferred by Siesser (1974 and 1975) on the basis of a radiometric date obtained from intertidally exposed dolostone in the northwestern part of Saldanha Bay and False Bay. The age of this rock was dated at 20 300 $\pm \frac{600}{630}$ years B.P. Kensly (1976) reports a raised beach deposit at Milnerton, dated at 35 000 years B.P.,

and in the course of this study the writer has recovered shell bearing calcrete from the former outflow channel at Kraalbaai which was dated independently at 26 130 $\pm$ 400 years B.P. (Pta - 1599) and 26 260 $\pm$ 310 years B.P. (Pta - 1600), respectively. The material was recovered about 3 m above present sea level. High interstadial sea levels are generally rejected on the basis of field evidence and theoretical calculations of ice volumes in relation to palaeo-temperatures inferred from oxygen isotope ratios (Donn et al., 1962; Mörner, 1971; Thom, 1973; Shackleton and Opdyke, 1973). Some studies, however, suggest an interstadial sea level close to the present, notably one by Milliman and Emery (1968), in which a high stand is indicated at 35 to 30 ka B.P.

For several reasons the writer is inclined to related all of the local marine deposits to the late Eemian as outlined earlier. Firstly, reports on high interstadial sea levels are extremely few. The study by Milliman and Emery (1968) would require reconsideration in the light of the new evidence concerning tectonic instability of the Atlantic coast of the United States (Winker and Howard, 1977). The shell-bearing rock recovered from the Milnerton (Kensley, 1976) and the former channel sites are both diagenetically affected and the dates should, therefore, be regarded as minimum ages only. In addition, the fossil warm-water assemblage in the Milnerton deposit is very similar to the general Eemian mollusc communities reported by Tankard (1975). The Kraalbaai material, in turn, is evidently linked to the basal shell bed of the fossil dune barrier.

On the other hand, Siesser (1975) sees no reason to mistrust his date 'per se'. In the opinion of the writer the date may well be accurate, but it does not necessarily imply a high stand of the sea at the time in question. In order to facilitate syngenetic precipitation of dolomite as proposed by Siesser (1975), the sea must have stood practically at its present position. However, even Milliman and Emery's sea level curve does not accommodate a sea level in this position at 20 000 years B.P.

An alternative interpretation would be the dissolution of former evaporitic deposits by groundwater and subsequent intergranular reprecipitation from the resulting high-saline brine in the course of evaporation near the surface. Since rainfall was almost certainly higher in this area during the glacial periods (viz. Schalke, 1973), a high groundwater level would not seem an incongruous assumption. Similar processes of post-depositional dolomitization by Mg-rich groundwater have recently been described by Randazzo

et al. (1977) in upper-Eocene carbonate shorelines of central Florida, and by Levy (1977) along the northern Sinai coastal plain. The date could thus reflect post-depositional dolomitization without requiring a high stand of the sea at the time under consideration.

6.3. HOLOCENE EVOLUTION OF SALDANHA BAY AND LANGEBAAN LAGOON

The Holocene evolution of Saldanha Bay and Langebaan Lagoon thus commenced in a semi-consolidated late Pleistocene dune landscape. The controversy regarding the course of the Holocene sea level recovery has been discussed in an earlier section of this study (viz. Section 5.1.2.), and it has been taken for granted here that, relative to South Africa, the sea had in fact recovered to its present position by about 6500 years B.P. This date is in excellent agreement with observations of Martin (1962 and 1968), who has inferred a higher Holocene stand of the sea between 6780 $\pm$ 160 years B.P. and at least 4000 years B.P. on the basis of pollen analyses and radiocarbon dates obtained on material from the Wilderness Lakes area along the South African south coast. The interpretation has received further support by investigations of Butzer and Helgren (1972). These authors suggest a high stand of the sea of at least + 2.5 m. As pointed out earlier, the writer believes that the evidence from Langebaan Lagoon requires a minimum rise of at least 3 m above the present in order to accommodate all of the features related to a high sea level stand. On the basis of this evidence the Holocene evolution of Saldanha Bay and Langebaan Lagoon is outlined below.

The Flandrian transgression rapidly reworked the fossil dune material encountered in the course of its advance. At a stand of -10 m, some 10 ka years B.P., it must have reached at least into the deeper parts of the inner bay although it was still some distance from the present coastline along the dune belt adjacent to the modern lagoon. The seismic data of Du Plessis and De la Cruz (1977) suggest that the inner bay deposits were strongly dissected by a number of deep gullies that drained the immediate hinterland. The physiographic design of the granite hills in the vicinity of Langebaan suggests the existence of a valley that ran through the gap between Langebaan village and Skaapeiland, draining the granite slopes of the upper lagoon through the wide Saldanha Bay valley.

The rising sea soon invaded this extension and formed a shallow arm

along the northeastern shoreline of the modern lagoon. Initially there was little erosion because the relatively small surface area of this proto-lagoon did not facilitate strong tidal current activity. However, erosion steadily increased with the increasing surface area of the lagoon since the outlet remained unchanged. By 6500 years B.P. the present sea level position had been reached and the incipient lagoon probably stretched in a long, but relatively narrow arm down to its present southern limit. The climate, at this stage, was several degrees warmer than today (Hammen et al., 1967; Mörner, 1973; Emiliani, 1955). This would have shifted the sheltered, coastal areas of the west coast into the spawning range of oysters and other thermophilic molluscs (Korringa, 1956; Zinsmeister, 1974). The lack of initial sedimentation and the warm climate gave rise to prolific growth of oyster reefs.

At about 6000 years B.P., or soon after, the sea breached the fossil barrier along the southern margin of the southern granite peninsula, thereby opening a tidal channel that connected Kraal-baai to the open sea. This event was followed by vigorous abrasion along the inner margin of the fossil barrier, in response to ebb-current scouring along the western shoreline, on its way to the Kraalbaai outlet. Since the ebb current dominated erosion and sediment transport, most of the reworked material appears to have been flushed from the system, thus allowing the rapid expansion of the oyster reefs.

In the meantime erosion also continued along the seaward side of the barrier and at the time when the initial Holocene regression commenced, probably around 5500 years B.P., the barrier had narrowed down to a few hundred metres in some places (viz. Fig. 151 and Fig. 212 below). With the onset of regression, erosion rates immediately began to drop off and sediment slowly began to stabilize along the more sheltered margins of the lagoon, especially in the south and southeast. These areas formed the starting-points of the modern salt marshes. At the seaward side the former undercut calcrete cliff was abandoned by progressive beach progradation.

It is not clear from the evidence around Langebaan Lagoon whether the general regression commenced in a number of stronger oscillations, as indicated along the coast of Mauritania (Einsele et al., 1974) or whether the sea withdrew more or less steadily. Whichever mode it followed, it certainly stood above present at about 3500 years B.P. (ca. + 1.5 - 2.0 m)

Fig. 212. The Holocene evolution of Langebaan Lagoon

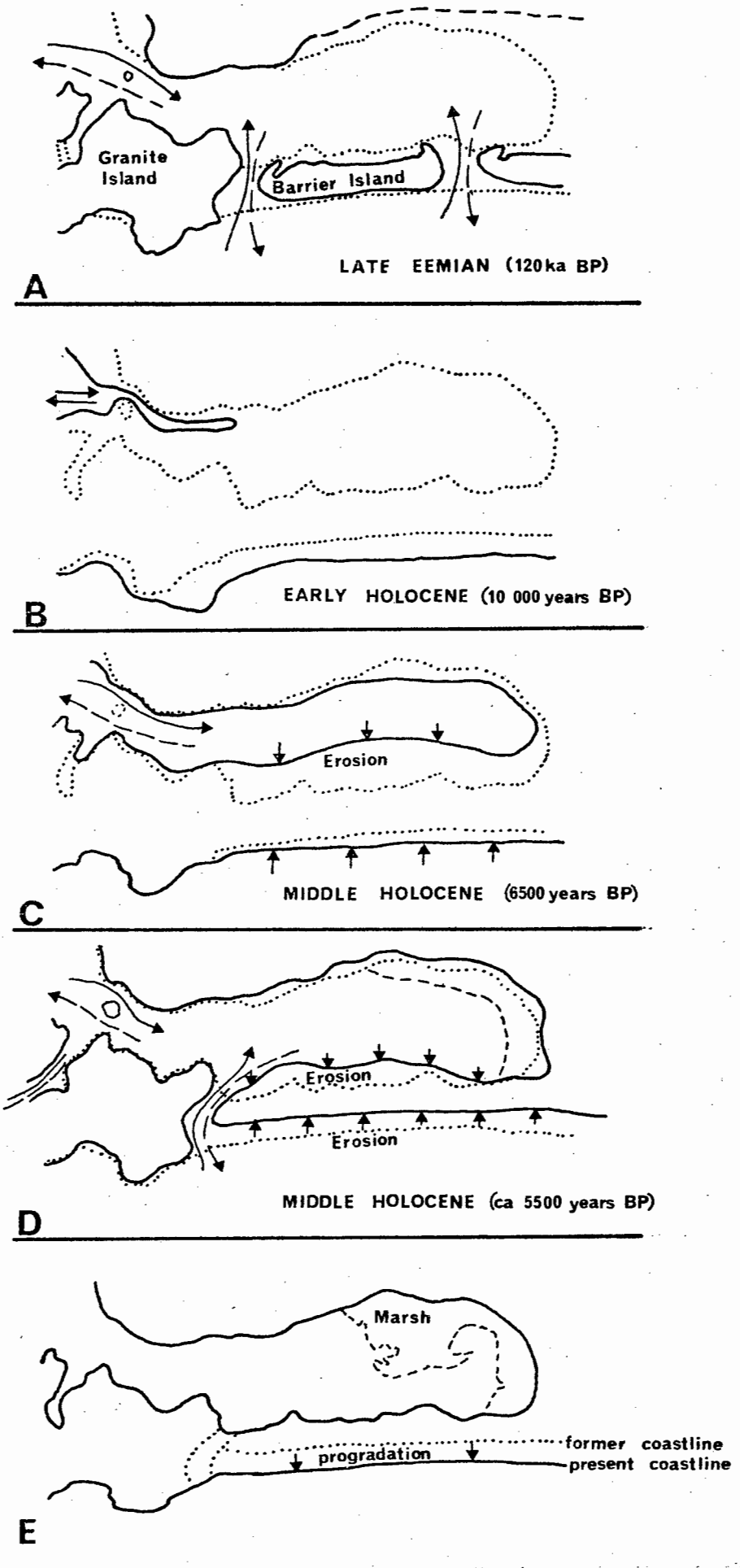

and was still 1.0 - 1.5 m higher 2000 years ago. At this stage the shoreline had almost reached its present position as indicated by the fossil beach ridge at the seaward side of the former outflow channel. The Kraalbaai channel fell dry sometime between 5000 and 2000 years B.P. The fact that the abandoned channel was not filled up with windblown sands would indicate that the coastal dune belts must have been stabilized by vegetation since this event. Martin (1968) and Butsor and Helgren (1972) postulate a dry climate between 7000 and 2000 years and wetter conditions after 2000 years B.P. In the light of this evidence, the writer concludes that the final stages of the Kraalbaai channel activity probably coincide with the latter date. In Saldanha Bay the abrasion platform would have reached its base level by that time, as suggested by the estimated abrasion rate (viz. Section 4.1.) Various stages of the lagoonal evolution, as outlined above, are illustrated in Fig. 212.

Langebaan Lagoon is thus clearly the outcome of selective erosion of a late-Pleistocene dune landscape. In a recent study the concept of a modern, northward prograding sand spit has been revived (Birch, 1977b). However, the field evidence is incompatible with this postulation and the concept is thus refuted.

With the closure of the Kraalbaai channel the high erosion rates will have dropped off appreciably. The remaining material, however, was no longer flushed from the system and sediment began to accumulate in areas of lower energy, especially around the fossil oyster reefs. These were soon mantled and ultimately smothered with a sediment blanket. The date of a fossil oyster at the top of a reef in the central lagoon places this event at about 1800 years B.P.

The readjustment of flow patterns, that followed the closure of the Kraalbaai channel, led to a shift of relative energy levels in various parts of the system and as a result, previously deposited sediments and probably also salt marshes were reworked. In this process fine and very fine sands were removed and carried into Saldanha Bay where they stabilized in the tidal delta and the sheltered and semi-exposed parts of the bay. A new equilibrium appears to have been reached before all of the fine sand was removed, thus explaining its wide distribution in the lagoon with a clear affinity towards the outflow channels and the tidal delta.

In the course of the depositional processes, the sediment transport mechanism has effectively separated and concentrated the bioclastic component in the northern part of the lagoon. This phenomenon is explained by the mode of transport of differently shaped sedimentary components. In Langebaan Lagoon the sediment is composed predominantly of a subrounded to well rounded terrigenous quartz population and an irregularly shaped skeletal carbonate component. The high drag on the irregularly shaped particles, i.e. their resistence to motion, results in traction transport of this component whereas the terrigenous particles are preferentially transported in upper bottom suspension. This differential response has led to the progressive concentration of one component relative to the other.

The modern sediment distribution in Saldanha Bay and Langebaan Lagoon thus represents a relict pattern inherited from the time when the two systems reached a new equilibrium, after the stabilization of sea level around its present position some 1800 years B.P. It would appear that subsequent depositional processes were so insignificant that they were unable to modify this inherited feature. Low modern sedimentation rates are convincingly demonstrated in Kraalbaai, where 2000 years of sedimentation have not resulted in substantial infilling of this low-energy, lagoonal embayment. That this process is still under-way is documented by the intertidal sand spit at the eastern boundary of Kraalbaai.

The modern stratigraphic framework of Langebaan Lagoon is summarized in Fig. 213.

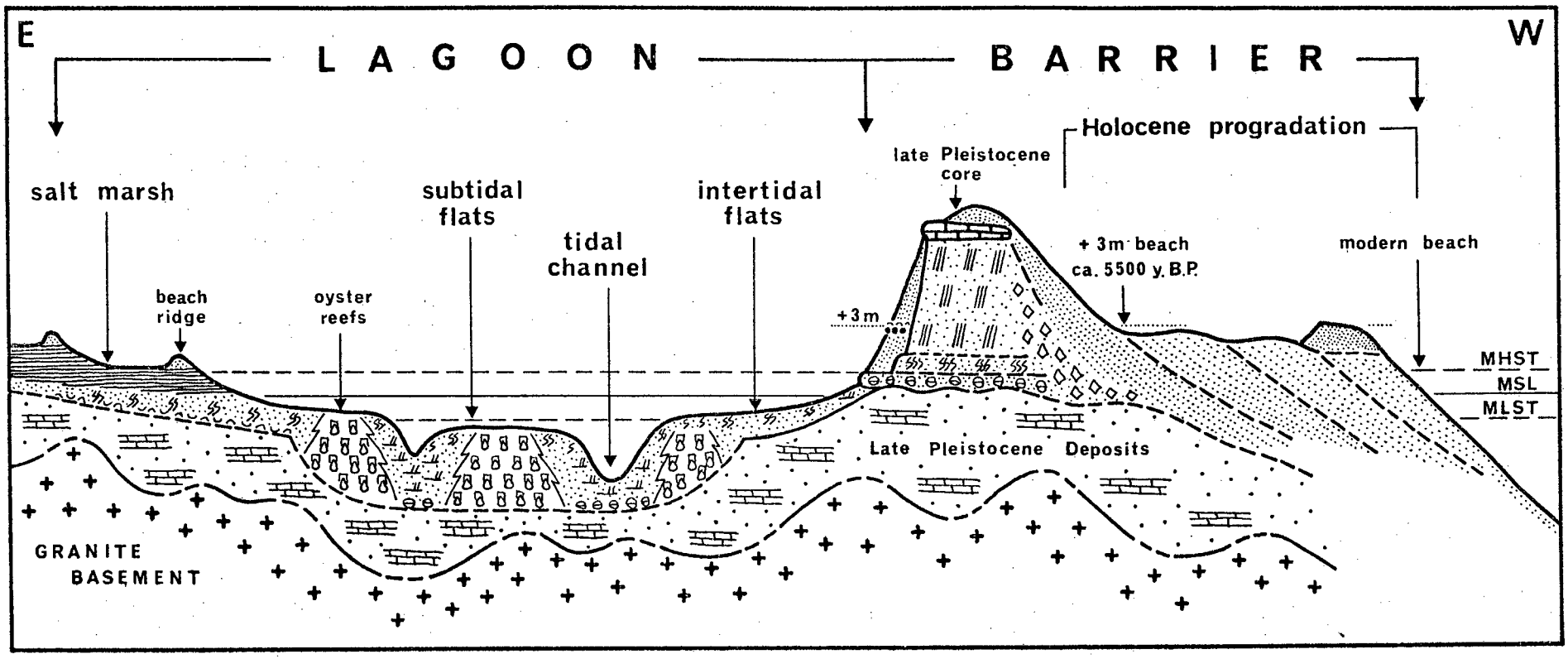

Fig. 213. The modern stratigraphic framework of Langebaan Lagoon

CHAPTER 7. REFERENCES

Albertson, M. 1953. Effects of shape on the fall velocity of gravel particles. Proc. 5th Iowa Hydraul. Conf., Iowa City.

Allen, J.R.L. 1965. A review of the origin and characteristics of Recent alluvial sediments. Sedimentology 5: 89-191.

Allen, J.R.L. 1968. Current Ripples. North-Holland Publ.Co., Amsterdam : 433pp.

Allen, J.R.L. 1970. Physical Processes of Sedimentation. Unwin University Books, London : 248pp.

Allen, J.R.L. 1974. Reaction, relaxation and lag in natural sedimentary systems: General principles, examples and reasons. Earth Sci. Rev. 10: 263-342.

Bachmann, D. 1959. Die Sedimentationswaage, ein neues schreibendes Gerät zur Feinheitsanalyse. Laboratoriumstechnik, Dechema - Monographien 31: 23-51.

Bagnold, R.A. 1956. The flow of cohesionless grains in fluids. Phil.Trans. Roy.Soc., Ser.A 249: 235-297.

Bagnold, R.A. 1966. An approach to the sediment transport problem from general physics. Prof.Pap.U.S.geol.Surv. 422-I: 37pp.

Bagnold, R.A. 1968. Deposition in the process of hydraulic transport. Sedimentology 10: 45-56.

Bang, N.D. 1974. The southern Benguela Current system : Finer oceanic structure and atmospheric determinants. Ph.D. thesis, University of Cape Town (unpublished).

Bascomb, C.L. 1968. A new apparatus for recording particle size distributions. J.sed.Petr. 38: 878-884.

Belderson, R.H., Kenyon, N.H., Stride, A.H., Stubbs, A.R. 1972. Sonographs of the sea floor. Elsevier, Amsterdam : 185pp.

Bennett, R.J. 1976. Adaptive adjustment of channel geometry. Earth Surface Processes 1: 131-150.

Berthois, L. 1962. Étude du comportement hydraulique du mica. Sedimentology 1: 40-49.

Bieneck, B., Huffmann, H., Meder, H. 1965. Korngrössenanalysen mit Hilfe von Sedimentationswaagen. Erdöl und Kohle 18(7): 509-513.

Birch, G.F. 1977a. Surficial sediments on the continental margin off the west coast of South Africa. Marine Geol. 23: 305-337.

Birch, G.F. 1977b. Surficial sediments of Saldanha Bay and Langebaan Lagoon. Trans.Geol.Soc.S.Afr. 79: 293-300.

Birch, G.F. 1977c. Phosphorites from the Saldanha Bay region. Trans.roy.Soc. S.Afr. 42(3/4): 223-240.

Bird, E.C.F. 1972. Coasts. Austr.National Univ.Press, Canberra : 246pp.

Blatt, H., Middleton, G., Murray, R. 1972. Origin of Sedimentary Rocks. Prentice-Hall, New York : 634pp.

Bloom, A.C. and Stuiver, M. 1963. Submergence of the Connecticut coast. Science 139: 332-334.

Boillot, G. 1964. Géologie de la Manche Occidentale. Fonds rocheux, dépôts Quarternaires, sédiments actuels. Ann.Inst.Océanogr. XLII/1: 1-220.

Boothroyd, J.C and Hubbard, D.K. 1974. Bedform development and distribution pattern, Parker and Essex Estuaries, Massachusetts. Coastal Research Centre, Univ. of Massachusetts, Miscellaneous Paper 1-74: 1-39.

Bouma, A.H. 1968. Methods for the Study of Sedimentary Structures. Wiley-Interscience, New York : 458pp.

Bradley, W.H. 1965. Vertical density currents. Science 150: 1423-1428.

Braithwaite, C.J.R. 1973. Settling behaviour related to sieve analysis of skeletal sands. Sedimentology 20: 251-262.

Bremner, J.M. and LeBlond, P.H. 1974. On the planimetric shape of Wreck Bay, Vancouver Is. J.sed.Petr. 44:1155-1165.

Brezina, J. 1969. Granulometer - A sediment analyzer directly writing size distribution curves. J.sed.Petr. 39: 1627-1631.

Broecker, W.S., Thurber, D.L., Goddard, J., Ku, T.-L., Matthews, R.K., Mesolella, K.J. 1968. Milankovitch hypothesis supported by precise dating of coral reefs and deep-sea sediments. Science 159: 297-300.

Brush, L.M. 1965. Sediment sorting in alluvial channels. In: Middleton, G.V. (ed.), Primary Sedimentary Structures and their Hydrodynamic Interpretation. SEPM, Spec.Publ. 12: 25-33.

Buckley, D.E. 1964. Mechanical analysis of macroscopic dispersal systems by means of a settling tube. Bedford Inst.Oceanogr., BIO 64-2: 1-33.

Burgers, J.M. 1941. On the influence of the concentration of a suspension upon the sedimentation velocity. Kon.Ned.Akad.Wetensch., Amsterdam, Proc. 44: 1045-1051 and 1177-1184.

Burgers, J.M. 1942. On the influence of the concentration of a suspension upon the sedimentation velocity. Kon.Ned.Akad.Wetensch., Amsterdam, Proc. 45: 9-16 and 126-128.

Butzer, K.W. and Helgren, D.M. 1972. Late Cenozoic evolution of the Cape coast between Knysna and Cape St. Francis, South Africa. Quat.Res. 2: 143-169.

Carr, E. 1976. Distribution pattern of the intertidal macrofauna at Langebaan Lagoon. B.Sc. (Hons.) project, Dept. of Zoology, Univ.Cape Town (unpl.).

Carver, R.E. 1971. Procedures in Sedimentary Petrology. Wiley-Interscience, New York : 653pp.

Channon, R.D. 1971. The Bristol Fall Column for coarse sediment grading. J.sed.Petr. 41: 867-870.

Chappell, J. 1974. Relationships between sea levels, O^{18} variations and orbital perturbations during the past 250 000 years. Nature 252: 199-202.

Chappell, J. and Polach, H.A. 1972. Some effects of partial recrystallization on ^{14}C dating late Pleistocene corals and molluscs. Quatern.Res. 2: 244-252.

Clifton, E.H., Hunter,R., Phillips, R. 1971. Depositional structures and processes in the non-barred high-energy nearshore. J.sed.Petr. 41: 651-670.

Clowes, A.J. 1950. An introduction to the hydrology of South African waters. Fish.Mar.Biol.Surv.Div., Investigational Report 12: 1-28.

Coetzee, J.A. 1967. Pollenanalytical studies in East and Southern Africa. Palaeoecology of Africa 3: 1-146.

Conybeare, C.E.B. and Crook, K.A.W. 1968. Manual of Sedimentary Structures. Bureau of Mineral Resources, Geology and Geophysics, Commonwealth of Australia, Bulletin No. 102: 1-327.

Cook, D.O. 1966. The probable error of sampling shallow marine sediments for textural analysis. Unpubl. Research Paper in Geology, Univ. of Southern California : 13pp.

Cook, D.O. 1969. Calibration of the University of Southern California automatically recording settling tube system. J.sed.Petr. 39: 781-786.

Cook, D.O. 1971. Depression in shallow marine sediment made by benthic fish. J.sed.Petr. 41: 577-578.

Davies, J.L. 1958. Wave refraction and the evolution of shoreline curves. Geophys. Studies 5.

Davies, J.L. 1964. A morphogenic approach to world shorelines. Zeitschr. f.Geomorph. 8: 127-142.

Davies, J.L. 1972. Geographical Variation in Coastal Development. Oliver & Boyd, Edinburgh.

Davies, O. 1973. Pleistocene shorelines in the western Cape and South west Africa. Ann.Ntl.Mus. 21: 719-765.

Day, J.H. 1959. The biology of Langebaan Lagoon : a study of the effect of shelter from wave action. Trans.roy.Soc.S.Afr. 35: 475-547.

Day, J.H. 1969. A Guide to Marine Life on South African Shores. Balkema, Cape Town, 300pp.

Dingle, R.V. 1971. The geology of the continental shelf between Lüderitz and Cape Town (South West Africa) with special reference to Tertiary strata. SANCOR Marine Geology Programme, Techn.Rep. 4: 14-37.

Doeglas, D.J. 1964. Interpretation of the results of mechanical analysis. J.sed.Petr. 16: 19-40.

Doeglas, D.J. 1968. Grain-size indices, classification and environment. Sedimentology 10: 83-100.

Dunbar, C.O. and Rogers, J. 1957. Principles of Stratigraphy. Wiley & Sons, New York : 356pp.

Duncan, C.P. and Nell, J.H. 1969. Surface currents off the Cape Coast. Div. Sea Fish.Investigational Report 76: 1-19.

Dunham, R.J. 1962. Classification of carbonate rocks according to depositional texture. In: Ham, W.E. (ed.), Classification of Carbonate Rocks. AAPG, Memoir 1: 108-121.

Du Plessis, A. and De la Cruz, A. 1977. Geophysical investigations in Saldanha Bay. Trans.roy.Soc.S.Afr. 42: 285-302.

Du Toit, A.L. 1917. Report on the phosphates of Saldanha Bay. Mem.geol.Surv. S.Afr. 10: 1-38.

Einsele, G. and Werner, F. 1972. Sedimentary processes at the entrance Gulf of Aden / Red Sea. "Meteor" Forsch.-Ergeb., Reihe C, 10: 39-62½

Einsele, G., Herm, D., Schwarz, H.U. 1974. Holocene eustatic (?) sea level fluctuations at the coast of Mauritania. "Meteor" Forsch.-Ergeb., Reihe C, 18: 43-62.

Emery, K.O. 1938. Rapid method of mechanical analysis of sand. J.sed.Petr. 8: 105-111.

Elouard, P. 1968. Le Nouakchottien, étage du Quaternaire de Mauritanie. Ann.Fac.Sc.Dakar 22: 121-138.

Emery, K.O. and Stevenson, R.E. 1950. Laminated beach sand. J.sed.Petr. 20: 220-223.

Emery, K.O. and Stevenson, R.E. 1957. Estuaries and Lagoons. I. Physical and chemical characteristics. Geol.Soc.Am. Memoir 67: 673-749.

Emiliani, C. 1955. Pleistocene temperatures. J.Geol. 63: 538-578.

Evans, G. 1965. Intertidal flat sediments and their environments of deposition in the Wash. Quart.J.Geol.Soc.London 121: 209-241.

Fairbridge, R.W. 1961. Eustatic changes of sea-level. Physics and Chemistry of the Earth Vol. 4, Pergamon Press, Oxford.

Fairbridge, R.W. 1971. Quaternary shoreline problems at Inqua, 1069. Quaternaria 15: 1-18.

Felix, D.W. 1969. An inexpensive recording settling tube for analysis of sands. J.sed.Petr. 39: 777-780.

Ferguson, R.I. 1973. Regular meander paths. Water Res. Research 9: 1079-1086.

Flemming, B.W. 1976a. Side-scan sonar : a practical guide. Int.Hydrogr.Rev. 53: 65-92.

Flemming, B.W. 1976b. Rocky Bank - evidence for a relict wave-cut platform. Ann.S.Afr.Mus. 71: 33-48.

Flemming, B.W. 1977a. Distribution of Recent sediments in Saldanha Bay and Langebaan Lagoon. Trans.roy.Soc.S.Afr. 42: 317-340.

Flemming, B.W. 1977b. Langebaan Lagoon - A mixed carbonate-siliclastic tidal environment in a semi-arid climate. Sed.Geol. 18: 61-95.

Flemming, B.W. and Wefer, G. 1973. Tauchbeobachtungen an Wellenrippeln und Abrasionserscheinungen in der Westlichen Ostsee südöstlich Bokniseck. Meyniana 23: 9-18.

Flemming, B.W. 1977c. Underwater sand dunes along the southeast African continental margin - observations and implications. Mar.Geol. (in press).

Folk, R.L. 1951. Stages of textural maturity in sedimentary rocks. J.sed.Petr. 21: 127-130.

Folk, R.L. 1965. Petrology of Carbonate Rocks. In: Petrology of Sedimentary Rocks. Hemphills, Austin : 159pp.

Folk, R.L. 1966. A review of grain-size parameters. Sedimentology 6: 73-93.

Folk, R.L. 1968. Petrology of Sedimentary Rocks. Hemphills, Austin: 170pp.

Folk, R.L. and Ward, W.C. 1957. Brazos River bar : A study in the significance of grain size parameters. J.sed.Petr. 27: 3-26.

Folk, R.L. and Robles, R. 1964. Carbonate sediments of Isla Perez, Alacran Reef Complex, Yucatan. J.Geol. 72: 255-292.

Fontein, F.J. 1960. Separation of solids particles according to size, shape or specific gravity in a wet medium. Geol.Mijnb. 39: 227-243.

Force, L.M. 1969. Calcium carbonate size distribution on the West Florida Shelf and experimental studies on the microarchitectural control of skeletal breakdown. J.sed.Petr. 39: 902-934.

Friedman, G.M. 1961. Distinction between dune, beach, and river sands from their textural characteristics. J.sed.Petr. 31: 514-529.

Friedman, G.M. 1962. On sorting, sorting coefficients, and lognormality of the grain-size distribution of sandstones. J.Geol. 70: 737-753.

Füchtbauer, H. 1959. Zur Nomenklatur der Sedimentgesteine. Erdöl und Kohle 12: 605-613.

Gaudette, H.E., Flight, W.R., Toner, L., Folger, D.W. 1974. An inexpensive titration method for the determination of organic carbon in Recent sediments. J.sed.Petr. 44: 249-253.

Gessler, J. 1970. Self-stabilizing tendencies of alluvial channels. ASCE, 96 (WW2).

Gibbs, R.J. 1972. The accuracy of particle-size analysis utilizing settling tubes. J.sed.Petr. 42: 141-145.

Gibbs, R.J. 1974. A settling tube system for sand-size analysis. J.sed.Petr. 44: 583-588.

Gibbs, R.J., Matthew, M.D., Link, D.A. 1971. The relationship between sphere size and settling velocity. J.sed.Petr. 41: 7-18.

Ginsburg, R.N. (ed.) 1975. Tidal Deposits. Springer-Verlag, Berlin : 428pp.

Ginsburg, R.N. and James, N.P. 1974. Holocene carbonate sediments of continental shelves. In: Burk, C.A. and Drake, C.L. (eds.), The Geology of Continental Margins : 137-156.

Graf, W.H. 1971. Hydraulics of Sediment Transport. McGraw-Hill, New York : 513pp.

Graf, W.H. and Acaroglu, E.R. 1966. Settling velocities of natural grains. Bull.Int.Ass.Sci.Hydraul. 11: 27-43.

Graf, J.B. 1976. Comparison of measured and predicted nearshore sediment grain-size distribution patterns, southwestern Lake Michigan, U.S.A.. Marine Geol. 22: 253-270.

Griffiths, J.C. 1951. Size versus sorting in some Caribbean sediments. J.Geol. 59: 211-243.

Griffiths, J.C. 1961. Measurement of the properties of sediments. J.Geol. 69: 487-498.

Griffiths, J.C. 1967. Scientific Method in Analysis of Sediments. McGraw-Hill, New York : 570pp.

Guilcher, A. 1969. Pleistocene and Holocene sea level changes. Earth Sci.Rev. 5: 69-97.

Gust, G. and Walger, E. 1976. The influence of suspended cohesive sediments on boundary-layer structure and erosive activity of turbulent seawater flow. Mar.Geol. 22: 189-206.

Hagan, G.M. and Logan, B.W. 1975. Prograding tidal-flat sequences : Hutchinson Embayment, Shark Bay, Western Australia. In: Ginsburg, R.N. (ed.), Tidal Deposits. Springer-Verlag, Berlin : 215-222.

Hammen, Th.v.d., Maarleveld, G.C., Vogel, J.C. Zagwijn, W.H. 1967. Stratigraphy , climatic succession and radiocarbon dating of the last glacial in the Netherlands. Geol.Mijnb. 46: 79-95.

Häntzschel, W. 1938. Bau und Bildung von Gross-Rippeln im Watten-Meer. Senckenbergiana 20: 1-42.

Harms, J.C. and Fahnenstock, R.K. 1965. Stratification, bed forms, and flow phenomena (with an example from the Rio Grande). In: Middleton, G.V. (ed.), Primary Sedimentary Structures and their Hydrodynamic Interpretation. SEPM, Spec.Publ. 12: 84-115.

Haughton, S.H. 1932. The late Tertiary and Recent deposits of the west coast of South Africa. Trans.Geol.Soc.S.Afr. 34: 19-57.

Haughton, S.H. 1969. Geological History of Southern Africa. Geol.Soc.S.Afr., Cape & Transvaal Printers, Cape Town : 535pp.

Hedgepeth, J.W. 1957. Classification of Marine Environments. Geol.Soc.Am. Memoir 67: 17-27.

Hendy, Q.B. 1970. A review of the geology and palaeontology of the Plio-/Pleistocene deposits at Langebaanweg, Cape Province. Ann.S.Afr.Mus. 56: 75-113.

Hjulström, F. 1935. Studies of the morphological activity of rivers as illustrated by the river Fyris. Bull.Geol.Inst.Univ.Uppsala 25: 221-527.

Horikawa, K. and Sunamura, T. 1970. A study of erosion of coastal cliffs and submarine bedrocks. Coastal Eng. in Japan 13: 127-139.

Howard, J.D., Mayou, T.V., Heard, R.W. 1977. Biogenic sedimentary structures formed by rays. J.sed.Petr. 47: 339-346.

Hoyt, J.H. 1967. Barrier Island formation. Geol.Soc.Am.Bull. 78: 1125-1136.

Humphries, D.W. 1961. A non-laminated miniature sample splitter. J.sed.Petr. 31: 471-473.

Imbrie, J. and Buchanan, H. 1965. Sedimentary structures in modern carbonate sands of the Bahamas. In: Middleton, G.V. (ed.), Primary Sedimentary Structures and their Hydrodynamic Interpretation. SEPM, Spec.Publ. 12: 149-172.

Inman, D.L. 1949. Sorting of sediments in the light of fluid mechanics. J.sed.Petr. 19: 51-70.

Jakobsen, B. 1962. The formation of ebb and flood channels in tidal channels described on basis of morphological and hydrological observations. Geogr. Tidsskr. 61.

Janke, N.C. 1965. Empirical formula for velocities and Reynolds Numbers of single settling spheres. J.sed.Petr. 35: 749-750.

Janke, N.C. 1966. Effect of shape upon the settling velocity of regular convex geometric particles. J.sed.Petr. 36: 370-376.

Jennings, J.N. 1955. The influence of wave action on coastal outline in plan. Austr. Geogr. 6: 36-44

Johnson, J.W. and Eagleson, P.S. 1966. Coastal Processes. In: Ippen, A.T. (ed.), Estuary and Coastline Hydrodynamics. McGraw-Hill, New York : 404-492.

Jones, J.R. and Cameron, B. 1976. Comparison between sieving and settling-tube determinations of sand sizes by using discriminant function analysis. Geology 4: 741-744.

Jopling, A.V. 1965. Laboratory Study of the distribution of grain sizes in cross-bedded deposits. In: Middleton, G.V. (ed.), Primary Sedimentary Structures and their Hydrodynamic Interpretation. SEPM, Spec.Publ. 12: 53-65.

Kennedy, W.Q. 1951. Sedimentary differentiation as a factor in the Moine-Torridonian correlation. Geol.Mag. 88: 257-261.

Kennedy, J.F. and Koh, R.C.Y. 1961. The relation between the frequency distributions of sieve diameters and fall velocities of sediment particles. J.Geophys.Res. 66: 4233-4246.

Kensley, B.F. 1976. A late Pleistocene raised beach from Milnerton, Cape. Conf. on Recent Progress in Later Cenozoic Studies in Southern Africa, S.Afr.Mus., Cape Town.

Kensley, B.F. 1972. Pliocene marine invertebrates from Langebaanweg, Cape Province. Ann.S.Afr.Mus. 60: 173-190.

King, C.A.M. 1974. Introduction to Marine Geology and Geomorphology. Edward Arnold, London : 309pp.

Klein, G.deVries 1970. Depositional and dispersal dynamics of intertidal sand bars. J.sed.Petr. 40: 1095-1127.

Klein, G. de Vries 1975. Epilogue. In: Ginsburg, R.N. (ed.), Tidal Deposits. Springer-Verlag, Berlin : 407-410.

Klein, G. de Vries 1976. Holocene Tidal Sedimentation. Benchmark Papers in Geology Vol. 50, Dowden, Hutchinson & Ross, Stroudsburg.

Kluger, J.W. 1972. Saldanha Bay - Wave Studies. CSIR Hydraulics Research Unit, Report MEG 1009.

Komar, P.D. 1976. Beach Processes and Sedimentation. Prentice-Hall, New Yersey.

Komar, P.D. and Miller, M.C. 1973. The threshold of sediment movement under oscillatory water waves. J.sed.Petr. 43: 1101-1110.

Kondrat'ev, N.E. 1953. Calculations of Wind Waves and Modifications of Reservoir Banks. Gidrometeoizdat, Moscow.

Koopmann, B. 1975. Siltmergel und Schillsande in der nördlichen Baie du Levrier (Mauretanien). Unpl. M.Sc. thesis, University of Kiel, FRG : 51pp.

Korringa, P. 1956. Oyster culture in South Africa. Investigational Report, Div.Sea Fish.S.Afr. 20: 1-86.

Krige, A.V. 1927. An examination of the Tertiary and Quaternary changes of sea-level in South Africa, with special stress on the evidence in favour of a recent world-wide sinking ocean level. Annals Univ. Stellenbosch V, Section A: 1-81.

Krumbein, W.C. 1934. The probable error of sampling for mechanical analysis. Am.J.Sci. 27: 204-214.

Krumbein, W.C. 1937. Sediments and exponential curves. J.Geol. 45: 577-601.

Krumbein, W.C. and Aberdeen, E. 1937. The sediments of Barataria Bay. J.sed. Petr. 7: 3-17.

Krumbein, W.C. and Pettijohn, F.J. 1938. Manual of Sedimentary Petrography. D.Appleton-Century, New York : 549pp.

Krumbein, W.C. 1942. Settling-velocity and flume-behaviour of non-spherical particles. Trans.Am.Geophys.Union 23: 621-632.

Krumbein, W.C. and Sloss, L.L. 1963. Stratigraphy and Sedimentation. Freeman, San Francisco : 660pp.

Kuenen, P.H. 1968. Settling convection and grain-size analysis. J.sed.Petr. 38: 817-831.

Larsonneur, C. 1975. Tidal deposits, Mont Saint-Michel Bay, France. In: Ginsburg, R.N. (ed.), Tidal Deposits. Springer-Verlag, New York, 21-30.

Lawson, R.I. and Day, G.F. 1969. Note on a non-laminated joint-free sample splitter. J.sed.Petr. 39: 373-375.

LeBlond, P.H. 1972. On the formation of spiral beaches. 13th Coastal Eng. Conf., Vancouver, Canada, Proceedings Vol. II: 1331-1345.

Lees, A. 1975. Possible influence of salinity and temperature on modern shelf carbonate sedimentation. Mar.Geol. 19: 159-198.

Lees, A. and Buller, A.T. 1972. Modern temperate-water and warm-water shelf carbonate sediments contrasted. Mar.Geol. 13: M67-M73.

Leont'yev, O.K. and Nikiforov, L.G. 1965. Reasons for the world-wide occurrence of barrier beaches. Oceanology 5: 61-67.

Leopold, L.B. and Maddock, T. 1953. The hydraulic geometry of stream channels and some physiographic implications. U.S.Geol.Surv.Prof.Paper 252.

Levy, Y. 1977. Description and mode of formation of the supra-tidal evaporite facies in Northern Sinai coastal plain. J.sed.Pter. 47: 463-474.

Ludwick, J.C. and Henderson, P.L. 1968. Particle shape and inference of size from sieving. Sedimentology 11: 197-235.

Mabbutt, J.A. 1956. The physiography and surface geology of the Hopefield fossil site. Trans.roy.Soc.S.Afr. 35: 21-58.

Maiklem, W.C. 1968. Some hydraulic properties of bioclastic carbonate grains. Sedimentology 10: 101-109.

Marchillon, E.K., Clamen, A., Gauvin, W.H. 1964. Oscillatory motion of freely falling disks. Phys.Fluids 7(12).

Martin, A.R.H. 1962. Evidence relating to the Quaternary history of the Wilderness lakes. Trans.Geol.Soc.S.Afr. 65: 19-42.

Martin, A.R.H. 1968. Pollen analysis of Groenvlei lake sediments, Knysna. Rev.Palaeobotany and Palynology 7: 107-144.

McKinney, C.R. and Silver, L.T. 1956. A joint-free sample splitter. Am. Mineralogist 41: 521-523.

McNown, J.S. and Malaika, J. 1950. Effects of particle shape on settling velocities at low Reynolds Numbers. Trans.Am.geophys.Union 31: 74-82.

McNown, J.S., Malaika, J., Pramanik, H. 1951. Particle shape and settling velocity. Proc. 4th Meeting Int.Ass.Hydr.Res., Bombay.

McNown, J.S. and Lin, P.N. 1952. Sediment concentration and settling velocity. Proc. 2nd Conf.Fluid Mechanics, Ohio State Univ. : 401-411.

Menard, H.W. 1950. Sediment movement in relation to current velocity. J.sed. Petr. 20: 148-160.

Menard, H., Dill, R., Hamilton, E., Moore, D., Shumway, G., Silverman, M., Stewart, H. 1954. Underwater mapping by Diving Geologists. AAPG Bull. 38: 129-147.

Middleton, G.V. 1967. Experiments on density and turbidity currents.3.The deposition of sediments. Can.J.Earth Sci. 4: 475-525.

Milliman, J.D. and Emery, K.O. 1968. Sea levels during the last 35 000 years. Science 162: 1121-1123.

Mitzutani, S. 1963. A theoretical and experimental consideration on the accuracy of sieving analysis. J.Earth Sci., Nagoya Univ. 11: 1-27.

Moore, R.C. 1949. Meaning of Facies. Geol.Soc.Am.Memoir 39: 1-34.

Moore, D.G. and Scruton, P.C. 1957. Minor internal structures of some recent unconsolidated sediments. AAPG Bull. 41: 2723-2751.

Moreland, C. 1963. Settling velocities of coal particles. Can.J.Chem.Eng. 41.

Morgans, J.F.S. 1956. Notes on the analysis of shallow-water soft substrata. J.Anim.Ecol. 25: 367-387.

Mörner, N.-A. 1971a. The Holocene sea level problem. Geol.Mijnb. 50: 699-702.

Mörner, N.-A. 1971b. The position of the ocean level during the interstadial at about 30 000 B.P. - a discussion from a climatic-glaciogenic point of view. Can.J.Earth Sci. 8: 132-143.

Mörner, N.-A. 1973. Climatic changes during the last 35 000 years as indicated by land, sea and air data. Boreas 2: 33-54.

Müller, G. 1967. Methods in Sedimentary Petrology. Schweizerbart, Stuttgart:283pp.

Munch-Peterson, R. 1950. Littoral drift formula. Bull. Beach Erosion Board 4: 1-31.

Murray, L.G., Joint, R.H., O'Shea, D.O.C., Foster, R.W., Kleinjan, L. 1970. The geological environment of some diamond deposits off the coast of South West Africa. In: Delany, F.M. (ed.), The geology of the East Atlantic continentla margin. 1. General and Economic Papers. Rept.Inst.geol.Sci. 70: 119-141.

Nelsen, T.A. 1974. An automated rapid sediment analyzer (ARSA). NOAA Techn. Memorandum ERL AOML-21: 26pp.

Nelson, C.S. 1977. Grain-size parameters of insoluble residues in mixed terrigenous-skeletal carbonate sediments and sedimentary rocks: some New Zealand examples. Sedimentology 24: 31-52.

Newman, W.S. and Rusnack, G.A. 1965. Holocene submergence of the eastern shore of Virginia. Science 148 (3676): 1464-1466.

Odén, S. 1915. Eine neue Methode zur mechanischen Bodenanalyse. Int Mitt. Bodenk. 5: 257-311.

Olausson, E. 1975. Methods for the chemical analysis of sediments. Manual of Methods in Aquatic Environment Research. Part I. FAO Fisheries Techn.Paper No. 137: 201-211.

Otto, G.H. 1933. Comparative tests of several methods of sampling heavy mineral concentrates. J.sed.Petr. 3: 30-39.

Page, H.G. 1955. Phi-millimetre conversion table. J.sed,Petr. 25: 258-292.

Parker, R,J. 1968. Eustatic shorelines of Saldanha Bay. Unpubl. B.Sc.(Hons.) project, University of Cape Town, 77pp.

Passega, R. 1957. Texture as characteristic of clastic deposits. AAPG Bull. 41: 1952-1984.

Passega, R. 1964. Grain size representation by CM patterns as a geological tool. J.sed.Petr. 34: 830-847.

Passega, R., Rizzini, A., Borghetti, G. 1967. Transport of sediment by waves, Adriatic coastal shelf, Italy. AAPG Bull. 51: 1304-1319.

Passega, R. and Byramjee, R. 1969. Grain-size image of clastic deposits. Sedimentology 13: 233-252.

Pearce, A.F. and Smith, D.W. 1974. Oceanographic survey off Saldanha Bay. NRIO (CSIR) Internal Report IG 74/12: 6pp.

Pettijohn, F.J. 1957. Sedimentary Rocks. Harper & Row, New York : 718pp.

Pettijohn, F.J. and Potter, P.E. 1964. Atlas and Glossary of Primary Sedimentary Structures. Springer-Verlag,Berlin: 370pp.

Pettijohn, F.J., Potter, P.E., Siever, R. 1972. Sand and Sandstone. Springer-Verlag, Berlin : 618pp.

Pettyjohn, E.S. and Christiansen, E.B. 1948. Effect of particle shape on free-settling rates of isometric particles. Chem.Eng.Progr. 44(2).

Phleger, F.B. 1969. Some general features of coastal lagoons. In: Castanares, A.A. and Phleger, F.B. (eds.), Coastal Lagoons, a Symposium. Universidad Nacional Autónoma, Mexico : 5-26.

Phleger, F.B. and Ewing, G.C. 1962. Sedimentology and oceanography of coastal lagoons in Baja California, Mexico. Geol.Soc.Am.Bull. 73: 145-182.

Plankeel, F.H. 1962. An improved sedimentation balance. Sedimentology 1: 158-163.

Poole, D.M. 1957. Size analysis of sand by sedimentation techniques. J.sed.Petr. 27: 460-468.

Potter, P.E. 1959. Facies model conference. Science 129: 1292-1294.

Prandtl, L. 1956. Führer durch die Strömungslehre. Vieweg Verlag, Braunschweig.

Prandtl, L. and Tietjens, O.G. 1934. Applied Hydro and Aeromechanics. Dover, New York.

Purdy, E.G. 1963. Recent calcium carbonate facies of the Great Bahama Bank, 1. Petrography and reaction groups. 2. Sedimentary facies. J.Geol. 71: 334-355 and 472-497.

Rabatin, J.G. and Gale, R.H. 1956. Determination of particle size with a simple recording sedimentation balance. Analyt.Chem. 28: 1314-1316.

Randazzo, A.F., Stone, G.C., Sarop, H.C. 1977. Diagenesis of Middle and Upper Eocene carbonate shoreline sequences, Central Florida. AAPG Bull. 61: 492-503.

Raudkivi, A.J. 1976. Loose Boundary Hydraulics. Pergamon, Oxford : 397pp.

Redfield, A.C. 1950. The analysis of tidal phenomena in narrow embayments. Papers in Physical Oceanography and Meteorol., MIT and Woods Hole Oceanogr. Inst. 11: 1-36.

Redfield, A.C. and Rubin, M. 1962. The age of saltmarsh peat and its relation to recent changes in sea level at Barnstable, Mass. Proc. Nat.Acad.Sci. 48: 1728-1735.

Reed, W.E., Le Fever, R., Moir, G.J. 1975. Depositional environment interpretation from settling velocity (Psi) distributions. Geol.Soc.Am.Bull. 86: 1321-1328.

Reiche, P. 1950. A survey of weathering processes and products. Univ.New Mexico Publ.Geol. 3: 1-95.

Reineck, H.-E. 1962. Reliefgüsse ungestörter Sandproben. Z.Pflanzenernähr., Düngung, Bodenkde. 99: 151-153.

Reineck, H.-E. 1963. Sedimentgefüge im Bereich der südlichen Nordsee. Abh.senckenbergische naturforsch.Gesellsch. 505: 1-138.

Reineck, H.-E. (ed.) 1970. Das Watt - Ablagerungs- und Lebensraum. Waldemar Kramer, Frankfurt a.M. : 142pp.

Reineck, H.-E. and Wunderlich, F. 1968. Classification and origin of flaser and lenticular bedding. Sedimentology 11: 99-104.

Reineck, H.-E. and Rosenboom, W. 1969. Stechkästen zur Entnahme von Watten- und Unterwasserproben. Natur und Museum 99: 45-55.

Reineck, H.-E. and Singh, I.B. 1972. Genesis of laminated sand and graded rhythmites in storm-sand layers of shelf mud. Sedimentology 18: 123-128.

Reineck, H.-E. and Singh, I.B. 1973. Depositional Sedimentary Environments. Springer-Verlag, Berlin : 439pp.

Retief, G. 1977. Tide Recordings - Langebaan Lagoon. Final Report for 6th General Meeting of Committee for Ecological Studies in the Langebaan Lagoon Area.

Richards, et al. 1970. Velocity of Galena and Quartz falling through water. Am.Inst.Mining Eng. 38.

Richter, R. 1936. Marken und Spuren im Hunsrückschiefer. II. Schichtung und Grundleben. Senckenbergiana 18: 215-244.

Riedl, R. 1968. Die Tauchmethode, ihre Aufgaben und Leistungen bei der Erforschung des Litorals; eine kritische Untersuchung. Helgol.wiss. Meeresunters. 15: 294-352.

Rigby, J.K. and Hamblin, W.K. 1972. Recognition of Ancient Sedimentary Environments. SEPM, Spec.Publ. 16: 130pp.

Rittenhouse, G. 1943. The transportation and deposition of heavy minerals. Geol.Soc.Am.Bull. 54: 1725-1780.

Rouse, H. 1936. Nomogram for the settling velocity of spheres. Nat.Res. Council Comm. on Sedimentation Publ. : 57-64.

Rubey, W. 1933. Settling velocities of gravel, sand and silt particles. Am.J.Sci. 25: 325-338.

Rusnack, G.A. 1960. Sediments of Laguna Madre, Texas. In: Shepard, F.P., Phleger,F.B., Van Andel, T.H. (eds.), Recent Sediments, Northwest Gulf of Mexico. AAPG, Tulsa, Oklahoma : 153-196.

Sahu, B. 1965. Theory of sieving. J.sed.Petr. 35: 750-753.

Sanford, R.S. and Swift, D.J.P. 1971. Comparison of sieving and settling techniques for size analysis using a Benthos Rapid Sediment Analyzer. Sedimentology 17: 257-264.

Sarnthein, M. 1971. Oberflächensedimente im Persischen Golf und Golf von Oman. II. Quantitative Komponentenanalyse der Grogfraktion. "Meteor" Forsch.-Ergebn., Reihe C, No. 5: 1-113.

Schäfer, W. 1956. Wirkungen der Benthos-Organismen auf den jungen Schichtverband. Senckenbergiana Lethaea 37: 183-263.

Schäfer, W. 1962. Aktuo-Paläontologie nach Studien in der Nordsee. Waldemar Kramer, Frankfurt a.M. : 666pp.

Schalke, H.J.W.G. 1973. The upper Quaternary of the Cape Flats area. Scripta Geol. 15: 1-55.

Schiller, L. 1932. Fallversuche mit Kugeln und Scheiben. Handbuch der Experimental-Physik IV/2, Akademische Verlagsgesellschaft, Leipzig.

Schlee, J. 1966. A modified Woods Hole rapid sediment analyzer. J.sed.Petr. 36: 403-413.

Schofield, J.C. 1964. Postglacial sea levels and isostatic uplift. N.Z.J. Geol.Geophys. 7: 359-370.

Scholl, D.W. and Stuiver, M. 1967. Recent submergence of South Florida; a comparison with adjacent coasts and other eustatic data. Geol.Soc.Am. Bull. 78: 437-454.

Schou, A. 1967. Estuarine research in the Danish moraine archipelago. In: Lauff, G.H. (ed.), Estuaries. Am.Ass.Adv.Sci.Publ. 83: 129-145.

Schulz, E.F., Wilde, R.H., Albertson, M.L. 1954. Influence of shape on the fall velocity of sedimentary particles. Missouri River Div.Corps Eng., U.S.Army, Sediment Ser. 5: 161pp.

Schulze, B.R. 1965. Climate of South Africa. Part 8. General Survey. W.B.28, Govt.Printer and Weather Bureau, Pretoria : 330pp.

Schumm, S.A. and Lichty, R.W. 1965. Time, space, and causality in geomorphology. Am.J.Sci. 263: 110-119.

Scott, J.S., Field, D.E., Colbett, L.S., Jones, F.W., Meilleur, A.G. 1963. Rapid sediment analyzer. Geol.Surv.Can.Prof.Paper 63-2, 41.Project : 19-20.

Seibold, E. 1963. Geological investigation of nearshore sand transport. In: Sears, M. (ed.), Progress in Oceanography 1: 1-70.

Seilacher, A. 1953. Studien zur Palichnologie. Neues Jahrb.Geol.Palaeontol., Abhandl. 96: 421-452.

Seilacher, A. 1954. Die geologische Bedeutung fossiler Lebensspuren. Z.Deut.Geol.Ges. 105: 214-227.

Seilacher, A. 1964. Biogenic sedimentary structures. In: Imbrie, J. and Newell, N. (eds.), Approaches to Paleoecology. Wiley & Sons, New York : 296-316.

Selley, R.C. 1970. Ancient Sedimentary Environments. Chapman & Hall, London : 237pp.

Sengupta, S. and Veenstra, H.J. 1968. On sieving and settling techniques for sand analysis. Sedimentology 11: 83-98.

Seward-Thompson, B.L. and Hails, J.R. 1973. An appraisal of the computation of statistical parameters in grain size analysis. Sedimentology 20: 161-169.

Shackleton, N.J. and Opdyke, N.D. 1973. Oxygen isotope and palaeomagnetic stratigraphy of Equatorial Pacific Core V28-238 : Oxygen isotope temperatures and ice volumes on a 10^5 year to 10^6 year scale. Quatern. Res. 3: 39-55.

Shannon, L.V. and Stander, G.H. 1977. Physical and Chemical characteristics of water in Saldanha Bay and Langebaan Lagoon. Trans.roy.Soc.S.Afr. 42: 441-459.

Shen, H.W. 1971. River Mechanics. H.W. Shen, Fort Collins, Colorado.

Shepard, F.P. 1954. Nomenclature based on sand-silt-clay ratios. J.sed.Petr. 24: 151-158.

Shepard, F.P. 1956. Marginal sediments of Mississippi Delta. AAPG, Bull. 40: 2537-2623.

Shepard, F.P. and Moore, D.G. 1954. Sedimentary environments differentiated by coarse-fraction studies. AAPG Bull. 38: 1792-1802.

Shepard, F.P. and Moore, D.G. 1955. Central Texas coast sedimentation : characteristics of sedimentary environment, recent history, and diagenesis. AAPG Bull. 39: 1463-1593.

Shepard, F.P. and Young, R. 1961. Distinguishing between beach and dune sands. J.sed.Petr. 31: 196-214.

Shepard, F.P. and Curray, J.R. 1967. Carbon 14 determinations of dea-level change in stable areas. In: Sears, M. (ed.), Progress in Oceanography 4.

Shields, A. 1935. Anwendung der Ähnlichkeitsmechanik und der Turbulenzforschung auf die Geschiebebewegung. Mitt.Preuss.Versuchsanst.f.Wasserbau und Schiffbau, Berlin, Heft 26: 1-26.

Siesser, W.G. 1972. Abundance and distribution of carbonate constituents in some South African coastal and offshore limestones. Trans.roy.Soc.S.Afr. 40: 261-277.

Siesser, W.G. 1974. Relict and Recent beachrock from Southern Africa. Geol. Soc.Am.Bull. 85: 1849-1854.

Siesser, W.G. 1975. Dolostone at Saldanha Bay : evidence for Pleistocene desiccation. Trans.Geol.Soc.S.Afr. 78: 361-365.

Siesser, W.G. and Rogers, J. 1970. An investigation of the suitability of four methods used in routine carbonate analysis of marine sediments. Deep-Sea Res. 18: 135-139.

Sigl, W. 1973. Der Golf von Manfredonia (Südliche Adria). I. Fazielle Differenzierung der Sedimente. Senckenbergiana marit. 5: 3-49.

Silvester, R. 1960. Stabilization of sedimentary coastlines. Nature 188: 467-469.

Silvester, R. 1970. Growth of crenulate shaped bays to equilibrium. ASCE Proc. 96 (WW2): 275-287.

Silvester, R. 1974. Coastal Engineering. II. Sedimentation, estuaries, tides, effluents, and modelling. Elsevier, Amsterdam.

Simons, D.B. and Richardson, E.V. 1962. Resistance to flow in alluvial channels. ASCE, Trans. 127: 927-953.

Simons, D.B., Richardson, E.V., Nordin, C.F. 1965. Sedimentary structures generated by flow in alluvial channels. In: Middleton, G.V. (ed.), Primary Sedimentary Structures and their Hydrodynamic Interpretation. SEPM, Spec.Publ. 12: 34-52.

Skolnik, H. 1959. An inexpensive sample splitter. J.sed.Petr. 29: 116-117.

Southard, J.B. 1975. Bed configurations. In: Harms et al. (eds.), Depositional environments as interpreted from primary sedimentary structures and stratification sequences. SEPM, Short course Lecture Notes 2: 5-43.

Steinbeck, J. 1951. The Log from the Sea of Cortez. Viking Press, New York : 282pp.

Straaten, L.M.J.U. van 1953. Megarippels in the Dutch Wadden Sea and in the Basin of Archachon (France). Geol.Mijnb. 15: 1-11.

Stringham, G.E., Simons, D.B., Guy, H.P. 1969. The behaviour of large particles falling in quiescent liquids. Prof.Paper U.S.geol.Surv. 562-C: 36pp.

Stuiver, M. and Daddario, J.J. 1963. Submergence of the New Yersey coast. Science 142: 951.

Sundborg, A. 1956. The River Klarälven : a study offluvial processes. Geograf. Ann. 38: 127-316.

Swift, D.J.P. 1970. Quaternary shelves and the return to grade. Mar.Geol. 8: 5-30.

Swift, D.J.P. and Ludwick, J.C. 1976. Substrate response to hydraulic process : grain-size frequency distribution and bedforms. In: Stanley, D.J. and Swift, D.J.P. (eds.), Marine sediment transport and environmental Management. Wiley-Interscience, New York : 602pp.

Talbot, W.J. 1947. Swartland and Sandveld. Oxford University Press, Cape Town.

Tankard, A.J. 1974. Varswater Formation of the Langebaanweg - Saldanha area, Cape Province. Trans.Geol.Soc.S.Afr. 77: 265-283.

Tankard, A.J. 1975a. Thermally anomalous late Pleistocene molluscs from the south-western Cape Province, South Africa. Ann.S.Afr.Mus. 69: 17-45.

Tankard, A.J. 1975b. Petrology and origin of the phosphorites and aluminum Phosphate rock of the Langebaanweg - Saldanha area, southwestern Cape Province. Ann.S.Afr.Mus. 65: 217-249.

Tankard, A.J. 1976. Pleistocene history and coastal morphology of the Ysterfontein - Elandsbaai area, Cape Province. Ann.S.Afr.Mus. 69: 73-119.

Tanner, W.F. 1976. Discussion : On the planimetric shape of Wreck Bay, Vancouver Is. - By J.M. Bremner and P.H. LeBlond. J.sed.Petr. 44: 1155-1165.

Teichert, C. 1958. Concept of Facies. AAPG Bull. 42: 2718-2744.

Teleki, P.G. 1972. Wave boundary layers and their relation to sediment transport. In: Swift,D.J.P., Duane, D.B., Pilkey, O.H. (eds.), Shelf Sediment Transport : Process and Pattern. Dowden, Hutchinson & Ross, Stroudsburg : 21-59.

Thom, B.G. 1973. The dilemna of high interstadial sea levels during the last glaciation. Progress in Geogr. 5: 167-246.

Thom, B.G. and Chappell, J. 1975. Holocene sea levels relative to Australia. Search 6: 90-93.

Trask, P. 1932. Origin and environment of source sediments of Pretoleum. Houston, Texas : 323pp.

Tyson, P.D. 1971. Outeniqualand : The George-Knysna area. The South African Landscape No. 2: 1-23.

Upson, J.E., Leopold, E.B., Rubin, M. 1964. Postglacial change of sea level in New Haven Harbour, Connecticut. Am.J.Sci. 262: 121-132.

Van Andel, Tj.H. van and Veevers, J.J. 1967. Morphology and sediments of the Timor Sea. Dept. of Nat.Development, Bureau of Mineral Resources, Geology and Geophysics, Bulletin 83: 173pp.

Vanoni, V.A. 1964. Measurements of critical shear stress for entraining fine sediments in a boundary layer. California Inst.Tech., W.M. Keck Lab. of Hydraulics and Water Resources, Rept. KH-R-7: 47pp.

Vause, J.E. 1959. Underwater geology and analysis of Recent sediments off the northwest Florida coast. J.sed.Petr. 29: 555-563.

Visher, G.S. 1965. Fluvial processes as interpreted from ancient and recent fluvial deposits. In: Middleton, G.V. (ed.), Primary Sedimentary Structures and their Hydrodynamic Interpretation. SEPM, Spec.Publ. 12: 116-132.

Visher, G.S. 1969. Grain size distribution and depositional processes. J.sed.Petr. 39: 1074-1106.

Visser, H.N. and Schoch, A.E. 1973. The geology and mineral resources of the Saldanha Bay area. Dept. of Mines, Geol.Surv.S.Afr. Memoir 63: 150pp.

Wadell, H. 1934. Some new sedimentation formulas. Physics 5: 181-191.

Wadell, H. 1936. Some practical sedimentation formulas. Geol.Fören. Stockholm Förh. 58: 397-408.

Walger, E. 1962. Die Korngrössenverteilung von Einzellagen sandiger Sedimente und ihre genetische Bedeutung. Geol. Rundschau 51: 494-507.

Walger, E. 1966. Critical remarks on sedimentation balances. 11th Int. Oceanogr.Congr.Abstracts: 390; Publ.House "Nanka", Moscow.

Walther, J. 1894. Lithogenesis der Gegenwart. Beobachtungen über Bildung der Gesteine an der heutigen Erdoberfläche. Dritter Teil einer Einleitung in die Geologie als historische Wissenschaft. Fischer Verlag, Jena: 535-1055.

Walton, W.R. 1955. Ecology of living benthonic Foraminifera, Todos Santos Bay, Baja California. J.Paleontology 29: 952-1018.

Wefer, G. and Flemming, B.W. 1976. Submarine Abrasion des Geschiebemergels vor Bokniseck (westl. Ostsee). Meyniana 28: 87-94.

Weller, J.M. 1960. Stratigraphic principles and practice. Harper & Row, New York, 725pp.

Willis,J.P., Fortuin, H.H.G., Eagle, G.A. 1977. A preliminary report on the geochemistry of recent sediments in Saldanha Bay and Langebaan Lagoon. Trans.roy.Soc.S.Afr. 42: 497-509.

Wilson, B.W. 1976. Effects of long period waves in harbours. Alfred E. Snape Memorial Lecture, 1975. Die Siviele Ingenieur in Suid-Afrika, Jan.1976.

Winker, C.D. and Howard, J.D. 1977. Correlation of tectonically deformed shorelines on the southern Atlantic coastal plain. Geology 5: 123-127.

Woods, P.J. and Brown, R.G. 1975. Carbonate sedimentation in an arid zone tidal flat, Nilemah Embayment, Shark Bay, Western Australia. In: Ginsburg, R.N. (ed.), Tidal Deposits. Springer-Verlag, Berlin: 223-234.

Wunderlich, W. 1967. Darstellende Geometrie II. BI Hochschultaschenbücher, Mannheim : 234pp.

Yalin, M.S. 1964. Geometrical properties of sand waves. ASCE Proc. HY5 90: 105-119.

Yalin, M.S. and Price, W.A. 1974. Formation of dunes by tidal flows. 14th Conf.Coastal Eng., Copenhagen, Denmark, Proceedings Vol.II: 991-1007.

Yasso, W.E. 1962. Geometry and development of spit-bar shorelines at Horseshoe Cove, Sandy Hook, New Jersey. U.S.Navy, Office of Naval Res. Geogr.Branch, Project NR 388-057, Techn.Rept. 5: 166pp.

Yasso, W.E. 1965. Plan geometry of headland-bay beaches. J.Geol. 73: 702-714.

Zeigler, J.M. and Gill, B. 1959. Tables and graphs for the settling velocity of quartz in water, above the range of Stoke' Law. Woods Hole Oceanogr.Inst. Techn.Rept. 36: 13pp.

Zenkovitch, V.P. 1967. Processes of Coastal Development. Oliver & Boyd, Edinburgh: 738pp.

Zinsmeister, W.J. 1974. A new interpretation of thermally anomalous molluscan assemblages of the California Pleistocene. J.Paleontology 48: 84-94.

CHAPTER 8. APPENDICES

1.1. SAMPLE LOCALITIES IN SALDANHA BAY

SAMPLE STAT.	GEOGR. COORDINATES LAT.	LONG.	WATER DEPTH
010101	33 00,20	17 57,00	00,0
02	00,33	56,88	00,0
03	-- --	-- -	-
04	00,88	57,21	7,0
010201	00,02	57,33	00,0
02	-	-	-
03	00,40	57,45	6,0
04	00,70	57,48	7,1
05	00,95	57,50	8,2
06	01,18	57,52	8,9
010301	32 59,88	57,69	00,0
02	-	-	-
03	33 00,18	57,74	5,4
04	00,44	57,77	6,5
05	00,70	57,78	7,6
06	00,93	57,79	8,8
07	01,17	57,78	9,4
010401	32 59,80	58,05	00,0
02	59,95	58,05	4,0
03	33 00,10	58,07	5,2
04	00,35	58,06	6,3
05	00,60	58,07	7,3
06	00,92	58,05	9,2
07	01,25	58,03	10,9
08	01,47	58,01	11,5
09	01,70	58,09	15,1
010501	32 59,75	58,40	00,0
02	59,92	58,39	3,8
03	33 00,14	58,38	5,4
04	00,48	58,37	7,0
05	00,80	58,35	9,3
06	01,10	58,30	11,8
07	01,41	58,26	14,1
08	01,69	58,29	15,8
010601	32 59,73	58,72	00,0
02	-	-	-
03	-	-	-
04	33 00,09	58,70	4,9
05	00,28	58,69	5,5
06	00,37	58,68	6,0
07	00,41	58,67	6,0
08	00,47	58,66	6,5
09	00,52	58,65	7,0
10	00,67	58,63	8,3
11A	00,97	58,59	11,5
11B	00,92	58,55	10,9
12	01,27	58,52	13,6
13	01,58	58,47	15,2

SAMPLE STAT.	GEOGR. COORDINATES LAT.	LONG.	WATER DEPTH
020101	32 59,74	17 59,08	00,0
02	59,96	59,03	5,1
03	33 00,23	59,00	6,8
04	00,52	58,93	7,5
05	00,68	58,90	8,5
06	00,90	58,86	10,5
07	01,21	58,79	13,1
08	01,51	58,71	15,0
020201	32 59,82	59,50	00,0
02	33 00,04	59,33	5,7
03	00,24	59,30	7,0
04	00,40	59,24	8,5
05	00,66	59,23	9,3
06	00,96	59,20	10,2
07	01,22	59,18	12,0
08	01,75	59,17	-
020301	32 59,92	59,80	00,0
02	33 00,28	59,55	6,8
03	00,51	59,48	8,0
020401	00,05	18 00,07	00,0
02	00,32	17 59,85	6,4
03	00,58	59,75	7,9
04	00,80	59,68	8,1
05	01,02	59,59	9,5
06	01,25	59,51	10,5
07	01,47	59,42	11,2
08	01,90	59,20	-
020501	00,21	18 00,33	00,0
02	00,34	00,13	5,0
03	00,64	00,17	7,5
04	00,91	00,05	9,1
05	01,16	17 59,95	10,0
06	01,39	59,84	11,6
07	01,62	59,74	12,5
08	01,85	59,64	14,0
09	02,09	59,53	16,0
020601	00,39	18 00,58	00,0
02	00,58	00,48	5,0
03	00,82	00,37	8,6
04	01,10	00,23	9,3
05	01,36	00,12	11,2
06	01,60	00,00	13,0
07	01,84	17 59,88	14,3
08	02,08	59,77	16,8
09	02,32	59,63	18,3
030101	00,58	18 00,82	00,0
02	00,73	00,73	4,5

SAMPLE STAT.	GEOGR. COORDINATES LAT.	LONG.	WATER DEPTH
03	33 00,86	18 00,65	8,1
04	01,02	00,57	9,8
05	01,17	00,49	10,3
06	01,30	00,42	10,5
07	01,43	00,34	11,5
08	01,56	00,28	12,0
09	01,82	00,13	14,2
10	02,06	00,01	14,2
11	02,32	17 59,87	16,0
12	02,60	59,73	17,4
030201	00,76	18 01,08	00,0
02	01,00	01,04	5,0
03	01,24	00,87	10,1
04	01,54	00,68	12,0
05	01,81	00,51	14,3
06	02,10	00,36	14,5
07	02,37	00,20	15,0
08	02,64	00,03	16,0
030301	00,96	01,32	00,0
02	01,27	01,32	6,0
03	01,48	01,18	10,1
04	01,79	00,94	12,7
05	02,09	00,74	15,1
06	02,38	00,57	14,0
07	02,65	00,38	14,0
030401	01,34	01,72	00,0
02	01,49	01,62	4,0
03	01,75	01,42	10,0
04	02,07	01,16	12,9
05	02,37	00,92	13,5
06	02,67	00,74	13,5
030501	01,69	01,98	00,0
02	01,90	01,78	6,0
03	02,10	01,57	10,0
04	02,34	01,35	12,9
05	02,65	01,12	11,0
030601	02,06	02,16	00,0
02	02,25	02,00	5,0
03	02,47	01,75	10,2
04	02,64	01,58	12,1
030701	02,40	02,25	00,0
02	02,50	02,05	5,5
040101	02,86	02,56	00,0
02	02,82	02,39	4,0
03	02,73	02,11	6,0

SAMPLE STAT.	GEOGR. COORDINATES LAT.	LONG.	WATER DEPTH
040201	33 03,15	18 02,59	00,0
02	03,09	02,41	4,0
03	02,98	02,19	6,8
04	02,84	01,82	10,0
05	02,72	01,49	12,1
040301	03,55	02,53	00,0
02	03,44	02,28	5,8
03	03,34	02,06	8,1
04	03,18	01,76	10,0
05	03,05	01,50	10,8
06	02,89	01,23	11,6
040401	03,85	02,48	00,0
02	03,72	02,25	5,2
03	03,50	01,84	8,5
04	03,36	01,60	9,9
05	03,16	01,27	10,8
06	02,90	00,83	12,6
040501	04,09	02,36	00,0
02	03,90	02,06	5,9
03	03,71	01,74	8,2
04	03,53	01,47	10,2
05	03,33	01,13	12,1
040601	04,25	02,30	00,0
02	04,08	02,05	5,3
03	03,89	01,77	7,0
04	03,73	01,54	9,0
05	03,53	01,23	11,4
06	03,30	00,90	14,0
07	03,09	00,59	14,4
08	02,92	00,22	15,9
040701	04,54	02,10	00,0
02	04,37	01,82	4,1
03	04,13	01,62	6,0
04	33 03,90	18 01,33	9,1
05	03,65	01,00	12,1
06	03,35	00,63	14,4
07	02,89	17 59,87	15,9
040801	04,80	18 01,88	00,0
02	04,67	01,68	3,2
03	04,49	01,00	2,0
04	04,32	01,36	5,2
05	04,10	01,00	9,0
06	03,84	00,71	12,4
07	03,50	00,33	15,4
08	03,24	00,05	16,8
040901	05,00	01,70	00,0
02	05,00	01,55	6,2
03	04,87	01,44	6,0
04	04,74	01,33	5,0
05	04,57	01,18	4,5
06	03,68	00,25	15,2
07	03,28	17 59,81	17,3
041001	05,27	18 01,80	00,0
02	05,32	01,71	14,0
03	05,25	01,61	6,5
04	05,25	01,49	5,0
05	05,22	01,30	4,3
06	05,07	01,17	5,0
07	04,85	01,12	6,0
08	04,71	00,87	7,5
09	03,75	00,00	15,9
10	03,52	17 59,79	17,3
041101	05,19	18 00,99	6,0
02	04,95	00,80	5,0
03	04,78	00,64	5,2
041201	05,30	00,73	5,0
02	05,10	00,35	1,5
041203	33 04,88	18 00,35	4,0
04	04,69	00,36	4,0
05	04,62	00,07	4,0
06	04,60	17 59,84	3,5
07	04,41	59,91	5,0
060001	02,48	58,49	-
02	02,37	58,62	-
03	02,23	58,80	-
04	02,28	58,96	-
05	02,07	58,85	16,0
06	02,82	59,58	18,2
07	03,18	59,48	-
08	03,10	58,49	-
09	01,55	57,07	00,0
10	01,54	56,71	00,0
11	02,96	59,04	22,1
12	03,70	59,04	19,6
13	03,26	58,02	27,0
14	03,97	58,02	24,5
15	04,53	57,74	29,5
16	03,97	57,04	38,0
17	02,96	57,04	32,0
18	02,24	56,74	23,4
19	02,96	56,05	25,5
20	03,50	56,50	38,8
21	03,97	56,05	42,8

1.2. SAMPLE LOCALITIES IN LANGEBAAN LAGOON

SAMPLE STAT.	GEOGR. COORDINATES LAT.	LONG.	SAMPLE STAT.	GEOGR. COORDINATES LAT.	LONG.	SAMPLE STAT.	GEOGR. COORDINATES LAT.	LONG.	SAMPLE STAT.	GEOGR. COORDINATES LAT.	LONG.
050101	33 05,45	18 01,87	050507	33 06,60	18 01,10	04	33 08,44	18 03,75	08	33 10,33	18 03,96
02	05,46	01,82	08	06,60	00,94	05	08,44	03,23	09	10,33	03,77
03	05,46	01,78				06	08,44	02,74			
04	05,47	01,72	050601	06,84	02,75	07	08,46	02,18	052005	10,60	05,12
05	05,47	01,64	02	06,84	02,55	08	08,47	01,70	06	10,60	04,82
06	05,63	01,39	03	06,84	02,46	09	08,41	01,58	07	10,60	04,52
07	05,65	01,05	04	06,85	02,23	10	08,39	01,53	08	10,60	04,23
08	05,47	01,08	05	06,85	02,00						
09	05,50	00,69	06	06,85	01,78	051302	08,71	05,47	052102	10,82	07,20
10	05,50	00,44	07	06,86	01,45	03	08,71	05,00	03	10,85	06,70
11	05,24	00,50	08	06,87	01,20	04	08,70	04,50	04	-	-
12	05,40	00,33	09	06,86	01,04	05	08,73	04,03	05	10,85	05,87
13	05,54	00,15	10	06,86	00,93	06	08,73	03,58	06	10,85	05,54
14	05,27	00,26	11	06,86	00,91	07	08,74	02,94	07	10,86	05,16
15	05,40	00,05				08	08,75	02,44	08	10,86	05,84
16	05,51	17 59,89	050701	07,11	03,10	09	08,75	01,88	09	10,85	04,50
17	05,32	59,84	02	07,13	02,94	10	08,67	01,67			
18	05,44	59,68	03	07,14	02,78	11	08,68	01,63	052202	11,10	07,38
19	05,51	59,49	04	07,15	02,48				03	11,10	06,99
20	05,40	59,41	05	07,16	02,20	051403	09,02	05,25	04	11,10	06,70
21	05,52	59,28	06	07,16	01,92	04	09,01	04,60	05	-	-
22	05,68	59,21	07	07,15	01,59	05	09,02	04,10	06	11,11	05,16
23	05,78	59,00	08	07,14	01,25	06	09,00	03,44	07	11,11	05,88
24	05,62	59,08	09	07,15	00,93	07	09,01	02,53	08	11,13	05,60
25	05,40	59,18	10	07,11	00,88	08	08,94	02,08	09	11,13	05,28
									10	11,12	05,04
050201	05,82	18 01,78	050801	07,35	03,40	051505	09,21	05,54			
02	05,85	01,71	02	07,35	03,12	06	09,24	05,19	052303	11,38	07,25
03	05,80	01,65	03	07,33	02,80	07	09,25	04,92	04	11,39	06,79
04	05,79	01,55	04	07,38	02,42	08	09,25	04,58	05	11,39	06,52
05	05,79	01,40	05	07,38	02,23	09	09,24	04,16	06	11,39	06,18
06	05,79	01,30	06	07,38	01,90	10	09,25	03,66	07	11,39	05,90
07	05,79	01,20	07	07,39	01,64	11	09,25	03,34	08	11,39	05,63
08	05,79	01,10	08	07,39	01,40	12	09,25	03,19	09	11,39	05,44
09	05,78	01,01				13	09,14	02,68			
10	05,78	00,92	050901	07,61	03,50				052402	11,65	07,10
			02	07,59	03,12	051605	09,49	05,10	03	11,63	06,69
050301	06,07	01,84	03	07,63	02,77	06	09,50	04,64	04	11,63	06,30
02	06,07	01,69	04	07,65	02,44	07	09,50	04,20	05	-	-
03	06,07	01,49	05	07,65	02,15	08	09,51	03,80	06	11,65	05,51
04	06,07	01,34	06	07,65	01,92	09	09,51	03,35			
05	06,07	01,23				10	09,51	03,16	052503	11,90	06,78
06	06,07	01,10	051001	07,88	03,89				04	11,91	06,44
07	06,08	00,90	02	07,89	03,44	051704	09,82	05,20	05	11,90	06,07
08	06,08	00,70	03	07,90	03,00	05	09,80	04,72	06	11,91	05,75
			04	07,93	02,52	06	09,79	04,37	07	11,92	05,43
050401	06,32	02,03	05	07,93	02,20	07	09,79	04,04			
02	06,32	01,90	06	07,93	01,85	08	09,80	03,68	052601	12,19	07,72
03	06,32	01,66				09	09,81	03,24	02	12,20	07,47
04	06,32	01,45	051101	08,15	04,58				03	12,20	06,96
05	06,32	01,08	02	08,17	04,04	051807	10,07	04,78	04	12,20	06,69
06	06,32	00,88	03	08,15	03,50	08	10,06	04,40	05	12,15	06,27
			04	08,17	02,84	09	10,07	04,05	06	12,17	05,76
050501	06,58	02,30	05	08,16	02,40	10	10,07	03,80			
02	06,58	02,24	06	08,17	02,07	11	10,07	03,60	052701	12,56	07,54
03	06,58	02,04	07	08,17	01,75				02	12,43	07,18
04	06,60	01,78				051905	10,33	05,03	03	12,44	06,62
05	06,60	01,56	051202	08,41	04,74	06	10,33	04,76	04	12,44	06,28
06	06,60	01,32	03	08,41	04,28	07	10,33	04,36			

APPENDIX 2

2.1. CHAPTER 3 (cont.)

3.3.3. MECHANICAL DESIGN

The mechanical design of the system (Fig. 15) consists of four main parts: a tube, a funnel section, an introduction device and a suspended collecting pan. In addition, a number of refinements help to simplify the operational procedure.

The tube, made of perspex or PVC, is 210 cm long with an internal diameter of 14 cm, giving an overall fall height of 200 cm. These measures are by no means coincidental and the writer believes that an optimum tube should have at least the above dimensions. Strictly controlled experimental tests concerning the accuracy of settling tubes were carried out by Gibbs (1972). He came to the conclusion that the minimum dimensions of a settling tube should be 140 cm in length with an internal diameter of 12 cm in order to achieve accurate results. Accuracy is here understood to be a function of the dimensions of the system. Thus, the length of a tube will define the time a sediment sample will have to separate its size components into their hydraulic fractions with sufficient resolution for recording purposes. The diameter of a tube, on the other hand, will define the maximum quantity of material that can be processed without being too strongly affected by the walls or by density currents (Burgers, 1941 and 1942; McNown and Lin, 1952; Bradley, 1965; Kuenen, 1968).

Gibbs (1974) has constructed a tube of these minimum dimensions calling it an "optimum settling tube system". However, a first disadvantage of this tube is the time involved in splitting a sample down to the specified quantity of 1 - 2 g. Whereas bulk sample splitters will rapidly and adequately split a sample down to about 10 g, its accuracy is not suitable for very much smaller splits, especially when dealing with coarse sediments. Micro-splitting, on the other hand, is a tedious and time-consuming exercise; a second disadvantage arises from the fact that splits of a few grams of coarse sediment may not contain representative grain numbers (Fig. 16-A and 16-B). Splits of about 8 - 10 g would eliminate this problem; but large quantities of sediment were shown to give progressively more inaccurate

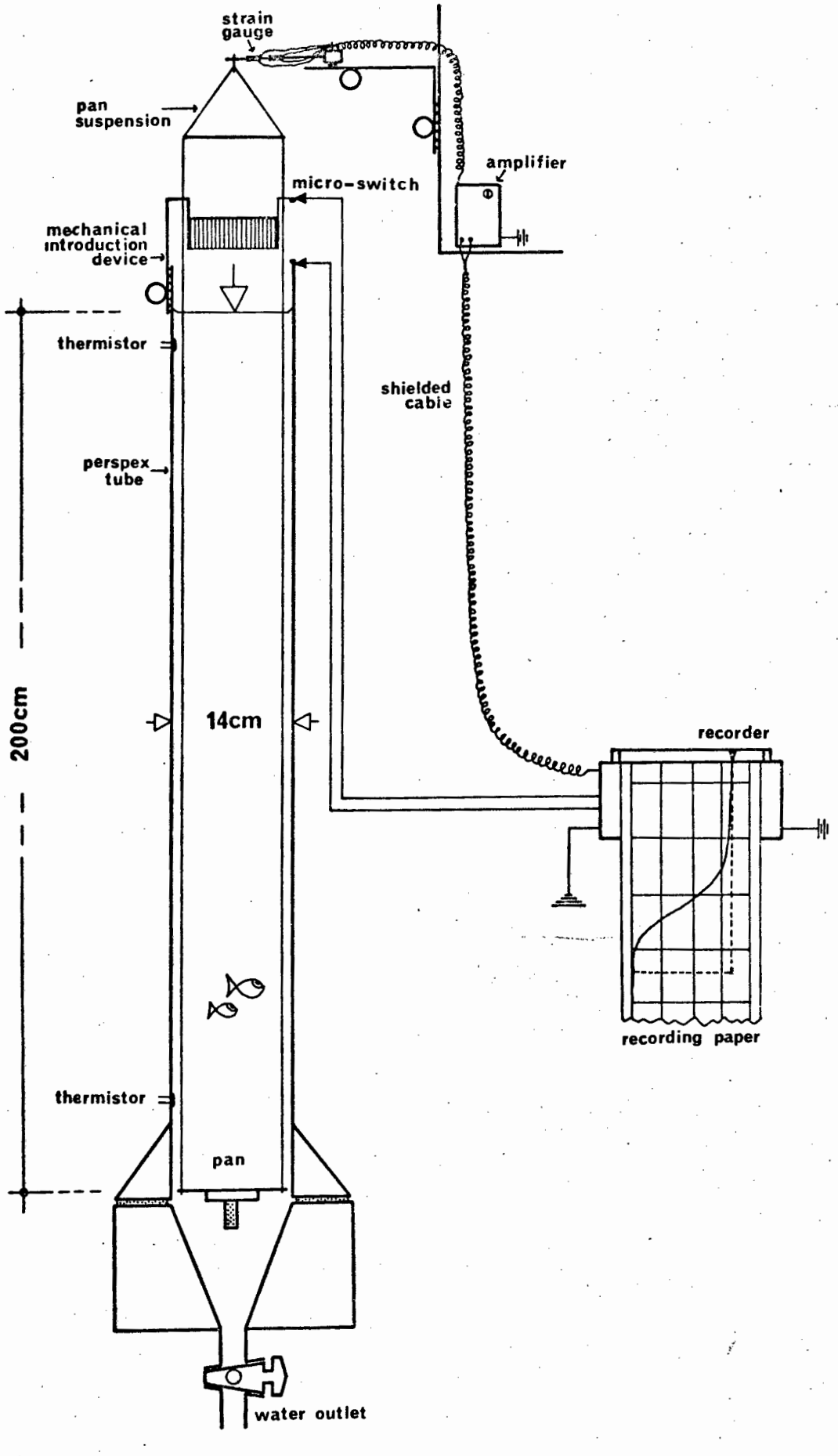

Fig. 15. Schematic sketch of the automatically recording settling tube system.

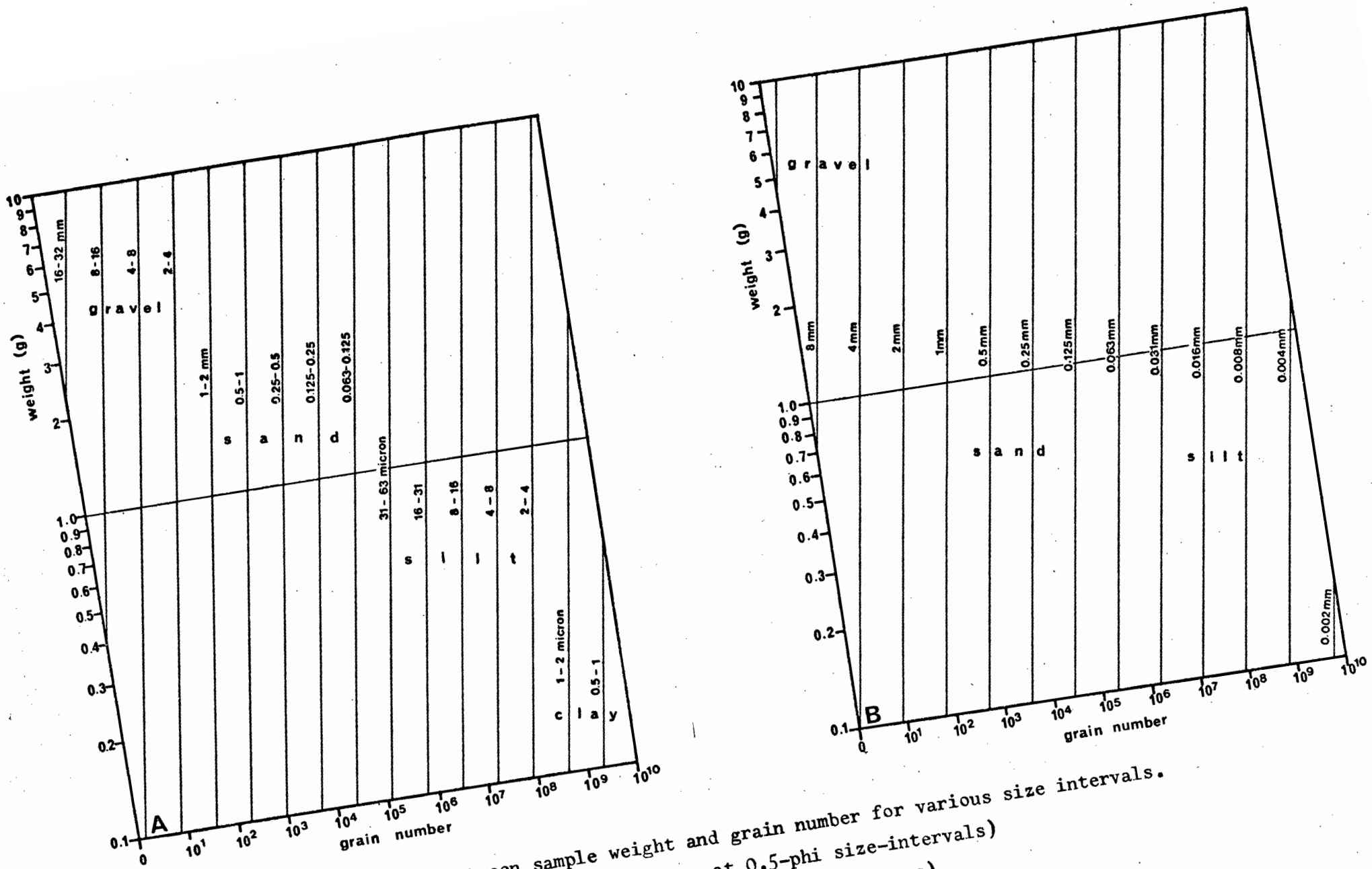

Fig. 16. The relationship between sample weight and grain number for various size intervals.
A. Carbonate sand (average grain numbers at 0.5-phi size-intervals)
B. Quartz sand (average grain numbers for specific diameters)

results when settled in small diameter tubes. Gibbs derived his minimum tube diameter by achieving accurate results with 1 - 3 g of sediment in a 12 cm diameter tube. This means simply that not more than 0.01 - 0.03 g/cm^2 should be settled. By keeping this mass/diameter ratio constant about 4 - 12 g of sediment could be settled in a tube with a 20 cm diameter. The writer would consider a tube of this diameter better suited than the minimum diameter proposed by Gibbs (1974). Unfortunately a tube of this diameter was unobtainable at the time of construction and microsplitting was, therefore unavoidable for the purpose of this study. However, a large diameter tube is being considered for the future.

A fall height of 200 cm has operational advantages, especially when processing coarse sediments because of their relatively high settling velocities. Adequate separation of successive size intervals will be achieved even for the coarsest sands. Still longer tubes become impracticable because the gain in accuracy does no longer compensate the longer processing times. Space problems would be another factor to consider since tubes over 2 m would no longer fit into average-sized rooms.

The funnel section seals off the bottom of the tube. It is constructed of strong material because the whole water column rests on it. PVC plates 10 mm thick were used to support the funnel which was lathed from a solid PVC block. The whole section, sealed off by a rubber gasket, is bolted to a perspex collar at the lower end of the tube. A stop-cock with sufficiently large diameter will flush the accumulated sediment whenever required.

The introduction device consists of a short tube section slightly smaller in diameter than the settling tube itself. Across one end a double layer of nylon mesh is glued to form a tight surface. The outer layer should have a mesh size below 63 microns whereas the inner mesh can be considerably coarser. The writer prefers this arrangement to plain discs used with some systems because the dry sediment will immediately fluidize from below through capilliary action when poured onto the mesh. The sediment is then evenly spread across the surface. It will adhere to the mesh when turned upside down due to surface tension. The inverted introduction device is placed onto a mechanical lowering stage and is lowered until the sediment touches the water surface in the tube. The sudden break of the surface tension will release the whole sediment instantaneously.

The collecting pan, also constructed of perspex, consists of a disc with a smaller diameter than the tube. In order to give the pan centering stability, a small flotation chamber underneath the disc is compensated with just enough lead shot to achieve negative buoyancy. The lower extension piece should not be longer than half the diameter of the tube in order to facilitate the tilting process when clearing the pan of accumulated sediment. The pan is suspended from two threads attached at opposite sides of the rim. The writer found nylon threads inadequate for this purpose, but good results were achieved with thin whipping twine which, after extensive use, has shown no sign of stretching. Above the tube the two threads are held apart by a solid crossbar from where they converge towards the hook on the cantilever.

3.3.4. ELECTRONIC DESIGN

The electronic design of the settling tube system consists basically of a mass indicator which can be separated into three units: a strain gauge unit, an amplifier and a strain gauge power supply.

The strain gauge unit consists of four strain gauges cemented to a cantilever of phosphor bronze. The cantilever is 80 mm long, 10 mm wide and 0.5 mm thick. These dimensions are quite arbitrary; however, the quality of the metal is important. It must have a low Young's modulus and low hysteresis, i.e. it must bend easily and return to its original position after bending. Two strain gauges are cemented to the top and two to the bottom of the cantilever. The whole unit is soldered to a mounting post of hex brass (Fig. 17-A and 17-B). The strain gauges are 20 mm long with a resistance of 120 ohms and a gauge factor of 2.09 (Kyowa Type KC-10-A1-11). They are connected in a bridge configuration (Fig. 18).

The amplifier used in this construction is an integrated circuit operational amplifier of the 725 type. The output of the strain gauge unit is of the order of a millivolt, which means that a gain of 1000 is needed in order to produce the 1 volt or so needed to drive most pen-recorders. The above device possesses the high open loop gain (over 10^5), low drift and noise which makes a gain-of-1000 amplifier quite feasible. The amplifier is connected in the standard inverted operational amplifier configuration, using the effective resistance of the strain gauge bridge as input resistance.

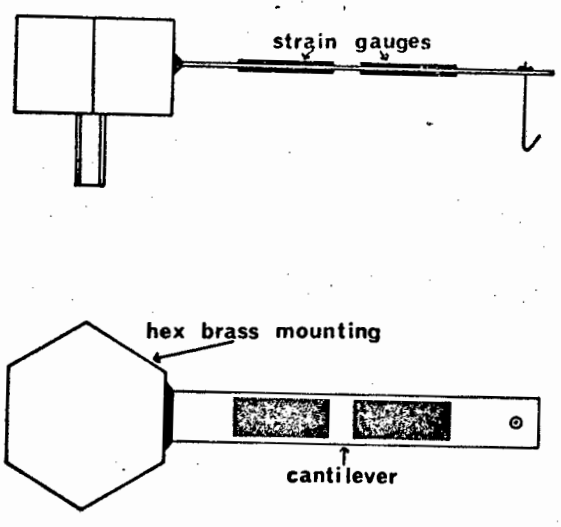

Fig. 17. The strain gauge unit

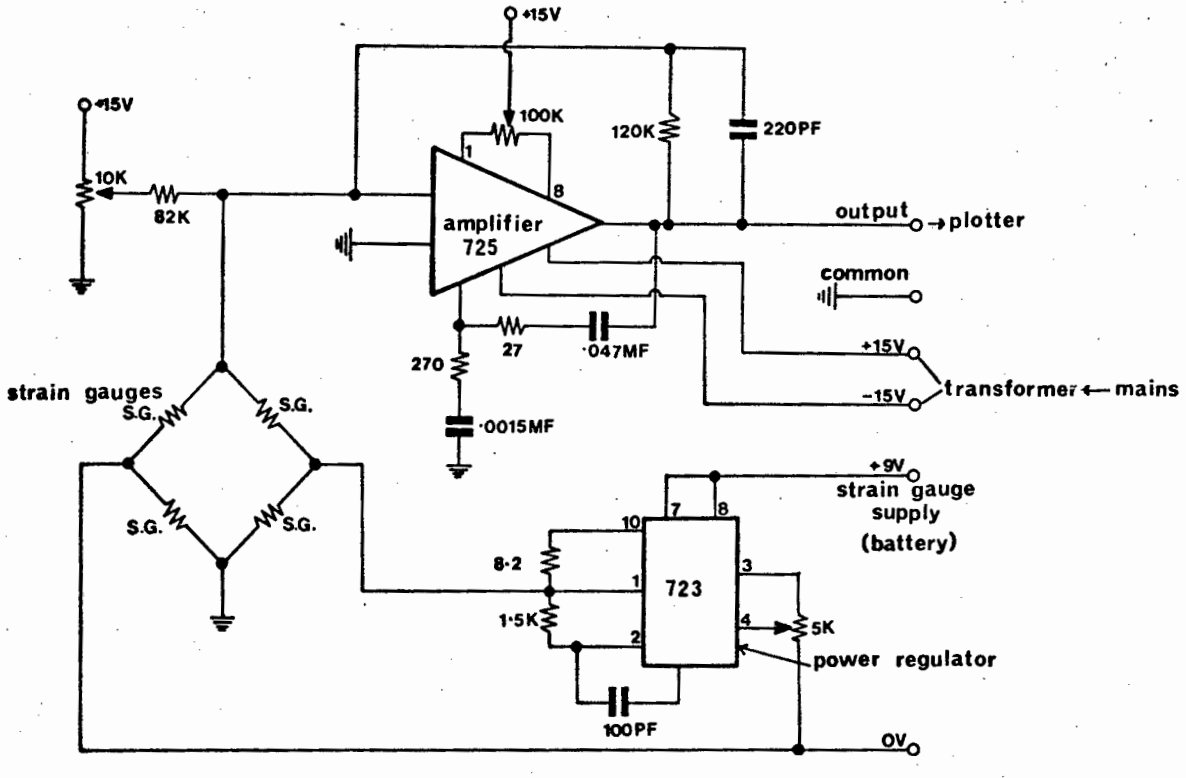

Fig. 18. Full circuitry of the strain gauge amplifier

The whole unit is mounted on perforated insulated board and no particular precaution needs to be observed beyond keeping inter-connections reasonably short and avoiding ground loops. The cable between the strain gauges and the amplifier is shielded as a precaution against hum pick-up. The variable resistors are all 10-turn wire-wound or cermet types. Single-turn trimpots are not suitable. The full circuitry is sketched in Fig. 18.

The strain gauge power supply has to provide approximately 3 volts to the strain gauges. The precise voltage is not important as long as it remains stable. The effective resistance of the strain gauge bridge is 120 ohms and thus the power supply must have a 25 mA capability at 3 volts. All these specifications are met in the 723 type of regulated power supply, which is connected in the low-voltage configuration.

The amplifier is operated from +15 and -15 volt supplies, derived from a single modular with 50 mA capability. These supplies are connected to a ground return. The strain gauges may be operated from any supply between 8 and 20 volts with 50 mA capability. The 9 volts indicated in Fig. 18 may be derived from a PM 9 dry battery which requires regular checks. A full parts list is added in Appendix 2.2. The whole system is calibrated in the following way:

(a) With strain gauge power supply OFF and amplifier power supply ON, adjust the 100 K potentiometer for zero output.

(b) With strain gauge power supply ON, adjust 5K potentiometer for 3 volt output (Pin 1) from 723.

(c) Adjust 10 K potentiometer for zero output with no load on the cantilever.

The strain gauge output is thus amplified and fed into a suitable pen recorder. The type used in the system described here is a Hitachi Model QPB 53 (1966), which has an amplification range from 0.001 - 10.0 volts and chart speeds of 240, 60 and 20 mm/min and mm/h, respectively. The cable between the strain gauge amplifier and the pen recorder has also been shielded as it was found to be a source for hum pick-up. Power to the pen recorder is fed through a voltage regulator in order to avoid the effects of power fluctuations in the mains. An advantage of the Hitachi recorder

is the paper width of 25 cm which gives excellent resolution of the recorded curve.

3.3.5. OPERATIONAL PROCEDURES

A sediment sample is split down to about 10 g using a bulk sample splitter. The subsample is then further reduced with a microsplitter of standardized design (e.g. Otto, 1936; McKinney and Silver, 1956; Skolnik, 1959; Humphries, 1961; Lawson and Day, 1969). The resulting split is cleaned of its mud by washing it through a 63 micron sieve. In order to disperse the muds more effectively, the sample can be pretreated with H_2O_2 and immersed in an ultrasonic bath provided this will not lead to the destruction of the sand-size particles, e.g. faecal pellets. It should be noted that although the mud fraction (< 63 microns) is not included in the coarse fraction size analysis, its total contribution to the sediment was recorded in each case as it contains important additional information about depositional environments.

A simple graph (Fig. 19) giving equivalent weights of various sediment types in water simplifies the selection of the correct amplification range on the paper recorder. This will ensure that with each split the maximum amplitude that will fit onto the paper is utilized for recording purposes. In this way it is avoided from shifting out of range or from choosing an amplification range that is too small.

The electrical system of the instrument is switched on some time before start of operation in order to allow temperature adjustment of the strain gauge system. This will avoid the initial drift of the servo-arm of the recorder. The temperature sensitivity of the system is felt especially in the lower amplification ranges when processing small splits of under 1 g at 20 mV or less. This disadvantage could be eliminated by placing the whole system into a constant temperature casing or by using an electrical balance in place of the strain gauge system. Both solutions, however, would have resulted in considerable additional expense which would have defeated the low cost objective of the construction. The tube was placed in a reasonably temperature-stable room. In addition, the computer program was adapted to cope with a wide range of room temperatures.

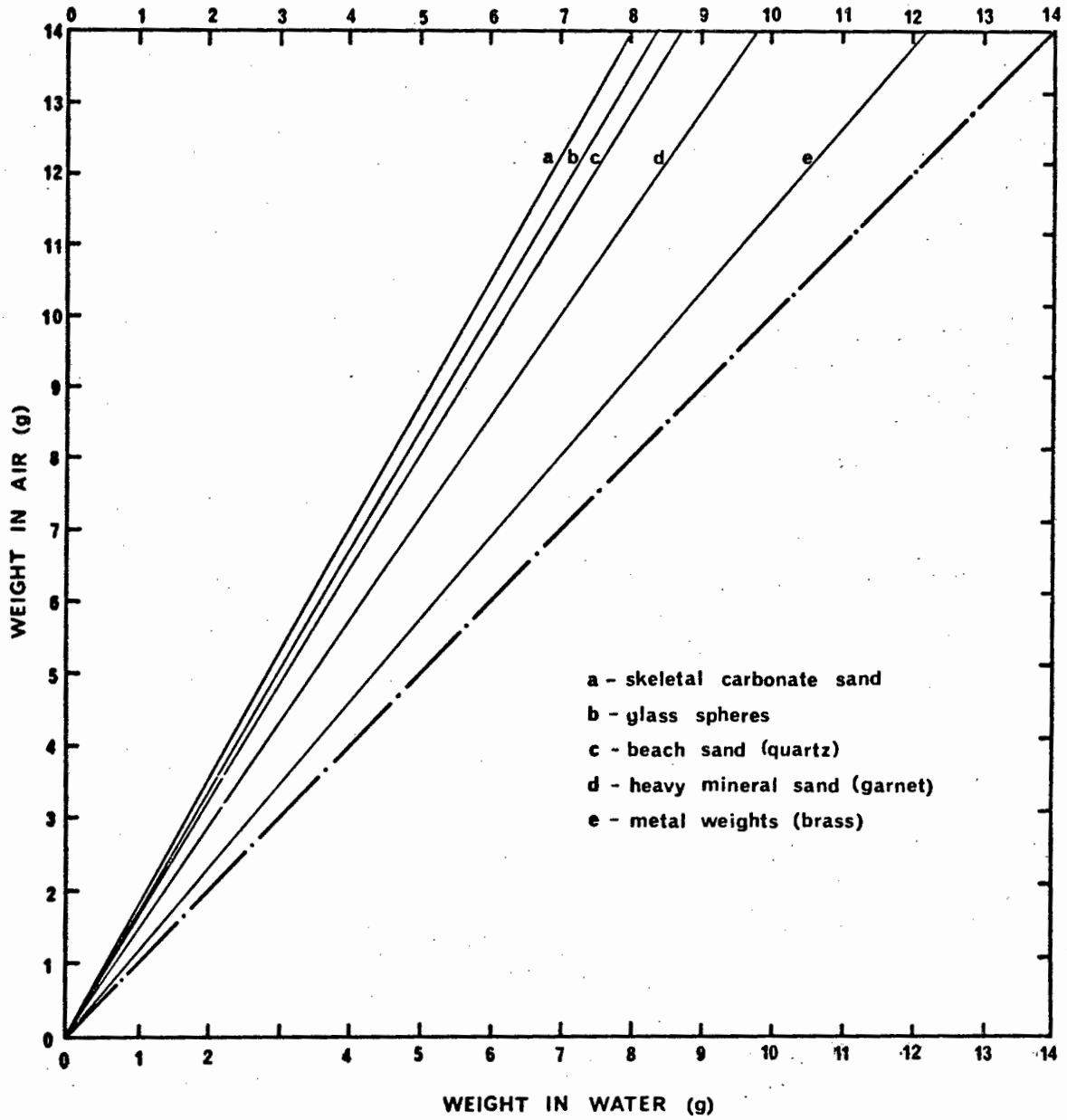

Fig. 19. The weight equivalents of various sediments in water

The sample is poured onto the wet mesh of the introduction device, fluidized and spread evenly across the surface. It is then turned upside down and placed in the inverted position on the lowering stage. The sediment particles are held in place by surface tension until they touch the water surface of the tube. In this manner sediments with maximum rounded particle sizes of up to 4 mm and considerably larger flat particles, e.g. shell fragments, can be processed. Prior to introduction the water temperature is recorded and the pen recorder is activated at the selected speed. At the same time the pen is adjusted to zero. For coarse sediments a high initial speed is advisable (e.g. at least 240 mm/min), whereas fine sediments can be run at lower chart speeds (e.g. 60 mm/min or even 20 mm/min). If the sediment is not well sorted then a run can be started at a high speed and switched down to a lower speed when the curve begins to level off appreciably. The point at which a speed change is undertaken must be carefully annotated in order to allow the correct calculation of settling velocities from this point onwards. In the prototype tube it was necessary to record the exact time of introduction by stopwatch. A mark was then made on the paper in line with the pen after a specified time interval, thus allowing the exact starting position to be calculated in relation to the chart speed. This problem could be overcome by triggering the chart at the time of introduction by means of a micro-switch.

When the curve has reached its maximum amplitude the recording process is interrupted and the next run is prepared. It is not necessary to clear the pan after each run because the strain gauge amplifier can be adjusted to zero with its variable resistor. In this way a minimum of 10 samples can be accumulated on the pan before clearing becomes necessary. This is achieved by disconnecting the threads of the pan from the hook on the cantilever and giving a bold tug on one of the threads. This will tilt the pan and immediately clear most of the sediment.

The recorded curve represents a continuous cumulative display of the mass of the particles as they settle onto the pan. The amplitude is in each case equivalent to 100% by weight. The settling velocity for any point on the curve is a function of the time that has passed since introduction, the height of the water column between the surface and the pan, and the density and viscosity of the fluid as determined by its temperature. Using the tables compiled by Zeigler and Gill (1959) or Gibbs et al., (1971)

the size in mm of the hydraulically equivalent quartz or glass sphere is looked up and converted into its phi-equivalent (Page, 1955). This conversion process from settling velocities into phi-equivalents is also known as the "psi-transformation" (Middleton, 1967; Reed et al., 1975).

The whole procedure of transforming settling velocities into grain sizes is accomplished by computer. Manual calculations are extremely time-consuming and prone to operator errors. In order to allow operation at virtually any expected room temperature, viscosity and density values have been programmed for temperatures between 10°C and 30°C. By automatically compensating for temperature differences an expensive constant temperature casing was avoided. The full computer program in Fortran IV used on the UCT-Univac computer facility is listed in Appendix 2.4.

3.3.6. CALIBRATION OF THE SETTLING TUBE SYSTEM

Once completed, the instrument was subjected to a series of tests in order to establish its accuracy, reproducibility, and comparability. After the important study of Gibbs (1972) it has become unnecessary to conduct extensive accuracy tests in terms of dimensional constraints. The dimensions of this tube were chosen such that they lay well within the accuracy limits defined by his experimental results.

Reproducibility was tested by running several splits of individual samples. Three different types of sediments were tested: a pure skeletal carbonate sand (Fig. 20-A), a mixed carbonate-quartz sand (Fig. 20-B) and a pure quartz sand (Fig. 20-C). All five splits of samples A and C were run at a constant temperature whereas each split of sample B was run at a different temperature. In each case reproducibility is excellent. This is particularly well reflected in standard deviation values of the reproducibility of individual statistical parameters (Table 2). The best reproducibility was achieved by the very fine quartz sand with standard deviations for the first three parameters well below 0.1 phi-intervals. This feature is readily explained by the homogeneity of the material and the low shape effects in the small size classes. The odd variety of shapes encountered in coarse skeletal carbonate sands (McNown and Malaika, 1950; Maiklem, 1968; Braithwaite, 1973) will obviously not be reproduced in the splitting process

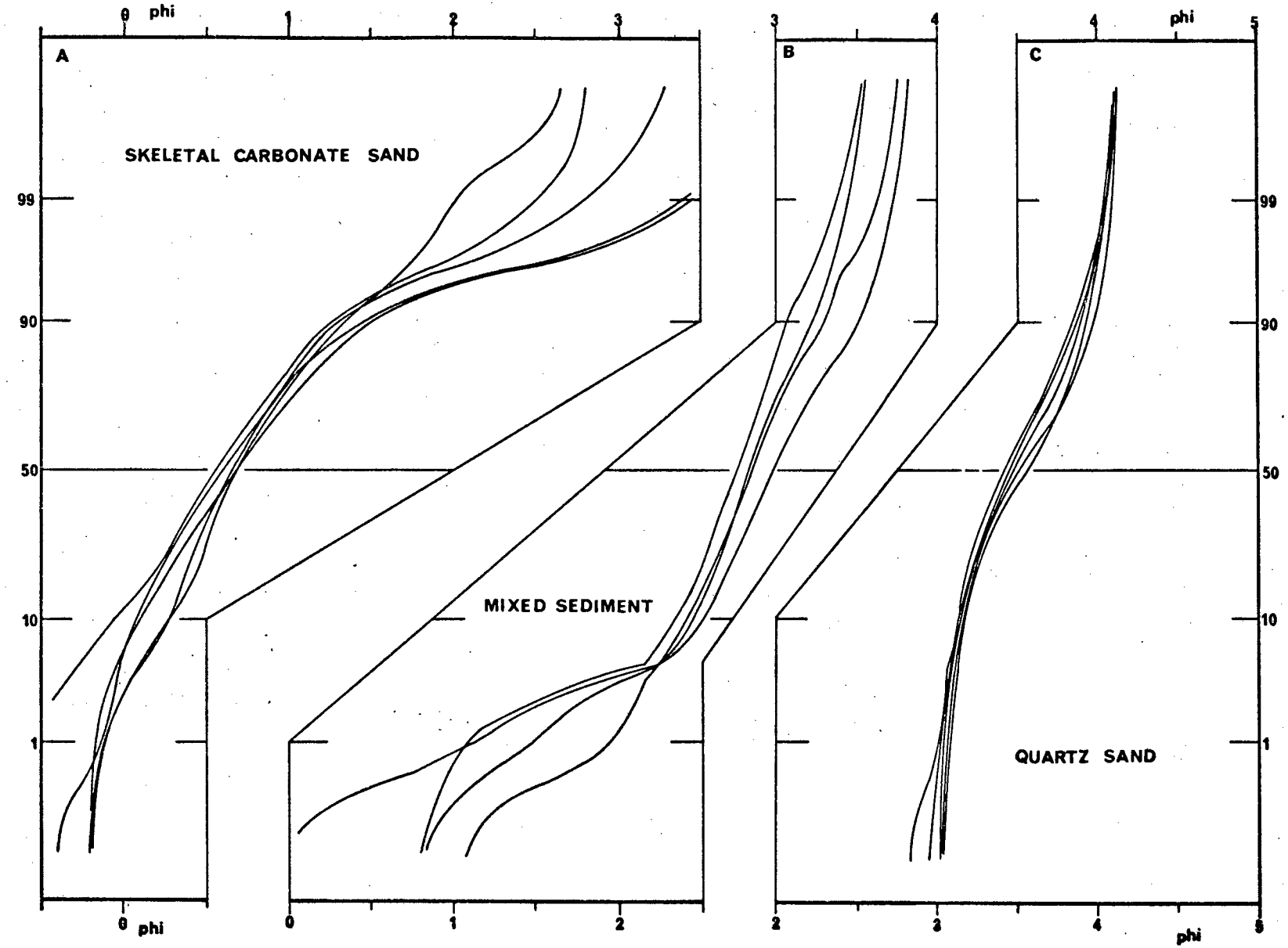

Fig. 20. Reproducibility tests on three different sediment types

as representatively as a fine homogenous sediment. This is especially noticeable in the tails of bioclastic sands where grain numbers decrease markedly and shapes of individual grains are not expected to reproduce statistically.

TABLE 2. Results of Reproducibility Tests

SAMPLE	MEAN	MEDIAN	SORTING	SKEWNESS	KURTOSIS
A-1	0.768	0.710	0.569	+0.700	+3.135
A-2	0.783	0.654	0.691	+0.959	+4.739
A-3	0.878	0.727	0.647	+0.928	+4.528
A-4	0.670	0.607	0.582	+0.409	+1.571
A-5	0.809	0.742	0.439	+0.410	+1.223
$\bar{X}$	0.782	0.688	0.585	+0.681	+3.039
S	0.075	0.056	0.096	0.267	1.626
B-1	2.825	2.834	0.346	-0.718	+4.923
B-2	2.851	2.852	0.342	-0.182	+1.426
B-3	2.710	2.751	0.360	-1.017	+6.704
B-4	2.962	2.979	0.472	-0.872	+6.488
$\bar{X}$	2.837	2.854	0.380	-0.697	+4.885
S	0.103	0.094	0.062	0.365	2.439
C-1	3.588	3.608	0.295	-0.048	-1.112
C-2	3.579	3.544	0.314	+0.077	-1.155
C-3	3.550	3.514	0.275	+0.131	-1.104
C-4	3.500	3.459	0.274	+0.226	-0.818
C-5	3.515	3.502	0.264	+0.110	-0.795
$\bar{X}$	3.546	3.525	0.284	+0.099	-0.997
S	0.039	0.055	0.020	0.099	0.175

After accuracy and reproducibility proved satisfactory, it remained to be investigated how well results from this system compared with those obtained elsewhere on a similar instrument. For this purpose a number of selected samples were sent to the Department of Geology, University if Kiel (West Germany), where a large settling tube has been operating for many years. Fig. 21

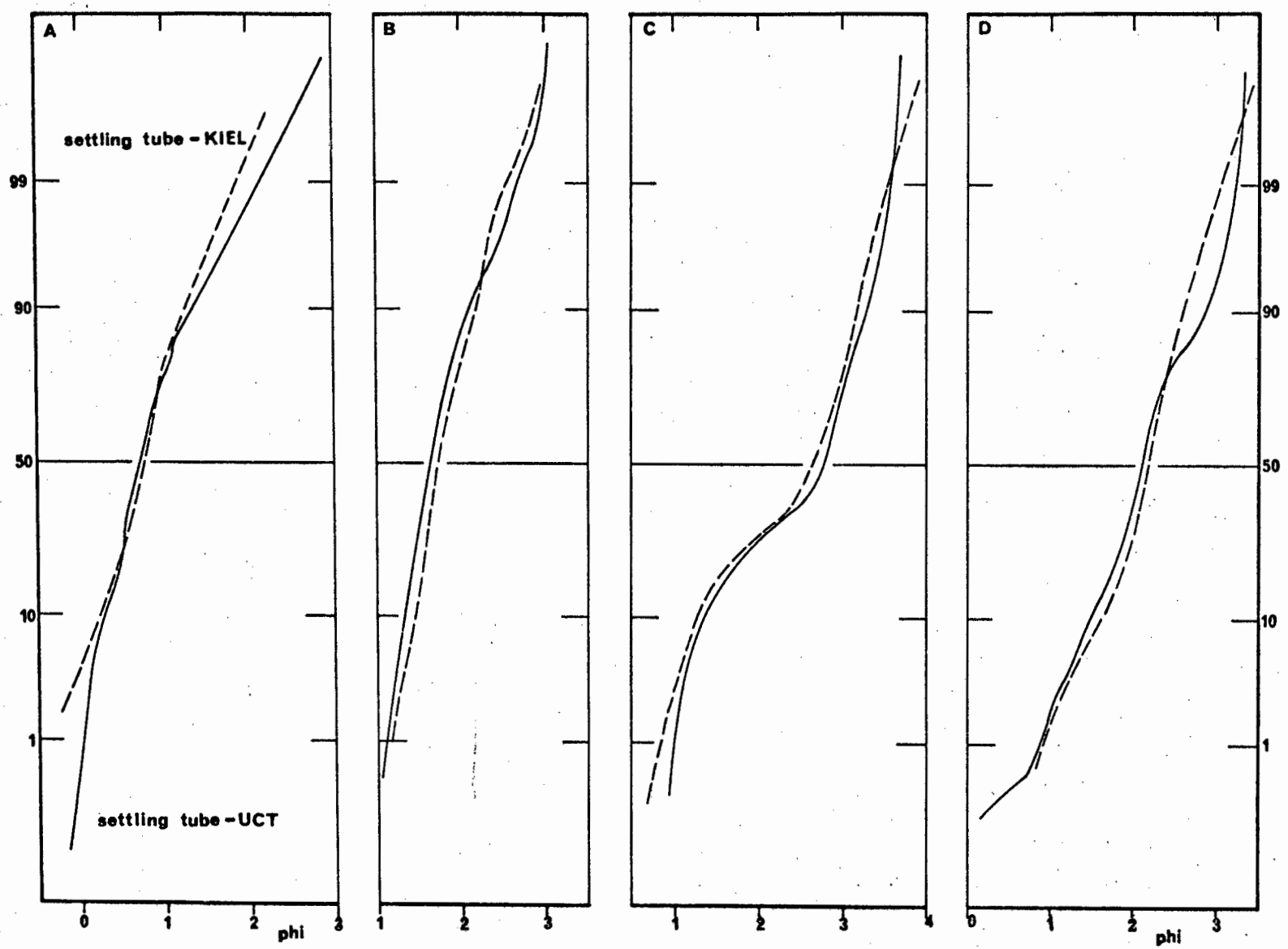

Fig. 21. The comparability of results obtained on the settling tube described here with those obtained elsewhere on splits of the same samples

demonstrates the excellent agreement between the two systems, which incidentally operate on a different transducer principle. Whereas this system uses strain gauges, the Kiel instrument operates with an inductive potentiometer. The deviations between the two curves lie in each case well within the normal range of reproducibility.

Further evidence for good performance of the system is given by two other examples where theoretic expectations were confirmed experimentally. The settling curve of glass spheres virtually coincides with the sieve curve (Fig. 14-B) and the modal shift of garnet sand by 0.5 phi-intervals (Fig. 14-C) compares well with the 0.6 phi calculated by Rittenhouse (1943).

3.3.7. ERROR ASSESSMENTS

Systematic as well as operator errors can enter the investigational procedures at various points of each subroutine. Since most of the interpretations and conclusions reached in the course of this study are directly or indirectly affected by the results obtained from the settling tube, the discussion of analytical techniques would be incomplete if the limits of potential errors were not carefully estimated.

3.3.7.1. Sampling Errors

A first error that can hardly be eliminated completely is introduced when recovering a sediment sample in the field. The expected "probable sampling error" has been carefully estimated (Krumbein, 1934; Cook, 1966; Griffiths, 1967) and if a strict sampling procedure is observed it can be reduced to an acceptable level.

In this study "in situ" sampling was given preference over conventional, remotely controlled sampling. It has been found that the error of the mean of a set of samples varies inversely as the square root of the number of samples (Krumbein and Pettijohn, 1938). Thus, in order to reduce the sampling error the writer recovered four randomly placed core samples at each locality. According to statistical law the probable sample error of the subsequently mixed sediment is reduced by 50% (Fig. 11). A larger number of samples at any given point would further reduce the probable sampling error; however, methodology also has its practical limits.

3.3.7.2. Splitting Error

Another source for errors is the splitting process where a bulk sample is reduced to the quantity required for a run in the settling rube. If mechanical splitters of the types discussed earlier are used then splitting errors will be negligible, provided that the final split still contains a statistically representative grain number (Tobi and Van der Plas, 1968). Normally even a single gram of sediment will contain several thousand sand grains thus warranting a representative split. Even the marginal case of a coarse bioclastic sand discussed earlier gave good reproducibility (Fig. 20-A and Table 2). A good estimate of expected grain numbers as a function of sample weight is presented in Fig. 16. The graph for quartz sand (Fig. 16-B) has been reproduced from Gibbs (1972) whereas the graph for skeletal carbonate sands (Fig. 16-A) is based on previous work of the writer (Flemming, 1976b).

3.3.7.3. Introduction Error

When introducing the sediment into the water column a system inherent error has to be accepted. It is from a practical point of view impossible to guarantee that all grains of the introduced sample will settle at exactly thesame time, regardless of the method applied. The procedure discussed above is probably as close as one can get to simultaneous introduction.

The significance of this error can best be estimated by observing the effect of time lag that may occur between individual grains. The simplest way of achieving this is by purposely assuming a wrong fall height and comparing the outcome with the true result. This experiment was simulated by computer. A sample previously run at 18°C with a true fall height of 200 cm was processed (a) by assuming a fall height of only 196 cm and (b) by assuming an excessive fall height of 206 cm (Fig. 22). The deviation from the true curve is surprisingly small, lying well within the normal scatter range of reproducibility. This result in fact supports the use of a 2 m tube. The introduction error will increase progressively the shorter the tube becomes. The actual error of introduction is expected to be exceedingly smaller than the extreme deviations assumed in the test.

3.3.7.4. Temperature Error

As outlined earlier, settling velocity is a function of the viscosity and the density of the fluid, which in turn is a function of water temperature. Since the water column is usually not quite homogenous as far as temperature is concerned, an error may be introduced by recording an erroneous temperature. Again the effects were observed in a similated computer experiment. The true settling velocities of a sample run at 18°C were processed assuming temperatures between 10°C and 30°C. From Fig. 23 it is quite evident that a conceivable temperature of 1°C or even 2°C has quite neglibible effects on the resulting curve.

An interesting aspect of this test was the observation that the error trend is not linear. The mean diameter decreases progressively faster with increasing water temperature, reflecting the decreasing viscosity and density of the medium. Sorting, on the other hand, appears to decrease with rising temperature while the size distribution shows a general trend towards negative skewness, at the same time becoming more leptocurtic (Fig. 24-A,B,C,D). This differential reaction of individual size parameters to temperature manipulations may indicate a definite influence on the size-sorting characteristics of sediments by the water temperatures at different latitudes. It would appear that the efficiency of size-sorting is very much a function of viscosity and density of the transporting medium. Theoretically this means that a given sediment would produce different size distribution characteristics when exposed for a given time period to similar transport mechanisms at the tropics and at the poles.

3.3.7.5. Recording Errors

Two basic errors can occur in the recording process. In order to avoid the inevitable error introduced by recording particles that have interfered with the wall of the tube, the pan was constructed such that these particles would not be collected, i.e. not all of the introduced sediment is collected and recorded. It was assumed that particles passing the pan are statistically representative of the total and would, therefore, not affect the final result. Although this error is difficult to assess directly, the excellent reproducibility of consecutive runs using splits of the same material seems to support the assumption.

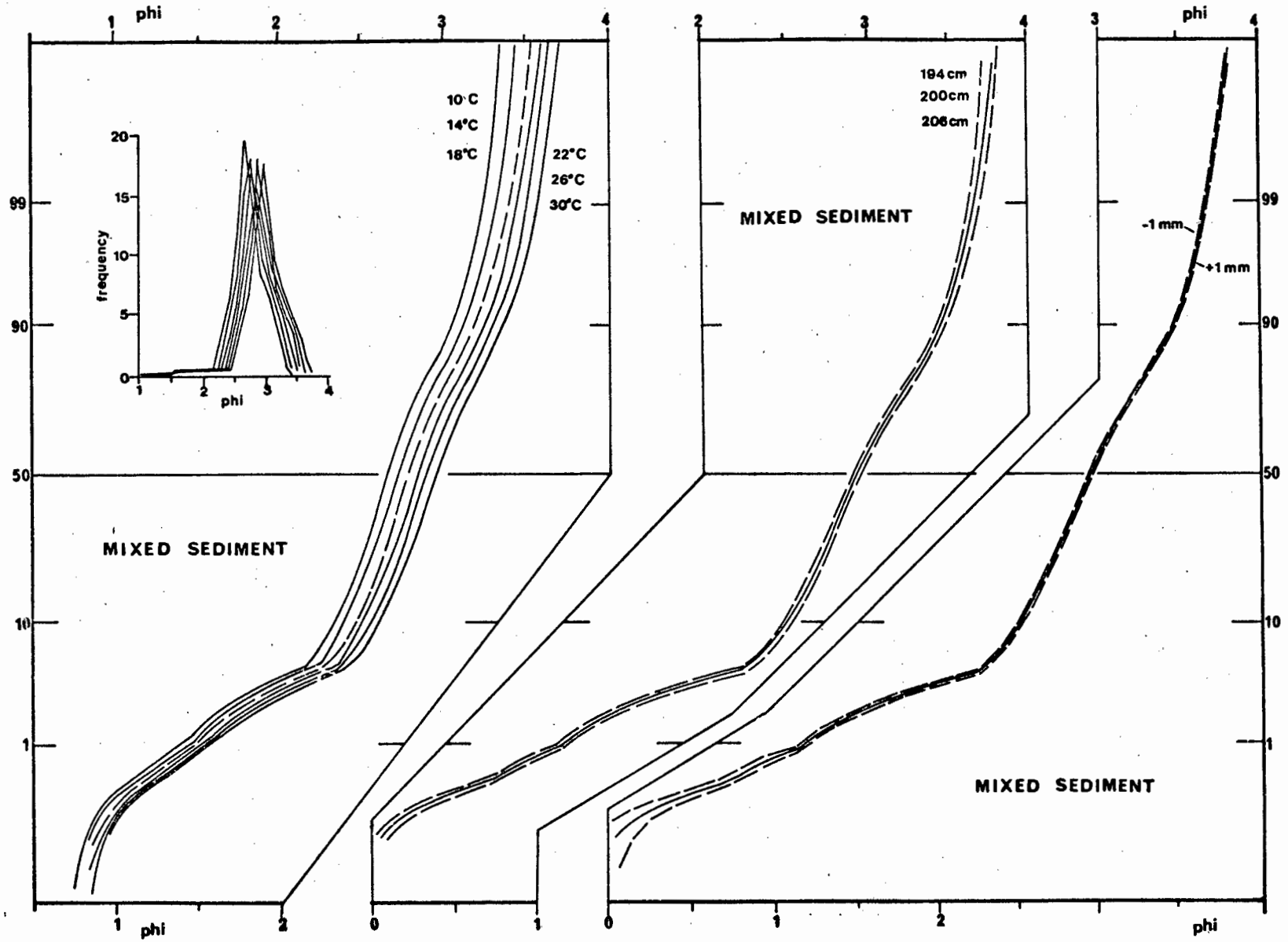

Fig. 23. The effect of temperature errors

Fig. 22. Errors in measuring the fall heights

Fig. 25. The effect of errors in sampling the recorded curve

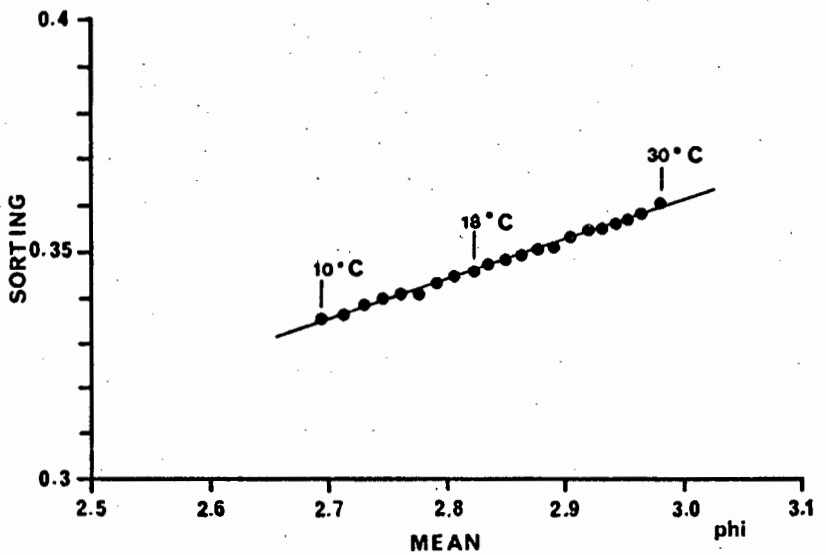

Fig. 24-A. The effect of temperature errors on sorting and mean diameter

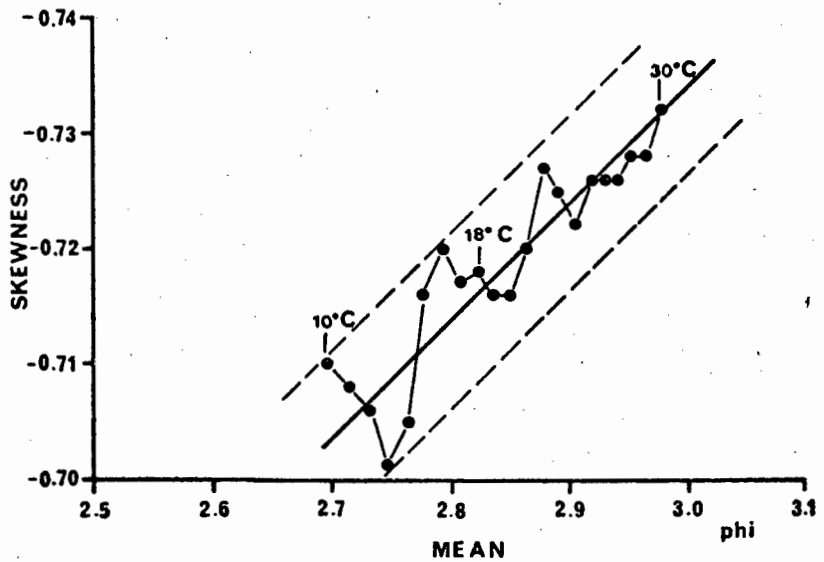

Fig. 24-B. The effect of temperature errors on skewness and mean diameter

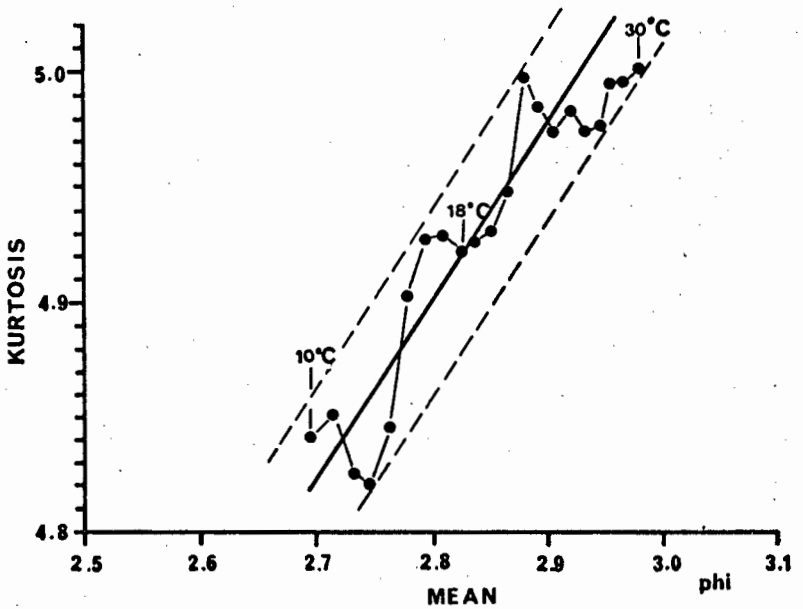

Fig. 24-C. The effect of temperature errors on Kurtosis and mean diameter

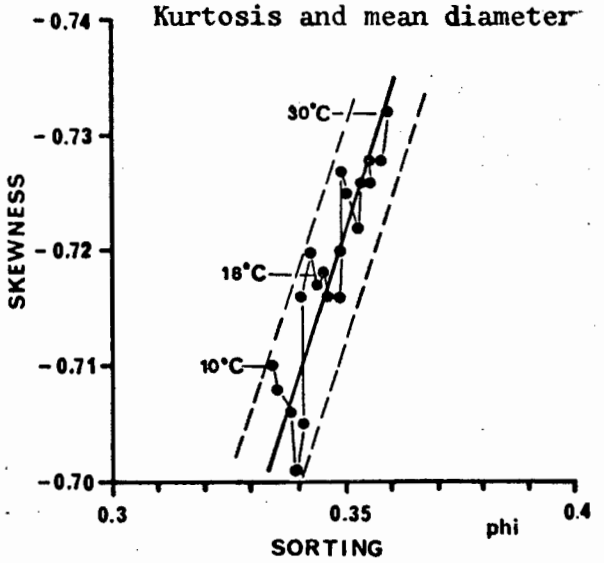

Fig. 24-D. The effect of temperature errors on skewness and sorting

A final operator error can occur when sampling the recorded curve for computer evaluation. For this purpose the distances between the starting line and 30 selected points on the curve are measured. These values are then fed into the computer for statistical processing. Assuming that a maximum measuring error of 1 mm in either direction could occur, the influence of such errors could again be assessed by a simulated computer experiment. Fig. 25 clearly demonstrates that this error is extremely small especially when dealing with medium or finer-grained sands. It increases slightly towards the coarser size fractions when using the 60 mm/min chart speed, thus demonstrating the necessity for high initial chart speeds when processing coarse sediments.

In order to demonstrate the effect of cumulative errors, a sample for which the true size distribution had previously been established was processed by computer introducing a series of conceivable errors as outlined above. In place of the true fall height of 200 cm an erroneous fall height of 202 cm was computed; instead of 18°C a temperature of 20°C was assumed; and an error of $\pm$ 1 mm was entered at random while sampling the curve. Fig. 26 convincingly demonstrates the irrelevance of cumulative errors that may under normal operational conditions enter into the final results. With the exception of Kurtosis all errors are confined to the second and third decimal places of the computed outputs. This surprisingly small overall deviation is explained by the systematic nature of most errors, which themselves are very small, and as a result, the final curve will, more or less, retain its original shape.

3.3.8. RESOLUTION LEVELS

The settling tube results are recorded in a continuous manner and theoretically it would be possible to convert settling velocities into equivalent grain sizes in an almost infinite number of discrete steps. For practical reasons, however, the curve is sampled at 30 specified intervals (Appendix 2.5.). The size distribution can then be computed at various resolution levels and the writer found that computation and presentation of size frequency data at 0.1 phi intervals provided the most practical solution. Fig. 27 illustrates the effect of resolution level on the computation of various size parameters.

Whereas the deviation normally increases as resolution decreases

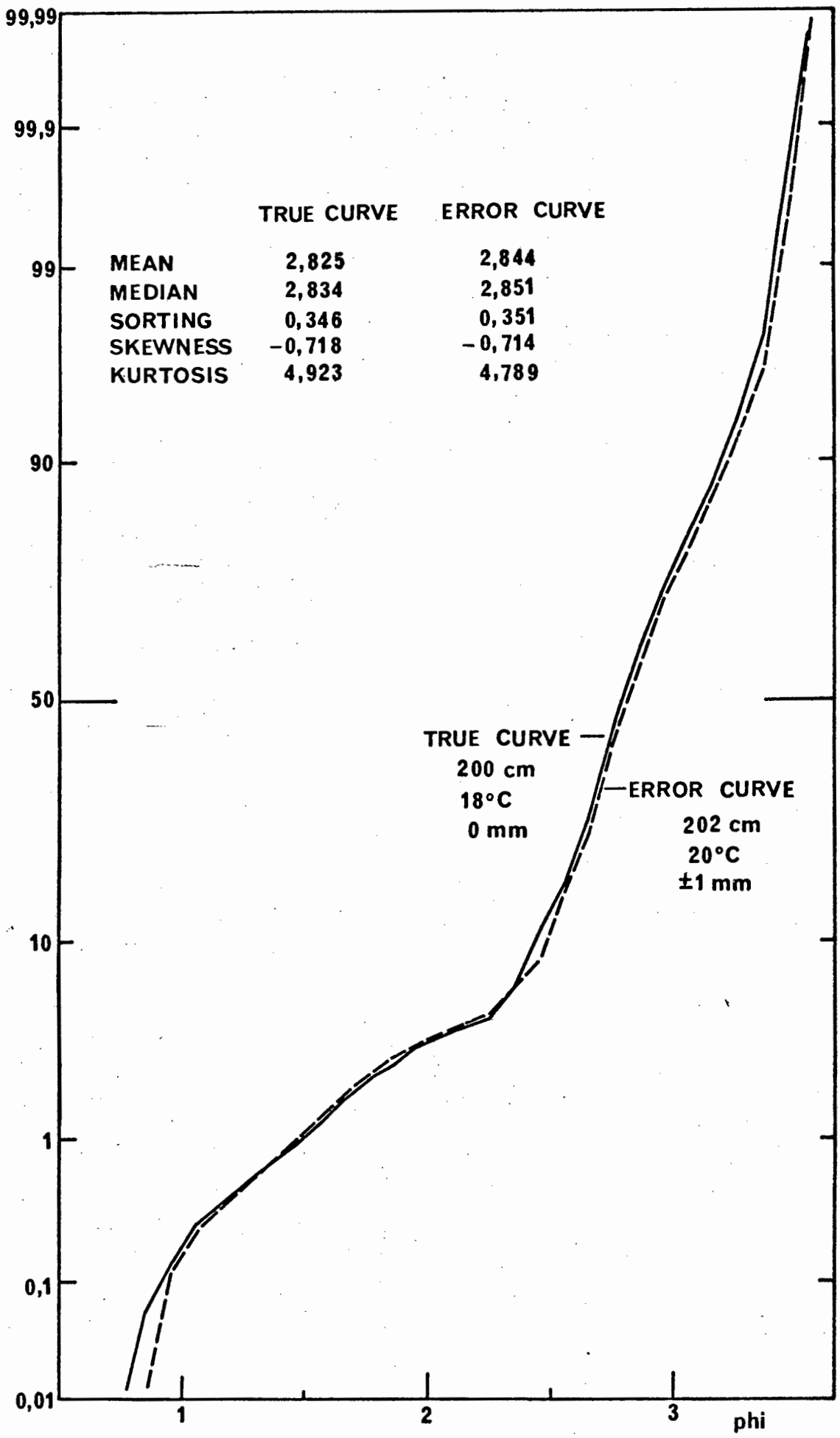

Fig. 26. The effect of cumulative errors on the size distribution

(e.g. from 0.1 to 1.0 phi-intervals), it appears to remain more stable at levels smaller than 0.1 phi. Fig. 28 demonstrates the effect of resolution on the size frequencies of two samples. Fig. 28-A presents the data at 0.1 phi-intervals, whereas Fig. 28-B presents the same data at 0.25 phi-intervals. Clearly the resolution of the size frequency curves is superior at the higher level.

2.2. PARTS LIST FOR THE STRAIN GAUGE UNIT

Resistors :

1 x 120 K ohms
1 x 27 ohms
1 x 270 ohms
1 x 82 K ohms
1 x 8.2 K ohms
1 x 1.5 K ohms

Capacitors :

1 x 220 pF
1 x 0.047 mF
1 x 0.0015 mF
1 x 100 pF

Miscellaneous :

1 x 15-0-15 volt power supply
1 x 8 - 20 volt dry battery
Circuit board, mounting hardware etc.

Ten-turn Trimpots :

1 x 10 K ohms
1 x 100 K ohms
1 x 5 K ohms

Integrated circuits :

1 x 725 operational amplifier
1 x 723 regulator

Strain Gauges :

4 x Kyowa Type KC-10-Al-11

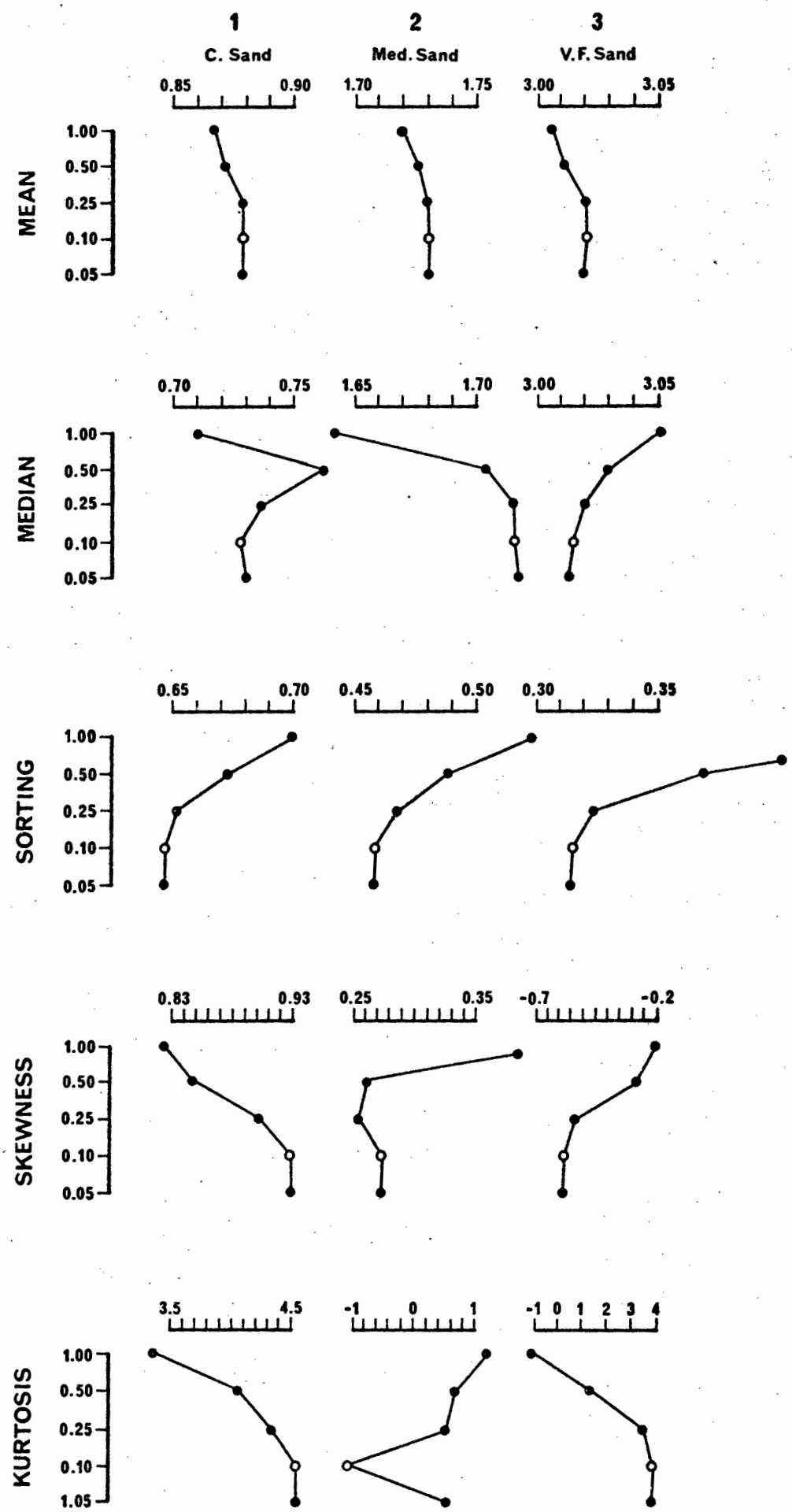

Fig. 27. Resolution at different phi-frequency intervals

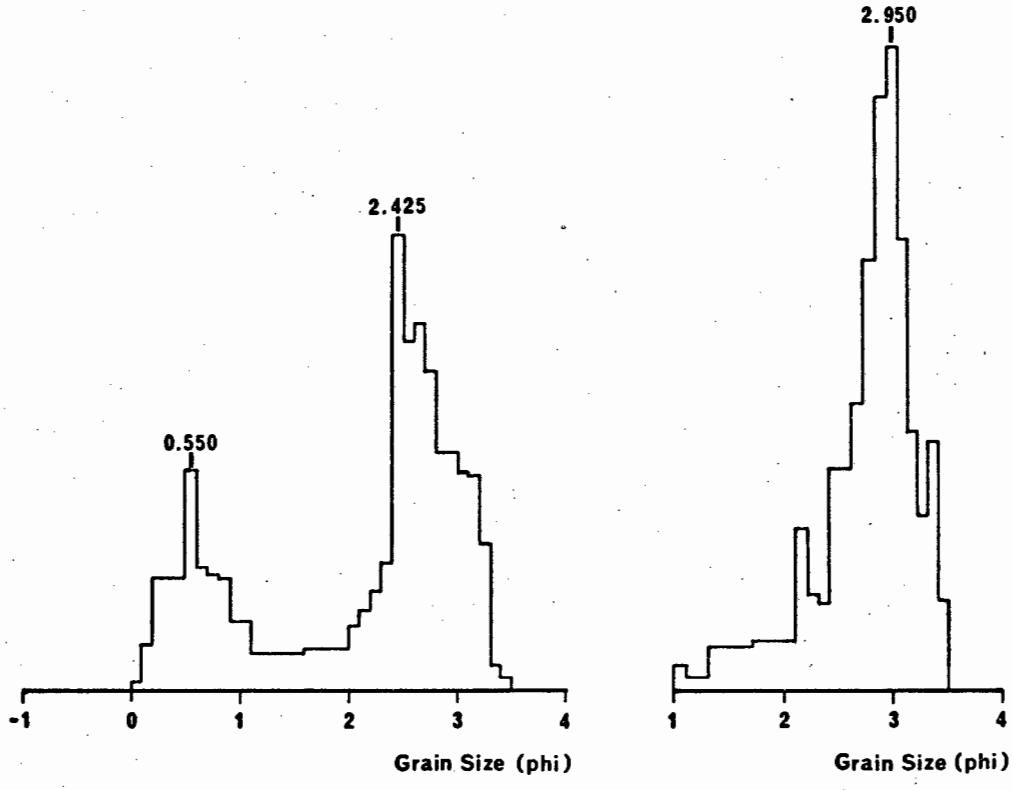

Fig. 28-A. Size-frequency distributions at 0.1-phi intervals

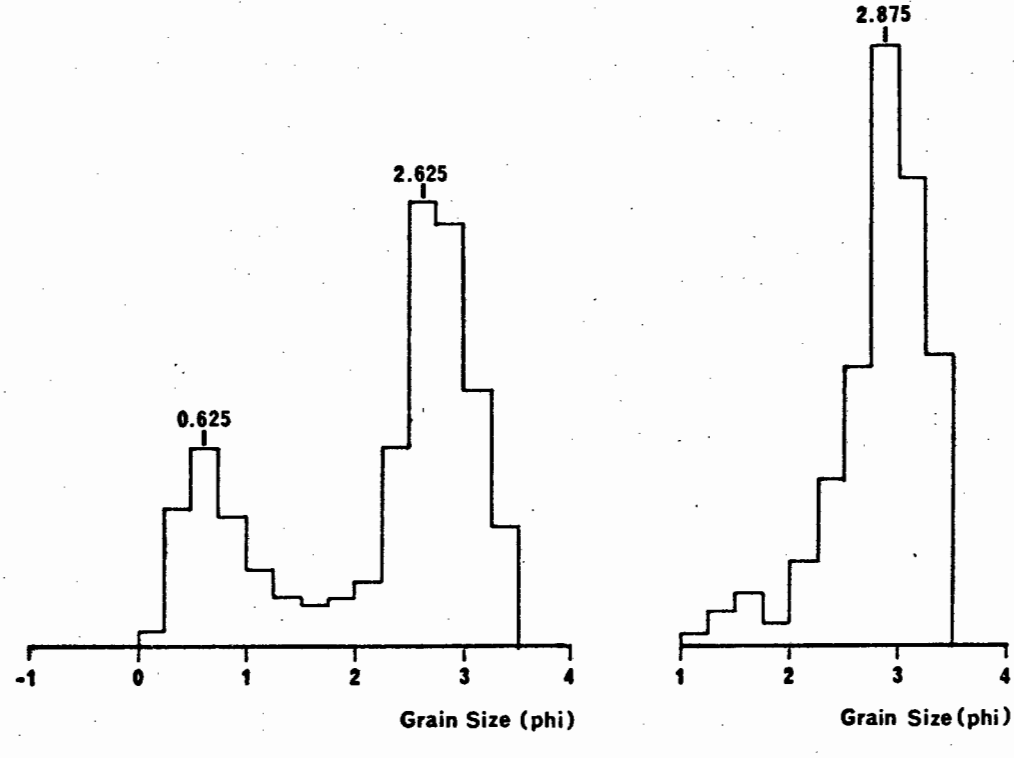

Fig. 28-B. Size-frequency distributions at 0.25-phi intervals

2.3. SIEVE - SETTLING DATA

PARAMETER	SIEVING	SETTLING
050106		
MEAN	2,53	2,76
MEDIAN	2,54	2,72
SORTING	0,24	0,41
SKEWNESS	-0,04	+0,11
KURTOSIS	1,04	1,07
050109		
MEAN	2,12	2,38
MEDIAN	2,35	2,52
SORTING	0,95	0,68
SKEWNESS	-0,34	-0,48
KURTOSIS	1,15	1,12
050112		
MEAN	1,08	1,64
MEDIAN	0,86	1,59
SORTING	1,22	1,06
SKEWNESS	0,25	-0,05
KURTOSIS	0,83	0,79
050118		
MEAN	0,83	1,37
MEDIAN	0,70	1,21
SORTING	0,93	0,83
SKEWNESS	0,24	0,31
KURTOSIS	1,04	0,83
050204		
MEAN	2,29	2,52
MEDIAN	2,29	2,49
SORTING	0,44	0,45
SKEWNESS	-0,03	-0,18
KURTOSIS	1,10	1,45
050209		
MEAN	0,99	1,60
MEDIAN	1,21	1,64
SORTING	1,47	0,80
SKEWNESS	-0,37	+0,18
KURTOSIS	1,57	1,02
050302		
MEAN	1,68	2,04
MEDIAN	1,71	1,98
SORTING	0,67	0,57
SKEWNESS	-0,06	0,10
KURTOSIS	1,23	0,98
050304		
MEAN	1,21	1,60
MEDIAN	1,28	1,67
SORTING	0,76	0,70
SKEWNESS	-0,15	-0,11
KURTOSIS	0,94	1,19

PARAMETER	SIEVING	SETTLING
050803		
MEAN	0,18	0,73
MEDIAN	0,02	0,55
SORTING	1,31	0,78
SKEWNESS	+0,35	+0,46
KURTOSIS	1,03	1,06
050403		
MEAN	2,19	2,37
MEDIAN	2,23	2,39
SORTING	0,59	0,65
SKEWNESS	-0,18	-0,43
KURTOSIS	1,06	1,62
050405		
MEAN	1,37	1,62
MEDIAN	1,42	1,67
SORTING	0,55	0,54
SKEWNESS	-0,27	-0,25
KURTOSIS	1,22	1,38
050502		
MEAN	2,61	2,86
MEDIAN	2,68	2,87
SORTING	0,40	0,46
SKEWNESS	-0,27	-0,17
KURTOSIS	0,94	1,10
050505		
MEAN	0,85	1,43
MEDIAN	1,20	1,47
SORTING	1,71	0,84
SKEWNESS	-0,37	-0,09
KURTOSIS	0,94	0,72
050508		
MEAN	1,37	1,74
MEDIAN	1,50	1,85
SORTING	0,80	0,66
SKEWNESS	-0,27	-0,17
KURTOSIS	0,88	0,98
050601		
MEAN	2,58	2,56
MEDIAN	2,80	2,99
SORTING	0,68	1,00
SKEWNESS	-0,64	-0,72
KURTOSIS	1,43	1,28
050605		
MEAN	1,86	2,19
MEDIAN	2,00	2,30
SORTING	0,92	0,54
SKEWNESS	-0,44	-0,40
KURTOSIS	1,56	1,12

PARAMETER	SIEVING	SETTLING
050607		
MEAN	2,04	2,21
MEDIAN	2,07	2,27
SORTING	0,60	0,50
SKEWNESS	-0,18	-0,34
KURTOSIS	1,40	1,29
050704		
MEAN	2,61	2,80
MEDIAN	2,68	2,80
SORTING	0,42	0,45
SKEWNESS	-0,29	-0,22
KURTOSIS	1,07	1,22
050708		
MEAN	1,44	1,62
MEDIAN	1,49	1,62
SORTING	0,85	0,67
SKEWNESS	-0,11	-0,11
KURTOSIS	0,94	0,86
040804		
MEAN	1,72	2,16
MEDIAN	1,70	2,14
SORTING	0,44	0,50
SKEWNESS	0,06	-0,03
KURTOSIS	1,10	1,17
050806		
MEAN	0,99	1,52
MEDIAN	1,00	1,46
SORTING	1,11	0,70
SKEWNESS	-0,08	+0,07
KURTOSIS	0,98	0,78
040902		
MEAN	0,83	2,91
MEDIAN	1,63	3,00
SORTING	2,28	0,58
SKEWNESS	-0,57	-0,32
KURTOSIS	0,77	1,10
040904		
MEAN	1,97	1,95
MEDIAN	1,98	1,99
SORTING	0,86	0,56
SKEWNESS	-0,04	-0,14
KURTOSIS	1,06	1,12
041005		
MEAN	1,85	1,83
MEDIAN	2,03	2,06
SORTING	1,07	0,75
SKEWNESS	-0,36	-0,61
KURTOSIS	1,03	1,41

2.4. COMPUTER PROGRAM FOR PSI-TRANSFORMARION OF SETTLING TUBE DATA

```
@PRT,S .SETTLE/TEMP
      1           DOUBLE PRECISION DIS(2,30),DUM,PHI,PSI,RL,FACT(8),S(3),CH(3),DENS(
      2          *21),VISC(21)
      3     C
      4           REAL NM(3,100)
      5     C
      6           DIMENSION SD(77)
      7           INTEGER STAR,BLANK,COM(3),CHA(3),TEMP
      8           COMMON NM,SD,VISC,DENS,COM,X,Y,DELT,STAR,BLANK,JKL,TEMP,IJKL,ITYPE
      9           DATA  ICDRD,ILNPT/8,5/
     10           DATA VISC/1.307D0,1.271D0,1.235D0,1.202D0,1.169D0,1.139D0,1.109D0,
     11          *1.081D0,1.053D0,1.027D0,1.002D0,0.9779D0,0.9548D0,0.9325D0,
     12          *0.9111D0,0.8904D0,0.8705D0,0.8513D0,0.8327D0,0.8148D0,0.7975D0/
     13           DATA DENS/.99973D0,.99961D0,.99959D0,.99945D0,.9992D0,.99905D0,
     14          *.99889D0,.99871D0,.99855D0,.99836D0,.99817D0,.99798D0,.99778D0,
     15          *.99758D0,.99736D0,.99713D0,.9969D0,.99664D0,.99638D0,.99607D0,
     16          *.99567D0/
     17           DATA SD/.007,.011,.016,.023,.034,.048,.069,.097,.135,.187,.256,
     18          *.347,.466,.621,.820,1.072,1.390,1.786,2.275,2.872,3.593,4.447,
     19          *5.480,6.681,8.176,9.680,11.510,13.567,15.866,18.406,21.186,
     20          *24.196,27.425,30.854,34.458,38.209,42.074,46.017,50.000,38*0.0/
     21           DATA STAR,BLANK/'*',' '/
     22           DATA FACT/.25D0,1.0D0,3.0D0,15.0D0,0.0D0,0.0D0,0.0D0,0.0D0/
     23           DO 20 K=1,21
     24          20 VISC(K)=VISC(K)/100.
     25     C    THIS SECTION READS THE VALUES NECESSARY TO PLOT THE DISTRIBUTIONS
     26     C    AND SETS UP THE PERCENTILES ON THE INPUTTED DATA.
     27           DO 2 I=1,38
     28          2 SD(39+I)=100.-SD(39-I)
     29           DIS(1,1)=0.0
     30           DIS(1,2)=0.5
     31           DIS(1,3)=1.0
     32           DO 5 I=4,15
     33          5 DIS(1,I)=DIS(1,I-1)+4.
     34           DO 6 I=16,30
     35          6 DIS(1,I)=100.0-DIS(1,31-I)
     36     C  X AND Y ARE THE SAMPLE COORDINATES, DELT IS THE PHI INTERVAL FOR
     37     C    CALCULATING THE DISTRIBUTION, TEMP IS THE WATER TEMPERATURE, COM IS
     38     C    THE SAMPLE LABEL, IJKL IS AN INDEX VARIABLE WHICH CONTROLS THE PRINTING
     39     C    OF THE DISTRIBUTIONS- '0' FOR THE FREQUENCY AND CUMULATIVE PLOTS,
     40     C    '1' FOR THE FEQUENCY ALONE, '2' FOR THE CUMULATIVE ALONE, AND '3' FOR
     41     C    NEITHER. THE PARAMETERS WILL ALWAYS BE PRINTED. IJK IS AN INDEX
     42     C    VARIABLE WHICH SHOULD ALWAYS BE BLANK, EXCEPT FOR THE LAST SET OF DATA.
     43      8    READ(ICDRD,9)  ITYPE,X,Y,DELT,TEMP,COM,IJKL,IJK
     44          9 FORMAT(1X,I1,2F7.0,1X,F8.0,1X,I2,1X,3A4,2I1)
     45     C     CH IS THE DISTANCE FROM THE ORIGIN IN MMS. OF THE BEGINNING OF
     46     C    EACH SPEED CHANGE, CH IS THE CHART SPEED NUMBER, RL IS THE ROD LENGTH
     47     C    IN CENTIMETERS.
     48           READ(ICDRD,10)  (CH(N),CHA(N), N = 1,3),RL
     49          10 FORMAT(1X,3(F5.0,1X,I1),1X,F6.0)
     50     C     DIS IS THE SET OF MEASURED DISTANCES OF THE PERCENTILES FROM THE
     51     C     ORIGIN IN MMS.
     52           READ(ICDRD,11)  (DIS(2,N), N = 1,30)
     53          11  FORMAT(16F5.0)
     54     C     THIS SECTION CALCULATES THE TIMES TO THE SPEED CHANGES.
     55           IF(CH(2).EQ.0.0) CH(2)=10**4
     56           IF(CH(3).EQ.0.0) CH(3)=10**4
     57           S(1)=0.0
     58           JI=CHA(1)
     59           S(2)=CH(2)*FACT(JI)
```

```
      JJ=CHA(2)
      JK=CHA(3)
      S(3)=(CH(3)-CH(2))*FACT(JJ)+S(2)
C     THIS SECTION CALCULATES THE PHI VALUES FOR THE PERCENTILES.
      DO 12 I=1,30
      IF(DIS(2,I).LE.CH(2)) DIS(2,I)=DIS(2,I)*FACT(JI)
      IF(DIS(2,I).GT.CH(2).AND.DIS(2,I).LE.CH(3))DIS(2,I)=(DIS(2,I)-CH(2
     1))*FACT(JJ)+S(2)
      IF(DIS(2,I).GT.CH(3))DIS(2,I)=(DIS(2,I)-CH(3))*FACT(JK)+S(3)
      DIS(2,I)=RL/DIS(2,I)
      DIS(2,I)=PHI(DIS(2,I))
      IF(ITYPE.EQ.0) DIS(2,I)=DIS(2,I)*20.
      IF(ITYPE.EQ.1) DIS(2,I)=PSI(DIS(2,I))
      DUM = DLOG10(DIS(2,I))
      DIS(2,I) = (-1.0 * DUM) / 0.30103
   12 CONTINUE
C     THIS SECTION CALCULATES THE DISTRIBUTION USING THE INPUTTED PHI INTERVAL.
      A=-5.0
   13 A=A+DELT
      IF(A.LE.DIS(2,1)) GO TO 13
      A=A-DELT*2.
      B=A
      I=0
   14 B=B+DELT
      I=I+1
      NM(1,I)=B
      IF(B.LT.DIS(2,30).AND.I.LT.100) GO TO 14
      JKL=I
      DO 15 I=2,JKL
      DO 16 J=2,30
      IF(NM(1,I).LE.DIS(2,J)) GO TO 115
   16 CONTINUE
  115 NM(3,I)=(NM(1,I)-DIS(2,J-1))/(DIS(2,J)-DIS(2,J-1))*(DIS(1,J)
     1-DIS(1,J-1))+DIS(1,J-1)
   15 CONTINUE
      IF(NM(1,JKL).GT.DIS(2,30)) NM(3,JKL)=100.0
      NM(2,1)=0.0
      NM(3,1)=0.0
      DO 17 I=2,JKL
   17 NM(2,I)=NM(3,I)-NM(3,I-1)
      CALL PARA
      IF(IJK.EQ.0) GO TO 8
      STOP
      END
```

```
@COPIN,S DUM.PARA,TPF$.PARA
 1 SYM
```

```
@PRT,S .PARA
```

```
      SUBROUTINE PARA
      DOUBLE PRECISION DENS(21),VISC(21)
C
      REAL NM(3,100),SD(77),N(4),M(4),MEAN,KURT,MED,
     1ANUM(100),DEC(9)
      INTEGER COM(3),PLOT(50), PL(77) ,STAR,BLANK,TEMP,IDEC(9)
      COMMON NM,SD,VISC,DENS,COM,X,Y,DELT,STAR,BLANK,JKL,TEMP,IJKL,ITYPE
      ILNPT = 5
      DO 1 I=1,JKL
    1 ANUM(I)=NM(1,I)-DELT/2.
      S=0.0
      DO 2 I=1,JKL
    2 S=S+NM(2,I)
      DO 3 I=1,4
```

```
      N(I)=0.0
    3 M(I)=0.0
      DO 4 I=1,4
      DO 4 J=2,JKL
    4 N(I)=N(I)+(NM(2,J)*ANUM(J)**I)/S
      M(2)=N(2)-N(1)**2
      M(3)=N(3)-3.*N(2)*N(1)+2.*N(1)**3
      M(4)=N(4)+N(1)*(-4.*N(3)+6.*N(1)*N(2)-3.*N(1)**3)
      MEAN=N(1)
      SORT=SQRT(M(2))
      SKEW=M(3)/(2.*SORT*M(2))
      KURT=M(4)/M(2)**2-3.
      DO 5 I=1,9
      A=I*10
      IDEC(I)=A
      DO 6 J=1,JKL
      B=J-1
      IF(NM(3,J).GT.A) GO TO 5
    6 CONTINUE
    5 DEC(I)=(A-NM(3,J-1))/(NM(3,J)-NM(3,J-1))*DELT+(NM(1,1)-DELT)
     1+B*DELT
      MED=DEC(5)
      WRITE(ILNPT,7)  COM,X,Y
    7 FORMAT('1',9X,3A4/10X,'X = ',F8.2,3X,'Y = ',F8.2)
      IF(ITYPE.EQ.0)  WRITE(ILNPT,8)
      IF(ITYPE.EQ.1)  WRITE(ILNPT,108)
    8 FORMAT(//10X,'DATA FOR OBTAINING A DISTRIBUTION CURVE'/10X,
     1'PHI INTERVAL',4X,'PERCENT',5X,'CUMULATIVE'/12X,'MIDPOINT',20X,
     2'PERCENT'//)
  108 FORMAT(//10X,'DATA FOR OBTAINING A DISTRIBUTION CURVE'/10X,
     1'PSI INTERVAL',5X,'PERCENT',5X,'CUMULATIVE'/12X,'MIDPOINT',20X,
     2'PERCENT'//)
      DO 9 I=2,JKL
    9 WRITE(ILNPT,10)  ANUM(I),(NM(J,I), J = 2,3)
   10 FORMAT(13X,F5.2,10X,F8.4,5X,F8.4)
      WRITE(ILNPT,11) (IDEC(I),I = 1,5),(DEC(J),J = 1,5),(IDEC(K),K = 6,
     *9),(DEC(L),L = 6,9)
   11 FORMAT(//10X,'DECILES'/9X,5(5X,I2,2X)/8X,5(4X,F5.2)//9X,
     14(5X,I2,2X)/8X,5(4X,F5.2))
      WRITE(ILNPT,12) MED,MEAN,SORT,SKEW,KURT
   12 FORMAT(/10X,'MOMENT MEASURES'/11X,'MEDIAN = ',F7.3/11X,'MEAN = ',
     1F7.3/11X,'SORTING = ',F7.3/11X,'SKEWNESS = ',F7.3/11X,'KURTOSIS =
     2',F7.3//)
      WRITE(ILNPT,13)
   13 FORMAT(10X,'REMARKS-')
      IJKL=IJKL+1
      GO TO (19,19,20,100),IJKL
   19 WRITE(ILNPT,14) COM
   14 FORMAT('1',10X,3A4//10X,'FREQUENCY DISTRIBUTION'//16X,
     1'FREQUENCY PERCENT'/12X,'0',9X,'5',8X,'10',8X,'15',8X,'20',
     28X,'25',/22X,'I',4(9X,'I')/12X,'I')
      DO 15 I=2,JKL
      IB=NM(2,I)/.5+.5
      DO 16 J=1,50
   16 PLOT(J)=BLANK
      IF(IB.GT.0.AND.IB.LE.50) PLOT(IB)=STAR
   15 WRITE(ILNPT,17)  ANUM(I),PLOT
   17 FORMAT(5X,F6.3,1X,'I',50A1/12X,'I')
      IF(IJKL.NE.1) GO TO 100
   20 IF(ITYPE.EQ.0)  WRITE(ILNPT,21)  COM
      IF(ITYPE.EQ.1)  WRITE(ILNPT,121)  COM
   21 FORMAT('1'/10X,'CUMULATIVE GRAIN-SIZE DISTRIBUTION FOR ',3A4//)
  121 FORMAT('1'/10X,'CUMULATIVE VELOCITY DISTRIBUTION FOR ',3A4//)
      WRITE(ILNPT,99)
```

```
      99 FORMAT(40X,'CUMULATIVE PERCENT'/11X,'.01',1X,'.05',   '.1',2X,'.5'
     1,2X,'1',6X,'5',2X,'10',5X,'30',3X,'50',3X,'70',5X,'90',2X,'95',
     25X,'99',1X,'99.5',2X,'99.95',2X,'99.99'/11X,'I',4X,'I',1X,'I',4X,
     3'I',2X,'I',6X,'I',2X,'I',7X,'I',4X,'I',4X,'I',7X,'I',2X,'I',6X,'I'
     4,2X,'I',4X,'I',1X,'I',4X,'I'/10X,'I')
         DO 93 I=2,JKL
         DO 97 J=1,77
      97 PL(J)=BLANK
         DO 94 J=1,77
         IF(NM(3,I).LT.SD(J).AND.NM(3,I).GE.0.007) GO TO 95
      94 CONTINUE
         GO TO 93
      95 IF(NM(3,I)-SD(j-1).GT.SD(J)-NM(3,I)) PL(J)=STAR
         IF(PL(J).NE.STAR) PL(J-1)=STAR
      93 WRITE(ILNPT,98)  NM(1,I),PL
      98 FORMAT(3X,F6.2,1X,'I', 77A1/10,'I')
     100 RETURN
         END
```

```
@COPIN,S DUM.FUNCTIONPSI,TPF$.FUNCTIONPSI
 1 SYM

@PRT,S .FUNCTIONPSI

      DOUBLE PRECISION FUNCTION PSI(R)
      DOUBLE PRECISION R,A,B,C,RHO,VISCO
      DOUBLE PRECISION VISC(21),DENS(21)
C
      REAL  NM(3,100),SD(77),X,Y
      INTEGER COM(3),STAR,BLANK,JKL,TEMP,IJKL,ITYPE
      COMMON NM,SD,VISC,DENS,COM,X,Y,DELT,STAR,BLANK,JKL,TEMP,IJKL,ITYPE
      RHO=DENS(5)
      VISCO=VISC(5)
      A=(((.0202/R)+.248)/1.82)*R*RHO
      B=6.*VISCO
      C=-4./3.*R**2*(2.65-RHO)*980.66
      PSI=(-1.*B+DSQRT(B**2-4.*A*C))/(2.*A)
      RETURN
      END
```

```
@COPIN,S DUM.FUNCTIONPHI/TEMP,TPF$.FUNCTIONPHI/TEMP
 1 SYM

@PRT,S .FUNCTIONPHI/TEMP

      DOUBLE PRECISION FUNCTION PHI(VEL)
      DOUBLE PRECISION A,B,C,RHO,VISCO,V,VEL
      DOUBLE PRECISION  VISC(21),DENS(21)
C
      REAL  NM(3,100),SD(77),X,Y
      INTEGER COM(3),STAR,BLANK,JKL,TEMP,IJKL
      COMMON NM,SD,VISC,DENS,COM,X,Y,DELT,STAR,BLANK,JKL,TEMP,IJKL,ITYPE
      I=TEMP-9
      RHO=DENS(I)
      VISCO=VISC(I)
      V=VEL
      A=(4./3.)*(2.65-RHO)*980.66
      B=(-0.248*RHO*V**2)/1.82
      C=-6.*VISCO*V-(.0202*RHO*V**2)/1.82
      PHI=(-1.*B+DSQRT(B**2-4.*A*C))/(2.*A)
      RETURN
      END
```

```
@FIN
```

RUNSTREAM :

	CARD
@RUN	(1)
@ASG,AX ABS.	(2)
@ELT,IL .DATA	(3)
⊬⊬⊬⊬⊬⊬⊬⊬⊬⊬⊬⊬⊬⊬⊬⊬⊬⊬⊬⊬⊬0.1⊬20⊬SB-010101⊬⊬⊬⊬1	(4)
⊬⊬⊬⊬⊬⊬⊬1xx123⊬2xx462⊬3⊬⊬200.	(5)
xxx24xxx33xxx40xxx97x99.5xx102110.5x115etc.	(6)
xx154xx160xx165171.5xx180etc.	(7)
@HDG,XN X.M,66,0,0	(8)
@XQT ABS.SETTLEPROG/TEMP	(9)
@ADD .DATA	(10)
@FIN	(11)

Cards 4,5,6,7, are the data cards :

Card 4 : begins with 22 blanks (⊬)
0.1 is the phi-interval at which the grain-size distribution is presented.
20 is an example for the water temperature in degrees Centigrade at which the sample was processed.
SB-010101 is an example for the sample code-number.
1 is the signal that the following data set is the last of a batch, up to ten of which are conveniantly processed simultaneously. The one (1) appears on the last data set only.

Card 5 : begins with 7 blanks (⊬).
1 is the speed factor one (here 240 mm/min).
123 is an example of the distance at which a speed change was introduced. The program can handle three speed factors (240 mm/min, 60 mm/min, 20 mm/min). The 2 designates the second speed factor.
200 is the height of the fall column in cm.

Cards 6 and 7 list the distances measured between the starting line and the recorded curve. 30 intervals are specified, expressing the sampled percentiles on the distorted time-velocity curve. Five digits are available for each value.

Card 6 : 0%, 0.5%, 1%, 5%, 9%, 13%, 17%, 21%, 25%, 29%, 33%, 37%, 41%, 45%, 49%, 51%,

Card 7 : 55%, 59%, 63%, 67%, 71%, 75%, 79%, 83%, 87%, 91%, 95%, 99%, 99.5%, 100%.

APPENDIX 3

3.1. SALDANHA BAY : GRAIN SIZE PARAMETERS OF THE TOTAL SEDIMENT

SAMPLE	MEAN	MD	QD	QH	SK	K	%VCS	%CS	%MS	%FS	%VFS	%MUD	1%	99%
010101	1,33	1,24	0,87	2,68	+0,17	-0,50	04,5	32,1	41,5	16,7	05,2	-	-0,32	3,12
02	0,51	0,18	1,16	2,11	+0,59	+0,39	38,7	41,1	04,9	13,0	02,3	-	-1,03	3,23
03	-	-	-	-	-	-	-	-	-	-	-	-	-	-
04	2,91	2,88	0,35	1,74	-0,21	+1,35	00,0	00,0	02,0	62,7	35,3	-	1,86	3,69
010201	1,36	1,21	0,89	2,78	+0,27	-0,54	01,0	41,7	33,4	18,2	05,7	-	-0,04	3,45
02	-	-	-	-	-	-	-	-	-	-	-	-	-	-
03	2,81	3,06	0,72	3,78	-0,69	+0,81	00,0	02,9	14,0	24,7	58,4	3,29	0,79	3,62
04	2,89	2,97	0,59	2,93	-1,26	+8,17	00,2	02,7	03,4	48,7	45,0	6,05	0,23	3,67
05	2,98	3,03	0,56	2,66	-0,44	+1,31	00,0	00,0	06,4	39,9	53,7	6,54	1,19	3,83
06	3,05	3,01	0,52	2,35	-0,43	+2,38	00,0	00,6	03,7	43,8	51,8	7,15	1,45	3,96
010301	2,67	3,01	0,91	4,87	-0,76	+0,93	00,3	11,4	07,2	30,0	51,1	-	0,18	3,58
02	-	-	-	-	-	-	-	-	-	-	-	-	-	-
03	2,89	3,08	0,74	3,70	-0,93	+3,08	00,0	04,4	08,3	25,4	61,9	1,87	0,25	3,81
04	2,99	3,04	0,44	2,09	-0,95	+5,23	00,0	00,5	04,9	39,1	55,5	2,43	1,37	3,62
05	3,26	3,24	0,47	1,86	-0,90	+7,06	00,0	00,6	02,2	15,8	81,4	4,56	1,30	4,01
06	2,97	3,00	0,44	2,11	-0,53	+1,86	00,0	00,0	04,1	46,1	49,8	5,75	1,43	3,65
07	2,94	3,04	0,62	3,06	-0,41	+0,44	00,0	00,6	08,0	39,1	52,3	6,03	1,12	3,86
010401	1,70	1,31	1,33	5,32	+0,04	-1,69	04,5	41,5	09,1	16,4	28,5	-	-0,39	3,55
02	3,21	3,24	0,50	2,06	-1,68	+14,86	00,0	01,8	01,6	06,3	90,3	-	0,49	3,81
03	3,29	3,28	0,37	1,42	-0,97	+7,48	00,0	00,0	00,0	15,0	85,0	0,99	1,55	3,93
04	3,49	3,45	0,29	0,98	+0,14	-0,60	00,0	00,0	00,0	16,0	84,0	2,73	2,82	4,12
05	3,31	3,27	0,26	0,99	+0,15	-0,89	00,0	00,0	00,0	12,0	88,0	2,67	2,78	3,82
06	2,82	2,98	0,79	4,11	-0,33	-0,49	00,0	01,9	16,1	32,7	49,3	4,41	0,89	3,94
07	2,66	2,68	0,63	3,41	-0,16	-0,65	00,0	00,0	17,6	48,5	33,9	5,76	1,17	3,72
08	2,25	2,24	0,84	4,42	-0,21	+0,02	01,4	05,6	29,6	40,5	22,9	15,80	-0,16	3,67
09	0,81	0,50	0,86	1,94	+0,64	+0,91	18,9	52,4	17,9	05,6	05,2	0,28	-0,22	3,11
010501	1,02	0,94	0,54	1,42	+0,34	+0,63	01,3	52,2	41,6	04,7	00,2	-	-0,01	2,54
02	3,53	3,55	0,34	1,11	-0,65	+3,55	00,0	00,0	00,4	04,2	95,4	1,55	2,24	4,04
03	3,47	3,44	0,28	0,94	+0,14	-0,50	00,0	00,0	00,0	03,4	96,6	0,56	2,82	4,04
04	3,44	3,43	0,27	0,95	+0,03	-0,84	00,0	00,0	00,0	04,5	95,5	-	2,95	3,83
05	3,30	3,29	0,32	1,24	-0,80	+5,81	00,0	00,0	01,1	05,9	93,0	1,77	1,94	3,83
06	2,40	2,36	0,72	4,01	-0,20	+0,38	00,1	04,0	20,7	49,2	26,0	3,32	0,26	3,67
07	2,92	2,96	0,60	2,98	-0,42	+1,27	00,0	01,0	06,3	45,4	47,3	14,82	0,98	3,89
08	2,67	2,79	0,67	3,59	-0,33	+0,14	00,0	02,2	15,0	46,5	36,3	1,87	0,71	3,75
010601	2,19	2,73	1,08	5,68	-0,21	-1,28	01,0	19,4	21,0	29,1	29,5	-	-0,05	3,64
02	-	-	-	-	-	-	-	-	-	-	-	-	-	-
03	-	-	-	-	-	-	-	-	-	-	-	-	-	-
04	3,48	3,48	0,22	0,73	+0,06	-0,92	00,0	00,0	00,0	00,3	99,7	0,55	3,05	3,87
05	2,90	3,26	1,09	5,45	-0,97	+2,34	03,7	08,6	02,6	03,2	81,9	1,31	-0,47	3,79
06	2,99	3,40	1,03	4,92	-0,70	+0,44	02,4	08,8	07,8	05,4	75,6	1,16	0,42	3,94
07	3,23	3,27	0,48	1,97	-1,85	+16,99	00,0	01,7	01,7	04,3	92,3	0,98	0,55	3,74
08	2,31	2,71	1,16	6,12	-0,41	-0,68	05,0	16,1	10,9	28,4	40,6	1,15	-0,34	3,58
09	-	-	-	-	-	-	-	-	-	-	-	-	-	-
10	2,89	3,04	0,81	4,04	-0,41	+0,23	00,0	03,4	08,2	37,7	50,7	8,09	0,54	3,94
11A	2,54	2,59	0,57	3,14	-0,25	-0,17	00,0	00,5	16,3	53,0	30,2	6,62	1,03	3,53
11B	2,67	2,85	0,81	4,33	-0,39	+0,07	00,1	03,8	17,1	36,8	42,2	2,73	0,38	3,82
12	-	-	-	-	-	-	-	-	-	-	-	-	-	-
13	-	-	-	-	-	-	-	-	-	-	-	-	-	-
020101	1,92	1,95	0,57	2,52	-0,03	-0,03	00,0	06,9	47,4	41,5	04,2	-	-	-
02	3,23	3,26	0,44	1,81	-1,83	+17,45	00,0	01,3	01,8	01,8	95,1	0,38	0,81	3,83

APPENDIX 3.1. (cont.)

SAMPLE	MEAN	MD	QD	QH	SK	K	%CS	%CS	%MS	%FS	%VFS	%MUD	1%	99%
03	3,29	3,28	0,28	1,09	-1,37	+18,50	00,0	00,0	00,8	03,9	95,3	1,06	2,55	3,74
04	3,24	0,42		1,70	-1,23	+9,41	00,0	00,4	02,6	05,5	91,5	1,69	1,35	3,84
05	3,07	3,24	0,67	3,00	-0,84	+1,74	00,0	00,0	13,1	03,8	83,1	1,47	1,16	3,83
06	3,21	3,29	0,51	2,13	-0,97	+3,78	00,0	00,0	06,1	06,6	87,3	2,75	1,36	3,83
07	2,91	3,20	0,82	3,90	-0,41	+0,03	00,0	02,9	12,8	30,4	53,8	4,15	0,51	4,05
08	-	-	-	-	-	-	-	-	-	-	-	-	-	-
020201	1,82	2,10	0,81	3,36	-0,28	-0,67	00,4	19,6	26,6	48,8	04,6	0,15	-0,20	3,24
02	3,31	3,29	0,28	1,09	-1,13	+14,94	00,0	00,1	00,5	04,0	95,4	0,78	2,45	3,75
03	3,34	3,34	0,33	1,24	-1,18	+14,20	00,0	00,2	00,6	05,0	94,2	1,53	2,35	3,88
04	3,13	3,21	0,60	2,58	-1,13	+5,62	00,0	02,1	04,8	07,3	85,8	1,36	0,79	3,96
05	3,12	3,27	0,68	2,94	-1,02	+3,85	00,0	02,9	03,4	09,6	81,2	1,60	0,65	3,86
06	3,03	3,27	0,72	3,31	-0,47	-0,19	00,0	00,0	13,8	18,7	67,5	1,66	1,23	3,99
07	3,25	3,34	0,51	2,06	-1,02	+4,60	00,0	00,2	04,2	08,4	87,2	4,23	1,25	3,84
08	-	-	-	-	-	-	-	-	-	-	-	-	-	-
020301	1,67	1,66	0,52	2,05	+0,13	-0,31	00,0	10,9	64,0	24,4	00,7	0,03	0,67	2,93
02	3,22	3,27	0,36	1,48	-0,92	+4,05	00,0	00,0	02,0	10,1	87,9	1,76	1,83	3,71
03	-	-	-	2,80	-	+3,64	-	-	-	-	-	2,08	0,74	3,89
020401	1,62	1,60	0,44	1,64	+0,35	+1,16	00,0	05,4	79,1	14,4	01,1	0,02	0,69	2,97
02	2,91	2,97	0,45	2,10	-0,25	+0,26	00,0	00,0	03,7	49,4	46,9	2,81	1,63	3,77
03	3,23	3,32	0,61	2,49	-1,42	+9,41	00,1	02,3	03,1	06,5	88,0	1,25	0,46	3,85
04	3,36	3,42	0,51	1,87	-1,21	+6,99	00,0	00,0	04,7	03,8	91,5	1,61	1,18	3,97
05	2,43	2,77	1,04	5,75	-0,13	-1,45	00,0	10,5	29,1	15,0	45,4	10,65	0,57	3,89
06	3,40	3,43	0,43	1,53	-1,23	+9,93	00,0	00,1	02,5	02,4	95,0	3,25	1,31	4,04
07	3,35	3,43	0,59	2,17	-1,28	+7,43	00,0	01,7	04,0	03,4	90,9	10,06	0,83	4,04
08	-	-	-	-	-	-	-	-	-	-	-	-	-	-
020501	1,68	1,72	0,38	1,48	-0,04	-0,58	00,0	08,5	71,0	19,5	01,0	0,01	0,90	2,35
02	3,23	3,20	0,20	0,80	-0,13	-	-	-	-	-	-	0,27	2,58	3,64
03	3,26	3,26	0,29	1,16	-1,10	+8,97	00,0	00,0	01,4	03,5	95,1	1,25	1,85	3,73
04	3,46	3,45	0,28	0,95	-0,91	+6,60	00,0	00,0	00,0	04,2	95,8	1,56	2,21	3,85
05	3,20	3,56	0,71	2,94	-0,92	+3,10	00,0	02,2	07,0	79,9		3,47	0,82	4,06
06	3,41	3,42	0,39	1,37	-0,82	+5,47	00,0	00,0	01,8	03,4	94,8	6,17	1,75	4,04
07	3,31	3,41	0,61	2,31	-1,26	+6,86	00,0	01,8	04,3	02,7	91,2	10,15	0,82	3,98
08	-	-	-	-	-	-	-	-	-	-	-	-	-	-
09	-	-	-	-	-	-	-	-	-	-	-	-	-	-
020601	1,71	1,90	0,68	2,70	-0,45	+0,30	01,9	16,9	41,5	36,7	03,0	0,02	-0,15	2,89
02	3,16	3,19	0,35	1,46	-1,24	+9,03	00,0	00,0	02,6	10,4	87,0	0,54	1,49	3,64
03	3,17	3,26	0,54	2,26	-1,24	+6,98	00,0	01,4	04,3	07,0	87,3	1,76	0,85	3,88
04	3,26	3,30	0,50	2,00	-1,66	+14,99	00,0	01,6	01,9	04,4	92,0	3,17	0,64	3,99
05	2,90	3,12	0,90	4,49	-0,83	+1,88	01,4	06,0	08,9	14,3	69,4	4,24	0,08	3,92
06	-	-	-	-	-	-	-	-	-	-	-	-	-	-
07	3,12	3,24	0,74	3,22	-0,86	+2,88	00,0	03,9	06,0	16,8	73,3	8,26	0,61	4,09
08	-	-	-	-	-	-	-	-	-	-	-	-	-	-
09	2,33	2,46	0,83	4,31	-0,27	-0,37	00,4	06,6	25,4	37,6	30,0	9,45	0,18	3,71
030101	2,22	2,32	0,75	3,96	-1,06	+6,09	03,7	04,0	09,0	75,2	08,1	0,02	-0,86	3,45
02	3,14	3,09	0,23	1,00	+0,44	+0,92	00,0	00,0	00,0	28,8	71,2	0,40	2,65	3,79
03	3,13	3,22	0,59	2,51	-1,34	+7,71	00,0	02,5	04,0	05,8	87,7	2,94	0,66	3,84
04	3,12	3,17	0,47	2,02	-1,11	+6,95	00,0	00,5	04,0	19,0	76,5	3,64	1,05	3,88
05	2,66	2,99	0,85	4,57	-0,45	-0,10	00,0	05,5	18,2	27,0	49,3	2,60	0,39	3,91
06	2,89	3,05	0,85	4,04	-0,40	+0,04	00,0	04,0	13,2	32,6	50,2	28,17	0,62	4,12
07	2,25	2,92	1,31	6,89	-0,28	-1,21	05,5	20,2	12,1	15,9	46,3	4,63	-0,23	3,93
08	3,07	3,19	0,72	3,41	-1,24	+6,54	00,4	03,8	03,7	09,0	83,1	8,04	0,11	3,89
09	3,29	3,34	0,57	2,21	-1,24	+7,44	00,0	01,6	04,0	03,2	91,2	18,39	0,83	4,01
10	2,38	2,61	1,01	5,55	-0,31	-0,64	00,3	14,4	15,8	38,1	31,4	17,62	0,03	3,83
11	2,53	2,88	0,86	4,77	-0,70	+1,19	01,4	06,7	14,5	41,3	36,1	2,04	-0,16	3,55

APPENDIX 3.1. (cont.)

SAMPLE	MEAN	MD	QD	QH	SK	K	%VCS	%CS	%MS	% FS	%VFS	%MUD	1%	99%
12	3,05	3,06	0,46	2,11	-0,54	+3,34	00,0	00,0	04,9	34,2	60,9	11,16	1,37	4,04
030201	2,49	2,47	0,40	2,21	-0,32	+1,93	00,0	00,4	09,2	72,9	17,5	0,02	1,36	3,23
02	3,23	3,25	0,47	1,92	-1,82	+17,23	00,0	01,5	01,8	03,9	92,8	0,83	0,69	3,79
03	3,35	3,35	0,38	1,41	-0,12	-	00,0	00,1	00,1	13,5	86,3	4,21	2,35	4,14
04	1,50	1,55	0,81	2,90	+0,01	+0,34	06,5	16,5	56,5	12,7	07,8	2,30	-0,20	3,39
05	3,28	3,36	0,59	2,31	-0,88	+3,54	00,0	00,1	06,3	09,0	84,6	15,78	1,12	4,04
06	3,01	3,09	0,60	2,86	-0,43	+0,50	00,0	00,0	08,9	32,3	58,8	7,61	1,35	4,02
07	2,90	2,98	0,51	2,54	-0,44	+0,70	00,0	00,0	07,9	43,7	48,4	1,22	1,47	3,78
08	1,18	1,01	0,83	2,35	+0,72	+1,75	06,0	43,4	38,0	06,6	06,0	2,16	-0,60	3,74
030301	2,36	2,42	0,53	2,86	-0,34	+0,42	00,0	02,1	19,6	63,3	15,0	0,02	0,79	3,25
02	3,10	3,09	0,27	1,15	-0,45	+2,59	00,0	00,0	00,3	33,5	66,2	0,22	2,09	3,55
03	3,26	3,24	0,40	1,59	-0,99	+9,97	00,0	00,4	01,5	09,5	88,6	3,06	1,68	3,94
04	3,37	3,35	0,29	1,06	+0,22	-0,73	00,0	00,0	00,0	07,4	92,6	9,57	2,90	3,98
05	1,03	1,06	0,72	1,85	+0,16	+0,04	07,4	37,8	43,0	10,8	01,0	0,27	-0,46	2,95
06	1,60	1,72	1,15	4,24	-0,73	-0,99	11,1	20,7	29,2	27,8	11,2	3,71	-0,52	3,71
07	2,99	2,97	0,37	1,85	-0,37	+2,92	00,0	00,0	03,0	52,3	44,7	2,48	1,68	3,82
				2,99	-0,27	-0,06	00,0	01,5						
030401	2,37	2,42	0,55	2,99	-0,27	-0,06	00,0	01,5	20,1	60,1	18,3	0,02	0,89	3,25
02	3,05	3,09	-	2,00	-1,90	+18,08	00,0	01,3	03,1	23,1	73,5	0,27	0,82	3,53
03	3,21	3,20	0,34	1,41	-0,67	+4,14	00,0	00,0	01,2	09,2	89,6	2,05	1,91	3,82
04	3,00	3,10	0,87	4,15	-1,35	+9,27	02,6	01,6	04,0	30,0	61,8	7,33	-1,05	4,05
05	0,81	0,78	0,78	1,73	+0,23	+0,06	16,0	46,2	29,7	07,7	00,4	1,85	-0,60	2,78
06	2,90	2,96	0,42	2,10	-0,77	+3,11	00,0	00,0	06,0	51,1	42,9	1,04	1,38	3,61
030501	1,47	1,12	1,10	3,90	+0,25	-1,19	01,0	45,7	28,3	00,4	24,6	0,00	-0,05	3,14
02	2,88	2,92	0,36	1,79	-0,54	+3,09	00,0	00,0	02,8	58,9	38,3	0,09	1,68	3,54
03	2,94	3,06	0,63	2,67	-0,98	+3,25	00,0	02,2	08,2	29,9	59,7	1,98	0,85	3,64
04	1,16	1,17	0,66	1,85	+0,37	+1,03	00,5	39,8	51,4	06,2	02,1	0,01	-0,07	3,15
05	1,33	1,09	0,91	2,81	+0,39	-0,11	03,4	41,0	34,4	13,7	07,5	4,87	-0,43	3,44
030601	1,23	1,08	0,73	2,11	+0,15	-1,06	02,4	43,8	34,4	19,2	00,2	0,00	0,03	2,65
02	3,00	3,00	0,40	1,90	-0,90	-	00,0	00,0	05,0	32,0	63,0	0,18	-	-
03	3,03	3,07	0,41	1,89	-0,92	+4,82	00,0	00,0	05,1	32,0	62,9	2,53	1,45	3,69
04	1,61	1,55	1,06	3,93	+0,06	-1,14	04,6	29,3	29,4	23,8	12,9	2,27	-0,38	3,49
030701	2,44	2,41	0,30	1,67	+0,18	+0,40	00,0	00,0	05,8	89,3	04,8	0,00	1,75	3,14
02	3,00	2,98	0,25	1,18	-0,05	+1,10	00,0	00,0	00,2	54,8	45,0	0,34	2,33	3,55
040101	0,33	0,18	0,62	1,03	+0,84	+3,23	23,5	64,4	08,8	03,3	00,0	0,01	-0,78	2,52
02	3,16	3,17	0,27	1,13	-0,69	+5,91	00,0	00,0	00,4	11,7	87,9	0,79	2,27	3,69
03	3,14	3,19	0,53	2,26	-1,96	+18,28	00,4	01,9	01,4	08,4	87,9	0,92	0,13	3,75
040201	1,05	0,95	0,54	1,39	+0,20	-0,89	00,0	52,5	43,1	04,4	00,0	0,01	0,16	2,14
02	3,16	3,12	0,32	1,36	-0,15	+1,06	00,0	00,0	00,0	32,1	67,9	1,14	2,09	3,83
03	3,19	3,15	0,34	1,42	-0,47	+3,42	00,0	00,0	00,9	25,6	73,5	1,59	1,97	3,75
04	2,90	3,02	0,58	2,90	-0,59	+0,81	00,0	00,0	11,8	35,1	53,1	2,43	1,28	3,74
05	0,79	0,70	0,78	1,72	+0,36	+0,76	14,8	51,9	26,3	05,3	01,7	1,13	-0,64	3,14
040301	0,34	0,26	0,38	0,64	+1,37	+9,70	08,4	86,8	03,4	01,4	00,0	0,02	-0,10	2,06
02	3,13	3,14	0,40	1,70	-1,28	+11,22	00,0	00,3	02,7	20,9	76,1	0,77	1,13	3,83
03	3,00	3,03	0,44	2,08	-1,11	+6,49	00,0	00,0	05,2	39,1	55,7	0,90	1,14	3,63
04	0,99	0,75	0,93	2,31	+0,63	+1,25	08,8	56,3	22,1	06,4	06,4	1,07	-0,43	3,68
05	2,72	2,92	0,73	3,84	-0,74	+1,54	00,0	04,9	11,1	46,3	37,7	1,01	0,47	3,65
06	2,85	3,03	0,66	3,59	-0,67	+0,97	00,0	00,8	13,5	32,0	53,7	4,58	0,97	3,65

APPENDIX 3.1. (cont.)

SAMPLE	MEAN	MD	QD	QH	SK	K	%VCS	%CS	%MS	%FS	%VFS	%MUD	1%	99%
040401	1,13	1,04	0,49	1,35	+0,82	+3,67	00,0	45,0	50,0	03,9	01,1	0,01	0,37	2,96
02	3,11	3,12	0,47	2,04	-1,52	+15,23	00,0	01,6	01,8	19,9	76,7	1,63	0,65	3,88
03	3,15	3,12	0,30	1,27	-0,12	+1,64	00,0	00,0	00,3	46,0	53,7	1,24	-2,26	3,82
04	3,16	3,13	0,26	1,09	+0,05	+0,62	00,0	00,0	00,0	28,0	72,0	1,52	2,38	3,77
05	3,15	3,15	0,45	1,91	-0,78	+5,11	00,0	00,1	03,4	21,5	75,0	3,82	1,31	3,93
06	3,08	3,09	0,56	2,52	-0,73	+4,53	00,0	01,6	03,7	34,0	60,8	-	0,82	4,11
040501	1,17	1,16	0,58	1,62	+0,41	+1,54	00,0	38,7	54,4	05,5	01,4	0,02	0,08	3,05
02	3,16	3,13	0,23	0,98	+0,19	+1,35	00,0	00,0	00,0	19,0	81,0	0,69	2,48	3,75
03	3,07	3,09	0,39	1,72	-1,19	+10,25	00,0	00,4	02,6	29,0	68,0	1,53	1,45	3,74
04	3,14	3,10	0,26	1,12	+0,24	+1,38	00,0	00,0	00,0	29,0	71,0	2,31	2,42	3,83
05	2,61	2,92	0,91	5,04	-0,50	+0,03	00,0	09,5	14,4	35,0	41,0	8,60	0,28	3,93
040601	1,57	1,53	0,34	1,25	+0,30	+0,23	00,0	02,8	86,5	10,7	00,0	0,01	0,90	2,44
02	3,03	3,13	0,66	3,06	-1,45	+9,06	00,7	03,2	03,0	16,9	76,2	0,89	0,09	3,79
03	3,08	3,12	0,42	1,85	-1,41	+11,01	00,0	00,8	02,8	26,5	69,9	0,94	1,14	3,58
04	3,19	3,17	0,24	1,02	+0,03	+0,32	00,0	00,0	00,0	20,0	80,0	1,74	2,49	3,73
05	3,24	3,20	0,30	1,22	-0,12	+1,40	00,0	00,0	00,0	12,3	87,3	6,35	2,22	3,92
06	2,47	3,08	1,28	7,13	-0,55	-0,03	04,8	15,0	09,4	12,2	58,6	11,21	-1,02	3,83
07	2,83	3,01	0,74	3,85	-0,85	+2,11	00,0	05,5	08,3	34,5	51,7	10,48	0,55	3,72
08	2,88	2,97	0,52	2,62	-0,97	00,0	00,8		07,1	47,0	45,1	-	0,97	3,54
040701	1,62	1,57	0,45	1,68	+0,13	-0,38	00,0	06,9	71,1	22,0	00,0	0,02	0,67	2,69
02	2,79	3,04	0,77	4,03	-0,91	+2,33	00,0	06,3	08,5	28,8	56,4	0,47	0,36	3,54
03	3,03	3,05	0,40	1,86	-1,51	-	00,0	00,9	02,2	40,5	56,4	0,42	-	-
04	3,03	2,98	0,30	1,37	+0,10	+1,05	00,0	00,0	00,0	54,1	45,9	1,53	2,19	3,75
05	3,06	3,04	0,26	1,18	+0,04	+0,12	00,0	00,0	00,0	44,3	55,7	2,82	2,38	3,62
06	2,98	2,92	0,34	1,62	+0,17	+0,19	00,0	00,0	00,0	62,4	37,6	6,83	2,18	3,82
07	3,07	3,12	0,78	3,47	-0,65	+2,18	00,0	03,7	06,9	28,6	60,8	-	0,46	4,23
040801	1,44	1,42	0,49	1,64	+0,03	-0,79	00,0	20,7	63,1	16,2	00,0	0,01	0,39	2,38
02	3,00	3,01	0,30	1,44	-0,27	+1,58	00,0	00,0	00,9	47,2	51,9	1,13	1,96	3,63
03	2,94	2,97	0,43	2,10	-0,87	+5,49	00,0	00,0	04,0	50,9	45,1	1,67	1,09	3,73
04	2,05	1,98	0,44	2,12	+0,50	+0,70	00,0	00,0	52,6	41,4	06,0	0,01	1,36	3,23
05	3,03	2,99	0,31	1,42	+0,21	-0,19	00,0	00,0	00,0	50,9	49,1	3,07	2,37	3,75
06	2,96	2,98	0,41	1,97	-0,75	+4,07	00,0	00,0	04,0	50,3	45,7	6,60	1,37	3,63
07	-	-	-	-	-	-	-	-	-	-	-	-	-	-
08	1,89	1,82	0,51	2,18	+0,43	+0,71	00,0	00,8	64,9	30,0	04,3	-	0,96	3,29
040901	2,42	2,57	0,64	3,57	-0,44	-0,15	00,0	04,0	17,6	64,8	13,6	0,02	0,75	3,44
02	1,73	2,11	1,14	4,61	-0,12	-1,34	04,7	30,3	13,2	39,0	12,8	0,90	-0,52	3,46
03	1,17	1,17	0,99	2,78	+0,06	-0,79	13,6	32,0	33,1	17,5	03,8	1,36	-0,73	3,30
04	2,11	2,07	0,73	3,66	-0,11	-0,04	00,0	08,2	38,5	40,8	12,5	0,88	0,41	0,88
05	2,56	2,72	0,60	3,31	-0,41	-0,19	00,0	00,8	20,7	53,6	24,9	1,28	0,99	3,43
06	-	-	-	-	-	-	-	-	-	-	-	-	-	-
07	0,71	0,13	1,33	2,78	+0,50	-0,47	38,9	33,2	04,7	12,8	10,4	8,43	-1,02	3,75
041001	2,70	2,78	0,43	2,27	-0,73	+2,06	00,0	00,0	09,4	71,3	19,3	0,02	1,33	3,33
02	1,58	1,71	0,72	2,63	-0,01	-0,14	01,7	19,4	53,5	21,9	03,5	0,11	-0,14	3,15
03	2,87	2,87	0,42	2,11	-0,35	+1,21	00,0	00,0	04,3	60,0	35,7	26,82	1,57	3,62
04	1,49	1,48	0,34	1,19	-0,10	+1,69	00,2	04,5	88,4	06,9	00,0	0,03	0,55	2,29
05	2,23	2,28	0,90	4,74	-0,18	-0,37	00,2	11,4	24,6	40,8	23,0	1,96	0,04	3,83
06	2,45	2,41	0,34	1,91	+0,31	+1,04	00,0	00,0	06,9	85,9	07,2	0,30	1,66	3,42
07	2,61	2,85	0,78	4,33	-0,73	+1,60	00,6	05,3	13,1	45,3	35,7	2,36	0,09	3,54
08	1,79	2,06	1,02	4,25	-0,14	-1,04	01,9	26,8	18,8	43,2	09,3	3,90	-0,13	3,62
09	-	-	-	-	-	-	-	-	-	-	-	-	-	-
10	2,93	2,89	0,26	1,13	+0,46	+1,52	00,0	00,0	00,0	68,5	31,5	4,63	2,36	3,73

APPENDIX 3.1. (cont.)

SAMPLE	MEAN	MD	QD	QH	SK	K	%VCS	%CS	%MS	%FS	%VFS	%MUD	1%	99%
041101	2,21	2,19	0,51	2,71	-0,05	+0,54	00,0	01,5	27,9	63,9	06,7	1,58	0,88	3,41
02	0,82	0,72	0,97	2,18	+0,12	-0,44	20,0	38,9	26,8	12,5	01,8	2,40	-1,21	3,08
03	2,28	2,41	0,51	2,69	-0,70	+2,71	00,2	03,1	18,3	74,1	04,3	1,00	0,54	3,05
041201	0,91	0,91	0,73	1,69	+0,10	-0,04	11,3	44,8	36,3	07,6	00,0	1,61	-0,67	2,65
02	1,45	1,57	0,90	3,04	-0,11	-0,69	06,0	26,3	38,0	26,5	03,2	1,92	-0,57	3,11
03	2,83	2,85	0,39	2,00	-0,45	+1,64	00,0	00,0	04,7	64,8	30,5	4,93	1,58	3,57
04	1,91	1,99	0,49	2,11	-0,57	+1,82	00,2	05,4	45,9	48,5	00,0	1,82	0,28	2,68
05	2,42	2,46	0,53	2,96	-0,41	-0,41	00,0	02,0	15,9	70,1	12,0	3,74	0,78	3,34
06	2,46	2,59	0,75	4,14	-0,57	+1,31	00,7	04,2	16,8	52,7	25,6	5,22	0,03	3,54
07	1,79	1,85	0,72	2,96	-0,07	-0,29	00,0	15,6	44,4	35,5	04,5	7,23	0,19	3,35
060001	-	-	-	-	-	-	-	-	-	-	-	-	-	-
02	-	-	-	-	-	-	-	-	-	-	-	-	-	-
03	-	-	-	-	-	-	-	-	-	-	-	-	-	-
04	-	-	-	1,10	-	-	-	-	-	-	-	1,63	2,36	3,45
05	1,64	1,55	0,63	2,40	+0,52	+2,13	00,4	08,0	74,5	11,4	05,7	3,73	0,28	3,58
06	2,74	2,84	0,57	2,98	-0,99	+4,04	00,0	02,7	07,9	60,9	28,5	11,03	0,66	3,44
07	-	-	-	-	-	-	-	-	-	-	-	-	-	-
08	-	-	-	-	-	-	-	-	-	-	-	-	-	-
09	1,39	1,45	0,55	1,77	-0,09	-0,23	00,4	23,7	64,1	11,8	00,0	0,01	0,08	2,55
10	1,31	1,41	0,57	1,72	-0,43	+0,58	03,5	20,8	67,4	08,3	00,0	0,01	-0,36	2,19
11	3,18	3,13	0,30	1,27	+0,08	-0,63	00,0	00,0	00,0	32,5	67,5	-	2,47	3,75
12	3,32	-	0,59	2,24	-0,19	-1,55	00,0	00,0	00,4	44,6	55,0	0,05	2,07	3,85
13	3,24	3,20	0,27	1,10	+0,14	-0,28	00,0	00,0	00,0	20,6	79,4	0,57	2,56	3,83
14	3,21	3,16	0,34	1,41	+0,14	-0,36	00,0	00,0	00,0	30,0	70,0	0,17	2,45	3,94
15	1,20	1,18	0,32	0,90	+0,25	+0,50	00,0	26,7	72,3	01,0	00,0	-	0,56	1,95
16	2,52	2,41	0,68	3,79	+0,11	-	00,0	00,0	28,2	42,9	28,9	3,00	-	-
17	1,59	1,53	0,30	1,10	+0,90	+3,92	00,0	00,3	91,6	08,1	00,0	0,04	1,03	2,54
18	1,34	1,33	0,43	1,34	+0,01	+0,01	00,2	22,6	70,7	06,5	00,0	-	0,32	2,25
19	0,90	0,88	0,42	0,97	+0,27	+0,60	00,4	63,2	35,7	00,9	00,0	-	0,06	1,94
20	3,32	3,31	0,39	1,46	-0,17	+0,35	00,0	00,0	00,4	18,1	81,5	3,81	2,18	3,96
21	0,36	0,35	0,20	0,34	+0,17	+0,79	02,0	97,6	00,4	00,0	00,0	(4,34)	-	-

LEGEND :

MEAN - mean settling diameter in phi
MD - median grain size (50th percentile) in phi
QD - standard sorting coefficient in phi
QH - relative sorting coefficient
SK - skewness of the size distribution
K - kurtosis of the size distribution
%VCS - proportion of very coarse sand in the total sediment
%CS - proportion of coarse sand
%MD - proportion of medium sand
%FS - proportion of fine sand
%VFS - proportion of very fine sand
%MUD - mud content of the total sediment
1% - first percentile in phi
99% - ninetyninth percentile in phi

3.2. SALDANHA BAY : GRAIN SIZE PARAMETERS OF THE TERRIGENOUS COMPONENT

SAMPLE	MEAN	MD	QD	QH	SK	K	%VCS	%CS	%MS	%FS	%VFS	1%	99%
010101	1,36	1,26	0,73	2,23	+0,34	+0,14	00,8	32,4	50,0	13,5	03,3	0,05	3,15
02	0,46	0,18	1,11	1,99	+0,70	+1,17	39,2	44,2	02,9	09,2	04,5	-1,11	3,45
03	-	-	-	-	-	-	-	-	-	-	-	-	-
04	3,04	2,98	0,35	1,59	+0,17	-0,27	00,0	00,0	00,3	51,3	49,4	2,35	3,74
010201	1,25	1,04	0,89	2,62	+0,40	-0,20	00,6	47,6	33,0	11,7	07,1	-0,10	3,35
02	-	-	-	-	-	-	-	-	-	-	-	-	-
03	2,79	2,98	0,74	3,92	-0,74	+1,38	00,0	04,6	10,9	36,3	48,2	0,57	3,62
04	3,08	3,03	0,32	1,40	+0,22	-0,74	00,0	00,0	00,0	47,8	52,2	2,55	3,74
05	3,04	3,00	0,37	1,70	+0,01	-0,06	00,0	00,0	00,4	49,6	50,0	2,19	3,75
06	3,18	3,12	0,32	1,26	+0,32	-0,56	00,0	00,0	00,0	34,8	65,2	2,66	3,83
010301	2,65	3,01	1,04	5,33	-0,73	+0,58	00,0	16,1	03,1	30,3	50,5	0,08	3,73
02	-	-	-	-	-	-	-	-	-	-	-	-	-
03	2,90	3,02	0,61	3,07	-1,09	+5,41	00,0	02,9	05,7	39,2	52,2	0,45	3,55
04	3,16	3,13	0,24	1,00	+0,16	-0,85	00,0	00,0	00,0	31,8	68,2	2,75	3.63
05	3,09	3,06	0,27	1,17	+0,16	-0,10	00,0	00,0	00,0	31,6	68,4	2,40	3,71
06	3,14	3,08	0,28	1,20	+0,33	-0,25	00,0	00,0	00,0	38,7	61,3	2,66	3,79
07	3,11	3,06	0,28	1,20	+0,30	+0,28	00,0	00,0	00,0	41,3	58,7	2,49	3,82
010401	1,57	0,78	1,45	5,39	+0,05	-1,85	09,0	42,1	02,3	20,4	26,2	-0,38	3,54
02	3,26	3,23	0,19	0,74	+0,34	-0,09	00,0	00,0	00,0	00,9	99,1	2,90	3,73
03	3,18	3,16	0,20	0,85	+0,16	-0,69	00,0	00,0	00,0	25,5	74,5	2,78	3,59
04	3,09	3,06	0,22	0,96	+0,19	-0,75	00,0	00,0	00,0	30,0	70,0	2,70	3,55
05	3,16	3,16	0,26	1,12	-0,43	+2,66	00,0	00,0	00,0	22,0	78,0	2,16	3,63
06	3,12	3,13	0,40	1,71	-0,63	+2,84	00,0	00,0	02,6	26,5	70,9	1,76	3,75
07	2,89	2,96	0,50	2,52	-0,33	-0,09	00,0	00,0	06,2	47,0	46,8	1,52	3,65
08	2,32	2,46	0,79	4,14	-0,35	-0,39	00,0	10,2	18,8	47,0	24,0	0,45	3,36
09	0,28	0,16	0,65	1,04	+0,46	+0,48	36,8	49,2	13,4	00,6	00,0	-0,77	1,93
010501	0,86	0,78	0,39	0,88	+0,44	+0,30	00,0	69,2	29,8	01,0	00,0	0,30	1,86
02	3,36	3,34	0,19	0,70	+0,18	-0,68	00,0	00,0	00,0	00,0	100,0	3,00	3,74
03	3,28	3,26	0,16	0,60	+0,22	-0,66	00,0	00,0	00,0	00,0	100,0	3,00	3,62
04	3,27	3,27	0,18	0,70	+0,11	-0,84	00,0	00,0	00,0	03,9	96,1	2,90	3,63
05	3,25	3,25	0,19	0,70	+0,04	-1,12	00,0	00,0	00,0	09,1	90,9	2,90	3,55
06	2,99	3,05	0,42	2,01	-0,29	+0,12	00,0	00,0	02,7	46,2	51,1	1,78	3,73
07	2,83	2,93	0,68	3,55	-0,82	+3,79	00,0	02,0	08,2	46,1	43,7	0,29	3,74
08	3,18	3,12	0,22	0,91	+0,50	+1,35	00,0	00,0	00,0	28,1	71,9	2,85	3,78
010601	2,51	2,82	0,80	4,45	-0,47	-0,52	00,0	09,1	16,1	40,2	34,6	0,79	3,44
02	-	-	-	-	-	-	-	-	-	-	-	-	-
03	-	-	-	-	-	-	-	-	-	-	-	-	-
04	3,26	3,25	0,16	0,64	+0,15	-0,89	00,0	00,0	00,0	00,4	99,6	2,95	3,55
05	3,29	3,29	0,15	0,58	+0,07	-1,03	00,0	00,0	00,0	00,0	100,00	2,96	3,45
06	2,86	3,15	0,99	5,08	-1,31	+5,69	04,8	04,4	02,0	09,2	79,6	-0,87	3,53
07	3,24	3,22	0,21	0,92	+0,40	+0,62	00,0	00,0	00,0	08,1	91,9	2,90	3,84
08	3,01	3,15	0,60	2,84	-1,00	+5,11	00,0	02,1	04,4	28,8	64,7	0,59	3,84
09	-	-	-	-	-	-	-	-	-	-	-	-	-
10	3,33	3,29	0,25	0,94	+0,29	-0,54	00,0	00,0	00,0	02,8	97,2	2,90	3,86
11A	3,09	3,14	0,37	1,62	-0,75	+2,87	00,0	00,0	03,1	36,6	60,3	1,78	3,64
11B	3,01	2,98	0,24	1,14	+0,34	+0,56	00,0	00,0	00,0	53,9	46,1	2,50	3,66
12	-	-	-	-	-	-	-	-	-	-	-	-	-
13	-	-	-	-	-	-	-	-	-	-	-	-	-
020101	2,04	2,05	0,44	2,03	+0,00	-0,59	00,0	00,3	45,9	53,4	00,4	1,16	2,93
02	3,27	3,25	0,18	0,69	+0,22	-0,73	00,0	00,0	00,0	00,5	99,5	2,96	3,64
03	3,32	3,31	0,17	0,63	+0,16	-0,66	00,0	00,0	00,0	00,0	100,0	3,00	3,64
04	3,33	3,33	0,15	0,57	+0,04	-0,92	00,0	00,0	00,0	00,1	99,9	2,97	3,63
05	3,28	3,28	0,20	0,79	-1,15	+17,63	00,0	00,0	00,4	00,6	99,0	2,95	3,63
06	3,26	3,27	0,31	1,20	-1,00	+7,87	00,0	00,0	01,3	03,7	95,0	1,85	3,79

APPENDIX 3.2. (cont.)

SAMPLE	MEAN	MD	QD	QH	SK	K	%VCS	%CS	%MS	%FS	%VFS	1%	99%
07	3,32	3,35	0,43	1,70	-1,88	+17,48	00,0	01,2	01,8	01,8	95,2	0,86	3,83
08	-	-	-	-	-	-	-	-	-	-	-	-	-
020201	2,25	2,47	0,78	4.09	-0,38	-0,31	00,0	10,9	19,6	50,3	09,2	0,28	3,42
02	3,30	3,28	0,20	0,78	+0,16	-0,70	00,0	00,0	00,0	03,3	96,7	2,90	3,73
03	3,25	3,23	0,20	0,80	+0,09	-0,90	00,0	00,0	00,0	08,9	91,1	2,80	3,63
04	3,30	3,29	0,16	0,62	+0,11	-0,89	00,0	00,0	00,0	00,4	99,6	2,96	3,63
05	3,25	3,24	0,18	0,73	+0,14	-0,63	00,0	00,0	00,0	06,9	93,1	2,90	3,63
06	3,34	3,32	0,19	0,70	+0,18	-0,72	00,0	00,0	00,0	00,1	99,9	2,96	3,74
07	3,37	3,35	0,21	0,75	+0,35	+0,11	00,0	00,0	00,0	00,0	100,0	3,00	3,95
08	-	-	-	-	-	-	-	-	-	-	-	-	-
020301	1,59	1,47	0,55	2,03	+0,21	-0,99	00,0	12,1	59,9	28,0	00,0	0,68	2,74
02	3,30	3,31	0,18	0,70	-0,04	-0,90	00,0	00,0	00,0	05,0	95,0	2,90	3,63
03	3,28	3,26	0,17	0,65	+0,17	-0,72	00,0	00,0	00,0	00,3	99,7	2,96	3,63
020401	1,68	1,68	0,28	1,08	+0,01	+0,15	00,0	00,7	86,0	13,3	00,0	0,97	2,24
02	3,08	3,04	0,30	1,33	+0,11	-1,04	00,0	00,0	00,0	46,7	53,3	2,48	3,63
03	3,43	3,41	0,21	0,74	+0,23	-0,63	00,0	00,0	00,0	00,0	100,0	3,06	3,89
04	3,52	3,52	0,22	0,71	+0,08	-0,88	00,0	00,0	00,0	00,0	100,0	3,10	3,94
05	3,27	3,40	0,62	2,42	-1,02	+4,41	00,0	01,1	05,5	10,6	82,8	0,93	3,94
06	3,35	3,38	0,44	1,63	-1,36	+10,88	00,0	00,0	02,9	02,1	95,0	1,12	3,94
07	3,49	3,49	0,35	1,15	-0,09	-0,28	00,0	00,0	00,0	04,8	95,2	2,53	4,12
08	-	-	-	-	-	-	-	-	-	-	-	-	-
020501	1,56	1,55	0,57	2,06	+0,18	-0,24	00,0	16,7	62,3	19,8	01,2	0,55	2,99
02	3,26	3,24	0,27	1,06	-0,60	+8,18	00,0	00,0	00,3	08,2	91,5	2,59	3,74
03	3,33	3,29	0,25	0,93	+0,24	-0,72	00,0	00,0	00,0	03,0	97,0	2,90	3,87
04	3,41	3,39	0,24	0,85	+0,18	-0,73	00,0	00,0	00,0	00,0	100,0	2,96	3,91
05	3,32	3,36	0,51	1,92	-1,46	+12,08	00,0	01,6	01,7	01,7	95,0	06,5	3,94
06	3,43	3,42	0,24	0,83	+0,09	-0,70	00,0	00,0	00,0	01,0	99,0	2,95	3,93
07	3,43	3,41	0,27	0,96	+0,16	-0,98	00,0	00,0	00,0	00,6	99,4	2,96	3,94
08	-	-	-	-	-	-	-	-	-	-	-	-	-
09	-	-	-	-	-	-	-	-	-	-	-	-	-
020601	1,52	1,81	0,95	3,37	+0,04	-1,20	03,3	32,8	21,6	36,3	06,0	-0,03	3,42
02	3,32	3,31	0,20	0,74	+0,15	-0,70	00,0	00,0	00,0	01,3	98,7	2,90	3,74
03	-	-	-	-	-	-	-	-	-	-	-	-	-
04	3,32	3,29	0,21	0,78	+0,17	-0,92	00,0	00,0	00,0	00,5	99,5	2,96	3,73
05	3,12	3,21	0,71	3,05	-1,75	+14,74	01,8	01,4	01,5	17,3	79,0	-0,52	3,84
06	-	-	-	-	-	-	-	-	-	-	-	-	-
07	3,40	3,40	0,27	0,95	+0,06	-1,04	00,0	00,0	00,0	04,4	95,6	2,88	3,91
08	-	-	-	-	-	-	-	-	-	-	-	-	-
09	3,06	3,07	0,46	2,08	-0,59	+3,59	00,0	00,3	03,6	36,1	60,0	1,43	3,95
030101	2,24	2,49	0,93	4,99	-0,68	+0,98	03,6	07,1	09,0	68,4	11,9	-0,16	3,63
02	3,25	3,22	0,21	0,85	+0,36	+0,24	00,0	00,0	00,0	08,9	91,1	2,87	3,83
03	3,32	3,31	0,21	0,84	+0,25	-0,18	00,0	00,0	00,0	00,9	99,1	2,95	3,85
04	3,29	3,27	0,26	0,99	+0,22	-0,71	00,0	00,0	00,0	13,6	86,4	2,85	3,83
05	3,08	3,11	0,38	1,68	-0,68	+2,18	00,0	00,0	02,7	30,3	67,0	1,85	3,63
06	3,22	3,28	0,56	2,27	-0,90	+4,16	00,0	00,4	05,6	14,0	80,0	1,23	3,99
07	3,45	3,40	0,30	1,02	+0,10	-0,06	00,0	00,0	00,0	07,5	92,5	2,66	4,05
08	3,32	3,24	0,32	1,22	+0,29	-0,77	00,0	00,0	00,0	17,8	82,2	2,84	4,02
09	3,52	3,48	0,28	0,93	+0,20	-0,80	00,0	00,0	00,0	00,4	99,6	3,05	4,12
10	2,86	3,08	0,85	4,38	-0,70	+1,79	00,5	05,0	08,1	26,2	60,2	0,11	3,98
11	3,16	3,11	0,20	0,80	+0,40	-0,29	00,0	00,0	00,0	28,7	71,3	2,85	3,59
12	3,20	3,18	0,19	0,80	+0,30	-0,09	00,0	00,0	00,0	15,0	85,0	2,80	3,64

APPENDIX 3.2. (cont.)

SAMPLE	MEAN	MD	QD	QH	SK	K	%VCS	%CS	%MS	%FS	%VFS	1%	99%
030201	2,90	2,92	0,36	1,81	-0,55	+4,73	00,0	00,3	01,3	63,4	35,0	1,85	3,59
02	3,35	3,31	0,26	0,95	+0,20	-0,88	00,0	00,0	00,0	03,9	96,1	2,87	3,29
03	3,32	3,31	0,32	1,22	-1,16	+18,98	00,0	00,2	00,2	10,0	89,6	2,49	3,83
04	2,20	1,89	0,66	3,48	+0,24	-0,42	00,2	00,6	59,3	24,7	15,2	1,05	3,58
05	3,47	3,42	0,32	1,07	+0,19	-0,93	00,0	00,0	00,0	00,6	99,4	2.95	4,12
06	3,32	3,26	0,31	1,15	+0,49	-0,03	00,0	00,0	00,0	08,9	91,1	2,86	3,95
07	3,03	3,00	0,20	0,92	+0,29	+0,21	00,0	00,0	00,0	51,0	49,0	2,55	3,53
08	1,34	1,29	1,22	3,60	-0,28	+0,52	11,9	13,1	51,1	12,7	11,2	-0,95	3,50
09	-	-	-	-	-	-	-	-	-	-	-	-	-
030301	2,70	2,83	0,51	2,69	-0,61	+0,86	00,0	00,3	12,3	57,4	30,0	+1,36	3,42
02	3,27	3,23	0,22	0,85	+0,26	-0,69	00,0	00,0	00,0	07,6	92,4	2,86	3,74
03	3,29	3,26	0,25	0,96	+0,20	-0,86	00,0	00,0	00,0	12,0	88,0	2,86	3,78
04	3,39	3,36	0,23	0,83	+0,19	-0,95	00,0	00,0	00,0	00,1	99,9	2,96	3,84
05	1,59	1,55	0,50	1,84	+0,04	-0,66	00,0	13,0	66,6	20,3	00,1	0,57	2,54
06	2,95	3,08	0,43	1,73	-1,08	+3,91	00,0	00,0	08,1	20,8	71,1	1,41	3,43
07	3,17	3,12	0,20	0,82	+0,64	+1,87	00,0	00,0	00,0	15,6	84,4	2,80	3,75
030401	2,88	2,93	0,41	2,05	-0,98	+6,34	00,0	00,5	03,7	60,1	35,7	1,18	3,53
02	3,31	3,28	0,17	0,65	+0,24	-0,56	00,0	00,0	00,0	00,1	99,9	2,96	3,65
03	3,41	3,36	0,27	0,95	+0,38	+0,10	00,0	00,0	00,0	00,1	99,9	2,96	4,09
04	3,45	3,38	0,29	1,00	+0,29	-0,81	00,0	00,0	00,0	00,4	99,6	2,96	4,04
05	1,64	1,48	1,25	4,31	-0,13	-0,75	11,1	17,5	33,6	12,4	25,4	-0,96	3,43
06	3,09	3,03	0,26	1.12	+0,69	+1,56	00,0	00,0	00,0	45,8	54,2	2,75	3,87
030501	0,92	0,53	0,84	2,00	+0,55	-0,37	00,1	72,0	06,9	21,1	00,0	0,05	2,72
02	3,13	3,10	0,20	0,87	+0,32	-0,36	00,0	00,0	00,0	32,0	68,0	2,76	3,62
03	3,32	3,29	0,24	0,92	+0,28	-0,48	00,0	00,0	00,0	03,0	97,0	2,90	3,86
04	1,58	1,50	0,78	2,90	+0,10	+0,80	03,2	14,2	61,9	13,5	07,2	-0,55	3,39
05	2,15	2,74	0,94	4,95	-0,18	-1,48	00,0	14,4	30,0	35,0	20,6	0,28	3,24
030601	0,92	0,61	0,85	2,06	+0,42	+00,0	04,8	66,2	11,4	16,7	00,9	-0,87	2,94
02	3,21	3,17	0,21	0,85	+0,41	+0,26	00,0	00,0	00,0	12,9	87,1	2,86	3,74
03	3,25	3,22	0,21	0,80	+0,22	-0,60	00,0	00,0	00,0	10,0	90,0	2,86	3,72
04	2,74	3,00	0,77	4,06	-0,63	+1,24	00,2	04,1	17,3	28,3	50,1	0,27	3,91
030701	2,87	2,84	0,21	1,03	+0,40	+0,69	00,0	00,0	00,0	77,0	23,0	2,46	3,44
02	3,14	3,11	0,18	0,80	+0,20	-0,79	00,0	00,0	00,0	29,0	71,0	2,80	3,53
040101	0,27	0,21	0,42	0,68	+1,65	+13,46	17,2	78,3	02,4	02,1	00,0	-0,25	2,39
02	3,31	3,27	0,20	0,78	+0,23	-0,82	00,0	00,0	00,0	00,5	99,5	2,96	3,73
03	3,29	3,26	0,22	0,83	+0,31	-0,34	00,0	00,0	00,0	02,3	97,7	2,90	3,83
040201	1,02	0,83	0,53	1,33	+0,51	+0,18	00,0	61,1	32,1	06,8	00,0	0,36	2,45
02	3,30	3,28	0,18	0,69	+0,12	-1,12	00,0	00,0	00,0	00,1	99,9	2,96	3,63
03	3,24	3,19	0,23	0,97	+0,37	-0,11	00,0	00,0	00,0	13,7	86,3	2,90	3,83
04	3,10	3,08	0,15	0,67	+0,20	-0,62	00,0	00,0	00,0	30,7	69,3	2,80	3,42
05	1,99	1,74	0,88	4,20	+0,18	-1,10	00,2	10,6	51,3	16,4	21,5	0,46	3,49
040301	0,32	0,28	0,21	0,34	+0,81	+4,23	00,5	98,0	01,5	00,0	00,0	-0,04	1,03
02	3,14	3,14	0,36	1,55	-1,39	+14,31	00,0	00,4	01,8	21,7	76,1	1,55	3,73
03	3,20	3,17	0,23	0,98	-0,22	-0,56	00,0	00,0	00,0	24,9	75,1	2,76	3,72
04	0,98	0,67	1,02	2,56	+0,42	-0,29	12,6	49,2	19,4	12,4	06,4	-0,46	3,35
05	3,10	3,07	0,18	0,80	+0,30	-0,45	00,0	00,0	00,0	35,5	64,5	2,76	3,52
06	3,15	3,10	0,19	0,82	+0,51	+0,60	00,0	00,0	00,0	24,8	75,2	2,86	3,65

APPENDIX 3.2. (cont.)

SAMPLE	MEAN	MD	QD	QH	SK	K	%VCS	%CS	%MS	%FS	%VFS	1%	99%
040401	1,11	0,99	0,42	1,13	+0,92	+3,82	00,0	51,9	42,1	05,7	00,3	0,57	2,53
02	3,14	3,13	0,20	0,86	+0,11	-1,01	00,0	00,0	00,0	30,3	69,7	2,76	3,52
03	3,21	3,20	0,17	0,73	+0,11	-0,89	00,0	00,0	00,0	08,3	91,7	2,83	3,54
04	3,21	3,20	0,18	0,77	+0,12	-0,94	00,0	00,0	00,0	12,9	87,1	2,85	3,55
05	3,25	3,20	0,25	1,04	+0,47	+0,35	00,0	00,0	00,0	14,2	85,8	2,86	3,93
06	3,22	3,13	0,26	1,10	+0,53	+0,02	00,0	00,0	00,0	14,7	85,3	2,83	3,84
07													
040501	1,17	1,13	0,57	1,62	+0,62	+2,66	00,3	37,3	55,1	05,4	01,9	0,25	3,16
02	3,29	3,26	0,24	0,94	+0,20	-0,78	00,0	00,0	00,0	11,6	88,4	2,86	3,83
03	3,33	3,32	0,23	0,90	+0,10	-0,95	00,0	00,0	00,0	06,9	93,1	2,90	3,74
04	3,25	3,21	0,23	0,94	+0,21	-0,82	00,0	00,0	00,0	13,9	86,1	2,86	3,73
05	3,14	3,14	0,37	1,59	-1,52	+18,76	00,1	00,3	01,6	23,9	74,1	1,65	3,65
040601	1,61	1,57	0,26	0,98	+0,25	-0,25	00,0	00,2	89,3	10,7	00,0	1,07	2,18
02	3,07	3,11	0,48	2,09	-1,30	+9,49	00,0	01,4	02,9	29,4	66,3	-0,83	3,82
03	3,27	3,25	0,17	0,66	+0,18	-0,63	00,0	00,0	00,0	02,3	97,7	2,90	3,63
04	3,18	3,16	0,23	0,95	+0,12	-1,04	00,0	00,0	00,0	29,5	70,5	2,76	3,63
05	3,19	3,19	0,21	0,88	-0,18	+0,35	00,0	00,0	00,0	15,9	84,1	2,53	3,54
06	3,06	3,12	0,47	2,11	-1,19	+6,11	00,0	00,0	06,2	18,7	75,1	1,26	3,64
07	2,98	3,07	0,47	2,26	-1,21	+6,31	00,0	00,7	05,8	27,7	65,8	1,03	3,54
08	3,03	3,00	0,14	0,69	+0,41	+0,50	00,0	00,0	00,0	51,9	48,1	2,76	3,35
040701	1,66	1,57	0,51	2,04	+0,46	+0,85	00,0	06,3	70,9	20,3	02,5	0,86	3,19
02	3,03	3,01	0,19	0,90	-0,22	+2,90	00,0	00,0	00,2	47,7	52,1	2,66	3,34
03	3,10	3,07	0,16	0,71	+0,24	-0,54	00,0	00,0	00,0	34,9	65,1	2,76	3,45
04	3,16	3,12	0,24	1,02	+0,34	-0,27	00,0	00,0	00,0	32,1	67,9	2,76	3,73
05	3,18	3,15	0,19	0,79	+0,27	-0,44	00,0	00,0	00,0	19,5	80,5	2,86	3,63
06	3,06	3,01	0,20	0,91	+0,53	+0,52	00,0	00,0	00,0	47,5	52,5	2,75	3,59
07	3,30	3,23	0,42	1,61	-0,82	+7,48	00,0	00,4	01,4	07,1	91,1	1,74	3,94
040801	1,39	1,36	0,44	1,42	+0,11	-0,76	00,0	23,6	67,0	09,4	00,0	0,66	2,25
02	3,43	3,41	0,21	0,74	-0,13	+0,10	00,0	00,0	00,0	02,9	97,1	2,79	3,74
03	3,15	3,13	0,21	0,89	+0,27	-0,43	00,0	00,0	00,0	29,0	71,0	2,76	3,63
04	1,96	1,91	0,34	1,43	+0,53	+1,21	00,0	00,0	61,0	38,1	00,9	1,46	2,95
05	3,18	3,14	0,25	1,05	+0,14	-0,35	00,0	00,0	00,0	27,4	72,6	2,66	3,69
06	3,17	3,12	0,21	0,88	+0,39	-0,15	00,0	00,0	00,0	27,6	72,4	2,80	3,69
07	-	-	-	-	-	-	-	-	-	-	-	-	-
08	3,14	3,11	0,17	0,75	+0,38	-0,10	00,0	00,0	00,0	27,5	72,5	2,85	3,54
040901	2,55	2,75	0,63	3,50	-0,61	+0,67	00,0	02,9	15,2	60,4	21,5	0,75	3,34
02	2,32	2,60	0,83	4,35	-0,38	-0,58	00,0	10,1	20,1	40,2	20,7	0,33	3,43
03	1,83	1,75	0,62	2,59	+0,15	-0,07	00,3	06,1	58,4	31,0	04,2	0,63	3,30
04	2,30	2,28	0,69	3,64	-0,05	-1,06	00,0	01,4	38,8	40,1	19,7	0,89	3,46
05	2,79	2,87	0,48	2,51	-0,69	+1,92	00,0	00,3	09,4	58,3	32,0	1,28	3,44
06	-	-	-	-	-	-	-	-	-	-	-	-	-
07	3,03	3,09	0,50	2,40	-0,84	+5,14	00,0	01,2	02,5	39,9	56,4	0,84	3,73
041001	2,91	2,96	0,40	2,00	-1,24	+7,72	00,0	00,3	04,3	54,4	41,0	1,13	3,43
02	1,53	1,51	0,64	2,27	+0,15	-0,52	00,0	24,1	54,9	19,6	01,4	0,33	2,99
03	-	-	-	-	-	-	-	-	-	-	-	-	-
04	1,55	1,51	0,35	1,28	+0,81	+4,05	00,0	01,7	90,3	09,4	00,6	0,88	2,83
05	2,06	2,14	0,70	3,48	-0,29	-0,16	00,3	10,3	30,4	53,1	05,9	0,38	3,21
06	2,58	2,54	0,25	1,38	+0,24	-0,59	00,0	00,0	00,1	92,0	07,9	2,15	3,05
07	2,80	2,84	0,45	2,37	-0,63	+3,04	00,0	00,7	03,9	63,4	33,0	1,26	3,48
08	2,09	2,23	0,88	4,41	-0,18	-0,70	00,2	13,7	24,6	46,1	15,4	0,13	3,73
09	-	-	-	-	-	-	-	-	-	-	-	-	-
10	3,13	3,10	0,16	0,70	+0,37	-0,06	00,0	00,0	00,0	26,5	73,5	2,85	3,53

APPENDIX 3.2. (cont.)

SAMPLE	MEAN	MD	QD	QH	SK	K	%VCS	%CS	%MS	%FS	%VFS	1%	99%
041101	2,39	2,33	0,49	2,72	+0,00	+0,13	00,0	00,4	20,6	67,2	11,8	1,18	3,43
02	0,57	0,52	0,92	1,75	+0,05	-1,10	32,6	32,1	29,0	06,3	00,0	-1,01	2,15
03	2,36	2,41	0,40	2,22	-0,31	+1,07	00,0	00,3	17,5	78,4	03,8	1,28	3,24
041201	0,92	0,91	0,66	1,54	+0,05	+0,38	04,8	50,8	38,0	06,3	00,1	0,76	2,48
02	1,51	1,62	0,80	2,87	-0,09	-0,55	02,9	27,9	37,1	29,8	02,3	-0,49	3,15
03	2,87	2,83	0,40	2,00	-0,10	+0,17	00,0	00,0	03,0	61,3	35,7	1,80	3,64
04	2,00	2,01	0,42	2,02	-0,08	+0,15	00,0	00,6	48,4	50,6	00,4	1,06	2,84
05	2,56	2,61	0,53	2,92	-0,25	+0,12	00,0	00,5	14,2	65,1	20,2	1,20	3,44
06	2,62	2,73	0,71	3,94	-0,38	+0,05	00,0	03,4	14,9	48,0	33,7	0,70	3,63
07	1,73	1,75	0,76	3,02	+0,11	-0,19	00,3	18,8	48,9	24,9	07,1	0,18	3,49
060001	-	-	-	-	-	-	-	-	-	-	-	-	-
02	-	-	-	-	-	-	-	-	-	-	-	-	-
03	-	-	-	-	-	-	-	-	-	-	-	-	-
04	2,98	2,95	0,18	0,87	+0,52	0,83	00,0	00,0	00,0	63,8	36,2	2,70	3,84
05	2,45	2,26	0,42	2,33	+0,58	+0,15	00,0	00,0	00,8	84,4	14,8	1,96	3,50
06	3,01	2,99	0,17	0,81	-0,39	+4,90	00,0	00,0	00,2	51,5	48,3	2,48	3,34
07	-	-	-	-	-	-	-	-	-	-	-	-	-
08	-	-	-	-	-	-	-	-	-	-	-	-	-
09	1,08	1,11	0,41	1,11	-0,14	-0,58	00,4	42,0	57,5	00,1	00,0	0,17	1,74
10	1,26	1,33	0,57	1,63	-0,22	+0,37	02,8	27,0	62,9	07,3	00,0	-0,25	2,44
11	-	-	-	-	-	-	-	-	-	-	-	-	-
12	2,99	2,97	0,14	0,67	+0,37	-0,22	00,0	00,0	00,0	58,9	41,1	2,75	3,32
13	3,09	3,04	0,20	0,85	+0,35	-0,39	00,0	00,0	00,0	42,0	58,0	2,76	3,54
14	3,11	3,07	0,19	0,84	+0,27	-0,24	00,0	00,0	00,0	34,3	65,7	2,68	3,54
15	-	-	-	-	-	-	-	-	-	-	-	-	-
16	3,00	3,15	0,51	2,43	-1,05	+5,28	00,0	01,1	03,8	23,7	71,4	0,92	3,62
17	1,51	1,60	0,34	1,20	-0,97	+3,14	00,0	10,6	89,0	00,4	00,0	0,38	1,93
18	-	-	-	-	-	-	-	-	-	-	-	-	-
19	-	-	-	-	-	-	-	-	-	-	-	-	-
20	3,22	3,15	0,26	1,06	+0,70	+1,51	00,0	00,0	00,0	15,2	84,8	2,86	3,98
21	3,17	3,13	0,21	0,89	+0,32	-0,41	00,0	00,0	00,0	24,9	75,1	2,77	3,65

3.3: SALDANHA BAY : GRAIN SIZE PARAMETERS OF THE BIOCLASTIC COMPONENT

SAMPLE	MEAN	MD	QD	QH	SK	K	%VCS	%CS	%MS	%FS	%VFS	1%	99%
010101	1,30	1,21	1,02	3,09	+0,01	-1,14	08,2	31,8	33,0	19,9	07,1	-0,69	3,09
02	0,55	0,19	1,21	2,33	+0,48	-0,38	38,2	38,0	06,9	16,8	00,1	-0,95	3,01
03	-	-	-	-	-	-	-	-	-	-	-	-	-
04	2,78	2,79	0,34	1,82	-0,58	+2,97	00,0	00,0	03,7	74,1	21,2	1,37	3,64
010201	1,46	1,37	0,88	3,03	+0,14	-0,88	01,4	35,8	33,8	24,7	04,3	0,02	3,55
02	-	-	-	-	-	-	-	-	-	-	-	-	-
03	2,83	3,13	0,69	3,61	-0,65	+0,25	00,0	01,2	17,1	13,1	68,6	1,01	3,62
04	2,71	2,92	0,85	4,46	-2,73	+17,09	02,4	03,4	06,8	49,6	37,8	-2,09	3,60
05	2,93	3,06	0,74	3,66	-0,88	+2,67	00,0	01,0	11,4	30,2	57,4	0,19	3,91
06	3,12	3,07	0,59	2,53	-0,58	+4,36	00,0	01,2	03,4	39,9	55,3	0,24	4,09
010301	2,68	3,01	0,78	4,10	-0,79	+1,27	00,6	06,7	11,3	29,7	51,7	0,28	3,43
02	-	-	-	-	-	-	-	-	-	-	-	-	-
03	2,87	3,13	0,87	4,41	-0,77	+0,76	00,0	05,9	10,9	11,6	71,6	0,05	4,07
04	2,82	2,94	0,64	3,31	-2,16	+11,31	00,0	01,0	09,8	46,4	42,8	-0,01	3,61
05	3,42	3,43	0,66	2,33	-1,96	+14,21	00,0	01,2	04,4	00,0	94,4	0,20	4,31
06	2,80	2,92	0,60	3,14	-1,39	+3,97	00,0	00,0	08,2	53,5	38,3	0,20	3,51
07	2,76	3,02	1,00	5,10	-1,11	+0,60	01,0	02,2	14,0	36,9	45,9	-0,25	3,90
010401	1,82	1,84	1,20	5,06	+0,03	-1,53	01,0	39,9	15,9	12,4	30,8	-0,40	3,56
02	3,16	3,24	0,81	3,42	-3,70	+29,81	02,0	03,6	03,2	11,7	79,5	-1,92	3,89
03	3,40	3,41	0,53	1,91	-2,10	+15,64	00,0	01,0	01,0	04,5	93,5	0,32	4,27
04	3,90	3,83	0,37	0,83	+0,10	-0,45	00,0	00,0	00,0	02,0	98,0	2,94	4,69
05	3,46	3,39	0,26	0,88	+0,74	-4,63	00,0	00,0	00,0	00,5	99,5	3,40	4,01
06	2,52	2,83	1,18	6,53	-0,02	-3,83	00,0	03,8	29,6	38,9	27,7	0,02	4,13
07	2,43	2,41	0,77	4,25	+0,01	-1,21	00,0	01,0	28,0	50,0	21,0	0,82	3,79
08	2,19	2,02	0,89	4,63	-0,08	+0,44	02,8	01,0	40,4	34,0	21,8	-0,77	3,98
09	1,34	0,83	1,06	3,30	+0,81	+1,34	01,0	55,6	22,4	10,6	10,4	+0,33	4,29
010501	1,18	1,11	0,69	1,96	+0,24	+1,00	02,6	35,2	53,4	08,4	00,4	-0,32	3,23
02	3,69	3,76	0,50	1,34	-1,47	+7,79	00,0	00,0	01,8	07,2	91,0	1,48	4,34
03	3,66	3,62	0,40	1,06	+0,07	-0,35	00,0	00,0	00,0	06,8	93,2	2,64	4,46
04	3,61	3,59	0,37	1,11	-0,05	-0,85	00,0	00,0	00,0	01,0	99,0	3,00	4,03
05	3,34	3,34	0,46	1,69	-1,63	+12,74	00,0	01,0	01,2	02,7	95,1	0,98	4,11
06	1,81	1,67	1,02	4,25	-0,12	+0,64	02,2	08,0	36,7	51,2	01,9	-1,26	3,61
07	3,00	2,99	0,53	2,52	-0,02	-1,25	00,0	00,0	04,4	44,7	50,9	1,67	4,04
08	2,16	2,47	1,12	5,63	-1,15	-1,06	02,0	04,4	30,0	61,9	01,7	-1,43	3,72
010601	1,87	2,65	4,67	19,8	+2,63	-2,04	02,0	29,7	25,9	18,0	24,4	-0,89	3,84
02	-	-	-	-	-	-	-	-	-	-	-	-	-
03	-	-	-	-	-	-	-	-	-	-	-	-	-
04	3,70	3,71	0,27	0,73	-0,03	-1,00	00,0	00,0	00,0	00,2	99,8	3,15	4,19
05	2,51	3,24	2,03	11,27	-2,01	+4,70	07,4	17,2	05,2	06,4	63,8	-3,90	4,13
06	3,13	3,64	1,08	4,63	-0,09	-4,81	00,0	13,2	13,6	01,6	71,6	1,71	4,35
07	3,20	3,32	0,76	3,17	-4,11	+33,36	02,0	03,4	03,4	00,5	90,7	-1,80	3,64
08	1,61	2,27	1,73	6,40	+0,19	-6,46	10,0	14,1	17,4	28,0	16,5	-1,27	3,32
09	-	-	-	-	-	-	-	-	-	-	-	-	-
10	2,45	2,79	1,37	7,60	-1,10	+1,00	02,0	06,8	16,4	70,6	04,2	-1,82	4,02
11A	1,98	2,04	0,76	3,60	+0,25	-3,21	00,0	01,0	29,5	69,4	00,1	0,28	3,42
11B	2,33	2,54	1,02	5,46	+0,23	-4,98	02,2	05,5	29,8	42,8	19,7	-1,74	3,98
12	-	-	-	-	-	-	-	-	-	-	-	-	-
13	-	-	-	-	-	-	-	-	-	-	-	-	-
020101	1,79	1,85	0,70	3,02	-0,06	+0,53	00,0	13,5	48,9	29,6	08,0	-	-
02	3,18	3,27	0,71	2,98	-3,87	+35,62	02,0	02,6	03,6	03,1	88,7	-1,34	4,02
03	3,27	3,28	0,40	1,58	-2,89	+37,65	00,0	00,0	01,6	07,8	90,6	2,1	3,84
04	3,14	3,18	0,69	2,93	-2,50	+19,74	01,0	00,8	05,2	10,9	82,1	-0,27	4,05
05	2,85	3,21	1,14	5,83	-0,54	-14,15	02,0	03,0	23,8	07,0	64,2	-0,63	4,03

APPENDIX 3.3. (cont.)

SAMPLE	MEAN	MD	QD	QH	SK	K	%VCS	%CS	%MS	%FS	%VFS	1%	99%
06	3,16	3,32	0,72	3,04	-0,95	-0,32	00,0	00,0	10,9	09,5	79,6	0,87	3,87
07	2,50	3,06	1,21	6,74	+1,07	-17,42	00,0	04,6	23,8	59,0	12,4	0,16	4,27
08	-	-	-	-	-	-	-	-	-	-	-	-	-
020201	1,41	1,73	0,85	2,73	-0,17	-1,03	02,8	26,3	33,6	37,3	00,0	-0,68	3,06
02	3,31	3,30	0,37	1,39	-2,43	+30,57	00,0	00,2	02,0	03,7	94,1	2,00	3,06
03	3,42	3,44	0,45	1,84	-2,45	+29,30	00,0	00,4	01,2	01,1	97,3	1,90	4,13
04	2,96	3,13	1,04	5,03	-2,36	+12,12	02,0	04,2	09,6	14,2	70,0	-1,38	4,29
05	2,99	3,31	1,18	5,92	-2,18	+8,33	03,0	05,8	06,8	12,3	66,3	-1,60	4,09
06	2,73	3,22	1,25	6,57	-1,12	+0,33	01,0	02,0	24,6	37,3	35,1	-0,50	4,24
07	3,13	3,33	0,82	3,50	-2,38	+9,09	01,0	02,4	08,4	16,8	71,4	-0,50	3,73
08	-	-	-	-	-	-	-	-	-	-	-	-	-
020301	1,75	1,85	0,49	1,99	+0,06	+0,37	00,0	09,7	68,1	20,8	01,4	0,66	3,12
02	3,15	3,22	0,54	2,30	-1,88	+9,00	00,0	01,5	04,0	14,2	80,0	0,76	3,79
03	-	-	-	-	-	-	-	-	-	-	-	-	-
020401	1,55	1,52	0,60	2,17	+0,69	+2,17	00,0	10,1	72,2	15,5	02,2	0,41	3,70
02	2,75	2,90	0,59	3,12	-0,60	+1,55	00,0	01,5	07,4	51,1	40,0	0,78	3,91
03	3,03	3,23	1,01	4,69	-3,07	+19,45	03,2	04,6	06,2	13,0	73,0	-2,14	3,81
04	3,21	3,33	0,80	3,33	-2,51	+14,85	01,5	03,0	08,4	07,1	80,0	-0,74	4,00
05	1,59	2,14	1,45	5,36	+0,76	-7,30	00,0	19,9	52,7	19,4	08,0	0,21	3,84
06	3,45	3,48	0,42	1,44	-1,10	+8,98	00,0	00,2	02,1	02,7	95,0	1,50	4,14
07	3,21	3,36	0,82	3,43	-2,48	+15,14	01,5	03,4	08,0	02,0	85,1	-0,87	3,96
08	-	-	-	-	-	-	-	-	-	-	-	-	-
020501	1,81	1,89	0,19	0,77	-0,25	-0,91	00,0	00,3	79,7	19,2	00,8	1,25	1,71
02	3,20	3,16	0,13	0,54	+0,34	-	-	-	-	-	-	2,57	3,54
03	3,18	3,23	0,34	1,41	-2,44	+18,66	00,0	00,0	02,8	04,0	93,2	0,80	3,59
04	3,50	3,50	0,31	1,04	-1,99	+13,93	00,0	01,5	02,5	05,4	90,6	1,46	3,79
05	3,09	3,36	0,90	3,97	-0,39	-5,88	00,0	02,8	12,3	12,9	64,8	0,99	4,18
06	3,39	3,43	0,54	1,91	-1,73	+11,64	00,0	01,0	02,6	05,8	90,6	0,55	4,15
07	3,19	3,41	0,94	3,93	-2,69	+14,70	03,0	03,6	08,6	04,8	80,0	-1,32	4,02
08	-	-	-	-	-	-	-	-	-	-	-	-	-
09	-	-	-	-	-	-	-	-	-	-	-	-	-
020601	1,90	1,99	0,40	1,73	-0,93	+1,79	01,5	02,0	60,4	36,1	00,0	-0,27	2,36
02	3,01	3,07	0,49	2,35	-2,63	+18,75	00,0	01,0	05,2	18,5	75,3	0,08	3,54
03	-	-	-	-	-	-	-	-	-	-	-	-	-
04	3,20	3,31	0,80	3,33	-3,50	+30,89	02,0	03,2	03,8	08,3	82,5	-1,68	4,25
05	2,69	3,10	1,08	5,75	+0,09	-10,97	01,0	10,6	16,3	11,3	59,8	0,68	4,00
06	-	-	-	-	-	-	-	-	-	-	-	-	-
07	2,82	3,09	1,23	6,34	-1,78	+6,80	03,0	07,8	12,0	27,2	50,0	-1,66	4,27
08	-	-	-	-	-	-	-	-	-	-	-	-	-
09	1,61	1,85	1,21	4,48	+0,05	-4,32	02,8	12,9	45,2	39,1	00,0	-1,07	3,47
030101	2,20	2,15	0,58	3,04	-1,43	+11,19	03,8	00,9	09,0	82,0	04,3	-1,56	3,27
02	3,04	2,97	0,26	1,18	+0,52	+1,60	00,0	00,0	00,0	48,7	51,3	2,43	3,75
03	2,94	3,13	0,96	4,71	-2,94	+15,61	02,0	03,0	08,0	10,7	76,3	-1,63	3,83
04	2,94	3,07	0,68	3,33	-2,44	+14,62	01,0	02,0	06,0	24,4	66,6	-0,75	3,93
05	2,24	2,88	1,32	6,94	-0,22	-2,37	02,0	09,0	33,7	23,7	31,6	-1,07	4,19
06	2,57	2,81	1,14	6,31	+0,09	-4,08	00,0	07,6	20,8	51,2	20,4	0,01	4,25
07	1,05	2,45	2,32	6,03	-0,67	-2,35	11,0	40,4	24,2	24,3	00,1	-3,12	3,81
08	2,81	3,14	1,11	5,86	-2,77	+13,85	03,8	07,6	07,4	00,2	81,0	-2,62	3,76
09	3,07	3,19	0,86	3,87	-2,68	+15,68	02,0	03,2	08,0	06,0	80,8	-1,39	3,90
10	1,90	2,15	1,17	5,07	+0,08	-3,07	01,0	23,0	23,5	50,0	02,5	-0,05	3,68
11	1,91	2,66	1,52	6,61	-1,80	+2,67	03,8	13,4	28,0	53,9	00,9	-3,17	3,51
12	2,89	2,94	0,73	3,67	-1,34	+6,78	01,0	02,0	09,8	50,4	36,8	-0,06	4,44

APPENDIX 3.3. (cont.)

SAMPLE	MEAN	MD	QD	QII	SK	K	%VCS	%CS	%MS	%FS	%VFS	1%	99%
030201	2,09	2,03	0,44	2,16	-0,08	-0,86	00,0	01,5	17,1	81,4	00,0	0,87	2,87
02	3,10	3,18	0,68	2,95	-3,84	+35,33	02,0	03,0	03,6	03,9	87,5	-1,49	3,66
03	3,38	3,38	0,44	1,57	+0,93	-	00,0	00,0	00,0	17,0	83,0	2,21	4,45
04	0,81	1,22	0,96	2,14	-0,23	+1,11	11,8	31,4	52,7	02,7	01,4	-1,45	03,2
05	3,09	3,30	0,87	3,78	-1,95	+8,01	02,0	03,2	12,6	15,4	66,8	-0,71	3,95
06	2,70	2,92	0,90	4,72	-1,34	+1,02	01,2	02,0	17,8	52,5	26,5	-0,16	4,09
07	2,77	2,97	0,82	4,29	-1,17	+1,18	00,0	02,0	15,8	36,4	45,8	0,39	4,03
08	1,03	0,73	0,45	1,14	+1,71	+2,98	01,5	72,7	23,4	00,5	01,8	-0,25	3,98
09	-	-	-	-	-	-	-	-	-	-	-	-	-
030301	2,02	2,01	0,55	2,58	-0,08	-0,01	00,0	03,9	26,9	68,2	01,0	0,22	3,08
02	2,94	2,96	0,31	1,51	-1,16	+5,88	00,0	00,0	01,6	58,4	40,0	1,32	3,36
03	3,23	3,21	0,55	2,08	-2,18	+20,80	00,0	02,8	03,0	07,0	87,2	0,50	4,10
04	3,36	3,34	0,35	1,30	+0,26	-0,51	00,0	00,0	00,0	14,7	85,3	2,84	4,12
05	0,47	0,57	0,94	1,82	+0,27	+0,74	14,8	62,6	19,4	01,3	01,9	-1,49	3,36
06	0,25	0,37	1,86	3,12	-0,38	-5,89	22,2	40,4	35,4	01,0	01,0	-2,45	3,99
07	2,82	2,82	0,54	2,80	-1,38	+3,96	00,0	02,0	06,0	87,0	05,0	0,56	3,89
030401	1,87	1,91	0,68	2,92	+0,45	-6,45	00,0	02,5	36,5	60,1	00,9	0,60	2,97
02	2,79	2,81	-	-	-4,04	+36,71	02,0	03,6	06,2	44,1	46,1	-1,32	3,41
03	3,02	3,05	0,42	1,95	-1,71	+8,18	00,0	01,5	02,4	18,3	77,8	0,86	3,55
04	2,55	2,83	1,45	8,07	-2,98	+19,36	05,2	03,2	08,0	59,6	24,0	-5,06	4,06
05	-0,03	0,09	0,31	0,41	+0,60	+0,86	20,9	73,9	04,2	01,0	00,0	-0,24	2,13
06	2,70	2,90	0,58	3,05	-2,23	+4,67	00,0	01,0	12,0	55,4	31,6	0,01	3,35
030501	2,01	1,71	1,35	6,45	-0,04	-2,02	01,9	19,4	49,7	00,0	29,0	-0,15	3,56
02	2,63	2,75	0,51	2,81	-1,40	+6,54	00,0	02,0	05,6	83,8	08,6	0,60	3,46
03	2,55	2,84	1,02	5,68	-2,23	+6,98	02,0	04,4	16,4	54,8	22,4	-1,20	3,42
04	0,74	0,83	0,54	1,22	+0,65	+1,26	04,0	64,4	30,6	01,0	00,0	+0,41	2,91
05	0,52	-0,56	0,88	1,64	+0,95	+1,27	06,8	64,6	25,6	02,0	01,0	-1,14	3,64
030601	1,53	1,56	0,60	2,18	-0,11	-2,12	00,0	21,4	57,4	21,2	00,0	0,93	2,36
02	2,79	2,83	0,60	3,13	-2,21	-	00,0	00,0	10,0	51,1	38,9	-	-
03	2,82	2,92	0,61	3,19	-2,06	+10,23	00,0	03,0	10,2	51,0	35,8	0,04	3,66
04	0,48	0,10	1,35	2,42	+0,74	-3,51	08,5	54,5	35,5	01,0	00,5	-1,03	3,07
030701	2,01	1,98	0,39	1,88	-0,05	+0,12	00,0	00,0	11,6	88,4	00,0	1,04	2,84
02	2,86	2,84	0,31	1,56	-0,30	+3,00	00,0	00,0	01,4	80,6	18,0	1,86	3,57
03													
040101	0,38	0,14	0,83	1,41	+0,04	-7,00	29,8	50,5	15,2	04,5	00,0	-1,31	2,65
02	3,02	3,06	0,33	1,55	-1,61	+12,64	00,0	00,0	02,8	22,9	74,3	1,58	3,65
03	2,98	3,12	0,84	4,03	-4,23	+36,90	02,8	03,8	02,8	14,5	76,1	-2,64	3,67
040201	1,08	1,07	0,54	1,45	-0,12	-1,96	01,0	43,9	54,1	01,0	00,0	-0,04	1,83
02	3,01	2,96	0,46	2,16	-0,42	+3,23	00,0	00,0	02,0	62,1	35,9	1,22	4,03
03	3,13	3,11	0,44	1,90	-1,31	+6,95	00,0	00,0	02,8	36,5	60,7	1,04	3,67
04	2,70	2,97	1,01	5,29	-1,37	+2,23	01,5	02,0	20,6	39,5	36,4	-0,24	4,06
05	-0,42	-0,33	0,68	0,71	+0,55	+2,63	29,4	66,3	03,3	02,0	00,0	-1,74	2,79
040301	0,36	0,25	0,55	0,93	+1,94	+15,17	13,3	78,4	05,3	02,0	01,0	-0,16	3,09
02	3,11	3,14	0,44	1,89	-1,18	+8,13	00,0	01,2	03,6	20,1	75,1	0,71	3,93
03	2,80	2,89	0,64	3,36	-2,44	+13,54	01,5	02,0	10,4	52,3	33,8	-0,48	3,54
04	1,00	0,83	0,83	2,08	+0,83	+2,79	05,0	63,4	24,8	00,4	06,4	0,40	4,01
05	2,33	2,77	1,27	6,81	-1,79	+3,53	03,0	09,8	22,2	54,1	10,9	-1,82	3,78
06	2,54	2,96	1,13	6,27	-1,85	+1,33	02,0	03,6	27,0	36,2	32,2	-0,92	3,65
040401	1,16	1,10	0,56	1,56	+0,72	+3,52	00,0	38,1	57,9	02,1	01,9	0,17	3,39
02	3,07	3,11	0,74	3,31	-3,14	+31,47	03,0	03,2	03,6	09,5	80,7	-1,46	4,24

APPENDIX 3.3. (cont.)

SAMPLE	MEAN	MD	QD	QH	SK	K	%VCS	%CS	%MS	%FS	%VFS	1%	99%
03	3,08	3,04	0,42	1,87	-0,36	+4,18	00,0	00,0	00,6	83,7	15,7	1,69	4,10
04	3,11	3,07	0,33	1,43	-0,01	+2,18	00,0	00,0	01,0	40,8	58,2	1,91	3,99
05	3,04	3,11	0,65	2,95	-2,02	+9,86	01,5	02,7	06,8	28,8	61,2	-0,24	3,93
06	2,94	3,06	0,86	4,24	-2,00	+9,05	02,0	03,2	07,4	51,3	36,3	-1,19	4,38
040501	1,16	1,19	0,59	1,65	+0,21	+0,41	01,0	38,8	53,7	05,6	00,9	-0,09	2,94
02	3,04	3,00	0,22	1,00	+0,19	+3,48	00,0	00,0	00,0	26,4	73,6	2,10	3,67
03	2,85	2,87	0,54	2,76	-2,47	+21,45	00,0	02,8	05,2	51,1	40,9	00,0	3,74
04	3,03	2,99	0,30	1,39	+0,26	+3,57	00,0	00,0	01,0	43,1	55,9	1,98	3,93
05	2,08	2,70	1,45	7,19	+0,52	-18,76	02,0	18,6	27,2	44,1	07,9	-1,09	4,21
040601	1,53	1,49	0,42	1,51	+0,34	+0,72	00,0	05,4	83,7	10,7	00,0	0,73	2,70
02	2,99	3,14	0,84	3,99	-1,60	+8,64	01,0	05,0	03,5	04,4	86,1	1,01	3,76
03	2,89	2,99	0,67	3,33	-2,99	+22,66	01,5	02,6	05,6	50,2	40,1	-0,62	3,53
04	3,20	3,18	0,26	1,08	-0,06	+1,69	00,0	00,0	00,0	10,5	89,5	2,22	3,83
05	3,29	3,21	0,39	1,51	-0,05	+2,46	00,0	01,0	01,0	08,7	89,3	1,91	4,30
06	1,88	3,04	2,10	9,07	+0,10	-6,17	09,6	30,0	12,6	05,7	42,1	-3,30	4,02
07	2,62	2,95	1,01	5,60	-0,48	-2,09	00,0	10,3	10,8	41,3	37,6	0,07	3,90
08	2,72	2,95	0,89	4,69	-2,35	+7,40	00,0	01,6	14,2	42,1	42,1	-0,82	3,73
040701	1,57	1,57	0,39	1,42	-0,20	-1,62	00,0	07,5	71,3	22,2	00,0	0,48	2,19
02	2,54	3,06	1,34	7,45	-1,60	+1,76	03,0	12,6	16,8	09,9	57,7	-1,94	3,74
03	2,96	3,02	0,64	3,09	-3,26	-	00,0	01,8	04,4	46,1	47,7	-	-
04	2,89	2,85	0,35	1,76	+0,14	+2,38	00,0	00,0	02,0	74,1	23,9	1,62	3,77
05	2,94	2,92	0,34	1,65	-0,20	+0,68	00,0	00,0	01,0	68,1	30,9	1,90	3,61
06	2,89	2,82	0,48	2,41	-0,19	-0,15	00,0	00,0	02,0	75,3	22,7	1,61	4,05
07	2,84	3,01	1,13	5,84	-0,48	-3,13	02,0	07,0	12,4	48,1	30,5	-0,82	4,52
040801	1,48	1,48	0,55	1,92	-0,05	-0,83	00,0	17,8	59,2	23,0	00,0	0,12	2,51
02	2,57	2,61	0,40	2,21	-0,40	+3,05	00,0	00,0	01,8	91,5	06,7	1,13	3,52
03	2,74	2,82	0,65	3,42	-2,00	+11,40	02,0	03,0	08,0	67,8	19,2	-0,58	3,83
04	2,14	2,04	0,54	2,82	+0,48	+0,19	00,0	00,0	44,2	44,7	11,1	1,26	3,51
05	2,88	2,84	0,36	1,81	+0,28	-0,03	00,0	00,0	00,0	74,4	25,6	2,08	3,81
06	2,76	2,84	0,60	3,15	-1,89	+8,29	01,0	02,0	08,0	70,0	19,0	-0,06	3,57
07	-	-	-	-	-	-	-	-	-	-	-	-	-
08	0,63	0,53	0,84	1,67	+0,47	+1,51	01,6	62,9	32,5	02,0	01,0	-0,93	3,04
040901	2,28	2,40	0,66	3,45	-0,27	-0,96	00,0	05,1	20,0	69,2	05,7	0,75	3,54
02	1,14	1,63	1,45	3,98	+0,14	-2,10	09,4	50,5	06,3	37,8	04,9	-1,37	3,49
03	0,51	0,60	1,36	2,47	-0,02	-1,50	26,9	57,9	07,8	04,0	03,4	-2,09	3,30
04	1,93	1,85	0,77	3,43	-0,17	+0,98	01,0	14,0	38,2	41,5	05,3	-0,07	3,40
05	2,34	2,57	0,71	3,83	-0,13	-2,29	00,0	01,3	32,0	48,9	17,8	0,70	3,42
06	-	-	-	-	-	-	-	-	-	-	-	-	-
07	-1,61	-2,83	2,17	1,45	+1,84	-6,08	74,8	15,3	06,9	02,0	01,0	-2,88	3,77
041001	2,49	2,61	0,47	2,58	-0,22	-3,61	00,0	00,0	11,8	87,2	01,0	1,53	3,23
02	1,64	1,92	0,81	3,05	-0,17	+0,24	03,4	14,7	52,1	24,2	05,6	-0,61	3,31
03	-	-	-	-	-	-	-	-	-	-	-	-	-
04	1,43	1,46	0,32	1,06	-1,02	-0,68	00,4	07,3	86,5	04,4	01,4	0,22	1,75
05	2,40	2,41	1,11	6,15	-0,07	-0,57	01,6	11,5	18,8	28,0	40,1	-0,30	4,45
06	2,33	2,29	0,44	2,33	+0,38	+2,66	00,0	00,0	13,7	79,8	06,5	1,17	3,79
07	2,42	2,86	1,11	6,15	-0,83	+0,16	02,2	08,9	22,3	27,2	38,4	-1,08	3,60
08	1,49	1,89	1,16	4,14	-0,11	-1,38	03,6	39,9	13,0	40,3	03,2	-0,39	3,51
09	-	-	-	-	-	-	-	-	-	-	-	-	-
10	2,73	2,68	0,35	1,85	+0,55	+3,10	00,0	00,0	01,5	88,5	10,0	1,87	3,93
041101	2,04	2,05	0,54	2,61	-0,11	+0,96	00,0	02,6	35,2	60,0	01,6	0,58	2,82
02	1,07	0,92	1,03	2,70	+0,19	+0,21	07,4	45,7	24,6	18,7	03,6	-1,41	4,01
03	2,21	2,41	0,62	3,28	-1,10	+4,34	01,4	04,9	19,1	69,8	04,8	-0,20	3,40

APPENDIX 3.3. (cont.)

SAMPLE	MEAN	MD	QD	QH	SK	K	%VCS	%CS	%MS	%FS	%VFS	1%	99%
041201	0,90	0,92	0,79	1,84	+0,14	-0,46	17,8	38,8	34,6	08,8	00,0	-0,58	2,82
02	1,40	1,51	0,99	3,20	-0,13	-0,84	09,1	24,7	38,9	23,2	04,1	-0,65	3,27
03	2,80	2,88	0,38	1,97	-0,81	+3,12	00,0	00,0	06,4	68,3	25,3	1,36	3,50
04	1,82	1,96	0,55	2,29	-1,06	+3,48	01,4	10,2	42,4	46,0	00,0	-0,50	2,52
05	2,28	2,31	0,54	2,85	-0,57	-0,93	00,0	03,5	17,6	75,1	03,8	0,36	3,24
06	2,30	2,46	0,78	4,11	-0,75	+2,56	01,4	05,0	18,7	57,4	17,5	-0,64	3,45
07	1,85	1,96	0,68	2,89	-0,26	-0,40	00,0	12,1	39,9	46,1	01,9	0,20	3,21
060001	-	-	-	-	-	-	-	-	-	-	-	-	-
02	-	-	-	-	-	-	-	-	-	-	-	-	-
03	-	-	-	-	-	-	-	-	-	-	-	-	-
04	-	-	-	-	-	-	-	-	-	-	-	2,02	3,42
05	0,83	0,84	0,84	1,89	+0,46	+4,10	02,8	70,0	22,2	03,0	02,0	-1,40	3,66
06	2,47	2,69	0,96	5,34	-1,58	+3,18	02,0	05,4	13,6	70,3	08,7	-1,16	3,54
07	-	-	-	-	-	-	-	-	-	-	-	-	-
08	-	-	-	-	-	-	-	-	-	-	-	-	-
09	1,70	1,79	0,70	2,79	-0,05	+0,12	01,4	04,4	70,7	22,5	01,0	-0,01	3,36
10	1,35	1,50	0,57	1,78	-0,65	+0,78	04,2	14,6	71,9	09,3	00,0	-0,47	1,94
11	-	-	-	-	-	-	-	-	-	-	-	-	-
12	3,66	4,65	1,05	2,99	-0,74	-2,88	00,0	00,0	02,8	30,3	66,9	1,39	4,38
13	3,39	3,35	0,35	1,27	-0,08	-0,17	00,0	00,0	00,0	02,0	98,0	2,36	4,12
14	3,30	3,24	0,48	1,86	+0,01	-0,48	00,0	00,0	00,0	25,7	74,3	2,22	4,34
15	-	-	-	-	-	-	-	-	-	-	-	-	-
16	2,05	1,66	0,86	4,17	+1,26	-	00,0	00,0	50,5	48,5	01,0	-	-
17	1,67	1,47	0,26	1,01	+2,77	+4,69	00,0	00,0	94,2	05,8	00,0	1,68	3,15
18	-	-	-	-	-	-	-	-	-	-	-	-	-
19	-	-	-	-	-	-	-	-	-	-	-	-	-
20	3,43	3,48	0,52	1,82	-1,04	-0,82	00,0	00,0	02,8	21,0	76,2	1,50	3,94
21	-2,45	-2,43	0,19	0,10	+0,01	+2,00	94,0	06,0	00,0	00,0	00,0	-	-

3.4. LANGEBAAN LAGOON : GRAIN SIZE PARAMETERS OF THE TOTAL SEDIMENT

SAMPLE	MEAN	MD	QD	QH	SK	K	%VCS	%CS	%MS	%FS	%VFS	%MUD	1%	99%
050101	2,84	2,89	0,31	1,55	-0,68	+2,51	00,0	00,0	03,1	65,2	31,7	00,0	1,71	3,33
02	2,95	2,94	0,37	1,80	-0,34	+0,62	00,0	00,0	02,3	57,2	40,5	00,4	1,90	3,54
03	2,83	2,83	0,35	1,75	-0,72	+1,69	00,0	00,0	08,0	64,1	27,9	00,3	1,50	3,44
04	0,76	0,80	0,38	0,80	-0,02	+0,80	03,3	69,9	26,4	00,4	00,0	00,0	-0,15	1,55
05	1,28	1,31	0,49	1,90	-0,04	+0,22	00,0	25,7	69,4	04,9	00,0	00,1	0,09	2,50
06	2,76	2,72	0,41	2,10	+0,11	+0,21	00,0	00,0	03,3	73,4	23,3	00,5	1,75	3,68
07	0,90	0,91	0,79	1,85	+0,31	+0,99	13,0	42,5	37,7	04,5	02,3	01,3	-0,56	3,36
08	0,94	0,95	0,64	1,50	+0,02	-0,56	09,4	43,7	40,3	06,6	00,0	00,7	-0,20	2,24
09	2,37	2,52	0,68	3,20	-0,48	+0,38	00,0	06,0	18,0	61,0	15,3	00,8	+0,43	3,40
10	2,34	2,65	0,84	3,60	-0,39	-0,41	00,3	09,0	23,4	44,6	22,7	03,4	+0,29	3,44
11	1,85	1,97	0,96	3,40	-0,15	-0,87	03,2	20,1	28,1	35,9	12,7	01,1	-0,29	3,39
12	1,64	1,59	1,05	3,30	-0,05	-0,65	04,8	26,8	31,7	25,1	12,3	00,1	-0,64	3,44
13	1,31	1,08	0,94	2,75	+0,27	-0,68	04,2	41,6	29,1	19,4	05,7	02,1	-0,35	3,35
14	1,04	0,79	1,00	2,50	+0,49	+0,11	07,5	54,8	20,5	08,1	09,1	00,2	-0,59	3,40
15	1,46	1,21	1,00	3,10	+0,31	-0,78	00,5	41,1	31,9	12,0	14,5	00,3	-0,02	3,46
16	1,13	0,83	0,99	2,60	+0,42	-0,38	06,5	52,0	21,0	13,0	07,5	00,4	-0,35	3,36
17	1,33	0,67	1,22	3,30	+0,20	-1,61	06,1	53,0	03,2	27,2	10,5	00,2	-0,27	3,23
18	1,37	1,21	0,83	2,60	+0,31	-0,51	00,1	39,2	38,4	17,2	05,1	00,5	+0,05	3,24
19	1,23	1,08	0,70	2,00	+0,30	-0,47	00,0	46,0	37,0	15,8	01,2	00,4	0,08	2,85
20	2,25	2,49	0,86	3,60	-0,42	-0,44	00,1	15,2	12,0	56,2	16,5	00,3	0,36	3,43
21	1,52	1,44	0,83	2,75	+0,17	-0,73	00,0	31,7	39,4	24,6	04,3	00,8	0,09	3,40
22	2,27	2,52	1,04	4,00	-0,29	-0,86	01,0	16,0	18,4	30,4	34,2	06,1	-0,05	3,64
23	2,49	2,72	0,93	4,00	-0,28	-0,63	00,3	07,4	22,5	32,2	37,3	07,7	0,26	3,75
24	2,37	2,42	0,68	3,20	-0,08	-0,82	00,0	02,1	29,4	47,4	21,1	01,4	0,88	3,57
25	1,99	2,12	0,78	3,20	-0,28	-0,46	00,0	14,6	29,9	48,9	06,6	00,1	00,9	3,24
050201	2,93	3,00	0,50	0,72	-1,09	+5,90	00,0	01,2	05,2	44,0	49,6	00,1	0,44	3,33
02	2,86	2,97	0,48	2,40	-1,19	+5,76	00,0	01,2	06,2	49,2	43,4	00,9	0,93	3,34
03	0,82	0,77	0,62	1,75	+0,24	+0,10	08,7	56,0	31,1	04,2	00,0	00,0	-0,35	2,25
04	2,52	2,49	0,45	2,30	-0,18	+1,33	00,0	00,5	08,5	77,2	13,8	00,2	1,09	3,45
05	1,75	1,73	0,61	2,35	+0,12	-0,16	00,0	10,4	57,9	28,4	03,3	00,1	0,38	3,16
06	1,81	1,80	0,62	2,40	+0,01	-0,38	00,0	10,0	52,4	34,5	03,1	00,3	0,38	3,13
07	2,59	2,62	0,45	2,30	-0,80	+4,82	00,0	01,8	05,1	79,7	13,4	00,3	0,75	3,34
08	1,61	1,35	0,78	2,75	+0,39	-0,39	00,0	20,9	50,8	20,5	07,8	00,8	0,51	3,41
09	1,60	1,64	0,80	2,80	-0,18	+0,09	04,1	16,0	48,9	27,6	03,4	00,6	-0,49	3,19
10	1,40	1,40	0,75	2,40	+0,10	+0,03	03,3	24,6	54,3	14,6	03,2	00,6	-0,24	3,25
050301	3,00	2,98	0,33	1,60	-0,17	+2,28	00,0	00,0	01,7	50,7	47,6	00,3	1,84	3,83
02	2,04	2,00	0,57	2,50	+0,10	-0,35	00,0	03,3	48,7	39,3	08,7	00,1	0,77	3,15
03	1,90	1,94	0,51	2,25	-0,29	+1,14	00,3	04,4	51,6	43,0	00,7	00,1	0,36	2,94
04	1,60	1,67	0,70	2,45	-0,11	+0,58	02,5	14,2	57,3	22,6	03,4	00,1	-0,24	3,33
05	1,79	1,84	0,52	2,15	-0,07	-0,00	00,0	07,8	58,9	32,5	00,8	00,3	0,57	2,94
06	1,57	1,62	0,66	2,30	-0,30	+1,26	03,0	12,7	62,7	21,2	00,4	00,1	-0,55	2,92
07	2,09	2,12	0,58	2,70	-0,19	+0,40	00,0	04,7	34,5	55,9	04,9	00,6	0,45	3,29
08	0,73	0,55	0,78	1,65	+0,46	+0,14	15,7	55,1	18,9	10,3	00,0	02,8	-0,42	2,65
050401	1,47	1,51	0,41	1,40	-0,41	+2,04	00,0	10,0	85,6	06,4	00,0	00,1	0,04	2,36
02	2,49	2,53	0,51	2,60	-0,23	+0,15	00,0	00,5	15,5	68,6	15,4	00,3	1,09	3,42
03	2,37	2,39	0,65	3,10	-0,43	+1,87	00,7	03,1	17,6	63,2	15,4	00,0	0,31	3,54
04	2,29	2,35	0,63	3,00	-0,22	-0,35	00,0	03,3	26,0	56,0	14,7	00,3	0,78	3,34
05	1,62	1,67	0,54	2,00	-0,25	+1,13	00,9	11,0	70,0	17,8	00,3	00,2	0,02	2,84
06	2,06	2,36	0,98	3,65	-0,41	-0,18	04,5	11,7	21,9	48,2	13,7	02,1	-0,48	3,43
050501	2,70	3,02	0,93	4,10	-0,96	+3,78	02,8	02,1	13,5	29,6	51,9	00,4	-0,94	3,69
02	2,86	2,87	0,46	1,65	-0,17	+0,30	00,0	00,0	04,1	58,8	37,1	00,5	1,53	3,74
03	2,83	2,83	0,35	1,75	-0,72	-	00,0	00,2	03,0	69,6	27,2	00,1	-	-
04	2,67	2,71	0,47	2,40	-0,57	+2,39	00,0	00,8	07,0	70,5	21,7	00,3	1,05	3,46
05	1,43	1,47	0,84	2,70	-0,09	-0,81	04,6	29,1	37,9	28,1	00,3	00,4	0,44	2,93
06	2,20	2,26	0,63	2,90	-0,32	+0,72	00,2	04,2	28,5	58,0	09,1	00,4	0,29	3,34
07	2,49	2,48	0,34	1,80	-0,00	-0,15	00,0	00,0	07,7	84,2	08,1	00,0	1,66	3,23
08	1,74	1,85	0,66	2,50	-0,17	-0,11	00,0	15,0	45,6	36,8	02,6	00,3	0,09	3,15

APPENDIX 3.4. (cont.)

SAMPLE	MEAN	MD	QD	QH	SK	K	%VCS	%CS	%MS	%FS	%VFS	%MUD	1%	99%
050601	2,56	2,99	1,00	4,20	-0,72	+0,77	02,8	09,5	10,2	28,2	49,3	00,5	-0,26	3,54
02	2,69	2,78	0,57	2,95	-0,47	+1,26	00,0	01,5	09,7	60,5	28,3	00,4	0,86	3,69
03	2,83	2,90	0,45	2,35	-0,70	+2,27	00,0	00,0	07,7	55,8	36,5	00,3	1,30	3,53
04	1,85	1,91	0,67	2,70	-0,08	00,43	00,0	11,7	44,1	39,2	05,0	00,3	0,24	3,15
05	2,19	2,30	0,54	2,50	-0,40	+0,36	00,0	03,8	24,4	68,1	03,7	00,2	0,66	3,09
06	1,34	1,30	0,60	1,90	+0,20	+0,35	00,8	28,7	58,1	11,8	00,6	00,3	0,02	2,89
07	2,21	2,27	0,50	2,40	-0,34	+0,89	00,0	03,6	20,7	70,9	04,8	00,7	0,77	3,10
08	1,96	1,93	0,90	3,35	-0,07	-0,73	01,1	13,6	37,6	34,5	13,2	01,5	-0,06	3,59
09	1,87	1,99	0,62	2,60	-0,19	-0,02	00,0	10,0	40,6	43,9	05,5	00,7	0,28	3,04
10	-	-	-	-	-	-	-	-	-	-	-	02,9	-	-
050701	2,63	2,85	0,76	3,60	-0,69	+1,19	00,0	06,4	11,1	48,1	34,4	00,7	0,37	3,60
02	2,40	2,65	0,76	3,40	-0,23	-1,00	00,0	04,0	29,4	42,5	24,1	00,5	0,75	3,53
03	2,51	2,72	0,69	3,30	-0,31	-0,36	00,0	02,4	23,5	50,4	23,7	01,0	0,79	3,63
04	2,80	2,80	0,45	2,25	-0,22	+0,64	00,0	00,0	04,4	65,4	30,2	00,4	1,44	3,64
05	2,35	2,40	0,57	2,80	-0,43	+1,23	00,0	03,4	16,5	68,6	11,5	00,5	0,49	3,41
06	2,14	2,43	0,78	3,30	-0,59	+0,57	01,0	10,8	19,2	64,4	04,6	00,5	-0,04	3,11
07	1,67	1,67	0,71	2,65	+0,00	-0,34	00,3	17,0	51,6	27,7	03,4	01,0	0,09	3,24
08	1,62	1,62	0,67	2,50	-0,11	-0,41	00,7	17,9	51,4	29,5	00,5	00,5	0,06	2,88
09	1,62	1,63	0,99	3,20	-0,04	-0,97	05,5	23,5	33,9	28,7	08,4	02,9	-0,35	3,33
10	1,48	1,40	0,67	2,30	+0,08	-0,84	00,0	26,4	48,0	25,6	00,0	00,1	0,12	2,79
050801	2,00	1,81	0,79	3,20	+0,16	-1,15	00,0	08,6	48,7	27,4	15,4	01,2	0,66	3,43
02	2,76	3,01	0,72	3,50	-0,57	+0,20	00,0	02,3	17,6	29,5	50,6	01,0	0,79	3,63
03	3,02	3,02	0,32	1,50	-0,58	+3,85	00,0	00,0	02,1	45,2	52,7	01,5	1,74	3,60
04	2,16	2,14	0,50	2,40	-0,03	+0,50	00,0	01,3	31,2	60,2	07,3	00,2	0,92	3,23
05	1,81	1,92	0,56	2,30	-0,31	+0,61	00,3	10,9	48,0	39,6	01,2	00,2	0,31	2,99
06	1,52	1,46	0,70	2,40	+0,07	-0,62	00,0	24,0	49,0	25,1	01,9	00,8	0,09	3,05
07	1,98	2,12	0,66	2,80	-0,32	+0,31	00,3	09,4	32,1	54,1	04,1	00,9	0,19	3,24
08	1,70	1,73	1,15	3,60	-0,10	-0,98	09,5	19,2	28,7	28,6	14,0	01,5	-0,61	3,73
050901	2,84	2,92	0,50	2,60	-0,52	+1,47	00,0	00,0	07,0	53,5	39,5	00,6	1,18	3,68
02	2,91	3,00	0,58	2,90	-0,32	+0,02	00,0	00,0	08,7	41,7	49,6	00,5	1,35	3,86
03	3,00	3,00	0,25	1,20	-0,89	+5,24	00,0	00,0	01,3	49,6	49,1	00,3	1,93	3,44
04	1,95	1,99	0,56	2,40	-0,14	+0,37	00,0	07,4	43,2	45,6	03,8	00,4	0,49	3,23
05	2,43	2,49	0,48	2,40	-0,49	+2,09	00,0	01,7	11,5	79,2	07,6	00,2	0,85	3,43
06	1,67	1,81	0,69	2,55	-0,91	+1,95	03,1	11,3	50,3	34,0	01,3	00,4	-0,54	3,04
051001	2,06	1,99	0,54	2,40	+0,28	+0,24	00,0	02,0	48,9	41,0	06,1	00,3	0,85	3,34
02	2,83	2,90	0,44	2,25	-0,01	+1,87	00,0	00,0	06,8	56,7	36,5	00,4	1,35	3,54
03	2,94	2,97	0,42	2,05	-1,08	+7,71	00,0	01,0	02,8	50,1	46,1	00,3	0,95	3,64
04	2,21	2,48	0,83	3,50	-0,13	-1,17	00,0	07,6	34,3	39,4	18,7	00,2	0,47	3,55
05	1,83	2,06	0,75	2,90	-0,61	+1,24	03,4	11,6	31,0	53,7	00,3	00,3	-0,67	2,75
06	2,39	2,60	0,75	3,40	-0,22	-0,67	00,0	04,1	24,9	50,2	20,8	01,7	0,68	3,69
051101	2,17	2,02	0,70	3,10	+0,10	-1,25	00,0	01,8	47,1	34,4	16,7	00,5	0,89	3,34
02	2,18	2,03	0,73	3,20	+0,06	-1,03	00,0	03,5	45,0	32,8	18,7	01,5	0,67	3,50
03	2,89	2,90	0,41	2,10	-0,50	+2,20	00,0	00,0	04,2	56,2	39,6	01,9	1,39	3,63
04	2,76	2,94	0,60	3,05	-0,49	+0,16	00,0	00,0	17,4	42,8	39,8	01,5	1,14	3,72
05	2,34	2,49	0,75	3,40	-0,81	+3,24	02,4	04,5	12,4	67,3	13,4	02,3	-0,44	3,44
06	1,44	1,38	0,68	2,25	+0,13	-0,59	00,0	29,5	48,0	21,7	00,8	01,9	0,10	2,94
07	1,65	1,55	0,57	2,15	+0,41	+0,79	00,0	07,2	70,3	18,9	03,6	01,5	0,60	3,24
051202	2,70	2,90	0,64	3,20	-0,36	-0,49	00,0	00,0	19,5	44,0	36,5	00,7	1,20	3,73
03	2,25	2,16	0,79	3,40	-0,05	-1,39	00,0	04,0	41,5	30,0	24,5	00,8	0,67	3,45
04	1,77	1,69	0,47	1,95	+0,43	+0,68	00,0	01,8	72,3	23,6	02,3	00,4	0,89	3,10
05	1,84	1,79	0,58	2,40	+0,28	+0,45	00,0	04,6	60,5	30,5	04,4	01,2	0,57	3,41
06	2,96	2,91	0,38	1,90	-0,39	+2,69	00,0	00,0	03,0	60,0	37,0	01,1	1,59	3,65
07	2,24	2,32	0,72	3,20	-0,19	-0,63	00,0	06,3	27,7	50,8	15,2	01,8	0,55	3,43
08	2,57	2,83	0,71	3,40	-0,34	-0,71	00,0	00,3	24,6	43,9	31,2	02,4	0,99	3,59

APPENDIX 3.4. (cont.)

SAMPLE	MEAN	MD	QD	QH	SK	K	%VCS	%CS	%MS	%FS	%VFS	%MUD	1%	99%
09	1,24	1,17	0,67	2,06	+0,41	+1,21	00,0	32,7	55,8	08,7	02,8	01,6	0,01	3,23
10	1,44	1,41	0,28	0,95	+0,46	+1,70	00,0	03,8	91,6	04,6	00,0	00,0	0,81	2,33
051302	2,41	2,39	0,63	3,05	-0,04	-0,90	00,0	00,3	29,2	48,4	22,1	00,6	1,04	3,65
03	2,69	2,98	0,75	3,60	-0,45	-0,46	00,0	01,1	21,6	30,3	47,0	00,7	0,95	3,63
04	2,74	2,92	0,63	3,15	-0,62	+0,71	00,0	01,4	14,7	43,5	40,4	01,3	0,92	3,63
05	1,85	1,80	0,49	2,10	+0,23	+0,20	00,0	03,3	64,5	30,4	01,8	00,6	0,74	3,02
06	1,82	1,72	0,71	2,80	+0,19	-0,53	00,0	11,6	53,5	27,3	07,6	00,5	0,33	3,31
07	2,48	2,61	0,59	2,95	-0,19	-0,81	00,0	00,0	23,7	55,3	21,0	01,0	1,13	3,43
08	2,11	2,02	0,62	2,75	+0,11	-0,97	00,0	01,0	48,0	40,5	10,5	01,1	0,95	3,26
09	1,86	1,87	0,37	1,60	-0,00	-0,17	00,0	00,5	64,4	35,1	00,0	00,5	0,98	2,65
10	1,57	1,51	0,38	1,40	+0,18	-0,25	00,0	04,9	80,3	14,8	00,0	00,7	0,77	2,42
11	1,65	1,64	0,27	1,05	+0,18	+0,36	00,0	00,0	90,0	10,0	00,0	00,0	1,05	2,30
051403	2,97	3,01	0,43	2,05	-1,11	+6,31	00,0	00,0	05,2	42,9	51,9	01,7	1,15	3,55
04	2,74	3,00	0,75	3,60	-0,38	-0,63	00,0	00,5	21,9	27,1	50,5	00,4	1,05	3,82
05	1,73	1,70	0,45	1,80	+0,40	+1,49	00,0	02,3	74,6	21,1	02,0	00,7	0,86	3,15
06	1,89	1,83	0,53	2,25	+0,42	+0,70	00,0	01,0	63,3	30,2	05,5	01,7	0,95	3,34
07	1,70	1,69	0,40	1,60	+0,16	+0,63	00,0	03,0	77,0	19,8	00,2	00,4	0,85	2,75
08	1,75	1,70	0,36	1,55	+0,14	-0,58	00,0	00,0	74,9	25,1	00,0	00,9	1,04	2,53
051505	2,85	2,93	0,41	2,05	-0,78	+3,01	00,0	00,0	05,9	57,1	37,0	00,5	1,35	3,49
06	3,13	3,19	0,55	2,50	-0,50	+0,92	00,0	00,0	06,3	26,4	67,3	01,4	1,47	3,97
07	2,13	2,65	1,05	4,00	-0,32	-0,78	03,6	13,3	24,2	37,1	21,8	01,0	-0,32	3,54
08	2,72	2,90	0,61	3,05	-0,55	+0,25	00,0	00,0	16,6	45,3	38,1	01,0	1,08	3,55
09	1,82	1,76	0,53	2,20	+0,43	+0,66	00,0	02,3	67,3	25,6	04,8	00,4	0,88	3,29
10	1,83	1,84	0,42	1,80	+0,07	-0,46	00,0	00,9	63,4	35,7	00,0	01,2	0,95	2,75
11	1,90	1,85	0,57	2,40	+0,29	+0,51	00,0	03,5	58,8	31,0	06,7	00,7	0,75	3,29
12	2,01	1,91	0,62	2,70	+0,23	-0,75	00,0	00,8	55,1	34,1	10,0	14,2	0,95	3,33
13	1,75	1,70	0,44	1,80	+0,44	-	00,0	00,9	75,4	21,8	01,9	00,6	-	-
051605	2,83	2,95	0,57	2,90	-0,57	+0,75	00,0	00,0	12,1	45,4	42,5	01,1	1,22	3,64
06	2,20	2,37	0,76	3,30	-0,18	-1,05	00,0	07,9	29,0	47,5	15,6	00,3	0,65	3,35
07	1,63	1,56	0,43	1,65	+0,69	+2,15	00,0	00,9	86,0	11,7	01,4	00,3	0,95	2,99
08	2,73	2,80	0,48	2,45	-0,60	+1,25	00,0	00,0	10,1	61,4	28,5	01,5	1,25	3,42
09	2,66	2,86	0,84	3,80	-0,84	+2,35	01,3	06,4	08,2	52,3	31,8	01,1	-0,01	3,75
10	1,91	1,86	0,49	2,20	+0,32	+0,15	00,0	00,7	60,9	34,6	03,8	69,0	0,96	3,15
051704	2,79	2,83	0,44	2,30	-0,52	+1,86	00,0	00,0	07,7	66,3	26,0	01,3	1,35	3,63
05	2,48	2,77	0,75	3,45	-0,28	-1,02	00,0	02,0	28,4	39,5	30,1	01,3	0,89	3,52
06	1,98	1,90	0,61	2,60	+0,14	-0,73	00,0	03,5	52,3	39,6	04,6	01,6	0,79	3,33
07	3,08	3,05	0,26	1,20	+0,28	+0,91	00,0	00,0	00,0	41,1	58,9	01,2	2,45	3,75
08	1,68	1,68	0,43	1,70	+0,11	+),73	00,0	05,0	73,9	20,4	00,7	01,5	0,61	2,84
09	1,82	1,78	0,52	2,25	+0,40	+0,69	00,0	02,7	64,5	28,6	04,2	00,9	0,86	3,33
051807	2,66	2,81	0,59	3,05	-0,57	+0,73	00,0	01,0	14,7	55,7	28,6	00,9	0,95	3,45
08	2,44	2,61	0,73	-	-0,39	-0,81	00,0	04,2	21,7	50,1	24,0	01,3	0,38	3,56
09	1,96	1,71	0,76	3,05	+0,26	-0,02	00,0	04,0	57,5	22,1	16,4	02,8	0,77	3,35
10	1,73	1,72	0,46	1,80	+0,27	-1,12	00,0	03,6	72,4	22,4	01,6	02,9	0,85	3,04
11	1,59	1,54	0,53	1,90	+0,25	+0,58	00,0	10,2	69,8	18,5	01,5	01,1	0,43	3,03
051905	2,97	2,98	0,38	1,80	-0,59	+2,41	00,0	00,0	03,4	49,0	47,6	01,0	1,62	3,54
06	3,10	3,14	0,44	2,00	-0,54	+1,62	00,0	00,0	03,6	26,6	69,8	06,7	1,65	3,79
07	2,58	2,82	0,70	3,45	-0,40	-0,61	00,0	01,0	24,1	43,2	31,7	03,1	0,95	3,56
08	1,71	1,69	0,41	1,70	+0,31	+0,52	00,0	01,0	79,0	19,6	00,4	02,1	0,95	2,85
09	1,71	1,62	0,65	-	+0,23	-0,22	00,2	13,3	54,1	28,4	04,0	00,4	0,65	3,34

APPENDIX 3.4. (cont.)

SAMPLE	MEAN	MD	QD	QH	SK	K	%VCS	%CS	%MS	%FS	%VFS	%MUD	1%	99%
052005	3,04	3,04	0,31	1,45	-0,65	+4,64	00,0	00,0	02,0	42,3	55,7	01,8	1,75	3,69
06	2,44	2,66	0,73	3,40	-0,22	-1,18	00,0	00,7	30,8	40,0	28,5	04,8	0,96	3,43
07	1,74	1,63	0,51	2,10	+0,53	+1,01	00,0	03,3	73,7	19,4	03,6	00,7	0,85	3,15
08	1,62	1,57	0,34	1,25	+0,40	+0,42	00,0	01,0	85,3	13,5	00,2	00,6	1,04	2,54
052102	2,36	2,49	0,58	2,80	-0,24	-0,39	00,0	01,8	26,4	59,1	12,7	11,6	0,85	3,34
03	2,96	2,92	0,26	1,25	+0,27	+1,27	00,0	00,0	00,0	65,5	34,5	08,9	2,26	3,65
04	-	-	-	-	-	-	-	-	-	-	-	-	-	-
05	2,64	2,87	0,65	3,25	-0,53	-0,06	00,0	01,7	18,4	49,0	30,9	09,4	1,05	3,54
06	3,22	3,17	0,32	1,35	+0,10	+0,04	00,0	00,0	00,1	27,1	72,8	03,0	2,34	3,93
07	1,60	1,54	0,44	1,70	+0,59	+2,34	00,0	04,0	81,4	12,7	01,9	01,6	0,78	3,15
08	1,60	1,55	0,42	1,60	+0,29	+0,85	00,0	06,5	78,9	14,4	00,2	01,4	0,66	2,84
09	1,82	1,81	0,46	2,00	+0,09	-0,14	00,0	03,5	60,8	35,1	00,6	00,6	0,76	2,93
052202	2,11	2,08	0,56	2,60	+0,04	-0,52	00,0	01,0	43,1	49,6	06,3	05,9	0,95	3,32
03	3,03	2,99	0,30	1,40	+0,13	+0,58	00,0	00,0	00,0	50,7	49,3	08,7	2,19	3,79
04	3,20	3,17	0,38	1,60	+0,03	-0,58	00,0	00,0	00,3	32,7	67,0	20,6	2,45	3,91
05	-	-	-	-	-	-	-	-	-	-	-	-	-	-
06	1,96	1,84	0,63	2,70	+0,28	-0,43	00,0	03,1	56,3	32,2	05,4	03,0	0,79	3,44
07	1,39	1,37	0,28	0,90	+0,67	+3,35	00,0	03,6	92,6	03,8	00,0	00,2	0,86	2,39
08	2,77	2,89	0,57	2,95	-1,00	+3,76	00,0	02,6	08,0	55,0	34,4	05,2	0,75	3,42
09	1,72	1,74	0,30	1,20	-0,04	-0,05	00,0	00,5	83,3	15,6	00,6	01,0	0,97	2,39
10	1,71	1,66	0,45	1,75	+0,41	+1,16	00,0	03,1	74,9	20,0	02,0	01,7	0,85	3,13
052303	2,09	1,97	0,61	2,75	+0,34	-0,09	00,0	00,5	52,2	36,5	10,8	10,9	0,99	3,56
04	2,53	2,74	0,71	3,40	-0,22	-0,92	00,0	00,4	26,6	41,8	31,2	02,6	1,05	3,69
05	3,13	3,11	0,25	1,20	-0,01	+1,93	00,0	00,0	00,0	27,1	72,9	13,7	2,35	3,75
06	2,03	1,83	0,68	2,90	+0,36	-0,48	00,0	00,5	59,8	27,5	12,2	04,7	0,98	3,64
07	1,89	1,77	0,58	2,40	+0,29	-0,63	00,0	00,8	64,2	30,9	04,1	02,0	0,96	3,13
08	1,83	1,79	0,50	2,20	+0,22	+0,07	00,0	02,9	64,9	29,8	02,4	01,1	0,78	3,02
09	2,03	2,00	0,55	2,50	+0,37	+0,79	00,0	01,0	51,3	40,4	07,3	01,4	0,95	3,44
052402	2,16	2,06	0,53	2,50	+0,24	+0,01	00,0	00,7	43,9	45,6	09,8	13,3	0,99	3,39
03	2,43	2,39	0,61	3,05	+0,04	-0,67	00,0	00,4	26,4	52,4	20,8	11,0	1,09	3,63
04	2,08	1,91	0,69	3,00	+0,26	-0,77	00,0	00,8	54,4	29,8	15,0	15,4	0,96	3,54
05	-	-	-	-	-	-	-	-	-	-	-	-	-	-
06	1,86	1,81	0,53	2,30	+0,34	+0,18	00,0	01,9	64,1	29,3	04,7	04,1	0,88	3,19
052503	1,89	1,88	0,39	1,75	+0,23	+0,65	00,0	00,4	65,1	33,8	00,7	02,4	1,05	2,94
04	2,20	2,11	0,56	2,60	+0,22	-0,24	00,0	00,5	41,4	48,3	09,8	13,1	1,06	3,48
05	2,33	2,26	0,58	2,80	+0,14	-0,66	00,0	00,3	32,4	51,9	15,4	16,3	1,25	3,53
06	1,96	1,96	0,50	2,25	+0,16	+0,50	00,0	02,7	51,9	39,7	05,7	06,7	0,85	2,99
07	1,77	1,76	0,44	1,80	+0,20	-	00,0	03,4	71,6	24,9	01,1	04,5	0,85	2,99
052601	2,50	2,58	0,46	2,40	-0,23	-0,45	00,0	00,0	16,8	70,0	13,2	18,4	1,36	3,31
02	2,27	2,27	0,65	3,00	+0,03	-0,76	00,0	00,9	36,3	49,2	13,6	24,8	0,95	3,59
03	2,75	2,83	0,36	1,90	-0,79	+2,67	00,0	00,0	07,1	75,3	17,6	76,1	1,56	3,33
04	2,25	2,24	0,40	2,05	-0,09	-0,30	00,0	00,2	26,5	70,3	03,0	09,3	1,26	2,99
05	2,07	2,00	0,37	1,80	+0,38	+0,53	00,0	00,1	49,4	48,1	02,4	12,4	1,37	3,07

3.5. LANGEBAAN LAGOON : GRAIN SIZE PARAMETERS OF THE TERRIGENOUS COMPONENT

SAMPLE	MEAN	MD	QD	QH	SK	K	%VCS	%CS	%MS	%FS	%VFS	1%	99%
050101	2,98	2,96	0,20	0,95	+0,07	+0,17	00,0	00,0	00,0	57,7	42,3	2,45	3,43
02	3,13	3,07	0,26	1,20	+0,27	-0,67	00,0	00,0	00,0	40,2	59,8	2,64	3,64
03	2,97	2,94	0,25	1,20	-0,23	+5,35	00,0	00,0	00,4	60,1	39,5	2,55	3,52
04	0,79	0,77	0,40	0,90	+0,50	+1,63	00,4	75,8	22,0	01,8	00,0	0,16	2,04
05	1,27	1,30	0,39	1,15	-0,11	+0,68	00,2	22,1	74,4	03,3	00,0	0,28	2,11
06	2,71	2,70	0,33	1,75	-0,12	+0,87	00,0	00,0	03,2	79,7	17,1	1,65	3,41
07	0,68	0,79	0,90	1,80	-0,10	-0,30	19,5	42,5	30,9	07,0	00,1	-1,00	2,54
08	0,78	0,88	0,75	1,60	-0,09	-0,72	18,4	37,0	40,4	04,2	00,0	-0,74	2,29
09	2,52	2,59	0,50	2,50	-0,36	+0,42	00,0	00,4	16,4	68,6	14,6	1,18	3,45
10	2,11	2,47	1,07	4,10	-0,43	-0,23	06,7	11,9	17,6	43,7	20,1	-0,65	3,59
11	1,90	2,01	0,81	3,10	-0,15	-0,82	00,4	17,2	32,0	42,2	08,2	0,12	3,23
12	1,73	1,55	0,86	3,05	+0,14	-1,12	00,0	22,8	40,0	27,4	09,8	0,28	3,37
13	1,58	1,36	0,88	2,90	+0,29	-0,89	00,0	36,2	32,7	20,8	10,3	0,24	3,35
14	0,90	0,74	1,00	2,30	+0,35	+0,03	15,0	48,9	21,0	09,6	05,5	-0,96	3,25
15	1,42	1,22	0,72	2,30	+0,24	-1,01	00,0	38,0	36,7	24,0	01,3	0,35	2,84
16	0,92	0,80	0,71	1,75	+0,34	-0,08	06,7	53,9	31,1	07,9	00,4	-0,29	2,74
17	1,33	0,72	1,14	3,10	+0,14	-1,63	04,0	49,1	06,4	34,6	05,9	-0,16	3,13
18	1,22	1,13	0,69	1,90	+0,34	+0,04	00,0	42,8	44,8	10,7	01,7	0,15	3,05
19	1,22	1,09	0,77	2,20	+0,45	+0,34	00,0	45,7	38,7	14,6	01,0	-0,05	3,31
20	2,44	2,58	0,72	3,30	-0,53	+0,48	00,0	07,9	12,1	59,0	21,0	0,56	3,44
21	1,63	1,62	0,76	2,60	+0,18	-0,82	00,0	26,1	43,7	25,2	05,0	0,39	3,19
22	2,35	2,50	0,88	3,80	-0,21	-0,92	00,0	10,1	21,8	37,9	30,2	0,54	3,69
23	2,48	2,67	0,91	4,00	-0,18	-1,00	00,0	07,9	24,5	30,6	37,0	0,59	3,89
24	2,24	2,32	0,89	3,75	-0,13	-0,85	00,0	04,2	35,3	36,2	24,3	0,36	3,77
25	2,19	2,17	0,55	2,50	-0,10	-0,59	00,0	01,4	37,1	52,7	08,8	0,89	3,17
050201	3,11	3,08	0,31	1,30	-0,58	+9,21	00,0	00,2	00,3	38,0	61,5	2,48	3,72
02	3,19	3,14	0,30	1,25	+0,25	-0,49	00,0	00,0	00,0	29,7	70,3	2,64	3,85
03	0,93	0,77	0,82	1,90	+0,82	+1,56	06,4	55,8	29,4	08,4	00,0	-0,15	3,33
04	2,63	2,59	0,37	1,90	-0,06	+0,08	00,0	00,0	03,9	75,9	20,2	1,62	3,32
05	1,71	1,65	0,59	2,30	+0,25	+0,11	00,0	08,6	64,7	22,9	03,8	0,45	3,14
06	1,82	1,77	0,70	2,80	+0,28	-0,02	00,0	08,7	56,6	28,5	06,2	0,46	3,53
07	2,77	2,78	0,42	2,10	-0,36	+1,32	00,0	00,0	06,4	66,8	26,8	1,31	3,49
08	0,86	0,91	0,84	1,90	+0,01	-0,34	16,6	38,0	35,0	10,4	00,0	-0,96	2,59
09	1,65	1,66	0,61	2,30	-0,16	-0,09	01,0	13,8	57,0	28,2	00,0	-0,05	2,72
10	1,50	1,48	0,55	1,90	+0,55	+0,33	00,4	18,0	65,6	15,4	00,6	0,21	2,85
050301	2,97	2,96	0,18	0,90	+0,10	-0,23	00,0	00,0	00,0	57,3	42,7	2,55	3,34
02	1,93	1,93	0,55	2,40	-0,04	-0,16	00,0	04,6	51,6	41,8	02,0	0,58	3,02
03	1,90	1,90	0,47	2,10	+0,04	-0,14	00,0	03,4	57,3	38,4	00,9	0,85	2,94
04	1,61	1,63	0,50	1,90	-0,01	-0,42	00,0	12,6	66,7	20,7	00,0	0,54	2,66
05	1,71	1,75	0,44	1,75	-0,03	-0,38	00,0	07,1	65,9	26,7	00,3	0,76	2,68
06	1,65	1,65	0,39	1,50	+0,01	-0,33	00,0	04,8	75,9	19,3	00,0	0,74	2,45
07	2,22	2,13	0,41	2,10	+0,39	+0,44	00,0	00,0	35,0	58,7	06,3	1,45	3,32
08	0,94	0,70	0,94	2,20	+0,50	+0,24	10,7	53,0	22,4	09,3	04,6	-0,35	3,44
050401	1,62	1,55	0,44	1,60	+0,67	+3,56	00,0	04,0	87,2	06,5	02,3	0,69	3,14
02	2,64	2,70	0,60	3,00	-0,37	+1,49	00,0	02,1	10,2	63,4	24,3	0,75	3,78
03	2,54	2,53	0,38	1,90	-0,13	+0,24	00,0	00,0	04,8	83,4	11,8	1,45	3,22
04	2,36	2,44	0,54	2,75	-0,30	-0,22	00,0	00,7	25,2	63,4	10,7	1,05	3,15
05	1,75	1,70	0,52	2,40	+0,65	+2,86	00,0	02,6	75,4	17,7	04,3	0,85	3,55
06	2,30	2,48	0,68	3,20	-0,43	+0,07	00,0	05,0	21,5	62,5	11,0	0,48	3,32
050501	2,64	2,78	0,59	3,00	-1,15	+5,03	00,0	05,2	04,9	70,8	19,1	0,45	3,24
02	2,95	2,90	0,27	1,30	+0,28	-0,46	00,0	00,0	00,0	62,9	37,1	2,45	3,55
03	-	-	-	-	-	-	-	-	-	-	-	-	-
04	2,67	2,70	0,28	1,40	-0,46	+1,39	00,0	00,0	03,2	86,3	10,5	1,76	3,14
05	1,79	1,91	0,79	2,95	-0,20	-0,44	00,9	16,4	38,0	40,5	04,2	-0,04	3,14
06	2,13	2,20	0,61	2,80	-0,28	-0,41	00,0	06,2	32,1	58,0	03,7	0,59	3,04
07	2,53	2,56	0,38	2,00	-0,58	+2,76	00,0	00,4	06,9	84,8	07,9	1,15	3.19
08	1,64	1,71	0,46	1,80	-0,20	-0,64	00,0	11,1	61,6	27,3	00,0	0,54	2,33

SAMPLE	MEAN	MD	QD	QH	SK	K	%VCS	%CS	%MS	%FS	%VFS	1%	99%
050601	2,83	2,85	0,35	1,70	-0,62	+3,06	00,0	00,0	03,6	63,6	32,8	1,55	3,43
02	2,62	2,71	0,50	2,50	-0,76	+3,10	00,0	01,8	08,0	70,3	19,9	0,79	3,33
03	2,81	2,86	0,42	2,00	-1,03	+5,11	00,0	00,0	06,7	66,5	26,8	1,15	3,44
04	1,74	1,86	0,58	2,25	-0,05	-0,73	00,0	15,1	48,3	35,6	01,0	0,58	2,95
05	2,20	2,28	0,55	2,60	-0,42	+1,23	00,0	04,8	21,1	69,2	04,9	0,53	3,29
06	1,27	1,30	0,51	1,50	-0,03	-0,50	00,0	30,8	60,5	08,7	00,0	0,16	2,25
07	2,26	2,31	0,59	2,80	-0,26	+0,30	00,0	05,4	20,6	67,3	06,7	0,74	3,52
08	1,79	1,77	0,67	2,60	+0,01	-0,76	00,0	13,5	48,7	35,5	02,3	0,38	3,04
09	1,74	1,83	0,66	2,60	-0,04	-0,30	00,3	16,0	45,5	33,1	05,1	0,45	3,13
10	1,88	2,78	1,60	4,70	-0,44	-0,86	21,3	05,9	09,0	30,5	33,3	-1,13	3,53
050701	2,96	2,94	0,26	1,30	-0,15	+1,88	00,0	00,0	00,6	59,1	40,3	2,26	3,51
02	2,36	2,43	0,72	3,25	-0,08	-0,99	00,0	02,1	32,3	43,7	21,9	0,85	3,63
03	2,48	2,64	0,53	2,70	-0,38	+0,30	00,0	02,7	21,2	55,9	20,2	0,55	3,49
04	2,91	2,94	0,33	1,60	-0,25	+0,08	00,0	00,0	00,9	56,7	42,4	1,95	3,52
05	2,53	2,51	0,46	2,40	-0,05	-0,25	00,0	00,2	11,3	71,5	17,0	1,46	3,43
06	2,39	2,51	0,54	2,70	-0,52	+0,83	00,0	02,3	18,0	71,8	07,9	0,85	3,25
07	1,61	1,60	0,71	2,50	+0,08	-0,63	00,0	21,1	51,1	25,0	02,8	0,25	3,09
08	1,59	1,63	0,64	2,30	-0,07	-0,37	00,1	18,8	54,2	26,3	00,6	0,09	2,91
09	1,61	1,57	0,93	3,10	+0,05	-0,87	02,8	25,9	37,0	24,5	09,8	-0,11	3,34
10	1,57	1,49	0,55	2,00	+0,14	-0,92	00,0	18,7	56,9	24,2	00,2	0,58	2,63
050801	2,01	1,84	0,75	3,10	+0,19	-0,97	00,0	04,8	51,1	30,8	13,3	0,74	3,56
02	2,87	3,00	0,52	2,60	-0,58	+0,77	00,0	00,0	10,1	40,4	49,6	1,35	3,64
03	3,08	3,03	0,22	1,00	+0,29	-0,47	00,0	00,0	00,0	44,1	55,9	2,66	3,54
04	2,19	2,14	0,39	2,00	+0,15	+0,05	00,0	00,0	28,4	68,2	03,4	1,29	3,03
05	1,95	2,02	0,51	2,25	-0,18	+0,55	00,0	06,6	40,9	48,7	03,8	0,66	3,04
06	1,54	1,49	0,60	2,10	+0,08	-0,55	00,0	20,2	56,0	23,4	00,4	0,34	2,84
07	2,09	2,13	0,47	2,25	-0,04	-0,01	00,0	00,0	38,0	58,8	03,2	1,01	3,17
08	1,68	1,76	1,06	3,40	-0,26	-0,21	07,5	17,5	33,6	31,3	10,1	-1,13	3,34
050901	2,95	2,92	0,28	1,40	+0,12	+0,20	00,0	00,0	00,3	60,9	38,8	2,45	3,61
02	2,74	2,90	0,56	2,90	-0,56	+0,51	00,0	00,0	12,7	48,8	38,5	1,19	3,44
03	3,09	3,05	0,20	0,90	+0,34	-0,27	00,0	00,0	00,0	40,9	59,1	2,73	3,55
04	1,98	2,03	0,54	2,30	-0,12	-0,18	00,0	06,3	40,9	49,2	03,6	0,75	3,12
05	2,51	2,55	0,37	2,00	-0,34	+0,38	00,0	00,0	10,1	82,1	07,8	1,46	3,14
06	1,73	1,81	0,62	2,40	+0,02	+0,15	00,2	13,0	53,9	29,5	03,4	0,36	3,24
051001	1,94	1,92	0,43	1,90	+0,11	-0,02	00,0	00,8	57,6	41,3	00,3	0,96	2,87
02	3,02	3,04	0,29	1,30	-0,37	+1,93	00,0	00,0	00,4	43,2	56,4	2,35	3,49
03	3,01	2,98	0,22	1,10	-0,01	+1,01	00,0	00,0	00,0	53,9	46,1	2,33	3,53
04	2,23	2,47	0,78	3,50	-0,07	-1,53	00,0	02,1	41,4	38,1	18,4	0,88	3,42
05	1,96	2,09	0,69	2,85	-0,26	-0,56	00,0	13,9	30,7	51,8	03,6	0,36	3,05
06	2,39	2,47	0,61	3,00	-0,12	-0,62	00,0	00,0	26,0	58,8	15,2	1,06	3,49
051101	2,22	2,02	0,65	3,00	+0,65	-1,30	00,0	00,3	48,9	32,0	18,8	1,15	3,35
02	2,14	1,99	0,60	2,75	+0,17	-1,08	00,0	00,4	50,1	37,3	12,2	1,05	3,25
03	2,99	2,96	0,21	1.00	+0,13	+0,16	00,0	00,0	00,0	55,7	44,3	2,46	3,45
04	2,80	2,91	0,49	2,60	-0,52	+0,64	00,0	00,0	11,7	52,6	35,7	1,46	3,55
05	2,34	2,45	0,59	2,85	-0,57	+1,07	00,0	06,0	13,6	71,8	08,6	0,65	3,15
06	2,89	2,91	0,38	1,80	-0,07	-0,75	00,0	00,0	00,3	56,5	43,2	2,06	3,64
07	1,75	1,64	0,74	1,96	+0,42	-0,19	00,0	00,2	73,8	25,6	00,4	1,06	2,85
08	2,67	2,80	0,53	2,70	-0,35	-0,55	00,0	00,0	15,6	52,1	32,3	1,44	3,41
051203	2,19	2,06	0,71	3,10	+0,02	-1,46	00,0	00,8	47,1	36,1	16,0	0,96	3,31
04	1,85	1,77	0,42	1,85	+0,43	+0,37	00,0	00,2	70,4	28,5	00,9	1,15	2,95
05	1,84	1,89	0,46	2,00	+0,42	+0,60	00,0	00,2	64,1	32,2	03,5	1,15	3,21
06	2,96	2,92	0,20	1,00	+0,34	-0,53	00,0	00,0	00,0	64,1	35,9	2,65	3,35
07	2,26	2,33	0,59	2,80	-0,16	-0,57	00,0	02,1	29,3	57,9	10,7	0,85	3,25
08	2,66	2,78	0,58	3,00	-0,52	+0,33	00,0	00,0	15,3	52,1	32,6	1,15	3,45
09	1,34	1,24	0,53	1,60	+0,61	+1,91	00,1	23,5	66,1	08,6	01,7	0,36	3,05
10	1,39	1,38	0,26	1,10	+0,29	+1,29	00,0	00,0	07,6	89,7	02,7	0,86	2,05

APPENDIX 3.5. (cont.)

SAMPLE	MEAN	MD	QD	QH	SK	K	%VCS	%CS	%MS	%FS	%VFS	1%	99%
051302	2,69	2,77	0,47	2,40	-0,16	-0,85	00,0	00,0	07,1	62,3	30,6	1,57	3,42
03	2,73	2,89	0,60	3,10	-0,50	+0,28	00,0	00,7	15,9	47,5	35,9	1,02	3,63
04	2,83	2,90	0,49	2,50	-0,73	+2,50	00,0	00,5	08,6	52,1	38,8	1,15	3,54
05	1,84	1,78	0,47	2,10	+0,41	+0,83	00,0	01,7	69,7	25,2	03,4	0,89	3,15
06	2,00	1,86	0,62	2,75	+0,31	-0,65	00,0	00,9	60,1	27,1	11,9	0,95	3,29
07	2,54	2,68	0,55	2,80	-0,21	-0,76	00,0	00,0	19,2	59,1	21,7	1,31	3,39
08	2,27	2,15	0,61	2,90	+0,12	-1,06	00,0	00,0	40,3	46,0	13,7	1,14	3,48
09	1,86	1,88	0,35	1,20	+0,08	+0,07	00,0	00,2	65,3	34,4	00,1	1,11	2,25
10	1,58	1,51	0,32	1,20	+0,30	-0,30	00,0	00,4	86,8	12,8	00,0	1,05	2,25
11	1,62	1,60	0,23	0,90	+0,28	+0,83	00,0	00,1	93,6	06,3	00,0	1,12	2,14
051403	3,12	3,08	0,20	0,90	+0,24	-0,19	00,0	00,0	00,0	35,9	64,1	2,75	3,54
04	2,79	2,91	0,49	2,50	-0,44	+0,01	00,0	00,0	11,0	47,9	41,1	1,53	3,54
05	1,86	1,74	0,53	2,25	+0,57	+1,07	00,0	00,6	70,7	22,8	05,9	1,05	3,35
06	1,99	1,88	0,51	2,30	+0,40	-0,13	00,0	00,2	58,4	36,6	04,8	1,16	3,16
07	1,70	1,68	0,35	1,30	+0,33	+0,63	00,0	00,1	81,2	18,5	00,2	1,06	2,65
08	1,78	1,68	0,51	2,10	+0,55	+0,79	00,0	00,5	75,0	20,4	04,1	1,05	3,14
051505	2,99	3,03	0,35	1,60	-0,63	+3,13	00,0	00,0	02,2	43,4	54,4	1,79	3,56
06	2,89	2,95	0,44	2,20	-0,43	+0,77	00,0	00,0	05,7	49,2	45,1	1,55	3,62
07	2,65	2,89	0,65	3,25	-0,43	-0,58	00,0	00,4	22,5	38,1	39,0	1,14	3,44
08	2,78	2,89	0,53	2,75	-0,49	+0,39	00,0	00,0	12,7	49,3	38,1	1,33	3,55
09	1,76	1,71	0,46	1,90	+0,33	+0,66	00,0	03,3	70,7	24,2	01,8	0,79	3,05
10	1,83	1,82	0,37	1,60	+0,14	-0,50	00,0	00,3	69,1	30,6	00,0	1,08	2,64
11	1,96	1,90	0,52	2,30	+0,36	+0,29	00,0	01,5	59,2	32,9	06,4	0,91	3,24
12	2,14	2,02	0,52	2,40	+0,26	-0,86	00,0	00,0	48,4	43,7	07,9	1,27	3,12
13	1,78	1,71	0,41	1,70	+0,63	+1,89	00,0	00,1	78,4	19,4	02,1	1,15	3,12
051605	2,67	2,77	0,63	3,10	-0,51	+0,81	00,0	01,7	15,6	54,5	28,2	0,85	3,64
06	2,27	2,41	0,70	3,20	-0,16	-0,99	00,0	03,7	31,6	48,9	15,8	0,78	3,44
07	1,60	1,53	0,39	1,50	+0,59	+1,75	00,0	01,9	86,1	11,7	00,3	0,89	2,76
08	2,94	2,93	0,24	1,20	-0,64	+6,44	00,0	00,0	00,6	59,9	39,5	2,25	3,35
09	1,89	1,83	0,46	2,10	+0,47	+1,06	00,0	00,4	66,1	30,1	03,4	1,05	3,24
10	1,99	1,88	0,49	2,20	+0,61	+1,34	00,0	00,1	62,3	31,6	06,0	1,26	3,45
051704	2,84	2,85	0,37	1,80	-0,16	+0,67	00,0	00,0	02,2	66,7	31,1	1,87	3,69
05	2,66	2,77	0,57	2,90	-0,38	-0,32	00,0	00,0	17,6	50,6	31,8	1,23	3,43
06	2,17	2,06	0,57	2,70	+0,21	-0,86	00,0	00,0	46,3	43,3	10,4	1,18	3,33
07	3,08	3,04	0,20	0,96	+0,44	+0,45	00,0	00,0	00,0	43,9	56,1	2,76	3,62
08	1,73	1,72	0,37	1,55	+0,19	+0,19	00,0	00,8	76,8	22,3	00,1	0,96	2,71
09	1,83	1,80	0,42	1,75	+0,27	-0,03	00,0	00,2	68,3	31,1	00,4	1,06	2,89
051807	2,68	2,78	0,48	2,50	-0,52	+0,54	00,0	00,0	11,9	62,2	25,9	1.29	3,33
08	2,42	2,57	0,63	3,10	-0,32	-0,54	00,0	01,5	23,8	58,3	16,4	0,89	3,34
09	1,98	1,71	0,72	2,90	+0,32	-1,06	00,0	00,5	62,5	22,1	14,9	1,05	3,34
10	1,81	1,71	0,51	2,20	+0,60	+1,33	00,0	00,3	73,4	20,8	05,5	0,98	3,29
11	1,60	1,55	0,44	1,70	+0,32	+0,46	00,0	06,3	77,5	15,8	00,4	0,75	2,74
051905	2,94	2,96	0,29	1,40	-0,41	+1,36	00,0	00,0	00,7	53,6	45,7	2,03	3,39
06	2,96	2,97	0,31	1,50	-0,82	+5,02	00,0	00,0	02,4	51,7	45,9	1,64	3,35
07	2,58	2,83	0,66	3,30	-0,41	-0,60	00,0	00,2	23,8	47,4	28,6	1,09	3,52
08	1,75	1,69	0,37	1,65	+0,32	-0,01	00,0	00,3	77,4	22,3	00,0	1,06	2,65
09	1,88	1,85	0,59	2,50	+0,20	-0,69	00,0	00,9	56,9	37,7	04,5	0,95	3,24
052005	3,16	3,14	0,21	0,95	+0,02	+1,66	00,0	00,0	00,1	20,8	79,1	2,67	3,62
06	2,54	2,76	0,65	3,15	-0,23	-1,08	00,0	00,1	27,0	43,3	29,6	1,17	3,48
07	1,73	1,64	0,46	1,90	+0,49	+0,62	00,0	00,6	76,9	21,6	00,9	0,97	2,95
08	1,65	1,61	0,38	1,50	+0,36	+0,59	00,0	01,9	80,8	16,9	00,4	0,89	2,55

APPENDIX 3.5. (cont.)

SAMPLE	MEAN	MD	QD	QH	SK	K	%VCS	%CS	%MS	%FS	%VFS	1%	99%
052102	2,26	2,36	0,63	2,95	-0,22	-0,59	00,0	00,9	31,3	57,1	10,7	0,95	3,34
03	2,95	2,92	0,21	1,10	+0,05	+0,18	00,0	00,0	00,0	63,6	36,4	2,34	3,35
04	-	-	-	-	-	-	-	-	-	-	-	-	-
05	2,59	2,87	0,68	3,30	-0,62	+0,47	00,0	03,4	17,8	47,1	31,7	0,55	3,33
06	3,00	2,97	0,25	1,20	+0,14	+0,24	00,0	00,0	00,1	53,9	46,0	2,46	3,54
07	1,65	1,56	0,40	1,65	+0,71	+2,36	00,0	00,2	84,6	14,0	01,2	1,05	3,02
08	1,60	1,59	0,32	1,20	+0,17	-0,23	00,0	00,8	87,9	11,3	00,0	0,96	2,34
09	1,83	1,83	0,34	1,50	+0,06	-0,53	00,0	00,0	70,2	29,8	00,0	1,06	2,53
052202	2,21	2,13	0,46	2,25	+0,25	-0,33	00,0	00,0	38,2	54,7	07,1	1.35	3,29
03	3,06	3,04	0,28	1,25	+0,16	-0,43	00,0	00,0	00,0	44,9	55,1	2,47	3,63
04	-	-	-	-	-	-	-	-	-	-	-	-	-
05	-	-	-	-	-	-	-	-	-	-	-	-	-
06	1,94	1,82	0,54	2,40	+0,37	-0,36	00,0	00,1	62,6	31,9	05,4	1,09	3,14
07	1,40	1,37	0,23	0,80	+0,25	-0,09	00,0	00,9	98,3	00,8	00,0	0,95	1,95
08	3,06	3,04	0,36	1,60	-0,39	+3,72	00,0	00,0	01,7	42,6	55,7	1,76	3,82
09	1,85	1,77	0,41	1,95	+0,59	+1,26	00,0	00,0	75,2	23,6	01,2	1,18	2,96
10	1,71	1,66	0,35	1,40	+0,40	+0,91	00,0	00,3	78,4	20,8	00,5	1,08	2,55
052303	2,01	1,97	0,46	2,10	+0,15	-0,34	00,0	00,8	52,2	45,3	01,7	0,98	3,01
04	2,60	2,81	0,65	3,20	-0,29	-0,79	00,0	00,0	24,4	44,6	31,0	1,14	3,55
05	3,24	3,20	0,18	0,80	+0,25	-0,15	00,0	00,0	00,0	01,0	99,0	2,95	3.65
06	2,04	1,89	0,60	2,60	+0,26	-0,92	00,0	00,1	57,4	32,9	09,6	1,15	3,22
07	1,85	1,71	0,55	2,40	+0,42	-0,19	00,0	00,0	69,2	26,8	04,0	1,07	3,15
08	1,93	1,84	0,50	2,40	+0,61	+1,37	00,0	00,2	64,0	31,1	04,7	1,25	3,47
09	1,96	1,95	0,43	2,00	+0,11	-0,55	00,0	00,0	54,6	45,4	00,0	1,07	2,85
052402	2,27	2,12	0,51	2,50	+0,45	+0,13	00,0	00,0	37,4	52,5	10,1	1,48	3,62
03	2,42	2,38	0,54	2,70	+0,10	-0,69	00,0	00,0	24,3	58,2	17,5	1,36	3,53
04	2,04	1,89	0,58	2,60	+0,27	-0,84	00,0	00,2	56,7	34,5	08,6	1,12	3,22
05	-	-	-	-	-	-	-	-	-	-	-	-	-
06	1,92	1,85	0,43	2,00	+0,41	+0,25	00,0	00,0	64,2	33,5	02,3	1,25	3,06
052503	1,93	1,87	0,36	1,70	+0,49	+0,96	00,0	00,0	65,5	33,6	00,9	1,26	2,95
04	2,27	2,19	0,45	2,30	+0,22	-0,80	00,0	00,0	34,7	57,6	07,7	1,51	3,22
05	2,41	2,35	0,50	2,50	+0,14	-0,87	00,0	00,0	24,3	59,5	16,2	1,47	3,35
06	2,05	1,93	0,54	2,50	+0,74	+2,02	00,0	00,0	57,5	34,8	07,7	1,26	3,64
07	1,78	1,74	0,36	1,50	+0,26	-0,17	00,0	00,2	74,2	25,6	00,0	1,15	2,63
052601	2,47	2,53	0,48	2,50	-0,17	-0,86	00,0	00,0	19,7	67,3	13,0	1,45	3,24
02	2,23	2,22	0,46	2,30	+0.08	-1,01	00,0	00,0	37,2	58,0	04,8	1,37	3,12
03	2,99	2,88	0,32	1,60	+0,29	+1,40	00,0	00,0	00,3	64,6	35,1	2,55	3,76
04	2,30	2,26	0,40	2,05	+0,17	-0,53	00,0	00,0	24,6	69,4	06,0	1,52	3,16
05	2,05	1,97	0,36	1,80	+0,85	+3,52	00,0	00,0	54,4	42,0	03,6	1,55	3,32
06	1,96	1,92	0,36	1,80	+0,21	-0,28	00,0	00,0	57,8	42,0	00,2	1,25	2,73

3.6. LANGEBAAN LAGOON : GRAIN SIZE PARAMETERS OF THE BIOCLASTIC COMPONENT

SAMPLE	MEAN	MD	QD	QH	SK	K	%VCS	%CS	%MS	%FS	%VFS	1%	99%
050101	2,69	2,82	0,42	2,10	-1,43	4,84	00,0	00,0	06,2	72,7	21,1	0,97	3,23
02	2,78	2,81	0,47	2,40	-0,95	1,91	00,0	00,0	04,6	74,2	21,2	1,16	3,44
03	2,68	2,73	0,44	2,30	-1,21	-1,97	00,0	00,0	15,6	68,1	16,3	0,45	3,36
04	0,74	0,84	0,36	0,75	-0,54	-0,03	06,0	64,0	30,0	00,0	00,0	-0,46	1,06
05	1,28	1,32	0,59	2,89	+0,04	-0,25	00,0	29,1	64,4	06,5	00,0	-0,10	2,89
06	2,80	2,75	0,49	2,40	-0,34	-0,45	00,0	00,0	03,4	67,1	29,5	1,85	3,95
07	1,12	1,05	0,68	1,80	+0,71	+2,29	06,5	42,5	44,5	02,0	04,5	-0,12	4,18
08	1,10	1,01	0,53		+0,13	-0,40	00,4	50,4	40,2	09,0	00,0	0,34	2,19
09	2,21	2,46	0,86	3,60	-1,31	+0,33	00,0	11,4	19,4	53,2	16,0	-0,32	3,35
10	2,58	2,82	0,60	3,00	-0,36	-0,59	00,0	00,0	29,2	45,5	25,3	1,23	3,29
11	1,80	1,92	1,11	3,65	-0,15	-0,91	06,0	23,0	24,2	29,6	17,2	-0,70	3,55
12	1,54	1,62	1,25	3,55	-0,24	-0,19	08,2	30,8	23,4	22,8	14,8	-1,64	3,51
13	1,05	0,79	1,00	2,50	+),24	-0,48	08,4	47,0	25,5	18,0	01,1	-0,94	3,35
14	1,19	0,84	1,00	2,70	+0,62	+),19	00,0	60,7	20,0	06,6	12,7	-0,22	3,55
15	1,50	1,19	1,30	3,60	+0,39	-0,54	01,0	44,2	27,1	00,0	27,7	-0,39	4,08
16	1,35	0,85	1,27	3,40	+0,49	-0,67	06,3	50,1	10,9	18,1	14,6	-0,41	3,98
17	1,34	0,62	1,30	3,50	+0,27	-1,59	08,2	56,9	00,0	19,8	15,1	-0,38	3,33
18	1,53	0,11	0,97	3,10	+0,29	-1,05	00,2	35,6	32,0	23,7	08,5	-0,05	3,43
19	1,21	1,07	0,64	1,80	+0,16	-1,28	00,0	46,3	35,3	17,0	01,4	+0,21	2,39
20	2,06	2,41	1,00	3,80	-0,30	-1,36	00,2	22,5	11,9	53,4	12,0	0,16	3,42
21	1,41	1,26	0,89	2,75	+0,16	-0,65	00,0	37,3	35,1	24,0	03,6	-0,21	3,61
22	2,18	2,54	1,21	4,40	-0,36	-0,80	02,0	21,9	15,0	22,9	38,2	-0,59	3,59
23	2,50	2,78	0,94	4,10	-0,38	-0,27	00,6	06,9	21,1	33,8	37,6	-0,07	3,61
24	2,50	2,52	0,47	2,40	-0,03	-0,78	00,0	00,0	23,5	58,6	17,9	1,40	3,37
25	1,80	2,06	1,02	3,50	-0,47	-0,34	00,0	27,8	22,7	45,1	04,4	-0,71	3,31
050201	2,76	2,92	0,68	3,30	-1,61	+2,59	00,0	02,2	10,1	50,0	37,7	-2,60	2,94
02	2,53	2,80	0,67	3,25	-2,62	+12,02	00,0	02,4	12,4	68,7	16,5	-0,78	2,83
03	0,71	0,77	0,42	0,85	-0,34	+0,44	11,0	56,2	32,8	00,0	00,0	-0,55	1,17
04	2,41	2,49	0,52	2,65	-0,29	+2,59	00,0	01,0	13,1	78,5	07,4	0,55	3,58
05	1,80	1,81	0,63	2,50	-0,02	+0,42	00,0	12,2	51,1	33,9	02,8	0,31	3,18
06	1,79	1,83	0,54	2,15	-0,25	-0,75	00,0	11,3	48,2	40,5	00,0	0,54	2,73
07	2,40	2,45	0,47	2,50	-1,23	+8,32	00,0	03,6	03,8	92,6	00,0	1,19	3,19
08	2,36	1,80	0,72	3,30	+0,77	-0,45	00,0	02,9	66,6	30,5	00,0	1,98	4,23
09	1,56	1,62	0,98	3,15	-0,19	+0,27	07,2	18,2	40,8	27,0	06,8	-0,93	3,66
10	1,30	1,32	0,95	2,75	+0,07	-0,26	06,2	31,2	43,0	13,8	05,8	-0,69	3,65
									03,4	44,1	52,5	1,13	4,32
050301	3,02	3,01	0,49	2,20	-0,44	+4,79	00,0	00,0	03,4	44,1	52,5	1,13	4,32
02	2,14	2,03	0,59	2,70	+0,24	-0,54	00,0	02,0	45,8	36,8	15,4	0,96	3,28
03	1,90	1,98	0,55	2,40	-0,61	+2,41	00,6	05,4	45,9	47,6	00,5	-0,13	2,94
04	1,59	1,71	0,90	3,05	-0,21	+1,59	05,0	15,8	47,9	24,5	06,3	-0,12	4,00
05	1,87	1,94	0,60	2,50	-0,12	+0,37	00,0	08,5	51,9	38,3	01,3	0,38	3,20
06	1,48	1,59	0,92	2,90	-0,60	+2,85	06,0	20,6	49,5	23,1	00,8	-1,84	3,39
07	1,96	2,11	0,75	3,00	-0,77	+0,36	00,0	09,4	34,0	53,1	09,8	-0,55	3,26
08	0,53	0,39	0,61	1,15	+0,42	+0,03	20,7	57,2	15,4	06,7	00,0	-0,49	1,86
050401	1,33	1,47	0,38	0,90	-1,50	+0,52	00,0	16,0	84,0	04,0	00,0	-0,61	1,58
02	2,35	2,35	0,41	2,10	-0,09	-1,19	00,0	00,0	19,7	73,8	06,5	1,43	3,06
03	2,20	2,23	0,94	3,80	-0,73	+3,50	01,4	06,2	30,4	43,0	19,0	-0,83	3,86
04	2,23	2,25	0,72	3,20	-0,14	-0,47	00,0	05,9	26,8	48,6	21,4	0,51	3,53
05	1,49	1,64	0,56	1,49	-1,14	-0,60	01,8	19,4	64,6	14,2	00,0	-0,80	2,13
06	1,81	2,24	1,27	4,10	-0,39	-0,43	09,0	18,4	22,3	33,9	16,4	-1,44	3,54
050501	2,76	3,25	1,23	4,90	-0,78	+2,53	00,0	04,6	10,0	09,9	84,7	-2,33	4,14
02	2,77	2,84	0,65	3,25	-0,62	+1,07	00,0	00,0	08,2	54,7	37,1	0,61	3,93
03	-	-	-	-	-	-	-	-	-	-	-	-	-
04	2,66	2,72	0,14	0,80	-0,68	+3,39	00,0	01,6	10,8	54,7	32,9	0,34	3,78
05	1,06	1,04	0,89	2,25	+0,01	-1,18	08,3	41,8	37,8	12,1	00,0	0,92	2,72

APPENDIX 3.6. (cont.)

SAMPLE	MEAN	MD	QD	QH	SK	K	%VCS	%CS	%MS	%FS	%VFS	1%	99%
050506	2,27	2,32	0,64	3,00	-0,37	+1,84	00,4	02,2	24,9	58,0	14,5	-0,01	3,64
07	2,45	2,41	0,30	1,55	+0,58	-3,06	00,0	00,0	08,1	83,6	08,3	2,17	3,27
08	1,84	1,99	0,86	3,20	-0,15	+0,42	00,0	18,9	29,6	46,3	05,2	-0,36	3,97
050601	2,30	3,14	1,65	5,10	-0,82	-1,51	05,6	19,0	16,8	07,2	51,4	-1,81	3,65
02	2,75	2,86	0,63	3,10	-0,18	-0,57	00,0	01,2	11,4	50,7	36,7	0,93	4,05
03	2,85	2,93	0,49	2,50	-0,38	-0,57	00,0	00,0	08,7	45,1	46,2	1,45	3,62
04	1,95	1,95	0,76	3,10	-0,12	-0,13	00,0	08,3	39,9	42,8	09,0	-0,10	3,35
05	2,18	2,33	0,52	2,50	-0,37	-0,51	00,0	02,8	27,7	67,0	02,5	0,79	2,89
06	1,41	1,29	0,69	2,25	+0,43	+1,20	01,6	26,6	55,7	14,9	01,2	-0,12	3,53
07	2,15	2,23	0,40	2,00	-0,42	+1,48	00,0	01,8	20,8	74,5	02,9	0,80	2,68
08	2,14	2,08	1,12	4,20	-0,14	-0,71	02,2	13,7	26,5	33,5	24,1	-0,50	4,14
09	1,99	2,15	0,59	2,65	-0,34	+0,26	00,0	03,7	35,7	54,7	05,9	0,11	2,95
10	-	-	-	-	-	-	-	-	-	-	-	-	-
11	-	-	-	-	-	-	-	-	-	-	-	-	-
050701	2,31	2,76	1,25	4,60	-1,23	+0,50	00,0	12,8	21,6	37,1	28,5	-1,52	3,69
02	2,43	2,87	0,81	3,60	-0,38	-1,01	00,0	05,9	26,5	41,3	26,3	0,65	3,43
03	2,54	2,79	0,85	3,90	-0,24	+1,01	00,0	02,1	25,8	44,9	27,2	1,03	3,77
04	2,68	2,66	0,56	2,90	-0,18	+1,20	00,0	00,0	07,9	74,1	18,0	0,93	3,76
05	2,18	2,29	0,69	3,05	-0,76	+2,70	00,0	06,6	21,7	65,7	06,0	-0,48	3,39
06	1,90	2,36	1,02	3,60	-0,66	+0,31	02,0	19,3	20,4	57,0	01,3	-0,93	2,97
07	1,72	1,74	0,71	2,70	-0,07	-0,05	00,6	12,9	52,1	30,4	04,0	-0,07	3,39
08	1,64	1,61	0,71	2,65	-0,15	-0,46	01,3	17,0	48,6	52,6	00,4	0,03	2,85
09	1,62	1,69	1,04	3,40	-0,14	-1,08	08,2	21,1	30,8	32,9	07,0	-0,59	3,32
10	1,39	1,30	0,79	2,45	+0,02	-0,76	00,0	34,1	39,1	26,9	00,0	-0,34	2,95
050801	1,98	1,78	0,82	2,25	+0,12	-1,32	00,0	12,4	46,3	24,0	17,5	0,58	3,30
02	2,65	3,01	0,92	4,20	-0,57	-0,37	00,0	04,6	25,1	18,6	51,6	0,23	3,62
03	2,97	3,00	0,42	2,00	-1,44	+8,16	00,0	00,0	04,2	46,3	49,5	0,82	3,66
04	2,14	2,14	0,61	2,75	-0,21	+0,95	00,0	02,6	34,0	52,2	11,2	0,55	3,43
05	1,67	1,82	0,61	2,30	-0,44	+0,67	00,6	15,2	55,1	29,1	00,0	-0,04	2,94
06	1,51	1,43	0,80	2,65	+0,06	-0,69	00,0	27,8	42,0	26,8	03,4	-0,16	3,26
07	1,87	2,10	0,86	3,20	-0,60	+0,63	00,6	18,8	26,2	49,4	05,0	-0,63	3,31
08	1,72	1,70	1,25	3,90	+0,06	-1,75	11,5	20,9	23,8	25,9	17,9	-0,09	4,12
050901	2,73	2,93	0,73	3,40	-1,15	+2,75	00,0	00,0	13,7	46,1	40,2	-0,09	3,75
02	3,09	3,10	0,59	2,80	-0,08	-0,46	00,0	00,0	04,7	34,6	60,7	1,51	4,28
03	2,91	2,95	0,29	1,40	-2,13	+10,74	00,0	00,0	02,6	58,3	39,1	1,13	3,33
04	1,92	1,96	0,58	2,50	-0,17	+0,92	00,0	08,5	45,5	42,0	04,0	0,23	3,34
05	2,35	2,42	0,59	2,90	-0,64	+3,80	00,0	03,4	12,9	76,3	07,4	0,24	3,75
06	1,60	1,82	0,76	2,65	-1,83	+3,75	06,0	09,6	46,7	37,7	00,0	-1,44	2,84
051001	2,18	2,07	0,65	2,90	+0,45	+0,49	00,0	03,2	40,2	40,7	11,9	0,74	3,81
02	2,65	2,75	0,59	3,00	+0,36	+1,81	00,0	00,0	13,2	70,2	16,6	0,35	3,59
03	2,87	2,97	0,61	3,10	-2,15	+14,40	00,0	02,0	05,6	46,3	46,1	-0,43	3,75
04	2,19	2,49	0,88	3,60	-0,19	-0,81	00,0	13,1	27,2	40,7	19,0	0,06	3,68
05	1,70	2,03	0,81	2,95	-0,96	+3,05	06,8	09,3	31,3	52,6	00,0	-1,70	2,45
06	2,39	2,73	0,88	3,90	-0,33	-0,71	00,0	08,2	23,8	41,6	26,4	0,30	3,89
051101	2,12	2,02	0,74	3,10	+0,03	-1,21	00,0	03,3	45,3	36,8	14,6	0,63	3,33
02	2,22	2,08	0,85	3,60	-0,05	-0,97	00,0	06,6	39,9	28,3	25,2	0,29	3,75
03	2,79	2,83	0,62	3,15	-1,13	+4,25	00,0	00,0	08,4	56,7	34,9	0,32	3,81
04	2,71	2,97	0,71	3,30	-0,47	-0,32	00,0	00,0	23,1	33,0	43,9	0,82	3,89
05	2,35	2,53	0,92	4,10	-1,07	+5,41	04,8	03,0	11,2	62,8	18,2	-1,53	3,73
06	-0,02	-0,16	0,99	1,30	+0,33	-0,43	00,0	59,0	39,4	01,6	00,0	-1,86	2,24
07	1,55	1,45	0,61	2,15	+0,41	+1,77	00,0	14,2	66,8	12,2	06,8	0,14	3,63
08	-	-	-	-	-	-	-	-	-	-	-	-	-

APPENDIX 3.6. (cont.)

SAMPLE	MEAN	MD	QD	QH	SK	K	%VCS	%CS	%MS	%FS	%VFS	1%	99%
051203	2,30	2,25	0,88	3,80	-0,12	-1,32	00,0	07,2	35,9	23,9	33,0	0,38	3,59
04	1,70	1,61	0,52	2,00	+0,43	+0,98	00,0	03,4	74,2	18,7	03,7	0,63	3,25
05	1,84	1,68	0,69	2,75	+0,14	+0,30	00,0	09,0	56,9	28,8	05,3	-0,01	3,61
06	2,96	2,90	0,56	2,80	-1,11	+5,90	00,0	00,0	06,0	55,9	38,1	0,53	3,95
07	2,21	2,32	0,85	3,50	-0,21	-0,69	00,0	10,5	26,1	43,7	19,7	0,25	3,61
08	2,48	2,87	0,83	3,80	-0,17	-1,76	00,0	00,6	33,9	35,7	29,8	0,83	3,73
09	1,15	1,09	0,80	2,10	+0,20	+0,51	00,0	41,8	45,5	08,8	03,9	-0,34	3,41
10	1,49	1,44	0,31	1,00	+0,64	+2,10	00,0	07,6	90,0	02,4	00,0	0,76	2,61
051302	2,14	2,00	0,79	3,30	+0,07	-0,95	00,0	00,6	51,3	34,5	13,6	0,51	3,88
03	2,66	3,06	0,89	4,10	-0,40	-1,19	00,0	01,5	27,3	13,1	58,1	0,88	3,63
04	2,66	2,94	0,77	3,60	-0,50	-1,07	00,0	02,3	20,8	34,9	42,0	0,69	3,72
05	1,86	1,81	0,50	2,10	+0,05	-0,43	00,0	04,9	59,3	35,6	00,2	0,59	2,89
06	1,63	1,58	0,80	2,80	+0,06	-0,42	00,0	10,7	46,9	27,6	03,3	-0,29	3,33
07	2,42	2,54	0,63	3,05	-0,18	-0,87	00,0	00,0	28,2	51,5	20,3	0,95	3,47
08	1,95	1,89	0,63	3,65	+0,11	-0,88	00,0	02,0	55,7	35,0	07,3	0,76	3,04
09	1,86	1,87	0,39	1,60	-0,08	-0,41	00,0	00,8	63,5	35,7	00,0	0,85	2,56
10	1,56	1,50	0,44	1,60	+0,05	-0,20	00,0	09,4	73,8	16,8	00,0	0,49	2,59
11	1,69	1,67	0,30	1,20	+0,09	-0,11	00,0	00,0	86,3	13,7	00,0	0,98	2,46
051403	2,83	2,94	0,66	3,25	-2,46	+12,80	00,0	00,0	10,4	49,9	39,7	-0,45	3,56
04	2,69	3,10	1,00	4,40	-0,31	-1,26	00,0	01,0	32,8	06,3	59,9	0,57	4,10
05	1,61	1,65	0,37	1,35	+0,23	+1,91	00,0	04,0	78,5	17,5	00,0	1,24	2,95
06	1,78	1,78	0,56	2,25	+0,44	+1,52	00,0	01,8	68,2	23,8	06,2	0,74	3,52
07	1,71	1,71	0,45	1,80	-0,02	+0,64	00,0	05,9	72,8	21,1	00,2	0,64	2,85
08	1,71	1,72	0,21	0,90	-0,27	-1,96	00,0	00,0	74,3	25,7	00,0	1,03	1,92
051505	2,71	2,82	0,48	2,50	-0,94	+2,89	00,0	00,0	09,6	70,8	19,6	0,91	3,42
06	3,37	3,43	0,66	2,50	-0,57	+1,07	00,0	00,0	06,9	03,6	89,5	1,39	4,32
07	1,62	2,41	1,45	4,10	-0,21	-0,99	07,2	26,2	25,9	36,1	04,6	-1,78	3,64
08	2,65	2,91	0,69	3,40	-0,61	+0,11	00,0	00,0	20,5	41,3	38,1	0,83	3,55
09	1,87	1,80	0,61	2,60	+0,54	+0,67	00,0	01,3	63,9	27,0	07,8	0,97	3,53
10	1,83	1,85	0,48	2,00	+0,01	-0,42	00,0	01,5	57,7	40,8	00,0	0,82	2,86
11	1,84	1,81	0,61	2,50	+0,22	+0,73	00,0	05,5	58,4	29,1	07,0	0,59	3,34
12	1,89	1,80	0,73	2,85	+0,20	-0,64	00,0	01,6	61,8	24,5	12,1	0,63	3,52
13	1,72	1,68	0,47	1,90	+0,26	-	00,0	01,7	72,4	24,2	01,7	-	-
051605	2,99	3,13	0,50	2,50	-0,64	+0,69	00,0	00,0	06,9	36,3	56,8	1,59	3,64
06	2,14	2,33	0,81	3,40	-0,19	-1,12	00,0	12,1	26,4	46,1	15,4	0,52	3,26
07	1,67	1,59	0,47	1,80	+0,78	+2,54	00,0	00,0	85,8	11,7	02,5	1,01	3,22
08	2,52	2,68	0,71	3,40	-0,55	-3,95	00,0	00,0	19,6	62,9	17,5	0,25	3,49
09	3,42	3,89	1,23	4,00	-2,14	+3,64	02,6	12,4	04,8	20,0	60,2	-1,07	4,29
10	1,83	1,85	0,49	2,10	+0,02	-1,04	00,0	01,3	59,5	37,6	01,6	0,66	2,85
051704	2,73	2,80	0,52	2,75	-0,89	+3,05	00,0	00,0	13,2	65,9	20,9	0,83	3,57
05	2,30	2,78	0,93	3,90	-0,18	-1,73	00,0	04,0	39,2	28,4	28,4	0,55	3,61
06	1,78	1,73	0,65	2,55	+0,07	-0,60	00,0	07,0	58,3	34,7	00,0	0,40	3,33
07	3,07	3,06	0,14	0,75	+0,13	+1,37	00,0	00,0	00,0	38,3	61,7	2,14	3,88
08	1,63	1,64	0,49	1,90	+0,03	+1,28	00,0	09,2	71,0	18,5	01,3	0,26	2,97
09	1,81	1,75	0,63	2,50	+0,53	+1,40	00,0	05,2	60,7	26,1	08,0	0,66	3,77
051807	2,64	2,83	0,70	3,30	-0,63	+0,92	00,0	02,0	17,5	49,2	31,3	0,61	3,57
08	2,47	2,63	0,83	3,70	-0,45	-1,07	00,0	06,9	19,6	41,9	31,6	-0,13	3.78
09	1,93	1,70	0,80	3,15	+0,20	+1,01	00,0	07,4	52,6	22,1	17,9	0,49	3,36
10	1,65	1,72	0,41	1,70	-0,05	-2,57	00,0	06,9	71,4	21,7	00,0	0,72	2,79
11	1,59	1,53	0,62	2,25	+0,19	+0,71	00,0	14,1	62,1	21,2	02,6	0,11	3,32

APPENDIX 3.6. (cont.)

SAMPLE	MEAN	MD	QD	QH	SK	K	%VCS	%CS	%MS	%FS	%VFS	1%	99%
051905	3,00	3,01	0,46	2,30	-0,76	+3,47	00,0	00,0	06,1	44,4	49,5	1,21	3,69
06	3,24	3,30	0,57	2,40	-0,26	-1,78	00,0	00,0	04,8	01,5	93,7	1,66	4,23
07	2,57	2,80	0,75	3,50	-0,39	-0,61	00,0	01,8	24,4	39,0	34,8	0,81	3,60
08	1,68	1,70	0,45	1,85	+0,30	+1,05	00,0	01,7	80,6	16,9	00,8	0,84	3,05
09	1,54	1,39	0,70	2,40	+0,26	+0,25	00,4	25,7	51,3	19,1	03,5	0,35	3,44
052005	2,92	2,94	0,42	2,10	-1,31	+7,62	00,0	00,0	03,8	63,8	32,4	0,83	3,76
06	2,33	2,57	0,81	3,60	-0,20	-1,27	00,0	01,3	34,6	36,7	27,4	0,75	3,38
07	1,75	1,63	0,56	2,20	+0,56	+1,41	00,0	06,0	70,5	17,2	06,3	0,73	3,35
08	1,59	1,53	0,30	1,15	+0,45	+0,25	00,0	00,1	89,8	10,1	00,0	1,19	2,53
052102	2,47	2,62	0,53	2,70	-0,26	+0,18	00,0	02,7	21,5	61,1	14,7	0,75	3,34
03	2,97	2,93	0,30	1,40	+0,48	+2,30	00,0	00,0	00,0	67,4	32,6	2,18	3,95
04	-	-	-	-	-	-	-	-	-	-	-	-	-
05	2,69	2,87	0,62	3,10	-0,43	-0,59	00,0	00,0	19,0	50,9	30,1	1,55	3,75
06	3,44	2,36	0,40	1,35	+0,07	-0,16	00,0	00,0	00,1	00,3	99,6	2,22	4,32
07	1,55	1,52	0,48	1,80	+0,48	+2,37	00,0	07,8	78,2	11,4	02,6	0,51	3,28
08	1,59	1,51	0,53	1,90	+0,42	+1,94	00,0	12,2	69,9	17,5	00,4	0,36	3,34
09	1,81	1,79	0,59	2,40	+0,13	+0,25	00,0	07,0	51,4	40,4	01,2	0,46	3,33
052202	2,02	4,26	0,66	2,75	-0,17	-0,70	00,0	02,0	48,0	44,5	05,5	0,55	3,35
03	3,00	2,95	0,32	1,60	+0,10	+1,59	00,0	00,0	00,0	56,5	43,5	1,91	3,95
04	-	-	-	-	-	-	-	-	-	-	-	-	-
05	-	-	-	-	-	-	-	-	-	-	-	-	-
06	1,98	1,87	0,72	2,90	+0,20	-0,50	00,0	06,1	50,0	32,5	05,4	0,49	3,74
07	1,39	1,36	0,33	1,10	+1,08	+6,80	00,0	06,3	86,9	06,8	00,0	0,77	2,83
08	2,46	2,74	0,79	3,60	-1,61	+3,81	00,0	05,2	14,3	67,4	13,1	-0,26	3,03
09	1,58	1,70	0,20	0,75	-0,66	-1,37	00,0	01,0	91,4	07,6	00,0	0,76	1,82
10	1,72	1,67	0,55	2,20	+0,42	+1,41	00,0	11,9	71,4	19,2	03,5	0,62	3,71
052303	2,16	1,96	0,76	3,25	+0,52	+0,16	00,0	00,2	52,2	27,7	19,9	1,00	4,11
04	2,46	2,67	0,77	3,50	-0,16	-1,04	00,0	00,8	28,8	39,0	31,4	0,96	3,83
05	3,02	3,02	0,32	1,50	-0,27	+4,02	00,0	00,0	00,0	53,2	46,8	1,75	3,85
06	2,02	1,77	0,77	3,10	+0,45	-0,05	00,0	00,9	62,2	22,1	14,8	0,81	4,06
07	1,94	1,83	0,60	2,60	+0,16	-1,08	00,0	01,6	59,2	35,0	04,2	0,85	3,11
08	1,72	1,75	0,51	2,00	-0,16	-1,23	00,0	05,6	65,8	28,5	00,1	0,31	2,57
09	2,10	2,01	0,66	2,90	+0,63	+2,13	00,0	02,0	48,0	35,4	14,6	0,83	4,03
052402	2,06	2,01	0,54	2,40	+0,04	-0,12	00,0	01,4	50,4	38,7	09,5	0,52	3,16
03	2,44	2,39	0,69	3,25	-0,12	-0,64	00,0	00,8	28,5	46,6	24,1	0,82	3,73
04	2,13	1,92	0,80	3,35	+0,25	-0,71	00,0	01,4	52,1	25,1	21,4	0,80	3,86
05	-	-	-	-	-	-	-	-	-	-	-	-	-
06	1,81	1,77	0,63	2,40	+0,25	+0,11	00,0	03,8	64,0	25,1	07,1	0,51	3,32
052503	1,86	1,89	0,42	1,80	-0,03	+0,34	00,0	00,8	64,7	34,0	00,5	0,84	2,93
04	2,12	2,03	0,67	2,50	+0,21	+),31	00,0	01,0	48,1	39,0	11,9	0,61	3,74
05	2,24	2,16	0,66	2,90	+0,13	-0,46	00,0	00,6	40,5	44,3	14,6	1,03	3,71
06	1,88	1,98	0,46	2,00	-0,42	-1,02	00,0	05,4	46,3	44,6	03,7	0,64	2,66
07	1,75	1,77	0,53	2,15	+0,13	-	00,0	06,6	69,0	24,2	02,2	0,55	3,35
052601	2,54	2,62	0,45	2,25	-0,29	-0,04	00,0	00,0	13,9	72,7	13,4	1,27	1,38
02	2,30	2,31	0,85	3,60	-0,02	-0,52	00,0	01,8	35,4	40,4	22,4	0,53	4,06
03	2,52	2,77	0,40	2,00	-1,76	+3,95	00,0	00,0	13,9	86,0	00,1	0,57	2,90
04	2,21	2,23	0,41	2,00	-0,35	-0,06	00,0	00,4	28,4	71,2	00,0	1,00	2,82
05	2,09	2,04	0,38	1,80	-0,10	-2,45	00,0	00,2	41,0	54,2	04,6	1,19	2,82
06	-	-	-	-	-	-	-	-					

APPENDIX 4

4.1. SALDANHA BAY : GEOCHEMICAL PARAMETERS OF THE TOTAL SEDIMENT

SAMPLE	%$CaCO_3$	%$C_{org.}$	%P_2O_5	%K_2O	SAMPLE	%$CaCO_3$	%$C_{org.}$	%P_2O_5	%K_2O	SAMPLE	%$CaCO_3$	%$C_{org.}$	%P_2O_5	%K_2O
010101	06,3	0,05	-	-	020101	47,4	0,08	-	-	04	31,2	0,27	0,53	1,02
02	05,8	0,11	-	-	02	27,9	0,16	0,34	1,02	05	47,7	0,25	0,55	0,99
03	-	-	-	-	03	29,7	0,23	0,33	1,15	06	45,6	1,22	0,61	1,16
04	08,6	0,63	0,30	1,89	04	17,4	0,25	0,29	1,38	07	66,0	0,43	0,79	1,48
					05	18,3	0,27	0,25	1,44	08	28,6	0,41	0,56	1,25
010201	13,2	0,05	-	-	06	29,9	0,31	0,36	1,35	09	30,0	0,50	0,64	1,57
02	-	-	-	-	07	57,9	0,29	0,44	1,22	10	71,4	0,83	0,50	1,02
03	05,2	0,32	0,24	1,93	08	-	-	-	-	11	59,4	0,23	0,54	0,57
04	09,5	0,39	0,25	1,93						12	68,0	0,46	0,69	0,63
05	36,6	0,32	0,33	1,47	020201	79,8	0,12	0,37	1,16					
06	31,2	0,36	0,45	1,47	02	21,2	0,17	0,32	1,18	030201	74,9	0,15	0,79	0,70
07	36,4	0,39	0,54	1,84	03	32,2	0,20	0,35	1,25	02	31,4	0,19	0,48	0,85
					04	29,6	0,20	0,33	1,18	03	36,1	0,25	0,60	1,01
010301	28,9	0,09	-	-	05	28,3	0,23	0,32	1,25	04	86,8	0,33	0,41	0,91
02	-	-	-	-	06	42,9	0,22	0,40	1,25	05	35,4	0,46	0,61	1,08
03	11,5	0,20	0,23	1,64	07	40,1	0,26	0,53	1,44	06	54,3	0,35	0,63	0,91
04	10,6	0,25	0,22	1,54	08	-	-	-	-	07	50,1	0,27	0,64	0,59
05	10,4	0,28	0,23	1,50						08	87,1	0,32	0,25	0,62
06	31,4	0,30	0,34	1,44	020301	73,2	0,09	0,28	1,58	09	-	-	0,25	0,71
07	33,1	0,35	0,48	1,54	02	29,3	0,24	-	-					
					03	36,2	0,23	0,37	1,22	030301	73,5	0,13	0,48	0,75
010401	36,2	0,08	-	-						02	27,0	0,14	0,49	0,75
02	32,4	0,20	0,34	1,16	020401	73,1	0,08	0,25	1,44	03	25,5	0,22	0,51	0,85
03	16,5	0,16	0,24	1,25	02	41,5	0,27	0,38	1,22	04	33,0	0,37	0,55	0,95
04	12,4	0,24	0,18	1,25	03	29,9	0,20	0,39	1,38	05	90,5	0,24	0,29	0,53
05	23,7	0,26	0,18	1,25	04	34,4	0,22	0,52	1,58	06	88,9	0,49	0,29	0,36
06	42,7	0,31	0,31	1,44	05	67,1	0,69	0,44	1,18	07	49,8	0,31	0,59	0,53
07	48,4	0,37	0,57	1,80	06	30,0	0,32	0,57	1,65					
08	58,2	0,72	0,49	1,91	07	32,2	0,50	0,67	1,65	030401	66,0	0,15	0,52	0,65
09	94,0	0,19	0,08	0,31	08	-	-	-	-	02	26,5	0,14	0,50	0,65
										03	30,3	0,21	0,51	0,89
010501	53,0	0,08	-	-	020501	73,6	0,09	0,25	1,52	04	43,8	0,33	0,22	0,89
02	34,7	-	0,45	1,42	02	31,4	0,17	0,35	1,08	05	91,9	0,36	0,19	0,36
03	40,6	0,15	0,38	1,06	03	30,0	0,23	0,21	1,18	06	41,2	0,27	0,58	0,55
04	16,7	0,25	0,18	1,25	04	30,1	0,25	0,52	1,51					
05	14,1	0,23	0,19	1,34	05	31,4	0,30	0,56	1,61	030501	72,3	0,12	-	-
06	63,6	0,32	0,38	1,28	06	25,5	0,38	0,69	1,69	02	42,7	0,13	0,57	0,59
07	48,7	0,74	0,36	1,71	07	27,5	0,48	0,68	1,75	03	37,3	0,23	0,56	0,82
08	77,5	0,26	0,39	0,44	08	-	-	-	-	04	89,8	0,21	0,18	0,43
					09	-	-	-	-	05	86,3	0,46	0,29	0,49
010601	38,1	0,07	-	-										
02	-	-	-	-	020601	75,1	0,13	0,33	1,61	030601	72,8	0,10	-	-
03	-	-	-	-	02	30,0	0,16	0,41	1,02	02	30,5	0,14	0,46	0,63
04	28,2	-	0,30	1,15	03	31,1	0,24	0,56	1,25	03	38,9	0,24	0,57	0,70
05	38,0	0,24	0,31	1,06	04	27,0	0,30	0,56	1,29	04	74,3	0,26	0,37	0,75
06	34,1	0,23	0,28	1,15	05	34,2	0,40	1,40	1.31					
07	19,0	0,27	0,25	1,15	06	-	-	-	-	030701	79,5	-	-	-
08	31,0	0,31	0,33	1,65	07	34,3	0,42	0,64	1,55	02	34,1	0,18	0,61	0,63
09	-	-	-	-	08	-	-	-	-					
10	57,0	0,40	0,35	1,08	09	76,4	0,34	0,45	0,72	040101	15,8	-	0,29	2,31
11A	53,0	0,33	0,44	0,67						02	37,3	0,21	0,51	0,75
11B	66,7	0,30	0,33	1,28	030101	74,0	0,12	0,53	1,22	03	31,5	0,16	0,54	0,85
12	-	-	-	-	02	29,8	0,16	0,45	0,92					
13	-	-	-	-	03	32,4	0,25	0,46	1,18					

APPENDIX 4.1. (cont.)

SAMPLE	%$CaCO_3$	%$C_{org.}$	%P_2O_5	%K_2O
040201	36,2	-	0,22	1,92
02	35,2	0,19	0,48	0,82
03	31,0	0,19	0,51	0,91
04	43,0	0,23	0,57	0,71
05	92,6	0,22	0,18	0,46
040301	25,1	0,05	0,33	1,72
02	17,1	0,12	0,40	0,92
03	25,0	0,15	0,44	0,82
04	83,5	0,17	0,33	0,86
05	48,5	0,26	0,49	0,99
06	60,5	0,38	0,53	0,65
040401	30,8	00,8	0,22	1,87
02	16,1	0,16	0,41	0,71
03	20,3	0,19	0,40	0,86
04	23,7	0,23	0,45	0,92
05	41,5	0,27	0,59	0,92
06	62,6	0,38	-	-
040501	28,7	0,06	0,27	1,28
02	14,0	0,15	0,42	0,70
03	16,7	0,16	0,38	0,92
04	20,3	0,19	0,43	0,92
05	51,2	0,38	0,46	0,89
06	-	-	0,61	0,63
040601	24,9	0,07	0,26	1,15
02	19,0	0,15	0,41	0,82
03	20,5	0,18	0,40	0,71
04	19,8	0,17	0,40	0,75
05	21,6	0,33	0,43	0,82
06	53,2	0,55	0,51	0,71
07	43,1	0,43	0,53	0,65
08	43,6	0,45	-	-
040701	31,0	0,08	0,31	1,28
02	23,5	0,14	0,44	0,82
03	18,6	0,14	0,43	0,71
04	19,3	0,17	0,41	0,75
05	23,3	0,24	0,39	0,82
06	48,1	0,40	0,54	0,65
07	63,7	0,75	-	-
040801	31,5	0,08	0,32	1,39
02	26,7	0,23	0,51	0,70
03	30,0	0,25	0,52	0,75
04	40,4	0,11	0,34	1,31
05	26,2	0,25	0,44	0,82
06	25,7	0,39	0,44	0,89
07	-	-	-	-
08	68,9	0,44	-	-
040901	36,9	0,10	0,51	1,01
02	46,3	0,21	0,34	0,95
03	62,2	0,19	0,25	1,01
04	34,1	0,16	0,46	1,35
05	36,7	0,19	0,42	1,12
06	-	-	-	-
07	90,3	0,30	0,22	0,35
041001	35,7	0,13	0,49	0,82
02	37,0	0,12	0,29	1,42
03	-	1,08	0,50	0,89
04	36,4	0,09	0,23	1,28
05	15,7	0,18	0,38	1,35
06	47,0	0,14	0,41	1,42
07	15,1	0,27	0,23	1,35
08	17,1	0,26	0,37	2,22
09	-	-	-	-
10	55,9	0,37	0,61	0,53
041101	41,9	0,19	0,39	1,81
02	08,6	0,24	0,94	2,02
03	36,3	0,17	0,40	1,98
041201	23,3	0,21	0,45	1,93
02	02,2	0,23	0,49	2,77
03	12,9	0,41	0,39	1,75
04	46,9	0,21	0,33	1,81
05	31,7	0,32	0,41	1,78
06	13,3	0,32	0,36	1,83
07	32,3	0,44	0,37	2,24
060001	-	-	-	-
02	-	-	-	-
03	-	-	-	-
04	53,6	0,30	0,69	0,49
05	93,5	0,41	0,36	0,40
06	59,9	0,79	0,50	0,60
07	-	-	-	-
08	-	-	-	-
09	81,4	0,07	0,21	0,84
10	57,1	0,08	0,41	0,72
11	-	-	-	-
12	54,5	-	-	-
13	43,5	-	-	-
14	47,2	-	-	-
15	-	-	-	-
16	82,2	-	-	-
17	96,1	-	-	-
18	-	-	-	-
19	-	-	-	-
20	62,0	-	-	-
21	(41,6)	-	-	-

4.2. LANGEBAAN LAGOON : GEOCHEMICAL PARAMETERS OF THE TOTAL SEDIMENT

SAMPLE	%$CaCO_3$	%$C_{org.}$	%P_2O_5	%K_2O	SAMPLE	%$CaCO_3$	%$C_{org.}$	%P_2O_5	%K_2O	SAMPLE	%$CaCO_3$	%$C_{org.}$	%P_2O_5	%K_2O
050101	28,5	0,11	0,51	0,82	06	45,5	0,14	0,33	1,25	03	10,1	0,17	0,18	0,43
02	35,6	0,18	0,53	0,72	07	42,5	0,14	0,38	1,25	04	13,6	0,11	0,17	0,56
03	30,9	0,18	0,51	0,75	08	35,9	0,14	0,28	1,52	05	12,6	0,15	0,19	0,62
04	23,0	0,08	0,28	1,30						06	06,7	0,14	0,26	0,99
05	28,8	0,13	0,26	1,22	050601	02,5	0,15	0,13	0,65	07	04,6	0,14	0,11	0,78
06	26,4	0,22	0,46	1,46	02	31,3	0,13	0,36	0,99	08	06,3	0,17	0,15	0,82
07	24,1	0,30	0,26	1,83	03	26,9	0,15	0,38	0,76	09	18,6	0,18	0,15	0,66
08	30,0	0,31	0,31	2,50	04	32,6	0,14	0,25	1,25	10	12,7	0,05	0,13	0,27
09	04,3	0,38	0,34	1,83	05	37,8	0,15	1,23	0,30					
10	03,7	0,32	0,26	1,98	06	40,2	0,23	1,47	0,26	051302	06,2	0,16	0,12	0,53
11	05,3	0,28	0,26	1,79	07	52,3	0,18	1,25	0,33	03	07,7	0,13	0,16	0,63
12	03,0	0,18	0,25	1,78	08	27,2	0,18	1,47	0,30	04	08,2	0,16	0,21	0,70
13	04,3	0,25	0,20	1,42	09	34,9	0,15	1,70	0,28	05	13,4	0,14	0,17	0,57
14	06,0	0,26	0,32	2,51	10	08,5	0,26	2,50	0,23	06	16,3	0,18	0,17	0,63
15	03,0	0,11	0,24	1,42						07	04,8	0,14	0,18	0,84
16	00,7	0,13	0,28	1,78	050701	10,9	0,28	0,63	0,10	08	06,0	0,14	0,15	0,70
17	01,9	0,13	0,12	1,52	02	08,8	0,14	0,72	0,09	09	28,4	0,13	0,25	0,46
18	02,1	0,15	0,29	1,88	03	11,3	0,21	0,76	0,29	10	18,8	0,12	0,21	0,43
19	02,3	0,13	0,20	1,47	04	28,8	0,14	0,95	0,38	11	22,0	0,06	0,18	0,30
20	02,7	0,20	0,37	2,02	05	36,0	0,16	1,18	0,29					
21	04,0	0,13	0,18	1,98	06	47,4	0,22	1,18	0,31	051403	06,4	0,27	0,19	0,78
22	10,6	0,71	0,20	1,98	07	40,9	0,16	1,42	0,25	04	03,8	0,14	0,20	0,66
23	02,7	0,43	0,18	2,55	08	19,6	0,16	1,83	0,26	05	04,4	0,11	0,13	0,43
24	07,4	0,16	0,20	2,51	09	05,6	0,30	3,13	0,25	06	11,6	0,14	0,15	0,43
25	06,6	0,14	0,20	2,67	10	03,2	0,08	1,98	0,17	07	26,6	0,11	0,26	0,36
										08	24,3	0,13	0,23	0,40
050201	24,8	0,13	0,50	0,72	050801	07,8	0,21	0,59	0,10					
02	26,6	0,35	0,47	0,72	02	09,4	0,12	0,72	0,17	051505	09,1	0,14	0,13	0,46
03	26,3	0,09	0,27	1,75	03	17,7	0,17	0,92	0,32	06	06,7	0,17	0,19	0,75
04	48,4	0,25	0,41	1,16	04	31,5	0,12	1,22	0,25	07	15,3	0,15	-	-
05	38,0	0,14	0,26	1,28	05	40,7	0,13	1,42	0,24	08	06,0	0,12	0,16	0,53
06	37,9	0,14	0,28	1,25	06	38,4	0,17	1,22	0,21	09	12,2	0,08	0,13	0,46
07	32,3	0,15	0,43	1,25	07	19,2	0,16	1,93	0,20	10	06,2	0,14	0,14	0,53
08	26,0	0,26	0,33	2,02	08	06,6	0,28	1,98	0,18	11	13,8	0,15	0,18	0,43
09	07,5	0,24	0,27	2,02						12	01,5	0,58	0,24	0,72
10	10,4	0,38	0,23	2,36	050901	10,3	0,14	0,76	0,21	13	18,3	0,21	0,20	0,43
					02	13,0	0,13	0,72	0,21					
050301	28,0	0,13	0,43	0,82	03	12,3	0,14	0,80	0,33	051605	03,1	0,15	0,15	0,63
02	41,6	0,11	0,28	1,25	04	39,2	0,16	1,18	0,24	06	08,2	0,13	0,20	0,70
03	41,1	0,11	0,31	1,28	05	39,4	0,15	1,31	0,34	07	05,8	0,09	0,11	0,78
04	42,1	0,12	0,23	1,35	06	07,9	0,15	2,10	0,13	08	05,2	0,15	0,18	0,72
05	47,5	0,15	0,25	1,35						09	05,1	0,15	0,14	0,40
06	39,7	0,10	0,24	1,35	051001	08,4	0,17	0,07	0,58	10	01,8	1,93	0,24	2,11
07	20,4	0,16	0,28	1,98	02	09,3	0,14	0,23	0,86					
08	03,1	0,24	0,14	2,70	03	11,4	0,13	0,31	0,80	051704	04,3	0,15	0,17	0,78
					04	17,0	0,13	0,24	0,82	05	06,5	0,13	0,19	0,72
050401	06,0	0,07	0,06	2,17	05	40,1	0,18	0,26	1,42	06	06,9	0,12	0,15	0,57
02	42,5	0,13	0,37	1,12	06	06,0	0,19	0,17	1,81	07	07,5	0,17	0,26	0,78
03	38,9	0,09	0,37	1,23						08	11,5	0,11	0,14	0,46
04	44,2	0,15	0,31	1,14	051101	04,0	0,18	0,09	0,53	09	03,4	0,42	0,15	0,63
05	40,1	0,15	0,23	1,25	02	03,5	0,20	0,10	0,57					
06	07,4	0,31	0,26	2,63	03	11,9	0,20	0,21	0,86	051807	03,1	0,15	0,18	0,72
					04	20,0	0,17	0,28	0,80	08	08,1	0,14	0,50	0,34
050501	08,0	0,12	0,14	0,82	05	22,0	0,18	0,29	1,57	09	04,6	0,17	0,14	0,43
02	33,5	0,16	0,42	0,92	06	05,8	0,14	0,15	1,81	10	14,0	0,18	0,13	0,30
03	30,0	0,11	0,39	0,86	07	09,5	0,15	0,30	0,89	11	12,1	0,10	-	-
04	27,2	0,14	0,36	1,18										
05	47,1	0,24	0,28	1,14	051202	08,6	0,19	0,37	0,66	051905	01,5	0,18	-	-